ADVANCED MICROBIAL BIOTECHNOLOGIES FOR SUSTAINABLE AGRICULTURE, VOLUME II

EDITED BY: Ying Ma, Helena Freitas, Christopher Rensing and Miroslav Vosatka

PUBLISHED IN: Frontiers in Microbiology

frontiers Research Topics

frontiers

ISSN 1664-8714
ISBN 978-2-83250-290-7
DOI 10.3389/978-2-83250-290-7

About Frontiers

Frontiers is more than just an open-access publisher of scholarly articles: it is a pioneering approach to the world of academia, radically improving the way scholarly research is managed. The grand vision of Frontiers is a world where all people have an equal opportunity to seek, share and generate knowledge. Frontiers provides immediate and permanent online open access to all its publications, but this alone is not enough to realize our grand goals.

Frontiers Journal Series

The Frontiers Journal Series is a multi-tier and interdisciplinary set of open-access, online journals, promising a paradigm shift from the current review, selection and dissemination processes in academic publishing. All Frontiers journals are driven by researchers for researchers; therefore, they constitute a service to the scholarly community. At the same time, the Frontiers Journal Series operates on a revolutionary invention, the tiered publishing system, initially addressing specific communities of scholars, and gradually climbing up to broader public understanding, thus serving the interests of the lay society, too.

Dedication to Quality

Each Frontiers article is a landmark of the highest quality, thanks to genuinely collaborative interactions between authors and review editors, who include some of the world's best academicians. Research must be certified by peers before entering a stream of knowledge that may eventually reach the public - and shape society; therefore, Frontiers only applies the most rigorous and unbiased reviews.
Frontiers revolutionizes research publishing by freely delivering the most outstanding research, evaluated with no bias from both the academic and social point of view. By applying the most advanced information technologies, Frontiers is catapulting scholarly publishing into a new generation.

What are Frontiers Research Topics?

Frontiers Research Topics are very popular trademarks of the Frontiers Journals Series: they are collections of at least ten articles, all centered on a particular subject. With their unique mix of varied contributions from Original Research to Review Articles, Frontiers Research Topics unify the most influential researchers, the latest key findings and historical advances in a hot research area! Find out more on how to host your own Frontiers Research Topic or contribute to one as an author by contacting the Frontiers Editorial Office: frontiersin.org/about/contact

ADVANCED MICROBIAL BIOTECHNOLOGIES FOR SUSTAINABLE AGRICULTURE, VOLUME II

Topic Editors:
Ying Ma, University of Coimbra, Portugal
Helena Freitas, University of Coimbra, Portugal
Christopher Rensing, Fujian Agriculture and Forestry University, China
Miroslav Vosatka, Institute of Botany (ASCR), Czechia

Citation: Ma, Y., Freitas, H., Rensing, C., Vosatka, M., eds. (2022). Advanced Microbial Biotechnologies for Sustainable Agriculture, Volume II. Lausanne: Frontiers Media SA. doi: 10.3389/978-2-83250-290-7

Table of Contents

frontiers in Microbiology

REVIEW
published: 30 November 2021
doi: 10.3389/fmicb.2021.775794

A Review of Ammonia-Oxidizing Archaea and Anaerobic Ammonia-Oxidizing Bacteria in the Aquaculture Pond Environment in China

Shimin Lu[1], Xingguo Liu[1]*, Chong Liu[1], Guofeng Cheng[1], Runfeng Zhou[1,2] and Yayuan Li[1,2]*

[1] Fishery Machinery and Instrument Research Institute, Chinese Academy of Fishery Sciences, Shanghai, China, [2] College of Fisheries and Life Science, Shanghai Ocean University, Shanghai, China

OPEN ACCESS

Edited by:
Christopher Rensing, Fujian Agriculture and Forestry University, China

Reviewed by:
Sebastià Puig, University of Girona, Spain
Norihisa Matsuura, Kanazawa University, Japan

****Correspondence:***
Shimin Lu
lushimin@fmiri.ac.cn
Xingguo Liu
liuxingguo@fmiri.ac.cn

Specialty section:
This article was submitted to Microbiotechnology, a section of the journal Frontiers in Microbiology

Received: *14 September 2021*
Accepted: *28 October 2021*
Published: *30 November 2021*

Citation:
Lu S, Liu X, Liu C, Cheng G, Zhou R and Li Y (2021) A Review of Ammonia-Oxidizing Archaea and Anaerobic Ammonia-Oxidizing Bacteria in the Aquaculture Pond Environment in China. Front. Microbiol. 12:775794. doi: 10.3389/fmicb.2021.775794

The excessive ammonia produced in pond aquaculture processes cannot be ignored. In this review, we present the distribution and diversity of ammonia-oxidizing archaea (AOA) and anaerobic ammonia-oxidizing bacteria (AnAOB) in the pond environment. Combined with environmental conditions, we analyze the advantages of AOA and AnAOB in aquaculture water treatment and discuss the current situation of pond water treatment engineering involving these microbes. AOA and AnAOB play an important role in the nitrogen removal process of aquaculture pond water, especially in seasonal low temperatures and anoxic sediment layers. Finally, we prospect the application of bioreactors to purify pond aquaculture water using AOA and AnAOB, in autotrophic nitrogen removal, which can reduce the production of greenhouse gases (such as nitrous oxide) and is conducive to the development of environmentally sustainable pond aquaculture.

Keywords: nitrogen removal, ammonia-oxidizing archaea, anammox, pond aquaculture, nitrous oxide

INTRODUCTION

China is the largest aquaculture country in the world, and the proportion of aquaculture in fish production increased to 73.7% in 2016 (Food and Agriculture Organization of the United Nations and Fisheries and Aquaculture Department, 2018). In 2019, pond aquaculture accounted for 48.9% of the national aquaculture output in China, among which, the output of freshwater pond and seawater pond aquaculture was 22.3 million tons and 2.5 million tons, respectively (Fisheries Bureau and Ministry of Agriculture and Rural Affairs of the People's Republic of China, 2020). In the process of pond aquaculture, the average nitrogen deposition rate of feed protein by aquatic animals is only about 30% (Ackefors and Enell, 1994); most organic nitrogen is retained in the pond aquaculture environment. Part of the organic nitrogen is transformed to NH_4^+-N by ammoniation of heterotrophic bacteria and is released into the aquaculture water, resulting in the pollution of aquaculture water and stress on the healthy growth of aquatic animals

(Randall and Tsui, 2002). The release of pond aquaculture water can also cause the eutrophication of the surrounding water environment. With the increase of pond aquaculture density and total yield, more and more ammonia is produced. Survey results showed that, in 2017, the ammonia emissions from aquaculture reached 22,300 tons in China, accounting for 10.31% of agricultural ammonia emissions (Ministry of Ecological Environment et al., 2020). At present, the amount of ammonia produced by aquaculture in China cannot be ignored.

Ammonia oxidation is the first step in the nitrification process, but also the rate-limiting step (Kowalchuk and Stephen, 2001). Traditionally, it was thought that ammonia oxidation mainly depends on ammonia-oxidizing bacteria (AOB). The relatively recent discovery of ammonia-oxidizing archaea (AOA) (Könneke et al., 2005) and anaerobic ammonia-oxidizing bacteria (AnAOB) (Mulder et al., 1995) not only substantially improved our understanding of the earth nitrogen cycle, but also provided new possibilities for nitrogen removal from pond aquaculture water. Compared with AOB, many new physiological characteristics appear in AOA and AnAOB. AOA have a higher affinity for ammonia, and the concentration of ammonia-saturated substrate is lower (Straka et al., 2019). AOA has very low requirements for dissolved oxygen (DO). At a DO concentration of just 0.4 μM, it can have high ammonia oxidation activity (Stahl and de la Torre, 2012). Compared with heterotrophic denitrification, low levels of organic carbon are involved in the anammox process (Mulder et al., 1995). When the water temperature is lower than 20°C, the activity of AOB decreases sharply (Hooper and Terry, 1973; Jiang and Bakken, 1999). However, AOA are not sensitive to temperature changes within a temperature range from 8 to 20°C (Stahl and de la Torre, 2012). The discovery of AOA and AnAOB provides an innovative tool for the advanced treatment of pond aquaculture water.

Here, we summarize the research status of AOA and AnAOB in aquaculture pond environments in chronological order and list the water quality characteristics of specific aquaculture ponds. Combined with the environmental conditions of the pond aquaculture, we analyze the advantages of AOA and AnAOB in aquaculture water treatment. In addition, we discuss the current state of pond water treatment application engineering, in which AOA and AnAOB are involved and prospect their application in the field of pond aquaculture. The purpose of this review is to explore the establishment of efficient pond aquaculture water treatment technology based on AOA or AnAOB.

DISTRIBUTION OF AMMONIA-OXIDIZING ARCHAEA AND ANAEROBIC AMMONIA-OXIDIZING BACTERIA IN A POND ENVIRONMENT

Ammonia-Oxidizing Archaea

Although AOA were found as early as 2005 (Könneke et al., 2005), it was not until 2012 that Shimin et al. (2012) reported their existence in a freshwater aquaculture pond environment. Based on AOA *amoA*, through the construction of a clone library, Lu (2014) found that 80% of AOA in the surface sediments of grass carp pond belonged to group I.1b; the other 20% of AOA belonged to group I.1a. However, all the AOA attached to the fibrous roots of *Ipomoea aquatica* in a grass carp pond belonged to group I.1b (Lu, 2014). In 2015, Srithep et al. (2015) found that there were groups I.1a and I.1b in the sediment of shrimp ponds, and the majority of AOA sequences fell closer to group I.1a. Lu et al. (2016) found that the AOA in the 0- to 2-cm sediment layer of *Megalobrama amblycephala* ponds belonged to a *Nitrososphaera* cluster, while those in the deeper sediment layers belonged to a *Nitrosopumilus* cluster. Using the same experimental method, in 2017, it was found that AOA species affiliated to *Nitrososphaera*-like and *Nitrososphaera* clusters in three *Mandarin* fish ponds (Zhou et al., 2017). In 2019, metagenome analysis showed that *Nitrosopumilus* and *Nitrososphaera* were major AOA groups in all sediment layers of a grass carp aquaculture pond (Deng et al., 2020). Based on AOA *amoA*, in 2021, through the Illumina MiSeq platform analysis method, a phylogenetic tree revealed that most of the AOA in shrimp pond sediment were members of *Nitrosopumilus* and *Nitrososphaera* (Wei et al., 2021). Studies showed that AOA could be grouped into five major clusters: *Nitrosopumilus* (also known as group I.1a AOA), *Nitrosotalea* (also known as group I.1a-associated AOA), *Nitrososphaera* (also known as group I.1b AOA), *Nitrososphaera* sister cluster, and *Nitrosocaldus* (also known as thermophilic AOA, ThAOA) (Pester et al., 2012). Therefore, groups I.1a and I.1b AOA are so far considered to be the dominant species in the pond environment.

Perhaps subjected to photoinhibition (Lu S. et al., 2020), the abundance of AOA in pond aquaculture water is very low. However, abundant AOA are widespread in the surface sediments of aquaculture ponds (**Table 1**). Lu (2014) found that the abundance of AOA *amoA* gene in the surface sediments (0–5 cm depth) of grass carp ponds in Central China ranged from 4.21 (±2.00) × 10^5 to 1.71 (±0.76) × 10^6 copy g^{-1}, about one order of magnitude higher than that of AOB. Lu et al. (2016) found that the abundance of the *amoA* gene ranged from 6.82 (±2.28) × 10^4 to 7.79 (±3.88) × 10^5 copies g^{-1} in a *M. amblycephala* pond at a 0- to 25-cm-deep sediment layer. Zhou et al. (2017) found that the average archaeal *amoA* gene copy number in three ponds feeding *Mandarin* fish was from 2.53 × 10^6 to 4.13 × 10^6 copies g^{-1} dry sediment. In 2020, it was found that the copy number of AOA *amoA* genes varied widely in shrimp sediment at different culture stages, ranging from 9.04 (± 0.32) × 10^5 to 1.92 (± 2.2) × 10^6 *amoA* gene copies per gram of dry sediment (Wei et al., 2021). At present, the existing research on the detection of AOA abundance in ponds was all based on the AOA *amoA* gene. Each AOA cell of groups I.1a and I.1b has one copy of the *amoA* gene (Liu, 2019), so it can be inferred that the abundance of AOA in pond sediments is 10^4–10^6 cell g^{-1} sediment.

Perhaps because of the difficulty in culturing AOA in the laboratory, there are few reports of AOA strains or high abundance cultures originating from fishponds. The research studies on the physical and chemical properties of AOA are almost all based on the statistical analysis of AOA and environmental factor data. For instance, it was found that

TABLE 1 | Studies on ammonia-oxidizing archaea (AOA) and anaerobic ammonia-oxidizing bacteria (AnAOB) in the pond environment.

Environment	AOA/ AnAOB	Community	Abundance	Potential rates	Reference
0–5 cm deep sediment of grass carp ponds	AOA	80% AOA belonged to the *Nitrososphaera* cluster and 20% AOA belonged to the *Nitrosopumilus* cluster	$4.22 \pm 2.00 \times 10^5$ to $1.71 \pm 0.76 \times 10^6$ *amoA* gene copies g^{-1} throughout the year	/	Lu, 2014
Ipomoea aquatica Forsk roots in grass carp ponds	AOA	100% AOA belonged to group I.1b	$5.41 \pm 0.25 \times 10^3$–$3.82 \pm 0.37 \times 10^4$ *amoA* gene copies g^{-1} *rhizosphere*	/	Lu, 2014
Shrimp pond sediment	AOA	More than 99.29% AOA in each sample fell within the *Nitrososphaera* group, the other AOA belonged to the *Nitrosopumilus* group	$9.04 \pm 0.32 \times 10^5$ to $1.92 \pm 2.2 \times 10^6$ *amoA* gene copies g^{-1} dry sediment	/	Wei et al., 2021
0–2 cm deep sediment from a *Megalobrama amblycephala* pond	AOA	100% AOA belonged to the *Nitrososphaera* cluster	$7.79 \pm 3.88 \times 10^5$ *amoA* gene copies g^{-1} sediment	/	Lu et al., 2016
10–15 cm and 20–25 cm deep sediment of a *Megalobrama amblycephala* pond	AOA	100% AOA belonged to the *Nitrosopumilus* cluster	$6.82 \pm 2.28 \times 10^4$ to $1.69 \pm 0.86 \times 10^5$ *aomA* gene copies g^{-1} sediment	/	Lu et al., 2016
Crab pond water	AOA	97% AOA belonged to the *Nitrosopumilus* cluster; 3% AOA belonged to the *Nitrososphaera cluster*	/	/	Zhang et al., 2016
Grass carp ponds	AOA	*Nitrosopumilus* and *Nitrososphaera* AOA were detected in water and sediment	/	/	Deng et al., 2020
Shrimp pond sediment	AOA	80% AOA were related to group I.1a, 20% AOA belonged to group I.1b Thaumarchaeota	About 100 amoA gene copies ng^{-1} DNA	/	Srithep et al., 2015
0–5 cm deep sediment of grass carp ponds in spring	AnAOB	/	$2.03 \pm 0.92 \times 10^5$ 16S rRNA gene copies g^{-1} sediment	/	Lu, 2014
0–5 cm deep sediment of grass carp ponds in summer	AnAOB	/	$3.91 \pm 1.92 \times 10^5$ 16S rRNA gene copies g^{-1} sediment	/	Lu, 2014
0–5 cm deep sediment of grass carp ponds in autumn	AnAOB	/	$4.56 \pm 1.51 \times 10^5$ 16S rRNA gene copies g^{-1} sediment	/	Lu, 2014
0–5 cm deep sediment of grass carp ponds in winter	AnAOB	/	$1.46 \pm 0.69 \times 10^5$ 16S rRNA gene copies g^{-1} sediment	/	Lu, 2014
Surface sediment of grass carp ponds	AnAOB	Candidate division *Zixibacteria* (35.5–42.4%), Candidatus *Latescibacteria* (8.5–10.4%), and *Desulfuromonadales* (9.9–10.4%) (*Geobacter*-like) were the dominant AnAOB	/	/	Deng et al., 2020
Freshwater aquaculture pond	AnAOB	Including Candidatus *Brocadia*, Candidatus *Kuenenia,* and Candidatus *Anammoxoglobus*, with Candidatus *Brocadia* being the dominant AnAOB genus	5.6×10^4 to 2.1×10^5 *hzs* gene copies g^{-1} sediment	3.7–19.4 nmol N_2 g^{-1} sediment day^{-1}; Contribution to sediment N_2 ranged from 1.2 to 15.3%	Shen et al., 2016
Shrimp aquaculture ponds	AnAOB	The phylogenetic tree of AnAOB based on *hzo* gene sequences showed relatedness to *Candidatus Kuenenia* and *Candidatus Scalindua* genera	10^6 to 10^7 *hzo* gene copies g^{-1} sediment	/	Nair et al., 2020
A semi-intensive shrimp pond	AnAOB	*Ca.* "*Kuenenia*"-like gene fragments were the major component of AnAOB	/	0.7 nmol N_2 cm^{-3} h^{-1}	Amano et al., 2011
Tropical aquaculture settlement ponds	AnAOB	/	/	0–7.07 nmol N cm^{-3} h^{-1}	Castine et al., 2012

"/" indicates no relevant data.

both the abundance and diversity of AOA were significantly negative to the concentration of ammonium in interstitial water (Zhou et al., 2017). Correlation analyses indicated a significant correlation between the abundance of AOA and total nitrogen (TN) and arylsulfatase, and AOA diversity was significantly correlated with β-glucosidase (Dai et al., 2018). The conclusion was that AOA communities in the surface sediments of aquaculture ponds were regulated by organic matter. The AOA community has a close relationship with total organic carbon (TOC), pH, total phosphorus, nitrate reductase, urease, acid phosphatase, and β-glucosidase (Wei et al., 2021).

Anaerobic Ammonia-Oxidizing Bacteria

Mulder et al. (1995) confirmed that anammox was driven by microorganisms by using isotope tracer technology. In the reaction process, AnAOB uses one molecule of ammonia and one molecule of nitrite to produce one molecule of nitrogen gas, and with no need to supplement an organic carbon source in the process. Later, it was found that anammox was responsible for 24–67% of nitrogen loss in marine sediments (Thamdrup and Dalsgaard, 2002). Moreover, the anammox phenomenon existed in many other environments, such as lakes (Schubert et al., 2006), rivers (Zhang et al., 2007), and soil (Zhu et al., 2011). In recent years, technology using anammox in wastewater treatment has been widely applied around the world (Lackner et al., 2014; Weralupitiya et al., 2021).

The anammox phenomenon is also associated with the pond aquaculture environment (**Table 1**). In 2011, it was reported that the rate of potential anammox activity was 0.7 nmol N_2 cm^{-3} h^{-1}, and corresponded to at most 2% of the denitrification. *Kuenenia*-like AnAOB were the major component recovered from shrimp pond sediment (Amano et al., 2011). Lu (2014) found AnAOB accompanied by AOA in the surface sediments of freshwater aquaculture ponds. The abundance of AnAOB 16S rRNA ranged from 1.46 ($\pm$ 0.69) $\times$ 10^5 to 4.56 ($\pm$ 1.51) $\times$ 10^5 copies g^{-1} sediment throughout the whole year, and the highest abundance occurred in the autumn when the water temperature was 18°C (Lu, 2014). Shen et al. (2016) found that the abundance of the AaAOB *hzs* gene ranged from 5.6 $\times$ 10^4 to 2.1 $\times$ 10^5 copies g^{-1} sediment in different freshwater aquaculture ponds, and this process contributed to 1.2-15.3% of sediment N_2 production. In the same year, both 16S rRNA and *hzo* gene diversity analyses indicated that the major AnAOB in the sediments of marine aquaculture zones were *Scalindua*-related species, although *Kuenenia*-like AnAOB could also be detected from one of the four selected sampling sites (Li and Gu, 2016). In 2018, AnAOB were stimulated with the supplementation of bicarbonate in shrimp aquaculture sediment. The enriched AnAOB achieved a maximum nitrogen removal efficiency rate of 1.00 $\pm$ 0.02 kg-N m^{-3} day^{-1} (Luong Van et al., 2018). Nair et al. (2020) found that the abundance of the AnAOB *hzo* gene ranged from 10^6 to 10^7 copies per gram of sediment, and the concentration of ammonia, nitrite, redox potential, and the total organic carbon showed a strong positive correlation with the abundance of AnAOB in zero water exchange aquaculture ponds. There is no doubt that Anammox is ubiquitous in pond sediments and plays an important role in the process of ammonia oxidation and denitrification. The predominant AnAOB species and its driving factors in the pond environment are still uncertain.

OPPORTUNITY FOR NITROGEN REMOVAL BY AMMONIA-OXIDIZING ARCHAEA AND ANAEROBIC AMMONIA-OXIDIZING BACTERIA IN AQUACULTURE PONDS

As mentioned above, AOA and AnAOB are widespread in the aquaculture pond environment, which means the nutrient elements of fishponds are suitable for the growth of AOA and AnAOB. Here, combined with the characteristics of the aquaculture pond, we analyze the feasibility of pond aquaculture water purification using AOA and AnAOB, from the perspective of DO, temperature, organic matter, ammonia, and pH.

Temperature

Pond aquaculture is widely distributed in China and Southeast Asian countries. Generally, fish, shrimp, or crab fry start feeding when the water temperature rises every spring. After the summer to the end of autumn or winter, when breeding conditions are unsuitable for feeding due to low water temperature, drainage is started and nets are used to capture activity. In one aquaculture year, the temperature of the pond water varies widely. For example, in Central China, in the largest pond aquaculture area in China, the water temperature ranges from 5 to 28°C throughout the year and is only 4–18°C in autumn and winter (Lu et al., 2015). AOB activities could be severely inhibited under low temperatures (<15°C) (Zhang et al., 2020). AOA can compensate for the deficiency of AOB ammonia oxidation activity at low temperatures. AOA is more resistant to low temperature, and it is reported that they are not sensitive to temperature changes within 8–20°C (Stahl and de la Torre, 2012). In freshwater pond sediment, it was found that the maximum abundance of AOA occurred in winter, when the water temperature was 4°C, while the maximum abundance of AOB occurred in the autumn, when the water temperature was 18°C (Lu et al., 2015), indicating that AOA makes a greater contribution to ammonia oxidation in the pond environment at low temperatures. Similar phenomena occurred in some biofilm reactors. It was evaluated that up to 94.9% of the overall ammonia oxidation could be attributed to AOA at 10°C, 48.2% of that was undertaken by AOA at 35°C (Lin et al., 2020).

As with AOA, AnAOB also can adapt to a wide range of temperatures. It was reported that anammox can take place at temperatures from 6 to 43°C; the reaction rate drops rapidly at temperatures lower than 15°C or higher than 40°C (Ma et al., 2016). Although few studies have reported that AnAOB can adapt to a low temperature pond environment, it was documented in some anammox reactors. For instance, in an up-flow anaerobic sludge blanket, a high nitrogen removal rate of 2.28 kg N m^{-3} day^{-1} was achieved at a temperature of 16°C (Ma et al., 2013). In a gel carrier with entrapped AnAOB, anammox activity still occurred at 6.3°C. The nitrogen conversion rates at 22 and 6.3°C were 2.8 and 0.36 kg N m^{-3} day^{-1}, respectively (Isaka et al., 2008). This discovery has developed our understanding of AOA and AnAOB in the nitrogen cycling of pond aquaculture at low seasonal temperatures.

Dissolved Oxygen

The aquaculture animals in fishponds need high concentrations of DO, and on sunny days, in surface aquaculture water, the DO is often in a supersaturated state, whereas the subsurface sediment of the pond is anoxic. It was reported that the depth of the DO detection limit was 500 μm in freshwater pond surface sediment, and the DO concentrations ranged from 0 to 48.01 μmol L^{-1} (Lu et al., 2016). In contrast to AOB,

AOA is more suitable for low DO in pond surface sediments. AOA often thrive at DO levels of ca. 3 μM and can achieve higher ammonia oxidation under oxygen-limited conditions (Stahl and de la Torre, 2012). AOA has an affinity for oxygen that is more typical of aerobic microorganisms (∼4 μM) and is unable to grow anaerobically under the culture conditions so far evaluated (Stahl and de la Torre, 2012). For example, the AOA enrichment of *Nitrososphaera viennensis* had kinetic km, $O_2 \approx 2.9$ μM (Straka et al., 2019); however, the oxygen half-saturation constant of AOB was 21.4–56.4 μM in continuous stirred tank reactors (Guisasola et al., 2005; Manser et al., 2005; Daebel et al., 2007; Jubany et al., 2008). AOA could outcompete AOB and occupy the corresponding niche under anoxic sediment.

Unlike AOA and AOB, AnAOB is a type of anaerobic ammonia-oxidizing microorganism, whose activity could be inhibited by the presence of oxygen (Liu et al., 2016). AnAOB needs substrate NO_2^--N, which could only be provided by AOA or AOB in a pond environment. Therefore, in the surface sediment, AnAOB always exists with AOA and AOB in the autotrophic nitrogen removal process. For example, AOA *Nitrosopumilus* sp., *Nitrososphaera* sp., AOB *Nitrosomonas* sp., and AnAOB Candidatus *Kuenenia* sp. were found to be the dominant ammonia-oxidizing communities in zero water exchange shrimp ponds (Nair et al., 2019, 2020). Throughout the year, there were AnAOB, AOA, and AOB in the surface sediments of the grass carp pond. Moreover, there was a significant positive correlation between the abundance of AOA *amoA* and AnAOB 16S rRNA genes in the winter, which indicates that there is a synergistic effect between AOA and AnAOB in pond sediments in winter (Lu, 2014).

The AnAOB activity could be inhibited by the presence of oxygen (Liu et al., 2016); so far, no anammox activity has been reported in pond aquaculture water. However, AnAOB can be detected in aerated systems, such as nitrogen-removing moving bed biofilters (van Kessel et al., 2010; Persson et al., 2014), rotating biological contactor and biofilters (Egli et al., 2003), and the simultaneous partial nitrification, anammox, and denitrification (SNAD) bioreactor (Lu J. et al., 2020). They probably inhabit the oxygen-depleted zones of aerated biofilters (Mulder et al., 1995), where an anoxic environment is created by AOA, AOB, and heterotrophic bacteria. AnAOB use nitrite and ammonia generated by heterotrophic denitrification and the dissimilatory nitrate reduction process (Hao et al., 2021) (**Figure 1A**), where nitrate concentration is high but ammonia and nitrite are scarce. Alternatively, AnAOB can use nitrite produced by AOA and AOB and ammonia generated by heterotrophic ammonification, in what is called the one-stage nitritation/anammox process (Li et al., 2018) (**Figure 1B**).

Because the anammox process takes ammonia as the electron donor and nitrite as the electron acceptor to directly generate nitrogen gas, there is no need to oxidize nitrite into nitrate, only oxygen is required in the ammonia oxidation process. Compared with the traditional nitrification-denitrification water treatment process, the total energy for aeration can be reduced by 60% (Moomen and Ahmed, 2018). Therefore, bioreactors based on AOA and AnAOB are expected to be used in the treatment of pond aquaculture water in the future.

Ammonia

In the pond aquaculture environment, the ammonia concentrations between aquaculture water and pore water of surface sediment are quite different. For example, the survey results of 10 grass carp ponds showed that the ammonia concentration in sediment pore water is 3.30 ± 0.88 mM L^{-1}, while the ammonia concentration in aquaculture water is only 0.16 ± 0.13 mM L^{-1} (Lu et al., 2015). From the perspective of tolerance to ammonia concentration, some AOA strains may not adapt to the high ammonia concentration level in sediment pore water. For example, a study on AOA isolated from a recirculating aquaculture system (RAS) showed that the ammonia concentration of 0.25–1 mM L^{-1} is suitable for the growth of AOA. When the concentration of ammonia reaches 2 mM L^{-1}, the growth of AOA appears to be inhibited (Sauder et al., 2018). In enrichment cultures, AOA-DW and AOA-AC5 showed the highest growth at the ammonia concentration of 1 and 2 mM L^{-1}, respectively (French et al., 2012). However, some AOA strains or cultures can endure higher ammonia concentrations, such as the high tolerances to NH_4^+ observed for *N. viennensis* (15 mM L^{-1}) (Tourna et al., 2011), Ca. *Nitrosoarchaeum koreensis* (10 mM L^{-1}), and a strain in the AOA AC2 enrichment culture (5 mM L^{-1}) (French et al., 2012). It was found that group I.1b AOA species could tolerate very high ammonium concentrations (Jung et al., 2021).

As mentioned above, the AOA of the pond aquaculture environment mainly belong to group I.1a and group I.1 b. The latest research also showed that the AOA of group I.1a and group I.1b had a wide range of cellular ammonia affinities (Jung et al., 2021). Group I.1a AOA displayed a high substrate affinity, and the ammonia apparent-half-saturation concentration Km(app), which ranged from ∼2.2 to 24.8 nM, can adapt to oligotrophic conditions, while several group I.1b species possess a wide range of affinities for NH_3 [Km(app) = ∼0.14 to 31.5 μM] (Jung et al., 2021). Compared with AOB, AOA may not have the advantage of using high-concentration ammonia. However, the AOA strains showed a higher affinity for ammonia than published AOB measurements (>20 μM) (Straka et al., 2019). Throughout the year, the concentrations of pond aquaculture water ammonia are less than 0.21 mM L^{-1} most of the time (**Table 2**). Therefore, AOA has greater advantages than AOB in the advanced treatment of aquaculture water with a low ammonia nitrogen concentration. Because pond aquaculture facilities are relatively simple, few reports exist on using bioreactors to treat pond aquaculture water based on AOA. However, it was well documented in a limit water exchange recirculating freshwater aquarium using a down-flow hanging sponge and up-flow sludge blanket system to remove nitrogen, in which only AOA was detected, and no AOB existed (Adlin et al., 2017).

Unlike AOA, AnAOB prefer to live in an environment with high concentrations of ammonium, and it was reported that AnAOB was inhibited only when ammonium concentrations are above 71.43 mM L^{-1} (Jin et al., 2012). As shown in **Table 2**, the concentration of pore water ammonia is never

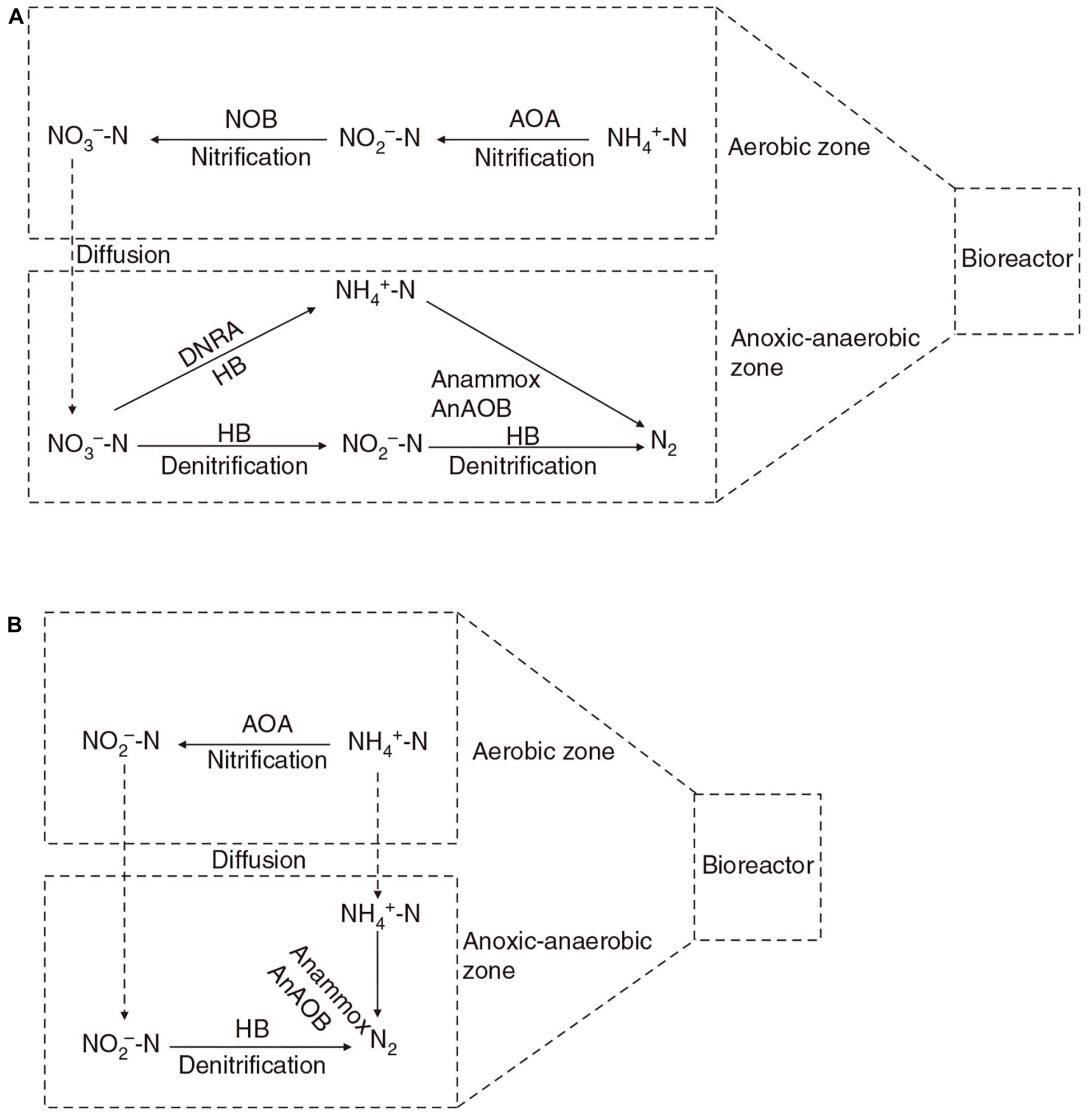

FIGURE 1 | Cooperative working mechanism of AOA and AnAOB in bioreactor. AOA, ammonia-oxidizing archaea; NOB, nitrite-oxidizing bacteria; AnAOB, anaerobic ammonia-oxidizing bacteria; HB, heterotrophic denitrifying bacteria; DNRA, dissimilatory nitrate reduction to ammonium process. Solid arrows represent different nitrogen cycling processes, and the dashed arrow represents diffusion in bioreactor. AnAOB use nitrite and ammonia generated by heterotrophic denitrification and dissimilatory nitrate reduction process in the anoxic–anaerobic zone of biofilm **(A)**, where the nitrate concentration is high but ammonia and nitrite are scarce. Alternatively, AnAOB can directly use nitrite produced by AOA and ammonia generated by heterotrophic ammonification, where nitrite-oxidizing bacteria are inhibited **(B)**.

higher than 7.14 mM L^{-1}, indicating that AnAOB could not be inhibited by the sediment ammonia. AnAOB can also grow well in an environment with low ammonia concentration, this phenomenon is apparent in a marine environment. For example, the ammonium concentration is no more than 0.1 mM L^{-1} in the deep water of the black sea, where the abundance of AnAOB ranged from 300 to 3,000 cells mL^{-1} in the suboxic zone, and consume more than 40% of the fixed nitrogen (Kuypers et al., 2003). As shown in **Table 2**, the concentration of ammonia in pond aquaculture water is generally maintained above 0.07 mM L^{-1}, indicating that the ammonia concentrations of the pond environment are suitable for AnAOB growth. As discussed above, a bioreactor may need to be established, when removing aquaculture water nitrogen using AnAOB and AOA.

Organic Matter

The AOB is a strictly chemoautotrophic microorganism and cannot use organic matter (Jin et al., 2012). However, a genomic bioinformatic analysis showed that AOA has the genetic potential for mixed trophic metabolism (Walker et al., 2010). AOA genomes encode five carbohydrate-active enzyme families: glycoside hydrolases, glycosyl transferases, carbohydrate esterases, carbohydrate-binding modules, and auxiliary activities (Liu, 2019). Moreover, it was found that the AOA genome

TABLE 2 | Characteristics of pond aquaculture water and pore water of sediment.

Pond	NH_4^+-N (mM L^{-1})	NO_2^--N (μM L^{-1})	NO_3^--N (μM L^{-1})	COD (mg L^{-1})	Reference
Surface water of grass carp ponds	0.07–0.18	1.43–17.14	15.00–59.29	/	Qin, 2016
Bottom water of grass carp ponds	0.07–0.19	1.43–17.14	17.86–60.71	/	Qin, 2016
Surface water of grass carp ponds in spring	0.09 ± 0.02	5.00 ± 2.14	9.29 ± 3.57	/	Lu et al., 2015
Surface water of grass carp ponds in summer	0.2 ± 0.07	24.29 ± 25.71	9.29 ± 2.86	/	Lu et al., 2015
Surface water of grass carp ponds in autumn	0.16 ± 0.13	9.28 ± 6.43	40.71 ± 18.57	/	Lu et al., 2015
Surface water of grass carp ponds in winter	0.07 ± 0.06	5.00 ± 2.14	40.71 ± 23.57	/	Lu et al., 2015
0.3 m below the surface water of shrimp pond	0.005 ± 0.002–0.008 ± 0.002	2.14 ± 0.64–10.07 ± 2.57	29.57 ± 5.93–55.43 ± 15.14	3.84 ± 0.24–4.62 ± 0.24	Li et al., 2021
At 0.6 m depth water of a *Penaeus vannamei* pond	0.004–0.07	11.43–55.71	8.57–32.14	/	Li et al., 2019
Freshwater aquaculture pond	0.04–0.07	/	/	2.9–4.0	Li and Li, 2009
An intensive pond aquaculture system	0.04 ± 0.004–0.13 ± 0.003	6.43 ± 0.00–43.57 ± 1.43	/	/	Bao et al., 2018
Mandarin fish ponds	0.01–0.14	/	3.57 ± 1.43–582.86 ± 11.43	8.32 ± 0.23–15.64 ± 1.20	Zhou et al., 2017
Shrimp ponds	0.03 ± 0.04–0.05 ± 0.07	−24.29 ± 42.14	3.57 ± 5.00–43.57 ± 57.14	53.5 ± 25.8–99.9 ± 23.9	Lin et al., 2010
Pore water of grass carp pond sediment	0.82 ± 0.17	2.14 ± 0.71	142.14 ± 27.86	/	Deng et al., 2020
Pore water of freshwater aquaculture pond sediment	1.2–3.4	2.14–0.004	11.43–25.71	/	Shen et al., 2016
Pore water of grass carp pond sediment in spring	1.69 ± 0.92	0.71 ± 0.00	8.57 ± 2.86	/	Lu et al., 2015
Pore water of grass carp pond sediment in summer	3.30 ± 0.88	7.86 ± 5.71	9.29 ± 2.86	/	Lu et al., 2015
Pore water of grass carp pond sediment in autumn	1.09 ± 0.41	0.71 ± 0.00	10.71 ± 2.14	/	Lu et al., 2015
Pore water of grass carp pond sediment in winter	1.44 ± 0.50	1.43 ± 0.00	12.86 ± 2.86	/	Lu et al., 2015
Pond sediment	4.96 ± 0.11	450.00 ± 99.29	1, 063.57 ± 70.71	/	Wei et al., 2021
Mandarin fish pond sediment	0.15 ± 0.01–0.28 ± 0.002	/	2.86 ± 0.00–35.71 ± 3.57	/	Zhou et al., 2017

"/" indicates no relevant data.

encodes organic transport protein families, such as the divalent anion Na^+ symporter family, which has the ability to transport extracellular succinate, malate, aspartic acid, α-ketoglutarate, etc. (Liu, 2019). Isolated AOA strains also showed mixed trophic phenomenon that can utilize some organic carbon compounds, such as α-ketoglutarate (Qin et al., 2014), cyanate (Palatinszky et al., 2015), urea (Tolar et al., 2016), and pyruvic acid (Tourna et al., 2011), although the association between these characterizations and the AOA genomic features has not been demonstrated. In addition, the AOA strain *Nitrososphaera gargensis* could degrade sulfonamide antibiotics through deamination, hydroxylation, and nitrification (Zhou et al., 2019). Perhaps, its ability to degrade and utilize organic compounds leads to its widespread presence in the pond sediment.

At present, residual bait and feces are directly left at the bottom of the aquaculture pond, and the aquaculture water is in close contact with the sediment. In most cases, the nitrate in the aquaculture water body will not accumulate in large quantities (**Table 2**). However, the organic matter of aquaculture water is often insufficient to support heterotrophic denitrification in the complete removal of nitrate from the water, without the sediment. It is reported that in the circulating water culture system of *Paralichthys olivaceus*, the concentration of nitrate even exceeds 35.71 mM L^{-1} (Honda et al., 1993). AnAOB are chemoautotrophic microorganisms with CO_2 as the main carbon source (Kuenen, 2008). In the anammox process, ammonia can be the electron donor, and little organic carbon is required. Autotrophic anammox can make up for the lack of heterotrophic denitrification function. It is generally thought that abundant organic matter has adverse effects on AnAOB (van de Graaf et al., 1996; Tang et al., 2010). It was reported that anammox activity can be inhibited, when the chemical oxygen consumption (COD) of pig manure effluent is >237 mg L^{-1} (Molinuevo et al., 2009). As shown in **Table 2**, the COD of pond aquaculture water is less than 100 mg L^{-1}. Hence, it can be inferred that the concentration of organic matter in pond aquaculture water will not inhibit AnAOB. Although at present, there is no report about suspended or attached AnAOB in pond aquaculture water, as mentioned above, AnAOB that could effectively be integrated in RAS biofilter systems had to be found (van Kessel et al., 2010). The organic matter composition of pond water is similar to that of RAS aquaculture water; both mainly originate from feces and residual bait. Therefore, it is very possible to purify pond aquaculture water by biofilter systems with attached AnAOB, coupling AOA and AOB, for autotrophic nitrogen removal, in the absence of sediment.

pH

The pH affects the ratio of ammonium ions (NH_4^+) to ammonia molecules (NH_3) and then affects the ammonia oxidation function of AOA (He et al., 2012). In the breeding season, the ideal pH range of a healthy freshwater pond within 24 h is 6.5–9.0 (Wurts and Durborow, 1992). At present, most studies

have shown that the best pH for the growth of group I.1a or group I.1b AOA is close to 7.0. For example, AOA strain JG1 belonging to group I.1b shows an optimal pH for ammonia oxidation of 6.5–7.0, the ammonia oxidation rate decreased below pH 6, and no sign of ammonia oxidation was observed at pH 5.5 or 8.0 (Kim et al., 2012). Three AOA cultures belonging to thaumarchaeal group I.1a grow at almost the same rate over a wide pH range of 6.5–9.0, with the highest growth rate occurring at pH 7 to 7.5 (French et al., 2012). On sunny days, the pH of surface pond water is not suitable for AOA growth. However, research has shown that the pH is very different between the surface and bottom water of aquaculture ponds in sunny weather. The pH of the bottom pond water is still close to 7.0 when the pH of the surface water approaches 9.0 (Deng et al., 2020). The pond bottom water can provide stable pH for the growth of AOA.

It has been reported that AnAOB have a physiological pH of 6.5 to 9.0 (Oshiki et al., 2016). The tolerance of AnAOB to pH is dependent on the species. For example, the optimal pH for Ca. *Brocadia sinica* was 7.0–8.8, while Ca. *Brocadia* sp. 40 had an optimal pH of 6.8–7.5 (Oshiki et al., 2016). The metabolic activity of AnAOB can be suppressed when the pH value is too high. It was found that the anammox bioreactor became destabilized when the effluent pH increased to 8.7–9.1, accompanied by the free ammonia concentration of 4.57–5.21 mM L^{-1} (Tang et al., 2009). In anammox reactors, a high pH should be avoided, a pH near neutral is the best option (Ma et al., 2016). As mentioned above, the pH of the bottom pond water is close to 7.0, which can meet the needs of both AOA and AnAOB.

Nitrous Oxide

Nitrous oxide (N_2O) is a strong greenhouse gas, which has a Ca. 300-times-higher warming impact than CO_2, responsible for 5–7% of the observed greenhouse effect (Rahn, 1997; Fux and Siegrist, 2004; Santoro et al., 2011). Tropospheric concentrations of N_2O are rising at a rate of ∼0.25% per year (Santoro et al., 2011). In biological wastewater treatment, microbial processes such as autotrophic nitrification and heterotrophic denitrification have been identified as major sources (Pw et al., 2012). It was documented that NO is an intermediate metabolite of AnAOB, but it cannot be further oxidized to N_2O, and AnAOB cannot produce N_2O (Fux and Siegrist, 2004; Kartal et al., 2010). AOB can produce N_2O during the oxidation of ammonia (NH_3) to nitrite (NO_2^-) and reduction of NO_2^- to N_2O in a process frequently termed "nitrifier-denitrification" (Ostrom et al., 2000). N_2O can also be produced by AOA; however, a study has shown that the total amount of N_2O accumulated by strains of group I.1a was far lower than that produced by AOB of *Nitrosomonas europaea*. The N_2O production of AOA strains was only 18% of that produced by *N. europaea*, when generating the same amount of NO_2^- (Jung et al., 2011). As mentioned above, AOA in the pond aquaculture environment mainly belongs to group I.1a and group I.1b, and AOB mainly belongs to *N. europaea* (Lu et al., 2019). Therefore, AOA replaces AOB for ammonia oxidation, and AnAOB replaces heterotrophic denitrification, to some extent, which can reduce the production of greenhouse gases and is conducive to the development of environmentally sustainable pond aquaculture.

CURRENT APPLICATION AND PROSPECTS OF AMMONIA-OXIDIZING ARCHAEA AND ANAEROBIC AMMONIA-OXIDIZING BACTERIA IN POND AQUACULTURE

Applications

To develop eco-friendly pond aquaculture, the impact of aquaculture tailwater on the surrounding water environment needs to be minimized. Now, many governments have formulated strict standards of aquaculture wastewater discharge. For example, in China, the government requires that the TN of freshwater pond tailwater should not exceed 0.21 mM L^{-1} (Requirement for Water Discharge from Freshwater Aquaculture Pond, SC/T9101-2007). Specific ecological engineering measures are taken for purifying pond aquaculture water, which includes *in situ* water treatment facilities, such as *in situ* biological floating beds (Lu, 2014) and ecological slopes (Liu X. et al., 2021), and ectopic water treatment facilities, such as artificial subsurface flow wetland (Liu X. et al., 2021) and settlement ponds (Castine et al., 2012). These engineering measures during nitrogen removal processes more or less involve AOA or AnAOB. For example, a biological floating bed is usually set up on the surface of the pond water to purify aquaculture water; the developed rhizosphere of the aquatic plants can create a good habitat for the growth of AOA and AOB and rely on their attachment to accelerate the nitrogen transformation of the aquaculture environment. The abundance of AOA in the floating bed rhizosphere of water spinach in grass carp ponds was up to ∼10^5 cell g^{-1} rhizosphere (Lu, 2014); however, at the same time, the abundance of AOA in the surrounding aquaculture water was below the detection limit (Lu, 2014). One of the purposes of a pond ecological slope is to promote the transformation of ammonia to nitrite using an attachment biofilm. At present, there is a lack of understanding of the water purification mechanism of the pond ecological slope, and the abundance and species of AOA on the pond ecological slope are still not clear. However, a large number of AOA and AOB are found in the biofilms of stream pebbles, which is similar to the pond environment (Merbt et al., 2017).

Perhaps, considering the cost of water treatment, a large-scale bioreactor has not been used to purify pond aquaculture water. However, laboratory-scale SNAD bioreactors and sequencing batch reactors (Lyles et al., 2008) have been studied for the treatment of aquaculture wastewater and have achieved a good result. Research has shown a bioreactor start-up for 180 days without adding extra organic carbon. After a 60-day operation, the bioreactor reached a stable stage with the average concentration of ammonia/nitrate/nitrite/COD in the effluent of 0.26/0.75/0.47/0.27 mg L^{-1} (Lu J. et al., 2020). Because they do not need extra organic carbon and are energy-saving, SNAD bioreactors have good prospects.

In the past decade, subsurface flow constructed wetlands (SSFCWs) have been used to treat the particulate and dissolved fraction of aquaculture wastewater from land-based fish farms (Snow et al., 2012). Recently, it was reported that AnAOB existed in the SSFCWs and that 77.72% of the AnAOB belong to Ca. *Brocadia* (Liu X.-G. et al., 2021). Before the pond aquaculture water enters the artificial subsurface flow wetland, it is often pretreated by sedimentation (Liu X. et al., 2021). It was reported that heterotrophic bacteria denitrification was the main driver of N_2 production, with anammox detected in two of four settlement ponds (Castine et al., 2012). Perhaps, too much organic carbon could inhibit the anammox of the settlement ponds. Heterotrophic bacteria can rapidly grow and compete for nitrite and living space with anammox under high organic loading conditions (Chamchoi et al., 2008; Jenni et al., 2014).

Prospects

Nitrogen pollution is one of the limiting factors of the sustainable and healthy development of the pond aquaculture model. The sediment is the main pollution source of pond aquaculture water, it should be removed from the aquaculture environment as far as possible by sedimentation, filtration, or other methods. Because the main components of pond aquaculture sediments are the feces and residual feed, which are rich in nitrogen, phosphorus, and other elements, the separated sediment can be used as raw material for agricultural organic fertilizer. For the micro-organic particles and dissolved organic matter that cannot be removed by physical methods in pond aquaculture water, it is recommended that they are removed by aquaculture water bioreactors, which are rich in AOA, AOB, and AnAOB. The bioreactor physical and chemical factors required by AOA and AnAOB, are easier to achieve compared with wetland, ecological floating bed, etc. In the bioreactors, the organic nitrogen of micro-organic particles and dissolved organic matter were degraded into ammonia and urea by heterotrophic bacteria. After ammonia oxidation and anaerobic ammonia oxidation, the organic nitrogen is finally formed into N_2. Because the nitrate of aquaculture water usually accumulates to a very high level without sediment (Honda et al., 1993), there is not enough organic carbon in the water for heterotrophic denitrification. AnAOB can carry out denitrification without an additional organic carbon source, which will save a lot of water treatment costs. The bioreactors can be moving bed biofilters, SNAD bioreactors, etc. (Lu J. et al., 2020). This bioreactor can greatly reduce N_2O emissions during pond aquaculture because the nitrogen removal process is mainly carried out by AOA and AnAOB. A schematic diagram of a pond aquaculture water treatment process to be established in the future is shown in **Figure 2**.

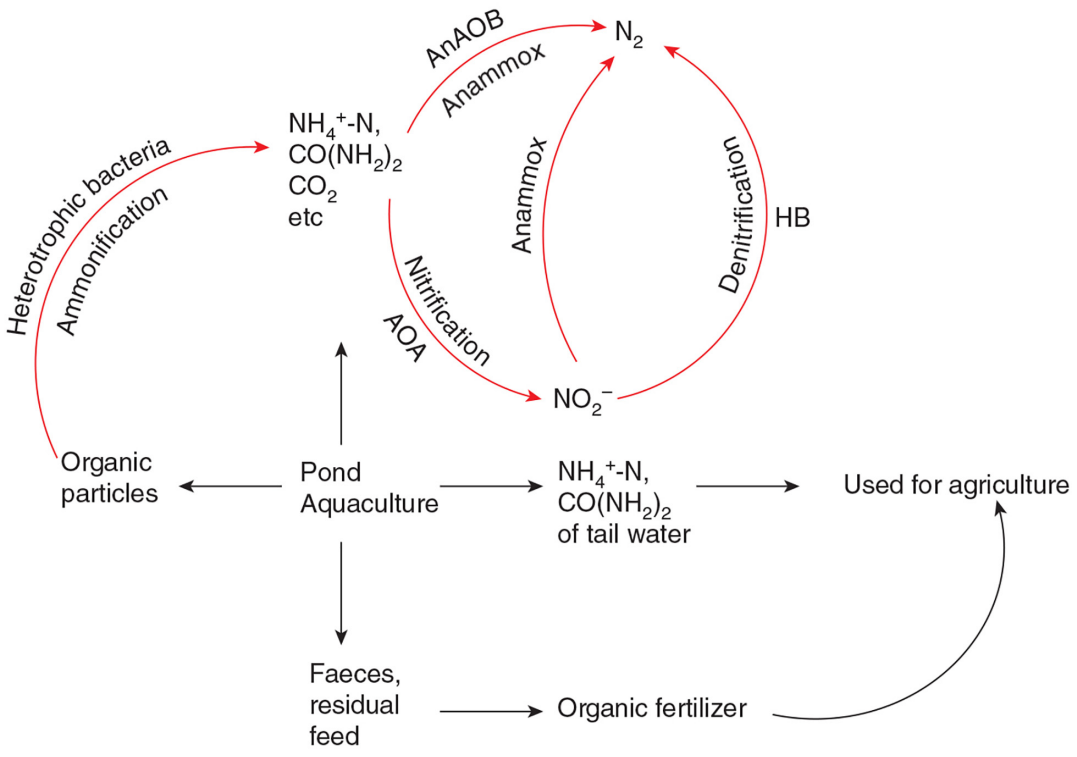

FIGURE 2 | Schematic diagram of a pond aquaculture water treatment process to be established in the future. AOA, ammonia-oxidizing archaea; AnAOB, anaerobic ammonia-oxidizing bacteria; HB, heterotrophic denitrifying bacteria. Red arrows represent different nitrogen cycling processes in the pond aquaculture water treatment process. Black arrows represent the flow direction of pond organic matter rich in nitrogen. Feces and residual feed are further processed and become agricultural organic fertilizer. Part of pond aquaculture tail water rich in NH_4^+ and $CO(NH_2)_2$ can be directly used for agricultural irrigation. Most NH_4^+ and $CO(NH_2)_2$ are directly generated by aquaculture animals or arise from ammonification by heterotrophic bacteria mainly removed via nitrification and anammox by AOA and AnAOB.

Challenges

As mentioned above, AOA and AnAOB have many advantages in pond aquaculture water treatment. For example, they can maintain high biological activity under low temperatures. In the process of nitrogen removal, there is no need for additional organic carbon. AOA and AnAOB can perform adherent growth, which is suitable for the establishment of a high-efficiency bioreactor. However, the following difficulties still need to be overcome in production practice:

(1) AOA and AnAOB are autotrophic microorganisms with a slow growth rate. The growth rate of AOA enrichments is approximately 0.23–0.36 day^{-1}, and the max growth rate of AnAOB is only 0.16 day^{-1} (Straka et al., 2019). The typical doubling times are approximately 15–30 days (Joss et al., 2009; Li et al., 2018). Generally, the start-up time of an AnAOB bioreactor exceeds 200 days (Ge et al., 2008; Yu et al., 2013; Adams et al., 2020), and the start-up time even exceeds a pond breeding cycle. (2) The discharge time of pond aquaculture tailwater is relatively concentrated, and the one-time drainage is large, which may require large-scale water treatment reactors, but these facilities are idle for most of the time, and the enriched AOA or AnAOB biofilm needs long-term maintenance. Compared with RAS aquaculture, the density of pond aquaculture is low. For example, in China, the average density of freshwater pond aquaculture is 8,400 kg km^2 when captured (Fisheries Bureau and Ministry of Agriculture and Rural Affairs of the People's Republic of China, 2020). In the first and middle stages of one aquaculture year, the aquaculture biomass is very small, the amount of feeding is low, and the aquaculture water can be completely treated by the self-purification ability of the environment, with no need for further treatment by peripheral equipment. Only in the late stage and at the end of one aquaculture year, especially when capturing, it is necessary to treat the discharge pond water. (3) It is difficult to screen and culture AOA and AnAOB, which are suitable for low-temperature aquaculture water. The pond aquaculture model is closely associated with temperature changes. Fish cultured at normal temperatures, such as grass carp and carp, are often captured when water temperatures are low. Although previous studies have shown that, some AOA and AnAOB can adapt to low-temperature environments. However, it is difficult to obtain AOA and AnAOB under normal temperature conditions. Perhaps, it is necessary to create low-temperature conditions for the growth of AOA and AnAOB over a long time, which is a great expense. How to obtain AOA and AnAOB enrichment cultures that are suitable for low-temperature conditions at a low cost is a major problem to be considered in the future.

CONCLUSION

Ammonia-oxidizing archaea and AnAOB exist widely in aquaculture pond sediment and play important roles in nitrogen removal processes, especially in low seasonal temperatures and anoxic sediment layers. Because AnAOB uses ammonia as the electron donor and little organic carbon source is required, anammox could compensate for the lack of heterotrophic denitrification function. The concentration of aquaculture water ammonia, organic matter, and pH fit the growth of AOA and AnAOB. However, AOA and AnAOB cannot grow well naturally in aquaculture water. It is very possible to purify the pond aquaculture water by bioreactors based on AOA and AnAOB for autotrophic nitrogen removal, which can reduce the production of greenhouse gas and is conducive to the development of environmentally sustainable pond aquaculture.

AUTHOR CONTRIBUTIONS

SL and XL contributed to conception and design of the study. CL wrote the first draft of the manuscript. RZ and YL wrote sections of the manuscript. All authors contributed to manuscript revision, read, and approved the submitted version.

FUNDING

This study was supported by the National Key Research and Development Program of China (No. 2018YFD0900701), the Natural Science Foundation of China (31702390), and China Agriculture Research System, Central Public Interest Scientific Institution Basal Research Fund, FMIRI of CAFS (No. 2021YJS007).

ACKNOWLEDGMENTS

We appreciate helpful suggestions from Liao Ming-jun (College of Resource and Environmental Engineering, Hubei University of Technology, Wuhan, China). We thank International Science Editing (http://www.internationalscienceediting.com) for editing this manuscript.

REFERENCES

Ackefors, H., and Enell, M. (1994). The release of nutrients and organic matter from aquaculture systems in Nordic countries. *J. Appl. Ichthyol.* 10, 225–241. doi: 10.1111/j.1439-0426.1994.tb00163.x

Adams, M., Xie, J., Xie, J., Chang, Y., and Zhang, T. C. (2020). The effect of carrier addition on Anammox start-up and microbial community: a review. *Rev. Environ. Sci Bio/Technol.* 19, 355–368. doi: 10.1007/s11157-020-09530-4

Adlin, N., Matsuura, N., Ohta, Y., Hirakata, Y., Maki, S., Hatamoto, M., et al. (2017). A nitrogen removal system to limit water exchange for recirculating freshwater aquarium using DHS–USB reactor. *Environ. Technol.* 39, 1577–1585. doi: 10.1080/09593330.2017.1333530

Amano, T., Yoshinaga, I., Yamagishi, T., Chu Van, T., Pham The, T., Ueda, S., et al. (2011). Contribution of anammox bacteria to benthic nitrogen cycling in a Mangrove forest and Shrimp Ponds, Haiphong, Vietnam. *Microb. Environ.* 26, 1–6. doi: 10.1264/jsme2.ME10150

Bao, W., Zhu, S., Guo, S., Li, W., and Ye, Z. (2018). Assessment of water quality and fish production in an intensive pond aquaculture system. *Trans. ASABE* 61, 1425–1433. doi: 10.13031/trans.12799

Castine, S. A., Erler, D. V., Trott, L. A., Paul, N. A., de Nys, R., and Eyre, B. D. (2012). Denitrification and anammox in tropical aquaculture settlement ponds: an isotope tracer approach for evaluating N_2 production. *PLoS One* 7:e42810. doi: 10.1371/journal.pone.0042810

Chamchoi, N., Nitisoravut, S., and Schmidt, J. E. (2008). Inactivation of ANAMMOX communities under concurrent operation of anaerobic ammonium oxidation (ANAMMOX) and denitrification. *Bioresour. Technol.* 99, 3331–3336. doi: 10.1016/j.biortech.2007.08.029

Daebel, H., Manser, R., and Guer, W. (2007). Exploring temporal variations of oxygen saturation constants of nitrifying bacteria. *Water Res.* 41, 1094–1102. doi: 10.1016/j.watres.2006.11.011

Dai, L., Liu, C., Yu, L., Song, C., Peng, L., Li, X., et al. (2018). Organic matter regulates ammonia-oxidizing bacterial and archaeal communities in the surface sediments of *Ctenopharyngodon idellus* aquaculture ponds. *Front. Microbiol.* 9:2290. doi: 10.3389/fmicb.2018.02290

Deng, M., Hou, J., Song, K., Chen, J., Gou, J., Li, D., et al. (2020). Community metagenomic assembly reveals microbes that contribute to the vertical stratification of nitrogen cycling in an aquaculture pond. *Aquaculture* 520:734911. doi: 10.1016/j.aquaculture.2019.734911

Egli, K., Bosshard, F., Werlen, C., Lais, P., Siegrist, H., Zehnder, A. J. B., et al. (2003). Microbial composition and structure of a rotating biological contactor biofilm treating ammonium-rich wastewater without organic carbon. *Microb. Ecol.* 45, 419–432.

Fisheries Bureau and Ministry of Agriculture and Rural Affairs of the People's Republic of China (2020). *China Fisheries Statistics Yearbook 2020*. Beijing: China Agricultural Press.

Food and Agriculture Organization of the United Nations and Fisheries and Aquaculture Department (2018). *The State of World Fisheries and Aquaculture: Meeting the Sustainable Development Goals*. Rome: Food and Agriculture Organization of the United Nations.

French, E., Kozlowski, J. A., Mukherjee, M., Bullerjahn, G., and Bollmann, A. (2012). Ecophysiological characterization of ammonia-oxidizing archaea and bacteria from freshwater. *Appl. Environ. Microbiol.* 78, 5773–5780. doi: 10.1128/AEM.00432-12

Fux, C., and Siegrist, H. (2004). Nitrogen removal from sludge digester liquids by nitrification/denitrification or partial nitritation/anammox: environmental and economical considerations. *Water Sci. Technol.* 50, 19–26. doi: 10.2166/wst.2004.0599

Ge, L., Yong, H., and Yi, Y. (2008). Literature review of start-up and performance of ANAMMOX bioreactors. *Environ. Pollut. Control.* 30, 83–86. (In Chinese).

Guisasola, A., Jubany, I., Baeza, J. A., Carrera, J., and Lafuente, J. (2005). Respirometric estimation of the oxygen affinity constants for biological ammonium and nitrite oxidation. *J. Chem. Technol. Biotechnol.* 80, 388–396. doi: 10.1002/jctb.1202

Hao, S. A., Rui, W. A., Yan, H. A., Zheng, W. A., Yang, Y., Chen, J. A., et al. (2021). The coupling of mixotrophic denitrification, dissimilatory nitrate reduction to ammonium (DNRA) and anaerobic ammonium oxidation (anammox) promoting the start-up of anammox by addition of calcium nitrate. *Bioresour. Techn.* 341:125822. doi: 10.1016/j.biortech.2021.125822

He, J.-Z., Hu, H.-W., and Zhang, L.-M. (2012). Current insights into the autotrophic thaumarchaeal ammonia oxidation in acidic soils. *Soil Biol. Biochem.* 55, 146–154. doi: 10.1016/j.soilbio.2012.06.006

Honda, H., Watanabe, Y., Kikuchi, K., Iwata, N., and Kiyono, M. (1993). High density rearing of Japanese Flounder, Paralichthys olivaceus with a closed seawater recirculation system equipped with a denitrification unit. *Aquac. Sci.* 41, 19–26.

Hooper, A. B., and Terry, K. R. (1973). Specific inhibitors of ammonia oxidation in *Nitrosomonas*. *J. Bacteriol.* 115, 480–485. doi: 10.1128/JB.115.2.480-485.1973

Isaka, K., Date, Y., Kimura, Y., Sumino, T., and Tsuneda, S. (2008). Nitrogen removal performance using anaerobic ammonium oxidation at low temperatures. *FEMS Microbiol. Lett.* 282, 32–38. doi: 10.1111/j.1574-6968.2008.01095.x

Jenni, S., Vlaeminck, S. E., Morgenroth, E., and Udert, K. M. (2014). Successful application of nitritation/anammox to wastewater with elevated organic carbon to ammonia ratios. *Water Res.* 49, 316–326. doi: 10.1016/j.watres.2013.10.073

Jiang, Q. Q., and Bakken, L. R. (1999). Comparison of *Nitrosospira strains* isolated from terrestrial environments. *FEMS Microbiol. Ecol.* 30, 171–186. doi: 10.1016/S0168-6496(99)00054-9

Jin, R.-C., Yang, G.-F., Yu, J.-J., and Zheng, P. (2012). The inhibition of the Anammox process: a review. *Chem. Eng. J.* 197, 67–79. doi: 10.1016/j.cej.2012.05.014

Joss, A., Salzgeber, D. V., Eugster, J., Koenig, R., Rottermann, K., Burger, S., et al. (2009). Full-scale nitrogen removal from digester liquid with partial nitritation and anammox in one SBR. *Environ. Sci. Technol.* 43, 5301–5306. doi: 10.1021/es900107w

Jubany, I., Carrera, J., Lafuente, J., and Baeza, J. A. (2008). Start-up of a nitrification system with automatic control to treat highly concentrated ammonium wastewater: experimental results and modeling. *Chem. Eng. J.* 144, 407–419. doi: 10.1016/j.cej.2008.02.010

Jung, M. Y., Park, S. J., Min, D., Kim, J. S., Rijpstra, W., Damste, J. S., et al. (2011). Enrichment and characterization of an autotrophic ammonia-oxidizing Archaeon of Mesophilic Crenarchaeal Group I.1a from an agricultural soil. *Appl. Environ. Microbiol.* 77, 8635–8647. doi: 10.1128/AEM.05787-11

Jung, M. Y., Sedlacek, C. J., Kits, K. D., Mueller, A. J., Wagner, M., and Hink, L. (2021). Ammonia-oxidizing archaea possess a wide range of cellular ammonia affinities. *ISME J.* doi: 10.1038/s41396-021-01064-z Online ahead of print.

Kartal, B., Tan, N., Van de Biezen, E., Kampschreur, M. J., Loosdrecht, M. V., and Jetten, M. (2010). Effect of nitric oxide on anammox bacteria. *Appl. Environ. Microb.* 76:6304. doi: 10.1128/AEM.00991-10

Kim, J.-G., Jung, M.-Y., Park, S.-J., Rijpstra, W. I. C., Damste, J. S. S., Madsen, E. L., et al. (2012). Cultivation of a highly enriched ammonia-oxidizing archaeon of thaumarchaeotal group I.1b from an agricultural soil. *Environ. Microbiol.* 14, 1528–1543. doi: 10.1111/j.1462-2920.2012.02740.x

Könneke, M., Bernhard, A. E., de la Torre, J. R., Walker, C. B., Waterbury, J. B., and Stahl, D. A. (2005). Isolation of an autotrophic ammonia-oxidizing marine archaeon. *Nature* 437, 543–546. doi: 10.1038/nature03911

Kowalchuk, G. A., and Stephen, J. R. (2001). Ammonia-oxidizing bacteria: a model for molecular microbial ecology. *Annu. Rev. Microbiol.* 55, 485–529. doi: 10.1146/annurev.micro.55.1.485

Kuenen, J. G. (2008). Anammox bacteria: from discovery to application. *Nat. Rev. Microbiol.* 6, 320–326. doi: 10.1038/nrmicro1857

Kuypers, M. M. M., Sliekers, A. O., Lavik, G., Schmid, M., Jorgensen, B. B., Kuenen, J. G., et al. (2003). Anaerobic ammonium oxidation by anammox bacteria in the Black Sea. *Nature* 422, 608–611. doi: 10.1038/nature01472

Lackner, S., Gilbert, E. M., Vlaeminck, S. E., Joss, A., Horn, H., and van Loosdrecht, M. C. M. (2014). Full-scale partial nitritation/anammox experiences - an application survey. *Water Res.* 55, 292–303. doi: 10.1016/j.watres.2014.02.032

Li, J., Guo, Y., Zhu, C., Ma, Z., Qin, J. G., Xie, X., et al. (2019). Effects of a partitioned aquaculture system on water quality and growth of Penaeus vannamei. *Aquac. Res.* 50, 1942–1951. doi: 10.1111/are.14081

Li, J., Li, J., Gao, R., Wang, M., Yang, L., Wang, X., et al. (2018). A critical review of one-stage anammox processes for treating industrial wastewater: optimization strategies based on key functional microorganisms. *Bioresour. Technol.* 265, 498–505. doi: 10.1016/j.biortech.2018.07.013

Li, M., and Gu, J.-D. (2016). The diversity and distribution of anammox bacteria in the marine aquaculture zones. *Appl. Microbiol. Biotechnol.* 100, 8943–8953. doi: 10.1007/s00253-016-7690-6

Li, T., Zhang, B., Zhu, C. B., Su, J. Q., and Qin, J. H. (2021). Effects of an ex situ shrimp-rice aquaponic system on the water quality of aquaculture ponds in the Pearl River estuary, China. *Aquaculture* 545:737179. doi: 10.1016/j.aquaculture.2021.737179

Li, W., and Li, Z. (2009). In situ nutrient removal from aquaculture wastewater by aquatic vegetable Ipomoea aquatica on floating beds. *Water Sci. Technol.* 59, 1937–1943. doi: 10.2166/wst.2009.191

Lin, Y.-F., Jing, S.-R., Lee, D.-Y., Chang, Y.-F., and Sui, H.-Y. (2010). Constructed wetlands for water pollution management of aquaculture farms conducting earthen pond culture. *Water Environ. Res.* 82, 759–768. doi: 10.2175/106143010X12609736966685

Lin, Z., Huang, W., Zhou, J., He, X., Wang, J., and Wang, X. (2020). The variation on nitrogen removal mechanisms and the succession of ammonia oxidizing archaea and ammonia oxidizing bacteria with temperature in biofilm reactors treating saline wastewater. *Bioresour. Technol.* 314:123760. doi: 10.1016/j.biortech.2020.123760

Liu, X., Shao, Z., Cheng, G., Lu, S., Gu, Z., Zhu, H., et al. (2021). Ecological engineering in pond aquaculture: a review from the whole-process perspective in China. *Rev. Aquac.* 13, 1060–1076. doi: 10.1111/raq.12512

Liu, X.-G., Wang, J., Wu, Z.-F., Cheng, G.-F., and Gu, Z.-J. (2021). Anaerobic ammonium oxidation bacteria in a freshwater recirculating pond aquaculture system. *Int. J. Environ. Res. Public Health* 18:4941. doi: 10.3390/ijerph18094941

Liu, Y., Ngo, H. H., Guo, W., Peng, L., Pan, Y., Guo, J., et al. (2016). Autotrophic nitrogen removal in membrane-aerated biofilms: archaeal ammonia oxidation versus bacterial ammonia oxidation. *Chem. Eng. J.* 302, 535–544. doi: 10.1016/j.cej.2016.05.078

Liu, L. (2019). Enrichment and Characteristics of Soil Ammonia-oxidizing Archaea and its Mechanism of High Ammonia Tolerance. PhD Thesis. Guangzhou: South China University of Technology library. (In Chinese).

Lu, J., Zhang, Y., Wu, J., and Wang, J. (2020). Nitrogen removal in recirculating aquaculture water with high dissolved oxygen conditions using the simultaneous partial nitrification, anammox and denitrification system. *Bioresour. Technol.* 305:123037. doi: 10.1016/j.biortech.2020.123037

Lu, S., Liu, X., Liu, C., Cheng, G., and Shen, H. (2020). Influence of photoinhibition on nitrification by ammonia-oxidizing microorganisms in aquatic ecosystems. *Rev. Environ. Sci. Bio-Technol.* 19, 531–542. doi: 10.1007/s11157-020-09540-2

Lu, S., Liao, M., Xie, C., He, X., Li, D., He, L., et al. (2015). Seasonal dynamics of ammonia-oxidizing microorganisms in freshwater aquaculture ponds. *Ann. Microbiol.* 65, 651–657. doi: 10.1007/s13213-014-0903-2

Lu, S., Liu, X., Liu, C., Wang, X., and Cheng, G. (2019). Review of ammonia-oxidizing bacteria and archaea in freshwater ponds. *Rev. Environ. Sci. Bio.* 18, 1–10. doi: 10.1007/s11157-018-9486-x

Lu, S., Liu, X., Ma, Z., Liu, Q., Wu, Z., Zeng, X., et al. (2016). Vertical segregation and phylogenetic characterization of ammonia-oxidizing bacteria and archaea in the sediment of a freshwater aquaculture pond. *Front. Microbiol.* 6:1539. doi: 10.3389/fmicb.2015.01539

Lu, S. (2014). *Study on the Ammonia-Oxidizing Microorganisms in the Freshwater Aquaculture Pond Environment.* PhD Thesis. Wuhan: Huazhong Agricultural University library. (In Chinese).

Luong Van, D., Song, B., Ito, H., Hama, T., Otani, M., and Kawagoshi, Y. (2018). High growth potential and nitrogen removal performance of marine anammox bacteria in shrimp-aquaculture sediment. *Chemosphere* 196, 69–77. doi: 10.1016/j.chemosphere.2017.12.159

Lyles, C., Boopathy, R., Fontenot, Q., and Kilgen, M. (2008). Biological treatment of shrimp aquaculture wastewater using a sequencing batch reactor. *Appl. Biochem. Biotechnol.* 151, 474–479. doi: 10.1007/s12010-008-8216-1

Ma, B., Peng, Y., Zhang, S., Wang, J., Gan, Y., Chang, J., et al. (2013). Performance of anammox UASB reactor treating low strength wastewater under moderate and low temperatures. *Bioresour. Technol.* 129, 606–611. doi: 10.1016/j.biortech.2012.11.025

Ma, B., Wang, S., Cao, S., Miao, Y., Jia, F., Du, R., et al. (2016). Biological nitrogen removal from sewage via anammox: recent advances. *Bioresour. Technol.* 200, 981–990. doi: 10.1016/j.biortech.2015.10.074

Manser, R., Gujer, W., and Siegrist, H. (2005). Consequences of mass transfer effects on the kinetics of nitrifiers. *Water Res.* 39, 4633–4642. doi: 10.1016/j.watres.2005.09.020

Merbt, S. N., Bernal, S., Proia, L., Marti, E., and Casamayor, E. O. (2017). Photoinhibition on natural ammonia oxidizers biofilm populations and implications for nitrogen uptake in stream biofilms. *Linmol. Oceanorg.* 62, 364–375. doi: 10.1002/lno.10436

Ministry of Ecological Environment, National Bureau of Statistics, and Ministry of Agriculture, and Rural Areas (2020). *Bulletin of the Second National Survey of Pollution Sources*. China: Ministry of Ecological Environment.

Molinuevo, B., Cruz Garcia, M., Karakashev, D., and Angelidaki, I. (2009). Anammox for ammonia removal from pig manure effluents: effect of organic matter content on process performance. *Bioresour. Technol.* 100, 2171–2175. doi: 10.1016/j.biortech.2008.10.038

Moomen, S., and Ahmed, E. (2018). Ammonia-Oxidizing Bacteria (AOB): opportunities and applications – a review. *Rev. Environ. Sci. Biol.* 17, 285–321. doi: 10.1007/s11157-018-9463-4

Mulder, A., van de Graaf, A. A., Robertson, L. A., and Kuenen, J. G. (1995). Anaerobic ammonium oxidation discovered in a denitrifying fluidized bed reactor. *FEMS Microbiol. Ecol.* 16, 177–183. doi: 10.1111/j.1574-6941.1995.tb00281.x

Nair, R. R., Boobal, R., Vrinda, S., Singh, I. S. B., and Valsamma, J. (2019). Ammonia-oxidizing bacterial and archaeal communities in tropical bioaugmented zero water exchange shrimp production systems. *J. Soils Sediment.* 19, 2126–2142. doi: 10.1007/s11368-018-2185-y

Nair, R. R., Rangaswamy, B., Sarojini, B. S. I., and Joseph, V. (2020). Anaerobic ammonia-oxidizing bacteria in tropical bioaugmented zero water exchange aquaculture ponds. *Environ. Sci. Pollut. Res.* 27, 10541–10552. doi: 10.1007/s11356-020-07663-1

Oshiki, M., Satoh, H., and Okabe, S. (2016). Ecology and physiology of anaerobic ammonium oxidizing bacteria. *Environ. Microbiol.* 18, 2784–2796. doi: 10.1111/1462-2920.13134

Ostrom, N. E., Russ, M. E., Popp, B., Rust, T. M., and Karl, D. M. (2000). Mechanisms of nitrous oxide production in the subtropical North Pacific based on determinations of the isotopic abundances of nitrous oxide and di-oxygen. *Chemosphere* 2, 281–290.

Palatinszky, M., Herbold, C., Jehmlich, N., Pogoda, M., Han, P., von Bergen, M., et al. (2015). Cyanate as an energy source for nitrifiers. *Nature* 524, 105–108. doi: 10.1038/nature14856

Persson, F., Sultana, R., Suarez, M., Hermansson, M., Plaza, E., and Wilen, B.-M. (2014). Structure and composition of biofilm communities in a moving bed biofilm reactor for nitritation-anammox at low temperatures. *Bioresour. Technol.* 154, 267–273. doi: 10.1016/j.biortech.2013.12.062

Pester, M., Rattei, T., Flechl, S., Groengroeft, A., Richter, A., Overmann, J., et al. (2012). amoA-based consensus phylogeny of ammonia-oxidizing archaea and deep sequencing of amoA genes from soils of four different geographic regions. *Environ. Microbiol.* 14, 525–539. doi: 10.1111/j.1462-2920.2011.02666.x

Pw, A., Jm, B., Aj, A., Le, B., and Hs, A. (2012). Mechanisms of N_2O production in biological wastewater treatment under nitrifying and denitrifying conditions. *Water Res.* 46, 1027–1037.

Qin, W., Amin, S. A., Martens-Habbena, W., Walker, C. B., Urakawa, H., Devol, A. H., et al. (2014). Marine ammonia-oxidizing archaeal isolates display obligate mixotrophy and wide ecotypic variation. *Proc. Nat. Acad. Sci. U S A.* 111, 12504–12509. doi: 10.1073/pnas.1324115111

Qin, Y. (2016). *The Effects of Green Fodder and Commercial Feed on Aquatic Microorganisms in the Grass Carp pond*. Master's degree dissertation. Wuhan: Huazhong Agricultural University library. (In Chinese)

Rahn, T. (1997). Stable isotope enrichment in stratospheric nitrous oxide. *Science* 278, 1776–1778.

Randall, D. J., and Tsui, T. K. N. (2002). Ammonia toxicity in fish. *Mar. Pollut. Bull.* 45, 17–23. doi: 10.1016/S0025-326X(02)00227-8

Santoro, A. E., Buchwald, C., Mcilvin, M. R., and Casciotti, K. L. (2011). Isotopic signature of N_2O produced by marine ammonia-oxidizing archaea. *Science* 333, 1282–1285. doi: 10.1126/science.1208239

Sauder, L. A., Engel, K., Lo, C.-C., Chain, P., and Neufeld, J. D. (2018). "Candidatus *Nitrosotenuis aquarius*," an ammonia-oxidizing archaeon from a freshwater aquarium biofilter. *Appl. Environ. Microbiol.* 84:e01430. doi: 10.1128/AEM.01430-18

Schubert, C. J., Durisch-Kaiser, E., Wehrli, B., Thamdrup, B., Lam, P., and Kuypers, M. M. M. (2006). Anaerobic ammonium oxidation in a tropical freshwater system (Lake Tanganyika). *Environ. Microbiol.* 8, 1857–1863. doi: 10.1111/j.1462-2920.2006.01074.x

Shen, L.-D., Wu, H.-S., Gao, Z.-Q., Ruan, Y.-J., Xu, X.-H., Li, J., et al. (2016). Evidence for anaerobic ammonium oxidation process in freshwater sediments of aquaculture ponds. *Environ. Sci. Pollut. Res.* 23, 1344–1352. doi: 10.1007/s11356-015-5356-z

Shimin, L., Mingjun, L., Min, Z., Pengzhi, Q., Congxin, X., and Xugang, H. (2012). A rapid DNA extraction method for quantitative real-time PCR amplification from fresh water sediment. *J. Food Agricul. Environ.* 10, 1252–1255.

Snow, A., Anderson, B., and Wootton, B. (2012). Flow-through land-based aquaculture wastewater and its treatment in subsurface flow constructed wetlands. *Environ. Rev.* 20, 54–69. doi: 10.1139/a11-023

Srithep, P., Khinthong, B., Chodanon, T., Powtongsook, S., Pungrasmi, W., and Limpiyakorn, T. (2015). Communities of ammonia-oxidizing bacteria, ammonia-oxidizing archaea and nitrite-oxidizing bacteria in shrimp ponds. *Ann. Microbiol.* 65, 267–278. doi: 10.1007/s13213-014-0858-3

Stahl, D. A., and de la Torre, J. R. (2012). Physiology and diversity of ammonia-oxidizing archaea. *Annu. Rev. Microbiol.* 66, 83–101. doi: 10.1146/annurev-micro-092611-150128

Straka, L. L., Meinhardt, K. A., Bollmann, A., Stahl, D. A., and Winkler, M.-K. H. (2019). Affinity informs environmental cooperation between ammonia-oxidizing archaea (AOA) and anaerobic ammonia-oxidizing (Anammox) bacteria. *ISME J.* 13, 1997–2004. doi: 10.1038/s41396-019-0408-x

Tang, C.-J., Zheng, P., Mahmood, Q., and Chen, J.-W. (2009). Start-up and inhibition analysis of the Anammox process seeded with anaerobic granular sludge. *J. Ind. Microbiol. Biotechnol.* 36, 1093–1100. doi: 10.1007/s10295-009-0593-0

Tang, C.-J., Zheng, P., Zhang, L., Chen, J.-W., Mahmood, Q., Chen, X.-G., et al. (2010). Enrichment features of anammox consortia from methanogenic granules loaded with high organic and methanol contents. *Chemosphere* 79, 613–619. doi: 10.1016/j.chemosphere.2010.02.045

Thamdrup, B., and Dalsgaard, T. (2002). Production of N_2 through anaerobic ammonium oxidation coupled to nitrate reduction in marine sediments. *Appl. Environ. Microbiol.* 68, 1312–1318. doi: 10.1128/AEM.68.3.1312-1318.2002

Tolar, B. B., Ross, M. J., Wallsgrove, N. J., Liu, Q., Aluwihare, L. I., Popp, B. N., et al. (2016). Contribution of ammonia oxidation to chemoautotrophy in Antarctic coastal waters. *ISME J.* 10, 2605–2619. doi: 10.1038/ismej.2016.61

Tourna, M., Stieglmeier, M., Spang, A., Konneke, M., Schintlmeister, A., Urich, T., et al. (2011). Nitrososphaera viennensis, an ammonia oxidizing archaeon from soil. *Proc. Nat. Acad. Sci. U S A.* 108, 8420–8425. doi: 10.1073/pnas.1013488108

van de Graaf, A. A., de Bruijn, P., Robertson, L. A., Jetten, M. S. M., and Kuenen, J. G. (1996). Autotrophic growth of anaerobic ammonium-oxidizing micro-organisms in a fluidized bed reactor. *Microbiology* 142, 2187–2187. doi: 10.1099/13500872-142-8-2187

van Kessel, M., Harhangi, H. R., van de Pas-Schoonen, K., van de Vossenberg, J., Flik, G., Jetten, M. S. M., et al. (2010). Biodiversity of N-cycle bacteria in nitrogen removing moving bed biofilters for freshwater recirculating aquaculture systems. *Aquaculture* 306, 177–184. doi: 10.1016/j.aquaculture.2010.05.019

Walker, C. B., de la Torre, J. R., Klotz, M. G., Urakawa, H., Pinel, N., Arp, D. J., et al. (2010). Nitrosopumilus maritimus genome reveals unique mechanisms for nitrification and autotrophy in globally distributed marine crenarchaea. *Proc. Nat. Acad. Sci. U S A.* 107, 8818–8823. doi: 10.1073/pnas.0913533107

Wei, D., Zeng, S., Hou, D., Zhou, R., Xing, C., Deng, X., et al. (2021). Community diversity and abundance of ammonia-oxidizing archaea and bacteria in shrimp pond sediment at different culture stages. *J. Appl. Microbiol.* 130, 1442–1455. doi: 10.1111/jam.14846

Weralupitiya, C., Wanigatunge, R., Joseph, S., Athapattu, B. C. L., Lee, T.-H., Biswas, J. K., et al. (2021). Anammox bacteria in treating ammonium rich wastewater: recent perspective and appraisal. *Bioresour. Technol.* 334:125240. doi: 10.1016/j.biortech.2021.125240

Wurts, W. A., and Durborow, R. M. (1992). Interactions of pH, carbon dioxide, alkalinity and hardness in fish ponds. *SRAC Publication* 464, 1–4.

Yu, Y.-C., Gao, D.-W., and Tao, Y. (2013). Anammox start-up in sequencing batch biofilm reactors using different inoculating sludge. *Appl. Microbiol. Biotechnol.* 97, 6057–6064. doi: 10.1007/s00253-012-4427-z

Zhang, J., Miao, Y., Zhang, Q., Sun, Y., Wu, L., and Peng, Y. (2020). Mechanism of stable sewage nitrogen removal in a partial nitrification-anammox biofilm system at low temperatures: microbial community and EPS analysis. *Bioresour. Technol.* 297:122459. doi: 10.1016/j.biortech.2019.122459

Zhang, Y., Ruan, X.-H., Op, den Camp, H. J. M., Smits, T. J. M., Jetten, M. S. M., et al. (2007). Diversity and abundance of aerobic and anaerobic ammonium-oxidizing bacteria in freshwater sediments of the Xinyi River (China). *Environ. Microbiol.* 9, 2375–2382. doi: 10.1111/j.1462-2920.2007.01357.x

Zhang, D., Weng, M., Qiu, Q., and Wang, C. (2016). Seasonal variations of ammonia-oxidizing archaea in two kinds of ponds of *Portunus trituberculatus*. *J. Biol.* 33, 21–26. (In Chinese).

Zhou, L.-J., Han, P., Yu, Y., Wang, B., Men, Y., Wagner, M., et al. (2019). Cometabolic biotransformation and microbial-mediated abiotic transformation of sulfonamides by three ammonia oxidizers. *Water Res.* 159, 444–453. doi: 10.1016/j.watres.2019.05.031

Zhou, Z., Li, H., Song, C., Cao, X., and Zhou, Y. (2017). Prevalence of ammonia-oxidizing bacteria over ammonia-oxidizing archaea in sediments as related to nutrient loading in Chinese aquaculture ponds. *J. Soils Sediments* 17, 1928–1938. doi: 10.1007/s11368-017-1651-2

Zhu, G., Wang, S., Wang, Y., Wang, C., Risgaard-Petersen, N., and Jetten, M. S. M. (2011). Anaerobic ammonia oxidation in a fertilized paddy soil. *ISME J* 5, 1905–1912. doi: 10.1038/ismej.2011.63

Conflict of Interest: The authors declare that the research was conducted in the absence of any commercial or financial relationships that could be construed as a potential conflict of interest.

Publisher's Note: All claims expressed in this article are solely those of the authors and do not necessarily represent those of their affiliated organizations, or those of the publisher, the editors and the reviewers. Any product that may be evaluated in this article, or claim that may be made by its manufacturer, is not guaranteed or endorsed by the publisher.

frontiers in Microbiology

ORIGINAL RESEARCH
published: 01 December 2021
doi: 10.3389/fmicb.2021.774438

Tea Plants With Gray Blight Have Altered Root Exudates That Recruit a Beneficial Rhizosphere Microbiome to Prime Immunity Against Aboveground Pathogen Infection

Qiaomei Wang[1,2,3], Ruijuan Yang[2,3,4], Wenshu Peng[2,3], Yanmei Yang[1], Xiaoling Ma[5], Wenjie Zhang[2,3], Aibing Ji[2,3], Li Liu[2,3], Pei Liu[1], Liang Yan[2,3] and Xianqi Hu[1]**

[1] College of Plant Protection, Yunnan Agricultural University, Kunming, China, [2] Puer Institute of Pu-Erh Tea, Pu'er City, China, [3] College of Pu'er Tea, West Yunnan University of Applied Sciences, Pu'er City, China, [4] College of Food Science and Technology, Yunnan Agricultural University, Kunming, China, [5] School of Biological and Chemical Science, Pu'er University, Pu'er City, China

OPEN ACCESS

Edited by:
Christopher Rensing,
Fujian Agriculture and Forestry University, China

Reviewed by:
Laith Khalil Tawfeeq Al-Ani,
Universiti Sains Malaysia, Malaysia
Chengyuan Tao,
Nanjing Agricultural University, China

***Correspondence:**
Liang Yan
jacky_4680@163.com
Xianqi Hu
xqhoo@126.com

Specialty section:
This article was submitted to Microbe and Virus Interactions with Plants, a section of the journal Frontiers in Microbiology

Received: 12 September 2021
Accepted: 13 November 2021
Published: 01 December 2021

Citation:
Wang Q, Yang R, Peng W, Yang Y, Ma X, Zhang W, Ji A, Liu L, Liu P, Yan L and Hu X (2021) Tea Plants With Gray Blight Have Altered Root Exudates That Recruit a Beneficial Rhizosphere Microbiome to Prime Immunity Against Aboveground Pathogen Infection. Front. Microbiol. 12:774438. doi: 10.3389/fmicb.2021.774438

Tea gray blight disease and its existing control measures have had a negative impact on the sustainable development of tea gardens. However, our knowledge of safe and effective biological control measures is limited. It is critical to explore beneficial microbial communities in the tea rhizosphere for the control of tea gray blight. In this study, we prepared conditioned soil by inoculating *Pseudopestalotiopsis camelliae-sinensis* on tea seedling leaves. Thereafter, we examined the growth performance and disease resistance of fresh tea seedlings grown in conditioned and control soils. Next, the rhizosphere microbial community and root exudates of tea seedlings infected by the pathogen were analyzed. In addition, we also evaluated the effects of the rhizosphere microbial community and root exudates induced by pathogens on the performance of tea seedlings. The results showed that tea seedlings grown in conditioned soil had lower disease index values and higher growth vigor. Soil microbiome analysis revealed that the fungal and bacterial communities of the rhizosphere were altered upon infection with *Ps. camelliae-sinensis.* Genus-level analysis showed that the abundance of the fungi *Trichoderma*, *Penicillium*, and *Gliocladiopsis* and the bacteria *Pseudomonas*, *Streptomyces*, *Bacillus*, and *Burkholderia* were significantly ($p < 0.05$) increased in the conditioned soil. Through isolation, culture, and inoculation tests, we found that most isolates from the induced microbial genera could inhibit the infection of tea gray blight pathogen and promote tea seedling growth. The results of root exudate analysis showed that infected tea seedlings exhibited significantly higher exudate levels of phenolic acids and flavonoids and lower exudate levels of amino acids and organic acids. Exogenously applied phenolic acids and flavonoids suppressed gray blight disease by regulating the rhizosphere microbial community. In summary, our findings suggest that tea plants with gray blight can recruit beneficial rhizosphere microorganisms by altering their root exudates, thereby improving the disease resistance of tea plants growing in the same soil.

Keywords: tea gray blight, foliar pathogen, rhizosphere microbiome, root exudates, induced systemic resistance

INTRODUCTION

The soil near plant roots, i.e., the rhizosphere, plays a key role in plant immunity and overall plant performance (Pineda et al., 2020) and in protecting above-ground plant tissues from pests and diseases (Edwards et al., 2019). Some rhizosphere soils can inhibit the occurrence of plant diseases even in the presence of virulent pathogens or under climatic conditions conducive to disease development (Weller et al., 2002; Mazzola, 2004). In such disease-suppressive soils, disease inhibition is related to the abundance of beneficial microorganisms (Mendes et al., 2011; Cha et al., 2016). While some beneficial microorganisms directly inhibit pathogens by producing antibacterial compounds, others indirectly inhibit pathogens by stimulating the plant immune system, a phenomenon termed induced systemic resistance (ISR) (Pieterse et al., 2014). *Pseudomonas simiae* WCS417 is probably the best-characterized microbe capable of eliciting ISR (Lundberg and Teixeira, 2018). It has been suggested that disease-suppressive soils are a consequence of the accumulation of beneficial microorganisms caused by repeated pathogen infection of aboveground plant parts (Schlatter et al., 2017; Yuan et al., 2018). *Arabidopsis thaliana* plants infected with the downy mildew pathogen recruited beneficial microorganisms that induced disease resistance and promoted growth, thus improving the survival chances of offspring growing in the same soil (Berendsen et al., 2018). Similarly, aphid and whitefly infestations led to the recruitment of beneficial bacteria that helped pepper plants cope with subsequent pathogen attacks (Lee et al., 2012; Kong et al., 2016).

In this process, root exudates are considered to play a regulatory role. During plant growth, the root system continuously releases root exudates, which are complex mixtures of soluble organic substances, into the rhizosphere (Zhao et al., 2015). Root exudates attract or inhibit specific microbial species to accumulate in the rhizosphere, forming a specific rhizosphere microbial community (Gu et al., 2016; Lundberg and Teixeira, 2018). Rhizosphere species and contents change with plant species and are closely related to plant health (Badri et al., 2013). For example, infection of *A. thaliana* leaves by *Pseudomonas syringae* pv. *tomato* increased the secretion of malic acid from the roots and enriched *Bacillus subtilis* in the rhizosphere (Rudrappa et al., 2008). In tomato, the presence of foliar pathogens increased the secretion of caffeic acid, leading to the reshaping of the rhizosphere microorganisms (Gu et al., 2016). *P. syringae* pv. *tomato*-infected *A. thaliana* recruited beneficial rhizosphere communities by secreting long-chain organic acids (Yuan et al., 2018). These findings suggest that plants can alter their root exudates when attacked to recruit beneficial microorganisms to generate a "soil memory" that benefits future plant performance in the same soil. However, the interaction mechanisms between different plants and pathogens are completely different. Studying the interaction mechanisms in different crops and their main pathogens will provide support for sustainable agricultural development (Kaplan et al., 2018; Mariotte et al., 2018).

Tea [*Camellia sinensis* (L.) O. Kuntze] is an important cash crop that plays an important economic role in planting areas (Arafat et al., 2017). Thus, improving tea yield and quality has an important economic impact (Wang et al., 2016). Tea gray blight is one of the most serious foliar diseases of tea plants (Wang et al., 2019). It is caused by *Pseudopestalotiopsis* spp., which severely affect tea yield and quality (Chen et al., 2017b). The disease mainly affects mature and old foliage, but can also affect young shoots (Maharachchikumbura et al., 2014). The harm of the disease is generally aggravated under high temperature and humidity, resulting in poor plant growth and decreased tea yields (Wang and Lu, 2008). At present, chemical pesticides are mainly used in the prevention and control of tea gray blight. However, these are associated with serious problems, including drug resistance in pathogens and pesticide residues (Hong et al., 2005). Although some progress has been made in the screening of antagonistic strains of tea gray blight (Hong et al., 2005, 2006; Li et al., 2010), little is known about sustainable agricultural control measures.

In this study, we aimed to investigate whether tea plants with aboveground *Pseudopestalotiopsis camelliae-sinensis* infection can recruit beneficial rhizosphere microbes by altering their root exudates to resist subsequent pathogen infection. Tea leaves were infected with *Ps. camelliae-sinensis*, and the microbial communities in the rhizosphere and bulk soils were evaluated by high-throughput 16S rRNA and ITS rRNA gene tag sequencing to evaluate whether infection of the aboveground plant parts would change the composition of rhizosphere microorganisms. Root exudates from infected and non-infected tea seedlings were collected and analyzed by LC-MS/MS to evaluate whether the exudate profile was changed after challenge with *Ps. camelliae-sinensis*. We next tested whether these compounds would affect plant resistance by regulating microorganisms. Finally, culturable beneficial microorganisms were isolated from the conditioned soil, and their abilities to induce disease resistance and promote plant growth were measured. Through these combined lines of investigation, we were able to explore how tea gray blight affects the tea plant root exudates to recruit beneficial microorganisms to the rhizosphere and induces systemic resistance to above-ground pathogens in tea plants.

MATERIALS AND METHODS

Isolation and Identification of the Pathogen Causing Tea Gray Blight

Infected tea leaves were collected from tea plantations in Pu'er City, Yunnan, China. Pathogenic fungi were isolated from the infected tea leaves according to previous methods (Chen et al., 2017b), with some modifications. Briefly, tea leaves with symptom spots of tea gray blight were cut into two 4-mm pieces, surface-sterilized with 75% alcohol for 1 min, washed with sterile water, disinfected with 1% sodium hypochlorite for 3 min, and finally washed with sterile water three times. Small pieces were placed on potato dextrose agar (PDA) plates containing 100 $\mu g\ ml^{-1}$ chloramphenicol. After 3 days of dark culture at 28°C, single mycelia were selected and transferred to PDA plates for dark culture at 28°C for 7–10 days. The isolated and purified strains were identified using morphological and molecular biological methods (Keith et al., 2006). Briefly, the size

(length and width) of conidia, intermediate cells, and apical and basal appendages were measured, and the color of the conidia and the number of apical and basal appendages were observed under a light microscope. For each strain, 30 conidia were observed. The strains were further identified with molecular methods. Briefly, genomic DNA was extracted from fresh mycelium of cultures grown on PDA for 7 days using the CTAB method according to the procedures reported by Than et al. (2008) and Chen et al. (2017a). Three pairs of primers (ITS, β-tubulin, and TEF) were used for PCR amplification. The primers are listed in **Supplementary Table 1**. The amplified products were separated on a 1% agarose gel and purified using the Gel Extraction Kit (Omega Bio-Tek, Norcross, GA, United States) according to the manufacturer's protocol. The purified PCR products were cloned into the pMD®19-T Vector (Takara, Japan). Positive transformants were sequenced at Shanghai Sangon Biotech (Shanghai, China). Neighbor-joining trees were constructed using MEGA 5.0 (Kumar et al., 2016).

The pathogenicity of the strains was determined on tea plants. Pathogen cakes with a diameter of 6 mm were placed on tea leaves with or without premade wounds with the mycelial side facing down and covered with sterile absorbent cotton to maintain a moist environment. Tea leaves with wounds covered with sterile PDA plugs were used as controls. Tea plants were randomly assigned to the different treatments, and after treatment, they were transferred to and randomly placed in the greenhouse. The humidity in the greenhouse was maintained above 80% to facilitate pathogen infection. Seven days after inoculation, pathogens were isolated from all tea leaves with symptomatic lesions.

Development of Conditioned Soils

The soil used in the study was collected in Pu'er City (22.48°N, 100.58°E; altitude, 1,390 m) in September 2019 at a tea plantation where Yunkang No. 10 tea plants have grown for 35 years. The surface soil (10–15 cm) was removed, and the layer between 15 cm and 30 cm was collected as natural soil (NS). The soil was transported to the laboratory, dried at room temperature, and sieved to remove debris (Yuan et al., 2018). The NS had the following characteristics: pH 4.8, available phosphate 8.6 mg kg^{-1}, available potassium 65 mg kg^{-1}, alkali-hydrolysable nitrogen 38.4 mg kg^{-1}, and organic matter 37,000 mg kg^{-1} soil. The soil was sterilized at 121°C for 2 h and transferred to sterile bags (6.0 cm × 6.0 cm × 12.0 cm) that were placed on seedling nursing trays (24 bags per tray).

Woody branches were cut from the tea plants, and each node was cut into a cutting (∼8 cm long), with one leaf preserved per cutting. The cuttings were immersed in 0.1% carbendazim and 0.1% rooting powder for 4 h and then planted in the bags on the seedling nursing trays (1 cutting per bag). All trays were sealed and arranged in a single greenhouse (28°C ± 2°C, 12-h/12-h light/dark cycle) and watered every 2 weeks.

After 18 months of growth, the seedlings were transferred to 36 pots (13 cm × 13 cm × 20 cm, 18 replicates per treatment) containing 3 kg of soil each. Plants in half of the pots (18 pots) were inoculated with *Ps. camelliae-sinensis* at 2 weeks post-transplantation. Four true leaves of each plant were cut with a sterilized blade, and a fungal cake with a diameter of 6 mm was put on the wound, which was then covered with sterile absorbent cotton to maintain a moist environment. The soil was covered with a plastic film to avoid contamination by *Ps. camelliae-sinensis*. Leaves of plants in the remaining 18 pots were wounded by cutting, and the wounds were covered with a sterile PDA plug as controls. Plants were randomly assigned to the treatments, and after treatment, the pots were transferred to and randomly placed in the greenhouse. The humidity in the greenhouse was maintained above 80% to facilitate pathogen infection.

Ps. camelliae-sinensis infection was allowed to develop for 10 days until the obvious round disease spot appeared on the tea leaves. Then, the aboveground parts of the tea plants were removed. Part of the rhizosphere and bulk soils were used for microbial diversity analysis, and the remaining soil was used to evaluate the feedback relationship between aboveground pathogen infection and the soil.

Soil Sample Collection and Soil Chemical Analyses

Rhizosphere soil was collected according to a previously reported method (Luo et al., 2019), with some modifications. The roots of the tea plants were dug out and the loose soil on the root surfaces was removed. The remaining soil within 1 mm from the root surface was collected as rhizosphere soil. Briefly, the roots were placed in a sterile tube containing 40 mL of 1× phosphate-buffered saline (PBS). After centrifugation at 12,000 rpm for 15 min, the precipitate was collected as rhizosphere soil. The soil left in the pot after the removal of the plants was defined as bulk soil. Six biological replicates of each treatment (24 samples) were collected and stored at −80°C until use. After removing the aboveground plant parts, 5 g bulk soil was collected from the conditioned and control soils for soil chemical analysis. The contents of available phosphorus (AP), available potassium (AK), nitrate (NO_3^-), and ammonia (NH_4^+), and pH were determined according to Bakker et al. (2015).

Sequence Analysis of the Complete ITS and 16S rRNA Genes

Total DNA was extracted from the soil samples using the PowerSoil® DNA isolation Kit (MO BIO Laboratories, Carlsbad, CA, United States) according to the manufacturer's instructions. DNA quality was evaluated using a NanoDrop 1000 spectrophotometer (Thermo Fisher Scientific, Wilmington, MA, United States), and the purified DNA was stored at −80°C until use. The complete fungal ITS and bacterial 16S rRNA genes were amplified from the total soil DNA using the ITS1/ITS4 and 27F/1492R primers, respectively, and sequenced using the PacBio platform at BIOMARKER (Beijing, China). PacBio Sequel subreads were demultiplexed and assembled into circular consensus sequences using SMRT link version8.0). The LIMA (v1.7.0) software was used to identify barcode sequences and remove chimeras to obtain high-quality consensus sequences (Callahan et al., 2016). QIIME2 (v2020.6) was used to denoise the data after quality control, using an amplicon sequence variant

threshold of 0.005%. After normalization, minimum data for all samples were subjected to community richness and diversity analyses (based on the alpha diversity index) and principal coordinate analysis (PCoA) in QIIME2.

Evaluation of the Effect of Conditioned Soil on Plant Performance

After the conditioned and control soils were dried for 1 week, 200 mL of Hoagland solution was added, and 18-month-old tea seedlings were transplanted into the soils. The pots were placed randomly in the greenhouse for cultivation. After 15 days, half of the seedlings were inoculated with *Ps. camelliae-sinensis* as described above. Seven days after inoculation, the size of spots was measured to calculate the disease incidence grade and disease index (DI). The incidence grade was calculated according to the formula in **Supplementary Table 2** (Wang and Lu, 2008; Wu et al., 2015), and the DI was calculated as follows:

$$\mathrm{DI} = \frac{\sum(\text{number of diseased plants in this index} \times \text{di})}{(\text{total number of plants investigated} \times \text{highest di})} \times 100\ \%.$$

For the half of the tea seedlings that were not inoculated with the pathogen, plant height was measured at 15 and 45 days after transplantation. The growth rate of the seedlings over 30 days was calculated to evaluate the effect of conditioned soil on growth.

Root Exudate Collection and Ultra-High Performance Liquid Chromatography-Tandem Mass Spectrometry Analysis

Tea root exudates were collected as previously described (Luo et al., 2020), with some modifications. Soil attached to the roots of healthy tea seedlings was gently rinsed off with sterile water, and the seedlings were transplanted into hydroponic pots containing 3 kg sterilized quartz sand that had been soaked in 10% HCl for 2–3 h, eluted with deionized water until the pH was stable at 6.5–7.0, and then sterilized. The pots were randomly placed in the greenhouse at a temperature of 28°C in the day and 23°C at night, and a 12-h/12-h light/dark cycle.

Tea seedlings were soaked in sterile water for 2 weeks and irrigated with 100 mL of Hoagland solutions every 3 days. Then, they were inoculated with *Ps. camelliae-sinensis* as described above and were transferred to glass bottles containing 500 mL of sterile water. The bottles were randomly placed in the greenhouse during the exudate collection period. Each treatment comprised three replicates, including six tea seedlings, and leaves inoculated with sterile PDA medium were used as controls. After incubation for 5 days, the liquid in six glass bottles was combined into a single sample and was defined as the root exudate. The collected liquid samples were filtered through a filter paper and 0.22-μm hydrophilic membrane.

The root exudates were extracted from the aqueous solution with 70% methanol and analyzed by UPLC-MS/MS as reported previously (Hu et al., 2018). Briefly, UPLC normal-phase chromatography was performed using a SHIMADZU Nexera X2, and MS data were collected using a 4500 QTRAP MS. Compounds were separated on an Agilent SB-C18 column (2.1 × 100 mm i.d., 1.8-μm particle sizes). Water (0.1% formic acid) and acetonitrile (0.1% formic acid) were employed as mobile phases A and B. The elution profile was: 0–9 min, 95–5% A in B; 9–10 min, 95% B; 10–10.1 min 5–95% A in B, 10.1–14 min 5% B. The mobile phase flow rate was 0.35 mL/min. The column temperature was maintained at 40°C, and the injection volume was 4 μL. In the AB 4500 QTRAP UPL-MS/MS system (AB SCIEX, CA, United States), the electrospray ionization temperature was 550°C, the capillary voltage was 5,500 V (positive ion mode)/−4,500 V (negative ion mode), and the curtain gas pressure was 50, 60, and 25 psi. All other MS parameters were left at their default values as suggested by the manufacturer. Data were analyzed using Analyst v1.6.3 (AB Sciex).

Preparation of Exudate-Conditioned Soils Using Exogenous Root Exudates

To investigate the effect of root exudates on soil microbial-mediated soil–plant feedback, we added exogenous root exudates to rhizosphere soil to prepare exudate-conditioned soils to evaluate the feedback effect of soil microorganisms on plant disease. The method used was modified from a previous report (Yuan et al., 2018). Briefly, we focused on four types of secretions: amino acids, flavonoids, phenolic acids, and alkaloids. Representative compounds of each exudate category were selected based on their abundance in root exudates after *Ps. camelliae-sinensis* infection. Amino acids represented the pathogen-repressed root exudates, and flavonoids, phenolic acids, and alkaloids represented the pathogen-induced root exudates. The final concentration of the mixture solutions in each group was 10 mM. Mixture solutions of pathogen-repressed exudates contained 2.0 mM L-glycyl-L-proline, 2.0 mM L-valine, 2.0 mM L-methylpiperidine-2-carboxylic acid, 2.0 mM L-tryptophan, and 2.0 mM 2-aminoisobutyric acid. Mixture solutions of pathogen-induced exudates contained 2.0 mM butin, 2.0 mM epicatechin, 2.0 mM paeonol, 2.0 mM 2′,4′,6′-trihydroxyacetophenone, and 2.0 mM putrescine.

Six hundred grams of soil was placed in pots, which were incubated at 30°C for 1 week to preculture the soil microorganisms. Then, the pots were randomly placed in a greenhouse at 28°C, and 60 mL of mixture solution was poured into the pots twice a week for 8 weeks (16 times in total). Three treatments were designed as follows: (1) pathogen-repressed (PR) group, (2) pathogen-induced (PI) group, and (3) water control (WC) group. Each treatment comprised three replicates.

Evaluation of the Effect of Exudate Compounds on Aboveground Plant Disease

After preparation and filtration as reported previously (Yuan et al., 2015), soil slurries were applied to 18-month-old tea seedlings to investigate their effect on the soil microbiome. Briefly, to prepare soil slurries, 350 g of exudate-conditioned soil was mixed with 3.5 L of sterile water and shaken on an

orbital shaker for 1 h. The mixture solutions were allowed to settle for 1 h, and the supernatant was centrifuged at 9,000 rpm for 10 min. The supernatant was defined as the soil slurry suspension containing microorganisms. Half of the suspensions were centrifuged again at 12,000 rpm for 15 min and then filtered through a 0.22-μm filter to remove most of the soil microorganisms. Filter-sterilized slurries were used as controls. Slurries were prepared from PR soil, PI soil, WC soil, and NS and mixtures of PR and PI soils at ratios of 9:1, 5:5, and 1:9 (v/v). Eighteen-month-old tea seedlings (prepared as described above) were transplanted into pots containing sterilized soil and 300 mL of unfiltered soil slurry, filtered and sterilized soil slurry, or sterile water. Three days after transplantation, 100 mL of Hoagland solution was added to provide nutrients for the growth of the tea seedlings. Two weeks later, *Ps. camelliae-sinensis* was inoculated onto the tea leaves as described above. Disease incidence in the tea seedlings was calculated 7 days after infection.

Isolation and Identification of Culturable Fungi and Bacteria in Conditioned Soil

Rhizosphere soil was collected as described above, and 10 g soil was added to 90 mL of PBS. The soil suspension was homogenized for 15 min, diluted from 10^{-1} to 10^{-5} (Yang et al., 2020), and 0.1 mL of each diluent was added to nutrient agar medium (NA, containing per L of distilled water: 15 g peptone, 5 g NaCl, 3 g beef extract, 15 g agar; pH 7) and rose Bengal medium (RBM, containing per L of distilled water: 5 g peptone, 10 g glucose, 1 g KH_2PO_4, 0.5 g $MgSO_4.7H_2O$, 15 g agar, 100 mL 1/3,000 rose Bengal solution, 0.1 g chloramphenicol) for bacterial and fungal culture, respectively (Zhou et al., 2014; Tchakounté et al., 2018). The NA and RBM plates were placed in incubators at 37 and 28°C, respectively, and incubated for 2–5 days. Then, single colonies were picked and inoculated onto NA (bacteria) or PDA (fungi) to obtain pure cultures, which were stored at 4°C until use. For strain identification, please refer to the method in sub-section "Isolation and Identification of the Pathogen Causing Tea Gray Blight." The primers used have been listed in **Supplementary Table 3**.

Screening of Beneficial Microbes in the Rhizosphere and Their Inhibitory Effect on the Pathogen Causing Tea Gray Blight

Microorganisms belonging to *Trichoderma*, *Gliocladiopsis*, *Penicillium*, *Streptomyces*, *Bacillus*, *Burkholderia*, and *Pseudomonas* with significantly increased abundance in conditioned soil were selected from the isolated and identified culturable strains. The selected beneficial strains were paired cultured with *Ps. Camelliae-sinensis*, and their inhibition percentage against the pathogen growth was tested (Liu et al., 2020). Briefly, a pathogen mycelium cake (6 mm diameter) was placed in the center of a PDA plate, and four culturable microbial cakes were placed around the pathogen at equal distances (20 mm). PDA plates with only the pathogen were used as control. Each treatment was repeated three times. All plates were cultured at 28°C for 3 days. The pathogen colony diameter was measured, and the inhibition rate of the culturable microbes on the growth of pathogen was calculated as follows:

$$\text{Growth inhibition rate (\%)} = 100 \times \frac{(\text{radial growth of control} - \text{radial growth of treated sample})}{\text{radial growth of control}}.$$

Evaluation of the Beneficial Microbes in Promoting the Growth of Plants and Alleviating Aboveground Disease

A pot experiment was used to evaluate the effects of the beneficial microbes in promoting tea seedling growth and inhibiting aboveground pathogen infection. The soil used was NS collected from the tea garden it was placed in pots (13 × 13 × 20 cm), and two 18-month-old tea seedlings were transferred in each pot. After 15 days, the pots were irrigated with either 300 mL (10^8 cfu mL^{-1}) suspension of the beneficial microbes or the same volume of sterile water as a control. Three days later, half of the tea seedlings were inoculated with *Ps. camelliae-sinensis*. Seven days after infection, the diameter of disease spots was measured to calculate the disease incidence grade and DI (inoculation and culture conditions were the same as described above). The remaining half of the tea seedlings were irrigated with the solution of beneficial microbes solutions and were allowed to grow for 30 days. Thereafter, their height was measured to evaluate the effect of the beneficial microbes on the growth of the tea seedlings. All treatments comprised three replicates, including six seedlings each.

Statistical Analysis

SPSS v26.0 (IBM SPSS Inc., Chicago, IL, United States) was used for data analysis. Before statistical analysis, data normality and homogeneity of variance were tested. Differences among the treatments were analyzed by one-way analysis of variance and Duncan's multiple-range test.

RESULTS

Pathogen Causing Tea Gray Blight

Ten strains of fungi were isolated from tea leaves showing typical symptoms of tea gray blight (i.e., leaf spots). Four of the strains showed obvious pathogenicity to tea leaves. Based on colony morphology, conidia characteristics, and ITS, β-tubulin, and TEF sequences, the four strains were identified as *Ps. camelliae-sinensis* (**Figures 1A,B**). When the identified strains were re-inoculated on tea leaves, 7 days later, they produced the typical tea gray blight spots on the leaves. Most of the strains did not produce any symptoms on non-wounded tea leaves. Control tea leaves with sterile PDA medium did not show any symptoms of tea gray blight, and *Ps. camelliae-sinensis* could not be isolated from these leaves (**Figure 1C**).

Effect of Conditioned Soil on Plant Performance

The results indicate that tea seedlings grown in conditioned soils showed a significantly lower DI than those grown in control soil

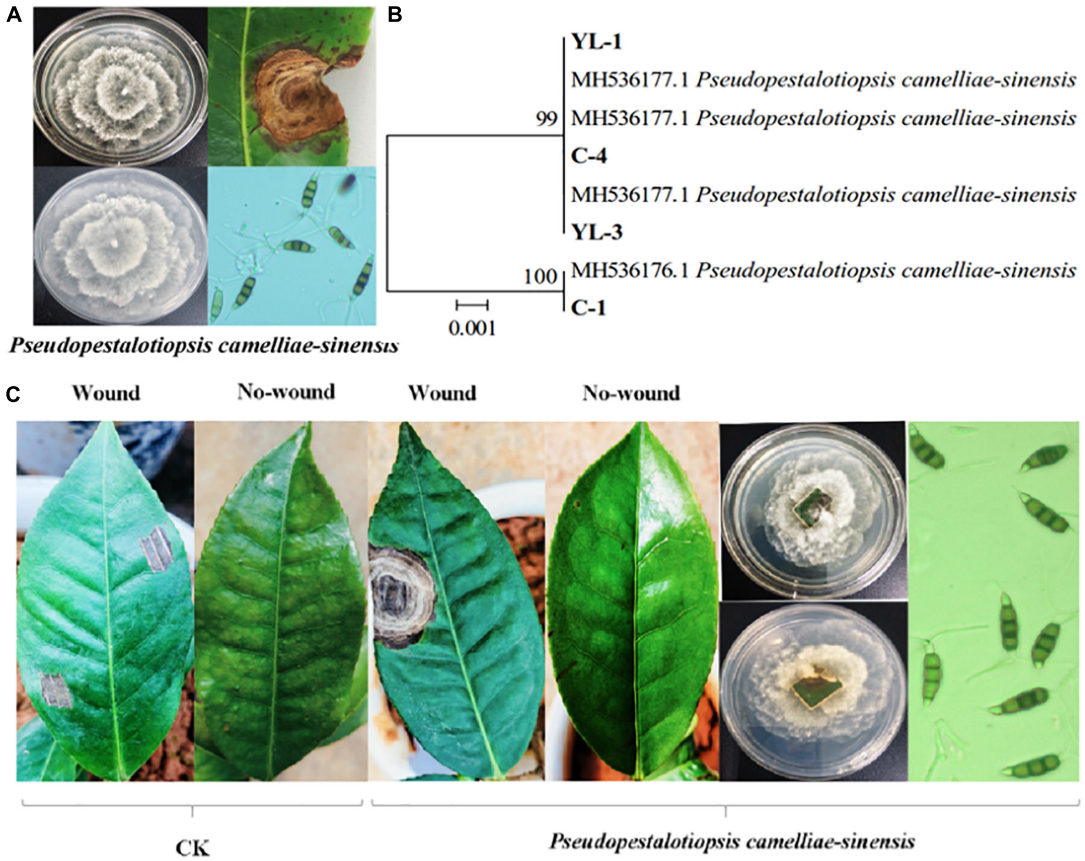

FIGURE 1 | Identification of the pathogen causing tea gray blight and pathogenicity tests. Colony morphology of, symptoms caused by, and conidia of *Ps. camelliae-sinensis*. **(A)** Hierarchical clustering based on β-tubulin gene sequences of pathogens **(B)**. *In-vitro* pathogenicity tests of tea leaves **(C)**.

($p < 0.05$; **Figure 2A**). In the absence of *Ps. camelliae-sinensis*, tea seedlings grown in conditioned soil showed significantly stronger growth than plants grown in control soil ($p < 0.05$; **Figure 2B**). This indicated that the conditioned soil could promote the growth of the tea seedlings. In addition, there was no significant ($p > 0.05$) difference in pH and nutrient content (NH_4^+, NO_3^-, AP, and AK) between conditioned and control soil (**Supplementary Table 4**). The data showed that nutrient availability did not drive differences in tea seedlings growth in soil regulation.

Effects of Aboveground Pathogen Infection on Soil Fungal and Bacterial Communities

Rhizosphere and bulk soils of conditioned and control soils were analyzed by PacBio sequencing. In total, 17,877 fungal OTUs and 18,179 bacterial OTUs were obtained for the analysis of the fungal and bacterial communities, respectively (**Supplementary Tables 5, 6**). PCoA results based on the Bray-Curtis statistic showed that the community structures of fungi and bacteria in rhizosphere soil were significantly different from those in bulk soil (**Figures 3A,B**). The difference in the microbial communities between conditioned and control bulk soils was small, whereas that between conditioned and control rhizosphere soils was larger (**Figures 3A,B**). Fungal abundance and diversity did not show significant differences between conditioned and control soils (**Figures 3C,E**). Compared to that in control soil, the bacterial abundance was significantly decreased in conditioned soil (**Figure 3D**), whereas the bacterial diversity did not show significant differences (**Figure 3F** and **Supplementary Figures 1A–D**).

Microbial Composition of Conditioned Soil

Aboveground pathogen infection altered the fungal and bacterial communities in the rhizosphere soil of tea seedlings at the phylum level (**Supplementary Figures 2–4**). As for rhizosphere fungi, the relative abundance of Ascomycota was significantly increased ($p < 0.01$), whereas that of Mucoromycota was significantly suppressed ($p < 0.01$) by aboveground pathogen infection (**Supplementary Figure 2**). In the bulk soil, the relative abundances of Ascomycota, Basidiomycota, and Glomeromycota were significantly increased ($p < 0.05$), whereas that of Chytridiomycota was significantly decreased ($p < 0.05$) (**Supplementary Figure 3**). For rhizosphere bacteria, seven phyla were significantly affected by aboveground plant infection; the

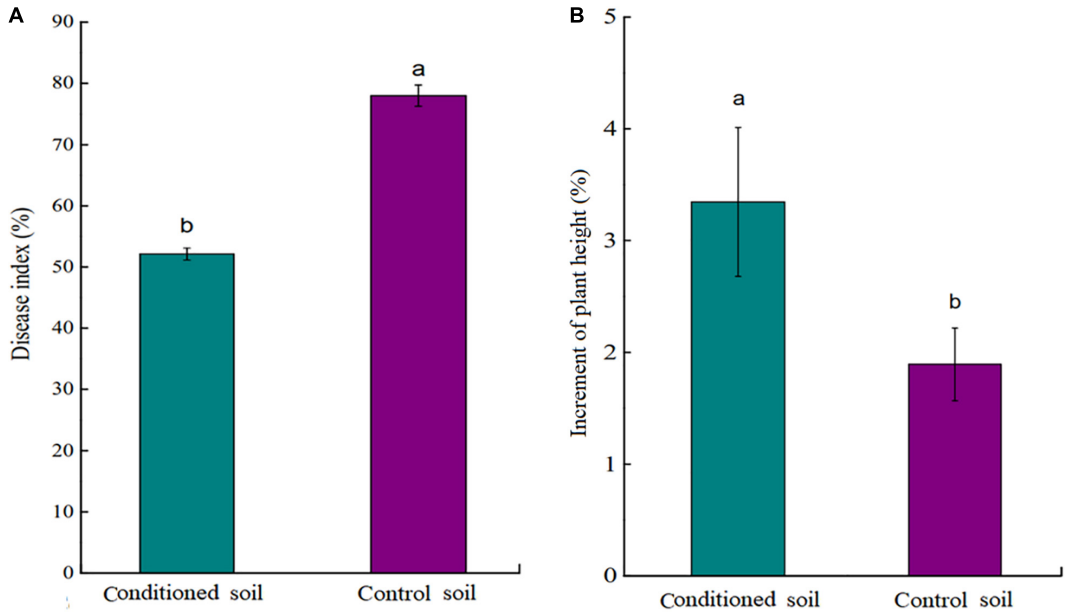

FIGURE 2 | (A) Disease index (DI) of tea seedlings grown in conditioned or control soil and challenged with *Ps. camelliae-sinensis* for 7 days. **(B)** Plant height of tea seedlings grown in conditioned or control soil for 30 days. a and b represent statistically significant differences between treatments as determined by Student's *t*-test ($p < 0.05$). Data are means ± SEs ($n = 6$).

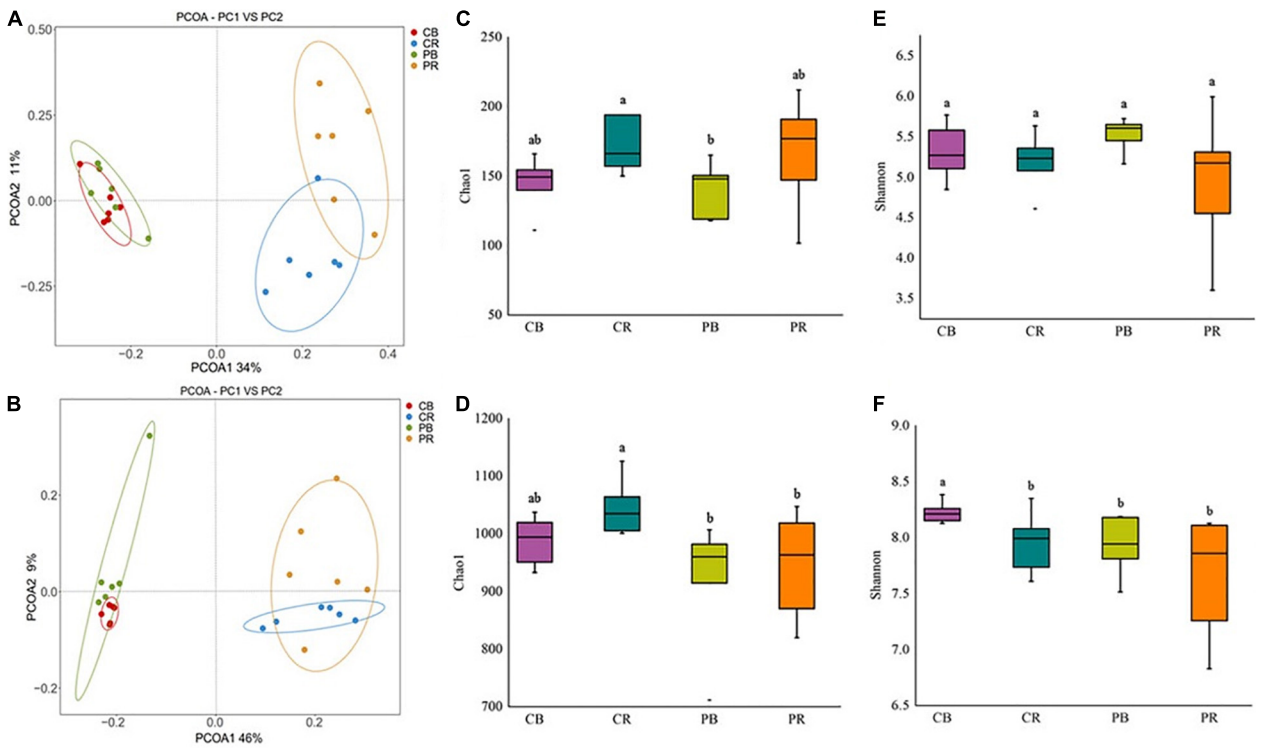

FIGURE 3 | Principal coordinate analysis (PCoA) of fungi **(A)** and bacteria **(B)**, community abundance and diversity indices of fungi **(C,E)** and bacteria **(D,F)** in conditioned and control soils. CB and CR represent control (C) bulk (B) and rhizosphere (R) soil, respectively. PB and PR represent conditioned (P) bulk (B) and rhizosphere (R) soil, respectively. Data are means ± SEs. a and b indicate significant differences among the soils ($p < 0.05$).

relative abundances of Proteobacteria and Gemmatimonadetes were significantly increased ($p < 0.05$), whereas those of Patescibacteria, Armatimonadetes, Planctomycetes, Bacteroidota, and Verrucomicrobia were significantly decreased ($p < 0.05$) (**Supplementary Figure 4**). In the bulk soil, there were no significant differences in bacteria at the phylum level.

At the genus level, 12 fungal genera showed significant differences between control and conditioned rhizosphere soils (**Figure 4A**). Compared with those in the control rhizosphere soil, the relative abundances of two genera of Basidiomycota were significantly increased, and two genera were significantly decreased in response to above-ground pathogen infection (**Figure 4A**). Five genera of Ascomycota were induced by aboveground pathogen infection, whereas two genera were inhibited (**Figure 4A**). Among them, *Trichoderma*, *Penicillium*, and *Gliocladiopsis*, which have biocontrol potential, were enriched in the conditioned rhizosphere soil, whereas, *Mortierella*, an important fungus promoting the transformation of soil nutrients, was inhibited by aboveground pathogen infection. As for bulk soil fungi, three phyla, including 15

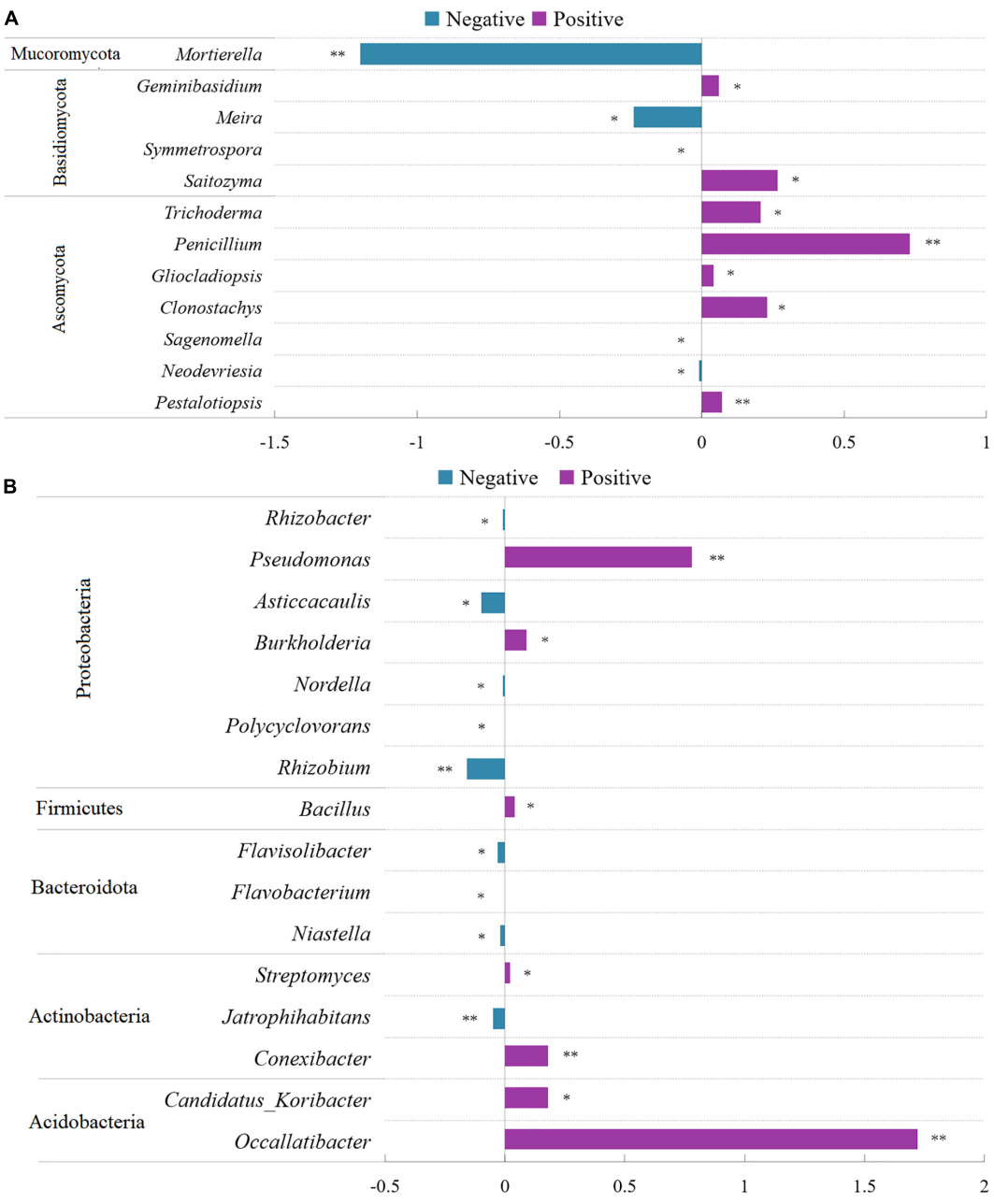

FIGURE 4 | Comparison of fungi **(A)** and bacterial **(B)** abundance differences between conditioned and control rhizosphere soils at the genus level. Data are means ± SEs. *$p < 0.05$, **$p < 0.01$ vs. control soil.

genera, showed significant alterations; the relative abundances of nine genera were significantly decreased in conditioned soil, whereas six genera were significantly increased (**Supplementary Figure 5**). The effects of aboveground pathogen infection on beneficial and harmful fungi in bulk soil were not significant.

As for rhizosphere bacteria, 16 bacterial genera showed significant differences between control and conditioned soils. They belonged to Acidobacteria, Actinobacteria, Bacteroidota, Firmicutes, and Proteobacteria. The relative abundances of seven genera were significantly increased, whereas nine genera were decreased in response to aboveground pathogen infection (**Figure 4B**). Of these genera, *Flavobacteria* and *Rhizobium*, which are associated with plant growth, were inhibited (**Figure 4B**). However, *Streptomyces*, *Bacillus*, *Burkholderia*, and *Pseudomonas,* which exert biocontrol effects, were significantly increased in the conditioned rhizosphere soil (**Figure 4B**). As for bulk soil bacteria, 6 phyla, including 18 genera, showed significant alterations; the relative abundances of 13 genera were significantly decreased, and those of five genera were significantly increased (**Supplementary Figure 6**).

Impact of Aboveground Pathogen Infection on Root Exudates of Tea Seedlings

Root exudates of healthy and infected tea seedlings were detected and analyzed by UPLC-MS/MS. In total, 544 compounds were identified across all samples (**Supplementary Table 7**), which could be divided into nine broad categories based on their chemical nature: lipids (102), phenolic acids (73), organic acids (72), amino acids and derivatives (68), flavonoids (66), nucleotides and derivatives (50), alkaloids (41), terpenoids (11), and others (61) (**Supplementary Figure 7**). All exudates identified were detected in both treatments. However, PCoA showed that the overall exudation pattern of the control tea seedlings differed from that of tea seedlings infected with *Ps. camelliae-sinensis* (**Supplementary Figure 8A**). A volcano plot showed that the expression of 198 compounds differed significantly (VIP $>$ 1) between the two treatments. The expression of 20 metabolites in the pathogen infection group was significantly upregulated compared to that in the control group, and the expression of 178 metabolites was significantly downregulated (**Figure 5A**).

When evaluated at the compound level, the 198 significantly altered metabolites included lipids (18), phenolic acids (24), organic acids (32), amino acids and derivatives (42), flavonoids (27), nuclei and derivatives (18), alkaloids (16), and others (21) (**Figure 5B** and **Supplementary Table 7**). When evaluated at the group level, amino acids and derivatives, organic acids, and alkaloids were found to be significantly higher ($p < 0.05$) in the control seedlings, whereas phenolic acids and flavonoids were significantly higher in the pathogen-inoculated seedlings (**Figure 5C**). *Ps. camelliae-sinensis* infection resulted in a significantly higher secretion of phenolic acids and flavonoids, whereas the secretion of amino acids and derivatives, organic acids, and alkaloids was reduced (**Figure 5C**). The alkaloid putrescine was the exception; it was significantly upregulated in pathogen-inoculated tea seedlings (**Supplementary Figure 8B**).

Disease-Suppressive Effect of the Exudate Compounds

Disease-suppressive effect of the exudate compounds showed that the DI of tea seedlings treated with PI slurry was significantly lower than that of tea seedlings treated with PR, NS, or WC slurries (**Figure 6A**). Importantly, soil slurry filtered to remove the microorganisms had no significant effect on the DI (**Figure 6B**), indicating that the microorganisms rather than exudate compounds ISR in the tea seedlings. To assess the amount of microbiome required for the induction of ISR, PI slurry was mixed into PR slurry at 90, 50, and 10% w/w. The results showed that 90 and 50% of the PI microbiome could at least partially inhibit the disease (**Figure 6C**).

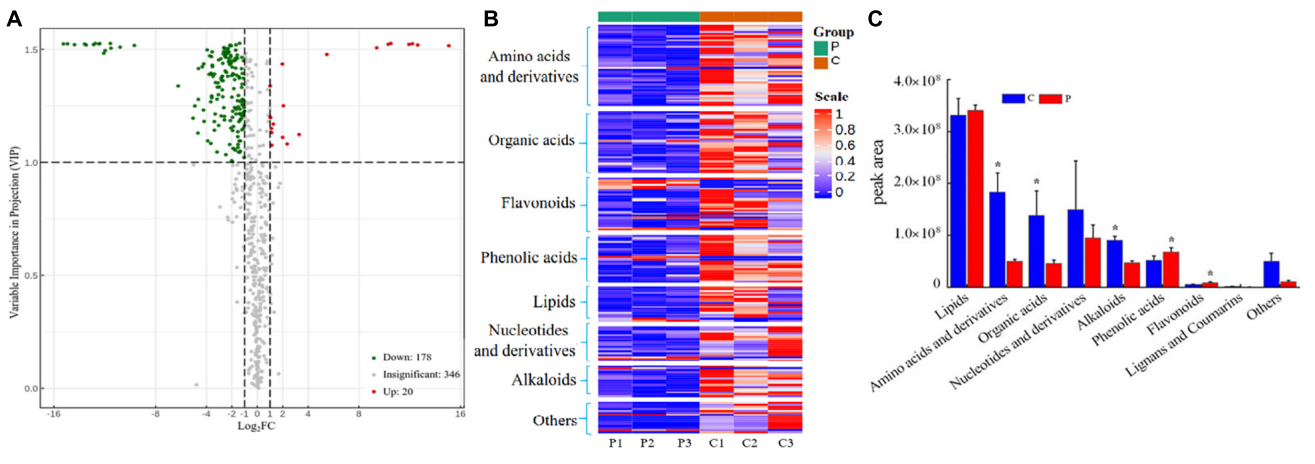

FIGURE 5 | (A) Volcano plot of differential expression of metabolites between the two treatments. VIP $>$ 1 indicates that metabolite expression is significantly different. **(B)** Heatmap of significantly differential substances in root exudates of control-treated and pathogen-inoculated tea seedlings. **(C)** Cumulative peak area of compound categories. "C" represents control treatment, "P" represents pathogen infection treatment. Data are means ± SDs of three replicates. *$p < 0.05$.

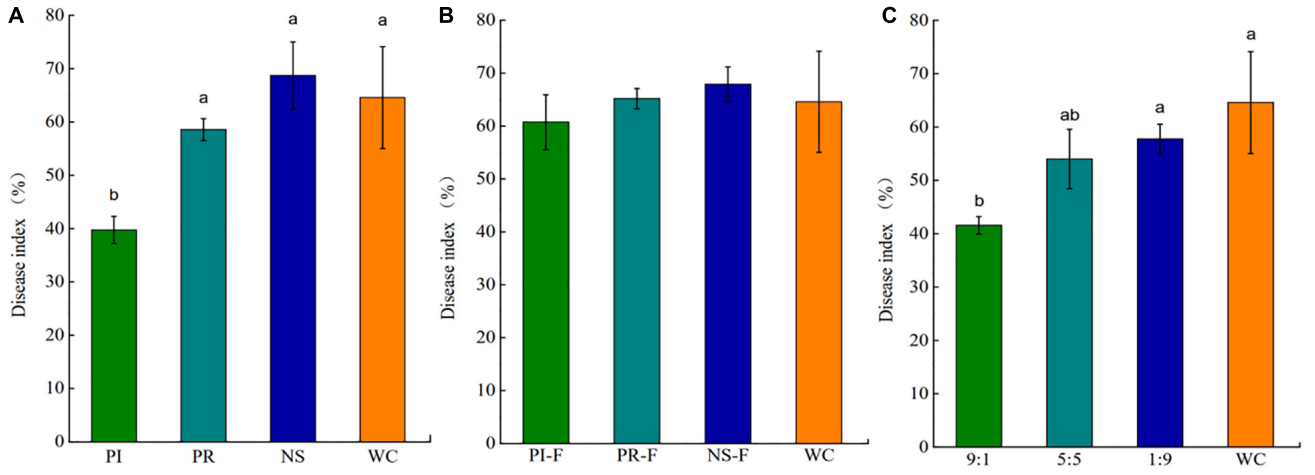

FIGURE 6 | Disease index (DI) of *Ps. camelliae-sinensis*-challenged tea seedlings growing on sterilized soil inoculated with slurries of pathogen-repressed (PR), pathogen-induced (PI), natural soil (NS), and water control (WC) **(A)**, filter-sterilized slurries of PR, PI, NC, and WC **(B)**, and PR and PI mixed at a ratio of 1:9, 5:5, or 9:1, and WC (v/v) **(C)**. Data are means ± SEs of six replicates. a, b, and c indicate significant differences ($p < 0.01$).

Growth Promotion and Disease Resistance Induction in Tea Seedlings by the Beneficial Microbes

Nine beneficial strains were isolated and screened from the conditioned rhizosphere soil. The three fungi were identified as *Trichoderma asperellum, Gliocladiopsis irregularis,* and *Penicillium citrinum* (**Figure 7A**), and six bacteria were identified as *Streptomyces ferralitis*, *S. olivochromogenes*, *B. velezensis*, *Burkholderia stagnalis*, *B. subtilis*, and *B. sporothermodurans* (**Figure 7B**).

The results of confrontation culture showed that all isolates showed antigenic activity toward *Ps. camelliae-sinensis* (**Supplementary Table 8**). Nine isolates were tested for their ISR-inducing effect on tea seedlings. All nine beneficial microorganisms could reduce the DI of tea seedlings, among which Z7 and X5 had the most obvious effect (**Figure 7C**). Growth test results showed that all microorganisms except X5 and X14 significantly promoted the growth of tea seedlings, with Z45 and X45 having the most obvious effect (**Figure 7D**).

DISCUSSION

Studies have shown that aboveground diseases in plants can affect the performance of their offspring by changing the composition of rhizosphere microorganisms (Yuan et al., 2018); however, different plant diseases caused different alterations in soil microorganisms (Lee et al., 2012; Cha et al., 2016; Gu et al., 2016; Kong et al., 2016; Berendsen et al., 2018). Here, we found that infection of tea seedling leaves by the tea gray blight pathogen can enhance disease defense in their offspring growing in the same soil. Further, we demonstrated that tea gray blight can indirectly promote the growth and disease defense of fresh tea seedlings in the same soil by changing root secretion patterns and recruiting beneficial microorganisms to the rhizosphere.

Tea Gray Blight Induces Disease Resistance in Tea Plants by Recruiting Beneficial Rhizosphere Microorganisms

Rhizosphere microbial reassembly caused by aboveground pathogen infection has been reported previously. Studies on Arabidopsis (Berendsen et al., 2018; Yuan et al., 2018) and pepper (Lee et al., 2012; Kong et al., 2016) have demonstrated that aboveground pathogen or insect attack can alter the community structure of rhizosphere microorganisms. In this study, aboveground *Ps. camelliae-sinensis* infection caused plant-mediated alterations in fungal and bacterial community structures in the rhizosphere; however, such an effect was not observed in bulk soil. Conversely, Yuan et al. (2018) found that the bacterial structure of bulk soil changed more significantly than that of rhizosphere soil after aboveground pathogen infection. However, this result was likely because these researchers only analyzed microbial communities in bulk soils of the next generation of plants challenged by pathogens, whereas we analyzed tea seedlings challenged by aboveground pathogen infection. Previous research has shown the directional selection of microorganisms by plant roots, and the rhizosphere, which is close to roots, may be more affected by host plants than bulk soil, which supports our results (Bulgarelli et al., 2013; Reinhold-Hurek et al., 2015). Further analysis of the microbial communities at the genus level demonstrated that some genera with potential biocontrol ability, such as *Trichoderma* (Huang et al., 2011), *Penicillium* (Yuan et al., 2021), *Gliocladiopsis* (Li, 2007), *Pseudomonas* (Trotel-Aziz et al., 2008; Park et al., 2015), *Streptomyces* (Wang, 2014; Chen et al., 2020; Hu et al., 2021), *Bacillus* (Trotel-Aziz et al., 2008; Tahir et al., 2017), and *Burkholderia* (Gao et al., 2015), were increased.

When we isolated these fungi and bacteria and tested their ability to induce ISR and promote growth, we found that nine isolated strains belonging to *Trichoderma*, *Penicillium*, *Gliocladiopsis*, *Pseudomonas*, *Streptomyces*, *Bacillus*, and

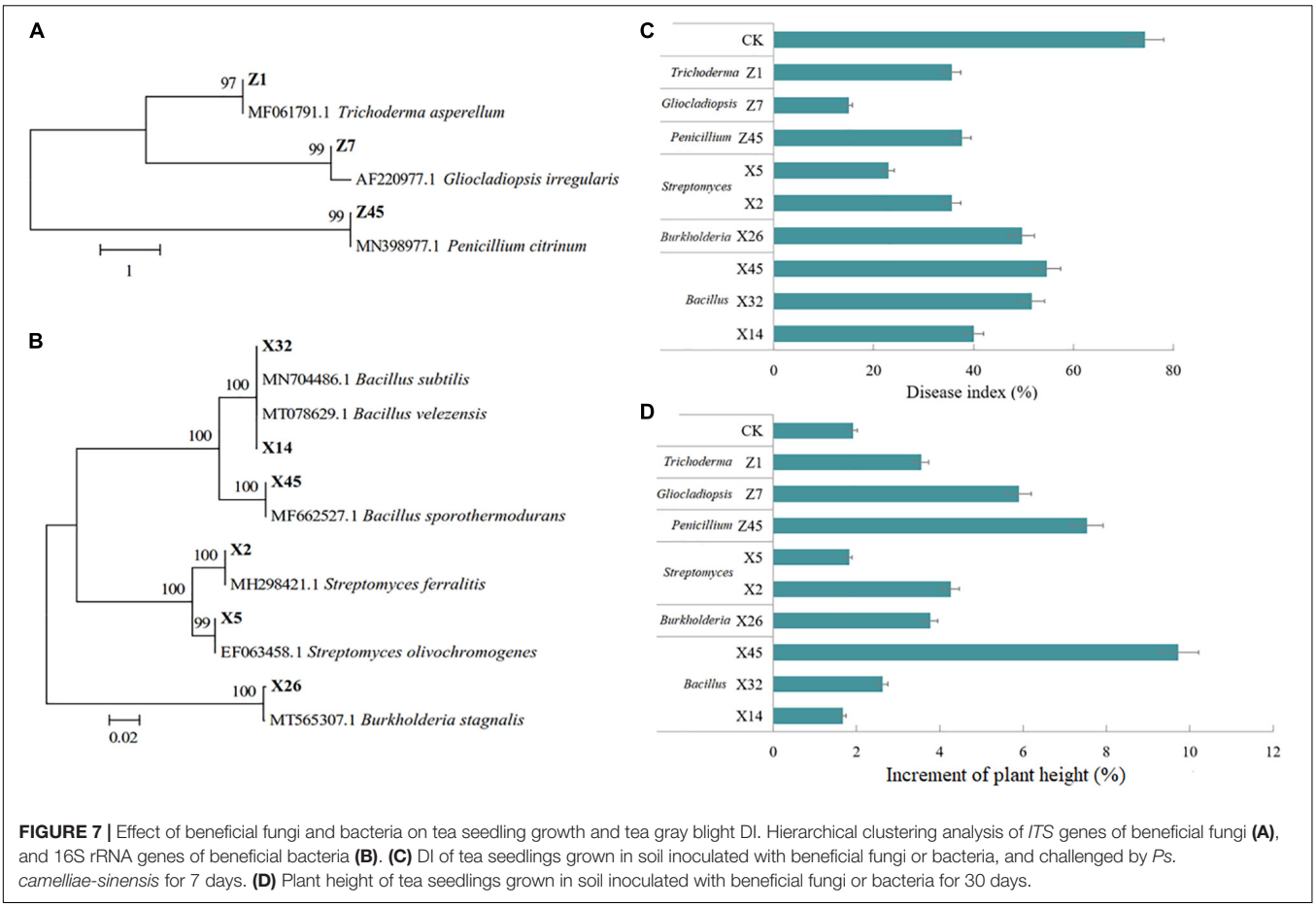

FIGURE 7 | Effect of beneficial fungi and bacteria on tea seedling growth and tea gray blight DI. Hierarchical clustering analysis of *ITS* genes of beneficial fungi **(A)**, and 16S rRNA genes of beneficial bacteria **(B)**. **(C)** DI of tea seedlings grown in soil inoculated with beneficial fungi or bacteria, and challenged by *Ps. camelliae-sinensis* for 7 days. **(D)** Plant height of tea seedlings grown in soil inoculated with beneficial fungi or bacteria for 30 days.

Burkholderia not only induced ISR against *Ps. camelliae-sinensis*, but also promoted the growth of tea seedlings. Overall, these findings indicate that increases in the abundances of these microbes are beneficial to tea seedlings as together, they not only induce ISR, but also promote growth in tea seedlings.

The above findings showed that tea seedlings infected with *Ps. camelliae-sinensis* can recruit specific microbes to aid in their defense. This finding was confirmed in our follow-up research. Tea seedlings were planted in conditioned and control soil and were then challenged with *Ps. camelliae-sinensis*. The results showed that the DI of tea seedlings in conditioned soil was lower than that of tea seedlings grown in the control soil. Recent studies in pepper (Lee et al., 2012; Kong et al., 2016), tomato (Gu et al., 2016), wheat (Dudenhffer et al., 2016), and Arabidopsis (Berendsen et al., 2018; Yuan et al., 2018) support this finding as aboveground pathogen infection triggered changes in rhizosphere microbial communities that ISR in plants. However, the previous studies showed that different foliar pathogens had different effects on rhizosphere microbial communities. A better understanding of the plant genetic basis of disease-induced beneficial root-related microbial recruitment can open up new possibilities for induced resistance research in crops. To our knowledge, this study is the first to demonstrate that tea gray blight can protect tea plants from subsequent aboveground pathogen infection by attracting beneficial microorganisms to the rhizosphere.

Tea Gray Blight Induces Disease Resistance in Tea Plants by Altering Their Root Exudates, Leading to the Recruitment of Rhizosphere Microorganisms

As for the mechanism of plant-mediated rhizosphere microbial community alterations, previous studies have shown that aboveground pathogen infections regulate rhizosphere microorganisms by altering the plant root exudates (Dudenhffer et al., 2016; Yuan et al., 2018). Further, studies have shown that the interaction mechanisms between different pathogens and plants are completely different (Gu et al., 2016; Hu et al., 2018; Stringlis et al., 2018). In this study, root exudates of tea seedlings infected by *Ps. camelliae-sinensis* were analyzed. The results showed that most of the root exudates, including amino acids and organic acids, were downregulated by aboveground pathogen infection (178 species). This result is inconsistent with findings reported by Yuan et al. (2018) who showed that *P. syringae* pv. *tomato* induced Arabidopsis to secrete amino acids and organic acids. However *Ps. camelliae-sinensis* inhibited the secretion of amino acids and organic acids by tea seedlings. It

has been suggested that such different findings may be related to differences in disease progression between pathogens (Camanes et al., 2015) and to metabolic differences between different plant species (Hong et al., 2012; Wang et al., 2016).

More importantly, 20 exudate substances, such as phenolic acids, flavonoids, and putrescine, were significantly upregulated by aboveground pathogen infection. Phenolic acids and flavonoids belong to the phenolic compounds. In fungus–plant interactions, plant phenolic compounds mainly serve as chemical defense substances. Accordingly, when plants are infected by pathogens, plant phenolic compounds accumulate significantly (Wang et al., 2016). Phenolic acids, flavonoids, and putrescine can function as antimicrobial and signaling molecules in the rhizosphere (Verma and Mishra, 2005; Steinkellner et al., 2007; Li et al., 2009). When we evaluated the effects of these compounds in the tea rhizosphere, we found that soil slurry conditioned with the compounds induced by aboveground pathogen infection could reduce the gray blight DI in tea seedlings. This disease resistance-inducing effect was lost in soil slurries from which the microbiome had been removed by filtration, indicating that the microbes, rather than the exudate compounds themselves, elicited resistance in the tea seedlings. Thus, root exudates can induce disease resistance by regulating the community structure of the rhizosphere microorganisms, as also reported by Yuan et al. (2018). This view is supported by research reported by Badri et al. (2013) who showed that sugars and amino acids act as general attractants to a broad range of microbes, whereas phenolic compounds act as specific substrates or signaling molecules for specific microbes, including *Rhizobium*, *Bacillus*, *Sphingomonas*, *Streptomyces*, and *Pseudonocardia*. Therefore, the upregulation of phenolic substances in the tea root exudates may have resulted in the recruitment and aggregation of beneficial microorganisms such as *Pseudomonas*, *Streptomyces*, and *Bacillus* in the tea rhizosphere.

The root exudates of tea plants growing in the natural environment are affected by a myriad of factors. Here, we only analyzed the compounds secreted by roots under controlled conditions and their functions in the rhizosphere. Although we did observe an association between the compounds studied and the functions they performed in the rhizosphere in vivo, further work is needed to clarify the interaction mechanism between secretions and specific microorganisms. Promoting rhizosphere-driven microbial function is a sustainable way to improve the health of tea plants. Exploring the roles of rhizosphere microorganisms in the development of tea plants can help design better disease-resistance strategies. Therefore, further studies are needed to explore the mechanisms of disease resistance induced by specific microorganisms and to reveal the pathways of signal transduction between species in the rhizosphere.

CONCLUSION

Aboveground infection by *Ps. camelliae-sinensis* triggers disease resistance to subsequent infection in tea seedlings by altering root exudates, leading to the recruitment of beneficial microbes in the rhizosphere. This ISR was mediated by different fungal and bacterial communities in soil pretreated with exudates from plants with aboveground pathogen infection. When tea seedlings were challenged with *Ps. camelliae-sinensis*, their root secretion profile changed, and the secretion of phenolic acids and flavonoids increased. The addition of a mixture of phenolic acids and flavonoids to the soil led to the induction of a response similar to that caused by aboveground pathogen infection. In other words, *Ps. camelliae-sinensis* infection can alter the root secretion of tea seedlings to recruit beneficial microorganisms to the rhizosphere and induce plants to produce systemic disease resistance.

DATA AVAILABILITY STATEMENT

The datasets presented in this study can be found in online repositories. The names of the repository/repositories and accession number(s) can be found below: NCBI (accession: PRJNA774068).

AUTHOR CONTRIBUTIONS

XH and LY conceived the study and directed the project. QW and RY performed the microbial isolation. QW and YY performed the microbial identification. WP, XM, and QW performed the root exudates analysis. AJ, WZ, and LL performed the microbial diversity sequencing and analysis. QW and PL performed all the tea seedling culture and inoculation experiments. XH, LY, and QW wrote the manuscript. All authors contributed to the article and approved the submitted version.

FUNDING

This work was partially funded by the Provincial special fund for agricultural development in 2021 (2017KJTX007).

SUPPLEMENTARY MATERIAL

The Supplementary Material for this article can be found online at: https://www.frontiersin.org/articles/10.3389/fmicb.2021.774438/full#supplementary-material

REFERENCES

Arafat, Y., Wei, X. Y., Jiang, Y. H., Chen, T., Saqib, H. S. A., Lin, S., et al. (2017). Spatial distribution patterns of root-associated bacterial communities mediated by root exudates in different aged ratooning tea monoculture systems. *Int. J. Mol. Sci.* 18:1727. doi: 10.3390/ijms18081727

Badri, D. V., Chaparro, J. M., Zhang, R., Shen, Q., and Vivanco, J. M. (2013). Application of natural blends of phytochemicals derived from the root exudates of arabidopsis to the soil reveal that phenolic-related compounds predominantly modulate the soil microbiome. *J. Biol. Chem.* 288, 4502–4512. doi: 10.1074/jbc.M112.433300

Bakker, M. G., Chaparro, J. M., Manter, D. K., and Vivanco, J. M. (2015). Impacts of bulk soil microbial community structure on rhizosphere microbiomes of Zea mays. *Plant Soil* 392, 115–126. doi: 10.1007/s11104-015-2446-0

Berendsen, R. L., Vismans, G., Yu, K., Song, Y., deJonge, R., Burgman, W. P., et al. (2018). Disease-induced assemblage of a plant-beneficial bacterial consortium. *ISME J.* 12, 1496–1507. doi: 10.1038/s41396-018-0093-1

Bulgarelli, D., Schlaeppi, K., Spaepen, S., Themaat, E. V., and SchulzeLefert, P. (2013). Structure and functions of the bacterial microbiota of plants. *Annu. Rev. Plant Biol.* 64, 807–838. doi: 10.1146/annurev-arplant-050312-120106

Callahan, B. J., McMurdie, P. J., Rosen, M. J., Han, A. W., Johnson, A. J., and Holmes, S. P. (2016). DADA2: high-resolution sample inference from Illumina amplicon data. *Nat. Methods* 13, 581–583. doi: 10.1038/nmeth.3869

Camanes, G., Scalschi, L., Vicedo, B., González-Bosch, C., and García-Agustín, P. (2015). An untargeted global metabolomic analysis reveals the biochemical changes underlying basal resistance and priming in solanumlycopersicum, and identifies 1-methyltryptophan as a metabolite involved in plant responses to botrytiscinerea and *pseudomonassyri*. *Plant J.* 84, 125–139. doi: 10.1111/tpj.12964

Cha, J. Y., Han, S., Hong, H. J., Cho, H., Kim, D., Kwon, Y., et al. (2016). Microbial and biochemical basis of a Fusarium wiltsuppressive soil. *ISME J.* 10, 119–129. doi: 10.1038/ismej.2015.95

Chen, J., Yang, Z. P., and Xia, Q. (2020). Effects of three strains of *Streptomyces* on the control of millet downy mildew at early stage. *J. Shanxi Agric. Univ.* 40, 82–88.

Chen, Y., Zeng, L., Shu, N., Jiang, M., Wang, H., and Huang, Y. (2017b). Pestalotiopsis-like species causing gray blight disease on Camellia sinensis in china. *Plant Dis.* 102, 98–106. doi: 10.1094/PDIS-05-17-0642-RE

Chen, Y., Qiao, W., Zeng, L., Shen, D. H., Liu, Z., Wang, S. H., et al. (2017a). Characterization, pathogenicity and phylogenetic analyses of Colletotrichum species associated with brown blight disease on Camellia sinensis in China. *Plant Dis.* 101, 1022–1028. doi: 10.1094/PDIS-12-16-1824-RE

Dudenhffer, J. H., Scheu, S., and Jousset, A. (2016). Systemic enrichment of antifungal traits in the rhizosphere microbiome after pathogen attack. *J. Ecol.* 104, 1566–1575. doi: 10.1111/1365-2745.12626

Edwards, J., Santos-Medellín, C., Nguyen, B., Kilmer, J., Liechty, Z., Veliz, E., et al. (2019). Soil domestication by rice cultivation results in plant-soil feedback through shifts in soil microbiota. *Genome Biol.* 20:221. doi: 10.1186/s13059-019-1825-x

Gao, M., Zhou, J. J., Wang, E. T., Chen, Q., Xu, J., and Sun, J. G. (2015). Multiphasic characterization of a plant growth promoting bacterial strain, *Burkholderia* sp. 7016 and its effffect on tomato growth in the fifield. *J. Integr. Agric.* 14, 1855–1863. doi: 10.1016/S2095-3119(14)60932-1

Gu, Y., Wei, Z., Wang, X. Q., Friman, V. P., Huang, J. F., and Wang, X. F. (2016). Pathogen invasion indirectly changes the composition of soil microbiome via shifts in root exudation profile. *Biol. Fertil. Soils* 52, 997–1005. doi: 10.1007/s00374-016-1136-2

Hong, Y. C., Lai, Y. B., Ye, W. N., Lin, P. X., and Hu, F. P. (2006). Mechanism of the control of tea grey blight disease by *Bacillus subtilis* strain TL2. *J. Tea Sci.* 2, 259–264.

Hong, Y. C., Xin, W., Lai, Y. B., Weng, X., and Hu, F. P. (2005). Isolation of endophytic antifungal and pesticide degrading bacteria from tea plant. *J. Tea Sci.* 25, 183–188.

Hong, Y. S., Martinez, A., Liger-Belair, G., Jeandet, P., Nuzillard, J. M., and Cilindre, C. (2012). Metabolomics reveals simultaneous influences of plant defence system and fungal growth in *Botrytis cinerea*-infected Vitis vinifera cv. Chardonnay berries. *J. Exp. Bot.* 63, 5773–5785. doi: 10.1093/jxb/ers228

Hu, L. F., Robert, C. A. M., Cadot, S., Zhang, X., Ye, M., Li, B., et al. (2018). Root exudate metabolites drive plant-soil feedbacks on growth and defense by shaping the rhizosphere microbiota. *Nat. Commun.* 9:2738. doi: 10.1038/s41467-018-05122-7

Hu, L. M., Xu, C. Y., Luo, J. Q., Zang, J. J., Lu, J. L., He, Z. P., et al. (2021). Screening, identification and biocontrol effect of a strain of *Streptomyces lavendulae* against Xanthomonas oryzae pv. oryzae. *Acta Phytopathol. Sin.* 1–16. doi: 10.13926/j.cnki.apps.000577

Huang, X., Chen, L., Ran, W., Shen, Q., and Yang, X. (2011). Trichoderma harzianum strain sqr-t37 and its bio-organic fertilizer could control Rhizoctonia solani damping-offff disease in cucumber seedlings mainly by the mycoparasitism. *Appl. Microbiol. Biotechnol.* 91, 741–755. doi: 10.1007/s00253-011-3259-6

Kaplan, I., Pineda, A., and Bezemer, M. (2018). "Application and theory of plant–soil feedbacks on aboveground herbivores," in *Aboveground–Belowground Community Ecology*, eds T. Ohgushi, S. Wurst, and S. N. Johnson (Charm: Springer), 319–343. doi: 10.1007/978-3-319-91614-9_14

Keith, L. M., Velasquez, M. E., and Zee, F. T. (2006). Identification and characterization of *Pestalotiopsis* spp. causing scab disease of guava, *Psidium guajava* in Hawaii. *Plant Dis.* 90, 16–23. doi: 10.1094/PD-90-0016

Kong, H. G., Kim, B. K., Song, G. C., Lee, S., and Ryu, C. M. (2016). Aboveground whitefly infestation-mediated reshaping of the root microbiota. *Front. Microbiol.* 7:1314. doi: 10.3389/fmicb.2016.01314

Kumar, S., Stecher, G., and Tamura, K. (2016). MEGA7.0: molecular evolutionary genetics analysis version 7.0 for bigger datasets. *Mol. Biol. Evol.* 33, 1870–1874. doi: 10.1093/molbev/msw054

Lee, B., Lee, S., and Ryu, C. M. (2012). Foliar aphid feeding recruits rhizosphere bacteria and primes plant immunity against pathogenic and non-pathogenic bacteria in pepper. *Ann. Bot.* 110, 281–290. doi: 10.1093/aob/mcs055

Li, J. (2007). *Antimicrobial Activity and Steroid Analysis of the Endophytic Fungi from Paris polyphylla var. yunnanensis*. Ph.D. thesis. Sichuan: Sichuan Agricultural University.

Li, S. R., Wei, Z. Z., Na, Z. Y., Xiong, N., and Yang, S. R. (2010). The application effect of Na's 778 indute on the tea tree. *Tea Commun.* 37, 13–15.

Li, Y., Peng, Q., Selimi, D., Wang, Q., Charkowski, A. O., Chen, Y., et al. (2009). The plant phenolic compound p-coumaric acid represses gene expression in the Dickeya dadantii type III secretion system. *Appl. Environ. Microbiol.* 75, 1223–1228. doi: 10.1128/AEM.02015-08

Liu, H. J., Su, Y. W., Fang, L., Luo, L. F., Wang, L. T., and Zhang, Z. L. (2020). The Effect and mechanism of fennel crop rotation on soil bacterial community to alleviate replant failure of *Panax notoginseng*. *Chin. J. Biol. Control* 36, 139–149.

Lundberg, D. S., and Teixeira, P. J. P. L. (2018). Root-exuded coumarin shapes the root microbiome. *Proc. Natl. Acad. Sci. U. S. A.* 115, 5629–5631. doi: 10.1073/pnas.1805944115

Luo, L. F., Guo, C., Wang, L., Zhang, J., Deng, L., Luo, K., et al. (2019). Negative plant-soil feedback driven by re-assemblage of the rhizosphere microbiome with the growth of *Panax notoginseng*. *Front. Microbiol.* 10:1597. doi: 10.3389/fmicb.2019.01597

Luo, L. F., Yang, L., Yan, Z. X., Jiang, B. B., Li, S., and Huang, H. C. (2020). Ginsenosides in root exudates of *Panax notoginseng* drive the change of soil microbiota through carbon source different utilization. *Plant Soil* 455, 139–153. doi: 10.1007/s11104-020-04663-5

Maharachchikumbura, S. S. N., Hyde, K. D., Groenewald, J. Z., Xu, J., and Crous, P. W. (2014). *Pestalotiopsis* revisited. *Stud. Mycol.* 79, 121–186. doi: 10.1016/j.simyco.2014.09.005

Mariotte, P., Mehrabi, Z., Bezemer, T. M., De Deyn, G. B., Kulmatiski, A., and Drigo, B. (2018). Plant–soil feedback: bridging natural and agricultural sciences. *Trends Ecol. Evol.* 33, 129–142.

Mazzola, M. (2004). Assessment and management of soil microbial community structure for disease suppression. *Annu. Rev. Phytopathol.* 42, 35–59. doi: 10.1146/annurev.phyto.42.040803.140408

Mendes, R., Kruijt, M., de Bruijn, I., Dekkers, E., vander Voort, M., Schneider, J. H. M., et al. (2011). Deciphering the rhizosphere microbiome for disease-suppressive bacteria. *Science* 332, 1097–1100. doi: 10.1126/science.1203980

Park, Y. S., Dutta, S., Ann, M., Raaijmakers, J. M., and Park, K. (2015). Promotion of plant growth by *Pseudomonas flfluorescens* strain SS101 via novel volatile organic compounds. *Biochem. Biophys. Res. Commun.* 461, 361–365. doi: 10.1016/j.bbrc.2015.04.039

Pieterse, C. M., Zamioudis, C., Berendsen, R. L., Weller, D. M., Van Wees, S. C., and Bakker, P. A. (2014). Induced systemic resistance by beneficial microbes. *Annu. Rev. Phytopathol.* 52, 347–375.

Pineda, A., Kaplan, I., Hannula, S. E., Ghanem, W., and Bezemer, T. M. (2020). Conditioning the soil microbiome through plant-soil feedbacks suppresses an aboveground insect pest. *New Phytol.* 226, 595–608. doi: 10.1111/nph.16385

Reinhold-Hurek, B., Bünger, W., Burbano, C. S., Sabale, M., and Hurek, T. (2015). Roots shaping their microbiome: global hotspots for microbial activity. *Annu. Rev. Phytopathol.* 53, 403–424. doi: 10.1146/annurev-phyto-082712-102342

Rudrappa, T., Czymmek, K. J., Paré, P. W., and Bais, H. P. (2008). Root-secreted malic acid recruits beneficial soil bacteria. *Plant Physiol. Nov.* 148, 1547–1556. doi: 10.1104/pp.108.127613

Schlatter, D., Kinkel, L., Thomashow, L., Weller, D., and Paulitz, T. (2017). Disease suppressive soils: new insights from the soil microbiome. *Phytopathology* 107, 1284–1297.

Steinkellner, S., Lendzemo, V., Langer, I., Schweiger, P., Khaosaad, T., and Toussaint, J. P. (2007). Flavonoids and strigolactones in root exudates as signals in symbiotic and pathogenic plant-fungus interactions. *Molecules* 12, 1290–1306. doi: 10.3390/12071290

Stringlis, I. A., Yu, K., Feussner, K., de Jonge, R., Van Bentum, S., Van Verk, M. C., et al. (2018). MYB72-dependent coumarin exudation shapes root microbiome assembly to promote plant health. *Proc. Natl. Acad. Sci. U. S. A.* 115, 5629–5631. doi: 10.1073/pnas.1722335115

Tahir, H. A. S., Qin, G., Hui, J. W., Waseem, R., Alwina, H., Li, M. W., et al. (2017). Plant growth promotion by volatile organic compounds produced by *Bacillus subtilis* SYST2. *Front. Microbiol.* 8:171. doi: 10.3389/fmicb.2017.00171

Tchakounté, G. V. T., Beatrice, B., Sascha, P., Henri, F., and Silke, R. (2018). Community structure and plant growth-promoting potential of cultivable bacteria isolated from cameroon soil. *Microbiol. Res.* 214, 47–59. doi: 10.1016/j.micres.2018.05.008

Than, P. P., Jeewon, R., Hyde, K. D., Pongsupasamit, S., and Taylor, P. W. J. (2008). Characterization and pathogenicity of *Colletotrichum* species associated with anthracnose on chilli (*Capsicum* spp.) in Thailand. *Plant Pathol.* 57, 562–572.

Trotel-Aziz, P., Couderchet, M., Biagianti, S., and Aziz, A. (2008). Characterization of new bacterial biocontrol agents *Acinetobacter*, *Bacillus*, *Pantoea* and *Pseudomonas* spp. mediating grapevine resistance against *Botrytis cinerea*. *Environ. Exp. Bot.* 64, 21–32. doi: 10.1016/j.envexpbot.2007.12.009

Verma, S., and Mishra, S. N. (2005). Putrescine alleviation of growth in salt stressed Brassica juncea by inducing antioxidative defense system. *J. Plant Physiol.* 162, 669–677. doi: 10.1016/j.jplph.2004.08.008

Wang, J. P., and Lu, D. S. (2008). Occurrence of tea grey spot disease and germinating characteristics of *Pestalotiopsis versicolor* conidiospores. *Amino Acids Biot. Res.* 30, 30–32.

Wang, S. Q. (2014). *Research on the Effects of Streptomyces JD211 on Rice Growth Promotion and Disease Prevention Mechanism*. Nanchang: Jiangxi Agricultural University.

Wang, S. S., Mi, X. Z., Wu, Z. R., Zhang, L. X., and Wei, C. L. (2019). Characterization and pathogenicity of *Pestalotiopsis* -like species associated with gray blight disease on *Camellia sinensis* in Anhui province, China. *Plant Dis.* 103, 2786–2797. doi: 10.1094/PDIS-02-19-0412-RE

Wang, Y., Qian, W. J., Li, N. N., Hao, X., Wang, L., Xiao, B., et al. (2016). Metabolic changes of caffeine in tea plant (*camellia sinensis* (L.) o. kuntze) as defense response to *colletotrichum fructicola*. *J. Agric. Food Chem.* 64, 6685–6693. doi: 10.1021/acs.jafc.6b02044

Weller, D. M., Raaijmakers, J. M., Gardener, B. B., and Thomashow, L. S. (2002). Microbial populations responsible for specific soil suppressiveness to plant pathogens. *Annu. Rev. Phytopathol.* 40, 309–348. doi: 10.1146/annurev.phyto.40.030402.110010

Wu, K., Yuan, S., Xun, G., Shi, W., Pan, B., Guan, H., et al. (2015). Root exudates from two tobacco cultivars affect colonization of ralstonia solanacearum and the disease index. *Eur. J. Plant Pathol.* 141, 667–677.

Yang, R. J., Wang, Q. M., Gong, W. Y., Zhao, M. M., and Yan, L. (2020). Distribution diversity of microbial communities in the Air of tea gardens and tea cellars in different habitats of jingmai mountain, Yunnan province. *J. Yunnan Agric. Univ.* 35, 659–666.

Yuan, H., Shi, B., Huang, T., Zhou, Z., Li, W., Hui, H., et al. (2021). Biological control of pear valsa canker caused by valsa pyri using *Penicillium citrinum*. *Horticulturae* 7:198. doi: 10.3390/horticulturae7070198

Yuan, J., Chaparro, J. M., Manter, D. K., Zhang, R., Vivanco, J. M., and Shen, Q. (2015). Roots from distinct plant developmental stages are capable of rapidly selecting their own microbiome without the influence of environmental and soil edaphic factors. *Soil Biol. Biochem.* 89, 206–209.

Yuan, J., Zhao, J., Wen, T., Zhao, M., Li, R., Goossens, P., et al. (2018). Root exudates drive the soil-borne legacy of aboveground pathogen infection. *Microbiome* 6:156. doi: 10.1186/s40168-018-0537-x

Zhao, Y. P., Wu, L. K., Chu, L. X., Yang, Y. Q., Li, Z. F., and Azeem, S. D. (2015). Interaction of Pseudostellaria heterophylla with Fusarium oxysporum f.sp.heterophylla mediated by its root exudates in a consecutive monoculture system. *Sci. Rep.* 5:8197. doi: 10.1038/srep08197

Zhou, Y., He, S., Gong, G., Zhang, S., Chang, X., Liu, N., et al. (2014). Soil fungal diversity in three nature reserves of jiuzhaigou county, sichuan province, china. *Ann. Microbiol.* 64, 1275–1290. doi: 10.1007/s13213-013-0772-0

Conflict of Interest: The authors declare that the research was conducted in the absence of any commercial or financial relationships that could be construed as a potential conflict of interest.

Publisher's Note: All claims expressed in this article are solely those of the authors and do not necessarily represent those of their affiliated organizations, or those of the publisher, the editors and the reviewers. Any product that may be evaluated in this article, or claim that may be made by its manufacturer, is not guaranteed or endorsed by the publisher.

frontiers in Microbiology

ORIGINAL RESEARCH
published: 16 December 2021
doi: 10.3389/fmicb.2021.777351

Interaction Between Halotolerant Phosphate-Solubilizing Bacteria (*Providencia rettgeri* Strain TPM23) and Rock Phosphate Improves Soil Biochemical Properties and Peanut Growth in Saline Soil

Huanhuan Jiang[1,2], Sainan Li[1], Tong Wang[2], Xiaoyuan Chi[2], Peishi Qi[3] and Gang Chen[1]**

[1] College of Life Sciences, Zhaoqing University, Zhaoqing, China, [2] Shandong Peanut Research Institute, Qingdao, China, [3] State Key Laboratory of Urban Water Resource and Environment, School of Environment, Harbin Institute of Technology, Harbin, China

OPEN ACCESS

Edited by:
Christopher Rensing,
Fujian Agriculture and Forestry University, China

Reviewed by:
Luz Bashan,
Centro de Investigaciones Biológicas del Noroeste (CIBNOR), Mexico
José David Flores Félix,
Universidade da Beira Interior, Portugal
Qurban Ali Panhwar,
Universiti Putra Malaysia, Malaysia

***Correspondence:**
Huanhuan Jiang
jhh0317@163.com
Gang Chen
447689336@qq.com

Specialty section:
This article was submitted to Microbiotechnology, a section of the journal Frontiers in Microbiology

Received: 15 September 2021
Accepted: 17 November 2021
Published: 16 December 2021

Citation:
Jiang H, Li S, Wang T, Chi X, Qi P and Chen G (2021) Interaction Between Halotolerant Phosphate-Solubilizing Bacteria (Providencia rettgeri Strain TPM23) and Rock Phosphate Improves Soil Biochemical Properties and Peanut Growth in Saline Soil. Front. Microbiol. 12:777351. doi: 10.3389/fmicb.2021.777351

Soil salinity has adverse effects on soil microbial activity and nutrient cycles and therefore limits crop growth and yield. Amendments with halotolerant phosphate-solubilizing bacteria (PSB) and rock phosphate (RP) may improve properties of saline soil. In this study, we investigated the effects of RP either alone or in combination with PSB (*Providencia rettgeri* strain TPM23) on peanut growth and soil quality in a saline soil. With the combined application of RP and PSB, plant length and biomass (roots and shoots) and uptake of phosphorus (P), nitrogen (N), and potassium (K) increased significantly. Soil Na^+ and Cl^- contents decreased in the PR alone or PR combined with PSB treatment groups. There were strongly synergistic effects of RP and PSB on soil quality, including a decrease in pH. The soil available N, P, and K contents were significantly affected by the PSB treatments. In addition, the alkaline phosphomonoesterases, urease, and dehydrogenase activities increased significantly compared with the untreated group; highest alkaline phosphomonoesterases activity was observed in the RP and PSB treatment groups. The composition of rhizosphere soil bacterial communities was determined using 454-pyrosequencing of the 16S rRNA gene. In the PR alone or PR combined with PSB treatment groups, the structure of the soil bacterial community improved with increasing richness and diversity. With PSB inoculation, the relative abundance of *Acidobacteria*, *Chloroflexi*, and *Planctomycetes* increased. The three phyla were also positively correlated with soil available N and root dry weight. These results suggested microbiological mechanisms by which the combined use of RP and PSB improved saline soil and promoted plant growth. Overall, the study indicates the combined use of RP and PSB can be an economical and sustainable strategy to increase plant growth in P-deficient and salt-affected soils.

Keywords: saline soil, rhizosphere, phosphate-solubilizing bacteria, rock phosphate, peanut growth, nutrient uptake, soil properties, bacterial community

INTRODUCTION

Saline soil is a serious global environmental problem that negatively affects agricultural production because of unfavorable soil physicochemical properties and nutrient deficiencies (Shrivastava and Kumar, 2015). Accumulation of excessive sodium ions can adversely affect soil nutrient cycles (Li et al., 2016), enzyme activity (Patel and Saraf, 2013), and microbial community diversity (Bharti et al., 2016). Phosphorus (P) is one of the most important macronutrients required for plant growth. However, most P in soil is in inorganic and organic forms with low solubility that are not available for plant uptake (Adnan et al., 2017). The low availability of P in saline soil is due to fixation when P is bound to calcium (Ca), aluminum, and iron (Tchakounté et al., 2020). Salt stress can also reduce plant uptake efficiency of P, which leads to losses in crop yields (Radhakrishnan et al., 2015). To overcome P deficiency, P fertilizers can provide adequate P to increase plant productivity, although excessive application can cause eutrophication and is not economical (Park et al., 2010). Therefore, in saline soils, management must be improved to increase the availability of P and also minimize its adverse effects. In sustainable agriculture, application of biofertilizers is one potential strategy to minimize the environmental problems associated with chemical fertilizers (Chang and Yang, 2009). The use of microbial inoculation combined with rock phosphate (RP) is recognized as a suitable strategy to improve saline soil properties and plant growth (Singh and Reddy, 2011); Phosphate-solubilizing bacteria (PSB) are an integral component of the soil P cycle and play a key role in dissolving different pools of soil P to increase P availability to plants. Many PSB can significantly increase plant growth in saline soils by releasing soluble P (Ramadoss et al., 2013; Wan et al., 2020). The most effective microbes at solubilizing P include some common genera of bacteria and fungi, such as *Pseudomonas*, *Bacillus*, *Micrococcus*, *Aspergillus*, *Penicillium*, and *Enterobacter* (Ghosh et al., 2016; Ludueña et al., 2018). Moreover, halotolerant PSB can facilitate plant adaptation and tolerance to salinity stress and subsequently improve plant growth (Vassilev et al., 2006). The main mechanism underlying inorganic phosphate mineralization is the production of low-molecular-weight organic acids. These acids acidify phosphate conjugate bases, thereby increasing their solubility as a result of the reduction of soil pH, while also chelating metals (Wei et al., 2018). In our previous work, a halotolerant PSB isolated from saline soil increased the availability of nutrients to plants, and in particular soil available P. The PSB used in that study, a strain of Providencia rettgeri, may thus have potential use as a biofertilizer to sustain the growth of peanut in salt-affected soil (Jiang et al., 2019). However, few studies have explored the potential of halotolerant PSB to dissolve multiple P sources.

Rock phosphate (RP) is a raw material used in manufacturing phosphatic fertilizers; it has been used as an alternative P source extensively due to its lower cost and as a support for sustainable agriculture (Xiao et al., 2011). However, the extremely poor solubility of RP limits its direct use as a soil amendment, especially in saline–alkaline soil. Previous studies have shown that RP can improve the physicochemical properties of saline soils and that inoculation with PSB enhances the effects (Baig et al., 2010). Adnan et al. (2020) found that compared with the application of only RP, the combination of RP and PSB increases maize P acquisition under salinity stress. Most studies now focus on using the combined application of RP and PSB to increase the growth of plants and improve soil physicochemical properties (Iqbal et al., 2019). Microbial communities are an integral part of soil ecosystems and are considered the main drivers of soil fertility and quality (van der Heijden and Wagg, 2013). However, microbial populations are often restricted by nutrient deficiencies in saline soils (García-Orenes et al., 2010). The use of PSB as bioinoculants has been shown to influence microbial communities that colonize the rhizosphere and further increase soil enzyme activity and nutrient contents (Li et al., 2014). According to Song et al. (2021), PSB enhanced the abundance of beneficial microorganisms and decreased the abundance of harmful microorganisms. PSB can secrete a growth-promoting substance or release a chemical signal to promote their own growth, thereby improving relative microbiology abundance and accelerating plant uptake of nutrients from the soil. Silva et al. (2017) reported that long-term RP fertilization also changes microbial community structure, with microorganisms related to P solubilization and acquisition increasing in abundance. Therefore, PSB can be used in the form of bioinoculants in agriculture to benefit the regulation of soil microbial communities. However, the effects of the interaction between RP and halotolerant PSB on rhizosphere microbial diversity remain poorly understood.

Peanut (*Arachis hypogaea* L.) is an economically valuable crop. However, high salt levels and P deficiency limit peanut production and ultimately lead to severe losses in yield (Sharma et al., 2016). Information on the combined application of halotolerant PSB and RP is lacking for peanuts grown in saline soils. In addition, the effects of the combined application of halotolerant PSB and RP on saline soil microbial communities have not been investigated. Our hypothesis, therefore, was that introducing PR in conjunction with PSB inoculation to saline soils would modify their properties and bacterial community. This treatment may be useful for increasing the available phosphorus content and promoting plant growth. Thus, the primary objective of this study was to evaluate the effects of the interaction between halotolerant PSB and RP on soil properties and peanut growth in a saline soil. Changes in bacterial community structure were examined to better understand the microbiological mechanisms underlying the improvements in soil properties and plant growth.

MATERIALS AND METHODS

Bacterial Strain Culture and Seed Treatment

Providencia rettgeri strain (TPM23) (Accession no. KX289656.1) is a halotolerant PSB described in our previous work (Jiang et al., 2019). The tricalcium phosphate medium (TPM) [10 g glucose, 0.5 g yeast extract, 0.5 g $(NH_4)_2SO_4$, 0.26 g KCl, 0.1 g $MgSO_4.7H_2O$, 0.2 g NaCl, 0.05 g $FeSO_4.7H_2O$, 0.2 mg

$MnSO_4.H_2O$, 5 g $Ca_3(PO_4)_2$, and 1,000 mL of distilled water] was added to flasks (200 mL). Then, 200 μL of the isolate were inoculated for 24 h at 28 ± 2°C with continuous shaking. Uninoculated medium was used as control. The bacterium suspension was adjusted to a final concentration of 10^8 colony forming units (CFU) per mL.

The peanut cultivar Huayu33 was provided by the Shandong Peanut Research Institution (China Qingdao). Seeds were sterilized in 75% ethanol and 10% $NaClO_3$ solutions for 1 and 10 min, respectively. After washing with sterilized distilled water, some seeds were cultured with the PSB isolate at 10^8 CFU/mL for 3 h. Seeds in uninoculated medium were the controls.

Pot Experiment

Soil samples were collected from sites known to have excessive salinity in the Yellow River delta area of Dongying Prefecture, Shandong, China (lat 37.5, long 118.3). We collected 10 samples at an interval of 1 m between each sampling point. The samples were scraped off from encrusted environmental surface soils. In addition, 15-cm soil cores were collected and mixed well. After air-drying at room temperature, soils were ground to pass through a 2-mm sieve. The characterization of the experimental soil used in the current study is described in **Table 1**. The main compound in RP is $CaSO_4$, which is acidic and contains the essential plant nutrients Ca, P, and sulfur. In addition, RP contains 15–20% P. Plastic pots (height, 25 cm; diameter, 25 cm) were filled with equal amounts (approximately 1.5 kg) of sieved soil. One group of pots contained only original soil (T0), and the other group contained original soil plus 20 g/kg RP (T1). After the soil was fully mixed, half the pots in each group were inoculated with 15 mL of PSB suspension (+PSB) at 10^8 CFU/mL, resulting in the treatments T0P and T1P. The other half in each group did not receive PSB inoculum (-PSB) but were mock-treated with 15 mL of sterilized water, resulting in the treatments T0 and T1. Five inoculated or control peanut seeds (prepared as described above) were sown in each pot (**Table 2**). After 7 days, the plants were thinned out to three plants per pot. The pot experiment was arranged in a two factor completely randomized design with three replicates per treatment. The experiment was conducted for 45 days in a growth chamber at 24 ± 1°C with a 16-h light and 8-h dark photoperiod (350 $\mu molm^{-2}$ s^{-1} light intensity), and a relative humidity of 50%. Samples were watered regularly with sterilized tap water twice a month.

Plant Growth and Yield Attributes

At maturity, peanut plants in three replicates from each treatment were harvested, and root and shoot lengths, as well as total branch number (TBN) and total leaf number (TLN), were determined. The roots and shoots were washed several times with sterilized distilled water. Plant material was dried at 80°C for 7 days, and dry weights were recorded. To determine total N (TN), total P (TP), and total K (TK) contents, peanut leaves were washed several times with sterilized distilled water and then oven-dried at 80°C for 48 h. Dried peanut leaves (0.1 g) were digested at 150°C for 2 h by the H_2SO_4-H_2O_2 cooking method. The content of total nitrogen was determined by the Kjeldahl method. The content of total phosphorus was determined by vanadate-molybdate-yellow colorimetry. The content of total potassium was determined by a flame photometer.

TABLE 1 | Soil characterization.

pH	Moisture content	TP	TN	TK	AP
	(%)	(mg/kg)	(mg/kg)	(mg/kg)	(mg/kg)
7.99	15.43	278.9	181.31	2300.21	9.31

TP, total P; TN, total N; TK, total K; AP, available P.

TABLE 2 | Pot experiment treatment for each experimental group.

Experimental group	Plant treatment method	Soil treatment method
T0	Seeds cultured in uninoculated medium	Original soil
T0P	Seeds cultured in PSB suspension	Original soil + PSB suspension
T1	Seeds cultured in uninoculated medium	Original soil + RP
T1P	Seeds cultured in PSB suspension	Original soil + RP + PSB suspension

Soil Physicochemical Properties and Enzyme Activities

After plants were harvested, soil was collected and analyzed for physicochemical properties and enzyme activities. Soil pH and electrical conductivity (EC) were determined using a pH meter (Hanna HI2221, Italy) and a conductometer (DDS-307A), respectively. Available N (AN) was extracted with 2 M KCl, and content was determined using the alkaline hydrolysis diffusion method (Mulvaney and Khan, 2001). Available P (AP) was extracted with 0.5 M $NaHCO_3$, and content was determined using molybdate colorimetry (Murphy and Riley, 1962). Available K (AK) was extracted with a CH_3COONH_4 solution, and content was measured by a flame photometer (AA-6300C, Shimadzu Japan). The activities of alkaline phosphomonoesterases (PP), dehydrogenase (DHA), and urease (UR) were determined by using ELISA kits (Shanghai Yuanye Biotechnology Co. Ltd., Shanghai, China).

Soil DNA Extraction and PCR Amplification

From the rhizosphere soil samples collected after peanut harvest, 2 g of soil from each replicate of the four treatments was collected. The V3–V4 region of the bacterial 16s RNA gene was amplified by PCR. After purification, PCR products were separated by electrophoresis on 2% agarose gel. Sequencing libraries were generated using a TruSeq® DNA PCR-Free Sample Preparation Kit (Illumina, United States) following the manufacturer's recommendations, and index codes were added. Library quality was assessed on a Qubit@ 2.0 Fluorometer

(Thermo Scientific) and an Agilent Bioanalyzer 2100 system. The library was sequenced on an Illumina HiSeq2500 platform, and 250-bp paired-end reads were generated.

Operational Taxonomic Unit-Based Sequence Analysis

Paired-end reads were assigned to samples based on their unique bar codes and truncated by cutting off the bar code and primer sequence. To obtain high-quality clean tags, QIIME[1] was used to perform quality filtering on the raw tags under specific filtering conditions. The effective tags were obtained after removal of chimera sequences. Sequences with ≥97% similarity were assigned to the same operational taxonomic unit abundances (OTUs). The observed-species, Chao1, ACE, Shannon, and Simpson indices of the bacterial communities were calculated in the QIIME software. To evaluate significant differences in soil bacteria between groups with a PSB suspension (T0P, T1P) and without PSB inoculation (T0, T1), *t*-tests were used. To evaluate the possible effects of soil environmental factors on bacterial communities, Pearson's coefficients of correlation (r) and significance (P) values were calculated between the most abundant bacterial phyla and peanut growth parameters and soil properties.

Statistical Analyses

Two-way ANOVA ($P < 0.05$; F-test) and Student's t-test ($P < 0.05$) were performed using SPSS v 13.0 (SPSS Inc., Chicago, IL, United States) software to determine the differences in pot experimental data among the different treatments. Differences were detected by the standard error of difference (SED).

RESULTS

Peanut Growth Parameters and Macronutrient Accumulation

The effect of RP with or without PSB on peanut growth efficiency was investigated. According to the two-way ANOVA, the effects of RP, PSB, and their interaction on peanut growth measures were significant ($P < 0.05$). Peanuts inoculated with PSB had greater root and shoot lengths compared with those without PSB, with or without RP (**Figure 1B**). Without PSB, RP had only slight effects on peanut biomass. However, when RP was combined with PSB inoculation, shoot and root dry biomass were also significantly affected by PSB inoculation (**Figure 1A**). Compared with the PR only treatment, the dry weight of roots increased by 13.61 and 55.91% and the dry weight of shoots increased by 42.81 and 10.62% in T0P and T1P, respectively. The same increasing trend was observed for TLN and TBN (**Figure 1C**).

Contents of TN, TP, and TK in peanut leaves are shown in **Figure 2**. The contents of TN and TP were different among the experimental groups with and without PSB inoculation ($P < 0.05$), but TK content was not affected ($P > 0.05$). The accumulation of nutrients was higher with PSB inoculation than without (**Figure 2**). The contents of TN, TP, and TK increased by 20.54, 83.98, and 12.08%, respectively, in the RP and PSB treatment compared with those in the RP only treatment.

Soil Physicochemical Properties

According to the two-way ANOVA, the effects of RP, PSB, and their interaction on rhizosphere soil physicochemical properties were significant ($P < 0.05$) (**Table 3**). Compared with the untreated group (T0), the soil pH in T1, T0P, and T1P decreased by 0.13, 0.48, and 0.62 units, respectively, and the EC value in the PSB treatment group was lower than that in the treatment group without PSB. The treatments significantly affected the soil contents of Ca^{2+}, Na^{+}, and Cl^{-}. The lowest Cl^{-} content was in the RP and PSB treatment groups. The treatments did not affect SO_4^{2-} content.

The effects of treatments on available nutrients in soil are shown in **Figure 3**. In the RP and PSB treatment, the contents were 184.90 mg/kg AN, 39.00 mg/kg AP, and 524.99 mg/kg AK. The difference was significant compared with no treatment, and the largest increase in soil AP (140.59%) was in the combined RP and PSB treatment.

Figure 4 shows the activity of the soil enzymes PP, UR, and DHA. Compared with uninoculated soil, inoculation with PSB increased UR activity by 2.61% (T0P) and 2.82% (T1P). The highest PP activity of 706.54 IU/L was in the RP and PSB treatment. Dehydrogenase had the lowest activity, and the differences were not significant between inoculated and uninoculated soils in all treatments.

Soil Microbial Community Diversity

This study is the first to investigate the effects of RP with or without PSB inoculation on the rhizosphere bacterial community of peanut (**Table 4**). The raw pyrosequencing data are accessioned at the NCBI SRA database with the BioProject accession number PRJNA777755. According to MiSeq analysis of the V3–V4 region of the bacterial 16S rRNA gene, the mean numbers of OTUs were 3,142 in T0, 2,879 in T1, 3,023 in T0P, and 2,674 in T1P. The mean Chao 1 and ACE indices were in the order T0 > T1 > T0P > T1P, indicating the level of community richness varied among the four treatments. The mean Shannon index indicated bacterial community diversity increased with PSB inoculation. The index ranged from 9.30 to 9.65 with PSB inoculation but from 8.92 to 8.97 without PSB inoculation. The results were similar for the Simpson index.

All valid sequences from the soil sample libraries were classified at the class and genus levels. At the class level, the top ten dominant classes were selected (**Figure 5**). The 10 dominant bacterial classes were Gammaproteobacteria, Alphaproteobacteria, Actinobacteria, Acidobacteria, Cytophagia, Deltaproteobacteria, Bacilli, Planctomycetacia, Betaproteobacteria, and Gemmatimonadetes. The dominant classes were the same in different treatments; however, the relative abundance of each class was different. The relative abundance of Alphaproteobacteria, Betaproteobacteria, and Deltaproteobacteria was higher in rhizosphere soils with PSB inoculation than in those without. By contrast, the relative

[1] http://qiime.org/index.html

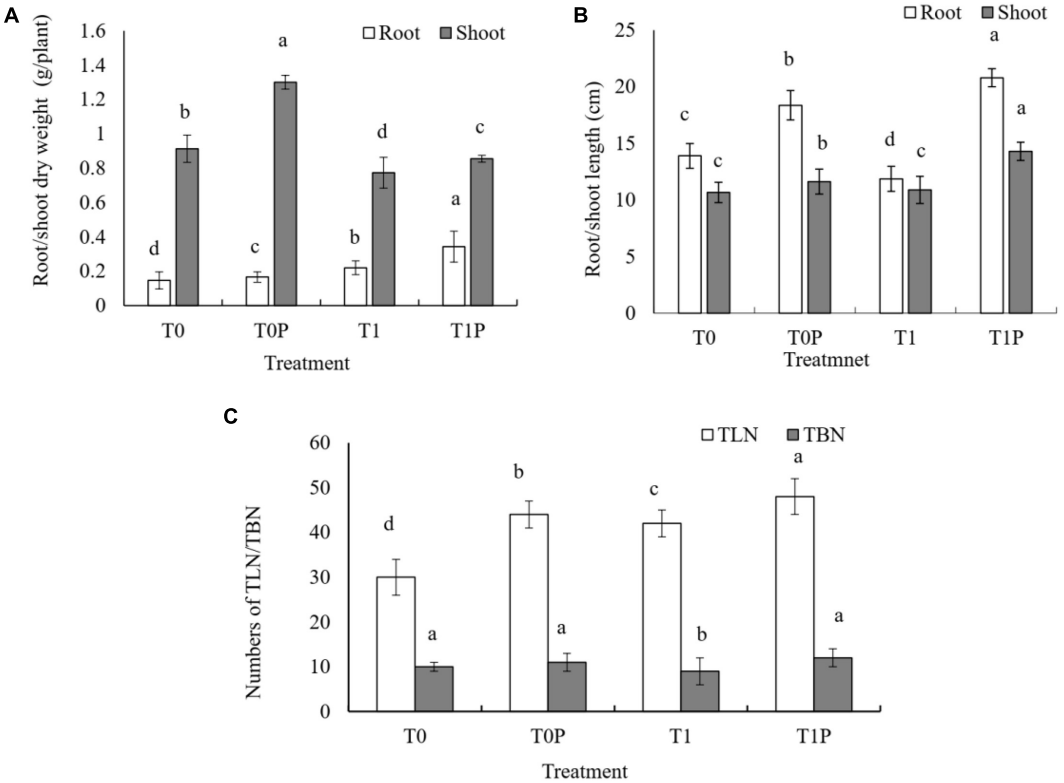

FIGURE 1 | Effects of rock phosphate (RP) and phosphate-solubilizing bacteria (PSB) on peanut **(A)** root and shoot dry weight (g plant^{-1}), **(B)** root and shoot length (cm), and **(C)** total leaf number (TLN) and total branch number (TBN). Treatments: T0, no additions, the control; T0P, with PSB inoculation only; T1, with RP amendment only; T1P, with RP and PSB. Values are the means of three replicates. Error bars represent ± standard deviation. Values sharing a common letter within the column are not significant at $P < 0.05$.

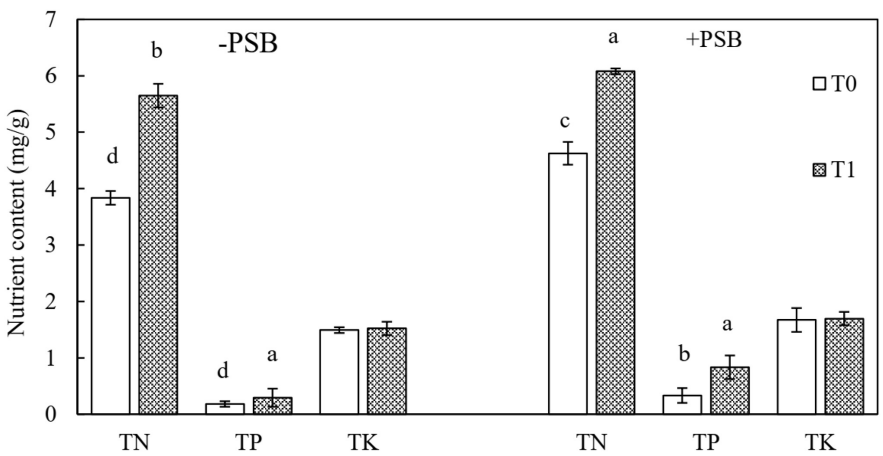

FIGURE 2 | Effects of rock phosphate (RP) and phosphate-solubilizing bacteria (PSB) on total N (TN), total P (TP), and total K (TK) accumulation (mg/g) in peanut leaves. Treatments: T0, without RP; T1, with RP; −PSB, without PSB; +PSB, with PSB. Values are the means of three replicates. Error bars represent ± standard deviation. Values sharing a common letter within the column are not significant at $P < 0.05$.

abundance of Gammaproteobacteria was higher in soils without PSB inoculation.

Figure 6 shows the relative abundance of bacteria at the genus level. The 10 dominant genera were *Arthrobacter*, *Skermanella*, *Sphingomonas*, *Pontibacter*, *Altererythrobacter*, *Kocuria*, *Devosia*, *Simiduia*, *Steroidobacter*, and *Bacillus*. The total abundance of the 10 dominant bacterial genera without PSB inoculation (T0, T1) was higher than that with inoculation (T0P, T1P). The lowest

TABLE 3 | Effects of rock phosphate (RP) and phosphate-solubilizing bacteria (PSB) on soil physicochemical properties.

Treatment		pH	EC	Ca^{2+}	Na^{+}	Cl^{-}	SO_4^{2-}
		–	μs/cm	g/kg	g/kg	g/kg	g/kg
-PSB	T0	7.96 ± 0.01[a]	1152.73 ± 39.84[b]	1.93 ± 0.02[c]	2.65 ± 0.01[a]	1.98 ± 0.02[a]	0.30 ± 0.01[b]
	T1	7.83 ± 0.02[b]	1281.53 ± 17.64[a]	2.85 ± 0.03[a]	0.13 ± 0.01[d]	0.35 ± 0.02[c]	0.37 ± 0.02[a]
+ PSB	T0P	7.48 ± 0.01[c]	1135.10 ± 11.22[d]	1.1 ± 0.02[d]	1.06 ± 0.01[b]	1.05 ± 0.01[b]	0.28 ± 0.01[c]
	T1P	7.34 ± 0.03[d]	1142.70 ± 27.69[c]	2.1 ± 0.03[b]	0.61 ± 0.01[c]	0.30 ± 0.01[c]	0.28 ± 0.01[c]

Treatments: T0, no additions, the control (−PSB); T1, with RP amendment only (−PSB); T0P, with PSB inoculation only (+PSB); T1P, with RP and PSB (+PSB). EC, electrical conductivity. Values are the means of three replicates. Error bars represent ± standard deviation. Values sharing a common letter within the column are not significant at $P < 0.05$.

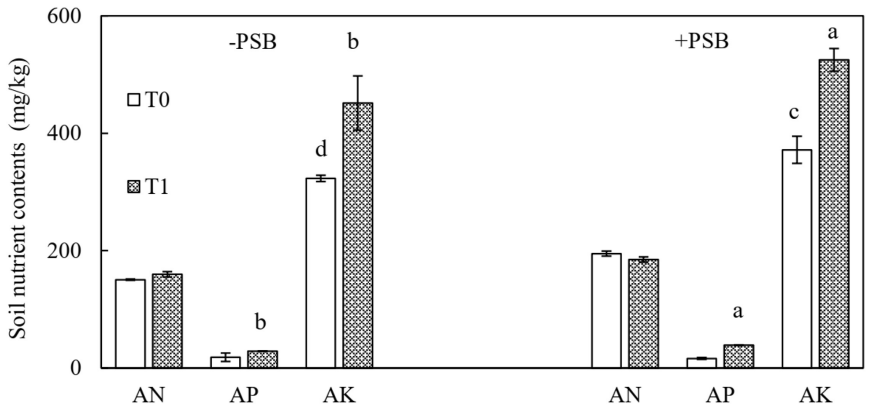

FIGURE 3 | Effects of rock phosphate (RP) and phosphate-solubilizing bacteria (PSB) on soil available nitrogen (AN), available phosphorus (AP), and available potassium (AK) contents (mg/kg). Treatments: T0, without RP; T1, with RP; −PSB, without PSB; +PSB, with PSB. Values are the means of three replicates. Error bars represent ± standard deviation. Values sharing a common letter within the column are not significant at $P < 0.05$.

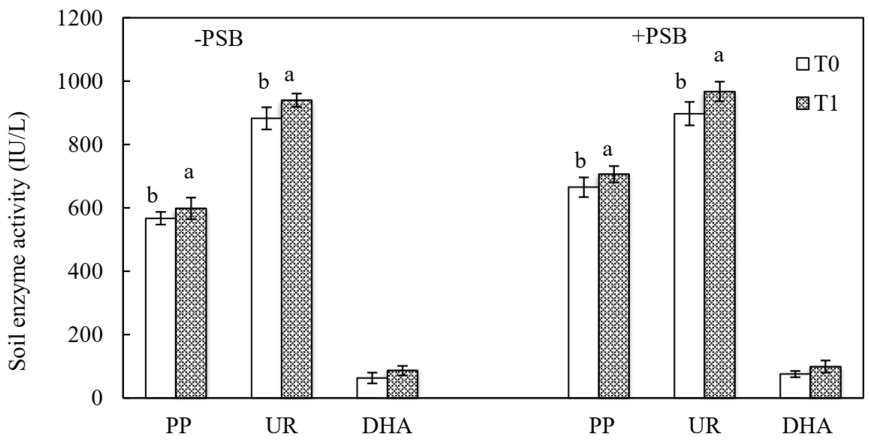

FIGURE 4 | Effects of rock phosphate (RP) and phosphate-solubilizing bacteria (PSB) on soil alkaline phosphomonoesterases (PP), urease (UR), and dehydrogenase (DHA) enzyme activities (IU/L). Treatments: T0, without RP; T1, with RP; −PSB, without PSB; +PSB, with PSB. Values are the means of three replicates. Error bars represent ± standard deviation. Values sharing a common letter within the column are not significant at $P < 0.05$.

total abundance of the 10 dominant genera of bacteria was in T0P, accounting for 10.64% of the total bacteria. The total abundance in T1 and T1P accounted for 18.42 and 17.48% of total bacteria, respectively. Therefore, the addition of PR and PSB greatly affected the relative abundance of the dominant genera of bacteria.

Figure 7 shows comparisons between two groups: T0 vs. T0P (**Figure 7A**) and T1 vs. T1P (**Figure 7B**). Within each comparison, significant differences in bacterial groups were determined using *t*-tests. Compared with T0, *Acidobacteria*, *Chloroflexi*, and *Nitrospirae* were more important in T0P ($P < 0.05$). By contrast, *Proteobacteria* and

TABLE 4 | Effects of rock phosphate (RP) and phosphate-solubilizing bacteria (PSB) on richness and diversity indices of soil bacterial communities.

Sample	Observed_species	Chao1	ACE	Shannon	Simpson
T0	3142.33 ± 43.99^{a}	4063.15 ± 111.21^{a}	4061.77 ± 54.96^{a}	8.97 ± 0.02^{c}	0.98 ± 0.00^{b}
T1	3029.33 ± 177.34^{b}	3903.36 ± 230.17^{b}	3911.65 ± 217.91^{b}	8.92 ± 0.18^{c}	0.99 ± 0.00^{a}
T0P	3023 ± 103.41^{b}	3549.44 ± 241.13^{c}	3578.69 ± 207.97^{c}	9.65 ± 0.32^{a}	0.99 ± 0.00^{a}
T1P	2674 ± 130.23^{c}	3262.13 ± 277.50^{d}	3227.01 ± 312.94^{d}	9.30 ± 0.0^{b}	0.99 ± 0.00^{a}

Treatments (following the treatment code is the replicate number): T0, no additions, the control; T1, with RP amendment only; T0P, with PSB inoculation only; T1P, with RP and PSB. Values sharing a common letter within the column are not significant at $P < 0.05$.

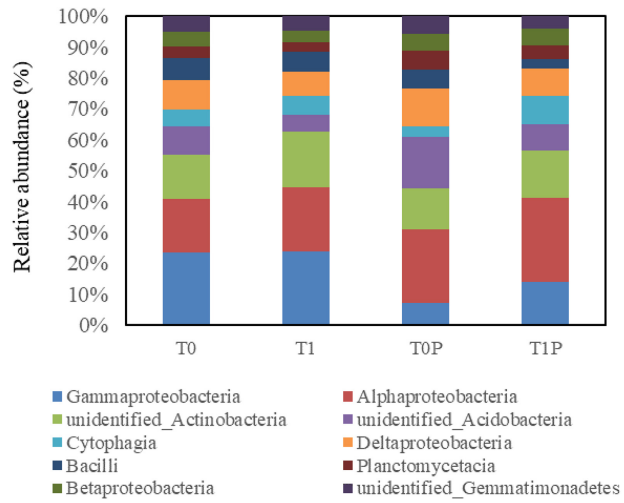

FIGURE 5 | Effects of rock phosphate (RP) and phosphate-solubilizing bacteria (PSB) on the relative abundance (%) of the 10 dominant classes of soil bacteria. The same 10 classes were dominant in all treatments. Treatments (following the treatment code is the replicate number): T0, no additions, the control; T0P, with PSB inoculation only; T1, with RP amendment only; T1P, with RP and PSB.

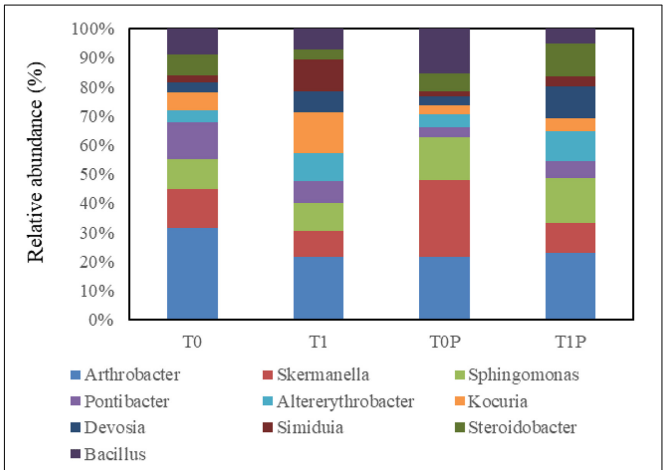

FIGURE 6 | Effects of rock phosphate (RP) and phosphate-solubilizing bacteria (PSB) on the relative abundance (%) of the 10 dominant genera of soil bacteria. The same 10 genera were dominant in all treatments. Treatments (following the treatment code is the replicate number): T0, no additions, the control; T0P, with PSB inoculation only; T1, with RP amendment only; T1P, with RP and PSB.

Hydrogenedentes were more important in T0. Compared with T1, *Planctomycetes*, *Verrucomicrobia*, *Nitrospirae*, *Cyanobacteria*, and *Armatimonadetes* were more important in T1P. Thus, PSB inoculation significantly affected those taxa. In all treatments, *Acidobacteria*, *Chloroflexi*, and *Planctomycetes* were enriched after inoculation with PSB.

Pearson's coefficients of correlation (r) and significance (P) values were calculated between the most abundant bacterial phyla and peanut growth parameters (**Table 5**) and soil properties (**Table 6**). The relative abundance of *Planctomycetes* was positively correlated with root length, and the relative abundances of *Acidobacteria*, *Chloroflex*, and *Planctomycetes* were positively correlated with root dry weight ($P < 0.05$; **Table 5**). Therefore, the three bacterial phyla likely had positive effects nutrient uptake and growth in peanut. The relative abundance of *Firmicutes* was negatively correlated with AP and AK and positively correlated with soil pH (**Table 6**). *Planctomycetes* was positively correlated with AN and negatively correlated with soil EC ($P < 0.05$). *Acidobacteria* and *Chloroflexi* were also positively correlated with AN. alkaline phosphomonoesterases, UR, and DHA activities were not correlated with the relative abundance of the bacterial phyla ($P > 0.05$). The results showed that PSB application significantly increased soil bacterial populations and favored those phyla that were associated with soil nutrient cycling.

DISCUSSION

Saline soils negatively affect plant growth because of nutrient deficiencies and salts (Yang et al., 2012). To address these problems, the combined application of RP and PSB as a potential substitute for chemical fertilizers has aroused considerable recent attention (Yadav et al., 2017). PSB play an important role in P cycling in soil–plant systems. Many PSB strains in the genera *Burkholderia, Enterobacter, Paenibacillus*, and *Pseudomonas* can potentially promote plant growth, by participating in various biological processes (Ait Barka et al., 2006). Shahzad et al. (2017) reported that the interaction between RP and PSB improved soil biochemical properties in dryland agriculture. However, the current study is the first to report that the interaction between RP and halotolerant PSB (*Providencia rettgeri* strain TPM23) improved soil biochemical properties and peanut production in a saline soil.

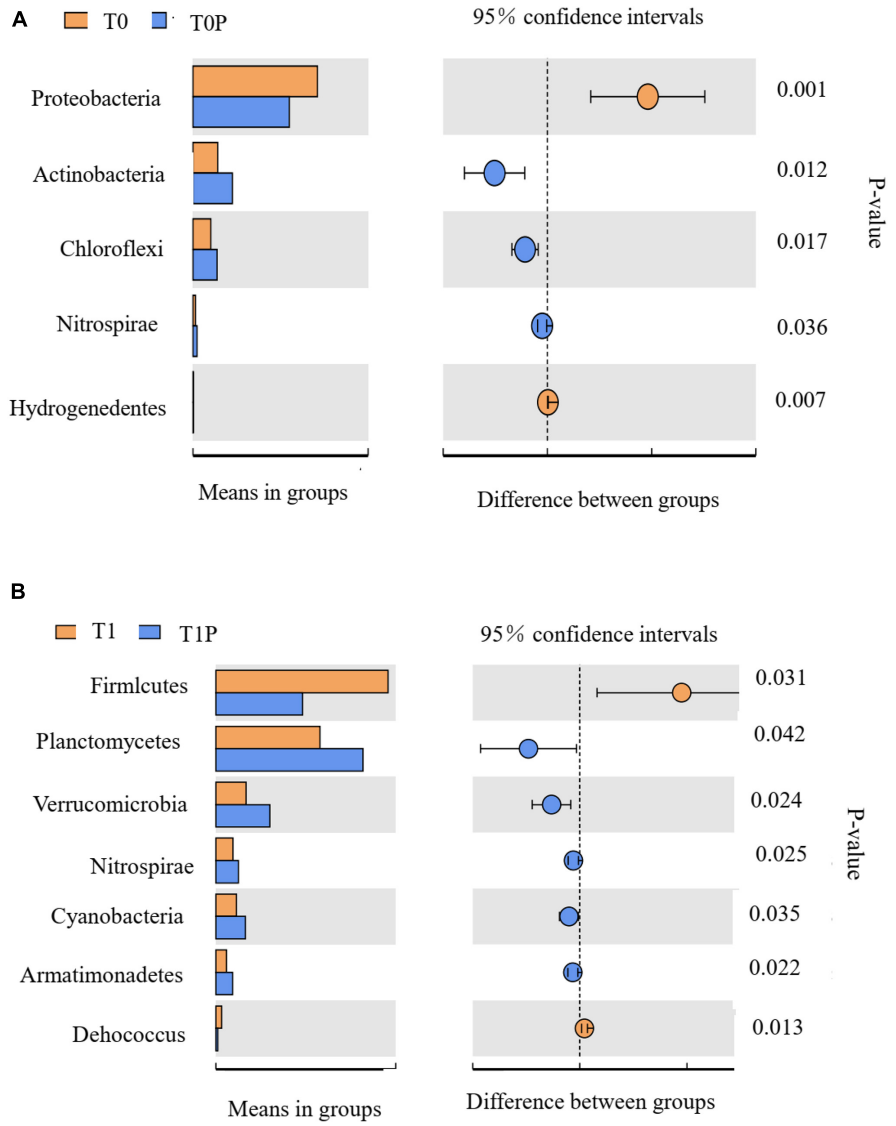

FIGURE 7 | Bacterial phyla with relative abundance significantly different in the comparison between **(A)** control soil with no additions (T0) and soil with only phosphate-solubilizing bacteria (PSB) (T0P) and between **(B)** soil with only rock phosphate (RP) amendment (T1) and soil with both RP and PSB (T1P). Significant differences in relative abundance were determined by *t*-tests. On the left: the abundance of taxa in each group, with each horizontal bar representing the mean value. On the right: the intergroup difference confidence level and the *P*-value for the significant difference in abundance.

The application potential of halotolerant PSB in agriculture is based on their ability to increase crop growth and eliminate the effects of stress without harming the environment (Shukla et al., 2012). The addition of P fertilizer can strengthen the effects of PSB because it provides a substrate that benefits the proliferation and survival of inoculated PSB (Yu et al., 2011). In this study, the growth of peanut in a saline soil increased under the combined the effect of RP and PSB. Other studies also indicate that PSB combined with an insoluble phosphate source can improve plant growth and yield as well as soil conditions (Gurdeep and Reddy, 2015; Mahanta et al., 2018). Estrada et al. (2013) and Yadav et al. (2014) found similar results with tricalcium phosphate or P_2O_5 amendments. Phosphorus uptake by plants reflects P availability in various treatments. In the present study, the combined application of PSB and RP significantly increased P uptake in comparison with only RP amendment or PSB inoculation. In addition, for the treatments with combined applications of PSB and RP with an increase in peanut growth parameters, N, P, and K accumulation increased significantly in leaves. Similarly, Khosravi et al. (2018) found that the co-application of plant growth-promoting rhizobacteria (PGPR) and RP significantly increased N, P, and K uptake rates in lettuce, which led to increases in biomass and length. Thus, the inoculation of seeds with PSB combined with a mineral P source is beneficial to crop growth, regardless of the type of mineral P. The application of RP provides a nutrient substrate for PSB, and

TABLE 5 | Pearson's coefficients of correlation (*r*) between the 10 most abundant phyla of soil bacteria and measures of peanut growth.

Phylum	RL	SL	RFW	SFW	SDW	RDW
	(cm)	(cm)	(g/plant)–	(g/plant)	(g/plant)	(g/plant)
Proteobacteria	−0.46	−0.09	0.14	−0.13	−0.32	**–0.54**
Actinobacteria	−0.07	−0.31	0.31	−0.11	0.37	−0.14
Acidobacteria	0.36	0.23	−0.36	0.14	0.17	**0.69**
Bacteroidetes	−0.10	0.24	0.20	0.05	−0.37	**–0.5**
Chloroflexi	0.25	−0.10	−0.37	0.02	0.21	**0.62**
Firmicutes	−0.13	−0.47	0.18	−0.26	0.11	−0.17
Planctomycetes	**0.59**	0.28	−0.08	0.32	0.17	**0.51**
Gemmatimonadetes	−0.27	−0.07	−0.47	−0.13	−0.16	0.1
Thaumarchaeota	0.30	−0.02	0.16	0.02	0.15	0.28
Thermomicrobia	0.34	−0.06	0.18	0.14	0.39	0.37

RL, root length; SL, stem length; RFW, root fresh weight; SFW, stem fresh weight; SDW, stem dry weight; RDW, root dry weight.
Bold type indicates a significant correlation ($p < 0.01$).

a large population of PSB can continuously dissolve the RP and release much more available P for plants, As a result, plant growth improves and biomass increases.

In addition to effects on plants, the complex interaction between PSB and RP also affects soil physicochemical properties. One of the main mechanisms leading to the dissolution of inorganic phosphate in soil is the reduction in rhizosphere pH due to the release organic acids (Rfaki et al., 2020). A small reduction in soil pH was observed with PSB inoculation or RP amendment compared with that in the control. However, the most significant reduction in pH was in the combined PSB and RP treatment. The greater reduction in pH might be because the RP was a substrate for PSB and associated with subsequent increases in microbial biomass would be increased excretion of organic acids, lowering the pH. The decrease in rhizosphere pH would then lead to the dissolution of P sources and increase the availability of P (Taktek et al., 2017). Moreover, according to Arora (2016), PSB can be used to decrease or exclude soil ions. Similarly, we found that Cl^- and Na^+ decreased in the combined RP and PSB treatment. The decrease might be because the Ca^{2+} of RP can react with Na^+ to form a calcium colloid, which increases the formation of soil aggregates and improves soil structure (Lebron et al., 2002; Chen et al., 2009). The solubility of the Na_2SO_4 is also greatly reduced compared with that of NaCl, which increases the salt-leaching of salinity components and inhibits soil processes. Thus, the application of RP and PSB reduced the pH while optimizing the salt–alkali ion composition. However, the content of Ca^{2+} increased with the addition of RP, likely because it was enriched with calcium ions.

Additionally, PGPR are exogenous bacteria introduced into soils to participate in soil processes such as the storage and release of nutrients (Ribeiro and Cardoso, 2012; Patel and Saraf, 2013). In this study, we found a higher level of AN, AP, and AK with PSB inoculation. Da Costa et al. (2015) also found a significantly higher level of AP when RP was combined with PSB, compared with other treatments. The PSB acidify soil by producing organic acids, which increases the solubility of P from RP (Yadav et al., 2015). In addition, PSB increases alkaline phosphomonoesterases activity to increase the solubility of P (Prabhu et al., 2018). In this study, the addition of PSB significantly affected soil enzyme activity. This result may have been related to the number and diversity of soil microorganisms, and that the metabolic activity of microorganisms can enhance soil enzyme activity. The secretion of organic acids and an increase in the root exudates can also increase soil enzyme activity. This result is consistent with that of Balota and Chaves (2010) who found that increases in soil enzyme activity are related to PGPR inoculation.

Soil microorganisms are critical to ecosystem functions and the maintenance of soil fertility. However, in saline soils, microbial populations are often restricted by nutrient deficiencies. Plant growth-promoting rhizobacteria (PGPR) are exogenous bacteria, and inoculation with PGPR can greatly affect existing soil microbial communities

TABLE 6 | Pearson's coefficients of correlation (*r*) between the 10 most abundant phyla of soil bacteria and soil chemical properties and enzyme activities.

Phylum	pH	EC	AN	AP	AK	PP	UR	DHA
		(μs/cm)	(mg/g)	(mg/g)	(mg/g)	(IU/L)	(IU/L)	(IU/L)
Proteobacteria	0.26	0.29	**–0.54**	−0.05	0.16	0.35	0.13	−0.07
Actinobacteria	0.21	0.30	−0.15	−0.13	−0.03	−0.21	0.04	0.13
Acidobacteria	−0.37	−0.38	**0.66**	0.21	−0.09	−0.16	−0.08	0.04
Bacteroidetes	−0.16	0.10	−0.28	0.23	0.32	0.45	0.22	0.29
Chloroflexi	−0.16	−0.33	**0.46**	−0.04	−0.22	−0.39	−0.14	−0.07
Firmicutes	**0.71**	0.19	−0.44	**–0.63**	**–0.54**	−0.47	−0.47	−0.63
Planctomycetes	−0.67	**–0.57**	**0.75**	0.47	0.22	0.15	0.08	0.25
Gemmatimonadetes	0.09	0.08	−0.03	−0.08	−0.15	−0.03	−0.05	−0.15
Thaumarchaeota	−0.07	−0.32	0.35	−0.13	−0.28	−0.40	−0.31	−0.16
Thermomicrobia	0	−0.16	0.31	−0.17	−0.26	−0.44	−0.19	−0.14

EC, electrical conductivity; AN, available nitrogen; AP, available phosphorus; AK, available potassium; PP, alkaline phosphomonoesterases activity; UR, urease activity; DHA, dehydrogenase activity.
Bold type indicates a significant correlation ($p < 0.01$).

(Jeong et al., 2013; Bharti et al., 2015; Sheridan et al., 2017). In this study, PSB inoculation strongly increased the α-diversity of bacterial communities. Such enrichment has been attributed to increased dissolution of chemical substrates with bio-inoculation, because released nutrients are then used by resident populations to promote their growth (Bharti et al., 2015). However, the distribution of sequences demonstrated that each rhizosphere bacterial community was unique, indicating that PSB inoculation stimulated the growth of additional bacterial taxa. In this study, the phyla *Proteobacteria*, *Acidobacteria*, *Actinobacteria*, *Chloroflexi*, *Bacteroidetes*, *Planctomycetes*, and *Gemmatimonadetes* dominated bacterial communities. Li et al. (2016) also found that most of these bacterial phyla were dominant in saline soils. However, the structure of rhizosphere-associated bacterial communities was different among treatments in this study. The application of RP and inoculation with PSB, as well as their interaction, were responsible for the differences. These results are consistent with those of Silva et al. (2017) who found an increase in bacterial communities in soils with long-term RP fertilization. Bacterial community structure was different between treatments with and without PSB inoculation. The differences might be because PSB inoculation was the major factor in determining the structure of bacterial communities in the saline soil. *Acidobacteria*, *Chloroflexi*, and *Planctomycetes* were most affected by treatment and were the dominant bacterial phyla in the combined RP and PSB treatment ($P < 0.05$). In addition, the three phyla were significantly positively correlated with root dry weight. Thus, the inoculation of PSB combined with RP favored the establishment of three dominant bacterial phyla and further promoted peanut growth. The phylum *Acidobacteria* is important in nutrient turnover and is also highly involved in rhizosphere physiological processes. In addition, the abundance of the *Planctomycetes* increases strongly following additions of inorganic P (Ganzert et al., 2011).

Luo et al. (2017) analyzed the functional genes and bacterial community structures associated with the P cycle and found that bacteria with the alkaline phosphomonoesterases gene *phoD* in soil are mainly composed of *Actinobacteria* and *Proteobacteria*. In this study, *Actinobacteria* were enriched after inoculation with PSB, which could lead to increases in alkaline phosphomonoesterases activity and thereby increase the availability of P in the saline soil. All the above results showed that the amendments affected the abundance and diversity of bacterial communities The application of PSB significantly increased the abundance of bacteria associated with soil nutrient cycling processes, which ultimately affects the health of saline soil.

CONCLUSION

In this study, halotolerant PSB (*Providencia rettgeri* strain TPM23) and RP effectively alleviated salt stress in peanut in saline soil. A strong synergistic effect was found between PSB inoculation and RP amendment for promoting plant growth and soil quality as well as microbial community diversity. The application of PSB significantly increased the populations of *Acidobacteria*, *Chloroflexi*, and *Planctomycetes*, which are phyla involved in nutrient cycling processes that could ultimately affect the health of the saline soil. Therefore, the combination of PSB and RP might be a low-cost and environmentally safe alternative strategy to remediate the problem of low nutrient availability in saline soils.

DATA AVAILABILITY STATEMENT

The datasets presented in this study can be found in online repositories. The names of the repository/repositories and accession number(s) can be found below: https://www.ncbi.nlm.nih.gov/genbank/, KX834965.

AUTHOR CONTRIBUTIONS

HJ and PQ designed the research. HJ and TW performed the experiment and data analysis. HJ wrote the manuscript. GC and SL participated in data download, manuscript revision, and document proofreading. XC guided the research. All the authors had read, edited and approved the final manuscript.

FUNDING

This study was supported by the Guangdong Province Undergraduate Training Program for Innovation and Entrepreneurship (S202010580048, S202110580049, and S202110580050), the Zhaoqing University Project (190060, 2020012526, and 2021011561), Science and Technology Program of Zhaoqing (2020SN015), and the China Agriculture Research System (CARS-14 to XC).

ACKNOWLEDGMENTS

We thank LetPub (www.letpub.com) for linguistic assistance and pre-submission expert review.

REFERENCES

Adnan, M., Fahad, S., Zamin, M., Shah, S., Mian, I. A., Danish, S., et al. (2020). Coupling phosphate-solubilizing bacteria with phosphorus supplements improve maize phosphorus acquisition and growth under lime induced salinity stress. *Plants* 9:900. doi: 10.3390/plants9070900

Adnan, M., Shah, Z., Fahad, S., Arif, M., Alam, M., Khan, I. A., et al. (2017). Phosphate-solubilizing bacteria nullify the antagonistic effect of soil calcification on bioavailability of phosphorus in alkaline soils. *Sci. Rep.* 7:16131.

Ait Barka, E., Nowak, J., and Clément, C. (2006). Enhancement of chilling resistance of inoculated grapevine plantlets with a plant growth-promoting rhizobacterium, *Burkholderia phytofirmans* strain PsJN. *Appl. Environ. Microbiol.* 72, 7246–7252. doi: 10.1128/AEM.01047-06

Arora, S. (2016). "Microbial approach for remediation and health management of salt affected soils," in *Natural Resource Management in Arid and Semi-Arid*

Ecosystem for Climate Resilient Agriculture, eds N. K. Pareek and S. Arora (New Delhi: Soil Conservation Society of India), 31–40.

Baig, K. S., Arshad, M., Zahir, Z. A., and Cheema, M. A. (2010). Short communication comparative efficacy of qualitative and quantitative methods for rock phosphate solubilization with phosphate solubilizing rhizobacteria. *Soil Environ.* 29, 82–86.

Balota, E. L., and Chaves, J. C. D. (2010). Enzymatic activity and mineralization of carbon and nitrogen in soil cultivated with coffee and green manures. *Rev. Bras. Ciênc. Solo* 34, 1573–1583. doi: 10.1590/s0100-06832010000500010

Bharti, N., Barnawal, D., Maji, D., and Kalra, A. (2015). Halotolerant PGPRs prevent major shifts in indigenous microbial community structure under salinity stress. *Microb. Ecol.* 70, 196–208. doi: 10.1007/s00248-014-0557-4

Bharti, N., Barnawal, D., Wasnik, K., Tewari, S. K., and Kalra, A. (2016). Co-inoculation of *Dietzia natronolimnaea* and *Glomus intraradices* with vermicompost positively influences *Ocimum basilicum* growth and resident microbial community structure in salt affected low fertility soils. *Appl. Soil Ecol.* 100, 211–225.

Chang, C., and Yang, S. (2009). Thermo-tolerant phosphate-solubilizing microbes for multi-functional biofertilizer preparation. *Bioresour. Technol.* 100, 1648–1658. doi: 10.1016/j.biortech.2008.09.009

Chen, L., Ramsier, C., Bigham, J., Slater, B., Kost, D., Lee, Y. B., et al. (2009). Oxidation of FGD-$CaSO_3$ and effect on soil chemical properties when applied to the soil surface. *Fuel* 88, 1167–1172. doi: 10.1016/j.fuel.2008.07.015

Da Costa, E. M., de Lima, W., Oliveira-Longatti, S. M., and de Souza, F. M. (2015). Phosphate-solubilising bacteria enhance *Oryza sativa* growth and nutrient accumulation in an oxisol fertilized with rock phosphate. *Ecol. Eng.* 83, 380–385. doi: 10.1016/j.ecoleng.2015.06.045

Estrada, G. A., Baldani, V. L. D., de Oliveira, D. M., Urquiaga, S., and Baldani, J. I. (2013). Selection of phosphate-solubilizing diazotrophic *Herbaspirillum* and *Burkholderia* strains and their effect on rice crop yield and nutrient uptake. *Plant Soil* 369, 115–129. doi: 10.1007/s11104-012-1550-7

Ganzert, L., Lipski, A., Hubberten, H., and Wagner, D. (2011). The impact of different soil parameters on the community structure of dominant bacteria from nine different soils located on Livingston Island, South Shetland Archipelago, Antarctica. *FEMS Microbiol. Ecol.* 76, 476–491. doi: 10.1111/j.1574-6941.2011.01068.x

García-Orenes, F., Guerrero, C., Roldán, A., Mataix-Solera, J., Cerdà, A., Campoy, M., et al. (2010). Soil microbial biomass and activity under different agricultural management systems in a semiarid Mediterranean agroecosystem. *Soil Tillage Res.* 109, 110–115.

Ghosh, R., Barman, S., Mukherjee, R., and Mandal, N. C. (2016). Role of phosphate solubilizing *Burkholderia* spp. for successful colonization and growth promotion of *Lycopodium cernuum* L. (Lycopodiaceae) in lateritic belt of Birbhum district of West Bengal, India. *Microbiol. Res.* 183, 80–91. doi: 10.1016/j.micres.2015.11.011

Gurdeep, K., and Reddy, M. S. (2015). Effects of phosphate-solubilizing bacteria, rock phosphate and chemical fertilizers on maize-wheat cropping cycle and economics. *Pedosphere* 25, 428–437.

Iqbal, A., Song, M., Shah, Z., Alamzeb, M., and Iqbal, M. (2019). Integrated use of plant residues, phosphorus and beneficial microbes improve hybrid maize productivity in semiarid climates. *Acta Ecol. Sin.* 39, 348–355. doi: 10.1016/j.chnaes.2018.09.005

Jeong, S., Moon, H. S., Shin, D., and Nam, K. (2013). Survival of introduced phosphate-solubilizing bacteria (PSB) and their impact on microbial community structure during the phytoextraction of Cd-contaminated soil. *J. Hazard. Mater.* 263, 441–449. doi: 10.1016/j.jhazmat.2013.09.062

Jiang, H., Qi, P., Wang, T., Chi, X., Wang, M., Chen, M., et al. (2019). Role of halotolerant phosphate-solubilising bacteria on growth promotion of peanut (*Arachis hypogaea*) under saline soil. *Ann. Appl. Biol.* 174, 20–30.

Khosravi, A., Zarei, M., and Ronaghi, A. (2018). Effect of PGPR, phosphate sources and vermicompost on growth and nutrients uptake by lettuce in a calcareous soil. *J. Plant Nutr.* 41, 80–89.

Lebron, I., Suarez, D. L., and Yoshida, T. (2002). Gypsum effect on the aggregate size and geometry of three sodic soils under reclamation. *Soil Sci. Soc. Am. J.* 66, 92–98.

Li, X., Rui, J., Mao, Y., Yannarell, A., and Mackie, R. (2014). Dynamics of the bacterial community structure in the rhizosphere of a maize cultivar. *Soil Biol. Biochem.* 68, 392–401. doi: 10.1016/j.soilbio.2013.10.017

Li, X., Sun, M., Zhang, H., Xu, N., and Sun, G. (2016). Use of mulberry–soybean intercropping in salt–alkali soil impacts the diversity of the soil bacterial community. *Microb. Biotechnol.* 9, 293–304. doi: 10.1111/1751-7915.12342

Ludueña, L. M., Anzuay, M. S., Angelini, J. G., McIntosh, M., Becker, A., Rupp, O., et al. (2018). *Strain Serratia* sp. S119: a potential biofertilizer for peanut and maize and a model bacterium to study phosphate solubilization mechanisms. *Appl. Soil Ecol.* 126, 107–112.

Luo, G., Ling, N., Nannipieri, P., Chen, H., Raza, W., Wang, M., et al. (2017). Long-term fertilisation regimes affect the composition of the alkaline phosphomonoesterase encoding microbial community of a vertisol and its derivative soil fractions. *Biol. Fertil. Soils* 53, 375–388. doi: 10.1007/s00374-017-1183-3

Mahanta, D., Rai, R. K., Dhar, S., Varghese, E., Raja, A., and Purakayastha, T. J. (2018). Modification of root properties with phosphate solubilizing bacteria and arbuscular mycorrhiza to reduce rock phosphate application in soybean-wheat cropping system. *Ecol. Eng.* 111, 31–43. doi: 10.1016/j.ecoleng.2017.11.008

Mulvaney, R. L., and Khan, S. A. (2001). Diffusion methods to determine different forms of nitrogen in soil hydrolysates. *Soil Sci. Soc. Am. J.* 65, 1284–1292. doi: 10.2136/sssaj2001.6541284x

Murphy, J., and Riley, J. P. (1962). A modified single solution method for the determination of phosphate in natural waters. *Anal. Chim. Acta* 27, 31–36. doi: 10.1021/ja038277x

Park, K., Lee, O., Jung, H., Jeong, J., Jeon, Y., Hwang, D., et al. (2010). Rapid solubilization of insoluble phosphate by a novel environmental stress-tolerant *Burkholderia vietnamiensis* M6 isolated from ginseng rhizospheric soil. *Appl. Microbiol. Biotechnol.* 86, 947–955. doi: 10.1007/s00253-009-2388-7

Patel, D., and Saraf, M. (2013). Influence of soil ameliorants and microflora on induction of antioxidant enzymes and growth promotion of *Jatropha curcas* L. under saline condition. *Eur. J. Soil Biol.* 55, 47–54. doi: 10.1016/j.ejsobi.2012.12.004

Prabhu, N., Borkar, S., and Garg, S. (2018). Phosphate solubilization mechanisms in alkaliphilic bacterium *Bacillus marisflavi* FA7. *Curr. Sci.* 114, 845–853. doi: 10.18520/cs/v114/i04/845-853

Radhakrishnan, R., Khan, A. L., Kang, S. M., and Lee, I. (2015). A comparative study of phosphate solubilization and the host plant growth promotion ability of *Fusarium verticillioides* RK01 and *Humicola* sp. KNU01 under salt stress. *Ann. Microbiol.* 65, 585–593. doi: 10.1007/s13213-014-0894-z

Ramadoss, D., Lakkineni, V. K., Bose, P., Ali, S., and Annapurna, K. (2013). Mitigation of salt stress in wheat seedlings by halotolerant bacteria isolated from saline habitats. *SpringerPlus* 2:6. doi: 10.1186/2193-1801-2-6

Rfaki, A., Zennouhi, O., Aliyat, F. Z., Nassiri, L., and Ibijbijen, J. (2020). Isolation, selection and characterization of root-associated rock phosphate solubilizing bacteria in moroccan wheat (*Triticum aestivum* L.). *Geomicrobiol. J.* 37, 230–241.

Ribeiro, C. M., and Cardoso, E. J. B. N. (2012). Isolation, selection and characterization of root-associated growth promoting bacteria in Brazil Pine (*Araucaria angustifolia*). *Microbiol. Res.* 167, 69–78. doi: 10.1016/j.micres.2011.03.003

Shahzad, S. M., Arif, M. S., Riaz, M., Ashraf, M., Yasmeen, T., Zaheer, A., et al. (2017). Interaction of compost additives with phosphate solubilizing rhizobacteria improved maize production and soil biochemical properties under dryland agriculture. *Soil Tillage Res.* 174, 70–80.

Sharma, S., Kulkarni, J., and Jha, B. (2016). Halotolerant rhizobacteria promote growth and enhance salinity tolerance in peanut. *Front. Microbiol.* 7:1600. doi: 10.3389/fmicb.2016.01600

Sheridan, C., Depuydt, P., De Ro, M., Petit, C., Van Gysegem, E., Delaere, P., et al. (2017). Microbial community dynamics and response to plant growth-promoting microorganisms in the rhizosphere of four common food crops cultivated in hydroponics. *Microb. Ecol.* 73, 378–393. doi: 10.1007/s00248-016-0855-0

Shrivastava, P., and Kumar, R. (2015). Soil salinity: a serious environmental issue and plant growth promoting bacteria as one of the tools for its alleviation. *Saudi J. Biol. Sci.* 22, 123–131. doi: 10.1016/j.sjbs.2014.12.001

Shukla, P. S., Agarwal, P. K., and Jha, B. (2012). Improved salinity tolerance of *Arachis hypogaea* (L.) by the interaction of halotolerant plant-growth-promoting rhizobacteria. *J. Plant Growth Regul.* 31, 195–206. doi: 10.1007/s00344-011-9231-y

Silva, U. C., Medeiros, J. D., Leite, L. R., Morais, D. K., Cuadros-Orellana, S., Oliveira, C. A., et al. (2017). Long-term rock phosphate fertilization impacts the microbial communities of maize rhizosphere. *Front. Microbiol.* 8:1266. doi: 10.3389/fmicb.2017.01266

Singh, H., and Reddy, M. S. (2011). Effect of inoculation with phosphate solubilizing fungus on growth and nutrient uptake of wheat and maize plants fertilized with rock phosphate in alkaline soils. *Eur. J. Soil Biol.* 47, 30–34. doi: 10.1016/j.ejsobi.2010.10.005

Song, J., Min, L., Wu, J., He, Q., Chen, F., and Wang, Y. (2021). Response of the microbial community to phosphate-solubilizing bacterial inoculants on *Ulmus chenmoui Cheng* in Eastern China. *PLoS One* 16:e247309. doi: 10.1371/journal.pone.0247309

Taktek, S., St-Arnaud, M., Piché, Y., Fortin, J. A., and Antoun, H. (2017). Igneous phosphate rock solubilization by biofilm-forming mycorrhizobacteria and hyphobacteria associated with *Rhizoglomus irregulare* DAOM 197198. *Mycorrhiza* 27, 13–22. doi: 10.1007/s00572-016-0726-z

Tchakounté, G. V. T., Berger, B., Patz, S., Becker, M., Fankem, H., Taffouo, V. D., et al. (2020). Selected rhizosphere bacteria help tomato plants cope with combined phosphorus and salt stresses. *Microorganisms* 8:1844. doi: 10.3390/microorganisms8111844

van der Heijden, M. G., and Wagg, C. (2013). Soil microbial diversity and agro-ecosystem functioning. *Plant Soil* 363, 1–5.

Vassilev, N., Vassileva, M., and Nikolaeva, I. (2006). Simultaneous P-solubilizing and biocontrol activity of microorganisms: potentials and future trends. *Appl. Microbiol. Biotechnol.* 71, 137–144. doi: 10.1007/s00253-006-0380-z

Wan, W., Qin, Y., Wu, H., Zuo, W., He, H., Tan, J., et al. (2020). Isolation and characterization of phosphorus solubilizing bacteria with multiple phosphorus sources utilizing capability and their potential for lead immobilization in soil. *Front. Microbiol.* 11:752. doi: 10.3389/fmicb.2020.00752

Wei, Y., Zhao, Y., Shi, M., Cao, Z., Lu, Q., Yang, T., et al. (2018). Effect of organic acids production and bacterial community on the possible mechanism of phosphorus solubilization during composting with enriched phosphate-solubilizing bacteria inoculation. *Bioresour. Technol.* 247, 190–199. doi: 10.1016/j.biortech.2017.09.092

Xiao, C., Chi, R., Li, X., Xia, M., and Xia, Z. (2011). Biosolubilization of rock phosphate by three stress-tolerant fungal strains. *Appl. Biochem. Biotechnol.* 165, 719–727. doi: 10.1007/s12010-011-9290-3

Yadav, H., Fatima, R., Sharma, A., and Mathur, S. (2017). Enhancement of applicability of rock phosphate in alkaline soils by organic compost. *Appl. Soil Ecol.* 113, 80–85. doi: 10.7717/peerj.11452

Yadav, H., Gothwal, R. K., Mathur, S., and Ghosh, P. (2015). Bioactivation of Jhamarkotra rock phosphate by a thermotolerant phosphate-solubilizing bacterium *Bacillus* sp. BISR-HY63 isolated from phosphate mines. *Arch. Agron. Soil Sci.* 61, 1125–1135. doi: 10.1080/03650340.2014.980239

Yadav, J., Verma, J. P., Jaiswal, D. K., and Kumar, A. (2014). Evaluation of PGPR and different concentration of phosphorus level on plant growth, yield and nutrient content of rice (*Oryza sativa*). *Ecol. Eng.* 62, 123–128. doi: 10.1016/j.ecoleng.2013.10.013

Yang, P. X., Li, M. A., Ming-Hui, C., Jia-Qin, X. I., Feng, H. E., Chang-Qun, D., et al. (2012). Phosphate solubilizing ability and phylogenetic diversity of bacteria from P-rich soils around Dianchi Lake drainage area of China. *Pedosphere* 22, 707–716. doi: 10.1016/s1002-0160(12)60056-3

Yu, X., Liu, X., Zhu, T. H., Liu, G. H., and Mao, C. (2011). Isolation and characterization of phosphate-solubilizing bacteria from walnut and their effect on growth and phosphorus mobilization. *Biol. Fertil. Soils* 47, 437–446. doi: 10.1007/s00374-011-0548-2

Conflict of Interest: The authors declare that the research was conducted in the absence of any commercial or financial relationships that could be construed as a potential conflict of interest.

Publisher's Note: All claims expressed in this article are solely those of the authors and do not necessarily represent those of their affiliated organizations, or those of the publisher, the editors and the reviewers. Any product that may be evaluated in this article, or claim that may be made by its manufacturer, is not guaranteed or endorsed by the publisher.

frontiers in Microbiology

ORIGINAL RESEARCH
published: 04 January 2022
doi: 10.3389/fmicb.2021.783925

Functional Investigation of Plant Growth Promoting Rhizobacterial Communities in Sugarcane

Mingjia Li[1†], Ran Liu[1†], Yanjun Li[1], Cunhu Wang[1], Wenjing Ma[1], Lei Zheng[1], Kefei Zhang[1], Xing Fu[1], Xinxin Li[1], Yachun Su[2], Guoqiang Huang[2], Yongjia Zhong[1] and Hong Liao[1]*

[1] Root Biology Center, Fujian Agriculture and Forestry University, Fuzhou, China, [2] National Engineering Research Center of Sugarcane, Fujian Agriculture and Forestry University, Fuzhou, China

Plant microbiota are of great importance for host nutrition and health. As a C_4 plant species with a high carbon fixation capacity, sugarcane also associates with beneficial microbes, though mechanisms underlying sugarcane root-associated community development remain unclear. Here, we identify microbes that are specifically enriched around sugarcane roots and report results of functional testing of potentially beneficial microbes propagating with sugarcane plants. First, we analyzed recruitment of microbes through analysis of 16S rDNA enrichment in greenhouse cultured sugarcane seedlings growing in field soil. Then, plant-associated microbes were isolated and assayed for beneficial activity, first in greenhouse experiments, followed by field trials for selected microbial strains. The promising beneficial microbe SRB-109, which quickly colonized both roots and shoots of sugarcane plants, significantly promoted sugarcane growth in field trials, nitrogen and potassium acquisition increasing by 35.68 and 28.35%, respectively. Taken together, this report demonstrates successful identification and utilization of beneficial plant-associated microbes in sugarcane production. Further development might facilitate incorporation of such growth-promoting microbial applications in large-scale sugarcane production, which may not only increase yields but also reduce fertilizer costs and runoff.

Keywords: sugarcane, root-associated microbes, beneficial function, nitrogen, growth promotion

OPEN ACCESS

Edited by:
Ying Ma,
University of Coimbra, Portugal

Reviewed by:
José David Flores Félix,
Universidade da Beira Interior, Portugal
Monali C. Rahalkar,
Agharkar Research Institute, India

****Correspondence:***
Yongjia Zhong
Yongjiazhong@fafu.edu.cn

† These authors have contributed equally to this work and share first authorship

Specialty section:
This article was submitted to Microbe and Virus Interactions with Plants, a section of the journal Frontiers in Microbiology

Received: *27 September 2021*
Accepted: *30 November 2021*
Published: *04 January 2022*

Citation:
Li M, Liu R, Li Y, Wang C, Ma W, Zheng L, Zhang K, Fu X, Li X, Su Y, Huang G, Zhong Y and Liao H (2022) Functional Investigation of Plant Growth Promoting Rhizobacterial Communities in Sugarcane. Front. Microbiol. 12:783925. doi: 10.3389/fmicb.2021.783925

INTRODUCTION

Plant-associated microbes colonize organs throughout host plants, with distinctive microbial communities forming in the different niches plants present, and the collection of organisms forming a holobiont (Tringe et al., 2005; Hassani et al., 2018). Within this intimate set of associations, plants provide microbes with photosynthates in exchange for a variety of beneficial features from microbes that confer improvements in host fitness across diverse environments (Dong et al., 2018). The composition of host associated microbial communities may act as an important determinant of plant health and yield through impacts on nitrogen fixation, phosphorus solubilization, 3-indoleacetic acid (IAA) production, root growth, and nutrient acquisition efficiency (Beckers et al., 2017; Wang et al., 2021). Recruitment and enrichment of the beneficial members of the plant microbial community are in turn determined by the available pool of soil microbiota, the host plant genotypes, and host plant nutrient status (Mendes et al., 2011; Zhong et al., 2019).

Sugarcane accounts for 90% of the sugar production in China (Li and Yang, 2015), and the byproducts can also be used for biomass energy production and animal husbandry (de Almeida et al., 2018; Vieira et al., 2020). Sugarcane is also a C_4 crop with high photosynthetic efficiency and rapid growth, which requires large amounts of mineral nutrients, especially nitrogen, to support growth and coordinate nutrient homeostasis with carbon fixation capacity (Gopalasundaram et al., 2012; Carvalho et al., 2014; de Oliveira et al., 2016). This has led to excessive nitrogen applications in sugarcane production (Boddey et al., 2003). A tradeoff of excessive nitrogen fertilization is serious environment impacts, including soil acidification, water eutrophication, and air pollution (Guo et al., 2010; Le et al., 2010; Liu et al., 2013). Hence, increasing sugarcane production while simultaneously protecting agroecosystems through more efficient nutrient acquisition and decreased fertilization are interconnected practical objectives for improving sugarcane production (Rosenblueth et al., 2018).

Although sugarcane plants need large amounts of nitrogen during vegetative growth, up to 70% of the total nitrogen required for its growth may be acquired through associated nitrogen fixation (Urquiaga et al., 1992). Multiple years of field trials in Brazil sugarcane production systems have demonstrated that associated nitrogen fixation can yield up to 40 kg/ha/y of nitrogen in these fields (Urquiaga et al., 2012). Hence, nitrogen fertilizer applications for sugarcane production in Brazil are significantly lower than in other countries due to the nitrogen fixation associated with Brazilian sugarcane (Boddey et al., 2003; Urquiaga et al., 2012). To date, nitrogen fixing bacteria isolated from sugarcane include *Beijerinckia* spp., *Azospirillum* spp., *Herbaspirillum* spp., *Gluconacetobacter* spp., *Enterobacter* spp., *Burkholderia* spp., *Klebsiella* spp., and so on (Döbereiner and Day, 1976; Boddey and Döbereiner, 1995; Baldani et al., 1997; Oliveira et al., 2009; Mehnaz, 2013; Carvalho et al., 2014; Lin et al., 2015; Muthukumarasamy et al., 2017; Guo et al., 2020). Beyond nitrogen fixation, plant-associated bacteria may also provide numerous other benefits for host plants (Oliveira et al., 2002; Saravanan et al., 2007; Ahmed and Holmström, 2014; Carvalho et al., 2014).

Over the last two decades, while knowledge of associated nitrogen fixation with sugarcane has greatly improved, most of this work focused on specific nitrogen fixing bacteria and lacked a systematic investigation of sugarcane associated communities (da Silva et al., 2018; Singh et al., 2019). Recently, with the development of high throughput sequencing technology, the structure and activities of sugarcane microbiome components have been gradually revealed (Bertalan et al., 2009; Pedrosa et al., 2011; Sant'Anna et al., 2011; Zhu et al., 2012; de Souza et al., 2016; Yeoh et al., 2016; da Silva et al., 2018; Dong et al., 2018; Schwab et al., 2018). In this study, we decipher the composition of a bacterial community in the root and rhizosphere of sugarcane using 16S rDNA sequencing. Then, potentially beneficial microbes were isolated from sugarcane roots and evaluated for plant growth promotion in both greenhouse pot experiments and a field trial. The results provide significant insights into interactions between sugarcane and root microbiota that may be and further harnessed to utilize beneficial microbes in sugarcane production.

MATERIALS AND METHODS

Sugarcane Growth and Cultivation

In order to investigate microbes specifically recruited from soil and enriched in the roots of commercial sugarcane variety ROC22, seedlings were propagated to the four-leaf stage in MS medium prior to transferring to rooting medium for another 2 weeks (**Supplementary Figure 1**). Transplanted sugarcane seedlings were then acclimatized for another 2 weeks to growth in liquid plant nutrition solution (Li et al., 2015) prior to transplanting into soils collected from a sugarcane farm managed by the Fujian Agriculture and Forestry University. Before planting, soils were filtered to remove larger residues and mixed well with equal volumes of sterile vermiculite, which was heated at 121°C for 40 min before use. Sugarcane seedlings were planted 1 seedling per pot (10 * 10 * 15 cm) in the soil mix described above. A total of 16 pots of sugarcane seedlings were reared in a growth chamber (day/night: 14 h/10 h, 26°C/24°C) under 37.5 $\mu E/m^2/s$ of daylight light intensity for 3 months before harvesting samples. During plant growth, liquid plant nutrient solution was supplied according to plant needs.

Rhizosphere and Root-Associated Microorganism Sampling

To sample the rhizosphere and root-associated microorganisms, sugarcane plants were removed from pots, with loosely attached soil being removed from roots prior to collecting rhizosphere soil firmly attached to the roots. Rhizosphere soils were collected through washing in 100 mL sterile phosphate buffer saline (PBS) solution and centrifugation at 12,000 rpm for 15 min (Bulgarelli et al., 2012, 2015; Zhong et al., 2019). After removing rhizosphere soil, roots were further treated with sonication for 20 min to remove microbes from the root surface (Lundberg et al., 2012), which were collected in three rinses of sterile water (**Supplementary Figure 2**). Each biological replicate of rhizosphere soil and sugarane root sample was collected from four independent sugarcane plants. In total, four biological replicates were collected for each rhizosphere soil and root.

DNA Extraction, Sequencing, and Analysis

Total DNA was extracted from rhizosphere soil and root samples using the PowerSoil DNA extraction kit (Mobio Laboratories, Carlsbad, CA, United States) according to the kit instructions. The DNA concentration was determined using the NanoDrop 1000 (Thermo Scientific, Waltham, EUA). Then, total DNA was subjected to polymerase chain reaction (PCR) (Majorbio Bio-pharm Technology Co., Ltd, Shanghai, China) prior to sequencing PCR fragments using an Illumina Miseq PE300 platform (Illumina, San Diego, CA, United States). Specifically, total DNA was used as PCR templates, and 16S amplicon libraries were generated using the PCR primers 799F (5′-AACMGGATTAGATACCCKG-3′), 1193R (5′-ACGTCATCCCCACCTTCC-3′), and 1392R (5′-ACGGGCGGTGTGTRC-3′), which span approximately 400 bp of the V5–V7 hypervariable regions of the prokaryotic 16S rDNA gene (Bulgarelli et al., 2012, 2015; Lundberg et al., 2012).

The QIIME2 software platform was used for bioinformatics analysis of raw data derived from the Illumina Miseq platform (Bolyen et al., 2019). Specifically, q2-demux and q2-cutadapt trim-pairs were used to remove barcodes and linkers (Martin, 2011) prior to merging paired-end reads in vsearch (Rognes et al., 2016). The quality-filter and deblur plugins in QIIME2 were used to carry out quality control (Quality Score > 25) and denoising, respectively (Amir et al., 2017). OTUs were clustered based on a 97% similarity threshold determined by the q2-feature-classifier using the SILIVA database (Yilmaz et al., 2014). The diversity plugin of QIIME2 was used to calculate the alpha diversity, weight-unifrac distance matrix, and Bray–Curtis distance matrix. The Vegan package (version: 2.5.6) in R (version: 4.0) (R core team) was used to perform ANOSIM (analysis of similarity) analysis. The calculation of *R* and *P*-values and the comparison of differences between groups were carried out by permutation testing with permutational anova, with the number of permutations set to 999. Two-sided Welch's *t*-tests with Benjaminii–Hochberg FDR corrections were conducted in the STAMP software (version: 2.1.3) to identify significant differences between sugarcane associated microbial groups (Parks et al., 2014). The Kruskal–Wallis rank-sum test, with an alpha value of 0.05 and a threshold value of 4.8, was used to test for significant differences between microbial groups using an online LEfSe (linear discriminant analysis effect size) program[1].

Phylogenetic Tree Construction

Sequences of 16S rDNA from isolates and similar sequences of known bacteria in GenBank database with NCBI BLAST program were downloaded and used for phylogenetic trees analysis in MEGA 7.0 (Kumar et al., 2016). ClustalX[2] was used for multiple alignments, and the neighbor-joining method in MEGA 7.0 was employed for genetic tree construction (Saitou and Nei, 1987) with 1000 replicates of bootstrap testing (Felsenstein, 1985). Finally, phylogenetic trees were visualized in iTol V4[3] (Letunic and Bork, 2019) or GraPhlAn (Asnicar et al., 2015).

Sugarcane Root-Associated Microbe Isolation and Identification

Roots of sugarcane plants grown in the pot cultures described above were used for root-associated microbe isolation. After harvesting sugarcane plants, root samples were collected after first shaking off loosely attached bulk soil, followed by removal of rhizosphere soil firmly attached to the roots through washing with 50 mL of sterile PBS solution for 15 min and centrifugation at 7000 rpm for 8 min (Bulgarelli et al., 2012, 2015). Then, 5 g of root tissues was homogenized in 15 mL of sterile PBS using a mortar and pestle in a laminar flow hood. Plant debris was removed by filtration, and the homogenized solution was considered as the collection of root-associated microbes. Homogenized solutions were diluted 1000-fold with sterile PBS. Finally, 100 μL of diluted microbial suspension was plated on a panel of four microbial isolation culture media and incubated at 28°C (Bai et al., 2015; Wang et al., 2021). The panel of isolation media consisted of two nitrogen free culture media, SNX (Hu et al., 2017) and JNFb (Baldani et al., 1992), and two other culture media containing nitrogen, TSB and M715 (Bai et al., 2015). Single colonies were picked out and streaked to new plates for further purification. Then, single colonies were picked once again from these solid medium plates. All collected isolates from root-associated compartments were subsequently stored in 40% glycerol at –80°C.

To identify potentially nitrogen fixing isolates, PCR assays were employed to identify the N_2 fixing marker gene (*NifH*) using the primer pair *NifH-F*: AAAGGYGGWATCGGYAARTCCACCAC and *NifH-R*: TTGTTSGCSGCRTACATSGCCATC AT (RöSch et al., 2002). For the determination of potential phosphate solubilizing capacity, isolates were cultured on Pikovskaya agar plates containing $Ca_3(PO_4)_2$ or phytin as the sole Pi source for 3 days at 28°C. The appearance of a transparent zone around a bacterial colony indicated the phosphate solubilizing capacity. The IAA biosynthesis capacity was measured in a color development assay (Littlewood and Bennett, 2003; Qin et al., 2011). Briefly, isolates were propagated in flasks containing liquid growth media for 3 days at 28°C, followed by centrifugation of 1 mL samples. Cell pellets were washed twice with 1 mL PBS and re-suspended to 10^7 cells/mL prior to mixing 1 mL of cell suspension with 10 mL of liquid medium containing 100 mol/mL of tryptophan. After incubating for 3 days, 50 μL of supernatant was collected and mixed with 50 μL of Salkowski buffer (4.5 g/L $FeCl_3$, 10.8 mol/L H_2SO_4). When the solution turns red, it has the ability to synthesize IAA. The colony morphology of SRB-109 was recorded using stereoscopic microscopy.

Application of Potential Beneficial Microbes in the Fields

For the field application of potentially beneficial microbes. Strains stored at –80°C were melted on ice, streaked on isolation culture medium, and then incubated at 28°C for 5–7 days. Single colonies were then picked off and inoculated in liquid culture medium at 28°C and shaken at 200 rpm until the concentration of bacteria liquid was 1×10^8 CFU/mL. Microbial cells were collected through centrifugation at 7000 rpm for 10 min. After discarding the supernatant, microbial cells were washed three times with low N (200 μM) nutrient solution and finally suspended in low N nutrient solution for later to the concentration of bacteria solution is 5×10^7 CFU/mL.

For sugarcane plant inoculations, seedlings of ROC22 sugarcane were collected at the six-leaf stage from tissue cultures and then immersed in prepared microbial solutions (5×10^7 CFU/mL) for 12 h prior to transplanting into pots filled with sterile substrate and vermiculite in equal proportions. Seedlings were co-cultured with microbial isolates in a growth chamber for 2 weeks, with pots supplied with 20 mL of low N (200 μM) nutrient solution each day (Li et al., 2018). A total of seven pots, with each containing one seedling, were cultivated for each microbial isolate. Control pots contained seedlings that were not inoculated with any microbial isolates. After 2 weeks in a

[1]http://huttenhower.sph.harvard.edu/galaxy/root/index

[2]http://www.clustal.org/

[3]https://itol.embl.de/

growth chamber, sugarcane seedlings were transplanted to the field with 50 cm spacing between plants for further growth; soil nutrient content and pH of field experimentation are shown in **Supplementary Table 1**. After cultivation for 120 days in the field, sugarcane plants were harvested for assessment of plant growth promotion.

Colonization Pattern of SRB-109 on Sugarcane Plants

SRB-109, an isolate from sugarcane roots exhibiting significant growth promotion effects, was selected for further study. To visualize the colonization patterns of SRB-109 on sugarcane plants, SRB-109 was labeled for GUS or red fluorescent protein (RFP) staining with *pMG103-NPTII-GUS* or *pMG103-NPTII-RFP* modified from *pMG103-NPTII-GFP* (Inui et al., 2000) using *Sph* I and *Eco*R I restriction endonuclease sites. Bacteria were labeled by electroporation (Liu S. et al., 2020). Positively transformed bacterial colonies were screened through kanamycin resistance and further identified using GUS staining.

Positively identified GUS labeled bacteria were cultured at 28°C in JNFb liquid medium supplied with 50 μg/mL of kanamycin and shaken at 200 rpm until the concentration of bacteria liquid was 1×10^8 CFU/mL. Bacterial inoculants were prepared through centrifugation at 7000 rpm for 8 min, prior to resuspension in low nitrogen liquid solution to 5×10^7 CFU/mL. Then, 5 mL of prepared inoculum (GUS labeled SRB-109) was added to the liquid nutrient solution of five acclimatized sugarcane plants. After 3 days of co-culturing with GUS labeled microbes, the colonization of SRB-109 throughout various organs of sugarcane plants such as leaves, roots, and whole plants was visualized with GUS staining according to the methods of Li et al. (2015), with the GUS signal being recorded using a stereo microscope (Zeiss Axio Zoom. V16).

Plant Growth Promoting Genes Identification With Polymerase Chain Reaction

To further confirm the plant growth promoting genes in SRB-109, the genome DNA of SRB-109 was used as a template, the primers specific target to the *nifH* (nitrogenase gene) (RöSch et al., 2002), *ACC* (1-aminocyclopropane-1-carboxylic acid deaminase) (Blaha et al., 2006), and *phoD* (Alkaline phosphatase D) (Sakurai et al., 2008).

RESULTS

Structure and Composition of Bacterial Communities Colonizing Root-Associated Compartments of Sugarcane Plants

16S rDNA sequencing spanning the V5–V7 regions was employed to investigate the composition of bacterial communities in the rhizospheres and roots of sugarcane plants. A total of 1,149,659 sequences were thusly obtained. After joining paired-end reads, sequences were subjected to quality control and denoising procedures. This yielded 127,810 high-quality 355 bp length reads. Operational taxonomic unit grouping was obtained through clustering of high-quality sequences at the 97% similarity threshold. Rarefaction curves of observed OTU plateaued after 60% sampling (**Supplementary Figure 3**), suggesting that the sequencing depth for all the samples was enough to cover most of the bacterial in the rhizosphere and root compartments. Bacterial community richness and evenness were significantly higher in the rhizosphere than in the roots, as reflected by the Chao 1 index, the Shannon index, observed numbers of OTU, and the Pielou evenness index (**Supplementary Figure 4**). This result suggests host involvement in determining root bacterial community members. Further structure analysis based on Bray_Curtis and Weighted unifrac tests all showed that bacterial communities in root compartments can be clearly separated from those in the rhizosphere compartment (**Figures 1A,B**). An ANOSIM analysis further showed that bacterial communities in the root compartment were significantly different from those in the rhizosphere (**Figures 1A,B**). All of these results reinforce the notion that roots of sugarcane actively select associated microbial communities.

Microbes Enriched by Sugarcane

To further investigate which microbes were specifically selected by sugarcane roots. Composition analysis at the phylum taxonomic level showed that *Proteobacteria* was the dominant bacteria in roots, with members of this group accounting for about 77.31% of the relative abundance of total bacteria in sugarcane roots (**Figure 1C**). In all, *Proteobacteria* (32.68% of rhizosphere bacteria; 77.31% of root bacterial), *Actinobacteria* (37.91%; 9.31%), *Chloroflexi* (7.88%; 5.02%), and *Firmicutes* (10.77%; 0.97%) were the dominant bacteria in the rhizosphere and root compartments of sugarcane plants. At the class taxonomic level, *Gammaproteobacteria* (47.91%; 14.45%) and *Alphaproteobacteri*a (26.79%; 15.63%) were the dominant bacteria in the root and rhizosphere compartments, respectively (**Figures 1C,D**). In addition, there were 870 OTUs existing in both the rhizosphere and root compartments, while 576 OTU were found exclusively in the root compartment (**Figure 1E**). The phylogenetic relationship of microbes detected through high throughput sequencing suggests that the sum of the sugarcane associated microbial community originated from a variety of phyla (**Figure 1F**).

To further investigate which microbes were significantly enriched by sugarcane, LEfSe analysis was employed. Results showed that *Gammaproteobacteria*, *Alphaproteobacteria*, *Burkholderiaceae*, *Rhizobials,* and *Burkholderia* were all significantly enriched in the root compartment, while *Actinobacteria*, *Intrasporangiaceae*, *Firmicutes,* and *Bacillus* were enriched biomarkers in the rhizosphere compartment (**Figure 2**). Meanwhile, STAMP results were similar to LEfSe results (**Supplementary Figure 5**). Taken together, the observations herein show that *Rhizobials* and *Burkholderia* were significantly enriched in the root compartment and *Bacillus* taxa were mainly enriched in the rhizosphere.

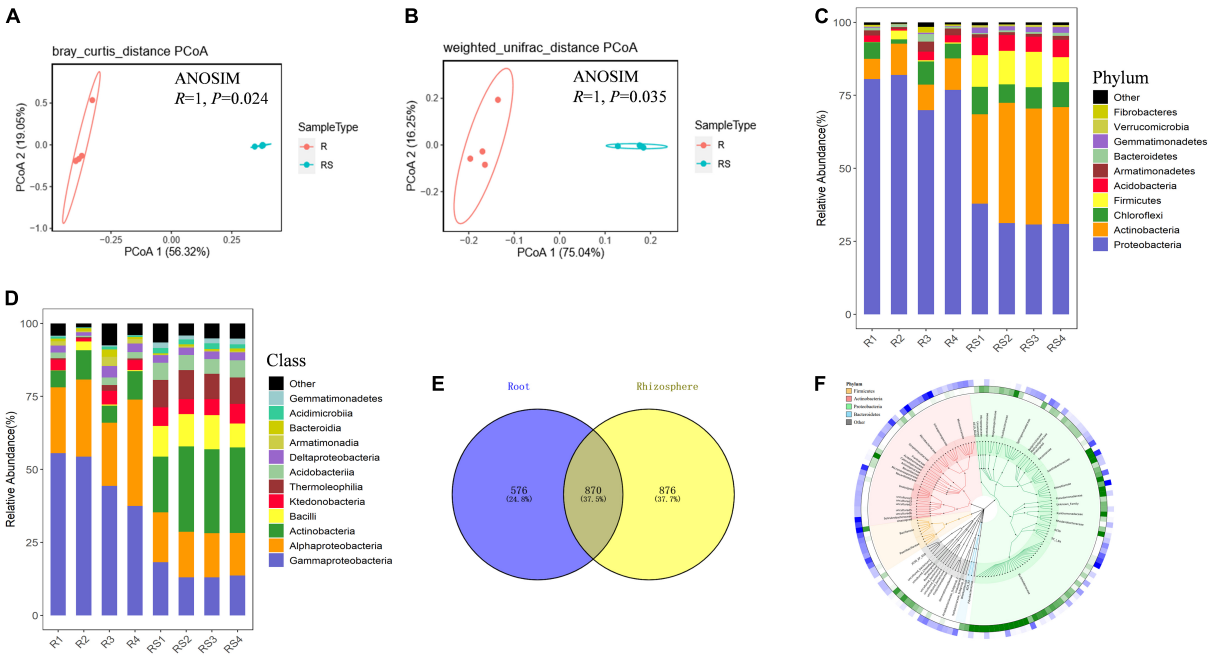

FIGURE 1 | Bacterial communities in the root-associated compartments of sugarcane. Samples were divided into rhizosphere and root samples according to the compartment of origin. Bacterial community composition was determined using 16S rDNA sequencing. Principal coordinates analysis (PCoA) was performed using Bray–Curtis distance **(A)** and weighted-unifrac distance **(B)** based on the OTU table. Analysis of similarity (ANOSIM) was performed based on the OTU tables of R and RS samples to calculate differences. In permutation tests, the number of permutations was 999. The composition of microorganisms was analyzed in the rhizosphere at the phylum level **(C)** and class level **(D)**. R, sugarcane root; RS, sugarcane rhizosphere; OTU, operational taxonomic unit. **(E)** Venn diagram of microbes in the rhizosphere and root compartments of sugarcane. **(F)** Cladogram of top 150 microbes (mean relative abundance) based on taxonomy. OTUs relative abundance of two compartments are shown in the outermost rings of the green and red heat map (root samples as green and rhizosphere samples as blue).

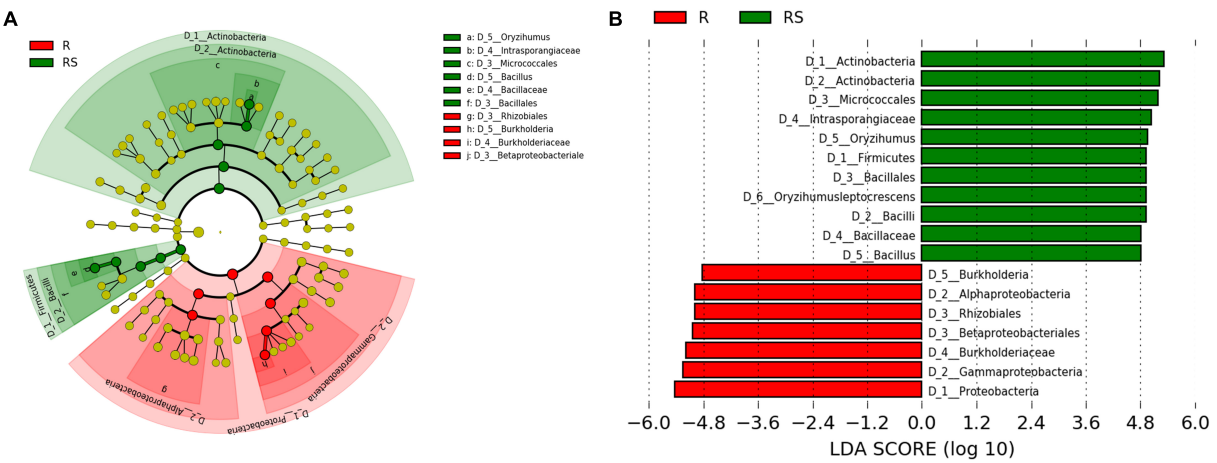

FIGURE 2 | Comparison of bacteria between the rhizosphere and root compartments. **(A)** Phylogenetic dendrogram of biomarkers in the R and RS sugarcane groups. Circles from inside to outside indicate bacterial taxonomic levels from phylum to genus. Yellow dots represent bacteria not significantly varying in abundance among treatments. Biomarker bacteria are colored according to their corresponding class colors on the right. **(B)** LDA scores of biomarker bacteria for each combination of sugarcane sites. LDA scores are shown as horizontal bars for the biomarker bacteria with an LDA score > 4.8 as listed on the left, Kruskal–Wallis rank sum test, $P < 0.05$. LDA, linear discriminant analysis.

Isolation and Identification of Beneficial Microbes in Sugarcane

To isolate microbes enriched within the root compartment of sugarcane plants, four bacterial culture media were employed, including two nitrogen-free and two of nitrogen-rich media. Isolation and purification procedures yielded a total of 519 isolates from sugarcane roots. These strains were tested for potential nitrogen fixation through PCR amplification of *nifH*

genes. Microbes with positive *nifH* gene PCR results were further screened for phosphate-solubilizing capacity and phytohormone IAA production as described in the methods. In these tests, 92 isolates were identified with potential nitrogen fixing capabilities. Among these potential nitrogen fixing members of the sugarcane root flora, 52 returned positive results in one or more of the three other functional assays. Of these, 17 isolates were able to produce IAA, 43 exhibited the capacity of solubilizing inorganic phosphate, and 43 could solubilize organic phosphate. Forty-one potential nitrogen fixing isolates returned positive results in at least two of the IAA production and phosphate solubilizing assays. Ten isolates yielded positive results in all four functional assays (**Figure 3A** and **Table 1**). All 92 of the potentially beneficial isolates were subjected to taxonomic assignments and phylogenetic analysis based on 16S rDNA sequences. These results showed that the 92 potentially beneficial strains were *Actinobacteria* (14.13%), *Bacilli* (28.26%), *Alphaproteobacteria* (10.86%), *Betaproteobacteria* (6.52%), *Gammaproteobacteria* (38.06%), and *Sphingobacteriia* (2.17%) (**Figure 3B** and **Supplementary Table 2**). The taxonomic grouping of these isolates was mostly consistent with the distribution of all dominant bacterial taxa in the root associated compartments of sugarcane plants (**Figure 1F**).

After conducting greenhouse assays of plant-microbe interactions, four isolates (SRB-13, SRB-33, SRB-109, SRB-112) displaying obvious growth promotion capacities were selected as candidate strains for further functional validation in a field experiment (**Supplementary Figure 6**). Phylogenetic analysis showed that the four selected strains were a *Xanthomonas* sp. (SRB-13), a *Staphylococcus* sp. (SRB-33), and 2 *Acinetobacter* sp. (SRB-109 and SRB-112) (**Figure 3B**). Relative to control treated plots, isolate SRB-109 significantly increased plant height by 27.6%, the leaf SPAD value by 11.7%, and the number of tillers by 6 ± 1. The only other isolate to produce significant improvements in sugarcane traits in these trials was SRB-33, which significantly increased plant height by 27.6% and the number of tillers by 7 ± 1 (**Supplementary Figures 8A–C**). No isolate significantly impacted dry weight of individual tillers relative to control tillers (**Figures 4A,B**). Nutrient acquisition relative to control plants was significantly enhanced with SRB-109 treatment by 35.7% for nitrogen and by 28.4% for potassium, but not for phosphorus with this isolate, nor for any nutrients with any of the other three tested isolates (**Figures 4C–E**). Taken together, these results suggest that SRB-109 may be the most promising isolate identified for promoting sugarcane growth and nutrient acquisition.

Colonization Patterns of SRB-109 on Sugarcane Plants

Since SRB-109 exhibited the most promising impacts on sugarcane growth-promotion capacity among tested isolates, this isolate was, therefore, selected for further study of interactions with sugarcane plants. Colony morphology showed SRB-109 with light yellow color, shiny smooth surface, and clear colony edge (**Supplementary Figure 7A**). And the plant growth promoting genes such as *phoD*, *ACC* deaminase and *nifH* (**Supplementary**

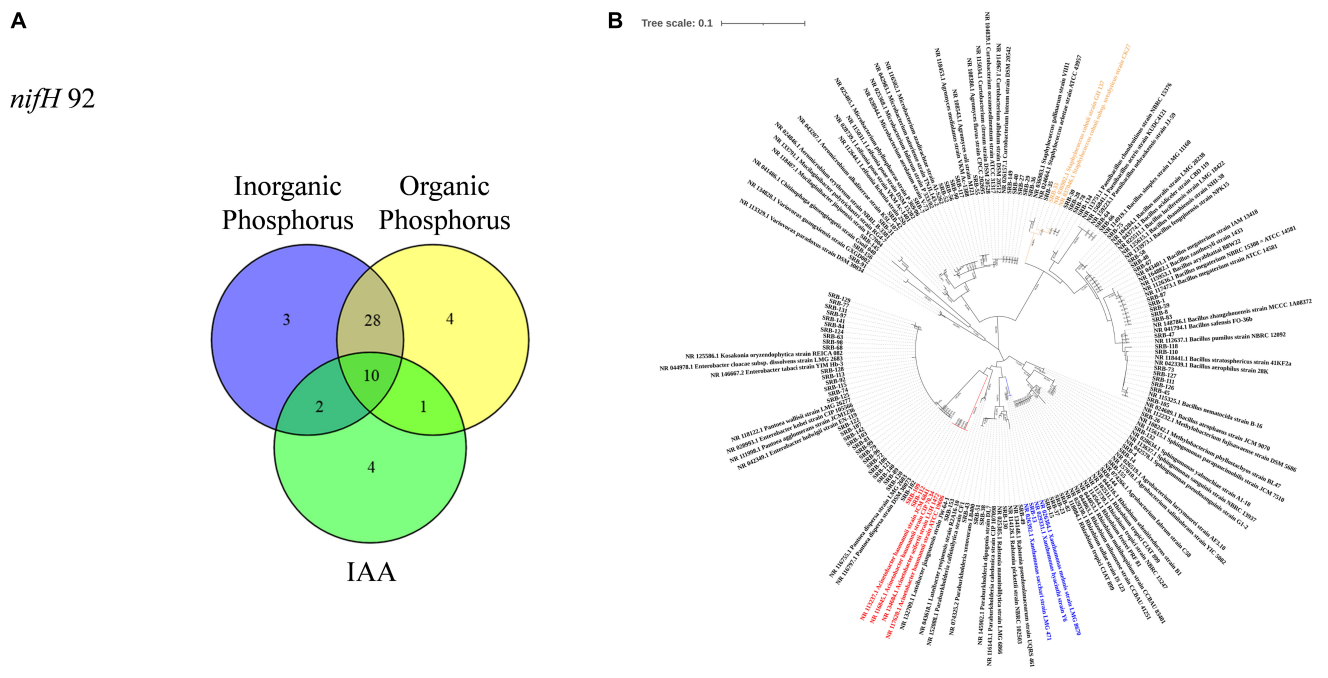

FIGURE 3 | Isolation and identification of microbes from roots of sugarcane. **(A)** Distribution of potentially beneficial functions among isolated root-associated microbes represented in a Venn diagram. **(B)** Phylogenetic tree was constructed using known sequences exhibited similar sequence similarity in GenBank database with NCBI BLAST program. Multiple sequence alignment was done using ClustalX 1.8 software package (http://wwwigbmc.ustrasbg.fr/BioInfo/clustalx), tree was constructed by neighbor-joining method using MEGA 7.0 (Kumar et al., 2016).

TABLE 1 | 16S rDNA sequence and functional characteristics of nitrogen-fixing bacteria in sugarcane roots.

Strain	Genus	Nitrogenase activity	IAA production	Inorganic phosphate solubilization	Organic solubilization
SRB-1	*Bacillus* sp.				
SRB-4	*Sphingomonas* sp.	+			
SRB-7	*Microbacterium* sp.				
SRB-8	*Bacillus* sp.				
SRB-13	*Xanthomonas* sp.		+	+	
SRB-14	*Sphingomonas* sp.				
SRB-15	*Rhizobium* sp.				
SRB-23	*Rhizobium* sp.				
SRB-26	*Methylobacterium* sp.				
SRB-27	*Curtobacterium* sp.				+
SRB-28	*Staphylococcus* sp.				
SRB-29	*Curtobacterium* sp.		+		
SRB-30	*Staphylococcus* sp.				
SRB-31	*Aeromicrobium* sp.				
SRB-33	*Staphylococcus* sp.	+			+
SRB-35	*Staphylococcus* sp.				
SRB-36	*Curtobacterium* sp.				
SRB-37	*Rhizobium* sp.		+		
SRB-38	*Paraburkholderia* sp.	+			
SRB-40	*Curtobacterium* sp.				
SRB-42	*Leifsonia* sp.				
SRB-43	*Paraburkholderia* sp.				
SRB-45	*Bacillus* sp.				
SRB-47	*Bacillus* sp.				
SRB-48	*Bacillus* sp.			+	
SRB-49	*Cupriavidus* sp.		+		+
SRB-51	*Paraburkholderia* sp.				
SRB-52	*Microbacterium* sp.				
SRB-55	*Agromyces* sp.				
SRB-56	*Microbacterium* sp.				
SRB-58	*Bacillus* sp.				
SRB-59	*Bacillus* sp.			+	+
SRB-63	*Enterobacter* sp.			+	
SRB-64	*Paenibacillus* sp.				
SRB-66	*Paenibacillus* sp.			+	+
SRB-67	*Bacillus* sp.				
SRB-68	*Enterobacter* sp.		+	+	+
SRB-72	*Enterobacter* sp.		+	+	+
SRB-73	*Bacillus* sp.				
SRB-74	*Enterobacter* sp.			+	+
SRB-75	*Brevibacterium* sp.				
SRB-77	*Enterobacter* sp.		+	+	+
SRB-78	*Paenibacillus* sp.		+	+	+
SRB-79	*Enterobacter* sp.		+	+	+
SRB-81	*Enterobacter* sp.		+	+	+
SRB-82	*Rhizobium* sp.		+	+	+
SRB-83	*Bacillus* sp.		+		
SRB-84	*Enterobacter* sp.		+	+	+
SRB-87	*Bacillus* sp.				
SRB-89	*Pantoea* sp.				
SRB-90	*Microbacterium* sp.				+
SRB-91	*Variovorax* sp.				

(Continued)

TABLE 1 | (Continued)

Strain	Genus	Nitrogenase activity	IAA production	Inorganic phosphate solubilization	Organic solubilization
SRB-92	*Enterobacter* sp.		+	+	+
SRB-96	*Enterobacter* sp.		+	+	+
SRB-97	*Enterobacter* sp.			+	+
SRB-98	*Enterobacter* sp.			+	+
SRB-99	*Enterobacter* sp.			+	+
SRB-102	*Acinetobacter* sp.			+	+
SRB-103	*Enterobacter* sp.			+	+
SRB-105	*Bacillus* sp.			+	+
SRB-106	*Pantoea* sp.			+	+
SRB-107	*Enterobacter* sp.			+	
SRB-109	*Acinetobacter* sp.	+		+	+
SRB-110	*Bacillus* sp.				
SRB-111	*Bacillus* sp.				
SRB-112	*Acinetobacter* sp.	+		+	+
SRB-113	*Enterobacter* sp.			+	+
SRB-115	*Enterobacter* sp.			+	+
SRB-117	*Microbacterium* sp.			+	+
SRB-118	*Bacillus* sp.				
SRB-120	*Pantoea* sp.				
SRB-121	*Pantoea* sp.			+	+
SRB-122	*Enterobacter* sp.			+	+
SRB-124	*Enterobacter* sp.			+	+
SRB-125	*Enterobacter* sp.			+	+
SRB-126	*Bacillus* sp.				
SRB-127	*Bacillus* sp.				
SRB-128	*Enterobacter* sp.			+	+
SRB-129	*Enterobacter* sp.			+	+
SRB-130	*Ralstonia* sp.			+	+
SRB-131	*Enterobacter* sp.			+	+
SRB-132	*Sphingomonas* sp.				
SRB-134	*Paenibacillus* sp.				
SRB-140	*Pantoea* sp.			+	+
SRB-141	*Enterobacter* sp.			+	+
SRB-142	*Enterobacter* sp.			+	+
SRB-144	*Shinella* sp.	+			+
SRB-145	*Mucilaginibacter* sp.			+	+
SRB-149	*Curtobacterium* sp.			+	+
SRB-153	*Luteibacter* sp.		+	+	
SRB-155	*Agrobacterium* sp.		+		
SRB-156	*Chitinophaga* sp.				

Figure 7B). Taxonomic identification using 16S rDNA showed that SRB-109 is an *Acinetobacter* sp. (**Figure 3B**). This isolate not only possesses a *NifH* gene but also exhibits the capacity to solubilize both inorganic and organic forms of normally insoluble phosphate (**Table 1**). Further investigation of SRB-109 colonization patterns using the labeled GUS and RFP reporter gene (**Supplementary Figure 9**) showed that 3 days after SRB-109/*pMG103-NPTII-GUS* inoculation, an obvious blue signal was detectable on the different tissues of roots, including root tips and root hairs, suggesting that SRB-109 could quickly colonize roots of sugarcane (**Figures 5A–C**), which was further confirmed by RFP labeled SRB-109 and visualized with confocal microscopy (**Figures 5K,L**). At the same time, the blue signal of GUS staining was also observed in sugarcane leaves, which suggests that SRB-109 may also colonize the aboveground parts of sugarcane plants (**Figures 5D–J**).

DISCUSSION

Plant-associated microbiota are essential for proper host plant growth and health (Niu et al., 2017). During the long history

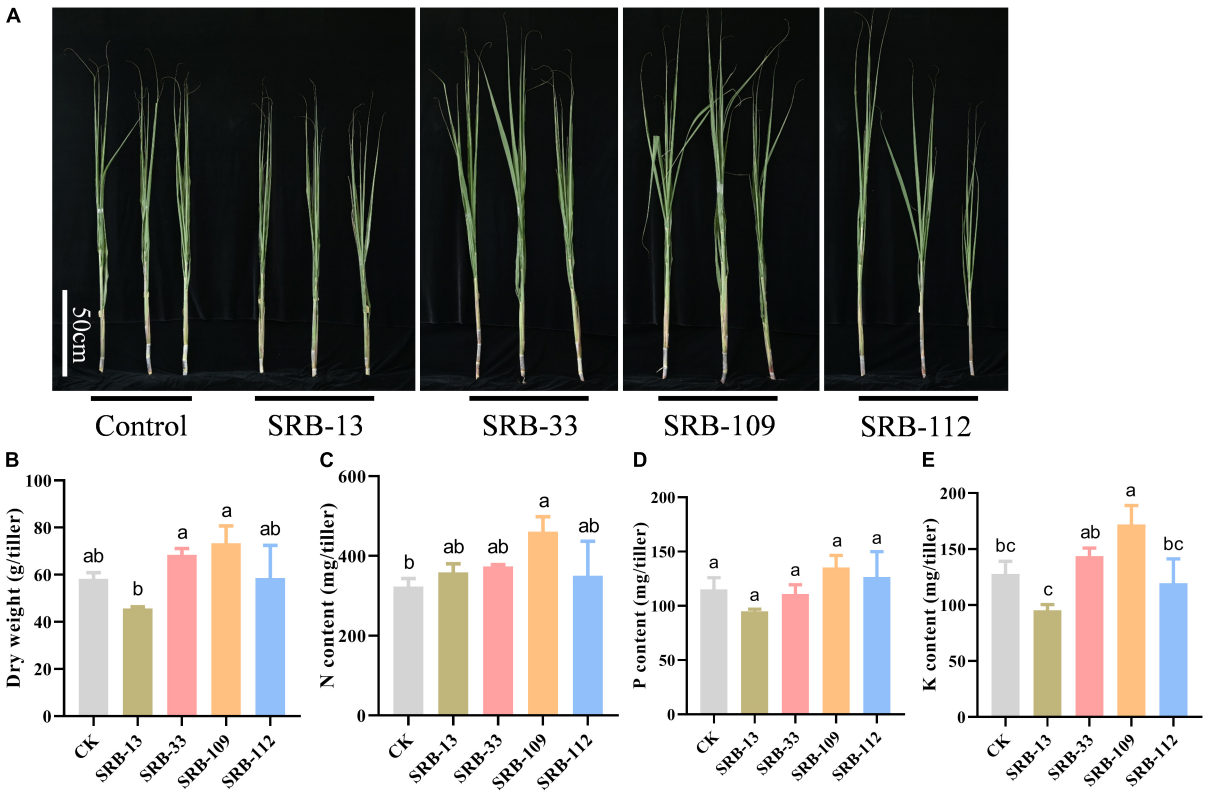

FIGURE 4 | Results of applying potentially beneficial microbes in a field experiment. **(A)** Growth performance of single stem of sugarcane plants in the field trial 120 days after inoculation with microbial isolates, bar = 50 cm. **(B)** Biomass of single stem of sugarcane under differnet treatment conditions. Total nitrogen content **(C)**, phosphate content **(D)**, and potassium content **(E)** of sugarcane plants under different microbial applications under field conditions. Different letters indicate significant differences among different treatments in Duncan's multiple range comparison test.

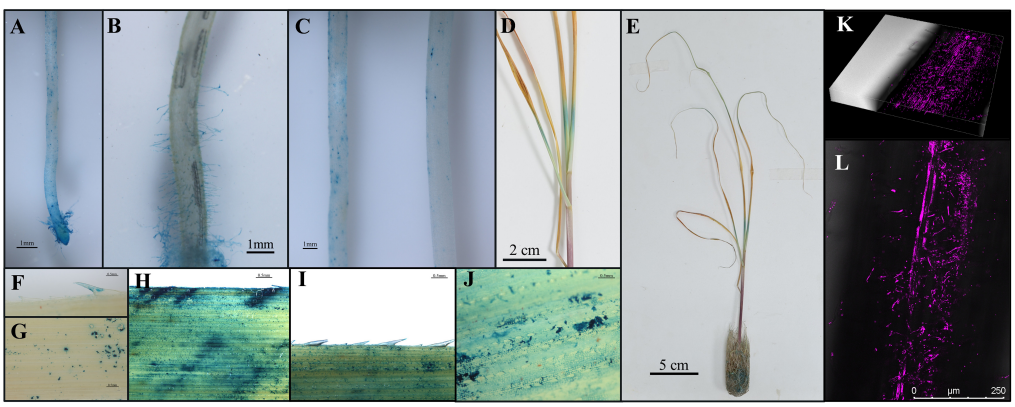

FIGURE 5 | Colonization pattern analysis of SRB-109 on sugarcane. GUS labeled SRB-109 was inoculated and co-cultured with sugarcane for 3 days in the growth chamber. Then, different organs of sugarcane plants were harvested for GUS staining. The blue color indicates the colonization of SRB-109 on different organs, including roots **(A–C)** and leaves **(D–G)**, along with GUS signals detected near inoculation wounds on leaves **(H–J)**. Results of colonization patterns of SRB-109 (RFP labeled) on the roots of sugarcane visualized with confocal microscopy **(K,L)**.

of co-evolution between host plants and their particular suites of microbiota, host plants have evolved several strategies to recruit specific microbes from surrounding soil environments (Mendes et al., 2011; Prashar et al., 2014). These strategies include changing rhizosphere soil pH and texture, production of antibiotic and Quorum-sensing mimicry substances, and specific signaling based on the composition of individual root exudates and cell debris (Marschner et al., 1986; Dennis et al., 2010). Overall, plant associated microbial community composition and activities result from the complex interactions

between soil types, geographic conditions, nutrient status, and genotypes of host plants and the available microbial pool (Zhang et al., 2019).

In this study, *Proteobacteria*, *Chloroflexi*, *Actinobacteria*, and *Firmicutes* were the dominant bacteria in the rhizosphere of sugarcane plants at the phylum taxonomic level (**Figure 1C**). Microbes in these phyla have previously been reported as the core microbiota of sugarcane plants along with *Bacteroidetes*, *Spirochaetae,* and *Verrucomicrobia* (Yeoh et al., 2016). The latter three listed taxa from the previous study were only found in low abundance in this study (**Figure 1C**), which may due to variation in the soil types and sugarcane genotypes between that published work and this report (Yeoh et al., 2016; Zhang et al., 2019; Liu W. et al., 2020). Consistent with previous studies, *Actinobacteria* was much more abundant than other taxa detected in the root compartments of sugarcane (**Figure 2**; Dong et al., 2018; Gao et al., 2019). At the genus level, *Leptothrix* sp. were the most abundant microbe in sugarcane roots, though its functions there remain mysterious due to a lack of reports on its functions or interactions with plants. In addition, *Burkholderia* sp. and *Bradyrhizobium* sp. also exhibited higher relative abundances in the sugarcane roots observed herein, with LEfSe analysis showing that these bacteria were significantly enriched in the roots relatvive to the rhizosphere. *Burkholderia* sp. and *Bradyrhizobium* sp. have also been detected from sugarcane plants cultivated in Yunnan Province, China (Dong et al., 2018), though they have been rare or absent in sugarcane grown in Brazil and Australia (de Souza et al., 2016; Yeoh et al., 2016; Gao et al., 2019; Liu W. et al., 2020). Previous work has also concluded that *Burkholderia* sp. and *Bradyrhizobium* sp. may be common plant growth promoting bacteria (Bernabeu et al., 2015; Cagide et al., 2018). However, these two genera were rarely isoalted in this study (**Figure 3B** and **Supplementary Figure 2**), which might be due to the composition of the culture medium used to isolate microbes (Bonnet et al., 2019). These results suggest that geographic location, culture conditions, and genotypic variation among of sugarcane plants coordinately regulate the composition of microbiota associated with the sugarcane hosts.

Pure culturing of microbes is important for accurate determination of specific microbial functions (Singh et al., 2019). Over the course of recent decades, with the development of high throughput next-generation sequencing, amplicon sequencing and metagenomics have been widely applied in microbial ecology investigations, with large numbers of microbes being discovered and assigned predicted functions (Giovannoni et al., 1990). To fully assess these predictions requires studying these microbes in controlled settings, typically in isolated cultures. Soil microbes have been historically perceived as largely unculturable (Woese et al., 1990). However, Bai et al. (2015) have demonstrated that 52–65% of *Arabidopsis* associated microbes may be cultured using proper culture media. More recent investigation suggests that up to 97.3% of microbes can be cultured, though most of them have not been investigated (Yang and Jia, 2021). Finally, in sugarcane, 56.1–64.5% of associated microbes may be isolated using broad spectrum microbial media (Armanhi et al., 2017). Therefore, culturing might not be as limiting to functionally characterizing microbial communities as previously perceived.

In this study, considering the importance of associated nitrogen fixation for sugarcane growth (Bai et al., 2015; Hu et al., 2017), two nitrogen-free and two nitrogen-rich media were used to culture and isolate microbes from root-associated compartments. In addition, nitrogen-fixing bacteria associated with sugarcane might also promote sugarcane growth even after the loss of nitrogen fixing capacity, which suggests that associated microbes could also promote plant growth independent of nitrogen fixation (Sevilla et al., 2001). Therefore, after the identification of the nitrogen fixation marker gene *NifH* (Gaby et al., 2018), microbes isolated in this study were also subjected to assays for other potentially beneficial functions relevant to the low phosphorus bioavailability acid soil regions of sugarcane production in South China (Kochian, 2012; **Figure 3A**). Since not all potentially beneficial microbes actually promote host plant growth, and given the complex interactions between microbes and host plants (Finkel et al., 2017; Wang et al., 2021), isolated microbe–plant interaction assays were necessary in this study to ultimately verify the potentially beneficial functions of isolated microbes. After co-culturing sugarcane seedlings with different selected microbes in greenhouse testing, four isolates were further observed under field conditions. The results of this field trial suggest that SRB-109 exhibited better plant growth-promotion than the other isolates identified in this study (**Figure 4**). Differences in the performance of the other isolates between greenhouse testing and the field trial might be due to the complex and dynamic field conditions (Finkel et al., 2017). Nevertheless, SRB-109, an apparent *Acinetobacter* sp. (**Supplementary Figure 8**), significantly promoted sugarcane growth in both greenhouse and field conditions. Laboratory assays suggested that SRB-109 might assist host plants in nutrient acquisition through solubilizing phosphate, as well as through fixing nitrogen (**Table 1**). However, whether the nitrogen fixing capacity of SRB-109 higher or lower than the previously identified sugarcane associative nitrogen fixing bacteria, such as *Azospirillum* spp. *Herbaspirillum* spp., *Gluconacetobacter* spp., *Enterobacter* spp., and *Burkholderia* spp., it will need further invesstigation and comparision of their nitrogen fixing capacity under the same treament conditions. Previous studies also suggest that *Acinetobacter* sp. may promote host plant growth through phytohormone production along with solubilizing phosphate (Kang et al., 2009; Rokhbakhsh-Zamin et al., 2011; Ishizawa et al., 2020). Consistently, in our study, the application of SRB-109 significanly enhanced the acquisition of nitrogen and potassium (**Figure 4**), which might be due to the functions of nitrogen fixation (**Table 1**). In addition, although phosphate solubilizing capacity in SRB-109 was significant in the lab, application of this isolate in the field did not significantly enhance phosphorus acquisition (**Figure 4D**). Further observation with GUS staining to determine which tissues SRB-109 colonizes suggests that SRB-109 can colonize sugarcane roots and root hairs, as well as, aboveground compartments. These observations indicate that SRB-109 establishes an intimate relationship with sugarcane that benefits the plants through gains in nutirent acquisition capabilities (**Figure 5**).

CONCLUSION

In this study, we used tissue culture of sugarcane seedlings and 16S rDNA sequencing of associated microbiota to systematically decipher the structure and composition of bacterial communities recruited and enriched from soils by sugarcane roots. Isolation of root-associated microbes and screening of the potentially beneficial members allowed for further evaluation of these isolates for the promotion of sugarcane growth in both greenhouse and field experiments. This led to the identification of SRB-109 as a rapid colonizer of both sugarcane roots and shoots that may significantly increase tillering and nitrogen acquisition by sugarcane plants. In this study, we outlined a strategy for functionally studying potentially beneficial plant-associated microbes, and demonstrated effects under field conditions. Building on these results might lead to applications of beneficial plant-associated microbes to decrease fertilizer use and promote the development of sustainable agriculture.

DATA AVAILABILITY STATEMENT

The 16s rDNA sequencing files for all samples used in this study have been deposited in the public database of the National Center for Biotechnology Information (NCBI) under project number BioProject ID: PRJNA748846.

AUTHOR CONTRIBUTIONS

YZ and HL designed the experiments and managed the projects. ML, RL, YL, CW, WM, LZ, KZ, and XF performed the experiments. XL, YS, and GH provided the tissue culture seedling and suggestion in the experiment and manuscript revision. YZ and ML performed the data analysis. YZ, HL, and ML wrote the manuscript. All authors contributed to the article and approved the submitted version.

FUNDING

ML and KZ were supported by the K+S Group scholarship from the International Magnesium Institute. This work was supported by the Natural Science Foundation of Fujian Province (2017J01603).

ACKNOWLEDGMENTS

We thank Z. X. Chen and M. J. Zeng for help during the outbreak of Coronavirus-2019 and help from other members in the Root Biology Center. We thank J. X. Xiang at the Yangzhong field experimental station of Fujian Agriculture and Forestry University for assistance with field trials. We also thank Thomas Walk for the valuable suggestions and comments and F. Tang at the Inner Mongolia Agricultural University for kindly providing the *pMG103-NPTII-GFP* construct.

SUPPLEMENTARY MATERIAL

The Supplementary Material for this article can be found online at: https://www.frontiersin.org/articles/10.3389/fmicb.2021.783925/full#supplementary-material

REFERENCES

Ahmed, E., and Holmström, S. J. M. (2014). Siderophores in environmental research: roles and applications. *Microb. Biotechnol.* 7, 196–208. doi: 10.1111/1751-7915.12117

Amir, A., Mcdonald, D., Navas-Molina, J. A., Kopylova, E., Morton, J. T., Zech Xu, Z., et al. (2017). Deblur rapidly resolves single-nucleotide community sequence patterns. *mSystems* 2:e00191–16. doi: 10.1128/msystems.00191-16

Armanhi, J. S. L., de Souza, R. S. C., Damasceno, N. B., de Araújo, L. M., Imperial, J., and Arruda, P. A. (2017). A community-based culture collection for targeting novel plant growth-promoting bacteria from the sugarcane microbiome. *Front. Plant Sci.* 8:2191. doi: 10.3389/fpls.2017.02191

Asnicar, F., Weingart, G., Tickle, T. L., Huttenhower, C., and Segata, N. (2015). Compact graphical representation of phylogenetic data and metadata with GraPhlAn. *PeerJ* 3:e1029. doi: 10.7717/peerj.1029

Bai, Y., Müller, D. B., Srinivas, G., Garrido-Oter, R., Potthoff, E., Rott, M., et al. (2015). Functional overlap of the *Arabidopsis* leaf and root microbiota. *Nature* 528, 364–369. doi: 10.1038/nature16192

Baldani, J., Caruso, L., Baldani, V. L. D., Goi, S. R., and Döbereiner, J. (1997). Recent advances in BNF with non-legume plants. *Soil Biol. Biochem.* 29, 911–922.

Baldani, V. L. D., Baldani, J. I., and Olivares, F. L. (1992). Identification and ecology of *Herbaspirillum seropedicae* and the closely related *Pseudomonas rubrisubalbicans*. *Symbiosis* 13, 65–73.

Beckers, B., Op De Beeck, M., Weyens, N., Boerjan, W., and Vangronsveld, J. (2017). Structural variability and niche differentiation in the rhizosphere and endosphere bacterial microbiome of field-grown poplar trees. *Microbiome* 5:25. doi: 10.1186/s40168-017-0241-2

Bernabeu, P. R., Pistorio, M., Torres-Tejerizo, G., Paulina, E. D. L. S., Galar, M. L., Boiardi, J. L., et al. (2015). Colonization and plant growth-promotion of tomato by *Burkholderia tropica*. *Sci. Hortic.* 191, 113–120. doi: 10.1016/j.scienta.2015.05.014

Bertalan, M., Albano, R., De Pádua, V., Rouws, L., Rojas, C., Hemerly, A., et al. (2009). Complete genome sequence of the sugarcane nitrogen-fixing endophyte *Gluconacetobacter diazotrophicus* Pal5. *BMC Genomics* 10:450. doi: 10.1186/1471-2164-10-450

Blaha, D., Prigent-Combaret, C., Mirza, M. S., and Moënne-Loccoz, Y. (2006). Phylogeny of the 1-aminocyclopropane-1-carboxylic acid deaminase-encoding gene acdS in phytobeneficial and pathogenic *Proteobacteria* and relation with strain biogeography. *FEMS Microbiol. Ecol.* 56, 455–470.

Boddey, R. M., and Döbereiner, J. (1995). Nitrogen fixation associated with grasses and cereals: recent progress and perspectives for the future. *Fertilizer Research* 42, 241–250.

Boddey, R. M., Urquiaga, S., Alves, B. J. R., and Reis, V. (2003). Endophytic nitrogen fixation in sugarcane: present knowledge and future applications. *Plant Soil* 252, 139–149. doi: 10.1023/a:1024152126541

Bolyen, E., Rideout, J. R., Dillon, M. R., Bokulich, N. A., Abnet, C. C., Al-Ghalith, G. A., et al. (2019). Reproducible, interactive, scalable and extensible microbiome data science using QIIME 2. *Nat. Biotechnol.* 37, 852–857. doi: 10.1038/s41587-019-0209-9

Bonnet, M., Lagier, J. C., Raoult, D., and Khelaifia, S. (2019). Bacterial culture through selective and non-selective conditions: the evolution of culture media

in clinical microbiology. *New Microbes. New Infect.* 34:100622. doi: 10.1016/j.nmni.2019.100622

Bulgarelli, D., Garrido-Oter, R., Münch, P. C., Weiman, A., Dröge, J., Pan, Y., et al. (2015). Structure and function of the bacterial root microbiota in wild and domesticated barley. *Cell Host Microbe* 17, 392–403. doi: 10.1016/j.chom.2015.01.011

Bulgarelli, D., Rott, M., Schlaeppi, K., Ver Loren Van Themaat, E., Ahmadinejad, N., Assenza, F., et al. (2012). Revealing structure and assembly cues for *Arabidopsis* root-inhabiting bacterial microbiota. *Nature* 488, 91–95. doi: 10.1038/nature11336

Cagide, C., Riviezzi, B., Minteguiaga, M., Morel, M. A., and Castro-Sowinski, S. (2018). Identification of plant compounds involved in the microbe-plant communication during the coinoculation of soybean with *Bradyrhizobium elkanii* and *Delftia* sp. strain JD2. *Mol. Plant Microbe Interact.* 31, 1192–1199. doi: 10.1094/mpmi-04-18-0080-cr

Carvalho, T. L. G., Balsemao-Pires, E., Saraiva, R. M., Ferreira, P. C. G., and Hemerly, A. S. (2014). Nitrogen signalling in plant interactions with associative and endophytic diazotrophic bacteria. *J. Exp. Bot.* 65, 5631–5642. doi: 10.1093/jxb/eru319

da Silva, P. R. A., Simões-Araújo, J. L., Vidal, M. S., Cruz, L. M., Souza, E. M., and Baldani, J. I. (2018). Draft genome sequence of *Paraburkholderia tropica* Ppe8 strain, a sugarcane endophytic diazotrophic bacterium. *Braz. J. Microbiol.* 49, 210–211. doi: 10.1016/j.bjm.2017.07.005

de Almeida, G. A. P., Ferreira, M. D. A., Silva, J. D. L., Chagas, J. C. C., Véras, A. S. C., De Barros, L. J. A., et al. (2018). Sugarcane bagasse as exclusive roughage for dairy cows in smallholder livestock system. *Asian Australas. J. Anim. Sci.* 31, 379–385. doi: 10.5713/ajas.17.0205

de Oliveira, R. I., de Medeiros, M. R. F. A., Freire, C. S., Freire, F. J., Neto, D. E. S., and de Oliveira, E. C. A. (2016). Nutrient partitioning and nutritional requirement in sugarcane. *Australian Aust. J. Crop. Science* 10, 69–75. doi: 10.3316/informit.936795392927333

de Souza, R. S. C., Okura, V. K., Armanhi, J. S. L., Jorrín, B., Lozano, N., da Silva, M. J., et al. (2016). Unlocking the bacterial and fungal communities assemblages of sugarcane microbiome. *Sci. Rep.* 6:28774. doi: 10.1038/srep28774

Dennis, P. G., Miller, A. J., and Hirsch, P. R. (2010). Are root exudates more important than other sources of rhizodeposits in structuring rhizosphere bacterial communities? *FEMS Microbiol. Ecol.* 72, 313–327. doi: 10.1111/j.1574-6941.2010.00860.x

Döbereiner, J., and Day, J. M. (1976). "Associative symbiosis in tropical grasses: characterization of microorganisms and dinitrogen fixing sites," in *Proceedings of the 1st International Symposium on Nitrogen Fixation*. (Pullman: Washington State University Press), 518–538.

Dong, M., Yang, Z., Cheng, G., Peng, L., Xu, Q., and Xu, J. (2018). Diversity of the bacterial microbiome in the roots of four Saccharum species: *S. spontaneum*, *S. robustum*, *S. barberi*, and *S. officinarum*. *Front. Microbiol.* 9:267. doi: 10.3389/fmicb.2018.00267

Felsenstein, J. (1985). Confidence limits on phylogenies: an approach using the bootstrap. *Evolution* 39, 783–791. doi: 10.1111/j.1558-5646.1985.tb00420.x

Finkel, O. M., Castrillo, G., Herrera Paredes, S., Salas González, I., and Dangl, J. L. (2017). Understanding and exploiting plant beneficial microbes. *Curr. Opin. Plant. Biol.* 38, 155–163. doi: 10.1016/j.pbi.2017.04.018

Gaby, J. C., Rishishwar, L., Valderrama-Aguirre, L. C., Green, S. J., Valderrama-Aguirre, A., Jordan, I. K., et al. (2018). Diazotroph community characterization *via* a high-throughput nifH amplicon sequencing and analysis pipeline. *Appl. Environ. Microbiol.* 84, e01512–e01517. doi: 10.1128/aem.01512-17

Gao, X., Wu, Z., Liu, R., Wu, J., Zeng, Q., and Qi, Y. (2019). Rhizosphere bacterial community characteristics over different years of sugarcane ratooning in consecutive monoculture. *Biomed. Res. Int.* 2019, 1–10. doi: 10.1155/2019/4943150

Giovannoni, S. J., Britschgi, T. B., Moyer, C. L., and Field, K. G. (1990). Genetic diversity in sargasso sea bacterioplankton. *Nature* 345, 60–63. doi: 10.1038/345060a0

Gopalasundaram, P., Bhaskaran, A., and Rakkiyappan, P. (2012). Integrated nutrient management in sugarcane. *Sugar. Tech.* 14, 3–20. doi: 10.1007/s12355-011-0097-x

Guo, D. J., Singh, R. K., Singh, P., Li, D. P., Sharma, A., Xing, Y. X., et al. (2020). Complete genome sequence of *Enterobacter* roggenkampii ED5, a nitrogen fixing plant growth promoting endophytic bacterium with biocontrol and stress tolerance properties, isolated from sugarcane root. *Front. Microbiol.* 22:580081. doi: 10.3389/fmicb.2020.580081

Guo, J. H., Liu, X. J., Zhang, Y., Shen, J. L., Han, W. X., Zhang, W. F., et al. (2010). Significant acidification in major Chinese croplands. *Science* 327, 1008–1010. doi: 10.1126/science.1182570

Hassani, M. A., Durán, P., and Hacquard, S. (2018). Microbial interactions within the plant holobiont. *Microbiome* 6:58. doi: 10.1186/s40168-018-0445-0

Hu, H. N., Ao, J. H., Huang, X. C., Li, X. X., and Liao, H. (2017). Evaluation on associative nitrogen fixation capability in different tissues of sugarcane. *Zhiwu Shengli Xuebao Plant Physiol. J.* 53, 437–444. doi: 10.13592/j.cnki.ppj.2016.0407

Inui, M., Roh, J. H., Zahn, K., and Yukawa, H. (2000). Sequence analysis of the cryptic plasmid pMG101 from Rhodo*pseudomonas palustris* and construction of stable cloning vectors. *Appl. Environ. Microbiol.* 66, 54–63. doi: 10.1128/aem.66.1.54-63.2000

Ishizawa, H., Ogata, Y., Hachiya, Y., Tokura, K. I., Kuroda, M., Inoue, D., et al. (2020). Enhanced biomass production and nutrient removal capacity of duckweed *via* two-step cultivation process with a plant growth-promoting bacterium, *Acinetobacter calcoaceticus* P23. *Chemosphere* 238:124682. doi: 10.1016/j.chemosphere.2019.124682

Kang, S. M., Joo, G. J., Hamayun, M., Na, C. I., Shin, D. H., Kim, H. Y., et al. (2009). Gibberellin production and phosphate solubilization by newly isolated strain of *Acinetobacter calcoaceticus* and its effect on plant growth. *Biotechnol. Lett.* 31, 277–281. doi: 10.1007/s10529-008-9867-2

Kochian, L. V. (2012). Rooting for more phosphorus. *Nature* 488, 466–467. doi: 10.1038/488466a

Kumar, S., Stecher, G., and Tamura, K. (2016). MEGA7: molecular evolutionary genetics analysis version 7.0 for bigger datasets. *Mol. Biol. Evol.* 33, 1870–1874. doi: 10.1093/molbev/msw054

Le, C., Zha, Y., Li, Y., Sun, D., Lu, H., and Yin, B. (2010). Eutrophication of lake waters in China: cost, causes, and control. *Environ. Manage.* 45, 662–668. doi: 10.1007/s00267-010-9440-3

Letunic, I., and Bork, P. (2019). Interactive tree of life (iTOL) v4: recent updates and new developments. *Nucleic Acids Res.* 47, 256–259. doi: 10.1093/nar/gkz239

Li, X., Zhao, J., Tan, Z., Zeng, R., and Liao, H. (2015). GmEXPB2, a cell wall beta-expansin, affects soybean nodulation through modifying root architecture and promoting nodule formation and development. *Plant Physiol.* 169, 2640–2653. doi: 10.1104/pp.15.01029

Li, X., Zheng, J., Yang, Y., and Liao, H. (2018). *Increasing NODULE SIZE*$_1$ expression is required for normal rhizobial symbiosis and nodule development. *Plant Physiol.* 178, 1233–1248. doi: 10.1104/pp.18.01018

Li, Y. R., and Yang, L. T. (2015). Sugarcane agriculture and sugar industry in China. *Sugar Tech.* 17, 1–8. doi: 10.1007/s12355-014-0342-1

Lin, L., Wei, C., Chen, M., Wang, H., Li, Y., Li, Y., et al. (2015). Complete genome sequence of endophytic nitrogen-fixing *Klebsiella variicola* strain DX120E. *Stand. Genomic Sci.* 10, 22. doi: 10.1186/s40793-015-0004-2

Littlewood, T. D., and Bennett, M. R. (2003). Apoptotic cell death in atherosclerosis. *Curr. Opin. Lipidol.* 14, 469–475. doi: 10.1097/00041433-200310000-00007

Liu, S., Liao, L. L., Nie, M. M., Peng, W. T., Zhang, M. S., Lei, J. N., et al. (2020). A VIT-like transporter facilitates iron transport into nodule symbiosomes for nitrogen fixation in soybean. *New Phytol.* 226, 1413–1428. doi: 10.1111/nph.16506

Liu, W., Jiang, L., Yang, S., Wang, Z., Tian, R., Peng, Z., et al. (2020). Critical transition of soil bacterial diversity and composition triggered by nitrogen enrichment. *Ecology* 101:e03053. doi: 10.1002/ecy.3053

Liu, X., Zhang, Y., Han, W., Tang, A., Shen, J., Cui, Z., et al. (2013). Enhanced nitrogen deposition over China. *Nature* 494, 459–462. doi: 10.1038/nature11917

Lundberg, D. S., Lebeis, S. L., Paredes, S. H., Yourstone, S., Gehring, J., Malfatti, S., et al. (2012). Defining the core *Arabidopsis thaliana* root microbiome. *Nature* 488, 86–90. doi: 10.1038/nature11237

Marschner, H., Römheld, V., Horst, W. J., and Martin, P. (1986). Root-induced changes in the rhizosphere: importance for the mineral nutrition of plants. *Z. Pflanzenernährung Bodenkunde* 149, 441–456. doi: 10.1002/jpln.19861490408

Martin, M. (2011). Cutadapt removes adapter sequences from high-throughput sequencing reads. *EMBnet J.* 17:10. doi: 10.14806/ej.17.1.200

Mehnaz, S. (2013). Microbes-friends and foes of sugarcane. *J. Basic Microbiol.* 53, 954–971. doi: 10.1002/jobm.201200299

Mendes, R., Kruijt, M., de Bruijn, I., Dekkers, E., van der Voort, M., Schneider, J. H., et al. (2011). Deciphering the rhizosphere microbiome for disease-suppressive bacteria. *Science* 332, 1097–1100. doi: 10.1126/science.1203980

Muthukumarasamy, R., Revathi, E., Vadivelu, M., and Arun, K. (2017). Isolation of bacterial strains possessing nitrogen-fixation, phosphate and potassium-solubilization and their inoculation effects on sugarcane. *Indian J. Exp. Biol.* 55, 161–170.

Niu, B., Paulson, J. N., Zheng, X., and Kolter, R. (2017). Simplified and representative bacterial community of maize roots. *Proc. Natl. Acad. Sci. U.S.A.* 114, E2450–E2459. doi: 10.1073/pnas.1616148114

Oliveira, A. L. M., Stoffels, M., Schmid, M., Reis, V. M., Baldani, J. I., and Hartmann, A. (2009). Colonization of sugarcane plantlets by mixed inoculations with diazotrophic bacteria. *Eur. J. Soil Biol.* 45, 106–113. doi: 10.1016/j.ejsobi.2008.09.004

Oliveira, A. L. M., Urquiaga, S., Döbereiner, J., and Baldani, J. I. (2002). The effect of inoculating endophytic N2-fixing bacteria on micropropagated sugarcane plants. *Plant Soil* 242, 205–215. doi: 10.1023/a:1016249704336

Parks, D. H., Tyson, G. W., Hugenholtz, P., and Beiko, R. G. (2014). STAMP: statistical analysis of taxonomic and functional profiles. *Bioinformatics* 30, 3123–3124. doi: 10.1093/bioinformatics/btu494

Pedrosa, F. O., Monteiro, R. A., Wassem, R., Cruz, L. M., Ayub, R. A., Colauto, N. B., et al. (2011). Genome of *Herbaspirillum seropedicae strain* SmR1, a specialized diazotrophic endophyte of tropical grasses. *PLoS Genet.* 7:e1002064. doi: 10.1371/journal.pgen.1002064

Prashar, P., Kapoor, N., and Sachdeva, S. (2014). Rhizosphere: its structure, bacterial diversity and significance. *Rev. Environ. Sci. Biol.* 13, 63–77. doi: 10.1007/s11157-013-9317-z

Qin, L., Jiang, H., Tian, J., Zhao, J., and Liao, H. (2011). Rhizobia enhance acquisition of phosphorus from different sources by soybean plants. *Plant Soil* 349, 25–36. doi: 10.1007/s11104-011-0947-z

Rognes, T., Flouri, T., Nichols, B., Quince, C., and Mahé, F. (2016). VSEARCH: a versatile open source tool for metagenomics. *PeerJ* 4:e2584. doi: 10.7717/peerj.2584

Rokhbakhsh-Zamin, F., Sachdev, D., Kazemi-Pour, N., Engineer, A., Pardesi, K. R., Zinjarde, S., et al. (2011). Characterization of plant-growth-promoting traits of *Acinetobacter* Species isolated from rhizosphere of *Pennisetum glaucum*. *J. Microbiol. Biotechnol.* 21, 556–566. doi: 10.1111/j.1439-0523.2012.01954.x

RöSch, C., Mergel, A., and Bothe, H. (2002). Biodiversity of denitrifying and dinitrogen-fixing bacteria in an acid forest soil. *Appl. Environ. Microbiol.* 68, 3818–3829. doi: 10.1128/aem.68.8.3818-3829.2002

Rosenblueth, M., Ormeño-Orrillo, E., López-López, A., Rogel, M. A., Reyes-Hernández, B. J., Martínez-Romero, J. C., et al. (2018). Nitrogen fixation in cereals. *Front. Microbiol.* 9:1794. doi: 10.3389/fmicb.2018.01794

Saitou, N., and Nei, M. (1987). The neighbor-joining method: a new method for reconstructing phylogenetic trees. *Mol. Biol. Evol.* 4, 406–425. doi: 10.1093/oxfordjournals.molbev.a040454

Sakurai, M., Wasaki, J., Tomizawa, Y., Shinano, T., and Osaki, M. (2008). Analysis of bacterial communities on alkaline phosphatase genes in soil supplied with organic matter. *Soil Sci. Plant Nut.* 54, 62–71.

Sant'Anna, F. H., Almeida, L. G., Cecagno, R., Reolon, L. A., Siqueira, F. M., Machado, M. R., et al. (2011). Genomic insights into the versatility of the plant growth-promoting bacterium *Azospirillum amazonense*. *BMC Genomics* 12:409. doi: 10.1186/1471-2164-12-409

Saravanan, V. S., Madhaiyan, M., and Thangaraju, M. (2007). Solubilization of zinc compounds by the diazotrophic, plant growth promoting bacterium *Gluconacetobacter diazotrophicus*. *Chemosphere* 66, 1794–1798. doi: 10.1016/j.chemosphere.2006.07.067

Schwab, S., Terra, L. A., and Baldani, J. I. (2018). Genomic characterization of Nitrospirillum amazonense strain CBAmC, a nitrogen-fixing bacterium isolated from surface-sterilized sugarcane stems. *Mol. Genet. Genomics* 293, 997–1016. doi: 10.1007/s00438-018-1439-0

Sevilla, M., Burris, R. H., Gunapala, N., and Kennedy, C. (2001). Comparison of benefit to sugarcane plant growth and 15N2 incorporation following inoculation of sterile plants with *Acetobacter diazotrophicus* wild-type and Nif- mutants strains. *Mol. Plant Microbe Interact.* 14, 358–366. doi: 10.1094/mpmi.2001.14.3.358

Singh, R., Ryu, J., and Kim, S. W. (2019). Microbial consortia including methanotrophs: some benefits of living together. *J. Microbiol.* 57, 939–952. doi: 10.1007/s12275-019-9328-8

Tringe, S. G., von Mering, C., Kobayashi, A., Salamov, A. A., Chen, K., Chang, H. W., et al. (2005). Comparative metagenomics of microbial communities. *Science* 308, 554–557. doi: 10.1126/science.1107851

Urquiaga, S., Cruz, K. H. S., and Boddey, R. M. (1992). Contribution of nitrogen fixation to sugar cane: Nitrogen-15 and nitrogen-balance estimates. *Soil Sci. Soc. Am. J.* 56, 105–114. doi: 10.2136/sssaj1992.03615995005600010017x

Urquiaga, S., Xavier, R. P., De Morais, R. F., Batista, R. B., Schultz, N., Leite, J. M., et al. (2012). Evidence from field nitrogen balance and 15N natural abundance data for the contribution of biological N2 fixation to Brazilian sugarcane varieties. *Plant Soil* 356, 5–21. doi: 10.1007/s11104-011-1016-3

Vieira, S., Barros, M. V., Sydney, A., Piekarski, C. M., de Francisco, A. C., Vandenberghe, L., et al. (2020). Sustainability of sugarcane lignocellulosic biomass pretreatment for the production of bioethanol. *Bioresour. Technol.* 299:122635. doi: 10.1016/j.biortech.2019.122635

Wang, C., Li, Y., Li, M., Zhang, K., Ma, W., Zheng, L., et al. (2021). Functional assembly of root-associated microbial consortia improves nutrient efficiency and yield in soybean. *J. Integr. Plant Biol.* 63, 1021–1035. doi: 10.1111/jipb.13073

Woese, C. R., Kandler, O., and Wheelis, M. L. (1990). Towards a natural system of organisms: proposal for the domains Archaea, Bacteria, and Eucarya. *Proc. Natl. Acad. Sci. U.S.A.* 87, 4576–4579. doi: 10.1073/pnas.87.12.4576

Yang, L. J., and Jia, Z. J. (2021). The history and definition of 99% unculturability paradigm and its assessment using nitrogen-fixing bacteria. *Acta Microbiol. Sin.* 61, 903–922. doi: 10.13343/j.cnki.wsxb.20200258

Yeoh, Y. K., Paungfoo-Lonhienne, C., Dennis, P. G., Robinson, N., Ragan, M. A., Schmidt, S., et al. (2016). The core root microbiome of sugarcanes cultivated under varying nitrogen fertilizer application. *Environ. Microbiol.* 18, 1338–1351. doi: 10.1111/1462-2920.12925

Yilmaz, P., Parfrey, L. W., Yarza, P., Gerken, J., Pruesse, E., Quast, C., et al. (2014). The SILVA and "all-species living tree project (LTP)" taxonomic frameworks. *Nucleic Acids Res.* 42, D643–D648. doi: 10.1093/nar/gkt1209

Zhang, J., Liu, Y.-X., Zhang, N., Hu, B., Jin, T., Xu, H., et al. (2019). NRT1.1B is associated with root microbiota composition and nitrogen use in field-grown rice. *Nat. Biotechnol.* 37, 676–684. doi: 10.1038/s41587-019-0104-4

Zhong, Y., Yang, Y., Liu, P., Xu, R., Rensing, C., Fu, X., et al. (2019). Genotype and rhizobium inoculation modulate the assembly of soybean rhizobacterial communities. *Plant Cell Environ.* 42, 2028–2044. doi: 10.1111/pce.13519

Zhu, B., Chen, M., Lin, L., Yang, L., Li, Y., and An, Q. (2012). Genome sequence of *Enterobacter* sp. strain SP1, an endophytic nitrogen-fixing bacterium isolated from sugarcane. *J. Bacteriol.* 194, 6963–6964. doi: 10.1128/jb.01933-12

Conflict of Interest: The authors declare that the research was conducted in the absence of any commercial or financial relationships that could be construed as a potential conflict of interest.

Publisher's Note: All claims expressed in this article are solely those of the authors and do not necessarily represent those of their affiliated organizations, or those of the publisher, the editors and the reviewers. Any product that may be evaluated in this article, or claim that may be made by its manufacturer, is not guaranteed or endorsed by the publisher.

frontiers in Microbiology

ORIGINAL RESEARCH
published: 18 February 2022
doi: 10.3389/fmicb.2022.828320

Effect of Ensiling Density and Storage Temperature on Fermentation Quality, Bacterial Community, and Nitrate Concentration of Sorghum-Sudangrass Silage

*Chunsheng Bai[1], Gang Pan[1], Ruoxuan Leng[1], Wenhua Ni[1], Jiyun Yang[1], Juanjuan Sun[2], Zhu Yu[3], Zhigang Liu[4] and Yanlin Xue[5,6]**

[1] College of Horticulture, Shenyang Agricultural University, Shenyang, China, [2] Institute of Grassland Research, Chinese Academy of Agricultural Sciences, Hohhot, China, [3] College of Grassland Science and Technology, China Agricultural University, Beijing, China, [4] Inner Mongolia Sihai Agriculture and Animal Husbandry Technology Co., Ltd., Baochang, China, [5] Inner Mongolia Engineering Research Center of Development and Utilization of Microbial Resources in Silage, Inner Mongolia Academy of Agriculture and Animal Husbandry Science, Hohhot, China, [6] Inner Mongolia Key Laboratory of Microbial Ecology of Silage, Inner Mongolia Academy of Agriculture and Animal Husbandry Science, Hohhot, China

OPEN ACCESS

Edited by:
Christopher Rensing,
Fujian Agriculture and Forestry University, China

Reviewed by:
Fuhou Li,
Lanzhou University, China
Xianjun Yuan,
Nanjing Agricultural University, China

***Correspondence:**
Yanlin Xue
xueyanlin_1979@163.com

Specialty section:
This article was submitted to Microbiotechnology, a section of the journal Frontiers in Microbiology

Received: 03 December 2021
Accepted: 10 January 2022
Published: 18 February 2022

Citation:
Bai C, Pan G, Leng R, Ni W, Yang J, Sun J, Yu Z, Liu Z and Xue Y (2022) Effect of Ensiling Density and Storage Temperature on Fermentation Quality, Bacterial Community, and Nitrate Concentration of Sorghum-Sudangrass Silage. Front. Microbiol. 13:828320. doi: 10.3389/fmicb.2022.828320

This study aimed to evaluate the fermentation quality, bacterial community, and nitrate content of sorghum-sudangrass silage with two ensiling densities [550 kg fresh weight (FW)/m^3 (low density, LD) and 650 kg FW/m^3 (high density, HD)] stored at two temperatures [10°C (low temperature, LT) and 25°C (normal temperature, NT)] for 60 days. The fermentation parameters, microbial counts, bacterial community, nutritional composition, and nitrate and nitrite levels were assessed. The pH and ammonia nitrogen (N) in all silages were below 4.0 and 80 g/kg total N, respectively. Compared with LT treatments, NT treatments had lower pH and lactic acid (LA) bacteria and yeasts counts and contained higher LA and LA/acetic acid (LA/AA) ($p < 0.05$). The LT-LD contained more ammonia–N than LT-HD ($p < 0.05$) and had higher nitrate and lower nitrate degradation than other treatments ($p < 0.05$). *Lactobacillus* was the most dominant genus with all treatments (57.2–66.9%). The LA, LA/AA, and abundances of *Pantoea*, *Pseudomonas*, and *Enterobacter* in the silage negatively correlated with nitrate concentration and positively correlated with nitrate degradation ($p < 0.05$). Moreover, pH and ammonia–N were positively correlated with nitrate concentration and negatively correlated with nitrate degradation ($p < 0.05$). Overall, all silage had satisfactory fermentation quality, and the silage with HD and NT had better fermentation quality and higher nitrate degradation. The bacterial communities in all silages were dominated by *Lactobacillus*. The nitrate degradation during the fermentation process might be related to the fermentation quality and the activity of *Pantoea*, *Pseudomonas*, and *Enterobacter* in silage.

Keywords: sorghum-sudangrass silage, storage temperature, ensiling density, fermentation quality, bacteria community, nitrate

INTRODUCTION

Sorghum-sudangrass is widely cultivated as a roughage for ruminants in arid and semiarid areas, because of its strong drought resistance, high water-use efficiency, and satisfactory biomass production (Han et al., 2015; McCary et al., 2020). Previous studies revealed that sorghum-sudangrass silage generally has high fermentation quality, that ensiling it with chemical additives improves *in vitro* digestibility and aerobic security, and that the inoculation of lactic acid (LA) bacteria (LAB) promotes fermentation and reduces yeasts count (Han et al., 2015; Diepersloot et al., 2021). Replacing 35 or 45% of whole-plant corn silage with sorghum-sudangrass silage in dietary dry matter (DM) improves dairy cow performance and optimizes the rumen environment (Dann et al., 2008).

Storage temperature and ensiling density are the main environmental factors that influence the fermentation quality, aerobic stability, and microbial community of silage (Weiss et al., 2016; Brüning et al., 2018; Sun et al., 2021a). Silage stored at high temperature (from 35 to 41°C) contains lower organic acid concentrations than those stored at 20 to 30°C (Weinberg et al., 1998; Kim and Adesogan, 2006; Weiss et al., 2016). Furthermore, a high packing density can positively affect the fermentation quality and aerobic stability of maize silage (Jungbluth et al., 2017; Brüning et al., 2018). Guan et al. (2020) revealed that *Lactobacillus* dominated the fermentation process in whole-plant corn silage stored at 30°C, but *Lactobacillus* exhibited decreasing abundance after 3 days of ensiling when the silage was stored at 45°C. Zhang et al. (2018) also reported that LAB genera were present as main taxa in alfalfa silage stored at 20 and 30°C but were minor taxa in silage stored at 40°C. Moreover, Sun et al. (2021a) found that increasing the ensiling density can increase the abundance of *Lactobacillus* in barley silage. However, no study has yet addressed the effect of temperature and density on the fermentation quality and microbial community of sorghum-sudangrass silage.

Nitrate accumulation in sorghum-sudangrass is a serious problem for livestock and human health; because there is high potential to accumulate nitrate in the background of large amount of nitrogen fertilizer application (Zhang et al., 1999; Harada et al., 2000). This also limits the application range of sorghum-sudangrass as animal feed. The nitrate content in plants is mainly associated with nitrogen fertilization, weather factors, and the growth stage (Drewnoski et al., 2019; Holman et al., 2019; Rashid et al., 2019). However, nitrate is not always toxic to animals and can cause toxicity when its concentration is greater than 3,000 mg/kg in forage (Roozeboom et al., 2019). Ensiling is adopted as an effective method to degrade nitrate in forage and to preserve forage based on anaerobic microbial fermentation (Khorasani et al., 1997). During fermentation, plant nitrate reductase, enterobacteria, and lactobacilli degrade nitrate to generate nitrite and nitric oxide as intermediates and then to ammonia and nitrous oxide as end-products (Spoelstra, 1985). To our knowledge, nitrate, nitrate degradation and the correlation between nitrate and fermentation quality or bacterial community have not been characterized in sorghum-sudangrass silage to date.

When harvesting sorghum-sudangrass in September in Shenyang, China, the temperature ranges from 10 to 25°C, and it is challenging to prepare silage with good fermentation quality. With reference to the typical temperatures during ensiling period in northeast China, sorghum-sudangrass was ensiled with two ensiling densities [550 and 650 kg fresh weight (FW)/m^3] and two storage temperatures (10 and 25°C). It was hypothesized that the differences in ensiling density and storage temperature will change the fermentation quality, microbial community, and nitrate content of sorghum-sudangrass silage. Thus, the sorghum-sudangrass silages prepared with two ensiling densities and stored at two ambient temperatures were analyzed for the fermentation parameters, microbial counts, bacterial community, nutrient composition, nitrate, and nitrite.

MATERIALS AND METHODS

Silage Preparation

Sorghum-sudangrass (*Sorghum bicolor* × *sudanense*, variety, BMR Octane) was planted on an experimental farm of Shenyang Agricultural University (123°25′E, 41°46′N, mean annual temperature of 6.5°C, annual precipitation of 700 mm) and was harvested at the flag leaf ligule of the stem elongation stage on 28 September 2018, from three fields as repeticates. The forage from each field was separately chopped to a length of 1–2 cm using a forage chopper (ZT0.8, Xinnong Machinery Co. Ltd., Donggang, China). After mixing homogeneously, the chopped forage from each field was randomly divided into four batches. Two batches were placed into two plastic silos (diameter × height, 20 × 30 cm) by hand with sterile gloves at a density of 550 kg FW/m^3 (low density, LD), respectively; the other two batches were also put into the two same siloes at a density of 650 kg FW/m^3 (high density, HD). After packing, the silo was closed using a plastic cover with a rubber O-ring and screw. After sealing, the two silos with the same density from each field were stored for 60 days in constant temperature incubators at 10°C (low temperature, LT) and 25°C (normal temperature, NT).

Fermentation Quality and Nutrient Composition

Silage silos were opened after 60 days of ensiling. A mixture of 20 g of silage and 180 ml of distilled water was homogenized for 100 s in a flap-type sterile homogenizer (JX-05, Shanghai Jingxin Industrial Development Co. Ltd., Shanghai, China) and filtered through four layers of cheesecloth to prepare silage extracts (Sun et al., 2021b). A pH meter with a glass electrode (PB-10, Sartorius Group, Göttingen, Germany) was used to detect the pH of the silage. Phenol-sodium hypochlorite colorimetry was used to detect the ammonia–N content (Broderick and Kang, 1980). The concentrations of LA, acetic acid (AA), propanoic acid (PA), and butyric acid (BA) in silage were assessed using a high-performance liquid chromatography (HPLC; Waters1525, Waters Corporation, Milford, MA, United States). The analysis conditions were as follows: chromatographic column, Carbomix H-NP5 (Sepax

Technologies, Inc., Newark, DE, United States); detector, refractive index detector (Waters2414, Waters Corporation, Milford, MA, United States); mobile phase, 2.5 mmol/L H_2SO_4; flow rate, 0.6 ml/min; column temperature, 55°C; sample volume, 10 μl (Nazar et al., 2021). The organic acid concentrations were obtained by comparing the curves of the silage extracts with the standard curve of standard substances.

The fresh material or silage was dried at 65°C for 48 h, followed by drying at 105°C until a constant weight was achieved. The DM content of the silage was corrected for the loss of volatiles during drying according to Weissbach and Strubelt (2008). Dried samples were passed through a 1-mm screen for further chemical analysis. Total nitrogen (TN) was measured by the Kjeldahl method using an autoanalyzer (Kjeltec 8400; FOSS Co. Ltd., Hillerød, Denmark) with copper sulfate as a catalyst (AOAC, 1990) and the crude protein (CP) concentration was calculated by multiplying the TN concentration by 6.25. The concentrations of neutral detergent fiber (NDF) and acid detergent fiber (ADF) were measured according to the Van Soest method (Van Soest et al., 1991) using an Ankom 2000 fiber analyzer (Ankom, Macedon, NY, United States), without using a heat stable amylase, and were expressed inclusive of ash. Water-soluble carbohydrates (WSCs) were determined using anthrone colorimetry (Thomas, 1977).

Microbial Counts and Bacterial Community

Fresh forage or silage (10 g) was placed into 90 ml of sterile distilled water and shaken at 4°C at 180 rpm for 30 min. Then, it was diluted successively to 10^{-1} to 10^{-6} to determine microbial counts according to Wang et al. (2021). The LAB, coliform bacteria, and yeast (molds) were enumerated on Man Rogosa Sharpe agar, Violet Red Bile agar, and Rose Bengal agar (Beijing Aoboxing Bio-tech Co. Ltd., Beijing, China), respectively, as reported by Cai et al. (1999).

Each silage sample (10 g) was placed into 90 ml of sterile distilled water and shaken using a cryogenic oscillator (THZ-98C, Shanghai Yiheng Scientific Instrument Co. Ltd., Shanghai, China) at 4°C and 180 rpm for 30 min. Then, it was filtered with a piece of four-layer gauze to obtain the filtrate, which was then centrifuged using a refrigerated centrifuge (ST 16R, Thermo Fisher Scientific, Inc., Waltham, MA, United States) at 4°C and 8,000 rpm for 15 min. Sediments enriched with bacteria were finally obtained for high-throughput sequencing (Wang et al., 2018). Total DNA of the bacterial community was extracted according to the instructions of the E.Z.N.A.® soil DNA kit (Omega Bio-tek, Norcross, GA, United States). A bead-beating step (Precellys® 24 tissue homogenizer, Bertin Instruments, Montigny-le-Bretonneux, France) was used to increase DNA recovery. The quality of DNA was assessed using spectrophotometry (ND 8000, NanoDrop® Technologies, Thermo Scientific, Waltham, MA, United States). Then, the variable region of V3–V4 of 16S ribosomal RNA (rRNA) was amplified with the primers 338F (5′-ACTCCTACGGGAGGCAGCAG-3′) and 806R (5′-GGACTACHVGGGTWTCTAAT-3′) (Sun et al., 2021a). The PCR reaction system included the following: 5× TransStartFastPfu buffer solution, 4 μl; 2.5 mM dNTPs, 2 μl; upstream primer (5 μM) and downstream primer (5 μM), 0.8 μl each; TransStart FastPfu DNA polymerase, 0.4 μl; template DNA, 10 ng; all supplemented with inactivated deionized water to 20 μl. The AxyPrep DNA Gel Extraction Kit (Axygen Biosciences, Union City, CA, United States) was used to purify the PCR products, and a Quantus™ Fluorometer (Promega, United States) was used for quantitative determination, using the MiSeq PE300 platform of the Illumina Company for sequencing (Shanghai Majorbio Bio-Pharm Technology Co. Ltd.). Next fastp[1] and FLASH[2] software were used to control quality and splice raw sequences, respectively. Furthermore, UPARSE software[3] was used to cluster sequences with 97% similarity in operational taxonomic units (OTUs). Then, RDP classifier[4] and Silva 16S rRNA database (v138) were used to analyze the microbial composition. Principal coordinates analysis of the abundance of bacterial communities (at genus level) in silage and the difference in bacterial communities (genus level) in silage was performed by R (version 3.2.1). The sequence data were deposited in the NCBI Sequence Read Archive under the accession number SRP272464.

Nitrate and Nitrite Concentrations

For this, 5 g of each dried sample was extracted with 250 ml of phosphate buffer ($Na_2HPO_4{\cdot}12H_2O$, 1.79 g; $NaH_2PO_4{\cdot}2H_2O$, 0.78 g; $NaClO_4$, 14.04 g; plus distilled water for a constant volume of 1 L) and then shaken at 180 rpm for 20 min and filtered. The nitrate and nitrite concentrations were assessed using HPLC (Waters1525, Waters Corporation, Milford, MA, United States). The analysis conditions according to the manufacturer's instructions for the chromatographic column were as follows: chromatographic column, NH2P-50 4E (Shimadzu Corporation, Tokyo, Japan); detector, UV detector (Waters2489, Waters Corporation, Milford, MA, United States); wavelength, 210 nm; mobile phase, phosphate buffer (identical with the extract); flow rate, 0.8 ml/min; column temperature, 40°C; sample volume, 10 μl. The nitrate degradation rate was calculated as follows: (nitrate in fresh materials − nitrate in silage) / nitrate in fresh materials × 100.

Statistical Analysis

Microbial counts were log-transformed before the statistical analysis. Data on fermentation quality, microbial counts, nutrient composition, nitrate, and nitrite were analyzed using a 2 × 2 factorial design. The model included two storage temperatures, two ensiling densities, and their interactions. A general linear model of statistical software SPSS (23.0) was used to perform two-way ANOVA for temperatures and densities, together with their interaction. One-way ANOVA was used to statistically analyze the difference among the treatments ($p < 0.05$). Meanwhile, the correlations between the nitrate concentration and nitrate degradation rate with fermentation parameters (pH, LA, AA,

[1]https://github.com/OpenGene/fastp, version 0.20.0.
[2]http://www.cbcb.umd.edu/software/flash,version1.2.7.
[3]http://drive5.com/uparse/,version7.1
[4]http://rdp.cme.msu.edu/,version2.2

LA/AA, and ammonia–N) or main bacterial genera (top 10 most abundant genera) were analyzed by R (version 3.2.1) at https://www.omicstudio.cn/tool/59.

RESULTS

Characteristics of Fresh Forage

The concentrations of CP, NDF, ADF, and WSC in sorghum-sudangrass before ensiling were 68.9, 564, 334, and 168 g/kg DM, respectively (**Table 1**). The nitrate content was 2,688 mg/kg, and nitrite was no detected.

Fermentation Quality and Nutrient Composition of Silage

The storage temperature mainly affected the pH, LA, and LA/AA of silage ($p < 0.05$), and the ensiling density mainly affected LA and ammonia–N ($p < 0.05$) (**Table 2**). Moreover, storage temperature and ensiling density interacted on ammonia–N ($p < 0.05$). The NT treatments had lower pH but higher LA and LA/AA than LT treatments ($p < 0.05$); moreover, the NT-HD contained greater LA than NT-LD ($p < 0.05$). The ammonia–N content in NT treatments was higher than that in LT-HD but lower than that in LT-LD ($p < 0.05$). The BA and PA contents were not detected with any of treatments (**Table 2**).

The storage temperature mainly affected the crude ash concentration of the silage ($p < 0.05$), and the storage temperature and ensiling density had main effects and interactions on the WSC ($p < 0.05$) (**Table 2**). The LT treatments contained higher WSC than HD treatments ($p < 0.05$); moreover, the WSC in the NT-LD was lower than that in the NT-HD ($p < 0.05$).

Microbial Counts and Bacterial Community in Silage

The storage temperature mainly affected the LAB and yeast counts of silage ($p < 0.05$), and the NT treatments had lower counts of LAB and yeast than the LT treatments ($p < 0.05$; **Table 3**). Molds were not detected with HD treatments; moreover, coliform bacteria were not detected with any of the treatments.

In total, 571,224 raw reads and 536,142 clean reads of the 16S rRNA genes were obtained from 12 silage samples according to sequencing data (**Table 3**). The average number of clean reads was 44,679 for each sample.

Storage temperature mainly affected OTUs, Ace and Chao 1 indexes, and coverage ($p < 0.05$); moreover, storage temperature and ensiling density interacted on Ace indexes ($p < 0.05$) (**Table 3**). The LT-LD had lower OTUs than the NT-TD ($p < 0.05$) and contained lower Ace and Chao 1 indexes but higher coverage than NT treatments ($p < 0.05$). Moreover, the NT-LD had higher Ace and Chao 1 indexes than the LT treatments ($p < 0.05$).

The NT treatments had clearly separated bacterial communities from LT treatments (**Figure 1**). The LT-LD and LT-HD had the separated bacterial communities; furthermore, the bacterial communities of NT-TD and NT-LD were clustered together.

Lactobacillus was the most dominant genus in LT-LD, LT-HD, NT-LD, and NT-HD, with abundances of 66.85, 57.16, 60.16, and 60.70%, respectively (**Figure 2**). The other common main bacterial genera (>1% abundance) were *Leuconostoc*, *Pantoea*, *Erwinia*, *Weissella*, *Rahnella*, and unclassified *Lactobacillales* in LT treatments and *Leuconostoc*, *Pantoea*, *Erwinia*, *Pseudomonas*, *Weissella*, *Rahnella*, *Enterobacter*, *Lactococcus*, and *Acinetobacter* in NT treatments. Compared with LT treatments, NT treatments had lower *Leuconostoc* but higher *Pseudomonas* and *Enterobacter* ($p < 0.05$) (**Figure 3**).

Nitrate and Nitrite Concentrations of Silage

Storage temperature and ensiling density had the main effects and interactions on the nitrate content and nitrate degradation rate of silage ($p < 0.05$; **Table 4**). The LT-LD contained more nitrate and lower nitrate degradation rate than other treatments ($p < 0.05$). Nitrite was not detected in any of the silage.

Correlation Between Nitrate and the Fermentation Quality and Bacterial Community

The nitrate concentration in silage was positively correlated with ammonia–N and pH ($p < 0.05$) and negatively correlated with *Pantoea*, *Pseudomonas*, *Enterobacter*, and *Lactococcus* ($p < 0.05$; **Figures 4A,B**). Moreover, the nitrate degradation rate was positively correlated with LA, LA/AA, *Pantoea*, *Pseudomonas*, *Enterobacter*, and *Lactococcus* ($p < 0.05$) and negatively correlated with pH and ammonia–N ($p < 0.05$).

TABLE 1 | Chemical composition of sorghum-sudangrass before ensiling ($n = 3$).

Items	Sorghum-sudangrass	SEM
DM (g/kg FW)	252	6.84
Crude protein (g/kg DM)	68.9	1.15
Neutral detergent fiber (g/kg DM)	564	4.85
Acid detergent fiber (g/kg DM)	334	7.35
Water soluble carbohydrates (g/kg DM)	168	5.29
Nitrate (mg/kg DM)	2,688	117.34
Nitrite (mg/kg DM)	ND	–

SEM, standard error of the mean; ND, not detected.

DISCUSSION

Material Characteristics and Silage Quality

In the present study, the fresh sorghum-sudangrass contained sufficient WSC (168 g/kg DM) as a fermentation substrate for microorganisms during the fermentation process, as reflected by the low pH and high LA content in NT treatments, with more than 24.0 g/kg of residual WSC (**Tables 1**, **2**). These were in line with the results in the work of Han et al. (2015) and Diepersloot et al. (2021). Nevertheless, the fresh materials in the present study

TABLE 2 | Fermentation quality and nutrient composition of sorghum-sudangrass silage (n = 3).

Items		LT		NT		SEM	Significance		
		LD	HD	LD	HD		T	D	T × D
Fermentation quality	pH	3.99^{a}	3.99^{a}	3.55^{b}	3.52^{b}	0.07	**	NS	NS
	Lactic acid (LA, g/kg DM)	28.3^{c}	31.5^{c}	63.1^{b}	74.0^{a}	6.06	**	*	NS
	Acetic acid (AA, g/kg DM)	20.1	17.8	19.7	22.3	0.93	NS	NS	NS
	Propionic acid (g/kg DM)	ND	ND	ND	ND	–	–	–	–
	Butyric acid (g/kg DM)	ND	ND	ND	ND	–	–	–	–
	LA/AA	1.41^{b}	1.81^{b}	3.21^{a}	3.36^{a}	0.26	**	NS	NS
	Ammonia–N (g/kg TN)	58.8^{a}	33.7^{c}	43.5^{b}	43.6^{b}	2.84	NS	*	**
Nutrient composition	Dry matter (g/kg FW)	245	262	274	280	10.5	NS	NS	NS
	Crude protein (g/kg DM)	64.6	66.0	60.5	62.7	1.11	NS	NS	NS
	Water soluble carbohydrates (g/kg DM)	67.6^{a}	68.2^{a}	24.0^{c}	45.8^{b}	5.79	**	*	*
	Neutral detergent fiber (g/kg DM)	568	582	574	590	4.00	NS	NS	NS
	Acid detergent fiber (g/kg DM)	366	371	362	378	6.37	NS	NS	NS
	Crude ash (g/kg DM)	73.9^{ab}	75.2^{a}	70.2^{ab}	69.6^{b}	0.85	*	NS	NS

LT, storage temperature at 10°C; NT, storage temperature at 25°C; LD, ensiling density at 550 kg/m^3; HD, ensiling density at 650 kg/m^3.
*Means with different superscripts in the same row (a–c) differ significantly ($p < 0.05$). SEM, standard error of the mean. ND, not detected; *$p < 0.05$; **$p < 0.01$; NS, not significant; T, storage temperature; D, ensiling density; T × D, interactive effect of storage temperature and ensiling density.*

TABLE 3 | Microbial counts, bacterial sequencing data, and alpha diversity of sorghum-sudangrass silage (n = 3).

Items		LT		NT		SEM	Significance		
		LD	HD	LD	HD		T	D	T × D
Microbial counts	Lactic acid bacteria (log_{10} cfu/g FM)	7.08^{a}	6.76^{a}	5.21^{b}	5.47^{b}	0.29	**	NS	NS
	Yeasts (log_{10} cfu/g FM)	6.34^{a}	6.14^{a}	3.98^{b}	4.08^{b}	0.38	**	NS	NS
	Molds (log_{10} cfu/g FM)	2.44	ND	2.33	ND	–	–	–	–
	Coliform bacteria (log_{10} cfu/g FM)	ND	ND	ND	ND	–	–	–	–
Sequencing data	Raw reads	46,103	45,334	52,155	46,816	1,947	NS	NS	NS
	Clean reads	42,211	40,532	50,720	45,251	2,065	NS	NS	NS
Alpha diversity	OTUs	84^{b}	106^{ab}	140^{ab}	146^{a}	11.5	*	NS	NS
	Shannon	1.593	1.908	1.919	1.933	0.085	NS	NS	NS
	Simpson	0.391	0.278	0.289	0.273	0.028	NS	NS	NS
	Ace	129^{c}	204^{bc}	320^{a}	242^{ab}	25.3	**	NS	*
	Chao 1	107^{c}	157^{bc}	234^{a}	210^{ab}	16.7	**	NS	NS
	Coverage	0.9995^{a}	0.9991^{ab}	0.9989^{b}	0.9988^{b}	0.0001	**	NS	NS

LT, storage temperature at 10°C; NT, storage temperature at 25°C; LD, ensiling density at 550 kg/m^3; HD, ensiling density at 650 kg/m^3.
*Means with different superscripts in the same row (a–c) differ significantly ($p < 0.05$). SEM, standard error of the mean. ND, not detected; *$p < 0.05$; **$p < 0.01$; NS, not significant; T, storage temperature; D, ensiling density; T × D, interactive effect of storage temperature and ensiling density.*

had lower DM contents than those in previous studies (252 vs. 254–256 and 349 g/kg) (Han et al., 2015; Diepersloot et al., 2021), because of the different harvesting stages (flag leaf ligule of stem elongation stage vs. after booting stage). Moreover, the nutrient compositions of sorghum-sudangrass at harvesting are also affected by the variety, irrigation levels, and nitrogen doses (Han et al., 2015; Kaplana et al., 2019).

According to the evaluating system for the fermentation quality of silage (Kaiser and Weiss, 2005), the scores with all treatments were 100, and their grade was first in the present study, owing to the lower contents of BA and AA in all silage (<3.0 and <30 g/kg DM, respectively). The normal storage temperature (25°C) might be a good temperature for higher LAB activity during the earlier fermentation process in silage, as reflected by the higher LA and lower pH in NT treatments (**Table 2**). Previous studies also revealed similar results regarding the effect of storage temperature on the fermentation characteristics of whole-plant corn silage (Zhou et al., 2016, 2019; Ferrero et al., 2021). However, the LAB in the final silage might be inhibited by the low pH condition (McDonald et al., 1991), which resulted in lower LAB count in NT treatments (**Table 3**). High ensiling density is favorable for reducing the porosity of forage granules in silos (Pitt and Muck, 1993; Toruk et al., 2009), emerging rapidly anaerobic environment, and mitigating WSC consumption during initial aerobic stage (Borreani et al., 2018). Moreover, in the present study, NT-HD contained greater LA than NT-LD (**Table 2**). These results indicated that HD contributes to the improvement in LAB fermentation in silage.

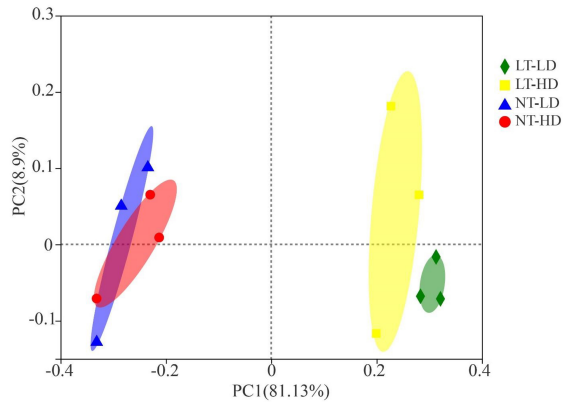

FIGURE 1 | Principal coordinates analysis of the bacterial community for sorghum-sudangrass silage (R^2 = 0.8362, p = 0.003; n = 3). LT, storage temperature at 10°C; NT, storage temperature at 25°C; LD, ensiling density at 550 kg/m^3; HD, ensiling density at 650 kg/m^3.

Lactic acid bacteria have lower activity in silage stored at LTs (Jungbluth et al., 2017), which might cause LT treatments contained lower organic acid concentrations than NT treatments. Nevertheless, the bacterial community in NT and LT treatments was absolutely dominated by homofermentative LAB (*Lactobacillus plantarum*) and heterofermentative LAB (*Lactobacillus brevis*), respectively (**Supplementary Figure 1**), and the LT treatments had more *Leuconostoc*, as heterofermentative LAB (**Figure 3**). Homofermentative LAB produce only LA, whereas heterofermentative LAB produce LA, AA, alcohols, and esters (Kung et al., 2018). These results suggest that, in the present study, the synergy of storage temperature and microbial dominant bacterial species resulted in higher LA and LA/AA in NT treatments than in LT treatments, with no difference in AA among all treatments (**Table 2**). Ammonia–N as a non-protein in silage indicates silage preservation during fermentation (Thomas et al., 1980). In the present study, all silages contained lower ammonia–N than the suggested contents (<60 g/kg TN vs. 80–120 g/kg TN) (Kung et al., 2018), because *Clostridium* activity is inhibited in silage with a pH below 4.2 (Driehuis et al., 2018). This was also reflected by the bacterial community (**Figure 2**). Moreover, Li et al. (2017) reported that the ammonia–N content in oat silage with 168.9 kg DM/m^3 (507 kg FW/m^3) of density increased as a decreasing storage temperature. Similarly, in the present study, LT-LD contained higher ammonia–N than NT-LD (**Table 2**). In the silage stored at low storage temperature, the microorganism has low activity, and the plant respiration is very low during initial aerobic phase; furthermore, there is relatively more air in silage with LD (McDonald et al., 1991; Toruk et al., 2009), and this silage has long the initial aerobic phase and slower fermentation rate. However, the proteolytic enzymes have a significant level of activity remaining under the condition of below 10°C and above pH 5.5 (Spoelstra, 1985). Those suggested that the low storage temperature might have negative effect on the ammonia–N content in silage with low ensiling density (≤500 kg FW/m^3). Brüning et al. (2018) reported that, storing at 12°C, the maize silage with high ensiling density contained less ammonia–N content than that with LD; moreover, in the present study, the LT-HD had lower ammonia–N than LT-LD (**Table 2**). There was no difference in ammonia–N content between NT-LD and NT-HD in the present study (**Table 2**); this was in line to the results of maize and sorghum silages stored at 25–28°C (Sucu et al., 2016). Moreover, the LT-HD had lower ammonia–N than NT-HD in the present study (**Table 2**). Those abovementioned implied that rising ensiling density can decrease the ammonia–N content in final silage stored at low storage temperature, the ensiling density has no effect on ammonia–N content in final silage stored at suitable temperature for fermentation (25–30°C), and reducing storage temperature decreases ammonia–N content in final silage with high ensiling density.

In the present study, the storage temperature and ensiling density had the main effects and interactions on the WSC

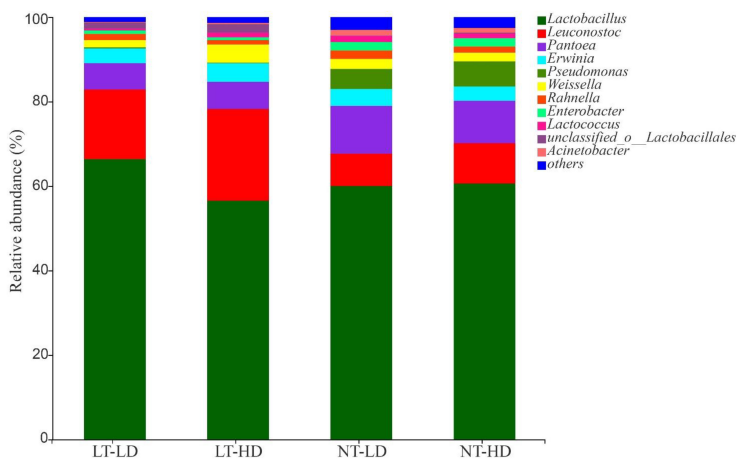

FIGURE 2 | Bacterial community (genus level) of sorghum-sudangrass silage (n = 3). LT, storage temperature at 10°C; NT, storage temperature at 25°C; LD, ensiling density at 550 kg/m^3; HD, ensiling density at 650 kg/m^3.

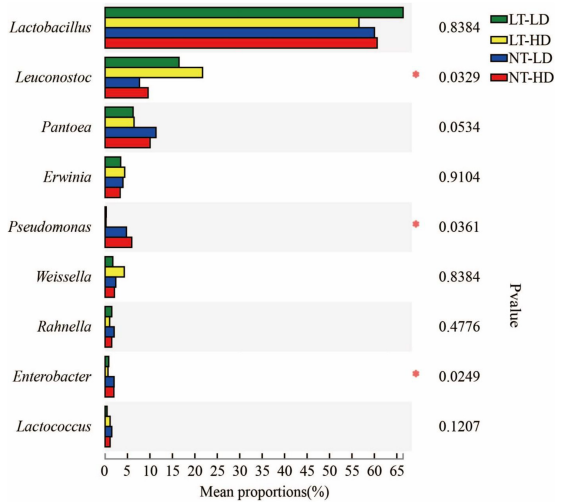

FIGURE 3 | Difference in bacterial community (genus level) of sorghum-sudangrass silage (n = 3). LT, storage temperature at 10°C; NT, storage temperature at 25°C; LD, ensiling density at 550 kg/m^3; HD, ensiling density at 650 kg/m^3. *p < 0.05.

concentration in the final silage (**Table 2**). The NT treatments contained more LA but less WSC than LT treatments (**Table 2**). This indicated that the bacteria in silage stored at 25°C tended to be more vigorous and utilized more WSC during the fermentation process. The reason for this might be that the microorganisms have greater activity in silage stored at NTs (20–30°C) than at LTs (less than 10°C) (Zhou et al., 2016; Jungbluth et al., 2017). Compared with NT-HD, the NT-LD contained less LA and WSC, but there was no difference in AA content (**Tables 2**, **3**), which showed that there might be more residual oxygen and active aerobes consumed more WSC at the early period of fermentation (Sucu et al., 2016; Anésio et al., 2017).

Microbial Counts and Bacterial Community in Silage

In the present study, compared with LT treatments, the NT treatments contained lower counts of LAB and yeasts, lower pH, and higher LA content (**Tables 2**, **3**). These results indicated that some microorganisms in the silage were inhibited during fermentation process under lower pH conditions (McDonald et al., 1991). This was also reflected by the correlation between the LAB and yeast counts and the pH and LA concentration (**Supplementary Figure 2**). Similar results were also reported in other studies (Ren et al., 2019; Wang et al., 2019a). Moreover, the LAB in LT treatments might develop tolerance of LT during fermentation process (60 days after ensiling), owing to specific conditions can contributed to the formation of the unique microorganisms (Pang et al., 2012). Molds were only detected in LD treatments, whereas mold count in HD treatments was below the detection limit (**Table 3**). The reason for this might be that the higher content of oxygen in silage with low ensiling density during the early ensiling period could lead to more mold residues (Tian et al., 2020).

The bacterial communities between LT and NT treatments were completely separated from each other. With low storage temperature, the communities in LD and HD treatments were adjacent to each other and clearly separated; however, the communities in NT-LD and NT-HD clustered together (**Figure 2**). These results indicated that storage temperature is the most important factor affecting the bacterial community, whereas ensiling density has less influence. Guan et al. (2020) also revealed that the storage temperature mainly affects the bacterial community of whole-plant corn silage. Zhou et al. (2016) and Wang et al. (2019a) further found that temperature treatment could cause the emergence of a separate bacterial community. These results indicated that storage temperature and ensiling density could induce the changes in the bacterial community structure of silage.

In the present study, *Lactobacillus* dominated the bacterial community of sorghum-sudangrass silage, with the highest abundance (**Figure 2**). Moreover, *Lactobacillus* is closely related to the LA content and pH of silage (Ni et al., 2018; Wang et al., 2019a) and is a characteristic of good fermentation (Guan et al., 2020). These results also explained the satisfactory fermentation quality of the silage in the present study. There was no difference in *Lactobacillus* in sorghum-sudangrass silage between high and LD (**Figure 3**); however, Sun et al. (2021a) reported that increasing density could enhance the abundance of *Lactobacillus* in barley silage. This difference might be due to differences in characteristics of forage before ensiling. Compared with NT treatments, the LT treatments contained more *Leuconostoc* and *L. brevis* as heterofermentative LAB (**Figure 2** and **Supplementary Figure 1**), which showed that heterofermentative LAB might be highly resistant to LT. In addition, the LT treatments had lower LA/AA and higher pH than NT treatments (**Table 2**). These results suggested that heterofermentative LAB

TABLE 4 | Nitrate concentration, nitrate degradation rate, and nitrite concentration of sorghum-sudangrass silage (n = 3).

Items	LT		NT		SEM	Significance		
	LD	HD	LD	HD		T	D	T × D
Nitrate (mg/kg DM)	1480^a	868^b	783^b	645^b	103	**	**	*
Nitrate degradation rate (%)	44.94^b	67.72^a	70.90^a	76.02^a	3.83	**	**	*
Nitrite (mg/kg DM)	ND	ND	ND	ND	–	–	–	–

LT, storage temperature at 10°C; NT, storage temperature at 25°C; LD, ensiling density at 550 kg/m^3; HD, ensiling density at 650 kg/m^3.
*Means with different superscripts in the same row (a–c) differ significantly (p < 0.05). SEM, standard error of the mean. ND, not detected; *p < 0.05; **p < 0.01; T, storage temperature; D, ensiling density; T × D, interactive effect of storage temperature and ensiling density.*

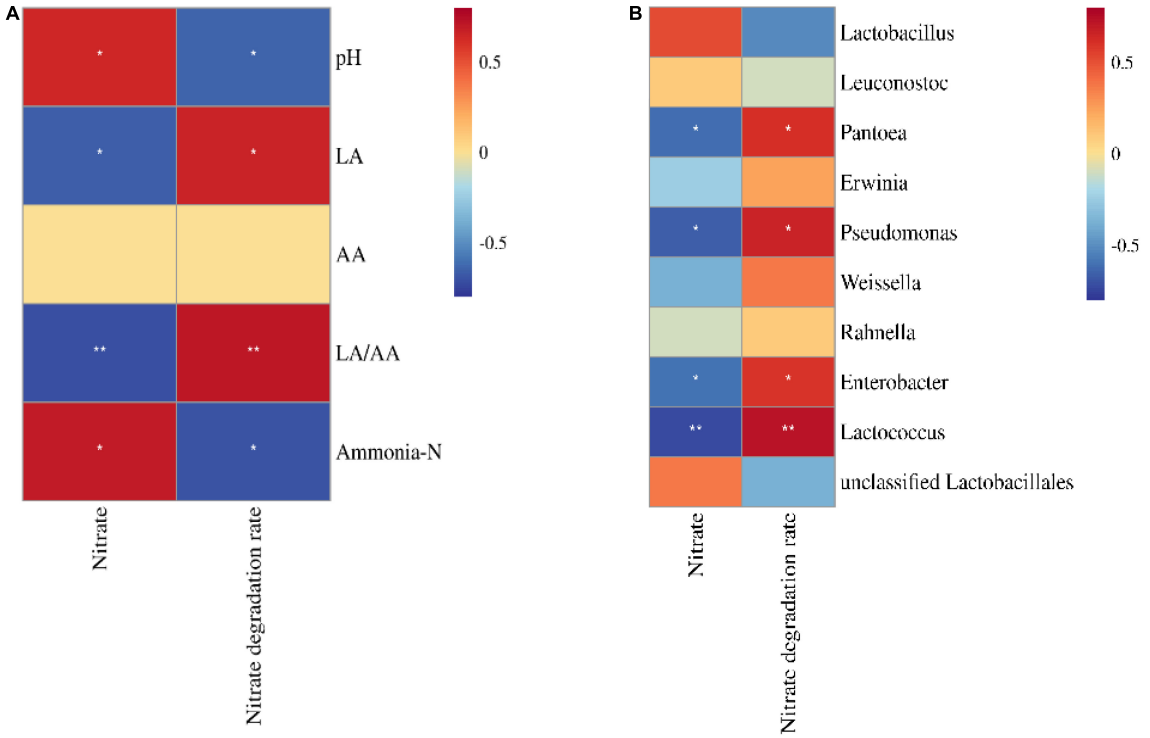

FIGURE 4 | Correlation heatmap of nitrate and nitrate degradation rate with fermentation parameters **(A)** and the bacterial community (top 10 bacterial genera, **B**) (n = 12). LA, lactic acid; AA, acetic acid. *$p < 0.05$; **$p < 0.01$.

might dominate the fermentation process of sorghum-sudangrass silage under low storage temperature (Cai et al., 1998). In the present study, *Pantoea* was one of the main bacterial genera (6.18–11.35%) in sorghum-sudangrass silage; moreover, *Pantoea* exhibits increasing abundance as the most dominant bacterial genus during the initial aerobic phase of whole-plant corn silage (Sun et al., 2021a). However, the effect of *Pantoea* on silage is not clear and requires further study. The NT treatments had higher *Pseudomonas* than LT treatments in the present study (**Figure 3**); this genus was also detected in mulberry leaf silage and Moringa oleifera leaf silage with high abundance (Wang et al., 2019b,c). The silage subjected to high temperature contained more *Pseudomonas* than silage at lower temperature (Wang et al., 2019c). Those indicated that the emergence of *Pseudomonas* in silage is likely related to the variety of raw materials and is also affected by temperature. The optimum temperature for *Enterobacter* proliferation is quite high (Weiss et al., 2016), which was regarded as one of the reasons for its lower abundance at 10°C. Similar results were also reported by Zhou et al. (2019).

Nitrate and Nitrite Concentrations of Silage

In the present study, fresh sorghum-sudangrass did not cause toxicity according to Roozeboom et al. (2019) (nitrate concentration <3,000 mg/kg). During fermentation, nitrite and nitric oxide, as intermediate products for nitrate degradation, can inhibit the growth of undesirable bacteria in the silage (Knicky and Sporndly, 2009), which explained the lack of *Clostridium* detected in silage in the present study (**Figure 2**). Nitrate begins to reduce immediately after ensiling, and nitrite and nitric oxide accumulate temporarily and disappear within 1 or 2 weeks (Spoelstra, 1985), as reflected by the lack of nitrite detected in silage in the present study (**Table 4**). The nitrate degradation rate in LT-LD was lower than that in LT-HD, but there was not difference between NT-LD and NT-HD (**Table 4**). Those indicated that high ensiling density improved nitrate degradation in the silage stored at LT but did not affect nitrate degradation at NT. Moreover, the nitrate degradation rate correlated positively with LA and LA/AA and positively with pH and ammonia–N (**Figure 4A**), suggesting that satisfactory fermentation quality contributed to nitrate degradation in silage. A previous study revealed that enterobacteria in silage are one of the main microbes that degrade nitrate during the fermentation process (Driehuis et al., 2018). In the present study, *Pantoea*, *Pseudomonas*, and *Enterobacter*, which are enterobacteria, were positively correlated with the nitrate degradation rate (**Figure 4B**); *Pseudomonas* and *Enterobacter* in NT treatments were more abundance than those in LT treatments (**Figure 3**). In addition, the optimal storage temperature for enterobacteria is higher than that for LAB (Weiss et al., 2016) and enterobacteria counts are greater in silage stored at 20°C compared with those at 10°C (Zhou et al., 2016). Those also explain that, in the present study, nitrate degradation was greater in NT treatments and influenced by the storage temperature (**Table 3**).

CONCLUSION

Sorghum-sudangrass silage has satisfactory fermentation quality and is safe in terms of the nitrate concentration. The silage stored at 25°C and with a density of 650 kg/m^3 had better fermentation quality and high nitrate degradation. *Lactobacillus* dominated the bacterial community, and storage temperature was the main factor affecting the bacterial community of the silage. The satisfactory fermentation quality contributed to the nitrate degradation of silage. *Pantoea*, *Pseudomonas*, and *Enterobacter* were the main bacterial genera degrading the nitrate in sorghum-sudangrass silage.

DATA AVAILABILITY STATEMENT

The original contributions presented in the study are included in the article/**Supplementary Material**, further inquiries can be directed to the corresponding author.

AUTHOR CONTRIBUTIONS

CB, JS, ZY, and YX designed the study and wrote the manuscript. CB, GP, RL, WN, JY, and ZL performed the experiments. JS, ZY, and YX reviewed and edited the manuscript. CB, GP, RL, and WN analyzed the data. ZY and YX funded and supervised the experiments. All authors reviewed the manuscript.

FUNDING

This work was funded by the National Natural Science Foundation of China (31872422, 31772674, and 32160342), the Inner Mongolia Science and Technology Plan (2020GG0049), and the National Forage Industry Technology System (CARS-34).

SUPPLEMENTARY MATERIAL

The Supplementary Material for this article can be found online at: https://www.frontiersin.org/articles/10.3389/fmicb.2022.828320/full#supplementary-material

Supplementary Figure 1 | Bacteria community (species level) of sorghum-sudangrass silage (n = 3). LT, storage temperature at 10°C; NT, storage temperature at 25°C; LD, ensiling density at 550 kg/m^3; HD, ensiling density at 650 kg/m^3.

Supplementary Figure 2 | Correlation networks among microbial counts and fermentation quality (n = 12). p-Value < 0.05.

REFERENCES

Anésio, A. H. C., Santos, M. V., da Silva, L. D., Silveira, R. R., Braz, T. G. S., and Pereira, R. C. (2017). Effects of ensiling density on chemical and microbiological characteristics of sorghum silage. *J. Anim. Feed Sci.* 26, 65–69. doi: 10.22358/jafs/69270/2017

AOAC (1990). *Official Methods of Analysis, Association of Official Analytical Chemists*, 15th Edn. Artington, VA: AOAC.

Borreani, G., Tabacco, E., Schmidt, R. J., Holmes, B. J., and Muck, R. E. (2018). Silage review: factors affecting dry matter and quality losses in silages. *J. Dairy Sci.* 101, 3952–3979. doi: 10.3168/jds.2017-13837

Broderick, G. A., and Kang, J. H. (1980). Automated simultaneous determination of ammonia and total amino acids in ruminal fluid and in vitro media. *J. Dairy Sci.* 63, 64–75. doi: 10.3168/jds.S0022-0302(80)82888-8

Brüning, D., Gerlach, K., Weiß, K., and Südekum, K.-H. (2018). Effect of compaction, delayed sealing and aerobic exposure on maize silage quality and on formation of volatile organic compounds. *Grass Forage Sci.* 73, 53–66. doi: 10.1111/gfs.12288

Cai, Y., Benno, Y., Ogawa, M., and Kumai, S. (1999). Effect of applying lactic acid bacteria isolated from forage crops on fermentation characteristics and aerobic deterioration of silage. *J. Dairy Sci.* 82, 520–526. doi: 10.3168/jds.S0022-0302(99)75263-X

Cai, Y. M., Benno, Y., Ogawa, M., Ohmomo, S., and Nakase, T. (1998). Influence of *Lactobacillus* spp. from an inoculant and of *Weissella* and *Leuconostoc* spp. from forage crops on silage fermentation. *Appl. Environ. Microbiol.* 64, 2982–2987. doi: 10.1128/aem.64.8.2982-2987.1998

Dann, H. M., Grant, R. J., Cotanch, K. W., Thomas, E. D., Ballard, C. S., and Rice, R. (2008). Comparison of brown midrib sorghum-sudangrass with corn silage on lactational performance and nutrient digestibility in Holstein dairy cows. *J. Dairy Sci.* 91, 663–672. doi: 10.3168/jds.2007-0521

Diepersloot, E. C., Pupo, M. R., Ghizzi, L. G., Gusmão, J. O., Heinzen, C. Jr., McCary, C. L., et al. (2021). Effects of microbial inoculation and storage length on fermentation profile and nutrient composition of whole-plant sorghum silage of different varieties. *Front. Microbiol.* 12:660567.

Drewnoski, M. E., Anderson, B. E., Kononoff, P. J., and Reynolds, M. B. (2019). *Nitrates in Livestock Feeding. C1779, Animal Agriculture / Beef.* Available online at: https://extensionpubs.unl.edu/publication/9000016365158/nitrates-in-livestock-feeding (accessed August 2021).

Driehuis, F., Wilkinson, J. M., Jiang, Y., Ogunade, I., and Adesogan, A. T. (2018). Silage review: animal and human health risks from silage. *J. Dairy Sci.* 101, 4093–4110. doi: 10.3168/jds.2017-13836

Ferrero, F., Tabacco, E., Piano, S., Casale, M., and Borreani, G. (2021). Temperature during conservation in laboratory silos affects fermentation profile and aerobic stability of corn silage treated with *Lactobacillus buchneri*, *Lactobacillus hilgardii*, and their combination. *J. Dairy Sci.* 104, 696–1713. doi: 10.3168/jds.2020-18733

Guan, H., Shuai, Y., Yan, Y., Ran, Q., Wang, X., Li, D., et al. (2020). Microbial community and fermentation dynamics of corn silage prepared with heat-resistant lactic acid bacteria in a hot environment. *Microorganisms* 8:719. doi: 10.3390/microorganisms8050719

Han, L. Y., Li, J., Na, R. S., Yu, Z., and Zhou, H. (2015). Effect of two additives on the fermentation, in vitro digestibility and aerobic security of Sorghum-sudangrass hybrid silages. *Grass Forage Sci.* 70, 185–194. doi: 10.1111/gfs.12092

Harada, H., Yoshimura, Y., Sunaga, Y., and Hatanaka, T. (2000). Variations in nitrogen uptake and nitrate-nitrogen concentration among sorghum groups. *Soil Sci. Plant Nutr.* 46, 97–104. doi: 10.1080/00380768.2000.10408766

Holman, J. D., Obour, A. K., and Mengel, D. B. (2019). Nitrogen application effects on forage sorghum production and nitrate concentration. *J. Plant Nutr.* 42, 2794–2804. doi: 10.1080/01904167.2019.1659321

Jungbluth, K. H., Trimborn, M., Maack, G., Büscher, W., Li, M., Cheng, H., et al. (2017). Effects of three different additives and two different bulk densities on maize silage characteristics, temperature profiles, co2 and o2–dynamics in small scale silos during aerobic exposure. *Appl. Sci.* 7:545. doi: 10.3390/app7060545

Kaiser, E., and Weiss, K. (2005). "A new systems for the evaluation of the fermentation quality of silage: silage production and utilization," in *Proccedings of the XIV International Silage Conference, a satellite workshop of the XX International Grassland Congress. Belfast, Northern Ireland, Proceedings*, (Belfast).

Kaplana, M., Karab, K., Unlukarac, A., Kaled, H., Buyukkilic Beyzie, S., Varolc, I. S., et al. (2019). Water deficit and nitrogen affects yield and feed value of sorghum sudangrass silage. *Agr. Water Manage.* 218, 30–36.

Khorasani, G. R., Jedel, P. E., Helm, J. H., and Kennelly, J. J. (1997). Influence of stage of maturity on yield components and chemical composition of cereal grain silages. *Can. Vet. J. Rev. Vet. Can.* 77, 259–267. doi: 10.4141/A96-034

Kim, S. C., and Adesogan, A. T. (2006). Influence of ensiling temperature, simulated rainfall, and delayed sealing on fermentation characteristics and

aerobic stability of corn silage. *J. Dairy Sci.* 89, 3122–3132. doi: 10.3168/jds.S0022-0302(06)72586-3

Knicky, M., and Sporndly, R. (2009). Sodium benzoate, potassium sorbate and sodium nitrite as silage additives. *J. Sci. Food Agric.* 89, 2659–2667. doi: 10.1002/jsfa.3771

Kung, L. Jr., Shaver, R. D., Grant, R. J., and Schmidt, R. J. (2018). Silage review: interpretation of chemical, microbial, and organoleptic components of silages. *J. Dairy Sci.* 101, 4020–4033. doi: 10.3168/jds.2017-13909

Li, P., Gou, W., Zhang, Y., Yang, F., You, M., Bai, S., et al. (2017). Fluctuant storage temperature increased the heterogeneous distributions of pH and fermentation products in large round bale silage. *Grassl Sci.* 65, 155–161. doi: 10.1111/grs.12232

McCary, C. L., Vyas, D., Faciola, A. P., and Ferraretto, L. F. (2020). Graduate student literature review: current perspectives on whole-plant sorghum silage production and utilization by lactating dairy cows. *J. Dairy Sci.* 103, 5783–5790. doi: 10.3168/jds.2019-18122

McDonald, P., Henderson, A. R., and Heron, S. J. E. (1991). *The Biochemistry of Silage*. Marlow: Chalcombe Publications.

Nazar, M., Wang, S., Zhao, J., Dong, Z., Li, J., Kaka, N. A., et al. (2021). Abundance and diversity of epiphytic microbiota on forage crops and their fermentation characteristic during the ensiling of sterile sudan grass. *World J. Microb. Biot.* 37:27. doi: 10.1007/s11274-020-02991-3

Ni, K. K., Zhao, J. Y., Zhu, B. G., Su, R. N., Pan, Y., Ma, J. K., et al. (2018). Assessing the fermentation quality and microbial community of the mixed silage of forage soybean with crop corn or sorghum. *Bioresour. Technol.* 265, 563–567. doi: 10.1016/j.biortech.2018.05.097

Pang, H., Tan, Z., Qin, G., Wang, Y., Li, Z., and Jin, Q. (2012). Phenotypic and phylogenetic analysis of lactic acid bacteria isolated from forage crops and grasses in the Tibetan Plateau. *J. Microbiol.* 50, 63–71. doi: 10.1007/s12275-012-1284-5

Pitt, R. E., and Muck, R. E. (1993). A diffusion model of aerobic deterioration at the exposed face of bunker silos. *J. Agric. Eng. Res.* 55, 11–26. doi: 10.1006/jaer.1993.1029

Rashid, G., Avais, M., Ahmad, S. S., Mushtaq, M. H., Ahmed, R., Ali, M., et al. (2019). Influence of nitrogen fertilizer on nitrate contents of plants: a Prospective aspect of nitrate poisoning in dairy animals. *Pak. J. Zool.* 51, 249–255. doi: 10.17582/journal.pjz/2019.51.1.249.255

Ren, F., He, R., Zhou, X., Gu, Q., Xia, Z., Liang, M., et al. (2019). Dynamic changes in fermentation profiles and bacterial community composition during sugarcane top silage fermentation: a preliminary study. *Bioresour. Technol.* 285:121315. doi: 10.1016/j.biortech.2019.121315

Roozeboom, K., Blasi, D., and Mengel, D. (2019). *Nitrate toxicity. Kansas State Univ. Coop. Ext. MF3029.* Available online at: http://bookstore.ksre.ksu.edu/pubs/mf3029.pdf (accessed August 2021).

Spoelstra, S. F. (1985). Nitrate in silage. *Grass Forage Sci.* 40, 1–11. doi: 10.1111/j.1365-2494.1985.tb01714.x

Sucu, E., Kalkan, H., Canbolat, O., and Filya, I. (2016). Effects of ensiling density on nutritive value of maize and sorghum silages. *Rev. Bras. Zootecn.* 45, 596–603. doi: 10.1590/s1806-92902016001000003

Sun, L., Na, N., Li, X., Li, Z., Wang, C., Wu, X., et al. (2021a). Impact of packing density on the bacterial community, fermentation, and in vitro digestibility of whole-crop barley silage. *Agriculture* 11:672. doi: 10.3390/agriculture11070672

Sun, L., Bai, C., Xu, H., Na, N., Jiang, Y., Yin, G., et al. (2021b). Succession of bacterial community during the initial aerobic, intense fermentation, and stable phases of whole-plant corn silages treated with lactic acid bacteria suspensions prepared from other silages. *Front. Microbiol.* 12:655095. doi: 10.3389/fmicb.2021.655095

Thomas, P. C., Chamberlain, D. G., Kelly, N. C., and Wait, M. K. (1980). The nutritive value of silages digestion of nitrogenous constituents in sheep receiving diets of grass-silage and grass silage and barley. *Br. J. Nutr.* 43, 469–479. doi: 10.1079/BJN19800114

Thomas, T. A. (1977). An automated procedure for the determination of soluble carbohydrates in herbage. *J. Sci. Food Agric.* 28, 639–642. doi: 10.1002/jsfa.2740280711

Tian, J., Xu, N., Liu, B., Huan, H., Gu, H., Dong, C., et al. (2020). Interaction effect of silo density and additives on the fermentation quality, microbial counts, chemical composition and in vitro degradability of rice straw silage. *Bioresour. Technol.* 297:122412. doi: 10.1016/j.biortech.2019.122412

Toruk, F., Gonulol, E., Ulger, P., and Kocabiyik, H. (2009). Dsensity, porosity and permeability rates of sunflower silage under different compaction conditions. *J. Anim. Vet. Adv.* 8, 1873–1877. doi: 10.1016/j.fsi.2009.06.017

Van Soest, P. J., Robertson, J. B., and Lewis, B. A. (1991). Methods for dietary fiber, neutral detergent fiber, and nonstarch polysaccharides in relation to animal nutrition. *J. Dairy Sci.* 74, 3583–3597. doi: 10.3168/jds.S0022-0302(91)78551-2

Wang, C., Han, H., Sun, L., Na, N., Xu, H., Chang, S., et al. (2021). Bacterial succession pattern during the fermentation process in whole-plant corn silage processed in different geographical areas of Northern China. *Processes* 9:900. doi: 10.3390/pr9050900

Wang, C., He, L. W., Xing, Y. Q., Zhou, W., Yang, F. Y., Chen, X. Y., et al. (2019a). Effects of mixing *Neolamarckia cadamba* leaves on fermentation quality, microbial community of high moisture alfalfa and stylo silage. *Microb. Biotechnol.* 12, 869–878. doi: 10.1111/1751-7915.13429

Wang, M., Xu, S., Wang, T., Jia, T., Xu, Z., Wang, X., et al. (2018). Effect of inoculants and storage temperature on the microbial, chemical and mycotoxin composition of corn silage. *Asian Australas. J. Anim. Sci.* 31, 1903–1912. doi: 10.5713/ajas.17.0801

Wang, Y., Chen, X. Y., Wang, C., He, L. W., Zhou, W., Yang, F. Y., et al. (2019b). The bacterial community and fermentation quality of mulberry (*Morus alba*) leaf silage with or without *Lactobacillus casei* and sucrose. *Bioresour. Technol.* 293:122059. doi: 10.1016/j.biortech.2019.122059

Wang, Y., He, L., Xing, Y., Zhou, W., Pian, R., Yang, F., et al. (2019c). Bacterial diversity and fermentation quality of *Moringa oleifera* leaves silage prepared with lactic acid bacteria inoculants and stored at different temperatures. *Bioresour. Technol.* 284, 349–358. doi: 10.1016/j.biortech.2019.03.139

Weinberg, Z. G., Szakacs, G., Ashbell, G., and Hen, Y. (1998). The effect of temperature and *Lactobacillus amylovorus* and *Lact. plantarum*, applied at ensiling, on wheat silage. *J. Appl. Microbiol.* 84, 404–408. doi: 10.1046/j.1365-2672.1998.00361.x

Weiss, K., Kroschewski, B., and Auerbach, H. (2016). Effects of air exposure, temperature and additives on fermentation characteristics, yeast count, aerobic stability and volatile organic compounds in corn silage. *J. Dairy Sci.* 99, 8053–8069. doi: 10.3168/jds.2015-10323

Weissbach, F., and Strubelt, C. (2008). Correcting the dry matter content of grass silages as a substrate for biogas production. *J. Agric. Eng.* 63:210.

Zhang, H., Redmon, L., Fuhrman, J. K., and Springer, T. (1999). Quick nitrate test for hybrid sudangrass and pearmillet hays. *Commun. Soil Sci. Plant Anal.* 30, 1573–1582. doi: 10.1080/00103629909370309

Zhang, Q., Yu, Z., Wang, X., and Tian, J. (2018). Effects of inoculants and environmental temperature on fermentation quality and bacterial diversity of alfalfa silage. *Anim. Sci. J.* 89, 1085–1109. doi: 10.1111/asj.12961

Zhou, Y., Drouin, P., and Lafreniere, C. (2016). Effect of temperature (5 − 25 °C) on epiphytic lactic acid bacteria populations and fermentation of whole-plant corn silage. *J. Appl. Microbiol.* 121, 657–671. doi: 10.1111/jam.13198

Zhou, Y., Drouin, P., and Lafreniere, C. (2019). Effects on microbial diversity of fermentation temperature (10 °C and 20 °C), long-term storage at 5 °C, and subsequent warming of corn silage. Asian Australas. *J. Anim. Sci.* 32, 1528–1539. doi: 10.5713/ajas.18.0792

Conflict of Interest: ZL is employed by Inner Mongolia Sihai Agriculture and Animal Husbandry Technology Co., Ltd.

The remaining authors declare that the research was conducted in the absence of any commercial or financial relationships that could be construed as a potential conflict of interest.

Publisher's Note: All claims expressed in this article are solely those of the authors and do not necessarily represent those of their affiliated organizations, or those of the publisher, the editors and the reviewers. Any product that may be evaluated in this article, or claim that may be made by its manufacturer, is not guaranteed or endorsed by the publisher.

frontiers in Microbiology

ORIGINAL RESEARCH
published: 18 February 2022
doi: 10.3389/fmicb.2021.802035

The Combination Analysis Between *Bacillus thuringiensis* Sip1Ab Protein and Brush Border Membrane Vesicles in Midgut of *Colaphellus bowringi* Baly

Dengtian Cao[1†], Changyixin Xiao[1†], Qian Fu[1†], Xinbo Liu[1], Rongmei Liu[1], Haitao Li[1,2] and Jiguo Gao[1*]*

[1] College of Life Sciences, Northeast Agricultural University, Harbin, China, [2] State Key Laboratory for Biology of Plant Diseases and Insect Pests, Institute of Plant Protection, Chinese Academy of Agricultural Sciences, Beijing, China

OPEN ACCESS

Edited by:
Ying Ma,
University of Coimbra, Portugal

Reviewed by:
Fengliang Jin,
South China Agricultural University, China
Dennis Ken Bideshi,
California Baptist University, United States

***Correspondence:**
Haitao Li
lihaitao@neau.edu.cn
Jiguo Gao
gaojiguo1961@hotmail.com

[†] *These authors have contributed equally to this work*

Specialty section:
This article was submitted to Microbial Symbioses, a section of the journal Frontiers in Microbiology

Received: *26 October 2021*
Accepted: *29 December 2021*
Published: *18 February 2022*

Citation:
Cao D, Xiao C, Fu Q, Liu X, Liu R, Li H and Gao J (2022) The Combination Analysis Between Bacillus thuringiensis Sip1Ab Protein and Brush Border Membrane Vesicles in Midgut of Colaphellus bowringi Baly. Front. Microbiol. 12:802035. doi: 10.3389/fmicb.2021.802035

The secretory insecticidal protein Sip1Ab and crystal protein Cry8Ca from *Bacillus thuringiensis* (Bt) are widely recognized for their coleopteran insecticidal activities. It is worthwhile to investigate the insecticidal mechanisms of these two proteins against *Colaphellus bowringi* Baly, which is a serious pest of cruciferous vegetables in China and other Asian countries. To that end, the genes encoding the Sip1Ab and Cry8Ca proteins were amplified from the strain QZL38 genome, then expressed in *Escherichia coli*, after which bioassays were conducted in *C. bowringi* larvae. After feeding these two proteins, the histopathological changes in the midguts of *C. bowringi* larvae were observed using transmission electron microscopy (TEM), and the Brush Border Membrane Vesicle (BBMV) was extracted for competition binding assays. TEM showed that ingestion of Sip1Ab caused a significant reduction in growth of the larvae, disruption of midgut microvilli, and expansion of intercellular spaces. Competition binding assays demonstrated that Sip1Ab bound to *C. bowringi* BBMV with a high binding affinity. However, a mixture of the two proteins in equal proportions showed no significant difference in insecticidal activity from that of Sip1Ab. These results could provide a molecular basis for the application of Sip1Ab in coleopteran insect control and contribute to the study of the Sip1Ab insecticidal mechanism as well.

Keywords: *Colaphellus bowringi*, Sip, *Bacillus thuringiensis*, BBMV, insecticidal mechanism, competition binding assay

INTRODUCTION

The cabbage beetle *Colaphellus bowringi* Baly (Coleoptera: Chrysomelidae) is a serious insect pest of crucifers in mountainous areas of China (Xue et al., 2002). Moreover, the application of chemical pesticides does not always effectively manage it (Gao et al., 2011; Shu et al., 2013).

Bacillus thuringiensis (Bt) is a Gram-positive bacterium belonging to the *Bacillus cereus* family. It can produce insecticidal proteins harmless to humans and the environment during growth and metabolism (Gómez et al., 2020). According to the protein location and secretion mode, these proteins are characterized as δ-endotoxins or exotoxins (Singh et al., 2021).

The δ-endotoxin is a protein with crystal structure encoded by the *crystal* (*cry*) and *cytolitic* (*cyt*) genes (Swiecicka et al., 2008). Current research shows that many *cry* genes have insecticidal activity against coleopteran pests, including *cry3*, *cry7*, *cry8*, *cry18*, *cry23*, *cry37*, and *cry43*. The *cry8* genes are currently the most studied, since they have specific insecticidal activity against many coleopteran insects, for example, the beetle family, the leaf beetle family, the weevil family, and so on (Jiang et al., 2017). In 1994, Beard et al. cloned a new insecticidal gene named *cry8ca1* from a *B. thuringiensis* strain with high toxicity to coleopteran beetles for the first time (Beard et al., 2001). On the basis of the established PCR-RFLP identification system of *cry8* genes, Liu and co-workers have cloned a novel *cry8C* gene from strain HBF-1, designated *cry8ca2* (AY518201) (Liu et al., 2004). Wu's Laboratory has established a purification method for the Cry8Ca2 active toxin, and bioassay results have suggested that the insecticidal protein had good activity against the larvae of *Anomala corpulenta* and *Anomala exoleta* Fald (Wu et al., 2007). To date, a series of Cry8 proteins which contain about 1,200 amino acids, with the molecular weight of approximately 130 kDa, have been identified to have the high insecticidal activity to coleopteran pests (Noguera and Ibarra, 2010).

Exotoxin is a metabolite which is secreted outside the cell during metabolism of Bt, such as Vegetative insecticidal protein (Vip) and Secreted insecticidal protein (Sip) (Palma et al., 2014). It is now well established from a number of studies that Sip has the insecticidal activity against coleopteran larvae. Donovan et al. (2006) reported that Bt strain EG2158 secreted the coleopteran active protein Sip1Aa, which had insecticidal activity against larvae of the potato beetle (*Leptinotarsa decemlineata*), the southern corn rootworm (*Diabrotica undecimpunctata howardi*), and the western corn rootworm (*Diabrotica virgifera virgifera*). The gene encoding Sip1Aa, which has been reported as the first member of Bt secreted proteins having activity against coleopteran larvae, was 1,104 bp in length and encoded a polypeptide of 367 amino acids (Donovan et al., 2006). In 2012, Liu and co-workers successfully cloned and identified another *sip* gene from strain QZL26 encoding a 39 kDa protein, which shared a 91.83% identity with Sip1Aa (Liu et al., 2012). In 2015, our laboratory identified a *sip* gene from strain DQ89, which was 1,095 bp and encoded a protein of 364 amino acids with a calculated mass of 42 kDa (Zhang et al., 2015). The protein expressed by this gene showed high toxicity to *C. bowringi* with a lethal concentration 50 (LC_{50}) of 1.542 μg/ml (Zhang et al., 2015). Sha et al. (2018) showed that Bt strain QZL38 contained a new *sip* gene designated as *sip1Ab* from 540 soil samples, which contained an open reading frame of 1,095 bp encoding a 364 amino acid polypeptide. The results of bioassays of four truncated mutant proteins indicated that the truncated protein SipA, from which the signal peptide (the first 30 amino acids) was removed, showed insecticidal activity against *C. bowringi*, with an LC_{50} of 1.078 μg/ml and showed no significant differences compared with Sip (Sha et al., 2018).

In previous studies, many Bt insecticidal proteins demonstrated synergistic or antagonistic effects (Lemes et al., 2017). Some studies have found that when Cry1Aa and Cry1Ac were mixed in various proportions, their insecticidal activities against *Lymantria dispar* varied. The insecticidal activity was increased by 3.8 times when the proteins were mixed in a proportion of 1:1, and it increased by 7.3 times when mixed in proportion of 1:2. However, a mixture of Cry1Aa and Cry1Ab showed antagonism (Xue et al., 2005). Moreover, a combination of Cry6Aa and Cry55Aa had significant synergistic toxicity to *Meloidogyne incognita*, and the insecticidal activity of these two proteins was increased five times when they were combined in a ratio of 1:1 (Peng et al., 2011). Additionally, in a study of the toxicity of Cry1 and Vip3A to *Diatraea saccharalis*, the proteins did not interact, but Cry1Ab and Cry1Fa had synergistic effects with Cry1Ca (Pavani, 2013).

Unlike Sip, the insecticidal mechanisms of the Cry and Vip toxins have been studied extensively. A study of the insecticidal mechanism of Cry toxins found that Cry was hydrolyzed and activated by a protease in the midgut of the target insect. The intestinal epithelium cell membrane was destroyed after the Cry toxins bound to a specific receptor, which led to the death of the insect pests (Deist et al., 2014). For the Vips, it has been found that Vip3Aa could bind to the intestinal cells of insects, then become activated by the alkaline midgut fluid, leading to cell fragmentation *via* binding to specific proteins in the midgut cells (Zhang et al., 2018). However, Wang et al. (2020) have indicated that the receptor for Sip might be located in the midgut of the *C. bowringi* larvae.

In previous research in our laboratory, it was found that strain QZL38 contained both the *cry8Ca* and *sip1Ab* genes (unpublished data), both of which may have synergistic or antagonistic effects. Given that, the *sip1Ab* and *cry8Ca* genes were cloned using the genome of QZL38 as a template, and the corresponding proteins were induced and expressed. By adding a mixture of the proteins Sip and Cry, changes in the midgut of *C. bowringi* larvae were observed under the electron microscope and compared with the group in which Sip alone was added. Competitive binding assays were carried out for further verification. One of the purposes of this investigation was the exploration of the relationship between Sip1Ab and the midgut of *C. bowringi* larvae; another was to verify whether Cry8Ca had a synergistic effect with Sip. This study indicates new directions for further research of protein interactions, and new resources for the prevention and control of coleopteran pests. It is hoped that this research will contribute to a deeper understanding of the insecticidal mechanism of the Sip toxin.

MATERIALS AND METHODS

Construction of Expression Vector

The genomic DNA of strain QZL38 was extracted by using the EasyPure® Bacteria Genomic DNA Kit (TransGen Biotech, Beijing, China) according to the manufacturer's protocol and quantified using a Nano Photometer P300 (Implen, Inc., Munich, Germany).

The *sip1Ab* (KP231523.1) and *cry8Ca* (GU270856.1) genes were amplified by polymerase chain reaction (PCR) from the

TABLE 1 | Primers used in this study.

Name	Sequence (5′→3′)
cry8CaF	GTGGTGGTGGTGGTGCTCGAGATGAGTCCAAATAATCAAAATGAGTATG
cry8CaR	CCGAATTCGAGCTCCGTCGACCTCTTCTTCTAACACGAGTTCTACACTTT
sipF	GTGGTGGTGGTGGTGCTCGAGGCAGAAACCAAGTCGCCAAA
sipR	CCGAATTCGAGCTCCGTCGACATTTCCACTTAAAATCTTTGTTTGAACA

Underlined nucleotides are the homology arms to pET21b.

QZL38 genomic DNA sample. KOD -Plus- DNA Polymerase (Toyobo Co., Ltd., Osaka, Japan) was used for all PCR reactions. The reaction system consisted of 1× -KOD- Plus buffer, 0.2 mM of dNTPs, 1 μM of $MgSO_4$, 0.3 μM of primer (for each), 200 ng of genomic DNA, and 1 U -KOD-Plus polymerase with a supplement of ddH_2O up to a total volume of 50 μl. Amplification was performed for 35 cycles after pre-denaturation at 95°C for 2 min. Cycling conditions were set to denaturation at 95°C for 15 s, annealing at 59°C for 30 s, and extension at 67°C for 90 s. The amplification products were analyzed by electrophoresis on a 1% (w/v) agarose gel and purified using an Axygen® DNA Gel Extraction Kit (Axygen Biosciences, Union City, CA, United States) following the manufacturer's instructions. The DNA sequences of the oligonucleotides used in this study are listed in **Table 1**.

Restriction digestion was performed on pET21b at *Xho* I and *Sal* I sites to obtain a linearized plasmid. The insert fragment and the linearized pET21b were blunted by using a ClonExpress™ II One Step Cloning Kit (Vazyme, Nanjing, China). The recombinant plasmids were then transformed into *Escherichia coli* DH5α using the heat-shock method, and the recombinant strains were incubated on solid LB medium (containing ampicillin) at 37°C for 12–16 h. Verification of successfully constructed plasmids was performed *via* colony PCR and sequencing.

Heterologous Expression of Sip1Ab and Cry8Ca

The recombinant plasmids were extracted using an Axygen® Plasmid Miniprep Kit. A second transformation was carried out in *E. coli* BL21 (DE3) using the same method as above. Plasmid pET21b without an inserted fragment was used as a control in downstream experiments. The obtained transformants were inoculated into 5 ml of LB medium supplemented with ampicillin and pre-cultured overnight at 37°C, shaking at 220 rpm. These liquid cultures were then inoculated with 1% (v/v) into a 500 ml flask containing 100 ml of LB medium supplemented with ampicillin and incubated at 37°C, 220 rpm to an optical density at 600 nm (OD_{600}) of 0.6. For inducing expression, isopropyl-β-D-thiogalactopyranoside (IPTG) was added into the cultures to a final concentration of 0.5 mM. After induction for 16 h at 16°C, 160 rpm, cells were harvested by centrifugation at 8,000 × *g* for 5 min at 4°C and washed at least twice with 10 mM phosphate buffered saline (PBS, pH 7.4). The cells were disrupted by ultrasonic treatment in an ice-water mixture for 3 s pulses for 10 min with 5 s intervals. Debris and unbroken cells were removed by centrifuging twice at 12,000 × *g* for 15 min at 4°C. The supernatant was filtered through a 0.22 μm filter and purified using a Ni-NTA Fast Start Kit (Qiagen, Hilden, Germany) according to the instructions in the manual.

Samples of the purified products were mixed with 2× SDS loading buffer [100 mM Tris–HCl pH 6.8, 200 mM β-mercaptoethanol, 4% (w/v) SDS, 2% (w/v) bromophenol blue, and 20% (v/v) Glycerol], immersed in a boiling water bath for 10 min, and centrifuged at 10,000 × *g* for 10 min. The supernatant was collected for protein separation using SDS-PAGE and visualized with a Coomassie blue stain. The protein concentration was determined using bovine serum albumin (BSA) as a standard following the user manual of the BSA Protein Assay Kit (TransGen Biotech, Beijing, China).

Insects and Bioassays

The *C. bowringi* standard used in this study was donated by the Institute of Plant Protection (IPP), Chinese Academy of Agricultural Sciences (CAAS). *C. bowringi* insect eggs were incubated in a biochemical incubator at 25°C for 4–5 days. Fresh rape leaves were picked, washed, and placed on filter paper. The initially hatched *C. bowringi* larvae were gently inserted with a brush, and 5–6 larvae were placed in each Petri dish, which was placed in a biochemical incubator at 25°C (Liu et al., 2014). An appropriate amount of sterilized water was sprayed in the biochemical incubator in the morning and evening to maintain the air humidity. The leaves and filter paper in the Petri dish were changed every 24 h in the initial stage (6 days before incubation); the new filter paper was wetted, and it was ensured that the filter paper and rape leaves had no water droplets. After the initial stage, the Petri dish and the dead larvae were cleaned every day and the leaves and filter paper in the Petri dish were replaced every 12 h. The insect bodies were immersed in a pre-cooled saline solution. Sip1Ab, Cry8Ca, and a mixture of Sip1Ab and Cry8Ca in equal proportions were separately solubilized in 20 mM phosphate buffer before use in the bioassays. An analysis of the toxicity to *C. bowringi* was conducted on second instar larvae with fresh rape using the leaf-dip bioassay (Omer et al., 1993). The trays were incubated at 25 ± 2°C, 70 ± 5% RH, and a 10/8 h light/dark cycle, and mortality was scored at the second day. The quantitative bioassays were replicated at least three times using different concentrations of Sip1Ab, Cry8Ca, and a mixture of Sip1Ab and Cry8Ca. An insecticidal protein solution of PBS buffer was used as the control. The pET21b plasmid was used as the negative control. The LC_{50} value was measured

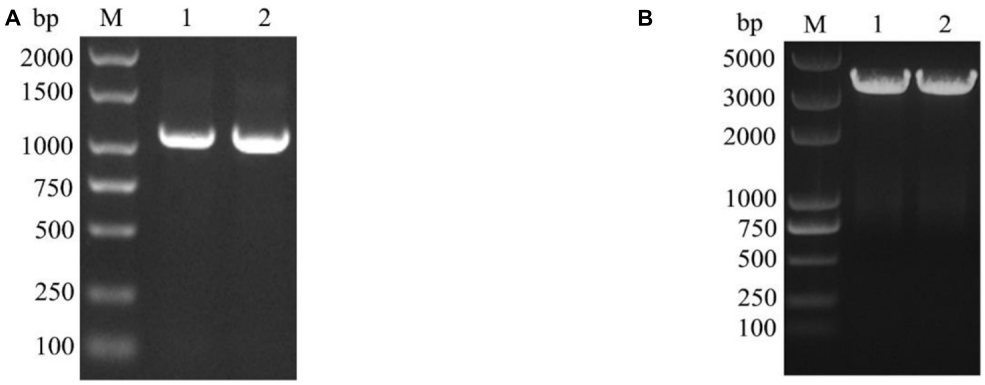

FIGURE 1 | Verification of the *sip1Ab* and *cry8Ca* by PCR. **(A)** M: DL2000 DNA Marker, 1 and 2: the amplified *sip1Ab* from QZL38 genome with sipF and sipR primers. **(B)** M: DL5000 DNA Marker, 1 and 2: the amplified *cry8Ca* from QZL38 genome with cry8CaF and cry8CaR primers.

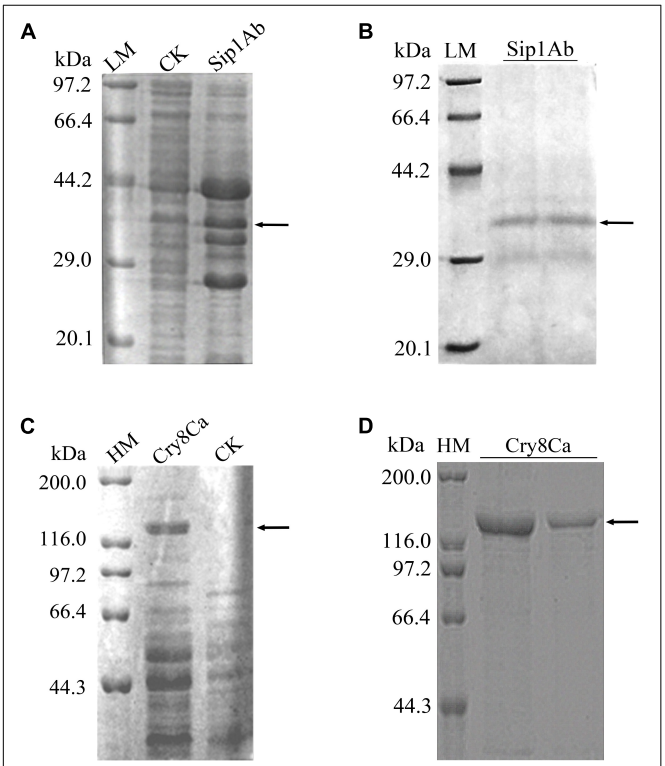

FIGURE 2 | Expression and purification of Sip1Ab and Cry8Ca. LM: Protein Molecular Weight Marker (Low) (Takara Biomedical Technology Co., Ltd., Beijing, China), HM: Protein Molecular Weight Marker (High) (Takara Biomedical Technology Co., Ltd., Beijing, China), CK: whole protein of pET21b-BL21 (DE3). Samples were subjected to SDS-PAGE followed by Coomassie Blue staining. **(A)** Expression of soluble Sip1Ab in *E. coli*. **(B)** The purified Sip1Ab. **(C)** Expression of soluble Cry8Ca in *E. coli*. **(D)** The purified Cry8Ca.

with SPSS software. It is generally believed that the toxicity ratio of LC_{50} measured is expected to be 0.5–2.6. A value higher than 1.5 was considered synergistic, and less than 0.5 as antagonistic.

Transmission Electron Microscope Observation

After starvation for 48 h, the *C. bowringi* larvae were fed the corresponding sensitive Bt proteins. Fresh and identical rapeseed leaves were selected. Protein samples were prepared and added with 0.1% detergent evenly smeared on both sides of the leaves with sterilized brushes. The leaves coated with protein samples were dried on the fresh-keeping film, and PBS buffer was applied as control. The concentration of Sip1Ab was 0.5 μg/ml. The sublethal worms and controls were dissected at 1, 2, and 3 days under microscopy. The midgut was immersed in PBS and diluted into 2.5% glutaraldehyde and fixed overnight at room temperature. The obtained midguts were prepared according to the method of transmission electron microscopy (TEM) sample preparation of Sinha et al. (2021). Uranium acetate peroxide dyeing was conducted for 10 min, lead acetate dyeing for 10 min, and a JEM-1230 (Joel, Tokyo, Japan) was used for electron microscopic observation.

Brush Border Membrane Vesicle Extraction

To obtain the *C. bowringi* Brush Border Membrane Vesicles (BBMVs), the insect midguts were poured into a pre-cooled conical flask, then 30 ml Buffer A (300 mmol/L mannitol, 5 mmol/L EGTA, 17 mmol/L Tris, and pH 7.5) was added. The mixture was subsequently ground on ice and placed on ice for 15 min after 30 ml $MgCl_2$ was added to the conical flask. Centrifugation (4,000 rpm) was conducted for 15 min. The supernatant was poured into a conical flask, and 15 ml $MgCl_2$ was added. The supernatant was placed on ice for 15 min and centrifuged at 4,000 rpm for 15 min. The supernatant was decanted into 50 ml centrifuge tube and centrifuged at 10,000 rpm for 30 min. The precipitate was dissolved in 1 ml Buffer B (150 mmol/L NaCl, 5 mmol/L EGTA, 20 mmol/L Tris, 1% CHAPS, and pH7.5). The total BBMV protein was quantified with a Bradford Protein Assay Kit (Merck, NJ, United States).

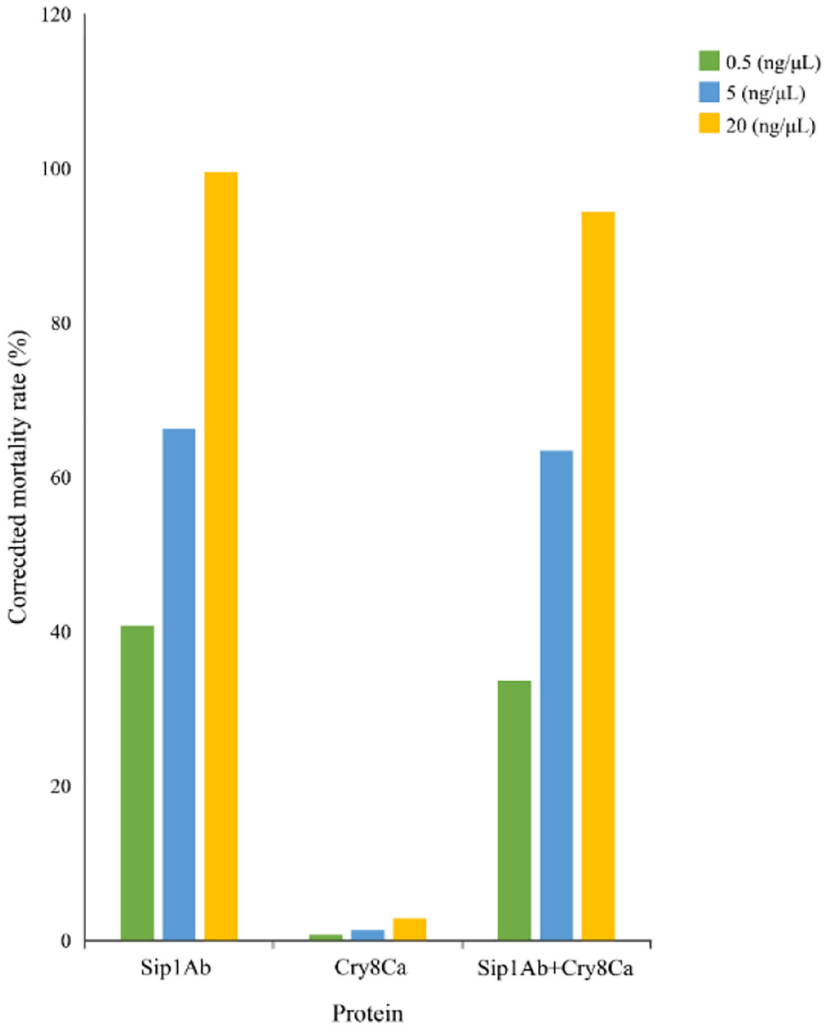

FIGURE 3 | Qualitative bioassay results of Sip1Ab and Cry8Ca against *Colaphellus bowringi*.

Ligand-Blotting Procedure

Proteins were biotinylated using the Pierce™ Cell Surface Protein Biotinylation and Isolation Kit (Thermo Fisher, MA, United States). Various concentrations of biotinylated Sip (NHS-Biotin-Sip) were added to BBMV in a range 25–100 nM at intervals of 25 nM. Additionally, 100 nM biotinylated Sip was separately added with a 10-, 15-, and 20-fold excess of unmarked Cry8Ca into the BBMV binding system. For the competitive binding assays, 0.1% BSA in PBS was added to all binding systems to make them up to 100 μl. All the systems were incubated for 1 h at room temperature. Unbound toxin was removed by centrifugation (10 min at 18,000 rpm), and the pellets were washed twice with PBS (pH 7.6, 0.1% BSA). The precipitate was suspended in 10 μl 1× SDS loading buffer, loaded on an SDS-PAGE gel, and electrotransferred to a PVDF membrane (GE Healthcare, MA, United States). The PVDF membrane was then incubated with Streptavidin-HRP (1:3000 dilutions) for 1 h at room temperature, followed by three wash cycles with PBST, 15 min per cycle. Binding was visualized using an ECL chemiluminescent kit (Thermo Scientific, MA, Untied States).

TABLE 2 | The bioassay results of Sip1Ab and Cry8Ca proteins against the *Colaphellus bowringi*.

Sample	LC_{50}(μ g ml^{-1})	95% confidence interval (μ g ml^{-1})
Sip1Ab	1.067	0.672–1.158
Cry8Ca	>200	–
Sip1Ab + Cry8Ca	1.462	0.855–1.361

RESULTS

Gene Cloning

The designed full-length primers sipF/sipR and cry8CaF/cry8CaR were used to amplify the *sip1Ab* and *cry8Ca*

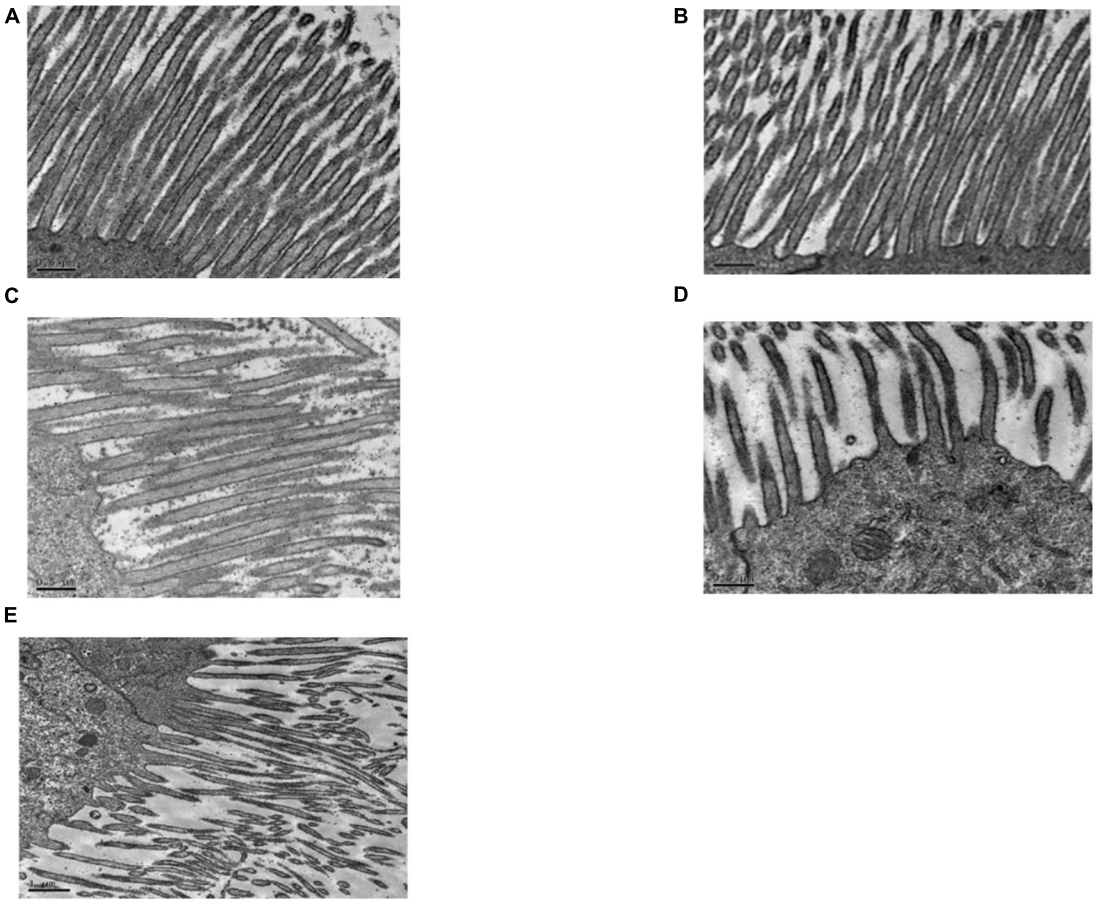

FIGURE 4 | Pathological effects of Sip1Ab and Cry8Ca on midgut microvilli of larvae of *Colaphellus bowringi* **(A)** Control group fed PBS for 3 days, **(B)** Cry8Ca treatment for 3 days, and **(C–E)**: 1, 2, and 3 days after treatment with Sip1Ab, respectively.

by PCR. The amplified fragments of a size of 1,044 and 3,522 bp were consistent with the expected fragment size. The agarose electrophoresis results are shown in the figure below (**Figure 1**).

Expression and Purification of Sip1Ab and Cry8Ca

Expression from recombinant plasmids *sip1Ab*-pET21b and *cry8Ca*-pET21b was induced by IPTG. With SDS-PAGE, the expressed products were shown to include a recombinant protein at approximately 37 kDa (**Figure 2A**) and 130 kDa (**Figure 2C**), indicating that both proteins were successfully expressed in *E. coli* BL21 (DE3). Subsequently, the His-tagged recombinant proteins were purified from the crude extract using Ni-NTA agarose affinity chromatography (GE Healthcare, MA, United States) (**Figures 2B,D**).

Bioassays

The expression from recombinant strains was induced by IPTG. In the qualitative bioassays for the insecticidal activity of the proteins, second-instar *C. bowringi* were used as the test insects, and in that of the protein expressed in *E. coli*, pET21b was used as the negative control. The protein concentrations for bioassay were 0.5, 5, and 20 mg/ml. Forty-eight insects were tested for each protein, and the death of the insects was assessed 48 h later. The experiment was repeated three times. The test results are shown in **Figure 3**.

The insecticidal activity of Cry8Ca and Sip1Ab is shown in **Table 2**. The results showed that the insecticidal activity of a mixture of Cry8Ca and Sip1Ab (1:1) showed no significant difference from that of Sip1Ab.

Observation of Midgut Histopathological Changes

Midgut Microvilli

Figure 4A shows that the midgut microvilli of healthy *C. bowringi* were dense, slender, and well-distributed and the membrane structure was normal. One day after treatment with Sip1Ab, the microvilli swelled and shed slightly and the structure was sparse (**Figure 4C**). After treatment with Sip1Ab for 2 days, a number of microvilli were exfoliated, and many vesicle structures were formed (**Figure 4D**). After 3 days of treatment with Sip, the microvilli were almost shed and disordered (**Figure 4E**). No significant change was seen in the group treated with Cry8Ca (**Figure 4B**).

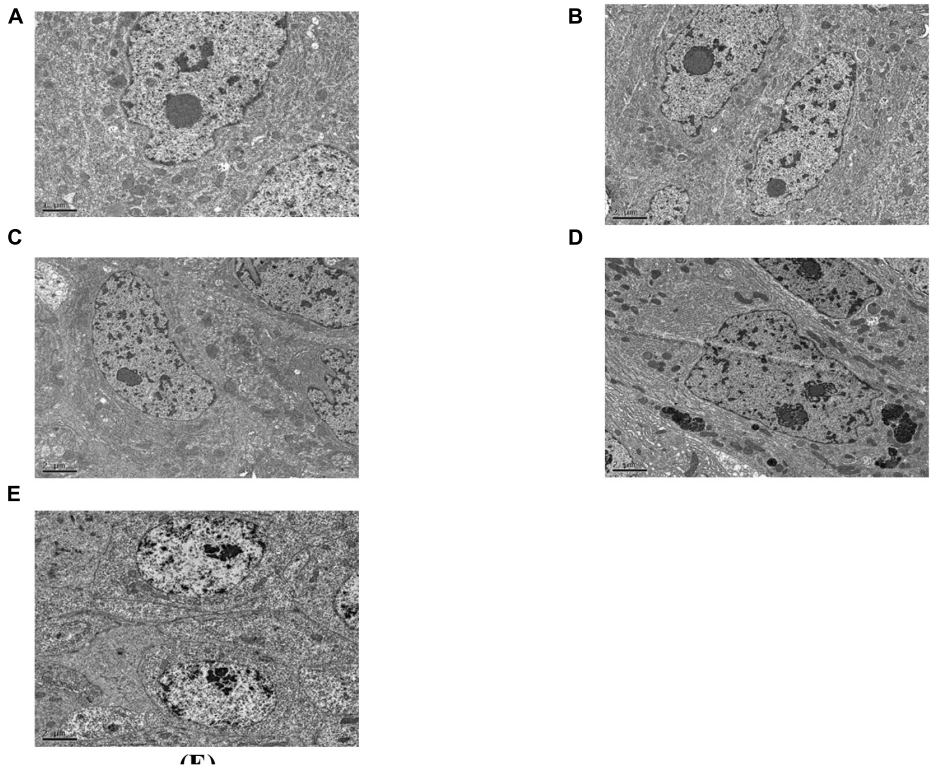

FIGURE 5 | Pathological effects of the Sip1Ab and Cry8Ca on midgut space of larvae of *Colaphellus bowringi* **(A)** Control group fed PBS for 3 days, **(B)** Cry8Ca treatment for 3 days, and **(C–E)**: 1, 2, and 3 days after treatment with Sip1Ab, respectively.

Midgut Intercellular Space

As can be seen in **Figure 5**, the gap between the two cells in the midgut of the healthy *C. bowringi* was very small, with sporadic vesicles (**Figure 5A**). After 3 days of treatment, the gap between the two cells in the midgut appeared to be unaffected by Cry8Ca (**Figure 5B**). After 1 day of treatment with Sip1Ab, the gap between the two cells in the midgut increased significantly, and the slight packing structure increased (**Figure 5C**). During 2–3 days of treatment with Sip1Ab, not only did the gap between the two cells in the midgut increase significantly, but also the break-up and separation of cell membranes appeared (**Figures 5D,E**).

Extraction of Brush Border Membrane Vesicles

About 5 g of midgut tissue was extracted from around 1,500 *C. bowringi* fifth instar larvae. BBMV was extracted from the *C. bowringi* midgut (**Figure 6**). The protein concentration was determined by the Bradford method.

Ligand Blotting

In the binding test, the binding of biotinylated Sip1Ab to *C. bowringi* BBMV was tested *in vitro*. The ligand-blotting analysis demonstrated the binding of biotin labeled toxin (Sip1Ab) to protein in the *C. bowringi* BBMV (**Figure 7**). The binding activity of Sip1Ab could be clearly observed at a concentration of 100 nM.

To determine whether Cry8Ca exhibits competition during interactions between Sip1Ab and *C. bowringi* BBMV, a mixture of these two proteins was added to the BBMV binding system. As shown in **Figure 8**, excess Cry8Ca up to 20× was unable to compete with the binding of Sip1Ab to *C. bowringi* BBMV, suggesting that this could be a unique binding protein for Sip1Ab toxin.

DISCUSSION

Colaphellus bowringi is a common agricultural pest which occurs in most parts of China, and mainly damages cruciferous vegetables such as the *Brassica rapa* Chinensis Group, *Raphanus sativus*, *Brassica oleracea* var. *botrytis*, *B. rapa* var. *botrytis*, and so on (Zhu et al., 2019). A series of studies has shown that Sip has high insecticidal activity against coleopteran pests such as *L. decemlineata* and *C. bowringi* (Donovan et al., 2006; Sha et al., 2018; Wang et al., 2020). This observation provides a foundation for the discovery of novel genes of Bt and for expanding its insecticidal spectrum. However, to date, *sip* has only been studied with mutants and truncated genes. Histopathological changes in the midgut due to poisoning by Sip toxin, and studies on the heterologous competition between Sip1Ab and another Bt toxin, have not yet been reported. So, TEM was used to observe the midgut tissue. Additionally, corresponding competition assays were carried out to gain more

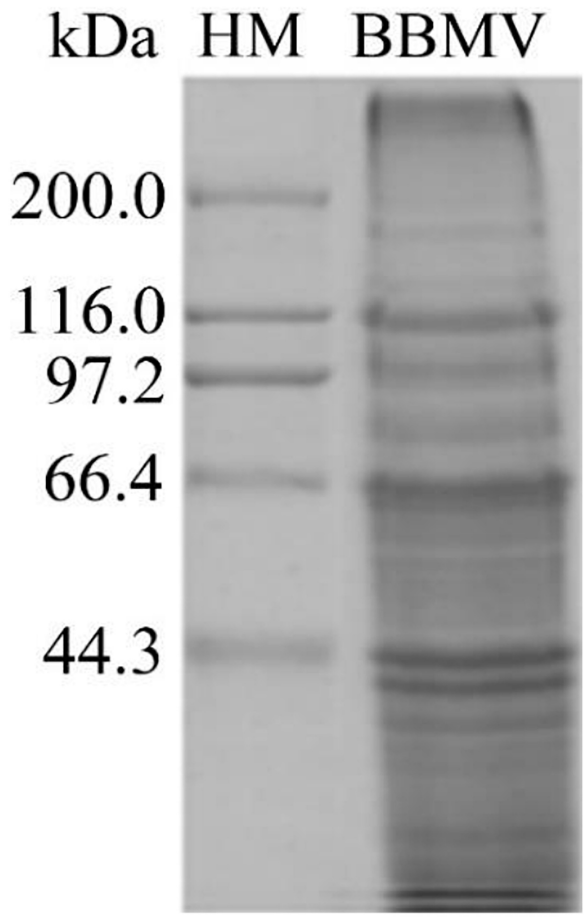

FIGURE 6 | Proteins in *C. bowringi* BBMV were separated by SDS-PAGE. HM: Protein Molecular Weight Marker (High).

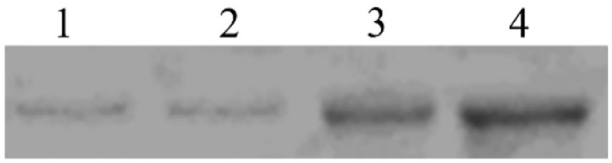

FIGURE 7 | Determination of saturated binding between biotinylated Sip toxin and *C. bowringi* BBMV. 1–4: 25, 50, 75, and 100 nM biotinylated Sip, respectively.

insight into the insecticidal mechanism of Sip and the biocontrol of *C. bowringi*. Extensive research has shown that Cry8Ca was reported to have high insecticidal activity against coleopteran beetles (Jiang et al., 2017). Since Bt strain QZL38 contained *sip1Ab* and *cry8Ca*, it was speculated that there was a linkage between these two toxins vis a vis toxicity to *C. bowringi*. According to the results of bioactivity assay, Sip1Ab is almost certainly has high insecticidal activity, while Cry8Ca may have no insecticidal activity against *C. bowringi*. Furthermore, compared with a mixture of Sip1Ab and Cry8Ca, no significant difference in

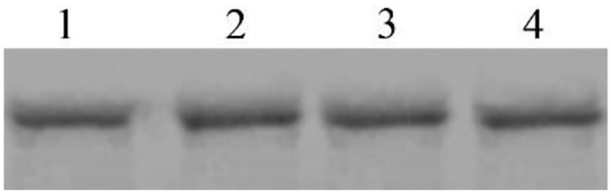

FIGURE 8 | Competitive determination of Cry8Ca between biotinylated Sip binding in *C. bowringi* BBMV. 1: 100 nM biotinylated Sip, 2–4: Biotinylated Sip + Cry8Ca in 10-, 15-, and 20-fold excess, respectively.

the LC_{50} of Sip1Ab was noted. A possible explanation is that no synergistic or antagonistic effect between these two toxins exists. Histopathological changes of the midgut were observed, further verifying the bioassay results. This inconsistency may be due to the different receptors for Sip1Ab and Cry8Ca in the midgut. In future investigations, on the one hand, it is possible that Sip1Ab and Cry8Ca have synergistic or antagonistic effects on the control of other coleopteran pests. For example, a study might be carried out on the basis of the known insecticidal activity of Sip against *L. decemlineata*. On the other hand, to develop a full picture of the correlation between Sip1Ab and Cry8Ca, additional studies could establish the basis of the insecticidal activity of Cry8Ca against *A. corpulenta* and *A. exoleta* Fald.

The midgut receptor was initially found to be a protein that could bind to membrane surface glycoproteins (Mayerson and Hall, 1986). Some studies have shown that a high affinity binding site exists between Bt toxins and BBMV in the larval midgut, and the corresponding effect was positively associated with the concentration of the toxins (Höfte and Whiteley, 1989). The findings of this study suggested that Sip interacted with BBMV. Analogous to the insecticidal mechanism of the Cry toxins, it is possible that the Sip toxins must be hydrolyzed by midgut proteases into active fragments to function. Further work should focus on determining the receptors for Sip1Ab in the BBMV *via* pull-down or yeast two hybrids. Nevertheless, Sip1Ab and Cry8Ca did not compete with each other in the combination assays. A possible explanation for this might be that Sip1Ab and Cry8Ca may have synergistic or antagonistic effects in different pests. Therefore, Sip1Ab may be beneficial for the avoidance of the risk of cross-resistance of insects to Cry8Ca toxins. Moreover, as has been observed in many laboratory and field pests, pyramiding with another toxin with a different mode of action and binding site would be desirable to circumvent the development of resistance to an insecticidal protein, and Sip toxins may be candidates for this.

CONCLUSION

In summary, while this study did not confirm that a specific receptor of Sip1Ab exists in the midgut, it did substantiate Sip1Ab has interactions with the BBMV. To the best of our knowledge, it is the first time pathological changes in the *C. bowringi* larvae midgut due to poisoning by Sip1Ab were observed using TEM. Additionally, the interaction between Sip1Ab and the

BBMV in the midgut was confirmed, which has advanced our understanding of the specific insecticidal mechanism of Sip1Ab. It can also provide genetic resources for the control of coleopteran pests and shine new and important light in the field of crossing resistance improvement strategy design.

DATA AVAILABILITY STATEMENT

The datasets presented in this study can be found in online repositories. The names of the repository/repositories and accession number(s) can be found in the article/supplementary material.

AUTHOR CONTRIBUTIONS

DC, CX, and QF: conceptualization. DC, XL, RL, and HL: methodology. CX: data analysis. DC and QF: writing—original draft preparation. CX and HL: writing—review and editing. JG: supervision, project administration, and funding acquisition. All authors have read and agreed to the published version of the manuscript.

FUNDING

This research was funded by Heilongjiang Provincial National Science Foundation (LH2020C007).

ACKNOWLEDGMENTS

Special acknowledgment is given to all the participants in this research and their relatives for their cordial guidance and material support during the laboratory work. We thank the Heilongjiang Provincial National Science Foundation (LH2020C007) and the open fund of State Key Laboratory of Biology for Plant Diseases and Insect Pests for support.

REFERENCES

Beard, C. E., Ranasinghe, C., and Akhurst, R. J. (2001). Screening for novel cry genes by hybridization. *Lett. Appl. Microbiol.* 33, 241–245. doi: 10.1046/j.1472-765x.2001.00982.x

Deist, B. R., Rausch, M. A., Fernandez-Luna, M. T., Adang, M. J., and Bonning, B. C. (2014). Bt toxin modification for enhanced efficacy. *Toxins (Basel)* 6, 3005–3027. doi: 10.3390/toxins6103005

Donovan, W. P., Engleman, J. T., Donovan, J. C., Baum, J. A., Bunkers, G. J., Chi, D. J., et al. (2006). Discovery and characterization of Sip1A: a novel secreted protein from Bacillus thuringiensis with activity against coleopteran larvae. *Appl. Microbiol. Biotechnol.* 72, 713–719. doi: 10.1007/s00253-006-0332-7

Gao, Y., Jurat-Fuentes, J. L., Oppert, B., Fabrick, J. A., Liu, C., Gao, J., et al. (2011). Increased toxicity of *Bacillus thuringiensis* Cry3Aa against crioceris quatuordecimpunctata, phaedon brassicae and colaphellus bowringi by a tenebrio molitor cadherin fragment. *Pest Manage. Sci.* 67, 1076–1081. doi: 10.1002/ps.2149

Gómez, I., Ocelotl, J., Sánchez, J., Aguilar-Medel, S., Peña-Chora, G., Lina-Garcia, L., et al. (2020). *Bacillus thuringiensis* Cry1Ab domain III β-22 mutants with enhanced toxicity to spodoptera frugiperda (J. E. Smith). *Appl. Environ. Microbiol.* 86:e01580-20. doi: 10.1128/aem.01580-20

Höfte, H., and Whiteley, H. R. (1989). Insecticidal crystal proteins of *Bacillus thuringiensis*. *Microbiol. Rev.* 53, 242–255. doi: 10.1128/mr.53.2.242-255.1989

Jiang, J., Huang, Y., Shu, C., Soberón, M., Bravo, A., Liu, C., et al. (2017). Holotrichia oblita midgut proteins that bind to *Bacillus thuringiensis* Cry8-like toxin and assembly of the H. oblita midgut tissue transcriptome. *Appl. Environ. Microbiol.* 83:e00541-17. doi: 10.1128/aem.00541-17

Lemes, A. R. N., Figueiredo, C. S., Sebastião, I., Marques da Silva, L., da Costa Alves, R., de Siqueira, H. A., et al. (2017). Cry1Ac and vip3aa proteins from *Bacillus thuringiensis* targeting cry toxin resistance in *Diatraea flavipennella* and *Elasmopalpus lignosellus* from sugarcane. *PeerJ* 5:e2866. doi: 10.7717/peerj.2866

Liu, X., Song, F., Wen, S., Wang, S., Huang, D., and Zhang, J. (2004). Study of microarray detection method of cry genes from *Bacillus thuringiensis*. *Sci. Agric. Sin.* 37, 987–992.

Liu, X. P., He, H. M., and Xue, F. S. (2014). The influence of female age on male mating preference and reproductive success in cabbage beetle, *Colaphellus bowringi*. *Insect Sci.* 21, 515–522. doi: 10.1111/1744-7917.12051

Liu, Y., Li, H., Liu, R., and Gao, J. (2012). Bt new gene sip cloning, expression, and bioinformatics analysis. *Biotechol. Bull.* 12, 101–105.

Mayerson, P. L., and Hall, M. O. (1986). Rat retinal pigment epithelial cells show specificity of phagocytosis in vitro. *J. Cell Biol.* 103, 299–308. doi: 10.1083/jcb.103.1.299

Noguera, P. A., and Ibarra, J. E. (2010). Detection of new cry genes of *Bacillus thuringiensis* by use of a novel PCR primer system. *Appl. Environ. Microbiol.* 76, 6150–6155. doi: 10.1128/aem.00797-10

Omer, A. D., Johnson, M. W., Tabashnik, B. E., Costa, H. S., and Ullman, D. E. (1993). Sweetpotato whitefly resistance to insecticides in hawaii: intra-island variation is related to insecticide use. *Entomol. Exp. Et Appl.* 67, 173–182. doi: 10.1111/j.1570-7458.1993.tb01666.x

Palma, L., Muñoz, D., Berry, C., Murillo, J., and Caballero, P. (2014). *Bacillus thuringiensis* toxins: an overview of their biocidal activity. *Toxins (Basel)* 6, 3296–3325. doi: 10.3390/toxins6123296

Pavani, C. D. (2013). *Efeitos Da Interação e Toxicidade Das Proteínas Cry1 e Vip3Aa De Bacillus thuringiensis, Berliner em Spodoptera frugiperda (J. E. Smith) (Lepidoptera: Noctuidae). Ph. D, Thesis*. Brazil: Universidade Estadual Paulista.

Peng, D., Chai, L., Wang, F., Zhang, F., Ruan, L., and Sun, M. (2011). Synergistic activity between *Bacillus thuringiensis* Cry6Aa and Cry55Aa toxins against meloidogyne incognita. *Microb. Biotechnol.* 4, 794–798. doi: 10.1111/j.1751-7915.2011.00295.x

Sha, J., Zhang, J., Chi, B., Liu, R., Li, H., and Gao, J. (2018). Sip1Ab gene from a native *Bacillus thuringiensis* strain QZL38 and its insecticidal activity against *Colaphellus bowringi* baly. *Biocontrol. Sci. Technol.* 28, 459–467. doi: 10.1080/09583157.2018.1460313

Shu, C., Su, H., Zhang, J., He, K., Huang, D., and Song, F. (2013). Characterization of cry9Da4, cry9Eb2, and cry9Ee1 genes from *Bacillus thuringiensis* strain T03B001. *Appl. Microbiol. Biotechnol.* 97, 9705–9713. doi: 10.1007/s00253-013-4781-5

Singh, D., Samiksha, Thayil, S. M., Sohal, S. K., and Kesavan, A. K. (2021). Exploration of insecticidal potential of cry protein purified from *Bacillus thuringiensis* VIID1. *Int. J. Biol. Macromol.* 174, 362–369. doi: 10.1016/j.ijbiomac.2021.01.143

Sinha, A., Ischia, G., Straffelini, G., and Gialanella, S. (2021). A new sample preparation protocol for SEM and TEM particulate matter analysis. *Ultramicroscopy* 230:113365. doi: 10.1016/j.ultramic.2021.113365

Swiecicka, I., Bideshi, D. K., and Federici, B. A. (2008). Novel isolate of *Bacillus thuringiensis* subsp. thuringiensis that produces a quasicuboidal crystal of cry1ab21 toxic to larvae of *Trichoplusia* ni. *Appl. Environ. Microbiol.* 74, 923–930. doi: 10.1128/aem.01955-07

Wang, J., Ding, M. Y., Wang, J., Liu, R. M., Li, H. T., and Gao, J. G. (2020). In silico structure-based investigation of key residues of insecticidal activity of sip1aa protein. *Front. Microbiol.* 11:984. doi: 10.3389/fmicb.2020.00984

Wu, H., Zhang, Y., Guo, S., Zhang, J., Wang, R., and Gao, J. (2007). A study on purification and activity of Cry8Ca2 protein from *Bacillus thuringiensis*. *Plant Protection* 33, 29–32.

Xue, F., Li, A., Zhu, X., Gui, A., Jiang, P., and Liu, X. (2002). Diversity in life history of the leaf beetle, *Colaphellus bowringi* baly. *Acta Entomol. Sin.* 45, 494–498.

Xue, J. L., Cai, Q. X., Zheng, D. S., and Yuan, Z. M. (2005). The synergistic activity between cry1aa and cry1c from *Bacillus thuringiensis* against spodoptera exigua and helicoverpa armigera. *Lett. Appl. Microbiol.* 40, 460–465. doi: 10.1111/j.1472-765X.2005.01712.x

Zhang, J., Li, H., Liu, R., Shu, C., and Gao, J. (2015). Explore sip gene from Bt strain DQ89 and its insecticidal activity against *Colaphellus bowringi* baly. *Chin. J. Biol. Control* 31, 598–602.

Zhang, J., Pan, Z. Z., Xu, L., Liu, B., Chen, Z., Li, J., et al. (2018). Proteolytic activation of *Bacillus thuringiensis* Vip3Aa protein by *Spodoptera exigua* midgut protease. *Int. J. Biol. Macromol.* 107, 1220–1226. doi: 10.1016/j.ijbiomac.2017.09.101

Zhu, L., Tian, Z., Guo, S., Liu, W., Zhu, F., and Wang, X. P. (2019). Circadian clock genes link photoperiodic signals to lipid accumulation during diapause preparation in the diapause-destined female cabbage beetles *Colaphellus bowringi*. *Insect. Biochem. Mol. Biol.* 104, 1–10. doi: 10.1016/j.ibmb.2018.11.001

Conflict of Interest: The authors declare that the research was conducted in the absence of any commercial or financial relationships that could be construed as a potential conflict of interest.

Publisher's Note: All claims expressed in this article are solely those of the authors and do not necessarily represent those of their affiliated organizations, or those of the publisher, the editors and the reviewers. Any product that may be evaluated in this article, or claim that may be made by its manufacturer, is not guaranteed or endorsed by the publisher.

frontiers in Microbiology

ORIGINAL RESEARCH
published: 15 March 2022
doi: 10.3389/fmicb.2022.823963

Straw Return and Nitrogen Fertilization to Maize Regulate Soil Properties, Microbial Community, and Enzyme Activities Under a Dual Cropping System

Li Yang[1†], Ihsan Muhammad[1†], Yu Xin Chi[1,2], Dan Wang[3] and Xun Bo Zhou[1]*

[1] *Guangxi Colleges and Universities Key Laboratory of Crop Cultivation and Tillage, Agricultural College, Guangxi University, Nanning, China,* [2] *The Key Laboratory of Germplasm Improvement and Cultivation in Cold Regions, College of Agronomy, Heilongjiang Bayi Agricultural University, Daqing, China,* [3] *College of Horticulture and Landscape, Tianjin Agricultural University, Tianjin, China*

OPEN ACCESS

Edited by:
Ying Ma,
University of Coimbra, Portugal

Reviewed by:
Giorgia Pertile,
Institute of Agrophysics (PAN), Poland
Bruno Brito Lisboa,
Department of Agricultural Research and Diagnosis, State Secretariat of Agriculture, Livestock and Irrigation, Brazil

***Correspondence:**
Xun Bo Zhou
xunbozhou@gmail.com

† These authors have contributed equally to this work

Specialty section:
This article was submitted to Microbe and Virus Interactions with Plants, a section of the journal Frontiers in Microbiology

Received: *28 November 2021*
Accepted: *18 January 2022*
Published: *15 March 2022*

Citation:
Yang L, Muhammad I, Chi YX, Wang D and Zhou XB (2022) Straw Return and Nitrogen Fertilization to Maize Regulate Soil Properties, Microbial Community, and Enzyme Activities Under a Dual Cropping System. Front. Microbiol. 13:823963. doi: 10.3389/fmicb.2022.823963

Soil sustainability is based on soil microbial communities' abundance and composition. Straw returning (SR) and nitrogen (N) fertilization influence soil fertility, enzyme activities, and the soil microbial community and structure. However, it remains unclear due to heterogeneous composition and varying decomposition rates of added straw. Therefore, the current study aimed to determine the effect of SR and N fertilizer application on soil organic carbon (SOC), total nitrogen (TN), urease (S-UE) activity, sucrase (S-SC) activity, cellulose (S-CL) activity, and bacterial, fungal, and nematode community composition from March to December 2020 at Guangxi University, China. Treatments included two planting patterns, that is, SR and traditional planting (TP) and six N fertilizer with 0, 100, 150, 200, 250, and 300 kg N ha^{-1}. Straw returning significantly increased soil fertility, enzymatic activities, community diversity, and composition of bacterial and fungal communities compared to TP. Nitrogen fertilizer application increased soil fertility and enzymes and decreased the richness of bacterial and fungal communities. In SR added plots, the dominated bacterial phyla were Proteobacteria, Acidobacterioia, Nitrospirae, Chloroflexi, and Actinobacteriota; whereas fungal phyla were Ascomycota and Mortierellomycota and nematode genera were *Pratylenchus* and *Acrobeloides*. Co-occurrence network and redundancy analysis (RDA) showed that TN, SOC, and S-SC were closely correlated with bacterial community composition. It was concluded that the continuous SR and N fertilizer improved soil fertility and improved soil bacterial, fungal, and nematode community composition.

Keywords: straw return, nitrogen fertilization, soil enzymes, soil microbes, soil properties

INTRODUCTION

Carbon sequestration and long-term sustainability can be improved with residues return to the field (Su et al., 2020a; Lu et al., 2021). Straw is mainly composed of carbon (C), nitrogen (N), and organic matter (OM) (Fan and Wu, 2020), which can effectively enhance soil fertility and mitigate the negative impacts of excessive synthetic fertilizers uses (Zhao et al., 2019;

Wang L. et al., 2021). Numerous studies have demonstrated that SR reduced mineral fertilizer application by enhancing nutrient efficiency and improved organic C inputs (Wu et al., 2020; Wang G. et al., 2021). Furthermore, SR has tremendous potential to improve soil health and micro-ecological environment (Su et al., 2020a). Straw decomposition is a complex process (Zhao and Zhang, 2018; Zhao et al., 2019), which is predominantly mediated by soil microorganisms with specialized functions (Zhao and Zhang, 2018). A variety of microbial communities play significant roles in the crop residues decomposition, such as bacteria preferring to decompose labile compounds and dominating straw degradation at the initial stage of decomposition (Mwafulirwa et al., 2021; Wu et al., 2021). In contrast, fungi decompose more abrasive materials principally in the final stages of decomposition (Marschner et al., 2011). The energy and C derived from the crop residues incorporated into the soil are distributed throughout the trophic levels, affecting different soil microorganisms such as soil bacteria, fungi, and nematodes (Chen et al., 2021).

In addition to a biotic component, the abiotic variables such as temperature and soil moisture, soil N, pH, and soil organic carbon (SOC) also affect the decomposition process and soil microbial activity, structure, and community (Geisseler and Scow, 2014; Kamble and Bååth, 2016). Guangxi is located south of China, which is a typical subtropical monsoon humid region and committed to a double-cropping system, where maize (*Zea mays* L.) is one of the main food crops (Huang et al., 2021). Straw decomposition and nutrient release are accelerated by the high temperature in this region (Ren et al., 2020). Residues incorporation into the soil decomposed more rapidly, which releases a variety of mineral nutrients that may be easily available and absorbed by plants (Muhammad et al., 2021). The straw C/N ratio is a factor that determines the rate of decomposition of the material, with lower C/N ratios favoring bacteria while higher fungi ratios can degrade more complex organic molecules such as lignin.

The activity of soil enzymes has long been considered as a fundamental indication of soil quality (Borase et al., 2020). Soil enzymatic activities are generated and released by soil microbes, which are responsible for organic matter degradation (Burns et al., 2013). The activity of soil enzymes can provide insight into the processes of microbial sensitivity to added C and N (Zhao et al., 2016; Muhammad et al., 2022). The addition of C and N to soil and field management approaches may affect different enzymes in different ways (Gong et al., 2021; Huang et al., 2021). Soil sucrase activity can help plants and soil bacteria use sucrose as an energy source by hydrolyzing it into glucose and fructose (Yu et al., 2018; Wu et al., 2020). Similarly, cellulose (S-CL) activity is significantly correlated with sucrase activity when organic matter was added to the soil, showing that the individual substrate can affect an enzyme-catalyzed biological reaction (Salazar et al., 2011). Thus, understanding the relationship between the impact of SR and N application on soil microorganisms and the production of soil enzyme activities is crucial and will provide insight into the fundamental mechanics of SOC changes under long-term SR.

Therefore, this study was conducted to investigate the effects of SR on the soil bacteria, fungi, and nematode communities, enzyme activities, and soil fertility. High-throughput DNA sequencing of PCR-amplified marker genes sequencing technology has recently provided significant insights into the diversity of the microbial community in various fertilizer management practices and SR decomposition (Zhao et al., 2016; Yuan et al., 2018). We conducted a field experiment in a subtropical region of China with two planting patterns (SR and TP) under N fertilizer application. The objectives of the study were (i) to investigate the impacts of N fertilization and SR on the soil microbial diversity and community composition; (ii) to determine the response of soil enzyme activity under various N levels and SR systems; and (iii) to understand how soil microbes and enzyme activities alter SOC and total N under SR and N application.

MATERIALS AND METHODS

Experimental Site

A field experiment was conducted at Agronomy Research Farm of Guangxi University, Nanning, Guangxi, China (22°50'N, 108°17′E) from March to December 2020. The region belongs to a sub-tropical monsoon climate, with a mean annual temperature of 21.7°C and a mean annual precipitation of 1,298 mm. The soil of the experimental site was classified as clay loam, with initial properties of 14.6 g kg^{-1} SOC, 0.8 g kg^{-1} total N, 42.7 mg kg^{-1} available P, 88.5 mg kg^{-1} available K, and pH 6.5 when sampling at 0–20 cm depth.

Experimental Design

The experiment was conducted in randomized complete block design in split-plot arrangement with three replications. The planting pattern was the main plot and N fertilization was the split-plot factor. The two planting patterns were straw return (SR; spring and autumn maize residue were mechanically crushed stalks in to 2–3 cm and mixed with soil in top 0–20 cm with rotary tillage) and traditional planting (TP; maize straw was removed from the field after harvested) since 2018. The six N fertilizer treatments were control (N0), 100 kg N ha^{-1} (N100), 150 kg N ha^{-1} (N150), 200 kg N ha^{-1} (N200), 250 kg N ha^{-1} (N250), and 300 kg N ha^{-1} (N300).

In 2020, the maize cultivar "Zhengda-619" was sown twice, the first time on March 11th and harvested on July 9th for spring maize, and the second time on August 2nd and harvested on November 30th for autumn maize. The plot size was 4.2 m × 4.2 m, with a planting density of 55,556 plants ha^{-1}, having 60 cm row to row space and 30 cm planting space. The recommended basal doses of phosphate fertilizer (calcium magnesium phosphate, P_2O_5 content of 18%) and potash fertilizer (KCl, K_2O content of 60%) were incorporated at a rate of 100 kg ha^{-1} into the soil before sowing. Two-thirds of the N from urea was applied prior to sowing, with the remaining one-third applied during the large trumpet period. Other field management measures were consistent with typical farming procedures.

Soil Sampling

Five random soil samples from 0 to 20 cm soil depth were obtained from each sub-plot at the jointing stage (V6) and mature stage (R6) before maize harvest. These soil samples were thoroughly mixed, sieved through a 2 mm mesh, and then divided into two parts, one of which was immediately stored at −80°C in the laboratory for molecular analysis. Additionally, the other portion of the soil samples was air-dried at room temperature and then sieved through 0.069 mm mesh for the analysis of enzyme activities, and/or sieved through 0.15 mm mesh for TN and SOC determination.

Soil Fertility and Enzyme Activities Analysis

Potassium dichromate volumetric and external heating techniques were used to quantify SOC (Chen et al., 2021), while soil TN was measured by the semi–micro kelvin method (Wang G. et al., 2021). The activities of soil enzymes, soil urease (S-UE), soil sucrase (S-SC), and soil cellulase (S-CL) were evaluated using Solarbio analytical kits BC0125, BC0245, and BC0155S, respectively (Science & Technology Co., Ltd., Beijing, China), as per the procedure of the manufacturer.

DNA Preparation, PCR Amplification, and High-Throughput Sequencing

Total genomic DNA was extracted through using the E.Z.N.A.® soil DNA Kit according to the manufacturer's instructions (Omega Bio-tek Inc., Norcross, GA, United States). The final DNA concentration and purity were determined using a Nano Drop 2000 UV-vis spectrophotometer (Thermo Scientific, Wilmington, United States), and the DNA quality was determined using 1% agarose gel electrophoresis. A Thermocycler PCR system was used to perform PCR amplification (Gene Amp 9700, ABI, United States). Bacterial primers 338F 5′-ACTCCTACGGGAGGCAGCAG-3′ and 806R 5′- GGACTACHVGGGTWTCTAAT-3′ were used to amplify the V3-V4 hypervariable sections of the 16S rRNA gene (Chen et al., 2018). The barcode primers ITS1F (5′-CTTGGTCATTTAGAGGAAGTAA-3′) and ITS2R (5′-GCTGCGTTCTTCATCGATGC-3′) were used to amplify the fungal rRNA gene in the ITS1 sequence region (Dang et al., 2020). The fungal ITS1 sequence region was used for nematode DNA gene amplification using the barcode primers NF1 5′-GGTGGTGCATGGCCGTTCTTAGTT-3′ and 18Sr2bR 5′-TACAAAGGGCAGGGACGTAAT-3′ (Xue et al., 2019). The PCR products from bacteria, fungi, and nematodes were extracted from a 2% agarose gel, purified using the AxyPrep DNA Gel Extraction Kit (Axygen Biosciences, Union City, CA, United States), and quantified using a QuantusTM Fluorometer (Promega, United States).

Processing of the Sequencing Data

All three PCR products (bacterial, fungal, and nematode) were purified, pooled in equimolar amounts and paired-end sequenced (2 × 300) on an Illumina MiSeq platform (Illumina, San Diego, CA, United States) by Majorbio Bio-Pharm Technology Co., Ltd. (Shanghai, China) (Zeng et al., 2020). UPARSE version 7.1 was used to cluster the processed sequences into operational taxonomic units (OTUs) that had at least 97% similarity (Gdanetz et al., 2017). The RDP Classifier method was used to assess the taxonomy of the bacterial sequences against the SILVA database (version 128/16S-bacteria database) and fungal against the United States database (version 7.00; fungal-database) with a confidence level of 70% (Zheng et al., 2020). The taxonomy of nematode sequences was analyzed by the RDP Classifier algorithm against the NCBI database (version NT/its-nematode database) using a confidence threshold of 70% (Xue et al., 2019).

Alpha and Beta Diversity Analysis

An OTU-based analytical technique was used to assess the bacterial, fungal, and nematode diversity in each sample. The OTU richness and diversity of each sample were assessed using QIIME software version v1.8.0, with a sequencing depth of 3% to measure the diversity index and species richness (alpha diversity).

Beta diversity analysis was used across all samples to estimate the community structure comparison index. The beta diversity of genotypes was calculated at the OTU level using weighted UniFrac distances and visualized using main coordinates analysis (PCoA). The QIIME tool was used to group and evaluate the weighted UniFrac distance matrices. They discovered evolutionary connections between various groups and the quantity of those samples.

Statistical Analyses

The results of enzymatic activities and nutrient contents were analyzed using two-way ANOVA under two planting patterns and six nitrogen fertilizer application rates. The least significant difference (LSD) was used to separate means and interactions, and statistical significance was evaluated at $P \leq 0.05$. The alpha diversity was calculated utilizing the Chao1 and Shannon diversity indices. Soil nutrient, enzyme activity, and alpha diversity were correlated using R package "pheatmap" (version 3.3.1). Beta diversity was estimated using the Bray-Curtis distance matrix and PCoA. Redundancy analysis (RDA) was used to examine the relationship between soil sample distribution and soil properties using R 4.0 package.[1] These analyses were carried out to assess community compositions across all samples using OTU composition and to depict the link between bacterial, fungal, and nematode communities and soil properties.

RESULTS

Soil Fertility and Enzyme Activities

Straw return had enhanced the soil SOC and TN under both spring and autumn maize cultivation (**Figure 1**). Compared to the TP treatment, SR significantly increased soil SOC content by 2.8–9.0% and TN content by 6.0–7.1% in both spring and autumn maize cultivated fields ($P < 0.05$). Averaged across SR, SOC and TN contents were 10.7 and 1.9 g kg^{-1} in a spring maize field, and 10.2 and 1.6 g kg^{-1} in an autumn maize field, respectively.

[1] https://cran.r-project.org/web/packages/rda/

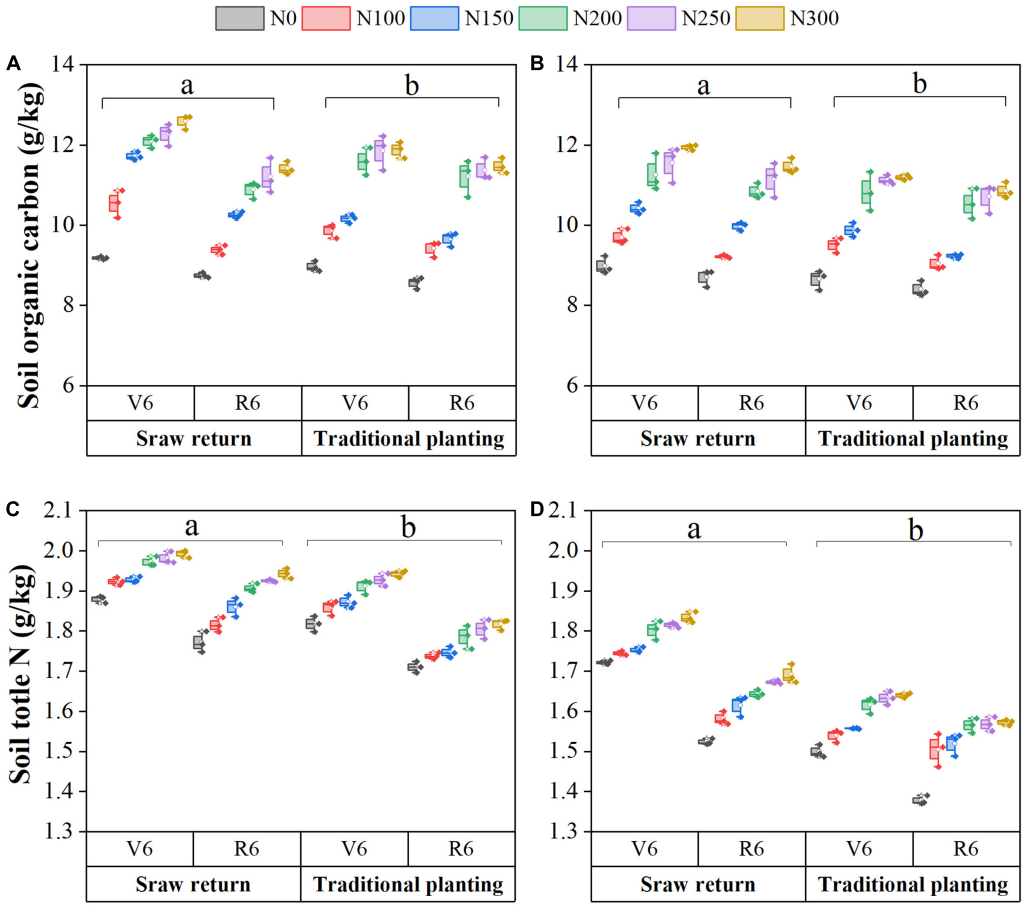

FIGURE 1 | Changes in soil physicochemical properties with straw returning and nitrogen fertilization under dual-cropping system. Soil organic carbon during spring **(A)** and autumn **(B)**, soil total nitrogen content in spring **(C)** and autumn **(D)**.

Our results showed that SOC contents significantly increased by 7.40 and 2.98% at the V6 stage in spring and autumn maize fields, respectively (**Figures 1A,B**). In contrast, TN contents decreased by 5.13% in a spring maize field and 6.6% in an autumn maize field (**Figures 1C,D**). In both spring and autumn maize fields, the SOC and TN contents generally increased with N fertilizer applications. The average SOC and TN contents of N100, N150, N200, N250, and N300 significantly increased compared to the N0 treatment ($P < 0.05$). These results demonstrated 8.8–32.1% changes in SOC and 3.1–8.5% changes in soil TN; however, no significant differences were observed between N200 and N250, and N250 and N300 treatments ($P > 0.05$).

The combined application of straw and nitrogen fertilizer (**Table 1**) improved soil enzyme activities for both seasons (S). Averaged across two stages, the SR increased S-UE, S-SC, and S-CL by 5.5, 3.5, and 5.8% in spring and 5.9, 18.4, and 12.2% in autumn, respectively (**Table 1**). Nitrogen fertilization significantly increased the soil enzyme activities in both planting patterns and seasons, suggesting that the S-UE, S-SC, and S-CL activities were significantly boosted in N300 compared to N0 treatment. However, the N250 treatment was not statistically different from N200 and N300, respectively. On an average basis, S-UE, S-SC, and S-CL activities were 290.1, 32.7, and 8.99 U g^{-1} in spring, and 216.3, 24.3, and 12.24 U g^{-1} in autumn, respectively. These results demonstrated that the S-UE and S-SC activities were higher in spring than in autumn, but the S-CL activity was lower. Moreover, the S-UE and S-SC activities were higher and S-CL activity was lower at the V6 stage than the R6 in both seasons.

Alpha Diversity of Soil Bacterial, Fungal, and Nematode Community

Based on the morphological traits, yield, soil organic carbon, nitrogen, and soil enzyme activities, highly significant differences were observed in response to 200 kg N ha^{-1} under both traditional and straw returning pattern. Therefore, the soil from the plot receiving 200 kg N ha^{-1} of maize field was adopted for soil bacterial, fungal, and nematode analysis.

After quality filtering, a total of 2,201 bacterial, 984 fungal, and 395 nematode OUTs were identified from 1415768, 1775268, and 1433535 RNA gene sequences, respectively. The bacterial OTUs number exhibited the trend SR-N0 > TP-N0 > SR-N200 > TP-N200 during spring and autumn seasons

TABLE 1 | Changes in soil enzyme activities with straw returning and nitrogen fertilization under dual-cropping system.

Season	Treatment	S-UE (U/g)		S-SC (U/g)		S-CL (U/g)	
		V6	R6	V6	R6	V6	R6
Spring	SR-N0	278.6 ± 12.2d	237.4 ± 12.1d	30.3 ± 0.2d	29.0 ± 0.6e	7.8 ± 0.0d	8.1 ± 0.0e
	SR-N100	310.6 ± 2.9c	246.2 ± 5.1cd	32.5 ± 0.1c	30.6 ± 0.2d	8.6 ± 0.1c	8.7 ± 0.0d
	SR-N150	326.4 ± 2.2bc	263.5 ± 2.4c	33.6 ± 0.2c	31.3 ± 0.4cd	8.8 ± 0.1c	9.3 ± 0.0c
	SR-N200	343.7 ± 7.5ab	293.3 ± 10.1b	35.7 ± 0.9b	32.4 ± 0.5bc	9.2 ± 0.1b	10.1 ± 0.1b
	SR-N250	353.6 ± 6.0a	304.7 ± 1.4ab	36.7 ± 0.8ab	33.8 ± 0.6ab	9.5 ± 0.1ab	10.4 ± 0.2ab
	SR-N300	354.3 ± 1.2a	318.7 ± 5.6a	38.5 ± 0.7a	34.5 ± 0.6a	9.7 ± 0.2a	10.7 ± 0.2a
	TP-N0	273.3 ± 13.4c	226.5 ± 5.1c	29.1 ± 0.7e	26.3 ± 0.7d	7.2 ± 0.2d	7.4 ± 0.0d
	TP-N100	301.5 ± 3.9c	241.0 ± 11.5bc	31.3 ± 0.8d	28.8 ± 0.8c	8.5 ± 0.1c	9.0 ± 0.1c
	TP-N150	317.7 ± 2.2b	246.7 ± 7.1bc	33.9 ± 0.9c	30.4 ± 0.2bc	8.7 ± 0.0bc	9.1 ± 0.0bc
	TP-N200	327.6 ± 4.9a	260.6 ± 3.9ab	34.4 ± 0.2bc	31.6 ± 0.9ab	8.9 ± 0.0ab	9.2 ± 0.0ab
	TP-N250	328.8 ± 2.3a	278.8 ± 4.5a	36.1 ± 0.4ab	33.3 ± 0.4a	9.0 ± 0.0a	9.3 ± 0.0a
	TP-N300	333.6 ± 4.8a	306.3 ± 11.8a	36.9 ± 0.5a	33.2 ± 0.7a	9.1 ± 0.1a	9.3 ± 0.0a
	P	NS	**	*	NS	NS	**
	N	**	**	**	**	**	**
	P × N	*	NS	NS	NS	**	**
Autumn	SR-N0	199.0 ± 1.5e	174.0 ± 0.9e	19.6 ± 0.2e	17.3 ± 0.5e	10.2 ± 0.1e	10.6 ± 0.3d
	SR-N100	215.9 ± 0.4d	185.3 ± 1.6d	22.5 ± 0.3d	20.9 ± 0.8d	11.4 ± 0.0d	11.5 ± 0.1c
	SR-N150	226.8 ± 1.5c	206.0 ± 1.3c	25.3 ± 0.6c	22.5 ± 0.4c	12.7 ± 0.0c	12.3 ± 0.1c
	SR-N200	243.7 ± 7.6b	232.4 ± 4.0b	30.3 ± 1.0b	29.5 ± 0.4b	13.7 ± 0.1b	14.3 ± 0.3bc
	SR-N250	249.2 ± 2.2ab	245.2 ± 4.2ab	32.2 ± 1.0ab	30.8 ± 0.1ab	14.1 ± 0.1ab	14.8 ± 0.2ab
	SR-N300	252.2 ± 1.4a	247.3 ± 0.2a	33.3 ± 0.5a	31.7 ± 0.3a	14.3 ± 0.3a	15.5 ± 0.5a
	TP-N0	193.4 ± 2.5d	162.9 ± 3.5d	15.2 ± 0.5d	10.6 ± 0.4c	7.9 ± 0.3d	9.6 ± 0.3d
	TP-N100	210.3 ± 2.9c	182.5 ± 0.4c	20.3 ± 0.8c	16.1 ± 0.5b	10.6 ± 0.1c	11.1 ± 0.1c
	TP-N150	219.5 ± 2.2b	195.8 ± 3.2b	23.2 ± 0.7b	17.3 ± 0.2b	11.6 ± 0.1b	11.9 ± 0.0b
	TP-N200	235.3 ± 3.7a	214.6 ± 0.8a	29.7 ± 0.7a	23.1 ± 0.4a	12.0 ± 0.2ab	12.7 ± 0.5a
	TP-N250	236.6 ± 0.5a	216.6 ± 0.5a	30.9 ± 0.6a	24.4 ± 0.4a	12.2 ± 0.2a	13.1 ± 0.0a
	TP-N300	242.0 ± 0.5a	219.5 ± 1.1a	31.4 ± 0.4a	24.6 ± 0.8a	12.3 ± 0.1a	13.4 ± 0.0a
	P	NS	*	NS	**	**	*
	N	**	**	**	**	**	**
	P × N	NS	**	*	NS	**	**

Different letters indicate significant differences between samples ($P < 0.05$). Values are means ± SE ($n = 3$).
**Significant at $P < 0.05$; **Significant at $P < 0.01$; NS, not significant.*
S–UE, soil urease activity; S–SC, soil sucrase activity; S–CL, soil cellulase activity. SR, TP, P, and N are straw return, traditional planting, planting pattern, and nitrogen, respectively.

(**Supplementary Figures 1A,B**). Whereas the trend for soil fungal OTUs number was SR-N0 > SR-N200 > TP-N0 > TP-N200 during spring, and SR-N0 > TP-N0 > SR-N200 > TP-N200 during autumn (**Supplementary Figures 2A,B**), and the nematode OTUs number exhibited the trend TP-N200 > TP-N0 > SR-N200 > SR-N during spring, and during autumn the OTUs number for SR-N0 and TP-N200 was found to be the same; however, SR-N0 has higher OTUs than SR-N200 (**Supplementary Figures 3A,B**). The results indicated that the SR plot resulted in higher bacterial diversity (Shannon index) in the autumn season, however, it was not significantly affected by N fertilization. The bacterial richness (Chao and ACE index) was not affected by planting pattern or N fertilization, except SR-N0 had significantly higher ACE compared to TP-N200 in the autumn season (**Table 2**). The fungal richness (Chao and ACE index) was significantly affected by seasons, planting pattern, and N fertilization. During the spring season neither planting pattern nor N fertilization had significant effect on fungal diversity and richness, except SR-N0 treatment had significantly lower diversity compared to other treatments. Similarly, the fungal diversity was significantly higher in the SR treatment compared to TP during the autumn season, whereas SR-N0 had noticeably higher fungal richness than TP-N200 (**Table 2**). In contrast, the bacterial, fungal, and nematode richness was significantly higher in TP during the spring season compared to SR treatments. However, SR-N200 treatment had significantly higher nematode Chao1 and ACE richness compared to SR-N0 treatment during the spring season. Moreover, our results showed that the nematode diversity was not significantly affected by seasons, planting pattern, and N fertilization (**Table 2**). No variation in alpha-diversity of bacterial and nematode communities was observed during the spring season ($P > 0.05$). However, bacterial and fungal diversity were significantly higher in SR than TP treatments during the autumn season in response to N fertilization application suggesting that bacterial and fungal are more sensitive to straw returning than nematode in the autumn season ($P < 0.05$). The multi-factor

analysis revealed that the bacterial ($P < 0.05$) and fungal alpha-diversity ($P < 0.01$) were significantly affected by planting pattern and seasons, respectively (**Table 2**).

Beta Diversity of Soil Bacterial, Fungal, and Nematode Community

The variations in bacterial, fungal, and nematode communities caused by SR and fertilization regime were explored using PCoA (**Figure 2**). The first two principal coordinates for the bacterial community represented 28.32 (PC1) and 21.38% (PC2) of total variation in spring (**Figure 2A**), and 35.07 (PC1) and 11.70% (PC2) in autumn maize fields (**Figure 2B**). These results demonstrated that the beta-diversity of bacterial community structure was significantly affected by planting pattern and N fertilization during the spring season; however, during the autumn season the SR-N200 and TP-N0 were overlapped and showed non-significant effect on soil bacterial community.

To assess the fungal beta diversity, the phylogenetic analysis of fungal composition was performed using unweighted UniFrac distances in spring (**Figure 2C**) and autumn (**Figure 2D**). The results of the current study revealed that autumn has more comparable community structure than the spring season. The PC1 and PC2 principal coordinates explained 24.2 and 17.8% of variation in spring and 27.7 and 18.1% of variation in autumn, respectively (**Figures 2C,D**). The application of N fertilizer in the spring altered the structure of the fungal community in a positive direction of PC2. The correlation between SR-N200 and SR-N0 treatments during both seasons was closer, while significant separation was observed for TP-N200 and TP-N0 treatments (**Figures 2C,D**). These results revealed that the fungal beta-diversity were strongly affected by both planting pattern and N fertilization during the autumn season (**Figure 2D**); however, the SR-N200 and SR-N0 treatments were not significantly different during the spring season ($P > 0.05$; **Figure 2C**).

The nematode community analysis indicated that the first and second principal coordinates represented 34.36 and 25.74% of the variation in spring (**Figure 2E**), and 36.79 and 27.53% of the variation in autumn, respectively (**Figure 2F**). The PCoA results indicated that during the spring season the SR-N200 treatment was not significantly different from other treatments. However, SR-N0 was significantly different from TP-N0 and TP-N200 treatments ($P < 0.05$; **Figure 2E**). During the autumn season the treatment SR-N0 was non-significant from the other treatments, but SR-N200 treatment was significantly separated from TP-N0 and TP-N200 treatments ($P < 0.05$; **Figure 2F**). These results suggest that the nematode community was not significantly affected by N fertilization, however, planting patterns have significant effect in both spring and autumn seasons.

Relative Abundance and Community Compositions

Soil Bacterial Abundance and Community Composition

In all treatments, including seasons, planting pattern, and nitrogen fertilizer application, 30 bacterial phyla were

TABLE 2 | Alpha–diversity of the soil bacterial, fungal, and nematode communities with straw return and nitrogen application.

		Bacteria			Fungi			Nemotode		
		Diversity	Richness		Diversity	Richness		Diversity	Richness	
		Shannon	Chao	ACE	Shannon	Chao	ACE	Shannon	Chao	ACE
Spring	SR-N0	6.61 ± 0.02a	2101.6 ± 27.6a	2080.6 ± 32.8a	4.17 ± 0.08b	576.9 ± 75.9a	567.8 ± 69.3a	1.39 ± 0.36a	6.33 ± 2.31c	5.04 ± 5.06c
	SR-N200	6.65 ± 0.04a	2091.5 ± 28.6a	2073.4 ± 27.7a	4.30 ± 0.03a	565.8 ± 79.0a	556.7 ± 77.3a	1.48 ± 0.47a	14.67 ± 2.89b	15.04 ± 3.54b
	TP-N0	6.59 ± 0.06a	2096.4 ± 17.0a	2080.7 ± 23.6a	4.37 ± 0.06a	545.7 ± 78.8a	535.4 ± 77.1a	1.61 ± 0.62a	22.83 ± 8.31a	29.97 ± 15.71a
	TP-N200	6.54 ± 0.06a	2047.8 ± 45.0a	2038.7 ± 28.0a	4.30 ± 0.02a	460.6 ± 86.1a	458.1 ± 85.4a	1.92 ± 0.27a	21.50 ± 1.8a	22.46 ± 1.33a
Autumn	SR-N0	6.61 ± 0.04a	2116.1 ± 21.7a	2101.4 ± 17.6a	4.60 ± 0.09a	691.9 ± 9.6a	682.7 ± 13.6a	1.72 ± 0.21a	19.33 ± 4.04a	19.33 ± 4.04a
	SR-N200	6.64 ± 0.02a	2084.2 ± 26.8a	2067.3 ± 16.9ab	4.56 ± 0.07a	580.9 ± 80.6ab	575.5 ± 80.6ab	1.29 ± 0.44a	15.17 ± 6.45a	11.42 ± 13.47a
	TP-N0	6.62 ± 0.06ab	2111.6 ± 17.3a	2090.0 ± 21.0ab	4.41 ± 0.03b	588.7 ± 78.6ab	579.8 ± 82.0ab	1.42 ± 0.46a	20.33 ± 3.51a	20.76 ± 2.93a
	TP-N200	6.51 ± 0.03b	2069.9 ± 38.1a	2038.3 ± 26.0b	4.41 ± 0.05b	493.9 ± 108.3b	485.39 ± 105.4b	1.81 ± 0.16a	21.83 ± 2.02a	22.61 ± 1.93a
Planting pattern (P)		*	NS	NS	NS	*	*	NS	NS	NS
Nitrogen (N)		NS	*	*	NS	**	**	NS	NS	NS
Season (S)		NS	NS	NS	**	*	**	NS	NS	NS
P × N		*	NS	NS	NS	NS	NS	NS	NS	NS
P × S		NS	NS	NS	**	NS	NS	NS	NS	NS
N × S		NS	NS	NS	NS	NS	*	*	NS	NS
P × N × S		NS	NS	NS	NS	NS	NS	*	NS	NS

Shannon, Chao, and ACE indexes were calculated based on phylogenetic distance at OTU level. Different letters indicate significant differences between samples ($P < 0.05$). Values are means ± SE ($n = 3$).

**Significant at $P < 0.05$; **Significant at $P < 0.01$; NS, not significant.*

SR, TP, P, N, and S are straw return, traditional planting, planting pattern, nitrogen, and season, respectively.

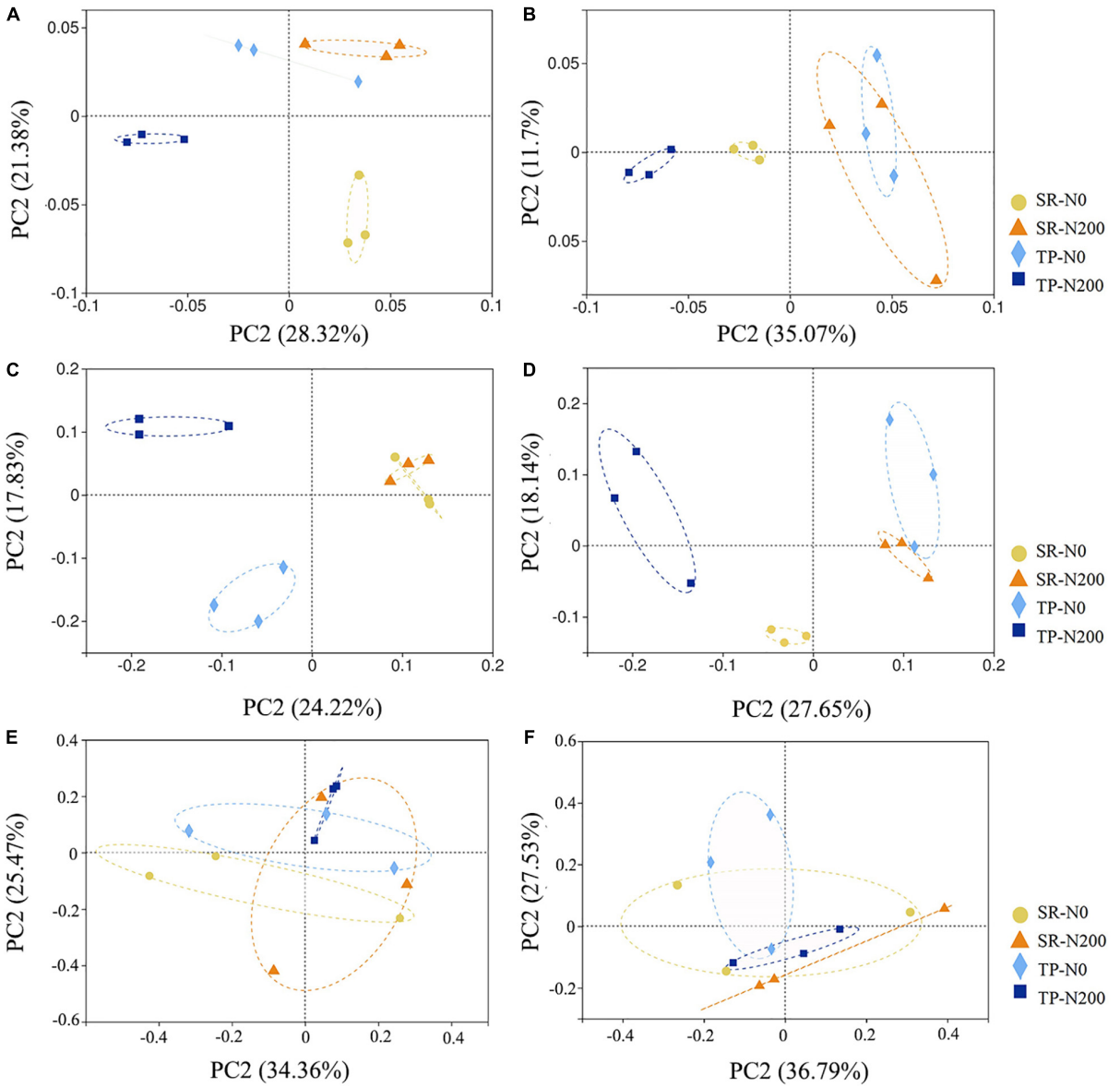

FIGURE 2 | Beta diversities of soil bacterial during spring **(A)** and autumn **(B)**, fungal diversity in spring **(C)** and autumn **(D)**, and nematode diversity in spring **(E)** and autumn **(F)** seasons were analyzed by principal coordinates analysis (PCoA) based on unweighted Unifrac phylogenetic distance metrics at the OTU level and displayed in scatter diagram, each treatment with three replications. SR-N0 = straw returning without N fertilizer application; SR-N200 = straw returning with 200 kg ha^{-1} N fertilizer application; TP-N0 = traditional planting without N fertilizer application; TP-N200 = traditional planting with 200 kg/ha nitrogen fertilizer application.

identified. In spring, 14 of the most abundant phyla were identified, accounting for 96.51–97.15% of all sequences (**Supplementary Figure 4A**). The microbial population was dominated by Proteobacteria (20.90–25.89%), followed by Acidobacterioia (18.56–22.47%), Chloroflexi (13.32–15.42%), and Actinobacteriota (16.41–16.79%). In autumn, 15 of the most abundant phyla were identified, accounting for 96.73–97.64% of all sequences (**Supplementary Figure 4B**). Like spring, the dominant bacterial phyla were Proteobacteria (21.06–23.26%), Acidobacterioia (13.68–23.88%), Chloroflexi (13.72–16.24%), and Actinobacteria (13.83–17.74%) in the autumn. In the SR-N0, SR-N200, TP-N0, and TP-N200 soils, Proteobacteria, Acidobacteriota, Actinobacteriota, and Chloroflexi were the top four most abundant bacterial phyla irrespective of planting seasons (**Figures 3A,B**). In SR-N200 soil, the Proteobacteria (22%), Acidobacteriota (22%), Actinobacteriota (16%), and Chloroflexi (14%) were the top four most abundant phyla in the spring planting pattern (**Figure 3A**). The abundance of Actinobacteriota and Chloroflexi were noticeably increased, whereas the abundance of Proteobacteria was markedly decreased in the TP-N200 soil compared to SR-N200 soil. In addition, the Proteobacteria

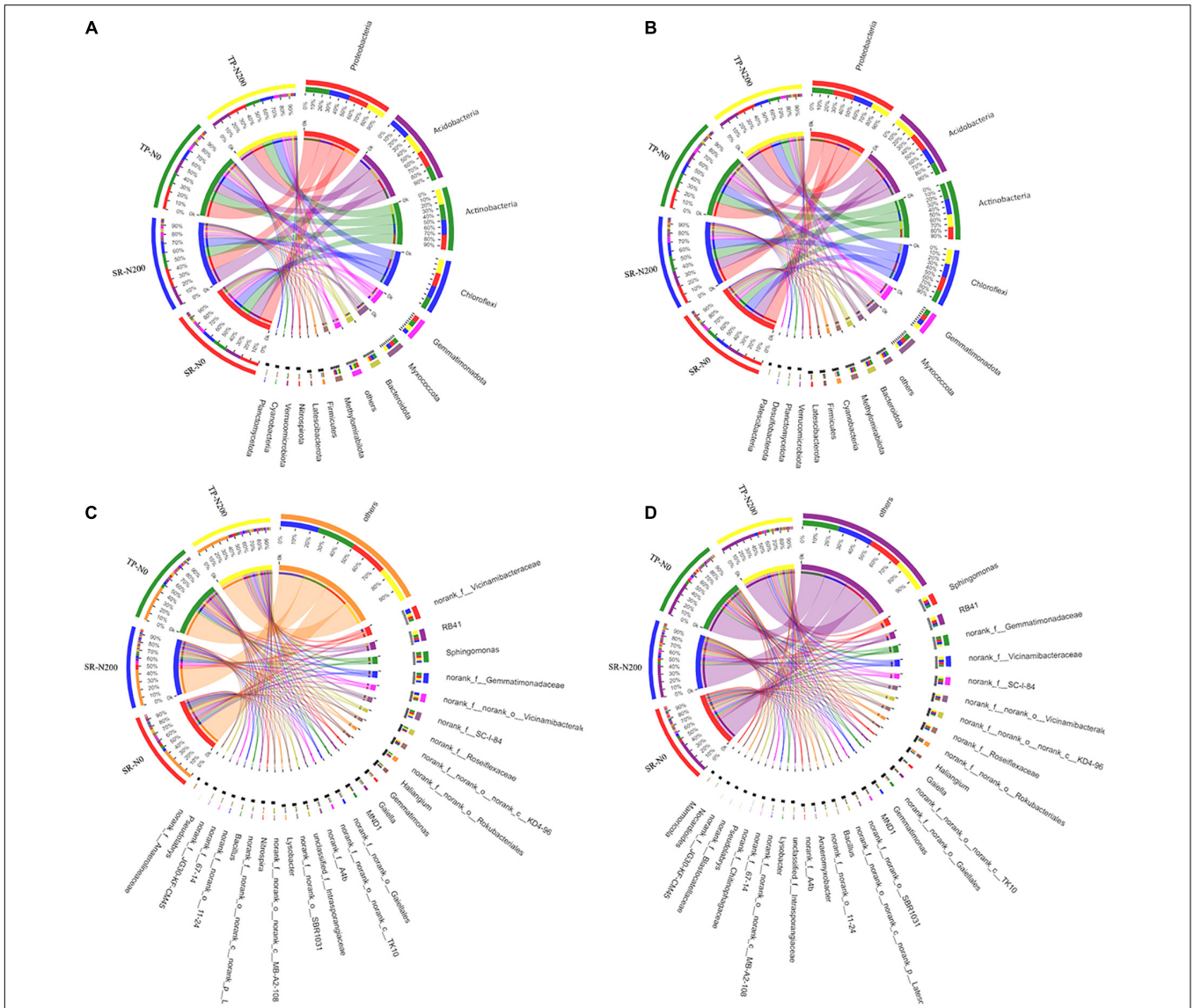

FIGURE 3 | Relative abundances of bacterial in spring **(A)** and autumn **(B)** communities at the phylum level, and abundance at the genes level in spring **(C)** and autumn **(D)** seasons. SR-N0 = straw returning without N fertilizer application; SR-N200 = straw returning with 200 kg ha^{-1} N fertilizer application; TP-N0 = traditional planting without N fertilizer application; TP-N200 = traditional planting with 200 kg/ha nitrogen fertilizer application.

and Actinobacteriota were potentially decreased, whereas the abundance of Acidobacteriota and Chloroflexi were increased in the SR-N0 soil compared to TP-N0 (**Figure 3A**). These results suggest that soil with SR and optimum N fertilization (200 N kg ha^{-1}) presents a significantly greater abundance of Proteobacteria, Acidobacteriota, and Chloroflexi in the spring season. Similarly, in the autumn season, the Proteobacteria, Acidobacteriota, Actinobacteriota, and Chloroflexi were the top four most abundant phyla in SR-N200 and TP-N200 soils (**Figure 3B**). The results of our current study suggest that the Acidobacteriota (24%) and Chloroflexi (16%) were markedly increased in the TP-N200 soil, but the abundance of Actinobacteriota (14%) was decreased compared to SR-N200 soil (**Figure 3B**).

At the genus level, the bacterial community structures showed significant differences among the different treatment and seasons (**Figures 3C,D**). For example, during the spring season in TP-N200 soil, the most dominant genera were norank_f_*Vicinamibacteraceae* (4.7%), RB41 (5.9%), and *Sphingomonas* (3.9%). Furthermore, suggesting that the TP-N0 soil significantly decreased the norank_f_*Vicinamibacteraceae* (3.3%) and *RB41* (4.1%), however, it increased the abundance of *Sphingomonas* (5%). Likewise, in the SR-N200 and SR-N0 soils the dominant bacterial genus was norank_f_*Vicinamibacteraceae* (6.9 and 4.1%), RB41 (3.4 and 3.8%) and *Sphingomonas* (3.2 and 4.1%), respectively, suggesting that the *RB41* and *Sphingomonas* were significantly dominant in SR-N0 soil compared to SR-N200 soil. During the autumn season, the TP-N200 soil has the

highest abundance of genera *Sphingomonas* (4.8%) and *RB41* (5.8%) compared to other treatments (**Figure 3D**). In addition, the abundance of *Sphingomonas* and *RB41* were significantly increased in TP having 200 N ha^{-1} than soil with no fertilization, however, the SR-N200 soil decreased the abundance of these genera compared to SR-N0 soil. These results indicated that the abundances of genera *Sphingomonas* and *RB41* were significantly decreased with N fertilization in an SR plot, however, they decreased under a TP plot (**Figure 3D**).

Soil Fungal Abundance and Community Composition

Various fungal phyla, including Ascomycota, Mortierellomycota, Chytridiomycota, Glomeromycota, Basidiomycota, and unclassified-fungal phyla, were found in all treatments, regardless of season, planting pattern, or nitrogen fertilizer application; however, Rozellomycota was only found in the spring season (**Supplementary Figures 5A,B**). Ascomycota, Mortierellomycota, and Chytridiomycota were found to be the most abundant fungal phyla in both seasons (**Figures 4A,B** and **Supplementary Figures 5A,B**). The phyla Ascomycota (75%) have the highest relative abundance among the fungal community, followed by Mortierellomycota (12%), unclassified (5.39%), and Chytridiomycota (1.75%). Our findings demonstrated that SR treatments have variable degrees of impact on the phylum-level composition of fungal communities. In the TP-N200 and SR-N200 soils, the Ascomycota (79 and 69%), Mortierellomycota (8.2 and 13%), and unclassified-fungi (6.7 and 11%) were the top three most abundant phyla in the spring season, respectively (**Figure 4A**). These results suggest that the abundance of Ascomycota decreased in SR-N200 soil, while Mortierellomycota and unclassified-fungi significantly increased compared to TP-N200 soil. In addition, the relative abundance of Ascomycota and Mortierellomycota were potentially increased, whereas the abundance of unclassified-fungi and Glomeromycota were decreased in the SR-N0 soil compared to TP-N0 (**Figure 4A**). These results demonstrated that SR increased the relative abundance of Ascomycota, Mortierellomycota, and Glomeromycota regardless of N fertilization. Similarly, in SR-N200 soil during autumn season, Ascomycota, Mortierellomycota, Chytridiomycota, and Basidiomycota were 76, 5.5, 9.4, and 2.5%, respectively (**Figure 4B**). However, in TP-N200 soil the relative abundance of Ascomycota, Mortierellomycota, Chytridiomycota, and Basidiomycota were 81, 7.3, 4.4, and 2.1%, respectively. The above results showed that the abundance of Ascomycota and Mortierellomycota was noticeably increased in TP-N220 soil whereas it was decreased in Chytridiomycota and Basidiomycota (**Figure 4B**).

At the genus level, the fungal community structure showed that *Mortierella*, *Chaetomium*, *Fusarium*, *Emericellopsis*, and *Gibberrella* were the most abundant genera in all the treatments (**Figure 4C**). The abundance of *Mortierella, Emericellopsis*, and *Gibberrella* was noticeably decreased in TP-N0 soil compared to TP-N200 soil, however, *Chaetomium* and *Fusarium* were increased. Likewise, in SR-N200 and SR-N0 soils the relative abundance of the top five genera were *Mortierella* (13 and 17%), *Chaetomium* (15 and 14%), *Fusarium* (3 and 6.4%), *Emericellopsis* (15 and 1%), and *Gibberrella* (3.5 and 12%), respectively. In the autumn season, the highest relative abundance of Ascomycota was observed in TP-N200 soil (81%), TP-N0 soil (81%), SR-N200 soil (76%), and SR-N0 soil (75%). Furthermore, the abundance of genera *Ascomycota* and *Mortierellomycota* were increased in the TP pattern, whereas the genre *Chytridiomycot* and *Basidiomycota* were decreased compared to SR (**Figure 4D**).

Soil Nematode Abundance and Community Composition

It was found that there were 15 different types of nematode genera in total during the spring season, and the most abundant genera were *Pratylenchus*, *Tylenchorhynchus*, *Acrobeloides*, *unclassified*, *Aphelenchus*, *Basiria*, and *Aporcella* (**Supplementary Figure 6A**). The dominant nematode genera in TP-N200, TP-N0, SR-N200, and SR-N0 were *Acrobeloides* (37%), *Tylenchorhynchus* (42%), *Pratylenchus* (42%), and *Tylenchorhynchus* (50%), respectively. In addition, the abundance of *Pratylenchus* (27%) and *Acrobeloides* (37%) were increased in TP-N200 soil but decreased the *Tylenchorhynchus* (0.028%) compared to TP-N0 soil and vice versa (**Figure 5A**). Similarly, the nematode genera *Pratylenchus, Acrobeloides,* and *Tylenchorhynchus* accounted for 42, 19, and 0% of the total abundance in SR-N200 soil, respectively. However, the relative abundance of *Tylenchorhynchus* was significantly higher in both TP-N0 and SR-N0 soils compared to the TP-N200 and SR-N200, suggesting that N fertilization negatively affected the abundance of *Tylenchorhynchus* (**Figure 5A**). In the autumn season, the most abundant nematode genera were *Prionchulus*, *Acrobeloides, Aporcella, Pratylenchus, Basiria,* and *Mesodorylaimus* (**Figure 5B** and **Supplementary Figure 6B**). The dominate genera in TP-N200, TP-N0, SR-N200, and SR-N0 were *Basiria* (19%), *Prionchulus* (40%), *Acrobeloides* (36%), and *Prionchulus* (28%). These results showed that the *Prionchulus* was significantly increased in an unfertilized plot; however, the *Aprocella* compared to an N fertilized plot decreased. Moreover, the relative abundance of genera *Tylenchorhynchus* and *Aphelenchus* was found significantly higher in the spring seasons, but significantly less abundance was observed in the autumn seasons (**Figures 5A,B**).

Relationships Between Bacterial, Fungal, and Nematode Community and Soil Environmental Properties

A multivariate RDA analysis indicated that soil environmental variables such as SOC, TN, S-UE, S-CL, and S-SC contributed to the distribution of the bacterial, fungal, and nematode OTUs (**Figure 6**). The first two RDA axes explained 39.17 and 27.11% variation in spring (**Figure 6A**) and autumn (**Figure 6B**), respectively. In addition, the relationship among the bacterial species and environmental factors, suggesting 25.52 and 13.65% variation in spring, and 17.82 and 9.29% variation in autumn for the first and second axes, respectively. The correlation analysis showed that the S-CS, TN, and S-UE significantly increased the bacterial phyla FCPU426 ($P < 0.01$) and significantly decreased Cyanobacteria ($P < 0.05$; **Supplementary Figure 7**). Moreover, S-CL significantly decreased FCPU426 ($P < 0.001$)

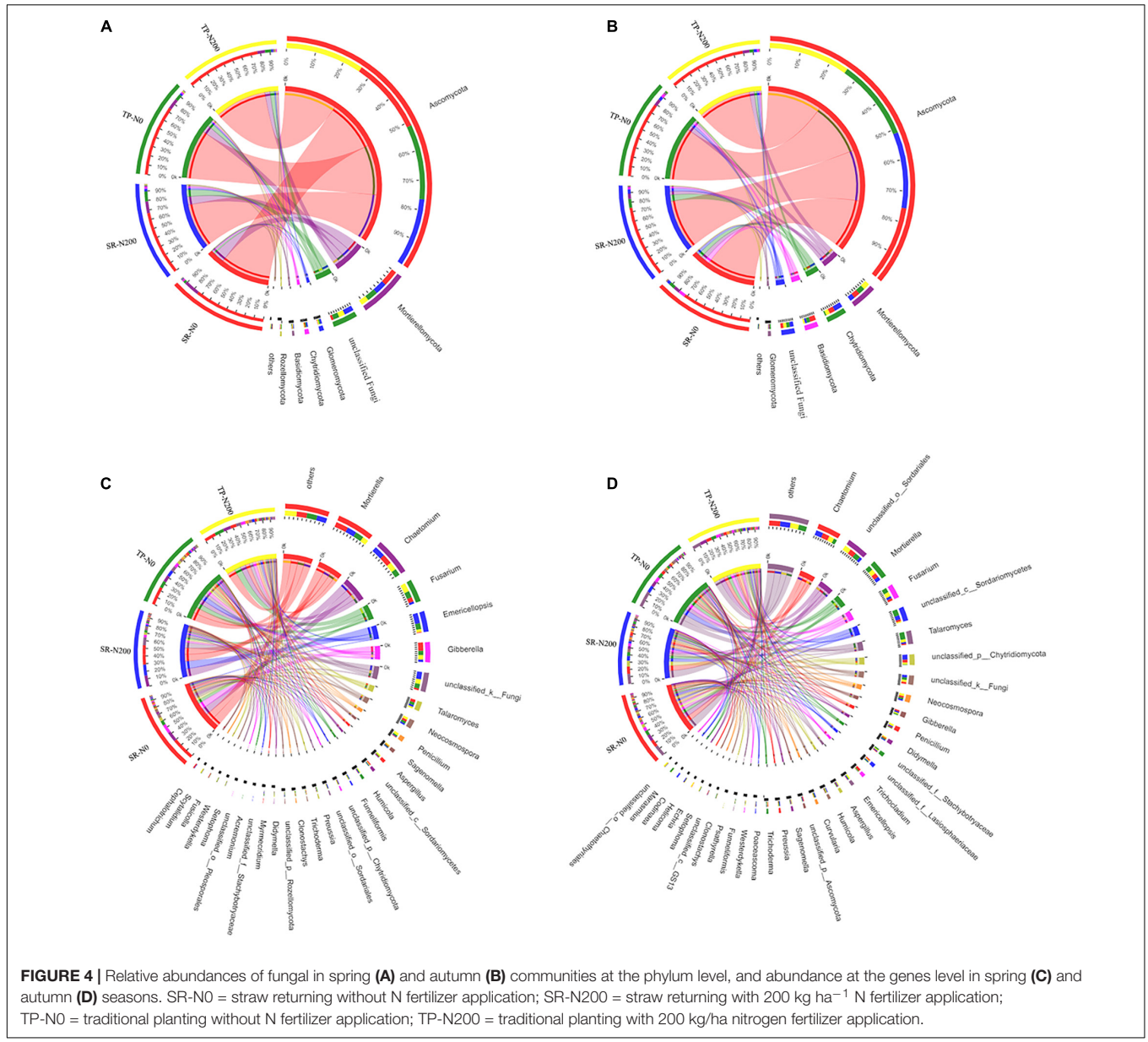

FIGURE 4 | Relative abundances of fungal in spring **(A)** and autumn **(B)** communities at the phylum level, and abundance at the genes level in spring **(C)** and autumn **(D)** seasons. SR-N0 = straw returning without N fertilizer application; SR-N200 = straw returning with 200 kg ha^{-1} N fertilizer application; TP-N0 = traditional planting without N fertilizer application; TP-N200 = traditional planting with 200 kg/ha nitrogen fertilizer application.

and Nitrospirota ($P < 0.05$), whereas SOC, S-CS, and S-UE increased Acidobacteriota. The relationship between changes in environmental factors and the relative abundances of fungal OTUs is shown in **Figures 6C,D**. In spring and autumn, the SOC, TN, S-UE, S-CL, and S-SC accounted for 45.51 and 55.88% of the overall variation, respectively. Furthermore, these results clearly demonstrated that the first and second axes account for 29.67 and 15.84% variation in spring, and 35.88 and 20.00% variation in autumn, respectively. Similarly, soil enzymes significantly affected the fungal phyla, the correlation analysis revealed that S-CL increased the abundance of Chytridiomycota and Basidiomycota ($P < 0.001$), while decreased Mucoromycota and Rozellomycota. In contrast, the abundance of Mucoromycota and Rozellomycota increased with TN and S-UC (**Supplementary Figure 8**). The first two axes suggested that environmental variables such as SOC, TN, S-UE, S-CL, and S-SC strongly influenced the distribution of the nematode OTUs. Redundancy analysis was used to understand the relationship between the nematode community and soil environmental characteristics (**Figures 6E,F**). These results demonstrated that the first two axes of RDA accounted for 26.04 and 10.89% variation in the spring season (**Figure 6E**), while 33.24 and 11.15% in the autumn season (**Figure 6F**). Soil enzyme activities, SOC, and TN were strongly associated with the nematode community distribution in TP-N200 and SR-N200 treatments during the spring season. However, soil enzymes and SOC were associated with SR-N0 and SR-N200 treatment in the autumn season, but TN was nearly correlated to TP-N0. The nematode genera *Pratylenchus* and unclassified *Aphelenchoididae* have positive correlation, while unclassified *Tylencholaimellidae*, *Prismatolaimus*, *Prionchulus*,

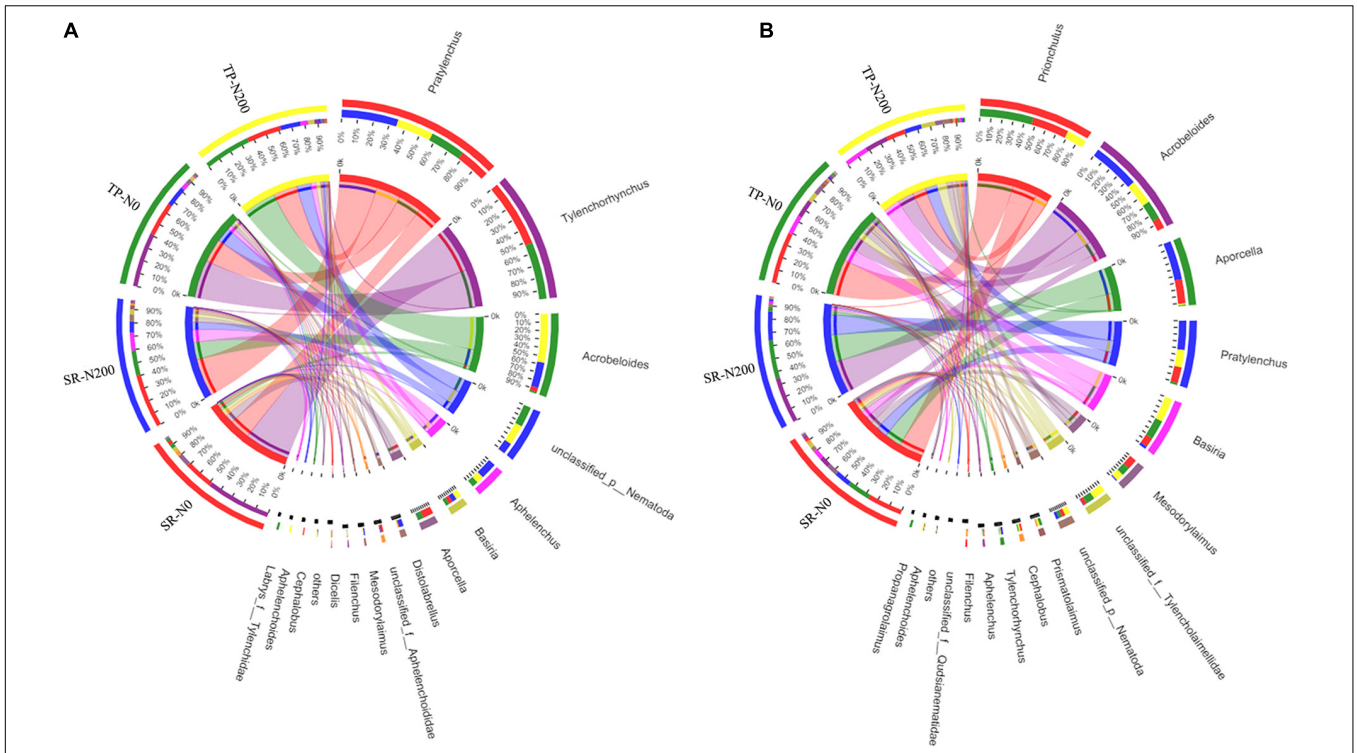

FIGURE 5 | Relative abundances of nematode at the genes level in spring **(A)** and autumn **(B)** seasons. SR-N0 = straw returning without N fertilizer application; SR-N200 = straw returning with 200 kg ha^{-1} N fertilizer application; TP-N0 = traditional planting without N fertilizer application; TP-N200 = traditional planting with 200 kg/ha nitrogen fertilizer application.

and *Mesodorylaimus* have negative correlation with S-CS, TN, and S-UE (**Supplementary Figure 9**). The co-occurrence network diagram further clarified the specific changes in soil fertility and correlation with bacterial, fungal, and nematode community structure under different planting patterns and N fertilizers (**Figure 7**). These results showed that S-SC has a positive relationship with bacterial phyla Chlorflexi, S-CL with Proteobacteria, and TN with Chloroflexi, Acidobacteria, and Actinobacteriota in SR-N200 soil. However, SOC has a positive relation with Chloroflexi and Actinobacteriota in TP-N200. The fungi and nematode have much more strong and positive correlation with soil enzymes, SOC, and TN in TP-N200 compared to SR-N200.

DISCUSSION

Changes in Soil Fertility and Enzyme Activities With Planting Pattern and N Fertilization

Soil organic carbon and N are the primary sources of energy and nutrients for microbial growth (Zhao et al., 2016). The SOC is derived from incorporated crop residues and rhizodeposited organic matter (Banger et al., 2010; Yang et al., 2012). Incorporated residues are decomposed rapidly and returned large amounts of N and C into the field, which lead to improve soil quality and boosted soil fertility (Liu et al., 2014). In addition, the application of N fertilizers increases soil TN and SOC compared to the control treatment (N0). Averaged across fertilization, the SR significantly increases SOC and TN during both seasons compared to the TP pattern (**Figure 1**). However, the spring season has a much higher SOC and TN content than that of the autumn season under both planting patterns. These findings showed that improved SOC and TN contents are mostly attributable to spring maize having more time to decompose the maize straw; however, straw obtained after spring maize harvesting had less time to decompose for the autumn maize (Liao et al., 2018; Zhao et al., 2021). These findings are in line with findings from earlier research (Chao et al., 2019), they also demonstrated that spring maize has higher soil fertility compared to autumn maize, which might be due to the straw incorporated into the soil having the proper time to decompose before sowing.

The soil enzymatic activities boosted in response to chemical fertilizer application and SR due to greater C demand for microbial development under high N content (Liu et al., 2021). Soil enzyme activity is more important in evaluating soil quality and plays an important role in nutrient recycling (Demisie et al., 2014). The increase in soil enzyme activities (**Table 1**) could be explained by changes in the microbial community composition, as well as improved soil microorganism metabolism and microbial activity stimulation by straw addition (Iovieno et al., 2009). Therefore, SR can produce organic supplements and increase microbial biomass, delivering sufficient energy and

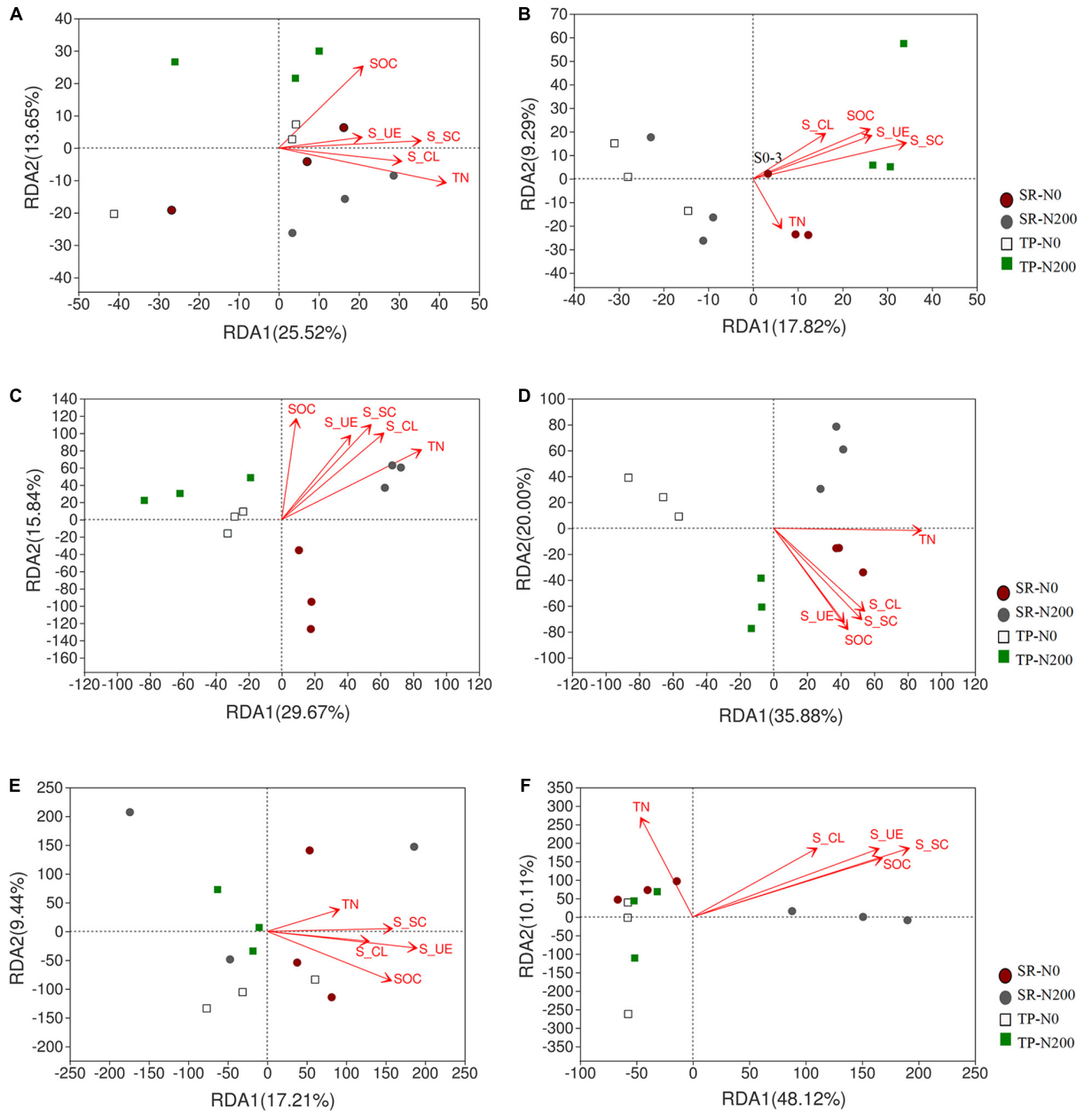

FIGURE 6 | The redundancy analysis (RDA) to identify the relationship of bacterial fungal and nematode OTUs taxa and soil properties. Bacterial in spring **(A)** and autumn **(B)**, fungal in spring **(C)** and autumn **(D)**, and nematode in spring **(E)** and autumn **(F)** seasons. S0 = straw returning without nitrogen fertilizer application; S200 = straw returning with 200 kg/ha nitrogen fertilizer application; T0 = traditional planting without nitrogen fertilizer application; T200 = traditional planting with 200 kg/ha nitrogen fertilizer application.

establishing an appropriate environment for the development of soil enzymes (Gianfreda et al., 2005).

Straw Returning Increases Bacterial, Fungal, and Nematode Diversity

Soil microbes, such as bacteria and fungi, have a major part in the decomposition of straw. Bacteria have a faster growth rate than fungi and play a bigger part in the early phases of decomposition while the fungi, on the other hand, play a bigger role in later stages of decomposition (Marschner et al., 2011; Wang L. et al., 2021). Straw returning increases the bacterial and fungal diversity during the autumn season; thereby changing the structure of the soil ecosystem and making it more stable and healthier (Yin et al., 2010). In the current study we find that the SR plot significantly increases the Shannon index of bacterial and fungal communities during the autumn season. Furthermore, Chao and ACE index of bacterial and fungal communities are

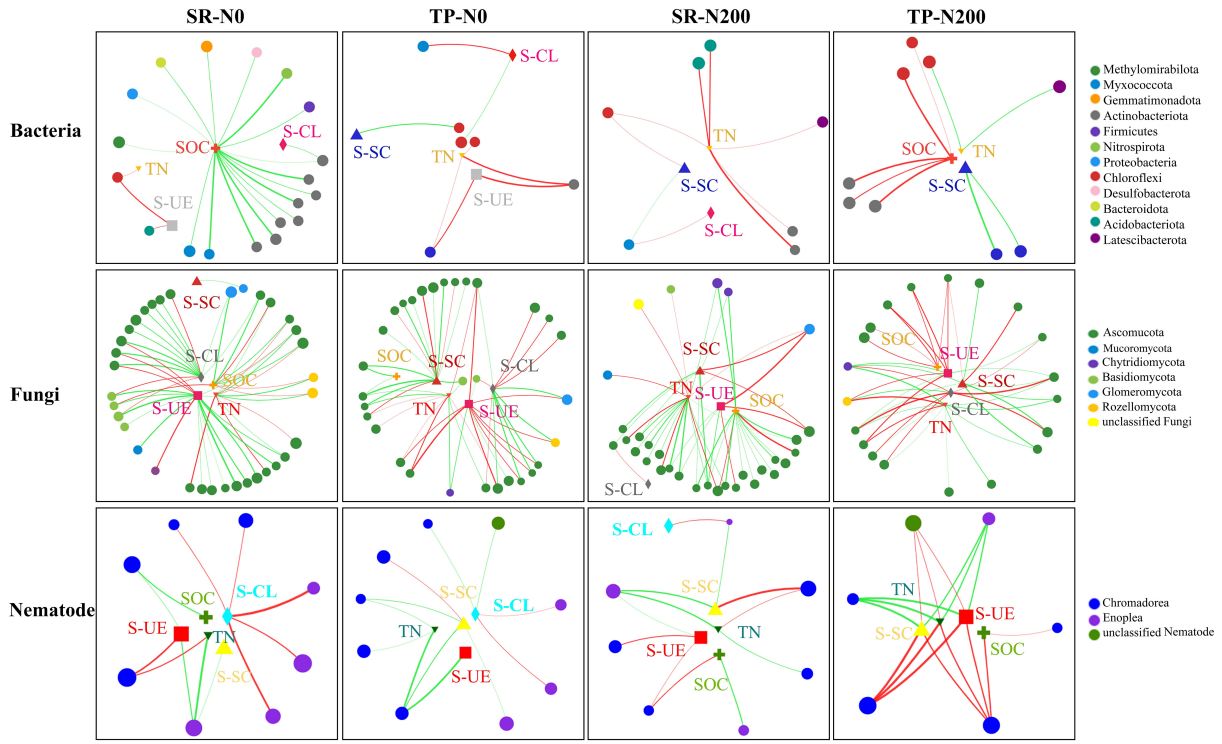

FIGURE 7 | Co-occurrence network diagram between bacterial and fungal taxa at the phyla level and nematode on the class level with soil fertility and enzymes under different treatments. Dot size indicates the value of relative abundances. Positive correlations are labeled with red lines and negative correlations are colored in green, thick lines are high correlations and little correlations have thin lines. Treatments: no nitrogen addition + straw addition (SR-N0), no nitrogen addition + traditional planting (TP-N0), no nitrogen addition + straw addition (SR-200), and traditional planting with nitrogen fertilizer application (TP-N200). TN, SOC, S-UE, S-CL, and S-SC represent total nitrogen content, soil organic carbon content, soil urease activity, soil sucrase activity, and soil cellulase activity.

significantly higher in SR-N0 than that of the TP-N200 treatment ($P < 0.05$; **Table 2**). These results suggest that SR improves soil bacterial and fungal diversity and richness. This may be attributed to the rapid growth rate of bacteria, which promotes straw decomposition in the early stages associated with a larger number of nematodes diversity in the SR plot (Zhang et al., 2012; Wang G. et al., 2021).

Our study finds that SR treatments significantly reduce soil nematode richness and diversity compared to TP treatments in the spring season, but SR-N200 has significantly higher soil nematode Chao and ACE indexes than that of the SR-N0 treatment (**Table 2**). Our findings are consistent with the findings of earlier researchers (Ferreira et al., 2021), who reported that fungal diversity and richness were unaffected by fertilization. Chemical fertilization, on the other hand, reduced bacterial diversity and richness, according to Feng et al. (2015). These results were also confirmed by Zhou et al. (2015), who found that long-term use of a single fertilizer reduces the diversity and richness of the soil bacterial community. In north China, the long-term uses of chemical and organic fertilizers increase the population of bacteria and fungi as reported by Li et al. (2017). As a result, straw addition with N fertilizer application have a key role in sustaining the diversity of soil bacteria, fungi, and nematode communities, which in turn may help to prevent the degradation of the soil microbial community structure and function over time (Sun et al., 2015).

Effect of Straw Returning on Bacterial, Fungal, and Nematode Communities Decomposition

The soil microbial community structure could be altered by SR and N fertilization (Li et al., 2017; Zhao et al., 2019). In this study, Proteobacteria, Acidobacteria, Nitrospirae, Chloroflexi, and Actinobacteria are the important components of the soil bacterial community (**Supplementary Figures 3A,B**), these results are supported by a previous study (Liu et al., 2020). However, the current study found no significant difference in the relative abundance of major soil bacteria phyla between SR and TP plots. The high number of Ascomycota taxa could be attributed to their easy colonization and rapid growth (Liu et al., 2017; Wang L. et al., 2021). In addition, SR has a considerable impact on the abundance of several fungi. Average abundances of fungal phyla Mucoromycota, Chytridiomycota, unclassified fungi, and Rozellomycota differ greatly in SR plots as compared to TP. Even though there were many different phyla in the soil, some of them were not dominating and their abundance was extremely low. In the SR plot, the relative abundances of Rozelloomycoa varied, these results are in line with recent findings

(Fan and Wu, 2020; Wang G. et al., 2021). *Pratylenchus*, *Tylenchorhynchus*, *Prionchulus*, and *Acrobeloides* were dominant and important genera of the soil nematode community (**Figures 5A,B**).

The bacterial and fungal community compositions are changed with N fertilization, planting pattern, and seasons. The most dominant bacterial phyla are Proteobacteria and Acidobacteria, and dominant fungal phyla were Ascomycota, Mucoromycota, and Chytridiomycota in both planting pattern and seasons. Furthermore, the phyla Chytridiomycota, unclassified fungi, and Glomeromycota are significantly increased in N200 kg N ha^{-1} compared to N0 irrespective of the planting pattern. Similarly N fertilizer application has significantly positive effects on the nematode abundances (**Supplementary Figure 3**). The abundance of genera *Pratylenchus* and *Acrobeloides* is noticeably increased in fertilized plots (N200 kg N ha^{-1}) compared to N0 treatment during both seasons. According to the finding of Allison and Martiny (2008), who reported that out of 38 publications 84% of studies suggest that the soil microbial communities are more sensitive to fertilization especially N.

Relationships of Bacterial, Fungal, and Nematode Community With Soil Fertility and Enzyme Activities

The Actinobacteria was the most dominant phylum of bacteria in SR-N0 compared to TP-N0, indicating that it is more prominent in straw decomposition than other microbial fractions (Chen et al., 2016; Li et al., 2017). Moreover, SR-N200 increases bacterial Acidobacteria at the phyla level compared to TP-N200. Different bacterial community compositions suggested that bacteria dominates soil C decomposition, these changes in bacterial fractions suggested that bacteria are important in the degradation of straw and the activity of enzymes (Zhao et al., 2016). The microbial community composition varies in plant growth, but also in reaction to the soil environment in the field, including nitrogen, organic carbon, and enzyme activity (Mouhamadou et al., 2013; Carrara et al., 2018; Hou et al., 2020). Our results show that the changes in the bacterial composition of the soil are identified in response to planting pattern and are closely related to N fertilizer application (**Figure 6**). Furthermore, the increase in diversity of bacterial composition in response to N fertilization is mostly attributable to changes in the relative abundance of certain bacterial phyla such as Chloroflexi, Actinobacteria, Acidobacteria, and Latescibacterota. The co-occurrence network analysis found that the abundance of Chloroflexi and Acidobacteria was closely related to TN in different planting patterns (**Figure 7**). These results are in line with the findings of other researchers (Fierer et al., 2007), who reported that these bacterial phyla have been linked to the soil C and N cycles.

Changes in the soil fungal community in response to SR could be more directly linked to changes in SOC and N derived from straws. As several different types of fungi are saprotrophic in the soil, acquiring SOC, N, and energy from incorporated crop residues (Su et al., 2020b). This might be one reason for the results of RDA that soil enzymes, SOC, and TN were found to be significantly correlated with soil fungal community variation (**Figures 6C,D**). These results further suggest that the most of soil enzymes and soil nutrients are significantly correlated with SR-N200 during spring and with SR-N0 during autumn. The current study results show that the fungal phylum Ascomycota is the most abundant phylum in SR-N0 compared to TP-N0, suggesting that Ascomycota predominated in the SR plot compared to other microbial segments (Ma et al., 2013; Yang et al., 2016). Additionally, at the phylum level, SR-N200 increased the fungal Chytridiomyeota division. Soil enzymes are essential for decomposing soil organic matter and unique to catalyze a specific biochemical reaction (Li et al., 2016). RDA results show differences in the enzymes affecting the changes of the nematode community, which is mainly influenced by S-UE and S-SC in spring (**Figure 6E**) and autumn (**Figure 6F**), respectively. Moreover, S-UE and S-CL had a positive impact on nematode communities at the genus level in SR-N0 and SR-N200 plots, and S-SC, S-UE, and SOC had positive impact in a TP-N200 plot (**Figure 5**).

CONCLUSION

This study investigates the impact of straw returning and N fertilizer on the composition and diversity of bacterial, fungal, and nematode communities, as well as their effects on soil enzymes, SOC, and TN of soil under maize plantation. The SOC, TN, S-UE, S-SC, and S-CL activities in the SR plot following N fertilization increase specifically at the V6 stage than the R6 in an SR plot. The SR incorporation is an important determinant in influencing the composition of the bacterial and fungal communities and improved soil fertility compared to TP. The most dominant soil bacterial and fungal species in spring and autumn were Proteobacteria and Ascomycota, and the most dominant nematode genera were *Pratylenchus* and *Prionchulus* in spring and autumn, respectively. RDA and co-occurrence network identified that TN, SOC, and S-SC were closely correlated with bacterial and fungal community composition. These findings will be helpful in framing the straw returning and N fertilizer application for improving soil fertility, bacterial, and fungal structure and communities on sustainable way and minimizing the degradation of soil in sub-tropical regions of China.

DATA AVAILABILITY STATEMENT

The datasets presented in this study can be found in online repositories. The names of the repository/repositories and accession number(s) can be found at: NCBI – PRJNA803963.

AUTHOR CONTRIBUTIONS

LY and XZ designed the experiment. LY performed the experiment and wrote the manuscript. YC and IM helped in data collection. DW data curation. IM writing–review and editing. XZ resources and supervision. All the authors have read and approved the final manuscript, agreed to the published version of the manuscript.

FUNDING

This study was financially supported by the National Natural Science Foundation of China (31760354) and the Natural Science Foundation of Guangxi Province (2019GXNSFAA185028).

SUPPLEMENTARY MATERIAL

The Supplementary Material for this article can be found online at: https://www.frontiersin.org/articles/10.3389/fmicb.2022.823963/full#supplementary-material

REFERENCES

Allison, S. D., and Martiny, J. B. (2008). Resistance, resilience, and redundancy in microbial communities. *PNAS* 105, 11512–11519. doi: 10.1073pnas.0801925105

Banger, K., Toor, G., Biswas, A., Sidhu, S., and Sudhir, K. (2010). Soil organic carbon fractions after 16-years of applications of fertilizers and organic manure in a Typic Rhodalfs in semi-arid tropics. *Nutr. Cycl. Agroecosyst.* 86, 391–399. doi: 10.1007/s10705-009-9301-8

Borase, D. N., Nath, C. P., Hazra, K. K., Senthilkumar, M., Singh, S. S., Praharaj, C. S., et al. (2020). Long-term impact of diversified crop rotations and nutrient management practices on soil microbial functions and soil enzymes activity. *Ecol. Indic.* 114:106322. doi: 10.1016/j.ecolind.2020.106322

Burns, R. G., Deforest, J. L., Marxsen, J., Sinsabaugh, R. L., Stromberger, M. E., Wallenstein, M. D., et al. (2013). Soil enzymes in a changing environment: current knowledge and future directions. *Soil Biol. Biochem.* 58, 216–234. doi: 10.1016/j.soilbio.2012.11.009

Carrara, J. E., Walter, C. A., Hawkins, J. S., Peterjohn, W. T., Averill, C., and Brzostek, E. R. (2018). Interactions among plants, bacteria, and fungi reduce extracellular enzyme activities under long-term N fertilization. *Glob. Chang. Biol.* 24, 2721–2734. doi: 10.1111/gcb.14081

Chao, P., Kan, Z. R., Peng, L., Qi, J. Y., Xin, Z., and Zhang, H. L. (2019). Residue management induced changes in soil organic carbon and total nitrogen under different tillage practices in the North China Plain. *J. Integr. Agric.* 18, 1337–1347. doi: 10.1016/S2095-3119(18)62079-9

Chen, B., Du, K., Sun, C., Vimalanathan, A., Liang, X., Li, Y., et al. (2018). Gut bacterial and fungal communities of the domesticated silkworm (Bombyx mori) and wild mulberry-feeding relatives. *ISME J.* 12, 2252–2262. doi: 10.1038/s41396-018-0174-1

Chen, C., Zhang, J., Lu, M., Qin, C., Chen, Y., Yang, L., et al. (2016). Microbial communities of an arable soil treated for 8 years with organic and inorganic fertilizers. *Biol. Fertil. Soils* 52, 455–467. doi: 10.1007/s00374-016-1089-5

Chen, L. F., He, Z. B., Wu, X. R., Du, J., Zhu, X., Lin, P. F., et al. (2021). Linkages between soil respiration and microbial communities following afforestation of alpine grasslands in the northeastern Tibetan Plateau. *Appl. Soil Ecol.* 161:103882. doi: 10.1016/j.apsoil.2021.103882

Dang, K., Gong, X., Zhao, G., Wang, H., Ivanistau, A., and Feng, B. (2020). Intercropping alters the soil microbial diversity and community to facilitate nitrogen assimilation: a potential mechanism for increasing proso millet grain yield. *Front. Microbiol.* 11:601054. doi: 10.3389/fmicb.2020.601054

Demisie, W., Liu, Z., and Zhang, M. (2014). Effect of biochar on carbon fractions and enzyme activity of red soil. *Catena* 121, 214–221. doi: 10.1016/j.catena.2014.05.020

Fan, W., and Wu, J. (2020). Short-term effects of returning granulated straw on soil microbial community and organic carbon fractions in dryland farming. *J. Microbiol.* 58, 657–667. doi: 10.1007/s12275-020-9266-5

Feng, Y., Chen, R., Hu, J., Zhao, F., Wang, J., Chu, H., et al. (2015). Bacillus asahii comes to the fore in organic manure fertilized alkaline soils. *Soil Biol. Biochem.* 81, 186–194. doi: 10.1016/j.soilbio.2014.11.021

Ferreira, D. A., Da Silva, T. F., Pylro, V. S., Salles, J. F., Andreote, F. D., and Dini-Andreote, F. (2021). Soil Microbial Diversity Affects the Plant-Root Colonization by Arbuscular Mycorrhizal Fungi. *Microb. Ecol.* 82, 100–103. doi: 10.1007/s00248-020-01502-z

Fierer, N., Bradford, M. A., and Jackson, R. B. (2007). Toward an ecological classification of soil bacteria. *Ecology* 88, 1354–1364. doi: 10.1890/05-1839

Gdanetz, K., Benucci, G. M. N., Pol, N. V., and Bonito, G. (2017). CONSTAX: a tool for improved taxonomic resolution of environmental fungal ITS sequences. *BMC Bioinformatics* 18:538. doi: 10.1186/s12859-017-1952-x

Geisseler, D., and Scow, K. M. (2014). Long-term effects of mineral fertilizers on soil microorganisms–A review. *Soil Biol. Biochem.* 75, 54–63. doi: 10.1016/j.soilbio.2014.03.023

Gianfreda, L., Rao, M. A., Piotrowska, A., Palumbo, G., and Colombo, C. (2005). Soil enzyme activities as affected by anthropogenic alterations: intensive agricultural practices and organic pollution. *Sci. Total Environ.* 341, 265–279. doi: 10.1016/j.scitotenv.2004.10.005

Gong, X., Dang, K., Lv, S., Zhao, G., Wang, H., and Feng, B. (2021). Interspecific competition and nitrogen application alter soil ecoenzymatic stoichiometry, microbial nutrient status, and improve grain yield in broomcorn millet/mung bean intercropping systems. *Field Crops Res.* 270:108227. doi: 10.1016/j.fcr.2021.108227

Hou, Q., Wang, W., Yang, Y., Hu, J., Bian, C., Jin, L., et al. (2020). Rhizosphere microbial diversity and community dynamics during potato cultivation. *Eur. J. Soil Biol.* 98:103176. doi: 10.1016/j.ejsobi.2020.103176

Huang, W., Wu, J. F., Pan, X. H., Tan, X., Zeng, Y. J., Shi, Q. H., et al. (2021). Effects of long-term straw return on soil organic carbon fractions and enzyme activities in a double-cropped rice paddy in South China. *J. Integr. Agric.* 20, 236–247. doi: 10.1016/S2095-3119(20)63347-0

Iovieno, P., Morra, L., Leone, A., Pagano, L., and Alfani, A. (2009). Effect of organic and mineral fertilizers on soil respiration and enzyme activities of two Mediterranean horticultural soils. *Biol. Fertil. Soils* 45, 555–561. doi: 10.1007/s00374-009-0365-z

Kamble, P. N., and Bååth, E. (2016). Comparison of fungal and bacterial growth after alleviating induced N-limitation in soil. *Soil Biol. Biochem.* 103, 97–105. doi: 10.1016/j.soilbio.2016.08.015

Li, S., Chen, J., Shi, J., Tian, X., Li, X., Li, Y., et al. (2017). Impact of straw return on soil carbon indices, enzyme activity, and grain production. *Soil Sci. Soc. Am. J.* 81, 1475–1485. doi: 10.2136/sssaj2016.11.0368

Li, S., Zhang, S., Pu, Y., Li, T., Xu, X., Jia, Y., et al. (2016). Dynamics of soil labile organic carbon fractions and C-cycle enzyme activities under straw mulch in Chengdu Plain. *Soil Tillage Res.* 155, 289–297. doi: 10.1016/j.still.2015.07.019

Liao, P., Huang, S., Van Gestel, N. C., Zeng, Y., Wu, Z., and Van Groenigen, K. J. (2018). Liming and straw retention interact to increase nitrogen uptake and grain yield in a double rice-cropping system. *Field Crops Res.* 216, 217–224. doi: 10.1016/j.fcr.2017.11.026

Liu, C., Gong, X., Dang, K., Li, J., Yang, P., Gao, X., et al. (2020). Linkages between nutrient ratio and the microbial community in rhizosphere soil following fertilizer management. *Environ. Res.* 184:109261. doi: 10.1016/j.envres.2020.109261

Liu, C., Lu, M., Cui, J., Li, B., and Fang, C. (2014). Effects of straw carbon input on carbon dynamics in agricultural soils: a meta-analysis. *Glob. Chang. Biol.* 20, 1366–1381. doi: 10.1111/gcb.12517

Liu, Y. X., Pan, Y. Q., Yang, L., Ahmad, S., and Zhou, X. B. (2021). Stover return and nitrogen application affected soil organic carbon and nitrogen in a double-season maize field. *Plant Biol.* 24, 387–395. doi: 10.1111/plb.13370

Liu, Z., He, T., Lan, Y., Yang, X., Meng, J., and Chen, W. (2017). Maize Stover Biochar Accelerated Urea Hydrolysis and Short-term Nitrogen Turnover in Soil. *Bioresources* 12, 6024–6039. doi: 10.15376/biores.12.3.6024-6039

Lu, J., Li, S., Wu, X., Liang, G., Gao, C., Li, J., et al. (2021). The dominant microorganisms vary with aggregates sizes in promoting soil carbon accumulation under straw application. *Arch. Agron. Soil Sci.* 28, 1–7. doi: 10.3390/agronomy11112126

Ma, A., Zhuang, X., Wu, J., Cui, M., Lv, D., Liu, C., et al. (2013). Ascomycota members dominate fungal communities during straw residue decomposition in arable soil. *PLoS One* 8:e66146. doi: 10.1371/journal.pone.0066146

Marschner, P., Umar, S., and Baumann, K. (2011). The microbial community composition changes rapidly in the early stages of decomposition of wheat residue. *Soil Biol. Biochem.* 43, 445–451. doi: 10.1016/j.soilbio.2010.11.015

Mouhamadou, B., Puissant, J., Personeni, E., Desclos-Theveniau, M., Kastl, E., Schloter, M., et al. (2013). Effects of two grass species on the composition of soil fungal communities. *Biol. Fertil. Soils* 49, 1131–1139. doi: 10.1007/s00374-013-0810-x

Muhammad, I., Wang, J., Sainju, U. M., Zhang, S., Zhao, F., and Khan, A. (2021). Cover cropping enhances soil microbial biomass and affects microbial community structure: a meta-analysis. *Geoderma* 381:114696. doi: 10.1016/j.geoderma.2020.114696

Muhammad, I., Yang, L., Ahmad, S., Zeeshan, M., Farooq, S., Ali, I., et al. (2022). Irrigation and nitrogen fertilization alter soil bacterial communities, soil enzyme activities, and nutrient availability in maize crop. *Front. Microbiol.* 13:833758. doi: 10.3389/fmicb.2022.833758

Mwafulirwa, L., Baggs, E. M., Russell, J., Hackett, C. A., Morley, N., Canto, C. D. L. F., et al. (2021). Identification of barley genetic regions influencingplant-microbe interactions and carbon cycling in soil. *Plant Soil* 468, 165–182. doi: 10.1007/s11104-021-05113-6

Ren, H., Feng, Y., Liu, T., Li, J., Wang, Z., Fu, S., et al. (2020). Effects of different simulated seasonal temperatures on the fermentation characteristics and microbial community diversities of the maize straw and cabbage waste co-ensiling system. *Sci. Total Environ.* 708:135113. doi: 10.1016/j.scitotenv.2019.135113

Salazar, S., Sánchez, L., Alvarez, J., Valverde, A., Galindo, P., Igual, J., et al. (2011). Correlation among soil enzyme activities under different forest system management practices. *Ecol. Eng.* 37, 1123–1131. doi: 10.1016/j.ecoleng.2011.02.007

Su, Y., He, Z., Yang, Y., Jia, S., Yu, M., Chen, X., et al. (2020a). Linking soil microbial community dynamics to straw-carbon distribution in soil organic carbon. *Sci. Rep.* 10:5526. doi: 10.1038/s41598-020-62198-2

Su, Y., Lv, J., Yu, M., Ma, Z., Xi, H., Kou, C., et al. (2020b). Long-term decomposed straw return positively affects the soil microbial community. *J. Appl. Microbiol.* 128, 138–150. doi: 10.1111/jam.14435

Sun, R., Guo, X., Wang, D., and Chu, H. (2015). Effects of long-term application of chemical and organic fertilizers on the abundance of microbial communities involved in the nitrogen cycle. *Appl. Soil Ecol.* 95, 171–178. doi: 10.1016/j.apsoil.2015.06.010

Wang, G., Bei, S., Li, J., Bao, X., Zhang, J., Schultz, P. A., et al. (2021). Soil microbial legacy drives crop diversity advantage: linking ecological plant-soil feedback with agricultural intercropping. *J. Appl. Ecol.* 58, 496–506. doi: 10.1007/s11368-021-03009-7

Wang, L., Wang, C., Feng, F., Wu, Z., and Yan, H. (2021). Effect of straw application time on soil properties and microbial community in the Northeast China Plain. *J. Soils Sediments* 21, 3137–3149.

Wu, H., Cai, A., Xing, T., Huai, S., Zhu, P., Xu, M., et al. (2021). Fertilization enhances mineralization of soil carbon and nitrogen pools by regulating the bacterial community and biomass. *J. Soils Sediments* 21, 1633–1643. doi: 10.1007/s11368-020-02865-z

Wu, L., Ma, H., Zhao, Q., Zhang, S., Wei, W., and Ding, X. (2020). Changes in soil bacterial community and enzyme activity under five years straw returning in paddy soil. *Eur. J. Soil Biol.* 100:103215. doi: 10.1016/j.ejsobi.2020.103215

Xue, B., Hou, L., and Xue, H. (2019). Research on the characteristics of soil nematode communities in alpine meadow in northern Tibet by using high-throughput sequencing. *Acta Ecol. Sin.* 39, 4088–4095.

Yang, H., Feng, J., Zhai, S., Dai, Y., Xu, M., Wu, J., et al. (2016). Long-term ditch-buried straw return alters soil water potential, temperature, and microbial communities in a rice-wheat rotation system. *Soil Tillage Res.* 163, 21–31. doi: 10.1016/j.still.2016.05.003

Yang, X., Ren, W., Sun, B., and Zhang, S. (2012). Effects of contrasting soil management regimes on total and labile soil organic carbon fractions in a loess soil in China. *Geoderma* 177, 49–56. doi: 10.1016/j.geoderma.2012.01.033

Yin, X., Song, B., Dong, W., Xin, W., and Wang, Y. (2010). A review on the eco-geography of soil fauna in China. *J. Geogr. Sci.* 20, 333–346. doi: 10.1007/s11442-010-0333-4

Yu, D., Wen, Z., Li, X., Song, X., Wu, H., and Yang, P. (2018). Effects of straw return on bacterial communities in a wheat-maize rotation system in the North China Plain. *PLoS One* 13:e0198087. doi: 10.1371/journal.pone.0198087

Yuan, Q., Hernández, M., Dumont, M. G., Rui, J., Scavino, A. F., and Conrad, R. (2018). Soil bacterial community mediates the effect of plant material on methanogenic decomposition of soil organic matter. *Soil Biol. Biochem.* 116, 99–109. doi: 10.1016/j.soilbio.2017.10.004

Zeng, X. Y., Li, S. W., Leng, Y., and Kang, X. H. (2020). Structural and functional responses of bacterial and fungal communities to multiple heavy metal exposure in arid loess. *Sci. Total Environ.* 723:138081. doi: 10.1016/j.scitotenv.2020.138081

Zhang, X., Li, Q., Zhu, A., Liang, W., Zhang, J., and Steinberger, Y. (2012). Effects of tillage and residue management on soil nematode communities in North China. *Ecol. Indic.* 13, 75–81. doi: 10.1016/j.ecolind.2011.05.009

Zhao, S., Fan, F., Qiu, S., Xu, X., He, P., and Ciampitti, I. A. (2021). Dynamic of fungal community composition during maize residue decomposition process in north-central China. *Appl. Soil Ecol.* 167:104057. doi: 10.1016/j.apsoil.2021.104057

Zhao, S., Li, K., Zhou, W., Qiu, S., Huang, S., and He, P. (2016). Changes in soil microbial community, enzyme activities and organic matter fractions under long-term straw return in north-central China. *Agric. Ecosyst. Environ.* 216, 82–88. doi: 10.1016/j.agee.2015.09.028

Zhao, S., Qiu, S., Xu, X., Ciampitti, I. A., Zhang, S., and He, P. (2019). Change in straw decomposition rate and soil microbial community composition after straw addition in different long-term fertilization soils. *Appl. Soil Ecol.* 138, 123–133. doi: 10.1016/j.apsoil.2019.02.018

Zhao, S., and Zhang, S. (2018). Linkages between straw decomposition rate and the change in microbial fractions and extracellular enzyme activities in soils under different long-term fertilization treatments. *PLoS One* 13:e0202660. doi: 10.1371/journal.pone.0202660

Zheng, L., Chen, H., Wang, Y., Mao, Q., Zheng, M., Su, Y., et al. (2020). Responses of soil microbial resource limitation to multiple fertilization strategies. *Soil Tillage Res.* 196:104474. doi: 10.1016/j.still.2019.104474

Zhou, J., Guan, D., Zhou, B., Zhao, B., Ma, M., Qin, J., et al. (2015). Influence of 34-years of fertilization on bacterial communities in an intensively cultivated black soil in northeast China. *Soil Biol. Biochem.* 90, 42–51. doi: 10.1016/j.soilbio.2015.07.005

Conflict of Interest: The authors declare that the research was conducted in the absence of any commercial or financial relationships that could be construed as a potential conflict of interest.

Publisher's Note: All claims expressed in this article are solely those of the authors and do not necessarily represent those of their affiliated organizations, or those of the publisher, the editors and the reviewers. Any product that may be evaluated in this article, or claim that may be made by its manufacturer, is not guaranteed or endorsed by the publisher.

frontiers in Microbiology

ORIGINAL RESEARCH
published: 30 March 2022
doi: 10.3389/fmicb.2022.861918

A Detoxification-Free Process for Enhanced Ethanol Production From Corn Fiber Under Semi-Simultaneous Saccharification and Fermentation

Yingjie Guo, Jiamin Huang, Nuo Xu, Hexue Jia, Xuezhi Li, Jian Zhao* and Yinbo Qu*

State Key Laboratory of Microbial Technology, Shandong University, Qingdao, China

Corn fiber, a by-product from the corn-processing industry, is an attractive feedstock for cellulosic ethanol because of its rich carbohydrate content (mainly residual starch, cellulose, and hemicellulose), abundant reserves, easy collection, and almost no transportation cost. However, the complex structure and components of corn fiber, especially hemicellulose, make it difficult to be effectively hydrolyzed into fermentable sugars through enzymatic hydrolysis. This study developed a simple and easy industrialized process without detoxification treatment for high-yield ethanol produced from corn fiber. Corn fiber was pretreated by dilute acid under the conditions optimized by Box-Behnken design (0.5% H_2SO_4 at 105°C for 43 min), and 81.8% of total sugars, including glucose, xylose, and arabinose, could be recovered, then the mixture (solid and hydrolysates) was directly used for semi-simultaneous saccharification and fermentation without detoxification, and ethanol yield reached about 81% of the theoretical yield.

Keywords: corn fiber, dilute sulfuric acid pretreatment, optimization, semi-simultaneous saccharification and fermentation, ethanol

OPEN ACCESS

Edited by:
Christopher Rensing, Fujian Agriculture and Forestry University, China

Reviewed by:
Binod Parameswaran, National Institute for Interdisciplinary Science and Technology (CSIR), India
Yong Sun, Northeast Agricultural University, China

****Correspondence:***
Xuezhi Li
lixz@sdu.edu.cn
Jian Zhao
zhaojian@sdu.edu.cn

Specialty section:
This article was submitted to Microbiotechnology, a section of the journal Frontiers in Microbiology

Received: *25 January 2022*
Accepted: *01 March 2022*
Published: *30 March 2022*

Citation:
Guo Y, Huang J, Xu N, Jia H, Li X, Zhao J and Qu Y (2022) A Detoxification-Free Process for Enhanced Ethanol Production From Corn Fiber Under Semi-Simultaneous Saccharification and Fermentation. Front. Microbiol. 13:861918. doi: 10.3389/fmicb.2022.861918

INTRODUCTION

Bioethanol, being a kind of fuel made from organic matter resulting from agriculture or forestry, is a sustainable resource with the advantages, such as cleanliness, renewable, and reduced dependence on petroleum imports (Lovett et al., 2011; Toor et al., 2020). In addition, as a fuel octane enhancing additive, bioethanol can diversify energy supplies while contributing significantly to reducing carbon and particle emissions (Moore et al., 2017). Currently, commercial bioethanol is mainly first-generation ethanol produced from starch- or sugar-containing feedstocks, such as corn, other grains, and sugar cane, which require huge cultivatable land while directly competing with the food supply (Nigam and Singh, 2011; Searchinger et al., 2018). The second-generation fuel ethanol uses renewable lignocellulose as raw materials, such as corn stover and other agricultural and forestry residues, but its commercial production has been limited by high production costs, including raw material costs, pretreatment costs, enzyme costs, and investment costs. The cost of raw materials is one of the most important factors affecting the commercial production of second-generation ethanol. Corn fiber is mainly composed of residual starch, cellulose, and hemicellulose. As a residue of the corn processing industry, it is estimated that the annual output of corn fiber reached 10.9 million tons in China (Jiang et al., 2018). In traditional corn ethanol facilities, corn fiber commonly

passes through the fermentation and distillation stages and ends up in the distiller's dried grains with solubles (DDGS) rather than being converted to ethanol, which reduces the total output of corn ethanol (Kurambhatti et al., 2018). Corn fiber is expected to become an attractive feedstock for cellulosic ethanol because of rich carbohydrates, abundant reserves, easy collection, and almost no transportation cost. According to reports, if corn fiber can be economically converted into ethanol, it will increase the total corn ethanol production by up to 13% on the existing basis while improving the protein content of DDGS (Bothast and Schlicher, 2005).

Unlike other lignocellulose, such as corn stover, hemicellulose is the most abundant component of corn fiber (about 40% of dry corn fiber weight), mainly composed of glucuronoarabinoxylan substituted by various side chains (Saha, 2003; Beri et al., 2020). It covers the surface of cellulose, thus affecting the accessibility of cellulase to cellulose. In contrast, because of the complex sugar compositions and structure of hemicellulose in corn fiber and the interaction between different components, it requires a complex hemicellulase system for completing the thorough degradation of hemicellulose (Agger et al., 2010). All the factors make corn fiber difficult to be effectively hydrolyzed into fermentable sugars by direct enzymatic hydrolysis. Therefore, pretreatment before enzymatic hydrolysis has been proposed to improve the enzymatic digestibility of corn fiber for obtaining high fermentable sugar yield (Kumar et al., 2009; Brodeur et al., 2011; Zhang et al., 2021). Till now, some methods used for pretreating corn fiber have been reported. For example, Bura et al. (2002) treated corn fiber by the steam explosion in a batch reactor at various degrees of severity and found that maximum total sugar yields of 81% could be obtained when corn fiber was pretreated at 190°C for 5 min with addition of 6% SO_2, and using the pretreated corn fiber as substrate, the ethanol concentration reached 6.9 g/L by enzymatic hydrolysis and fermentation at 2% solid content, but the conversion of hemicellulose sugar is lower than 60%. Juneja et al. (2021) performed a two-step pretreatment of corn fiber separated from whole stillage, including liquid hot water pretreatment (LHW) and disk milling. It was shown that, under optimal conditions, the yields of glucose, xylose, and arabinose after enzymatic hydrolysis were 96.18, 72.39, and 66.33%, respectively, but only 21.54 g/L of ethanol concentration was reached after fermentation at 20% solid content. Both steam explosion and LHW require high temperature and pressure, as well as pressure equipment, but the conversion of hemicellulose in pretreated corn fiber was still low. In contrast, the pretreatment conditions of high temperature and high pressure also led to the formation of fermentation inhibitors through further degradation of sugar products.

Many literature showed that dilute acid pretreatment could effectively degrade hemicellulose of lignocellulose materials (Noureddini and Byun, 2010; Jiang et al., 2015; Mikulski and Kłosowski, 2018; Santos et al., 2018), thus the method has been used for pretreating corn fiber to obtain the high conversion of cellulose and hemicellulose, but the monosaccharides would be further degraded during the pretreatment to form inhibitors, such as furfural and 5-hydroxymethylfurfural (HMF). For example, Iram et al. (2019) pretreated DDGS with dilute acid, and the yield of total reducing sugar (TRS) reached 0.382 g/g DDGS; besides TRS, furfural and HMF were also produced during the acid pretreatment. Li et al. (2019) used the combination of acid pretreatment with distillation to *in situ* pretreat whole stillage containing corn fiber and recycled it to the liquefaction step, which improved the ethanol yield by 6.3% compared to the traditional process, and the cellulose conversion was 77.5%, but similarly, many inhibitors were also produced, which led to incomplete fermentation. Noureddini and Byun (2010) used dilute sulfuric acid to treat corn fiber and found that the highest yield of monosaccharides (63.1 g sugar/100 g corn fiber) was obtained when the pretreatment was conducted at 5% of biomass loading (w/w), 1.5% of sulfuric acid concentration (v/v), and 140°C, but the concentration of furfural in pretreatment liquor was also high (3.8 mg/ml) after pretreatment under the conditions. Besides, their results also showed that the formation of furfural could be significantly decreased when pretreatment temperature dropped from 140 to 120°C during the dilute sulfuric acid pretreatment of corn fiber.

Although the inhibitors produced by the dilute acid pretreatment, for example, acetic acid, formic acid, furfural, HMF, and phenolic compounds, limit the applicability of the hydrolysate for subsequent biotransformation (Hendriks and Zeeman, 2009; Yemiş and Mazza, 2011; Lee et al., 2017), and detoxification treatment must be conducted before fermentation to decrease their adverse effects on subsequent saccharification and fermentation, the dilute acid pretreatment is still an attractive approach for improving enzymatic digestibility of corn fiber because of high content and complex structure of hemicellulose in corn fiber. However, the pretreatment process still needs to be further improved to more effectively improve the enzymatic digestibility of corn fiber while minimizing sugar loss and inhibitors formation. To achieve this goal, in this study, we optimized dilute sulfuric acid pretreatment conditions, including temperature, acid concentration, and reaction time, by using the response surface method (RSM), then, the pretreated corn fiber with hydrolysates was directly used for the production of ethanol without detoxification by semi-simultaneous saccharification and fermentation (semi-SSF) process to assess the feasibility of the integrated process for ethanol production using corn fiber as feedstock. In the semi-SSF process, the cellulase from *Penicillium oxalicum,* which has more abundant hemicellulase activities than the cellulase from *Trichoderma reesei* (Gao et al., 2021), was used in the pre-hydrolysis of corn fiber-rich in hemicellulose components and subsequent SSF process, and *Saccharomyces cerevisiae* LF2, an engineered strain with glucose and xylose metabolism, was used in the fermentation of hydrolysates for obtaining high ethanol yield by simultaneous conversion of glucose and xylose to ethanol.

MATERIALS AND METHODS

Materials and Strains

Corn fiber was obtained from Juneng Golden Corn Co. Ltd., (Shouguang, China). It was ground using an MF 10 basic Microfine grinder (IKA, Germany) with a 2.0-mm-hole

diameter sieve, then stored in a sealed polyethylene bag at −20°C before use.

The liquid chromatography standards, including glucose, galactose, arabinose, xylose, mannose, galacturonic acid, glucuronic acid, furfural, HMF, and acetic acid, were purchased from Sigma-Aldrich Co. LLC (St. Louis, MO, United States). Reagent grade sulfuric acid (98%), anhydrous sodium acetate, sodium hydroxide, and ethanol were obtained from Sinopharm Chemical Reagent Co. Ltd. (Shanghai, China).

Penicillium oxalicum MCAX, an engineered strain in our laboratory (Gao et al., 2021), was used to produce cellulases.

Saccharomyces cerevisiae LF2 is capable of metabolizing xylose and glucose was maintained in our group. It was provided by Professor Xiaoming Bao from Qilu University of Technology, Shandong.

Analysis of Chemical Compositions of Corn Fiber

The chemical compositions of corn fiber were determined according to the National Renewable Energy Laboratory (NREL) protocols. The extractives were quantified according to the analytical method NREL/TP-510-42619 (Sluiter et al., 2005a), and the ash was determined by the incineration method described by Sluiter et al. (2005b). The contents of cellulose, hemicellulose (xylose, arabinose, and galactose), lignin, and acetyl group were determined by two-step hydrolyzing corn fiber with H_2SO_4 of 72% (w/w) and 4% (w/w), respectively, according to the analytical method NREL/TP-510-42618 (Sluiter et al., 2008a). The starch was quantified according to the analytical method NREL/TP-510-42619 (Sluiter and Sluiter, 2005). The protein was quantified according to the analytical method NREL/TP-510-42625 (Hames et al., 2008). The sample collected during the determination of acetyl group content was filtered by 0.22 μm Millipore Syringe Filters (Jinteng, China), and the filtrate was used to analyze glucuronic acid by high-performance liquid chromatography (HPLC) (Shimadzu, Japan), which was equipped with Shimadzu's 20A refractive index detector. An Aminex HPX-87H column (300 × 7.8 mm) (Bio-Rad, Richmond, CA, United States) was used to separate the compounds at 60°C. The mobile phase was 0.005 M H_2SO_4 with a 0.5 ml/min flow rate.

Enzyme Preparation

The cellulase used in this study was produced by *P. oxalicum* MCAX according to the method suggested by Gao et al. (2021). The strain MCAX was cultivated in 50 ml of seed medium [g/L, wheat bran: 20, peptone: 10, glucose: 10, $(NH_4)_2SO_4$: 2, KH_2PO_4: 3, and $MgSO_4$: 0.5] in 300 ml Erlenmeyer flasks for 24 h at 30°C and 200 rpm on a rotary shaker. Then, the culture was inoculated into a fermentation medium [g/L, wheat bran: 30, bean cake powder: 15, microcrystalline cellulose: 30, $(NH_4)_2SO_4$: 2, KH_2PO_4: 5, and $MgSO_4$: 0.5] with an inoculation ratio of 10% (v/v) and incubated at 30°C and 200 rpm for 6 days. After fermentation, the supernatant was obtained by centrifugation at 10,000 rpm for 10 min and used as crude cellulase. The hydrolytic activities of the crude cellulase were as follows: filter paper activity (FPA) 6 stocktickerFPU/ml, xylanase 783 IU/ml, arabinofuranosidase 5 IU/ml, and β-xylosidase 1 IU/ml.

Pretreatment of Corn Fiber

Pretreatment of corn fiber with dilute sulfuric acid was performed in a laboratory-scale vertical pressure steam sterilizer (Deqiang, China). A total of 4 g of corn fiber and dilute acid solution was thoroughly mixed in 50 ml flasks with 12 ml of reaction volume. Based on preliminary experiments, the following experimental conditions were tested: temperature of 105–125°C, H_2SO_4 concentration of 0.2–0.5% (w/v), and time of 10–60 min. The experiments were designed by a Box-Behnken RSM using Design-Expert version 8.0.6.1 software and are shown in **Table 2**.

For the significance analysis of different factors in the pretreatment, p-value was obtained by ANOVA and used for determining statistically significant. $p > 0.05$ indicates that the factor is not significant; $p \leq 0.05$ indicates that it is significant; and $p \leq 0.01$ indicates that it is very significant.

After pretreatment, the flasks were cooled down to room temperature. A part of the pretreated corn fiber slurries was collected to analyze the contents of furfural, HMF, formic acid, and acetic acid.

Saccharification

The saccharification was performed at 5% (w/v) substrate concentration in 50 ml flasks with a reaction volume of 20 ml. The pretreated corn fiber slurries were first adjusted to pH 5.0 with 10 M NaOH solution, mixed well with crude cellulase solution and acetate buffer of pH 4.8 in flasks, and incubated at 48°C in a thermostat air bath shaker set at 150 rpm. The samples were taken at reaction times of 0, 12, 24, and 48 h, respectively, and 72 h to analyze the concentrations of monomeric sugars in the enzymatic hydrolysates.

All experiments were performed in triplicate, and the average values are given in this study.

Acclimation of Yeast for Obtaining Resistant Strain

The hydrolysate of corn fiber was treated with dilute acid under the optimum pretreatment conditions, which contains 4.60 g/L glucose, 3.92 g/L xylose, 0.44 g/L furfural, 1.04 g/L formic acid, and 1.62 g/L acetic acid. For acclimation of the yeast, four different acclimation media were used. One of the media consisted of hydrolysate that was not diluted. The three other media were prepared by diluting hydrolysate to a concentration of 25, 50, and 75% (v/v), respectively. In each acclimation medium, 15.0 g/L glucose, 0.40 g/L $(NH_4)_2SO_4$, and 1.00 g/L yeast extract were added. *S. cerevisiae* LF2 was first inoculated into YPD medium for activation of 24 h at 30°C, then take 2 ml of inoculum, centrifuge, and transfer the yeast cells to a 50 ml Erlenmeyer flask containing 20 ml of the acclimation medium with the lowest inhibitors concentration and incubated at 30°C to the glucose content in the medium less than 90% of the initial glucose content. After that, the strain was further transferred to the next acclimation medium with a higher inhibitors' concentration and cultured according to the procedure above

until the highest inhibitors concentration. To make the yeast better adapt to the change of inhibitor concentration, the acclimation of yeast in each inhibitor concentration was repeated more than four times.

Semi-Simultaneous Saccharification and Fermentation

The inoculum was prepared by growing *S. cerevisiae* LF2 in a YPD medium containing 20 g/L glucose, 20 g/L peptone, and 10 g/L yeast extract at 30°C, 200 rpm for 24 h in a thermostat air bath shaker. The inoculum with an OD of 2.0 at 600 nm was used as seed culture, and the inoculation volume was 5% (v/v).

The semi-SSF experiment was performed in a 50 ml sealed Erlenmeyer flask by a rubber plug with a needle. First, the pretreated corn fiber slurries were adjusted to pH 5.0 with 10 M NaOH, and the pre-hydrolysis was conducted at 20% (w/v) solid consistency, 48°C, pH 5.0 for 12 h using cellulase of 10 FPU/g (DM). After pre-hydrolysis, the reaction system temperature was adjusted to 30°C, and 5% (v/v) of seed was inoculated to the reaction system. Fermentation was carried out in a thermostat air bath shaker with a rotation rate of 200 rpm. The samples were taken periodically to determine the concentrations of glucose, xylose, and ethanol.

Analytical Methods

The FPA and the activities of xylanase, β-xylosidase (*p*NPXase), and α-arabinofuranosidase (*p*NPAase) of culture supernatants were measured using a Whatman No.1 filter paper, insoluble xylan (beech), *p*-nitrophenyl-β-D-xylopyranoside, and *p*-nitrophenyl-α-L-arabinofuranoside as the substrates, respectively, according to the methods presented by Gao et al. (2021). One unit (U) of enzyme activity was defined as the amount of enzyme that liberates 1 μmol of reducing sugars (for FPA and xylanase) equivalent or *p*-nitrophenol (for *p*NPAase and *p*NPXase) per minute under the assay conditions.

The samples collected in the pretreatment, enzymatic hydrolysis, and fermentation stages, respectively, were centrifuged at 10,000 rpm for 10 min. The supernatants were used for analyzing the contents of glucose, xylose, formic Acid, acetic acid, furfural, HMF, and ethanol using HPLC (LC-20AT, refractive index detector RID-20A, Shimadzu, Kyoto, Japan) With an Aminex HPX-87H column (Bio-Rad, Hercules, CA, United States) at 60°C using a mobile phase of 5 mM H_2SO_4 at a rate of 0.5 ml/min (Sluiter et al., 2008b). For the samples from the enzymatic hydrolysis and fermentation stage, the supernatants were first boiled for 10 min for inactivating enzyme. The sugar yields (%) were calculated according to the following formula:

$$\%\ \mathrm{Yield}_{\mathrm{Sugar}} = (C_{\mathrm{HPLC}} \times V \times CF) / (W \times \mathrm{Content}_{\mathrm{Sugar}} \times 1000) \times 100, \quad (1)$$

where C_{HPLC} is the concentration of sugar as determined by HPLC, mg/ml; V is the volume of the reaction system, ml; CF (conversion factor) is 0.9 for C-6 sugars and 0.88 for C-5 sugars; W is the weight of the substrate in the reaction system, g; and $\mathrm{Content}_{\mathrm{Sugar}}$ is the percentage of the polymeric sugar in corn fiber.

RESULTS AND DISCUSSION

Chemical Compositions of Corn Fiber

Table 1 provides the chemical compositions of corn fiber. The corn fiber contains starch, cellulose, and hemicellulose with a total carbohydrate content of 71.22 ± 1.27%. The major components were hemicellulosic sugars (xylose, arabinose, and galactose), and their total contents reached about 40%. These data were consistent with the previously reported results (Kim et al., 2008; Eylen et al., 2011). Compared with the chemical components of corn stover and corn cob (Eylen et al., 2011), the corn fiber had similar total glucan content to corn stover (30.6%) and corn cob (34.8%) and similar xylan content to corn stover (19%). But unlike corn cob and corn stover, a considerable part of the glucose in corn fiber was derived from starch, not just cellulose. In contrast, the contents of other hemicellulose sugars in corn fiber were significantly higher than that in corn stover and corn cob, which means that the degradation of corn fiber may require a more complex enzyme system with more abundant hemicellulase components.

Pretreatment of Corn Fiber With Dilute Sulfuric Acid

From batch kinetics studies, it was found that the factors affecting acid pretreatment included the type of biomass, the type of acid, acid concentration, reaction time, and reaction temperature (Rahman et al., 2006). Among them, the operating conditions, including reaction time, temperature, and acid concentration, would significantly affect the efficiency of dilute acid pretreatment (López-Arenas et al., 2010). In this study, RSM incorporating variables of temperature, time, and acid concentration was used to optimize the pretreatment process parameters for maximizing the enzymatic conversion of carbohydrate in corn fiber to monosaccharides and minimizing the formation of inhibitors. The complete list of runs and responses is provided in **Table 2**. Five experimental runs were replicated at the center point of the design to confirm any

TABLE 1 | Composition of corn fiber (%, dry basis).

Components	Contents
Starch	13.50 ± 1.24
Cellulose	18.54 ± 1.71
Xylan	20.73 ± 1.79
Arabinose	14.49 ± 1.15
Galactose	3.96 ± 0.32
Lignin	4.07 ± 0.45
Extractives	4.43 ± 0.23
Ash	0.55 ± 0.14
Protein	8.25 ± 0.06
Acetyl group	2.28 ± 0.12
Uronic acid	0.93 ± 0.12

differences in the estimation procedure as a measure of precision. **Table 2** shows the yields of formic acid, acetic acid, and furfural after pretreatment and the yields of glucose, xylose, and arabinose after pretreatment and following enzymatic hydrolysis. **Figure 1** shows the response surface plots of glucose, xylose, and arabinose yields under different pretreatment conditions. ANOVA of the models for glucose, xylose, arabinose, furfural, formic acid, and acetic acid is given in **Table 3**. The regression equations of different products were as follows, respectively.

Glucose = + 334.95 – 0.49 × Temp. + 4.69 × Time + 8.45 × Acid conc. – 9.53 × Temp. × Time – 6.38 × Temp. × Acid conc. – 2.60 × Time × Acid conc.

Xylose = + 132.21 + 19.61 × Temp. + 14.86 × Time + 19.06 × Acid conc. – 0.64 × Temp. × Time + 1.19 × Temp. × Acid conc. – 0.66 × Time × Acid conc. + 1.56 × Temp.2 – 7.19 × Time 2 – 3.91 × Acid conc.2

Arabinose = + 110.82 + 5.20 × Temp. + 4.97 × Time + 6.71 × Acid conc. – 4.23 × Temp. × Time −3.00 × Temp. × Acid conc. – 2.97 × Time × Acid conc. – 0.62 × Temp.2 – 4.26 × Time 2 – 2.29 × Acid conc.2

Furfural = + 3.07 + 0.57 × Temp. + 0.19 × Time – 0.14 × Acid conc. – 0.24 × Temp. × Time – 7.500E-003 × Temp. × Acid conc. + 0.018 × Time × Acid conc. + 0.061 × Temp.2 – 0.014 × Time 2 – 0.39 × Acid conc.2

Formic acid = + 5.30 + 0.33 × Temp. + 0.14 × Time + 0.23 × Acid conc. + 0.16 × Temp. × Time + 0.17 × Temp. × Acid conc. + 0.047 × Time × Acid conc.

Acetic acid = + 8.25 + 2.90 × Temp. + 1.69 × Time + 2.65 × Acid conc. + 0.73 × Temp. × Time + 0.93 × Temp. × Acid conc. + 1.10 × Time × Acid conc.

where sugars and inhibitors appear as yield (mg/g) and the variables are Temp. (temperature, °C), Time (in min), and Acid conc. (acid concentration, %, w/v).

It is shown in **Figure 1** and *p*-values in ANOVA that the yield of glucose obtained from the enzymatic hydrolysis of pretreated corn fiber was sensitive to acid concentration ($p = 0.0372 \leq 0.05$) but not to pretreatment time ($p = 0.2119 > 0.05$) and temperature ($p = 0.8922 > 0.05$), but the yield of xylose was significantly very sensitive to reaction time ($p < 0.0001$), temperature ($p < 0.0001$), and acid concentration ($p < 0.0001$). Initially, the increase in pretreatment temperature is in favor of the conversion of xylan to xylose in subsequent enzymatic hydrolysis, but a high pretreatment temperature led to the dehydration reaction of xylose accelerated, thus decreased xylose production but increased furfural content (**Table 2**), which is similar to the results reported in some literature (Kabel et al., 2007; Noureddini and Byun, 2010).

In contrast, it was found that the yields of glucose and xylose (based on the original content in corn fiber) were 10.5 and 38.3%, respectively, in the pretreatment stage, and the yields of glucose and xylose were 95.5 and 72.4% after enzymatic hydrolysis, indicating that xylan was more dissolved out in the pretreatment stage. Avci et al. (2013) also reported the difference in production behavior between glucose and xylose. They found that after being treated with dilute sulfuric acid a considerable part of xylan was directly hydrolyzed into xylose, while glucose was mostly produced by enzymatic hydrolysis. This is similar to our results. In the study, maximum xylose of 171 mg/g corn

TABLE 2 | Pretreatment factors and experiment results in the experiments designed by the central composite design from response surface methodology.

Run	Factors			Responses (mg/g)*					
	Temp. (°C)	Time (min)	Acid conc. (%, w/v)	Glucose	Xylose	Arabinose	Formic acid	Acetic acid	Furfural
1	125	10	0.35	328	132	110	5.27	9.13	3.93
2	115	60	0.50	333	151	111	5.58	13.6	2.70
3	115	10	0.50	344	125	109	5.37	7.87	2.19
4	115	10	0.20	329	89.5	92.0	5.06	5.07	2.66
5	105	35	0.20	318	91.5	92.4	4.83	3.84	2.35
6	125	35	0.50	340	171	117	5.97	14.5	3.11
7	115	35	0.35	345	135	113	5.39	8.25	2.93
8	105	60	0.35	354	122	111	5.01	5.85	2.78
9	115	60	0.20	328	119	105	5.08	6.43	3.10
10	105	35	0.50	354	131	114	5.02	7.58	2.26
11	115	35	0.35	339	136	112	5.48	9.71	3.13
12	125	35	0.20	329	126	108	5.12	7.08	3.23
13	115	35	0.35	347	133	112	5.42	7.97	3.20
14	115	35	0.35	338	130	109	5.41	7.70	3.07
15	125	60	0.35	334	162	114	6.05	13.8	3.73
16	115	35	0.35	326	127	107	5.14	7.74	3.02
17	105	10	0.35	310	89.5	89.8	4.88	4.09	2.03

**Based on per gram dry corn fiber.*

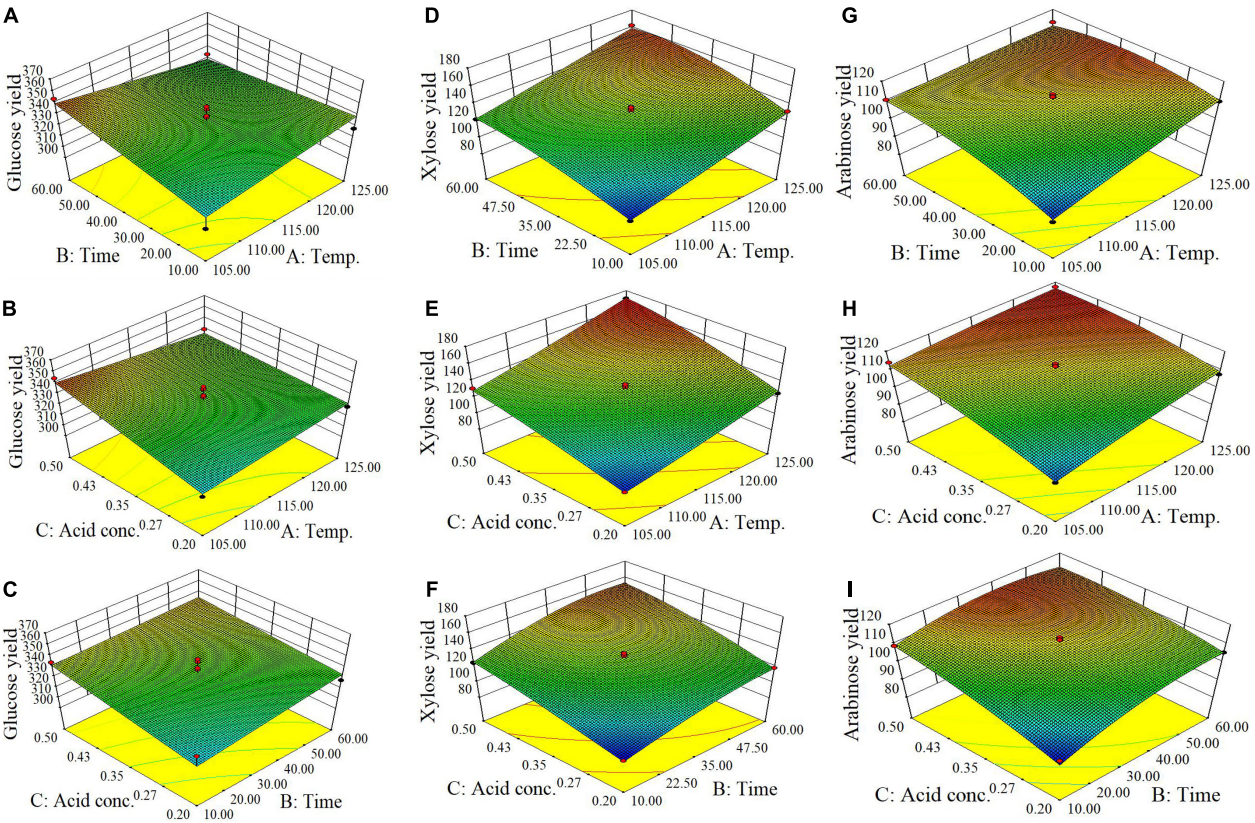

FIGURE 1 | Response surface plots of yields of glucose **(A–C)**, xylose **(D–F)**, and arabinose **(G–I)** (mg/g corn fiber) obtained from the Box-Behnken design of RSM.

fiber was obtained by pretreatment at 125°C for 35 min using 0.5% (m/v) H_2SO_4. Similar to xylose, as shown in **Figure 1I**, the yield of arabinose was also sensitive to pretreatment temperature ($p = 0.0011 \leq 0.01$), time ($p = 0.0014$), and acid concentration ($p = 0.0002$).

Overall, for three main sugars in corn fiber (glucose, xylose, and arabinose), the highest yield of total sugars was produced by pretreatment at 125°C for 35 min using 0.5% (w/v) H_2SO_4 and enzyme hydrolysis, including glucose of 340 mg, xylose of 171 mg, and arabinose of 117 mg, respectively, on the basis of per gram corn fiber. This amount was approximately 85.4% of the three sugars present in the corn fiber.

Furfural and HMF were generated from xylose and glucose in the pretreatment process through a further dehydration reaction, respectively (Jönsson and Martín, 2016). It was found that furfural formation was also most sensitive to pretreatment temperature ($p < 0.0001$), but not to acid concentration ($p = 0.949 > 0.05$), maybe because sulfuric acid only acts as a catalyst to provide an acidic environment. The highest furfural content of 3.93 mg/g corn fiber was found after pretreatment at 125°C for 10 min with 0.35% sulfuric acid (**Table 2**). Extending pretreatment time from 10 min to 60 min under conditions of 0.35% sulfuric acid and 125°C, furfural content in pretreatment liquid decreased, maybe due to further decomposition of furfural. It was also found that the yield of formic acid, a degradation product of furfural (Yang et al., 2012), increased (**Table 2**). In addition, Yemiş and Mazza (2011) also reported that the too-long reaction time could cause the condensation reaction of furfural to form other products. However, no HMF was detected in any hydrolysate from the acid pretreatment process, possibly because little glucose was degraded during the acid pretreatment under pretreatment conditions used in the paper. Acetic acid was also detected in hydrolysates after the acidic pretreatment (**Table 2**), which comes from the shedding of acetyl groups in hemicellulose (Ibbett et al., 2011), and its content was also sensitive to reaction time ($p < 0.0001$), temperature ($p < 0.0001$), and acid concentration ($p < 0.0001$). Longer reaction time, higher reaction temperature, and acid concentration can promote acetic acid formation.

It was found that, although the pretreatment can obtain the highest amounts of sugars at 125°C for 35 min using 0.5% H_2SO_4, there was also the higher production of formic acid (5.97 mg/g corn fiber), acetic acid (14.5 mg/g corn fiber), and furfural (3.11 mg/g corn fiber), which may result in the inhibitory effect on microbial growth in subsequent ethanol fermentation. To obtain the maximum sugars while minimizing the formation of inhibitory compounds as much as possible, based on the RSM analysis (**Figure 1** and **Tables 2**, **3**), it was determined that the suitable pretreatment conditions for the corn fiber were the acid concentration of 0.5%, reaction temperature of 105°C,

TABLE 3 | ANOVA Table of the adjusted models from dilute sulfuric acid pretreated and enzyme hydrolyzed corn fiber.

Source	Sum of squares	DF	Mean square	*F* value	*p*-Value
Glucose					
Model	1301.93	6	216.99	2.19	0.1304
Residual	989.62	10	98.96		
Lack of fit	711.74	6	118.62	1.71	0.3146
R^2	0.5681				
Xylose					
Model	1.156E-003	9	1.284E-004	85.43	<0.0001
Residual	1.052E-005	7	1.504E-006		
Lack of fit	4.006E-006	3	1.335E-006	0.82	0.5470
R^2	0.9910				
Arabinose					
Model	1023.70	9	113.74	14.80	0.0009
Residual	53.78	7	7.68		
Lack of fit	23.89	3	7.96	1.07	0.4572
R^2	0.9501				
Furfural					
Model	3.94	9	0.44	11.19	0.0022
Residual	0.27	7	0.039		
Lack of fit	0.23	3	0.077	7.24	0.0429
R^2	0.9350				
Formic acid					
Model	1.70	6	0.28	15.66	0.0001
Residual	0.18	10	0.018		
Lack of fit	0.11	6	0.019	1.07	0.4951
R^2	0.9038				
Acetic acid					
Model	156.64	6	26.11	65.27	<0.0001
Residual	4.00	10	0.40		
Lack of fit	1.23	6	0.20	0.30	0.9105
R^2	0.9751				

and reaction time of 43 min. Under this condition, the yield of glucose, xylose, and arabinose reached 354 mg/g corn fiber, 133 mg/g corn fiber, and 114 mg/g corn fiber, respectively, which is equivalent to 81.8% of the total amount of the three sugars present in the corn fiber. Although the yield (81.8%) was slightly lower than the highest sugar yield (85.4%) obtained at 125°C for 35 min using 0.5% H_2SO_4, the amounts of inhibitors produced in the mild pretreatment significantly decreased, for example, decreased by 25.7% for furfural, 45.6% for acetic acid, and 14.2% for formic acid, respectively.

Semi-Simultaneous Saccharification and Fermentation of Pretreated Corn Fiber for Producing Ethanol

Assessment of Inhibition Effect of Hydrolysate

According to the reports from the literature, furfural concentration greater than 0.2 mg/ml or acetic acid concentration greater than 5 mg/ml could be severely toxic to the growth of *S. cerevisiae* (Sanchez and Bautista, 1988; Larsson et al., 1999; Kim et al., 2013). In the system of multiple inhibitors coexisting, the interaction of these inhibitors could enhance the toxicity, leading to the greater inhibition of microbial growth and fermentation than any single inhibitor (Palmqvist and Hahn-Hägerdal, 2000; Hou et al., 2018). To high efficiently produce ethanol using the pretreated corn fiber as substrate, in this study, using two hydrolysates from corn fiber pretreated by dilute acid under optimum conditions (0.5% H_2SO_4, 105°C for 43 min) and the conditions for obtaining the highest total sugars yields (0.5% H_2SO_4, 125°C for 35 min), respectively, we first assessed the inhibition effect of hydrolysates on the growth of *S. cerevisiae* LF2 by investigating the effect on ethanol fermentation. The hydrolysates were preadjusted to pH 5.0 with 10 M NaOH solution, and *S. cerevisiae* LF2 was inoculated into the hydrolysates. It was shown in **Figure 2** that the growth of *S. cerevisiae* LF2 was obviously inhibited in the hydrolysates, in which the growth of *S. cerevisiae* LF2 was strongly inhibited in the hydrolysate from pretreated corn fiber at 125°C using 0.5% (w/v) H_2SO_4 for 35 min, and almost no ethanol was produced in the whole fermentation period. For the hydrolysate from corn fiber pretreated in optimum conditions, ethanol was just produced after about 60 h of fermentation.

Acclimation and Fermentation Assessment of Yeast

To shorten the lag growth period of *S. cerevisiae* LF2 during semi-SSF of hydrolysate, strain domestication was conducted by continuously and gradually increasing hydrolysate concentration in acclimation medium for making the *S. cerevisiae* LF2 adapt to this environment with inhibitors. After multiple habituated cultures, the tolerance of *S. cerevisiae* LF2 to inhibitors was greatly improved. The performances of the domesticated strain and parent strain were compared by cultivation in the acclimation media with the highest concentration of inhibitors, in which glucose was supplemented to 50.0 g/L in the media. As shown in **Figure 3**, using the domesticated strain, the ethanol concentration in fermentation liquid was significantly increased compared to the parent strain (23.5 g/L *vs.* 18.8 g/L), and the lag period decreased from 60 to 12 h, which could meet the requirements of semi-SSF, thus, in the following experiments, the domesticated strain was directly applied to ethanol fermentation of pretreated corn fiber without pre-detoxification treatment.

Semi-Simultaneous Saccharification and Fermentation of Pretreated Corn Fiber for Ethanol Production

Semi-simultaneous saccharification and fermentation was used to evaluate ethanol production potential using corn fiber as substrate under the best pretreatment conditions. Compared to the SSF process, a pre-hydrolysis step was first carried out prior to SSF under the optimal conditions of enzymatic hydrolysis, which help to promote enzymatic hydrolysis and liquefaction of cellulosic substrate. The pretreated corn fiber was pre-hydrolyzed with the cellulase preparation for 12 h at 48°C and pH 5.0 before yeast was inoculated. **Figure 4** shows the changes in glucose, xylose, and ethanol concentrations concerning time during the semi-SSF. It was shown that traces of ethanol in fermentation liquid (0.20 g/L) began to be detected at 24th hour, and after that, glucose was continuously consumed up to the concentration of 0 at 96th hour. Xylose concentration started decreasing when its

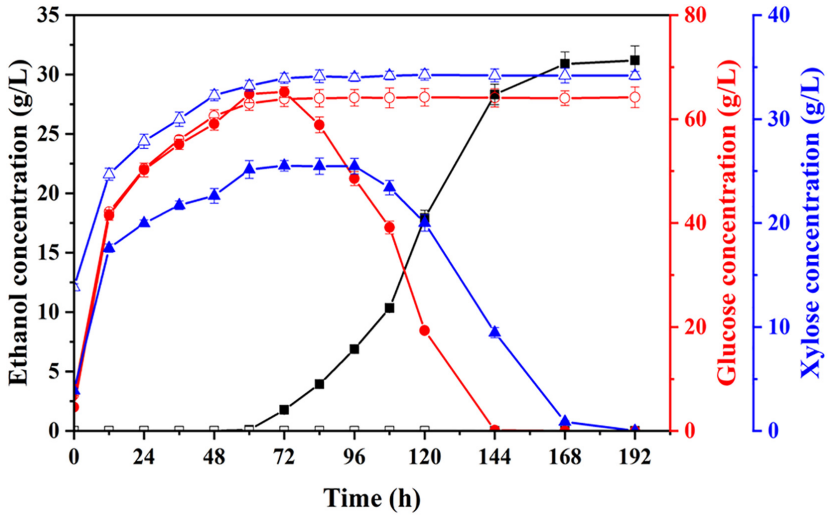

FIGURE 2 | Changes in concentrations of ethanol, glucose, and xylose during fermentation of pretreated corn fiber by dilute acid under different pretreatment conditions for assessing inhibitors' effect on fermentation. Ethanol, square; glucose, circle; xylose, triangle; pretreatment with 0.5% H_2SO_4 at 105°C for 43 min, solid; and pretreatment with 0.5% H_2SO_4 at 125°C for 35 min, hollow.

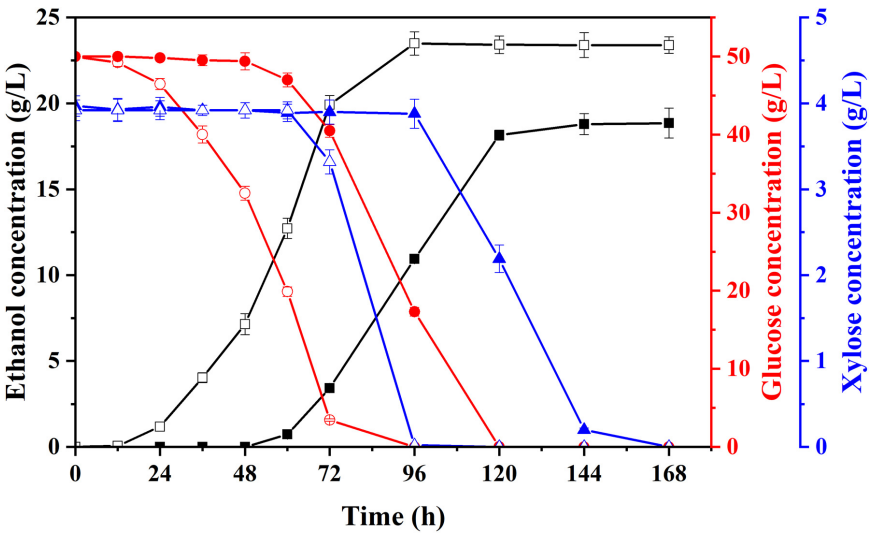

FIGURE 3 | Changes in concentrations of ethanol, glucose, and xylose of parent strain (solid) and domesticated yeast (hollow) in acclimation medium with the highest inhibitors concentration supplemented with glucose. Ethanol, square; glucose, circle; xylose, triangle.

concentration was close to that of glucose, and it was consumed completely at the end of fermentation. Finally, the ethanol concentration of 40.14 g/L was obtained, and ethanol yield was approximately 81% of the theoretical yield. However, in this study, the total fermentation time was long (about 144 h), and the rate of xylose conversion was still low. Thus, in further work, the *S. cerevisiae* LF2 will be further improved to decrease the lag period of strain, and the enzyme system will be modified to improve the rate of xylose conversion.

Some results from literature about cellulosic ethanol production using corn fiber as feedstock through different pretreatment and saccharification-fermentation process are summarized in **Table 4**. It was shown that, in the existing research, detoxification treatments, such as water washing, biodetoxification, and overliming, were usually used after acidic and alkaline pretreatment. For example, Shrestha et al. (2010) used water washing to detoxify the mild NaOH or steam pretreated corn fiber, and the ethanol concentration of 3.30 and 2.66 g/L, respectively, was obtained after fermentation under the condition of 4.3% solid content. However, its solid content and final ethanol concentration were too low for practical application. Gáspár et al. (2007) also used water washing for detoxification of corn fiber pretreated by KOH. The ethanol concentration reached 12.50 g/L after fermentation at 5% solid

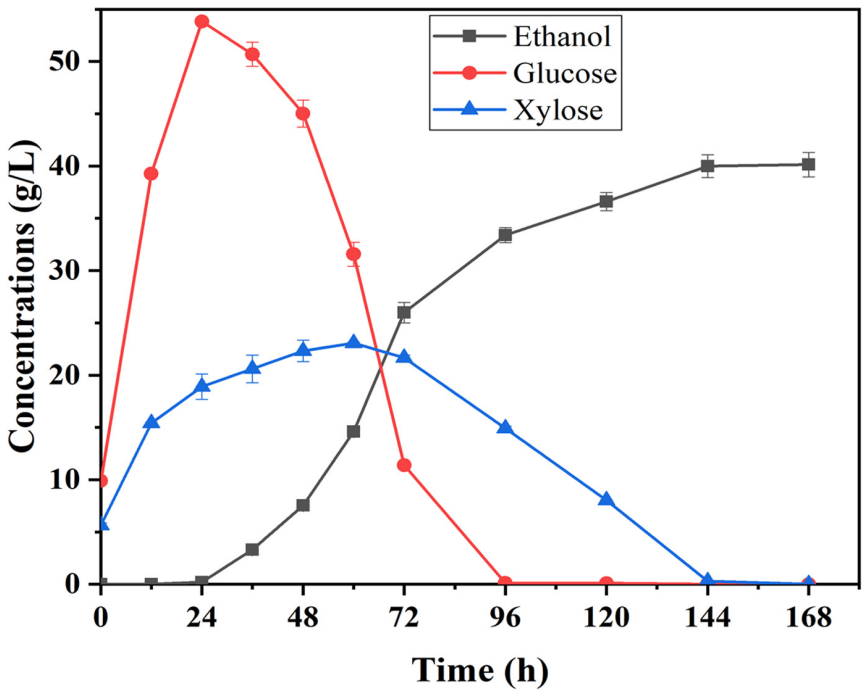

FIGURE 4 | Time courses of sugar utilization and ethanol production during semi-SSF with *S. cerevisiae* LF2 and corn fiber pretreated at 105°C; 0.5% H_2SO_4 for 43 min; fermentation conditions: 20% (w/v) of solid content, 30°C and pH 5.0.

TABLE 4 | Comparison of cellulosic ethanol production from corn fiber feedstock.

Pretreatment condition	Detoxification	Fermentation process	Solid content (w/v) (%)	Dosage of enzymes (per gram dry matter)	Ethanol production (g/g)	Ethanol concentration (g/L)	References
Alkaline pretreatment with 2% (w/w) NaOH at 30°C, for 2 h; Steaming at 100 °C for 2 h, 20% (w/w)	Water washing	SSF	4.3	10 FPU Spezyme CP	0.077*; 0.062*	3.30; 2.66	Shrestha et al., 2010
Alkaline pretreatment with 1% KOH at 120°C for 1 h under pressure (2 bar)	Water washing	Semi-SSF	5	25 FPU Celluclast 1.5 L and 25 IU Novozyme 188	0.062**	12.50	Gáspár et al., 2007
Steam explosion with 6% SO_2 at 190°C for 5 min	Overliming	SHF	2	8.3 FPU Celluclast 1.5 L, 10.1 IU Novozym 188 and 50-80 IU glucoamylase	0.490*	6.89	Bura et al., 2002
Acid pretreatment with 4% citric acid at 165°C for 2 min	Biodetoxification	Semi-SSF	25	10 FPU Cellic CTec2	0.280**	70.20	Zhang et al., 2021
Extrusion (300 rpm, 140°C)	None	Semi-SSF	7.1	5.9 FPU Cellulclast 1.5 L, 38.0 CBU β-glucosidase, 0.8 FBG Viscozyme L	0.410*	29.08	Myat and Ryu, 2014
Liquid hot water pretreatment at 180°C for 10 min and wet disk milling	None	SSF	20	0.05 g Cellulase	0.11*	21.54	Juneja et al., 2021
Liquid hot water at 160°C for 20 min	Water washing	SHF	7.8	5 FPU Novozyme 188 and 5 FPU Celluclast 1.5L	0.260*	20.00	Mosier et al., 2005
Acid pretreatment with 0.5% H_2SO_4 at 105°C for 43 min	None	Semi-SSF	20	10 FPU MCAX	0.201**	40.14	This study

**g/g pretreated corn fiber; **g/g initial corn fiber, calculated from the mass balance data provided in these literature.*

content by semi-SSF process. However, because most of the hemicellulose was dissolved in the alkali pretreatment process and wasted after water washing, the ethanol yield was very low, only 0.062 g/g initial corn fiber. Bura et al. (2002) reported that the inhibitors in the hydrolysate could be completed removed by detoxifying steam explosion-pretreated corn fiber

with overliming treatment, but fermentation was conducted at only 2% of solid content, which was too low to be suitable for practical application. Although water washing and overliming can remove inhibitors, they also increase process steps and costs while generating problems, such as wastewater and the loss of sugars. Different from this, Zhang et al. (2021) adopted biodetoxification by inoculating *Paecilomyces variotii* to remove inhibitors produced by citric acid pretreatment, and the ethanol concentration reached 70.2 g/L using semi-SSF at 25% of solid content, and ethanol production reached 0.280 g/g initial corn fiber. Although less wastewater is produced due to biological detoxification rather than water washing and overliming, high citric acid dosage (4%) and reaction temperature (165°C) during pretreatment and too-long biodetoxification as strain growth and inactivation after detoxification influenced the economy of the process. Li et al. (2019) used the combination of acid pretreatment with distillation to *in situ* pretreat whole stillage containing corn fiber. The pretreated stillage was recycled to the liquefaction step with the addition of cellulase, or hydrolyzed using cellulase and then recycled to the liquefaction step, or hydrolyzed using cellulase followed by C6/C5 sugar co-fermentation. Compared with the traditional dry milling process, the highest ethanol yield increased by 6.3%, and the conversion of cellulose reached 77.5%. However, a large number of inhibitors in the pretreatment liquid resulted in incomplete fermentation. Myat and Ryu (2014) used thermal-mechanical extrusion to pretreat corn fiber, which reduced the crystallinity and polymerization degree of cellulose in corn fiber, and the final ethanol concentration reached 29.08 g/L. Juneja et al. (2021) used the combination of liquid hot water pretreatment with wet disk milling to pretreat corn fiber, resulting in a final ethanol concentration of 21.54 g/L at 20% of solid content. Due to the lack of chemical pretreatment, there were fewer inhibitors in these two pretreatments so that ethanol fermentation could be carried out without detoxification. But these pretreatments required higher energy consumption because of mechanical milling and high temperature compared to the process used in this study, and the final ethanol concentration was also lower than that in this study.

Overall, this study proposed a simple and low-cost process used to produce ethanol from corn fiber. In this process, mild pretreatment with dilute acid can enable the saccharification and fermentation process to directly be conducted without detoxification while ensuring the low loss of sugars during pretreatment, which was conducive to ensure the high ethanol yield, high final ethanol concentration (as high solid content after pretreatment), and no wastewater problem in pretreatment stage. These advantages show that this process has a good prospect of industrial application.

CONCLUSION

This study developed a simple production process for cellulosic ethanol using corn fiber. In this process, an optimized mild dilute acid pretreatment process ensured the high sugar recovery and fewer inhibitor production while high enzymatic digestibility of substrate, and the mixtures of solid and hydrolysates from pretreatment were directly transported into subsequent enzymatic hydrolysis and fermentation process without detoxification treatment for achieving high-efficiency conversion of sugar to ethanol and obtaining high ethanol yield at 20% of solid content through the semi-SSF process using acclimated yeast. This process could be easily industrialized with low equipment investment, fewer process steps, and no pretreatment wastewater problem.

DATA AVAILABILITY STATEMENT

The raw data supporting the conclusions of this article will be made available by the authors, without undue reservation.

AUTHOR CONTRIBUTIONS

YG and JZ designed the study. YG performed the experiment, analyzed the data, and wrote the manuscript. JH, NX, and HJ participated in part of the experiments. YQ revised the manuscript. JZ and XL conceived the study and edits for the manuscript. All authors contributed to the creation of the manuscript.

FUNDING

This study was financially supported by grants from the National Natural Science Foundation of China (No. 31870562), Natural Science Foundation of Shandong Province, China (ZR2019ZD19), and the Key Research and Development Project of Shandong Province (2019GSF107009).

ACKNOWLEDGMENTS

We would like to thank Xiangmei Ren from the State Key Laboratory of Microbial Technology of Shandong University for help and guidance in HPLC.

REFERENCES

Agger, J., Viksø-Nielsen, A., and Meyer, A. S. (2010). Enzymatic xylose release from pretreated corn bran arabinoxylan: differential effects of deacetylation and deferuloylation on insoluble and soluble substrate fractions. *J. Agric. Food Chem.* 58, 6141–6148. doi: 10.1021/jf100633f

Avci, A., Saha, B. C., Dien, B. S., Kennedy, G. J., and Cotta, M. A. (2013). Response surface optimization of corn stover pretreatment using dilute phosphoric acid for enzymatic hydrolysis and ethanol production. *Bioresour. Technol.* 130, 603–612. doi: 10.1016/j.biortech.2012.12.104

Beri, D., York, W. S., Lynd, L. R., Peña, M. J., and Herring, C. D. (2020). Development of a thermophilic coculture for corn fiber conversion to ethanol. *Nat. Commun.* 11:1937. doi: 10.1038/s41467-020-15704-z

Bothast, R. J., and Schlicher, M. A. (2005). Biotechnological processes for conversion of corn into ethanol. *Appl. Microbiol. Biotechnol.* 67, 19–25. doi: 10.1007/s00253-004-1819-8

Brodeur, G., Yau, E., Badal, K., Collier, J., Ramachandran, K. B., and Ramakrishnan, S. (2011). Chemical and physicochemical pretreatment of lignocellulosic biomass: a review. *Enzyme Res.* 2011:787532. doi: 10.4061/2011/787532

Bura, R., Mansfield, S. D., Saddler, J. N., and Bothast, R. J. (2002). SO_2-catalyzed steam explosion of corn fiber for ethanol production. *Appl. Biochem. Biotechnol.* 98-100, 59–72. doi: 10.1007/978-1-4612-0119-9_5

Eylen, D. V., Dongen, F., Kabel, M., and Bont, J. (2011). Corn fiber, cobs and stover: enzyme-aided saccharification and co-fermentation after dilute acid pretreatment. *Bioresour. Technol.* 102, 5995–6004. doi: 10.1016/j.biortech.2011.02.049

Gao, L., He, X., Guo, Y., Wu, Z., Zhao, J., Liu, G., et al. (2021). Combinatorial engineering of transcriptional activators in *Penicillium oxalicum* for improved production of corn-fiber-degrading enzymes. *J. Agric. Food Chem.* 69, 2539–2548. doi: 10.1021/acs.jafc.0c07659

Gáspár, M., Kálmán, G., and Réczey, K. (2007). Corn fiber as a raw material for hemicellulose and ethanol production. *Process Biochem.* 42, 1135–1139. doi: 10.1016/j.procbio.2007.04.003

Hames, B., Scarlata, C., and Sluiter, A. (2008). *Determination of Protein Content in Biomass; Jan, Report No. TP-510-42625*. Golden, CO: National Renewable Energy Laboratory.

Hendriks, A. T. W. M., and Zeeman, G. (2009). Pretreatments to enhance the digestibility of lignocellulosic biomass. *Bioresour. Technol.* 100, 10–18. doi: 10.1016/j.biortech.2008.05.027

Hou, J., Qiu, Z., Han, H., and Zhang, Q. (2018). Toxicity evaluation of lignocellulose-derived phenolic inhibitors on *Saccharomyces cerevisiae* growth by using the QSTR method. *Chemosphere* 201, 286–293. doi: 10.1016/j.chemosphere.2018.03.008

Ibbett, R., Gaddipati, S., Davies, S., Hill, S., and Tucker, G. (2011). The mechanisms of hydrothermal deconstruction of lignocellulose: new insights from thermal–analytical and complementary studies. *Bioresour. Technol.* 102, 9272–9278. doi: 10.1016/j.biortech.2011.06.044

Iram, A., Cekmecelioglu, D., and Demirci, A. (2019). Optimization of dilute sulfuric acid, aqueous ammonia, and steam explosion as the pretreatments steps for distillers' dried grains with solubles as a potential fermentation feedstock. *Bioresour. Technol.* 282, 475–481. doi: 10.1016/j.biortech.2019.03.009

Jiang, K., Li, L., Long, L., and Ding, S. (2018). Comprehensive evaluation of combining hydrothermal pretreatment (autohydrolysis) with enzymatic hydrolysis for efficient release of monosaccharides and ferulic acid from corn bran. *Ind. Crops Prod.* 113, 348–357. doi: 10.1016/j.indcrop.2018.01.047

Jiang, L., Zheng, A., Zhao, Z., He, F., Li, H., and Liu, W. (2015). Obtaining fermentable sugars by dilute acid hydrolysis of hemicellulose and fast pyrolysis of cellulose. *Bioresour. Technol.* 182, 364–367. doi: 10.1016/j.biortech.2015.01.032

Jönsson, L., and Martín, C. (2016). Pretreatment of lignocellulose: formation of inhibitory by-products and strategies for minimizing their effects. *Bioresour. Technol.* 199, 103–112. doi: 10.1016/j.biortech.2015.10.009

Juneja, A., Noordam, B., Pel, H., Basu, R., Appeldoorn, M., and Singh, V. (2021). Optimization of two-stage pretreatment for maximizing ethanol production in 1.5G technology. *Bioresour. Technol.* 320, 124380. doi: 10.1016/j.biortech.2020.124380

Kabel, M. A., Bos, G., Zeevalking, J., Voragen, A. G. J., and Schols, H. A. (2007). Effect of pretreatment severity on xylan solubility and enzymatic breakdown of the remaining cellulose from wheat straw. *Bioresour. Technol.* 98, 2034–2042. doi: 10.1016/j.biortech.2006.08.006

Kim, S. K., Park, D. H., Song, S. H., Wee, Y., and Jeong, G. (2013). Effect of fermentation inhibitors in the presence and absence of activated charcoal on the growth of *Saccharomyces cerevisiae*. *Bioprocess Biosyst. Eng.* 36, 659–666. doi: 10.1007/s00449-013-0888-4

Kim, Y., Mosier, N. S., Hendrickson, R., Ezeji, T., Blaschek, H., Dien, B., et al. (2008). Composition of corn dry-grind ethanol by-products: DDGS, wet cake, and thin stillage. *Bioresour. Technol.* 99, 5165–5176. doi: 10.1016/j.biortech.2007.09.028

Kumar, P., Barrett, D. M., Delwiche, M. J., and Stroeve, P. (2009). Methods for pretreatment of lignocellulosic biomass for efficient hydrolysis and biofuel production. *Ind. Eng. Chem. Res.* 48, 3713–3729. doi: 10.1021/IE801542G

Kurambhatti, C. V., Kumar, D., Rausch, K. D., Tumbleson, M. E., and Singh, V. (2018). Increasing ethanol yield through fiber conversion in corn dry grind process. *Bioresour. Technol.* 270, 742–745. doi: 10.1016/j.biortech.2018.09.120

Larsson, S., Palmqvist, E., Hahn-Hägerdal, B., Tengborg, C., Stenberg, S., Zacvhi, G., et al. (1999). The generation of fermentation inhibitors during dilute acid hydrolysis of softwood. *Enzyme Microb. Technol.* 24, 151–159. doi: 10.1016/S0141-0229(98)00101-X

Lee, J. E., Vadlani, P. V., and Faubion, J. (2017). Corn bran bioprocessing: development of an integrated process for microbial lipids production. *Bioresour. Technol.* 243, 196–203. doi: 10.1016/j.biortech.2017.06.065

Li, X., Xu, Z., Yu, J., Huang, H., and Jin, M. (2019). In situ pretreatment during distillation improves corn fiber conversion and ethanol yield in the dry mill process. *Green Chem.* 21:1080. doi: 10.1039/C8GC03447H

López-Arenas, T., Rathi, P., Ramírez-Jiménez, E., and SalesCruz, M. (2010). Factors affecting the acid pretreatment of lignocellulosic biomass: batch and continuous process. *Comput. Aided Chem. Eng.* 28, 979–984. doi: 10.1016/S1570-7946(10)28164-6

Lovett, J. C., Hards, S., Clancya, J., and Snell, C. (2011). Multiple objectives in biofuels sustainability policy. *Energy Environ. Sci.* 4, 261–268. doi: 10.1039/C0EE00041H

Mikulski, D., and Kłosowski, G. (2018). Efficiency of dilute sulfuric acid pretreatment of distillery stillage in the production of cellulosic ethanol. *Bioresour. Technol.* 268, 424–433. doi: 10.1016/j.biortech.2018.08.005

Moore, R., Thornhill, K., Weinzierl, B., Sauer, D., D'Ascoli, E., Kim, J., et al. (2017). Biofuel blending reduces particle emissions from aircraft engines at cruise conditions. *Nature* 543, 411–415. doi: 10.1038/nature21420

Mosier, N. S., Hendrickson, R., Brewer, M., Ho, N., Sedlak, M., Dreshel, R., et al. (2005). Industrial scale-up of pH-controlled liquid hot water pretreatment of corn fiber for fuel ethanol production. *Appl. Biochem. Biotechnol.* 125, 77–97. doi: 10.1385/abab:125:2:077

Myat, L., and Ryu, G. H. (2014). Characteristics of destarched corn fiber extrudates for ethanol production. *J. Cereal Sci.* 60, 289–296. doi: 10.1016/j.jcs.2014.06.006

Nigam, P. S., and Singh, A. (2011). Production of liquid biofuels from renewable resources. *Prog. Energy Combust. Sci.* 37, 52–68. doi: 10.1016/j.pecs.2010.01.003

Noureddini, H., and Byun, J. (2010). Dilute-acid pretreatment of distillers' grains and corn fiber. *Bioresour. Technol.* 101, 1060–1067. doi: 10.1016/j.biortech.2009.08.094

Palmqvist, E., and Hahn-Hägerdal, B. (2000). Fermentation of lignocellulosic hydrolysates. II: inhibitors and mechanisms of inhibition. *Bioresour. Technol.* 74, 25–33. doi: 10.1016/S0960-8524(99)00161-3

Rahman, S. H. A., Choudhury, J. P., and Ahmad, A. L. (2006). Production of xylose from oil palm empty fruit bunch fiber using sulfuric acid. *Biochem. Eng. J.* 30, 97–103. doi: 10.1016/j.bej.2006.02.009

Saha, B. C. (2003). Hemicellulose bioconversion. *J. Ind. Microbiol. Biotechnol.* 30, 279–291. doi: 10.1007/s10295-003-0049-x

Sanchez, B., and Bautista, J. (1988). Effects of furfural and 5-hydroxymethylfurfural on the fermentation of *Saccharomyces cerevisiae* and biomass production from *Candida guilliermondii*. *Enzyme Microb. Technol.* 10, 315–318. doi: 10.1016/0141-0229(88)90135-4

Santos, V. T. O., Siqueira, G., Milagres, A. M. F., and Ferraz, A. (2018). Role of hemicellulose removal during dilute acid pretreatment on the cellulose accessibility and enzymatic hydrolysis of compositionally diverse sugarcane hybrids. *Ind. Crops Prod.* 111, 722–730. doi: 10.1016/j.indcrop.2017.11.053

Searchinger, T. D., Wirsenius, S., Beringer, T., and Dumas, P. (2018). Assessing the efficiency of changes in land use for mitigating climate change. *Nature* 564, 249–253. doi: 10.1038/s41586-018-0757-z

Shrestha, P., Khanal, S. K., Pometto, A. L. III, and van Leeuwen, J. H. (2010). Ethanol production via in situ fungal saccharification and fermentation of mild alkali and steam pretreated corn fiber. *Bioresour. Technol.* 101, 8698–8705. doi: 10.1016/j.biortech.2010.06.089

Sluiter, A., Ruiz, R., Scarlata, C., Sluiter, J., and Templeton, D. (2005a). *Determination of Extractives in Biomass; Jan, Report No. TP-510-42619*. Golden, CO: National Renewable Energy Laboratory.

Sluiter, A., Hames, B., Ruiz, R., Scarlata, C., Sluiter, J., and Templeton, D. (2005b). *Determination of Ash in Biomass; Jan, Report No. TP-510-42622*. Golden, CO: National Renewable Energy Laboratory.

Sluiter, A., Hames, B., Ruiz, R., Scarlata, C., Sluiter, J., Templeton, D., et al. (2008a). *Determination of Structural Carbohydrates and Lignin in Biomass; Jan, Report No. TP-510-42618*. Golden, CO: National Renewable Energy Laboratory.

Sluiter, A., Hames, B., Ruiz, R., Scarlata, C., Sluiter, J., and Templeton, D. (2008b). *Determination of Sugars, Byproducts, and Degradation Products in Liquid*

Fraction Process Samples; Jan, Report No. TP-510-42632. Golden, CO: National Renewable Energy Laboratory.

Sluiter, A., and Sluiter, J. (2005). *Determination of Starch in Solid Biomass Samples by HPLC; Jan, Report No. TP-510-42624*. Golden, CO: National Renewable Energy Laboratory.

Toor, M., Kumar, S. S., Malyan, S. K., Bishnoi, N. R., Mathimani, T., Rajendran, K., et al. (2020). An overview on bioethanol production from lignocellulosic feedstocks. *Chemosphere.* 242, 125080. doi: 10.1016/j.chemosphere.2019.125080

Yang, W., Li, P., Bo, D., and Chang, H. (2012). The optimization of formic acid hydrolysis of xylose in furfural production. *Carbohydr. Res.* 357, 53–61. doi: 10.1016/j.carres.2012.05.020

Yemiş, O., and Mazza, G. (2011). Acid-catalyzed conversion of xylose, xylan and straw into furfural by microwave-assisted reaction. *Bioresour. Technol.* 102, 7371–7378. doi: 10.1016/j.biortech.2011.04.050

Zhang, B., Zhan, B., and Bao, J. (2021). Reframing biorefinery processing chain of corn fiber for cellulosic ethanol production. *Ind. Crops Prod.* 170:113791. doi: 10.1016/j.indcrop.2021.113791

Conflict of Interest: The authors declare that the research was conducted in the absence of any commercial or financial relationships that could be construed as a potential conflict of interest.

frontiers in Microbiology

ORIGINAL RESEARCH
published: 31 March 2022
doi: 10.3389/fmicb.2022.823704

Agricultural Jiaosu: An Eco-Friendly and Cost-Effective Control Strategy for Suppressing *Fusarium* Root Rot Disease in *Astragalus membranaceus*

*Youhui Gao[1], Yue Zhang[2], Xiaoqian Cheng[1], Zehui Zheng[1,3], Xuehong Wu[4], Xuehui Dong[1], Yuegao Hu[1] and Xiaofen Wang[1]**

[1] College of Agronomy and Biotechnology, China Agricultural University, Beijing, China, [2] Biotechnology Research Institute, Beijing Academy of Agriculture and Forestry Sciences, Beijing, China, [3] Biology Institute, Qilu University of Technology, Shandong Academy of Sciences, Jinan, China, [4] College of Plant Protection, China Agricultural University, Beijing, China

OPEN ACCESS

Edited by:
Ying Ma,
University of Coimbra, Portugal

Reviewed by:
Manoj Kumar Solanki,
University of Silesia in Katowice, Poland
Ana C. Sampaio,
Universidade de Trás-os-Montes e Alto Douro, Portugal

***Correspondence:**
Xiaofen Wang
wxiaofen@cau.edu.cn

Specialty section:
This article was submitted to Microbiotechnology, a section of the journal Frontiers in Microbiology

Received: *28 November 2021*
Accepted: *07 March 2022*
Published: *31 March 2022*

Citation:
Gao Y, Zhang Y, Cheng X, Zheng Z, Wu X, Dong X, Hu Y and Wang X (2022) Agricultural Jiaosu: An Eco-Friendly and Cost-Effective Control Strategy for Suppressing Fusarium Root Rot Disease in Astragalus membranaceus. Front. Microbiol. 13:823704. doi: 10.3389/fmicb.2022.823704

Root rot caused by the pathogenic fungi of the *Fusarium* genus poses a great threat to the yield and quality of medicinal plants. The application of Agricultural Jiaosu (AJ), which contains beneficial microbes and metabolites, represents a promising disease control strategy. However, the action-effect of AJ on *Fusarium* root rot disease remains unclear. In the present study, we evaluated the characteristics and antifungal activity of AJ fermented using waste leaves and stems of medicinal plants, and elucidated the mechanisms of AJ action by quantitative real-time PCR and redundancy analysis. The effects of AJ and antagonistic microbes isolated from it on disease suppression were further validated through a pot experiment. Our results indicate that the AJ was rich in beneficial microorganisms (*Bacillus*, *Pseudomonas*, and *Lactobacillus*), organic acids (acetic, formic, and butyric acids) and volatile organic compounds (alcohols and esters). It could effectively inhibit *Fusarium oxysporum* and the half-maximal inhibitory concentration (IC_{50}) was 13.64%. The antifungal contribution rate of the microbial components of AJ reached 46.48%. Notably, the redundancy analysis revealed that the *Bacillus* and *Pseudomonas* genera occupied the main niche during the whole inhibition process. Moreover, the abundance of the *Bacillus*, *Pseudomonas,* and *Lactobacillus* genera were positively correlated with the pH-value, lactic, formic and butyric acids. The results showed that the combined effects of beneficial microbes and organic acid metabolites increased the efficacy of the AJ antifungal activity. The isolation and identification of AJ's antagonistic microbes detected 47 isolates that exhibited antagonistic activities against *F. oxysporum in vitro*. In particular, *Bacillus subtilis* and *Bacillus velezensis* presented the strongest antifungal activity. In the pot experiment, the application of AJ and these two *Bacillus* species significantly reduced the disease

incidence of *Fusarium* root rot and promoted the growth of *Astragalus*. The present study provides a cost-effective method to control of *Fusarium* root rot disease, and establishes a whole-plant recycling pattern to promote the sustainable development of medicinal plant cultivation.

Keywords: Agricultural Jiaosu, antifungal activity, *Astragalus membranaceus*, *Fusarium* root rot, sustainable agriculture

INTRODUCTION

Medicinal plants are important for human health and disease management. However, their consecutive monocultures have led to a very serious decline in soil quality and to an increase in soil-borne diseases (Wu et al., 2019). Root rot, caused by fungi of the *Fusarium* genus, is the most destructive soil-borne disease in monoculture systems (Klein et al., 2016; Tao et al., 2020), especially affecting the yield and quality of traditional Chinese herbs whose root and rhizomes are harvested for consumption, such as, *Astragalus membranaceus*. This plant, known as Huangqi in China, is one of the most widely used traditional Chinese herbs, and has been commonly infected by root rot caused by *Fusarium* spp. in recent years (Fu et al., 2014; Li et al., 2021). Crop rotation (Wang et al., 2015; Xiong et al., 2016), resistant cultivars (Pinaria et al., 2010), fungicides (Dignam et al., 2016) and soil fumigation (Gao et al., 2019) can control the pathogen to a certain extent. However, these measures are often impractical to apply to perennial medicinal plants because of their expensive, time consuming, and involve excessive labor-costs, and also because of their negative impact on food security and on the environment. At present, the control of soil-borne diseases should not focus only on eliminating pathogens, but also on regulating the microbial ecosystem. From the perspective of ecological balance, social security, and control efficiency, biological agents represent the optimal method to control *Fusarium* root rot (Liu et al., 2021). Many antagonistic microorganisms isolated from disease suppressive soils or rhizosphere soils of healthy plants (Dignam et al., 2016), such as *Bacillus* spp. (Khan et al., 2018; Wang et al., 2020), *Pseudomonas* spp. (Luo et al., 2019), *Lactobacillus* spp. (Magnusson et al., 2003), and *Penicillium* spp. (Usman et al., 2013), have been proved to be effective in disease suppression. However, these potentially antagonistic microbes have not been widely employed to control *Fusarium* root rot in medicinal plants, due to their instability and high-cost (Xiong et al., 2017). Therefore, a more stable, efficient, and low-cost control strategy is needed. A promising method is the application of Agricultural Jiaosu (AJ), a mix of beneficial microbes combined with metabolites.

The AJ is a microbial ecosystem produced through fermentation using organic waste as substrate (Zhang et al., 2020). It is widely used in agricultural production in China, especially in organic farming system, due to its low cost, stability, and simple operational. Previous studies have shown that AJ contains beneficial microorganisms, such as *Lactobacillus*, *Bacillus*, *Pseudomonas,* and *Pichia* spp., and organic acids, such as lactic and acetic acids (Arun and Sivashanmugam, 2015, 2017; Rahman et al., 2020). A number of studies reported that the application of AJ led to an increased biomass and quality of plants (Zhu et al., 2020), an increase in soil nutrients (Tong and Liu, 2020) and a change in the diversity of soil microbes (Wei et al., 2020). Moreover, our previous studies found that AJ can effectively inhibit soil-borne fungal pathogens for a long time (Zhang et al., 2020). However, the mechanisms underlying the AJ-induced disease suppression remain unclear. At the same time, it is also urgent to take measures to strengthen the antifungal activity of AJ, such as the optimization of fermented materials. Medicinal plants, especially those with anti-inflammatory properties, contain natural antifungal compounds. Their waste leaves and stems are considered as high-quality organic materials for AJ fermented because of their unique medicinal ingredients and easy decomposition.

In this study, *Astragalus membranaceus* was used as model crop and *Fusarium oxysporum* as model pathogen to reveal the mechanism of action of AJ and its effects on the suppression of *Fusarium* root rot. For this purpose, (1) the microbial and physicochemical properties of AJ fermented using the waste leaves and stems of medicinal plants were determined. (2) The antifungal activity of AJ against *F. oxysporum in vitro* was evaluated, and the relationships between beneficial microbes and physicochemical factors during the inhibition process were explored. (3) The main antagonistic microorganisms of AJ were isolated and their antifungal activity was evaluated *in vitro*. (4) The ability of AJ and antagonistic strains to suppress *Fusarium* root rot was verified *in vivo*. The aim of this study was to reveal the biocontrol mechanism of AJ, and may be useful to support this promising strategy for the control of soil-borne diseases in the future.

MATERIALS AND METHODS

An overview of the study methods is shown in **Supplementary Figure 1**. AJ preparation and characteristic detection methods were detailed presented in Sections "Agricultural Jiaosu Preparation and Pathogen Culture" and "Characterization of Agricultural Jiaosu." Design and methods of AJ's antifungal activity and biocontrol mechanism investigation were introduced in Sections "*In vitro* Antifungal Activity of Agricultural Jiaosu Against *F. oxysporum*" and "Dynamic Changes in Pathogen, Antagonistic Microorganisms, Organic Acids, and pH-Value During the Agricultural Jiaosu Inhibition Process." Methods of screening AJ's antagonistic strains in Section "Screening and Combination Effect of Antagonistic Strains Against

F. oxysporum." Design and methods for pot experiment in Section "*In vivo* Antifungal Assay of Agricultural Jiaosu and Antagonistic Strains by Greenhouse Pot Experiment."

Agricultural Jiaosu Preparation and Pathogen Culture

The main organic material used for AJ preparation consisted in the leaves and stems of medicinal plants, which included *Astragalus membranaceus*, *Radix scutellariae*, *Radix Sophorae flavescentis,* and *Bupleurum chinense*. The plant materials were collected in Lingqiu County, Datong City (located in Shanxi Province, China), and were cut into segments of 1–2 cm. Then, they were mixed together with brown sugar and deionized water at a ratio of 3:1:10 in a 5 L airtight glass container, and were kept at 35°C for 3 months to allow anaerobic fermentation. The mixed materials presented a pH of 6.29 and the following acid concentrations: lactic acid, 5.65 g/L; formic acid, 2.64 g/L; acetic acid, 4.55 g/L; propionic acid, 3.03 g/L; butyric acid, 0.50 g/L (the detection methods are shown in Section "Physicochemical Analysis"). After 3 months, the supernatant was used for subsequent experiments (Jiang et al., 2021).

The fungal pathogen *F. oxysporum* was isolated from the roots of an infected *A. membranaceus* plant (collected in Datong City, Shanxi Province, China) using a *Fusarium*-selective medium. The pathogen was cultured on PDA medium, added with 150 mg/L streptomycin, in the dark at 25°C for up to 5 days prior to use.

Characterization of Agricultural Jiaosu

After 90 days of fermentation, the characteristics of AJ were evaluated based on two aspects, (I) the microbial community structure of AJ (including both bacterial and fungal), and (II) the physicochemical properties, including pH, organic acids and volatile organic compounds (VOCs). Three replicates (one sample for each replicate) were performed for each experiment.

Microbiological Analysis

Microbial DNA was extracted using the OMEGA Soil DNA Kit (M5635-02) (Omega Bio-Tek, Norcross, GA, United States). The quantity and quality of the extracted DNA was measured using a NanoDrop NC 2000 spectrophotometer (Thermo Fisher Scientific, Waltham, MA, United States) and agarose gel electrophoresis, respectively. The primers used for bacteria were 338F (5′-ACTCCTACGGGAGGCAGCA-3′) and 806R (5′-GGACTACHVGGGTWTCTAAT-3′), and those used for fungi were ITS1F (CTTGGTCATTTAGAGGAAGTAA) and ITS2 (GCTGCGTTCTTCATCGATGC). PCR program: 98°C 3 min, 98°C 30 s 25 cycles, 53°C 30 s, 72°C 45 s, and 72°C 5 min by a thermocycler PCR system. Illumina Miseq sequencing were conducted as described by Xu et al. (2021).Community structure was analyzed at the phylum and genus levels using the SILVA Release 132 database[1] (Zhao et al., 2017) and UNITE Release 8.0 database[2] (Koljalg et al., 2013).

[1]http://www.arb-silva.de

[2]http://unite.ut.ee/index.php

Physicochemical Analysis

The pH values of AJ were determined by a micro-pH meter (Mettler-Toledo, Greifensee, Switzerland). The concentrations of organic acids (formic, acetic, lactic, and propionic acids) were analyzed using a high performance liquid chromatography (HPLC) system equipped with an ion-exchange column (Aminex HPX-87H; 300 mm × 7.8 mm, Bio-Rad Laboratories, Hercules, CA, United States) and a diode array detector (SPD-M20A, Shimadzu, Kyoto, Japan). The details of the chromatographic procedure and conditions are described in Cai et al. (2018).

The AJ's VOCs were determined by headspace solid-phase microextraction coupled to gas chromatography mass spectrometry (HS-SPME/GC-MS) (Sanchez-Palomo et al., 2005). Briefly, the SPME fiber coatings used in this study is 50/30 μm PDMS/CAR/DVB (2 cm). 8 ml of AJ was placed it into a 15 mL extraction bottle, and 2.5 g NaCl was added to improve the extraction efficiency (Butkhup et al., 2011). Fibers were then exposed to the headspace of the extraction bottle for 40 min at 80°C. After extraction, the SPME fiber was inserted into the hot injector port (at 250°C) of the GC-MS system for 5 min where the extracted chemicals were desorbed thermally and transferred directly to the analytical column. The GC-MS analysis was performed on an Agilent gas chromatograph (model 7890A; Shiyanjia Lab, Zhejiang, China) coupled to a mass selective detector (model 5975C). Compounds were separated on a HP-5MS capillary column (30.0 m × 250 μm i.d.; 0.25 μm film thickness); the GC-MS conditions are described in Zhao et al. (2021). The compounds were identified based on the match of their GC retention times, retention indices and mass spectrum with the NIST11 library (Mohamad et al., 2018). The peak area of each compound was normalized using the area normalization method, and the relative abundance of each compound was calculated.

In vitro Antifungal Activity of Agricultural Jiaosu Against *F. oxysporum*

Effect of Agricultural Jiaosu Dosage on the Antifungal Activity Against *F. oxysporum*

The antifungal activity of AJ was assessed through the agar plate diffusion method as previously described (Zhang et al., 2020). Briefly, PDA medium containing different AJ concentrations (5, 10, 15, 25, 35, and 50%, respectively) was prepared with AJ supernatant. The PDA medium without AJ was used as blank control (CK). Three replicates were performed for each treatment. After the medium solidified, a plug with a diameter of 6-mm containing *F. oxysporum* mycelium, which was obtained from a 5-day-old PDA culture, was placed at the center of each plate. These plates were incubated for 5 days in the dark at 25°C. The growth of the plug was measured every 24 h. The inhibition rate was calculated using the following formula (Aeron et al., 2011; Mohamad et al., 2018):

$$\text{Inhibition rate (\%)} = \frac{(\text{Fck} - \text{Ft})}{(\text{Fck} - \text{F0})} \times 100 \quad (1)$$

where F*ck* and F*t* represent the colony diameter of the fungal mycelium in the control and treatment, respectively, and F*0* is the diameter of the test fungus agar disks (6 mm).

In order to better measure the effectiveness of AJ, its half-maximal inhibitory concentration (IC_{50}) was calculated. Briefly, taking the concentration of AJ as the *x*-value and the colony diameter of the pathogen at 120 h as the *y*-value, a quadratic regression analysis was carried out to obtain the fitting curve and polynomial. Then, half of the colony diameter of CK was considered as the *y*-value and was brought into the equation to calculate the corresponding *x*-value, which is the IC_{50} of AJ against *F. oxysporum* (Zhang et al., 2020).

Effect of the Microbial Components of Agricultural Jiaosu on the Antifungal Activity Against *F. oxysporum*

The inhibitory effect of the AJ's microbial components against *F. oxysporum* was evaluated. Three different treatments were applied as follows: AJ, added 10% AJ; sterilized-AJ, added 10% sterilized AJ; CK, no AJ. Each treatment was repeated three times. According to the above-method in Section "Effect of Agricultural Jiaosu Dosage on the Antifungal Activity Against *F. oxysporum,*" the inhibition rate was determined after 5 days, and the contribution rate of different components to the inhibition of the pathogen was calculated using the following formula:

$$\text{OCR } \% = \frac{\text{IR}s}{\text{IR}} \times 100 \quad (2)$$

$$\text{MCR } \% = 1 - \text{OCR} \quad (3)$$

where OCR is contribution rate of other components, IR*s* is the inhibition rate of the sterilized-AJ treatment, IR is the inhibition rate of the AJ treatment, and MCR is the contribution rate of microbial components.

Dynamic Changes in Pathogen, Antagonistic Microorganisms, Organic Acids, and pH-Value During the Agricultural Jiaosu Inhibition Process

To reveal the biocontrol mechanism of AJ during the inhibition process, an antifungal assay was carried out in potato dextrose broth (PDB) medium with the following treatments: AJ, 10% AJ treatment; and CK, without AJ as a control. The same amount of *F. oxysporum* mycelium block (6 mm diameter) was inoculated in each treatment (three mycelium blocks/100 mL). Three independent biological replicates were used for each treatment. The samples were collected at 0, 12, 24, 36, 48, 60, and 72 h to determine the pH-value and the concentrations of organic acids. Here, *Lactobacillus*, *Bacillus,* and *Pseudomonas* genera were selected as representatives of AJ's antagonistic microorganisms, and their gene concentrations were determined by quantitative real-time PCR (qPCR).

The pH-value and organic acids were measured using the methods mentioned above in Section "Physicochemical Analysis." The abundances of *F. oxysporum*, *Lactobacillus*, *Bacillus,* and *Pseudomonas* communities were quantified with the EF1H/EF2T (O'Donnell et al., 1998), F_alllact_IS/R_alllact_IS (Haarman and Knol, 2006), BacF/BacR (Mori et al., 2004), and Ps-for/Ps-rev primers (Garbeva et al., 2004), respectively (**Supplementary Table 1**); qPCR was carried out with the Applied Biosystems 7500 qPCR System (Applied Biosystems, CA, United States) by using the SYBR Green I fluorescent dye detection in 20-μL volumes containing 10 μL SYBR real-time PCR premixture (2×), and 0.4 μL of both forward and reverse primers (Wei et al., 2018). The PCR protocol was set as follows: 95°C for 5 min; followed by 40 cycles at 95°C for 15 s and 60°C for 30 s. The copy number of thee target genes was calculated based on previously described by Zhou and Wu (2018).

Screening and Combination Effect of Antagonistic Strains Against *F. oxysporum*

Isolation and Identification of Antagonistic Strains

In order to identify the main antagonistic strains of AJ, the culturable bacteria and fungi were isolated using beef extract peptone agar medium and PDA medium containing 150 mg/L streptomycin. Bacteria and fungi were both incubated in the dark: the former at 35°C for 2–3 days, and the latter at 25°C for 3–4 days. These isolated bacteria and fungi were named from B1 to Bn, and from F1 to Fn, respectively. All microbial isolates were tested for their ability to inhibit fungal growth using a dual culture assay, following the method described in a previous study (Sun et al., 2021). The inhibition rate of the microbial isolates was calculated using the method described in Section "Effect of Agricultural Jiaosu Dosage on the Antifungal Activity Against *F. oxysporum.*"

The above assays detected seven isolates with high inhibition levels against *F. oxysporum*, their total genomic DNA was extracted using the Ezup Column Bacteria Genomic DNA Purification Kit (Sangon, Shanghai, China), following the manufacturer's instructions. The 16s rRNA was amplified using the universal bacterial primers 27F (5′AGAGTTTGATCCTGGCTCAG-5′) and 1492R (5′-GGTTACCTTGTTACGACTT-3′). The amplicon was purified and sequenced by Sangon Biological Engineering Co., Ltd. (Shanghai, China) (Tamegai et al., 1997; Rameshkumar and Nair, 2009). The generated sequences were submitted to the NCBI GenBank, and were compared with gene sequences published in the NCBI website using the BLAST algorithm (Altschul et al., 1990). Distances were calculated according to standard parameters (Kumar et al., 2016), and phylogenetic trees were inferred using the neighbor-joining method with MEGA 7.0 (Saitou and Nei, 1987).

Antifungal Effect of Antagonistic Strain Combination Against *F. oxysporum*

Among the seven bacterial strains with the highest antagonistic ability, five were identified as *Bacillus* spp. and two as *Lysinibacillus* spp. Their antagonistic activity against *F. oxysporum* was examined by agar plate diffusion assay,

including B1, B20, B23, B44, B50, B30, B38, 2L (equal proportion combination of the two *Lysinibacillus* isolates), 5B (equal proportion combination of the five *Bacillus* isolates), 2L + 5B (equal proportion combination of the seven bacterial isolates). Firstly, the seven strains were grown in beef extract peptone broth and were incubated at 35°C for 48 h, then, the 200 μL bacterial suspensions (isolated independently or in combination) were evenly spread on the surface of PDA plates, and a 6-mm plug of actively growing *F. oxysporum* mycelium was placed at the center of these plates containing the bacterial suspensions. Plates containing only sterile water were used as controls. Each treatment was repeated three time. All treatments were incubated in the dark at 25°C for 5 days. The mycelium growth of the pathogen was determined by measuring the colony diameter. The inhibition rate of the microbial isolates was calculated using the method described in Section "Effect of Agricultural Jiaosu Dosage on the Antifungal Activity Against *F. oxysporum*."

In vivo Antifungal Assay of Agricultural Jiaosu and Antagonistic Strains by Greenhouse Pot Experiment

The capacity of AJ and antagonistic strains to control *Astragalus* root rot was evaluated *in vivo*. The pot experiments with *Astragalus* were performed using the following five treatments: CK, not inoculated with *F. oxysporum* or biological agents; F, each plant inoculated with 1 mL of *F. oxysporum* suspension (10^5 CFU/mL); F + AJ, each plant inoculated with 1 mL of *F. oxysporum* suspension (10^5 CFU/mL) and 1 mL of 10% AJ; F + B1, each plant inoculated with 1 mL of *F. oxysporum* (10^5 CFU/mL) and 1 mL of *B. velezensis* suspensions (10^6 CFU/mL); F+B20, each plant inoculated with 1 mL of *F. oxysporum* (10^5 CFU/mL) and 1 mL of *B. subtilis* suspensions (10^6 CFU/mL). Each treatment included three replicates (pots) with twenty *Astragalus* seedlings per replicate. *Astragalus* seeds [*Astragalus membranaceus* (Fisch.) Bge. var. *mongholicus* (Bge.) Hsiao] were surface-sterilized with NaClO (3%; v: v) for 5 min and washed five times in sterile distilled water, and were then germinated on moist filter paper at 25°C in the dark (Wei et al., 2019). After 3 days, the germinated seeds were transferred to polyethylene plastic pots (100 mm × 150 mm × 120 mm) filled with 800 g of nutritional soil. The pots were randomly placed in a greenhouse at 28°C ± 2°C, 60–70% relative humidity, and a 16-h light/8-h dark cycle for 6 weeks until the end of the experiment (Chen et al., 2018).

After 2 weeks, all treatments—except for the CK treatment—were inoculated with *F. oxysporum* via root irrigation (Gao et al., 2019), and the control was treated with an equal volume of sterile PDA medium. The biocontrol agents were inoculated immediately after pathogens inoculation in the F + AJ, F + B1, and F + B20 treatments. Subsequently, biocontrol agents were applied once every 7 days for a total of three applications. The CK and F groups were treated with an equal volume of sterile water as controls. Plant characteristics were evaluated 4 weeks after pathogen inoculation, and they included: plant height, chlorophyll content (SPAD-502, Minolta), root length, root diameter, fresh weight and dry weight. The disease incidence was calculated based on the following formula (Zhai et al., 2021):

$$\text{Disease incidence (\%)} = \frac{\text{the number of diseased plants}}{\text{total number of investigated plants}} \times 100 \quad (4)$$

Statistical Analyses

Statistical significance (ANOVA) was analyzed in SPSS 23.0 (IBM Corporation, NY, United States) and was established at a *P*-value less than 0.05. The figures were produced using Origin 2018 (OriginLab Corporation, Northampton, MA, United States), Excel 2019 (Microsoft Corporation, Seattle, WA, United States) and Adobe illustrator CC2019 (Adobe, San Jose, CA, United States). The analysis of the microbial community structure, and redundancy analysis were performed on the Personal Genes cloud Platform, freely available online.

RESULTS

Characteristics of Agricultural Jiaosu

Microbial Community

The AJ's bacterial and fungal communities were analyzed through the Illumina sequencing of 16S rRNA and ITS gene amplicons, which obtained a total of 4,262 bacterial ASVs and 587 fungal ASVs (**Supplementary Table 2**). Bacterial and fungal good's coverage indexes were 0.9975, and 0.9998, respectively. Chao1, Simpson, Shannon and Pielou's evenness indexes were higher for bacteria than for fungi (**Supplementary Table 3**). The results showed that the diversity, richness, and evenness of AJ's bacteria were higher than those of fungi. Further analysis showed that the phyla representing more than 1% of the bacteria in the AJ included Firmicutes (65.12%), Proteobacteria (20.90%), Bacteroidetes (11.61%), and Actinobacteria (1.03%) (**Figure 1A**). Among the fungal community, the majority of species belonged to the phyla Ascomycota (56.95%) and Basidiomycota (32.33%) (**Figure 1B**). *Lactobacillus* and *Aspergillus* with potential biocontrol functions were the most abundant bacterial and fungal genus, accounting for 52.35, and 32.28% of the total, respectively (**Supplementary Table 4**). Moreover, other genera with potential biocontrol functions were also identified in the microbial community, such as *Pseudomonas*, *Bacillus*, *Burkholderia*, *Pichia*, and *Penicillium* (**Figures 1C,D**).

Physicochemical Properties

The AJ fermentation for 90 days, the pH value of AJ was 3.26 ± 0.01. The main organic acid was acetic acid, with a concentration of 13.08 ± 0.67 g/L. The concentration of formic, propionic, and butyric acids were 0.02 ± 0.00 g/L, 0.96 ± 0.19 g/L, and 0.63 ± 0.01 g/L, respectively. Lactic acid was not detected. Moreover, a total of 29 VOCs were detected by GCMS analysis (**Supplementary Table 5**), including 8 alcohols, 4 phenols, 11 esters, 2 hydrocarbons, 2 ketones, 1 ether and 1 amine. Esters and alcohols were the main compound

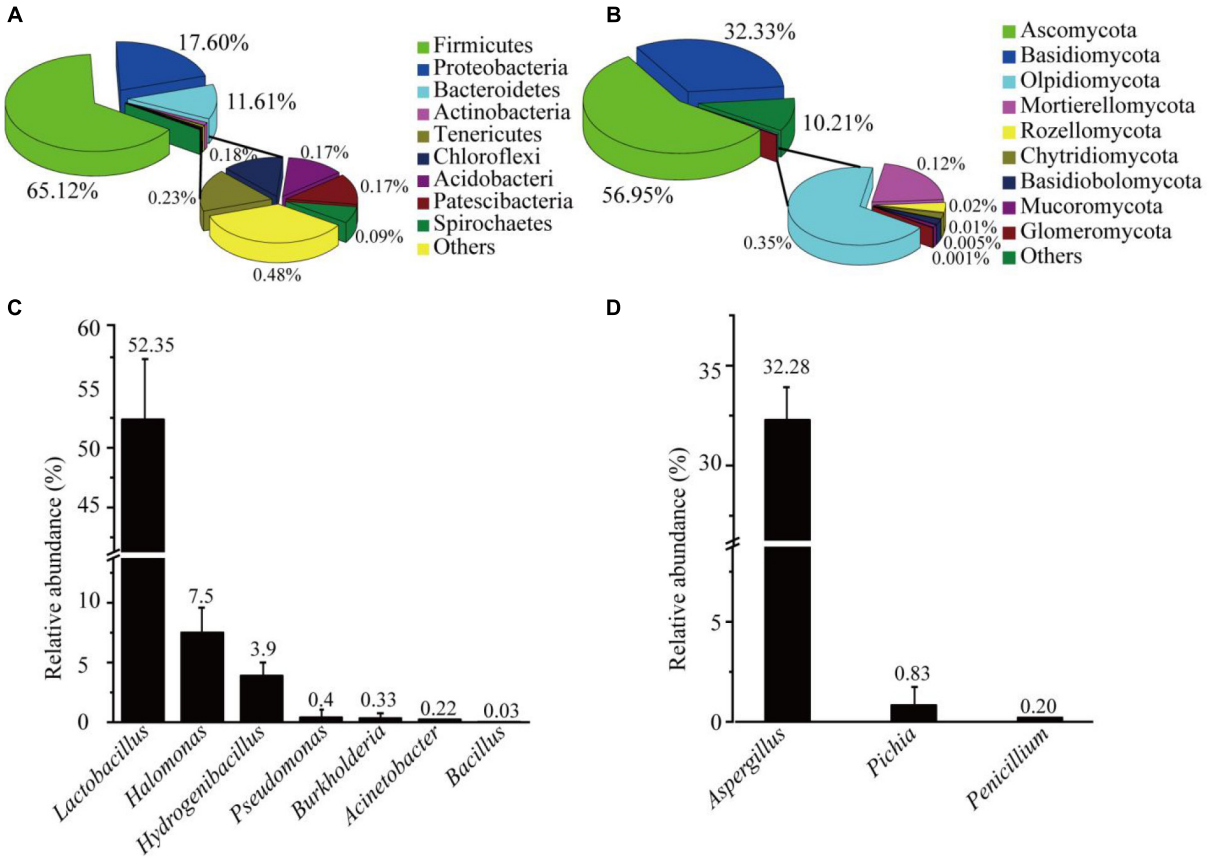

FIGURE 1 | Microbial community structure of AJ: **(A)** bacterial community at the phylum level; **(B)** fungal community at the phylum level; **(C)** relative abundance of bacteria with potential biological control functions; **(D)** relative abundance of fungi with potential biological control functions. Values in the bar plot are expressed asmean ± standard deviation (n = 3).

types, accounting for 63.88% of the 29 detected compounds. It was concluded that 3-heptanol, 6- methyl-, phenol, 4-ethyl-2- methoxy-, L-.alpha.-terpineol, 1-Octen-3-ol, methyl salicylate, and phenol, 2-methoxy-6-(2-propenyl)- were the main VOCs in the AJ, accounting for 14.00, 9.07, 7.85, 7.61, 6.84, and 4.80%, respectively.

Antifungal Activity of Agricultural Jiaosu Against *F. oxysporum*

The inhibitory effect of the AJ dosage was tested against *F. oxysporum* as shown in **Figure 2A**. The higher the dose of AJ, the stronger the inhibition of *F. oxysporum*. When the dosage was higher than 25%, the growth of the pathogen was almost completely inhibited and the inhibition rate reached up to 95.97% at 120 h. The 5, 10, and 15% AJ treatments had the strongest inhibitory effect at 48 h, and the inhibition rates were 25.45, 63.64, and 78.18%, respectively (**Figure 2B**). The IC_{50} was calculated based on the above experimental data. The fitting formula obtained was: $y = 0.0328x^2 - 2.6289x + 57.59$, $R^2 = 0.9851$; and the IC_{50} of AJ against *F. oxysporum* was 13.64% (**Supplementary Figure 2**). Notably, when the inhibitory effect of different AJ components was tested, it was found that the inhibition rate of sterilized-AJ was only 27.10%, and the antifungal contribution rate of microorganisms was 46.48% (**Figure 2C**).

Dynamic Changes in Pathogen, Antagonistic Microorganisms, Organic Acids and pH-Value During the Agricultural Jiaosu Inhibition Process

To further reveal the antifungal mechanisms of AJ, three commonly antagonistic microbial genera (*Lactobacillus*, *Bacillus*, and *Pseudomonas*) were selected as representatives of AJ's beneficial microorganisms. The qPCR results showed that AJ can effectively reduce the density of *F. oxysporum*, and the pathogen's total abundance was approximately 21.14-fold higher in CK compared to the AJ treatment. The *F. oxysporum* gene copy number in CK rapidly increased from 4.93×10^1 copy/μL at 0 h to 7.96×10^5 copy/μL at 36 h (3.85×10^5 copy/μL more than the level observed in the AJ treatment) (**Figure 3A**). Then, the dynamic changes in the antagonistic microorganisms in the AJ treatment were quantified. After 36 h, with the increase of *F. oxysporum*, the gene copy number of *Bacillus* and *Pseudomonas* increased rapidly, surpassing *Lactobacillus* and occupying the niche in

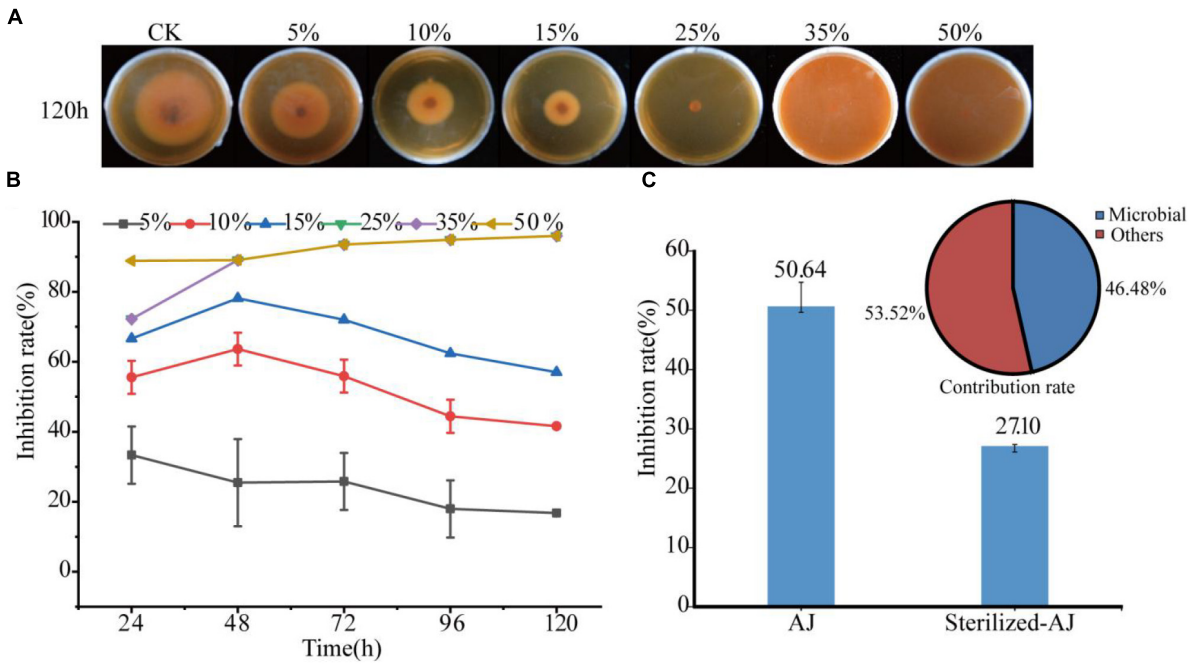

FIGURE 2 | Antifungal activity: **(A)** antifungal test photos taken at 120 h; **(B)** inhibition rate of different dosages of AJ at different times; **(C)** inhibition rate and contribution rate of different AJ components. AJ, 10% AJ; sterilized-AJ, 10% sterilized AJ. Data are mean ± standard deviation, $n = 3$.

AJ treatment. Among these genera, the density and increasing range of *Bacillus* were the largest (**Figure 3B**). By comparing the differences in organic acids between the AJ and CK treatments and the dynamic changes of pH value, it was found that the addition of AJ decreased the pH and promoted the accumulation of lactic and acetic acids (**Figure 3C**). In the redundancy analysis, among all the physicochemical properties, the arrow of pH were the longest, indicating that pH is the key predictor of antagonistic microorganism changes. Furthermore, *Lactobacillus*, *Bacillus*, and *Pseudomonas* were positively correlated with each other; Lactic, formic and butyric acids also had a positively relationship with antagonistic microorganism changes (**Figure 3D**).

Isolation and Identification of Antagonistic Microbes

A total of 53 bacterial strains and 12 fungal strains were isolated from AJ. The inhibitory effect of all isolates was tested against *F. oxysporum* (values listed in **Table 1**), and a total of 47 isolates showed antagonistic activity against the *F. oxysporum*. Among them, the inhibition rates of isolates B1, B20, B23, B30, B38, B44, and B50 were above 20%, specifically, 43.16, 37.63, 24.21, 28.55, 28.95, 30.53, and 32.11%, respectively. Their antifungal activity is shown in **Figure 4A**, and the identified phylogenetic tree is shown in **Figures 4B,C**. The results indicate the presence of five *Bacillus* strains and two *Lysinibacillus* strains. Furthermore, the antifungal effect of antagonistic strains independently or in combination against *F. oxysporum* was determined. **Figure 4D** indicates that the antifungal effect of *Bacillus* spp. was significantly higher than *Lysinibacillus* spp. ($P < 0.05$), and B1 and B20 alone had the strongest antifungal effect ($P < 0.05$).

Inhibition Effect of Agricultural Jiaosu and Isolated Strains in the Pot Experiment

In order to identify the effectiveness of AJ and antagonistic strains *in vivo*, the root rot disease incidence, plant height, chlorophyll content, root length, root diameter, fresh weight, and dry weight of *Astragalus* were further analyzed during the pot experiment. The experimental results showed that the application of AJ, or antagonistic strains B1 and B20 significantly reduced the disease incidence of root rot and promoted the growth of *Astragalus* (**Figure 5**). Compared with the F treatment, the disease incidence in F + AJ was reduced by 61.43% ($P < 0.05$), while the values for the F + AJ, F + B1, and F + B20 treatments were 30.00, 45.00, and 45.00%, respectively (**Figure 5A**). The F + AJ, F + B1, and F + B20 treatments determined a more significant increase in the fresh and dry weights of leaves and stems (**Figures 5B,C**), plant height (**Figure 5D**), chlorophyll content (**Figure 5E**) and root diameter (**Figure 5F**) of *Astragalus* compared to the F treatment ($P < 0.05$). Moreover, F + AJ and F + B1 treatments also produced a more significant increase in the fresh weight and length of roots compared the F treatment (**Figures 5B,F**) ($P < 0.05$).

DISCUSSION

Fusarium root rot is a critical factor restricting the sustainable production of medicinal plants. AJ as a promising biological

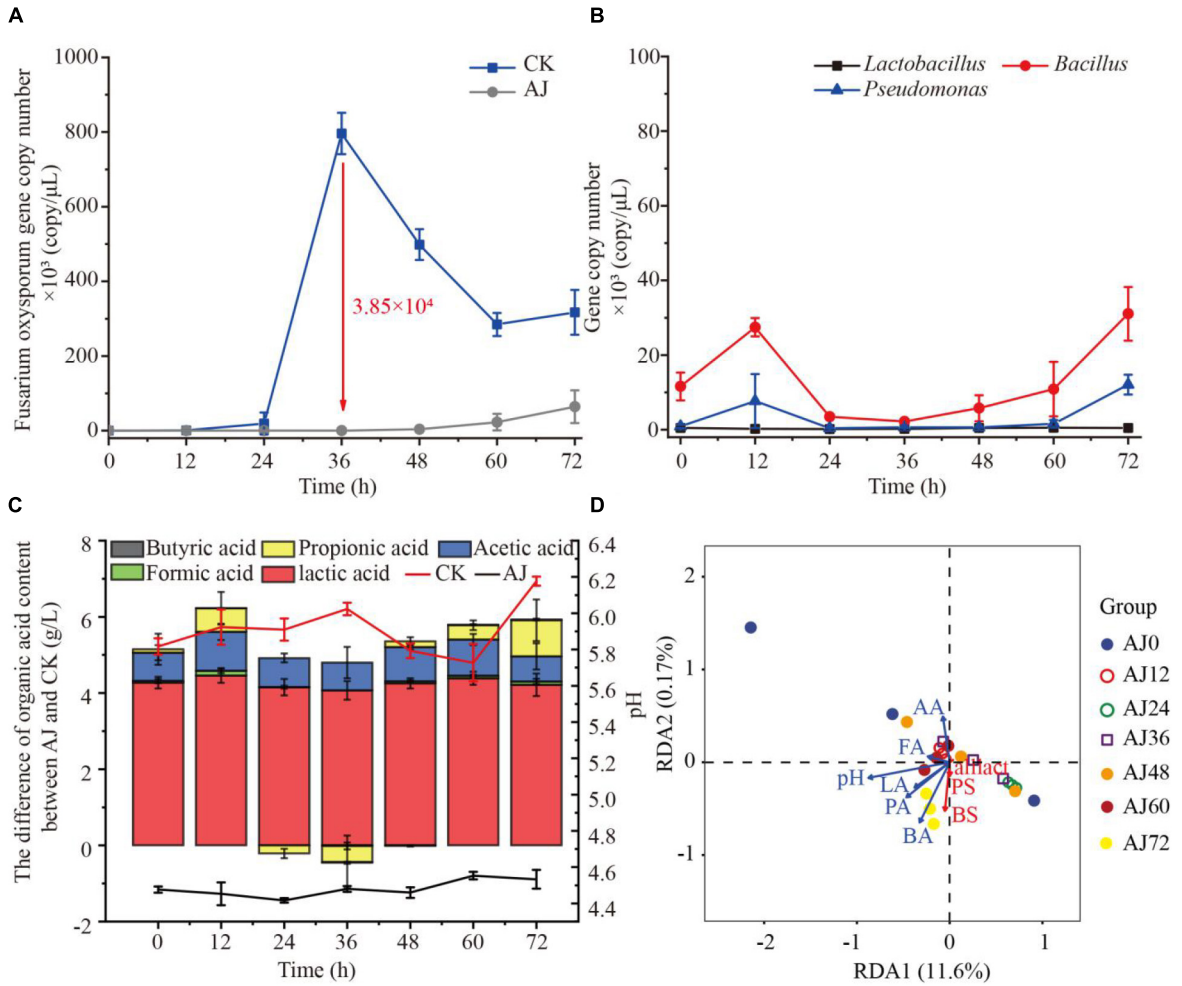

FIGURE 3 | Dynamic changes observed in microorganisms and physicochemical factors during the inhibition process. **(A)** Dynamic changes in *Fusarium oxysporum* gene copy number; **(B)** dynamic changes in *Lactobacillus*, *Bacillus* and *Pseudomonas* gene copy number during AJ treatment; **(C)** dynamic changes of pH and differences in organic acids content between AJ and CK; **(D)** redundancy analysis of physicochemical factors and beneficial microorganism in AJ treatment during the inhibition process. LA, lactic acid; FA, formic acid; AA, acetic acid; PA, propionic acid; BA, butyric acid; BS, *Bacillus*; PS, *Pseudomonas*; LS, *Lactobacillus*; CK, without AJ treatment; AJ, with 10% AJ treatment. Data are mean ± standard deviation, $n = 3$.

agent gradually attracted attention. In the present study, it was found that the AJ fermented using medicinal plants aboveground was rich in beneficial microorganisms and metabolites such as organic acids, esters, alcohols, and that it can effectively inhibit the growth of *F. oxysporum*. In addition, beneficial microorganisms and organic acid metabolites may be the main driving factors of AJ's antifungal action, and *B. subtilis* and *B. velezensis* were identified as the strongest antagonistic strains. Pot experiments confirmed that AJ and antagonistic strains can reduce the incidence of root rot and promote the growth of *Astragalus*.

Agricultural Jiaosu's Potential Capability to Suppress Soil-Borne Fungal Diseases

Biological control using beneficial microorganisms is a safe and effective method for suppressing soil-borne diseases (Mohamad et al., 2018). Previous studies have reported that AJ is a microbial ecosystem rich in beneficial microorganisms (such as *Lactobacillus* spp., *Pichia* spp., and others) and organic acids (such as lactic, acetic acids and others), and that it can effectively inhibit fungal pathogens (Rahman et al., 2020; Zhang et al., 2020). In this study, the waste leaves and stems of medicinal plants with anti-inflammatory effects were used as the fermentation material to enhance the antifungal activity of AJ. The MiSeq sequencing results showed that the core microbiome of AJ comprised Firmicutes, Proteobacteria, Bacteroidetes, and Actinobacteria. Among them, the relative abundance of Firmicutes and Proteobacteria was the highest (**Figure 1A**). These data are in line with previous reports, suggesting that Firmicutes and Proteobacteria dominate the entire bacterial community of AJ (Zhang et al., 2020). Previous studies have also shown that these two phyla were more abundant in healthy soils, they directly contributed to the pathogen

TABLE 1 | Antifungal activity of 65 isolates against *Fusarium oxysporum*.

IsolatesID	Myceliumdiameter (mm)	Inhibition rate (%)	Isolates ID	Mycelium diameter (mm)	Inhibition rate (%)
B1	**24.00 ± 0.12^{r}**	**43.16 ± 0.04^{a}**	B34	36.75 ± 0.04^{f-j}	2.89 ± 0.01^{l}
B2	45.50 ± 0.09^{de}	–	B35	36.25 ± 0.13^{f-k}	4.47 ± 0.04^{j-l}
B3	39.00 ± 0.87^{d-f}	–	B36	38.00 ± 0.10^{e-g}	–
B4	34.50 ± 0.09^{g-m}	10.00 ± 0.03^{e-l}	B37	33.00 ± 0.21^{i-m}	14.74 ± 0.07^{d-j}
B5	39.00 ± 0.17^{d-f}	–	**B38**	**28.50 ± 0.15^{n-q}**	**28.95 ± 0.05^{bc}**
B6	34.50 ± 0.05^{g-m}	10.00 ± 0.02^{e-l}	B39	38.00 ± 0.21^{e-g}	–
B7	32.67 ± 0.18^{j-n}	15.79 ± 0.06^{d-h}	B40	34.25 ± 0.29^{g-m}	10.79 ± 0.09^{e-l}
B8	46.50 ± 0.21^{ab}	–	B41	32.00 ± 0.10^{k-o}	17.89 ± 0.03^{d-f}
B9	33.75 ± 0.13^{g-m}	12.37 ± 0.04^{e-l}	B42	45.00 ± 0.19^{bc}	–
B10	37.25 ± 0.05^{f-i}	1.32 ± 0.06^{kl}	B43	35.50 ± 0.05^{f-l}	6.80 ± 0.02^{g-l}
B11	34.50 ± 0.05^{g-m}	10.00 ± 0.02^{e-l}	**B44**	**28.00 ± 0.10^{o-q}**	**30.53 ± 0.03^{bc}**
B12	31.50 ± 0.08^{l-p}	19.47 ± 0.04^{de}	B45	32.25 ± 0.15^{k-n}	17.11 ± 0.05^{d-f}
B13	32.00 ± 0.19^{k-o}	17.89 ± 0.06^{d-f}	B46	33.75 ± 0.38^{g-m}	12.37 ± 0.12^{e-l}
B14	33.75 ± 0.13^{g-m}	12.37 ± 0.04^{e-l}	B47	37.50 ± 0.25^{e-h}	0.53 ± 0.08^{kl}
B15	33.50 ± 0.15^{h-m}	13.16 ± 0.05^{e-k}	B48	32.50 ± 0.09^{j-n}	16.32 ± 0.03^{d-g}
B16	37.50 ± 0.21^{e-h}	0.53 ± 0.07^{kl}	B49	33.75 ± 0.11^{g-m}	12.37 ± 0.03^{e-l}
B17	32.75 ± 0.08^{j-n}	15.53 ± 0.03^{d-h}	**B50**	**27.50 ± 0.43^{p-r}**	**32.11** ± 0.14^{bc}
B18	42.75 ± 0.25^{b-d}	–	B51	31.33 ± 0.05^{l-p}	19.47 ± 0.02^{de}
B19	46.50 ± 0.32^{ab}	–	B52	33.00 ± 0.12^{i-m}	14.74 ± 0.04^{d-i}
B20	**25.75 ± 0.08^{qr}**	**37.63 ± 0.03^{ab}**	B53	32.75 ± 0.19^{j-n}	15.53 ± 0.06^{d-h}
B21	35.75 ± 0.13^{f-l}	6.05 ± 0.04^{h-l}	F1	31.50 ± 0.38^{d}	13.27 ± 0.13^{a}
B22	37.25 ± 0.28^{f-i}	1.32 ± 0.09^{j-l}	F2	31.00 ± 0.10^{d}	14.97 ± 0.03^{a}
B23	**30.00 ± 0.00^{m-p}**	**24.21 ± 0.00^{cd}**	F3	48.50 ± 0.15^{a}	–
B24	42.50 ± 0.25^{cd}	–	F4	33.00 ± 0.12^{cd}	8.16 ± 0.04^{a}
B25	34.50 ± 0.09^{g-m}	10.00 ± 0.03^{e-l}	F5	34.50 ± 0.50^{b-d}	3.06 ± 0.17^{a}
B26	35.50 ± 0.15^{f-l}	6.84 ± 0.05^{g-l}	F6	48.50 ± 0.35^{a}	–
B27	49.25 ± 0.13^{a}	–	F7	35.50 ± 0.36^{b-d}	–
B28	34.50 ± 0.15^{g-m}	10.00 ± 0.05^{e-l}	F8	36.00 ± 0.10^{b}	–
B29	34.00 ± 0.21^{g-m}	11.58 ± 0.07^{e-l}	F9	30.00 ± 0.00^{d}	18.37 ± 0.00^{a}
B30	**28.63 ± 0.20^{n-q}**	28.55 ± 0.06^{bc}	F10	32.00 ± 0.00^{d}	11.56 ± 0.00^{a}
B31	36.00 ± 0.10^{f-k}	5.26 ± 0.03^{j-l}	F11	37.00 ± 0.40^{b-d}	–
B32	34.75 ± 0.04^{f-l}	9.21 ± 0.01^{f-l}	F12	39.50 ± 0.15^{bc}	–
B33	37.75 ± 0.23^{e-h}	–			

Data are presented as means ± standard deviation. Different letters within each row indicate statistically significant differences ($P < 0.05$, $n = 3$) based on Duncan's tests. The ANOVA of mycelium diameters of bacteria and fungi were analyzedseparately. "–" indicates no antifungal activity. Antifungal activity of the seven bacterial strains with the highest antagonistic ability are bolded.

inhibition (Huang et al., 2019; Wei et al., 2019), and AJ addition significantly increased the relative abundance of Firmicutes in organic fertilizers (Jiang et al., 2021). In regards to fungi, Ascomycota and Basidiomycota were the dominant phyla found in AJ (**Figure 1B**), and previous studies have also shown that these phyla have a higher relative abundance in soil after AJ irrigation (Wei et al., 2020). Moreover, in the present study, it was found AJ was rich in potential antagonistic microorganisms, such as *Lactobacillus*, *Pseudomonas*, *Burkholderia*, *Acinetobacter*, *Bacillus*, *Aspergillus*, *Pichia*, and *Penicillium* (**Figures 1C,D**), and numerous previous studies indicated that they can control soil-borne pathogens through competition, antibiosis, parasitism, and induced systemic resistance, which have been widely used to protect crops from disease (Van Wees et al., 2008; Usman et al., 2013; Gao et al., 2021).

Furthermore, microbial metabolites containing many antifungal compounds, also play an important role in biological control. These metabolites are easy to decompose and coexist in the environment, and they can also promote interactions and communication between organisms, improve plant growth, induce systemic resistance, and inhibit the growth of pathogenic fungi (Gao et al., 2017). The fermentation of AJ is a process in which microorganisms decompose sugar and organic materials, and metabolites gradually accumulate, especially organic acids. The results of this study showed that AJ had a low pH value, and was rich in organic acids (such as acetic, formic and butyric acids). It has been proved that organic acids can inhibit soil-borne fungi, such as *F. oxysporum*, by acidifying the environment and changing the cell membrane permeability of pathogen (Momma et al., 2006). Accumulating evidence suggests that VOCs can act as antimicrobial agents, and are important for the regulation of the interactions between pathogens and beneficial microorganisms (Raza et al., 2021). GCMS analysis identified 29 unique VOCs

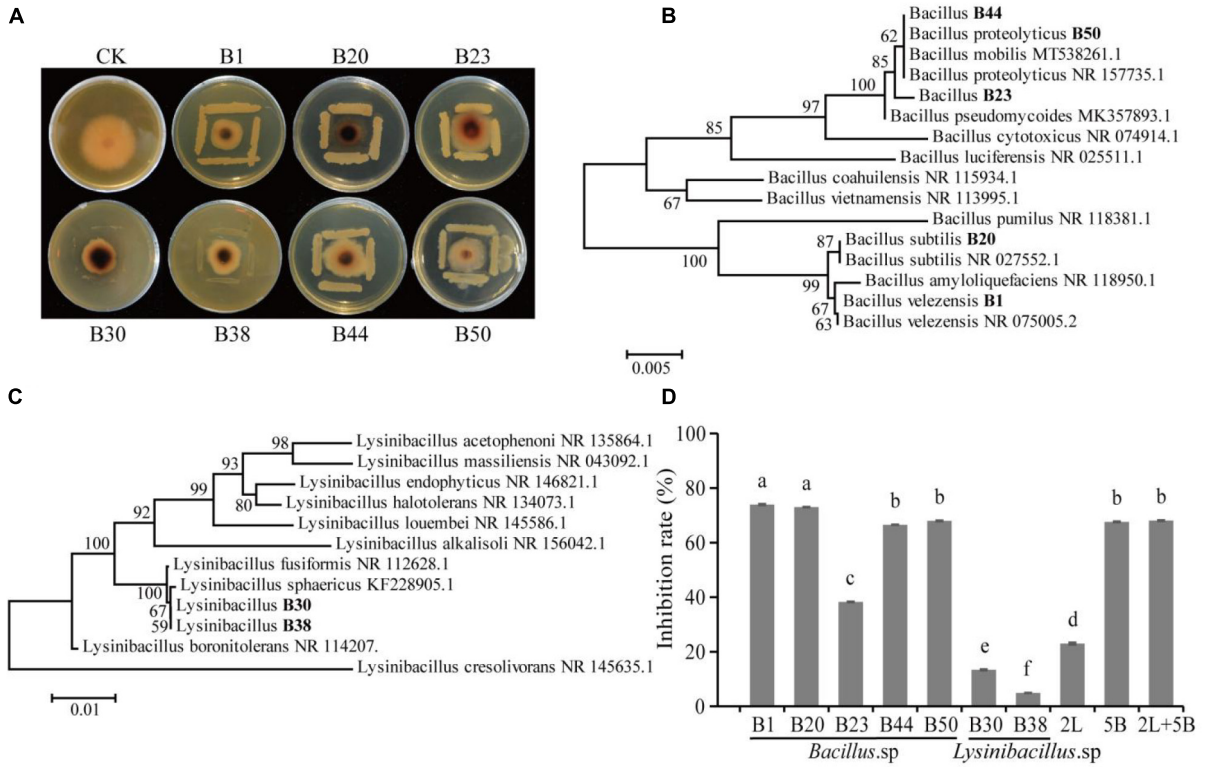

FIGURE 4 | Isolation and identification of antagonistic microbes. **(A)** Antagonistic activity of isolates against *F. oxysporum*; **(B)** hierarchical clustering of *Bacillus* spp.; **(C)** hierarchical clustering of *Lysinibacillus* spp.; **(D)** antifungal effect of antagonistic strains alone or in combination against *F. oxysporum* (2L, equal proportion combination of two *Lysinibacillus* isolates; 5B, equal proportion combination of five *Bacillus* isolates; 2L + 5B, equal proportion combination of seven bacterial isolates). Values in the bar plot are expressed as the mean with standard deviation ($n = 3$). Different letters on the bars indicate statistically significant differences ($P < 0.05$) based on Duncan's tests.

in the AJ, consisting mainly of esters (11) and alcohols (8) (**Supplementary Table 5**). In this study, the inhibitory effect of AJ on *F. oxysporum* was studied for the first time, and it was confirmed that, the higher the dose of AJ is, the stronger the inhibition of *F. oxysporum* (**Figure 2B**). This is consistent with the results we previously reported (Zhang et al., 2020), which indicated that AJ can effectively inhibit plant pathogenic fungi, and that the antifungal activity is positively correlated with dosage. All these results suggest that AJ has a great potential capability to suppress soil-borne fungal diseases, and its application will be a promising strategy for disease control.

Main Driving Factors of Agricultural Jiaosu Controlling *Fusarium* Root Rot

The AJ is a complex fermentation solution (Arun and Sivashanmugam, 2015, 2017), and its antifungal activity is caused by many factors. However, the main antifungal factor of AJ has not been reported in the literature. Our results indicate that AJ's microbial components were critical for the effective suppression of *Fusarium* root rot, and its antifungal contribution rate was 46.48% (**Figure 2C**), indicating that these microbial components may be the main driving factor of AJ's antifungal activity. Interestingly, it was found that the population densities of *Bacillus* and *Pseudomonas* genus increased rapidly and occupied a niche in the dynamic inhibition process induced by the AJ treatment, and the density and increasing range of *Bacillus* were the largest (**Figure 3B**). At the same time, the gradual accumulation of organic acid metabolites—especially lactic acid and acetic acid—lead to a decreased in the pH value (**Figure 3C**). Previous studies have reported that the beneficial microbes suppress fungal diseases by forming organic acids, which in turn lower the environmental pH (Yu et al., 2019). Redundancy analysis revealed that such microorganisms are positively correlated with lactic, formic, butyric acids, and pH value, and that the population densities of *Bacillus*, *Pseudomonas* and *lactobacillus* are correlated with each other (**Figure 3D**). These data imply that the combined effects of beneficial microbes (such as *Bacillus*, *Pseudomonas* and *Lactobacillus*) and organic acid metabolites (such as lactic, acetic, formic, and butyric acids) may represent the main driving factors and biocontrol mechanism through which AJ effectively suppresses *Fusarium* root rot.

Further isolation and identification of antagonistic strains revealed 47 AJ's strains with antagonistic activity against *F. oxysporum*. Among seven isolates with the highest antifungal activity, five isolates belonged to the *Bacillus* genus. In

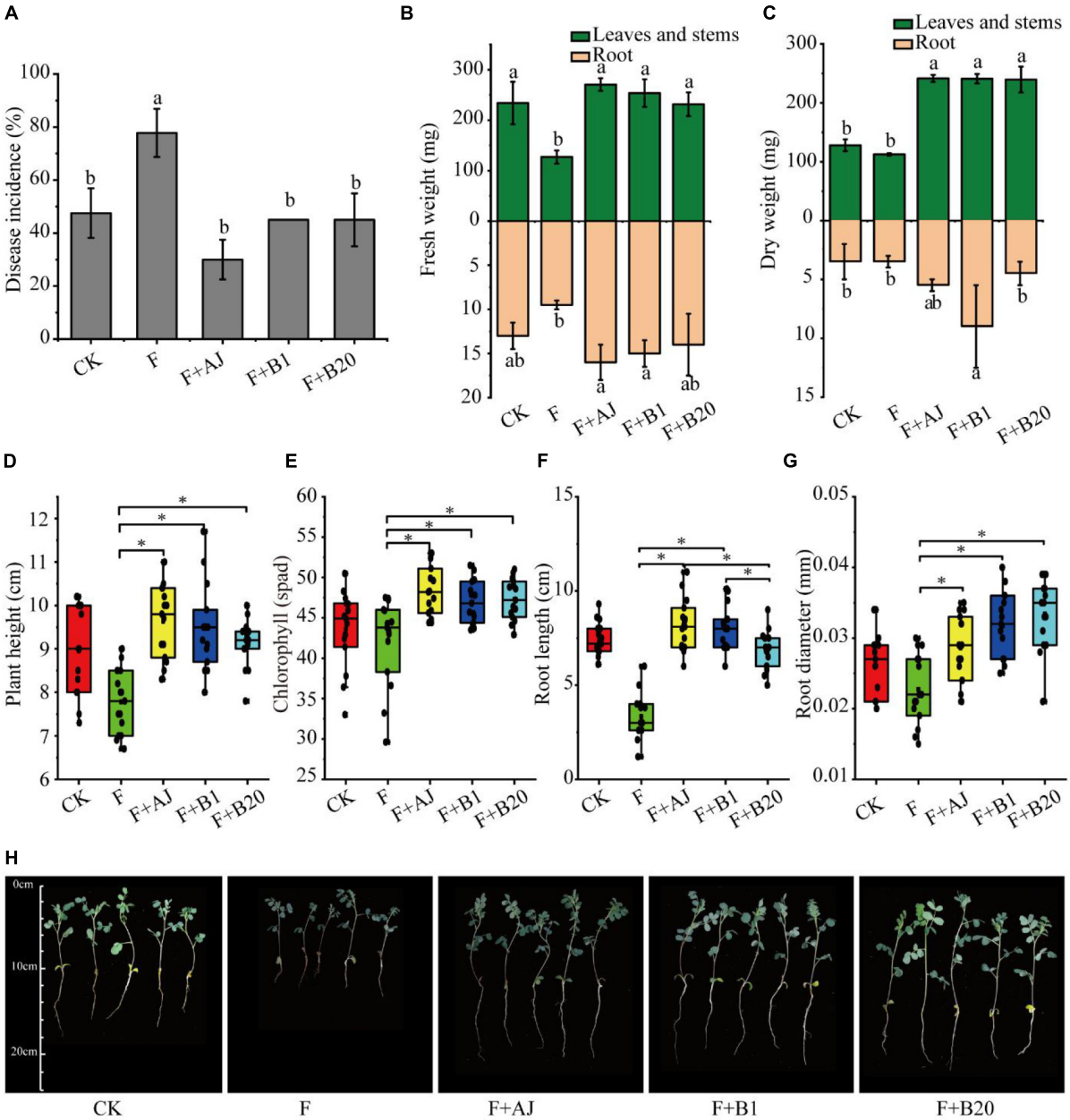

FIGURE 5 | Disease incidence of root rot and growth indexes of *Astragalus*. **(A)** Disease incidence of root rot; **(B)** fresh weight; **(C)** dry weight; **(D)** plant height; **(E)** chlorophyll content; **(F)** root length; **(G)** root diameter; **(H)** growth states of *Astragalus* in different treatments. CK, no *F. oxysporum* and no biological control; F, *F. oxysporum* inoculation alone; F + AJ, *F. oxysporum* inoculation and 10% AJ control; F + B1, *F. oxysporum* inoculation and *B. velezensis* control; F + B20, *F. oxysporum* inoculation and *B. subtilis* control. Data are mean ± standard deviation, $n = 15$. Different letters and the symbol * on the bars indicate statistically significant ($P < 0.05$) differences based on Duncan's tests.

particular, *B. subtilis* and *B. velezensis* were identified as the most effective antagonistic strains (**Figure 3** and **Table 1**). A number of well-known fungal antagonists belong to this genus, which has also been identified as the dominant genus in organic fertilizers treated by AJ treatment (Jiang et al., 2021). Among the *Bacillus* species, the above-mentioned *B. subtilis* and *B. velezensis* are ideal for the formulation of biocontrol agents, and can provide resistance against many pathogens by producing spores, biofilms and antibiotic substances (Cho et al., 2018; Charron-Lamoureux et al., 2020). In this study, the pot experiment confirmed that AJ treatments can significantly suppress *Fusarium* root rot; in fact, the disease incidence was 61.43% lower than that observed in the F treatment. Moreover, AJ treatments significantly increased the plant height, root length, root diameter, chlorophyll content, and the fresh and dry weights of *Astragalus* (**Figure 5**). Although the

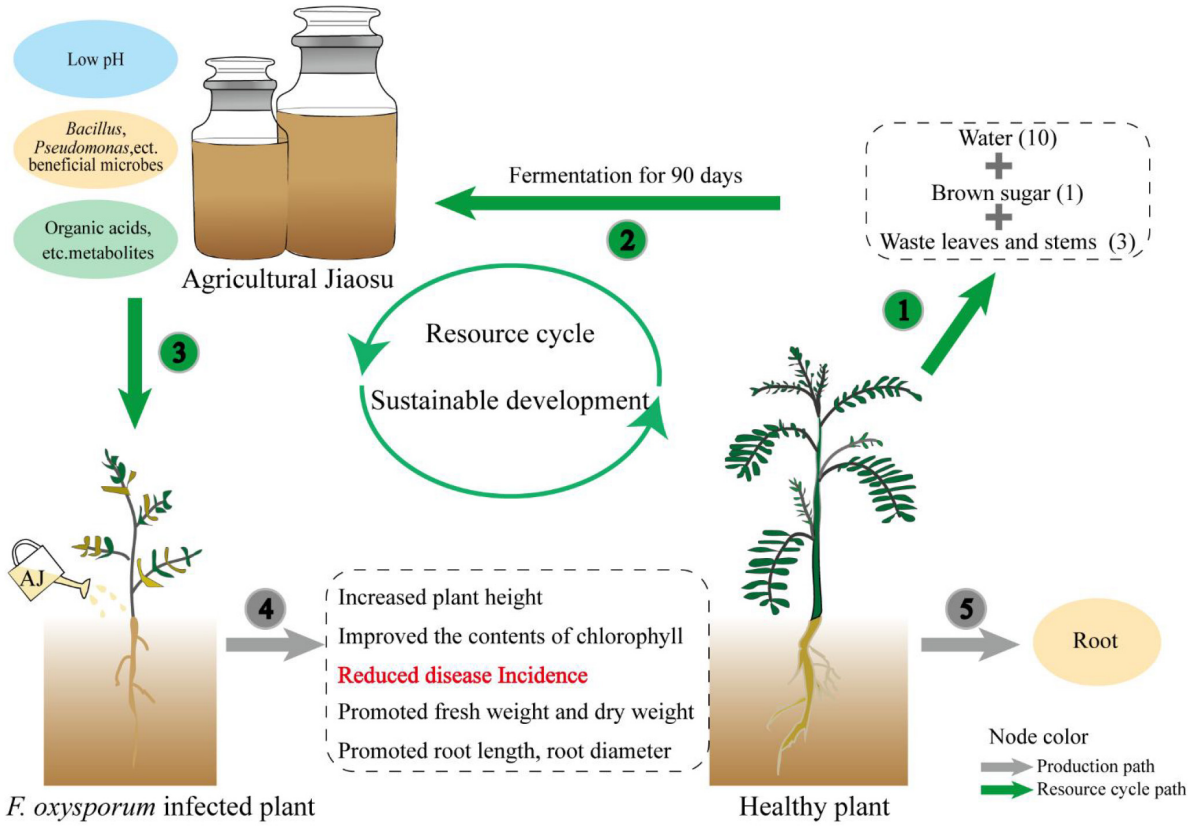

FIGURE 6 | Conceptual model illustrating how the application of AJ can establish a whole plant recycling pattern to promote the sustainable development of medicinal plants.

B. subtilis and *B. velezensis* isolates also significantly reduced the incidence of root rot, their control efficacy was slightly lower than that obtained in the AJ treatment (**Figure 5A**). It is well known that the performance of an individual antagonist may be unstable under different environmental conditions, and this applies also to *B. subtilis* and *B. velezensis* (Kalantari et al., 2018).

Agricultural Jiaosu Can Solve the Bottleneck of the High-Cost of Biological Agents Through Resource Recycling Patterns

The effectiveness of antagonists is generally accepted, however, their wide application is limited by their high cost and instability. The preparation and storage of antagonistic microorganisms require strict aseptic conditions and high requirements in terms of technology and equipment, which undoubtedly represent a huge economic investment. In contrast, AJ is a low-cost and easy-to-operate mixed microbial fermentation technique. It is easily prepared by the fermenting organic waste, sugar and water (Rani et al., 2020), and it does not require expensive equipment. Its lower pH reduces the risk of contamination during the fermentation process (Bartkiene et al., 2020), and our research has proved that it has a strong disease suppression capability. Therefore, this novel biotechnology can solve the bottleneck of the high cost of biological agents (Zhang et al., 2020). As shown in the conceptual model (**Figure 6**), the waste stems and leaves of medicinal plants can be used to prepare an AJ with a low pH value, beneficial microorganisms, and metabolites, which then can function as a biocontrol agent to suppress *Fusarium* root rot, and promote the growth of medicinal plants. The whole plant recycling pattern can convert agricultural waste into biological agents, promote the recycling of waste resources back into the soil, and conducive to the sustainable development of agriculture (Arun and Sivashanmugam, 2015). Thus, AJ can be used as a low-cost, stable, and practical biological agent to replace fungicides and expensive antagonists.

CONCLUSION

The results of this study showed that the AJ fermented using medicinal plants above-ground had a low pH value, and was rich in beneficial microorganisms, and metabolites, such as organic acid, esters and alcohols, etc. AJ can effectively inhibit *F. oxysporum* by the combined effects of beneficial microbes (such as *Bacillus*, *Pseudomonas,* and *Lactobacillus*) and organic acid metabolites (such as lactic acid, formic acid, and butyric acid). The application of AJ and *Bacillus* spp., isolated from AJ,

can significantly suppress *Fusarium* root rot, and promote the growth of *Astragalus membranaceus*. These results suggest that AJ should be considered as a cost-effective way to manage soil-borne diseases and promote agricultural sustainable development.

DATA AVAILABILITY STATEMENT

The original contributions presented in the study are included in the article/**Supplementary Material**, further inquiries can be directed to the corresponding author.

AUTHOR CONTRIBUTIONS

YG, YZ, and XFW conceived and designed the experiments. YG and XC performed the experiments. YZ and XC contributed reagents, materials, and analysis tools. YG, ZZ, and YZ analyzed the data. YG wrote the manuscript. XFW, XHW, XD, ZZ, and YH revised the manuscript. All authors approved the final version of the article for publication.

FUNDING

This research was supported by the Science and Technology Support Project of Datong City, Shanxi Province (2019001).

ACKNOWLEDGMENTS

We thank Haiyu Han, from the Propaganda Department of Lingqiu County (Datong City, Shanxi Province), for providing the leaves and stems of medicinal plants was used on the present research. We also thank Xiaoping Liu, from Luzhou agriculture and rural bureau (Luzhou City, Sichuan Province), for his help in AJ preparation.

SUPPLEMENTARY MATERIAL

The Supplementary Material for this article can be found online at: https://www.frontiersin.org/articles/10.3389/fmicb.2022.823704/full#supplementary-material

Supplementary Figure 1 | Research roadmap.

Supplementary Figure 2 | The half-maximal inhibitory concentration (IC50) of AJ.

Supplementary Table 1 | Amplification primers used in this study.

Supplementary Table 2 | Processed sample data information to analyze bacterial and fungal community of AJ.

Supplementary Table 3 | Alpha diversity of bacterial and fungal community of AJ.

Supplementary Table 4 | The relative abundance of top 10 bacterial and fungal genus.

Supplementary Table 5 | Volatile organic compounds (VOCs) of AJ.

REFERENCES

Aeron, A., Dubey, R. C., Maheshwari, D. K., Pandey, P., Bajpai, V. K., and Kang, S. C. (2011). Multifarious activity of bioformulated *Pseudomonas fluorescens* PS1 and biocontrol of *Sclerotinia sclerotiorum* in indian rapeseed (*Brassica campestris* L.). *Eur. J. Plant Pathol.* 131, 81–93. doi: 10.1007/s10658-011-9789-z

Altschul, S. F., Gish, W., Miller, W., Myers, E. W., and Lipman, D. J. (1990). Basic local alignment search tool. *J. Mol. Biol.* 215, 403–410. doi: 10.1006/jmbi.1990.9999

Arun, C., and Sivashanmugam, P. (2015). Investigation of biocatalytic potential of garbage enzyme and its influence on stabilization of industrial waste activated sludge. *Process Saf. Environ. Prot.* 94, 471–478. doi: 10.1016/j.psep.2014.10.008

Arun, C., and Sivashanmugam, P. (2017). Study on optimization of process parameters for enhancing the multi-hydrolytic enzyme activity in garbage enzyme produced from preconsumer organic waste. *Bioresour. Technol.* 226, 200–210. doi: 10.1016/j.biortech.2016.12.029

Bartkiene, E., Bartkevics, V., Pugajeva, I., Borisova, A., Zokaityte, E., Lele, V., et al. (2020). Challenges associated with byproducts valorization-comparison study of safety parameters of ultrasonicated and fermented plant-based byproducts. *Foods* 9:614. doi: 10.3390/foods9050614

Butkhup, L., Jeenphakdee, M., Jorjong, S., Samappito, S., Samappito, W., and Chowtivannakul, S. (2011). HS-SPME-GC-MS analysis of volatile aromatic compounds in alcohol related beverages made with mulberry fruits. *Food Sci. Biotechnol.* 20, 1021–1032. doi: 10.1007/s10068-011-0140-4

Cai, Y., Wang, J., Zhao, Y., Zhao, X., Zheng, Z., Wen, B., et al. (2018). A new perspective of using sequential extraction: to predict the deficiency of trace elements during anaerobic digestion. *Water Res.* 140, 335–343. doi: 10.1016/j.watres.2018.04.047

Charron-Lamoureux, V., Therien, M., Konk, A., and Beauregard, P. B. (2020). *Bacillus subtilis* and *Bacillus velezensis* population dynamics and quantification of spores after inoculation on ornamental plants. *Can. J. Microbiol.* 66, 664–669. doi: 10.1139/cjm-2020-0174

Chen, S., Yu, H., Zhou, X., and Wu, F. (2018). Cucumber (*Cucumis sativus* L.) seedling rhizosphere *Trichoderma* and *Fusarium* spp. communities altered by vanillic acid. *Front. Microbiol.* 9:2195. doi: 10.3389/fmicb.2018.02195

Cho, M. S., Jin, Y. J., Kang, B. K., Park, Y. K., Kim, C., and Park, D. S. (2018). Understanding the ontogeny and succession of *Bacillus velezensis* and *B. subtilis* subsp. *subtilis* by focusing on kimchi fermentation. *Sci. Rep.* 8:7045. doi: 10.1038/s41598-018-25514-5

Dignam, B. E. A., O'Callaghan, M., Condron, L. M., Raaijmakers, J. M., Kowalchuk, G. A., and Wakelin, S. A. (2016). Challenges and opportunities in harnessing soil disease suppressiveness for sustainable pasture production. *Soil Biol. Biochem.* 95, 100–111. doi: 10.1016/j.soilbio.2015.12.006

Fu, J., Wang, Z., Huang, L., Zheng, S., Wang, D., Chen, S., et al. (2014). Review of the botanical characteristics, phytochemistry, and pharmacology of *Astragalus membranaceus* (Huangqi). *Phytother. Res.* 28, 1275–1283. doi: 10.1002/ptr.5188

Gao, Y., Lu, Y., Lin, W., Tian, J., and Cai, K. (2019). Biochar suppresses bacterial wilt of tomato by improving soil chemical properties and shifting soil microbial community. *Microorganisms* 7:676. doi: 10.3390/microorganisms7120676

Gao, Y., Zheng, Z., Zhang, Y., Hu, Y., and Wang, X. (2021). Mechanism of rhizosphere micro-ecology in controlling soil-borne fungal diseasea: a review. *J. China Agric. Univ.* 26, 100–113. doi: 10.11841/j.issn.1007-4333.2021.06.11

Gao, Z., Zhang, B., Liu, H., Han, J., and Zhang, Y. (2017). Identification of endophytic *Bacillus velezensis* ZSY-1 strain and antifungal activity of its volatile compounds against *Alternaria solani* and *Botrytis cinerea*. *Biol. Control* 105, 27–39. doi: 10.1016/j.biocontrol.2016.11.007

Garbeva, P., Veen, J. A., and Elsas, J. D. (2004). Assessment of the diversity, and antagonism towards *Rhizoctonia solani* AG3, of *Pseudomonas* species in soil from different agricultural regimes. *FEMS Microbiol. Ecol.* 47, 51–64. doi: 10.1016/S0168-6496(03)00234-4

Haarman, M., and Knol, J. (2006). Quantitative real-time PCR analysis of fecal *Lactobacillus* species in infants receiving a prebiotic infant formula. *Appl. Environ. Microbiol.* 72, 2359–2365. doi: 10.1109/76.856451

Huang, X., Zhou, X., Zhang, J., and Cai, Z. (2019). Highly connected taxa located in the microbial network are prevalent in the rhizosphere soil

of healthy plant. *Biol. Fertil. Soils* 55, 299–312. doi: 10.1007/s00374-019-01350-1

Jiang, J., Wang, Y., Yu, D., Yao, X., Han, J., Cheng, R., et al. (2021). Garbage enzymes effectively regulated the succession of enzymatic activities and the bacterial community during sewage sludge composting. *Bioresour. Technol.* 327:124792. doi: 10.1016/j.biortech.2021.124792

Kalantari, S., Marefat, A., Naseri, B., and Hemmati, R. (2018). Improvement of bean yield and *Fusarium* root rot biocontrol using mixtures of *Bacillus*, *Pseudomonas* and *Rhizobium*. *Trop. Plant Pathol.* 43, 499–505. doi: 10.1007/s40858-018-0252-y

Khan, N., Martinez-Hidalgo, P., Ice, T. A., Maymon, M., Humm, E. A., Nejat, N., et al. (2018). Antifungal activity of *Bacillus* species against *Fusarium* and analysis of the potential mechanisms used in biocontrol. *Front. Microbiol.* 9:2363. doi: 10.3389/fmicb.2018.02363

Klein, E., Katan, J., and Gamliel, A. (2016). Soil suppressiveness by organic amendment to *Fusarium* disease in cucumber: effect on pathogen and host. *Phytoparasitica* 44, 239–249. doi: 10.1007/s12600-016-0512-7

Koljalg, U., Nilsson, R. H., Abarenkov, K., Tedersoo, L., Taylor, A. F., Bahram, M., et al. (2013). Towards a unified paradigm for sequence-based identification of fungi. *Mol. Ecol.* 22, 5271–5277. doi: 10.1111/mec.12481

Kumar, S., Stecher, G., and Tamura, K. (2016). MEGA7: molecular evolutionary genetics analysis version 7.0 for bigger datasets. *Mol. Biol. Evol.* 33, 1870–1874. doi: 10.1093/molbev/msw054

Li, Z., Bai, X., Jiao, S., Li, Y., Li, P., Yang, Y., et al. (2021). A simplified synthetic community rescues *Astragalus mongholicus* from root rot disease by activating plant-induced systemic resistance. *Microbiome* 9:217. doi: 10.1186/s40168-021-01169-9

Liu, Y., Tian, Y., Yue, L., Constantine, U., Zhao, X., Zhou, Q., et al. (2021). Effectively controlling *Fusarium* root rot disease of *Angelica sinensis* and enhancing soil fertility with a novel attapulgite-coated biocontrol agent. *Appl. Soil Ecol.* 168:104121. doi: 10.1016/j.apsoil.2021.104121

Luo, L., Guo, C., Wang, L., Zhang, J., Deng, L., Luo, K., et al. (2019). Negative plant-soil feedback driven by re-assemblage of the rhizosphere microbiome with the growth of *Panax notoginseng*. *Front. Microbiol.* 10:1597. doi: 10.3389/fmicb.2019.01597

Magnusson, J., Strm, K., Roos, S., Sjgren, J., and Schnürer, J. (2003). Broad and complex antifungal activity among environmental isolates of lactic acid bacteria. *FEMS Microbiol. Lett.* 219, 129–135. doi: 10.1016/S0378-1097(02)01207-7

Mohamad, O. A. A., Li, L., Ma, J. B., Hatab, S., Xu, L., Guo, J. W., et al. (2018). Evaluation of the antimicrobial activity of endophytic bacterial populations from chinese traditional medicinal plant Licorice and characterization of the bioactive secondary metabolites produced by *Bacillus atrophaeus* against *Verticillium dahliae*. *Front. Microbiol.* 9:924. doi: 10.3389/fmicb.2018.00924

Momma, N., Yamamoto, K., Simandi, P., and Shishido, M. (2006). Role of organic acids in the mechanisms of biological soil disinfestation (BSD). *J. Gen. Plant Pathol.* 72, 247–252. doi: 10.1007/s10327-006-0274-z

Mori, K., lriye, R., hirata, M., and takamizawa, K. (2004). Quantification of *Bacillus* species in a wastewater treatment system by the molecular analyses. *Biotechnol. Bioprocess Eng.* 9, 482–489. doi: 10.1007/BF02933490

O'Donnell, K., Cigelnik, E., and Casper, H. H. (1998). Molecular phylogenetic, morphological, and mycotoxin data support reidentification of the quorn mycoprotein fungus as *fusarium venenatum*. *Fungal Genet. Biol.* 23, 57–67. doi: 10.1006/fgbi.1997.1018

Pinaria, A. G., Liew, E. C. Y., and Burgess, L. W. (2010). *Fusarium* species associated with vanilla stem rot in Indonesia. *Australas. Plant Pathol.* 39, 176–183. doi: 10.1071/AP09079

Rahman, S., Haque, I., Goswami, R. C. D., Barooah, P., Sood, K., and Choudhury, B. (2020). Characterization and FPLC analysis of garbage enzyme: biocatalytic and antimicrobial activity. *Waste Biomass Valorization* 12, 293–302. doi: 10.1007/s12649-020-00956-z

Rameshkumar, N., and Nair, S. (2009). Isolation and molecular characterization of genetically diverse antagonistic, diazotrophic red-pigmented vibrios from different mangrove rhizospheres. *FEMS Microbiol. Ecol.* 67, 455–467. doi: 10.1111/j.1574-6941.2008.00638.x

Rani, A., Negi, S., Hussain, A., and Kumar, S. (2020). Treatment of urban municipal landfill leachate utilizing garbage enzyme. *Bioresour. Technol.* 297:122437. doi: 10.1016/j.biortech.2019.122437

Raza, W., Wei, Z., Jousset, A., Shen, Q., and Friman, V.-P. (2021). Extended plant metarhizobiome: understanding volatile organic compound signaling in plant-microbe metapopulation networks. *mSystems* 6:e0084921. doi: 10.1128/mSystems.00849-21

Saitou, N., and Nei, M. (1987). The neighbor-joining method: a new method for reconstructing phylogenetic trees. *Mol. Biol. Evol.* 4, 406–425. doi: 10.1093/oxfordjournals.molbev.a040454

Sanchez-Palomo, E., Diaz-Maroto, M. C., and Perez-Coello, M. S. (2005). Rapid determination of volatile compounds in grapes by HS-SPME coupled with GC-MS. *Talanta* 66, 1152–1157. doi: 10.1016/j.talanta.2005.01.015

Sun, R.-L., Jing, Y.-L., de Boer, W., Guo, R.-J., and Li, S.-D. (2021). Dominant hyphae-associated bacteria of *Fusarium oxysporum* f. sp. *cucumerinum* in different cropping systems and insight into their functions. *Appl. Soil Ecol.* 165:103977. doi: 10.1016/j.apsoil.2021.103977

Tamegai, H., Li, L., Masui, N., and Kato, C. (1997). A denitrifying bacterium from the deep sea at 11000-m depth. *Extremophiles* 1, 207–211. doi: 10.1007/s007920050035

Tao, C., Li, R., Xiong, W., Shen, Z., Liu, S., Wang, B., et al. (2020). Bio-organic fertilizers stimulate indigenous soil *Pseudomonas* populations to enhance plant disease suppression. *Microbiome* 8:137. doi: 10.21203/rs.3.rs-18216/v2

Tong, Y., and Liu, B. (2020). Test research of different material made garbage enzyme's effect to soil total nitrogen and organic matter. *IOP Conf. Ser. Earth Environ. Sci.* 510:042015. doi: 10.1088/1755-1315/510/4/042015

Usman, F., Shaukat, S. S., Abid, M., and Hussain, F. (2013). Rhizosphere fungi of different vegetabies and their antagonistic acticity against pathogenic fungi of brinjal and spinach. *Int. J. Biol. Biotechnol.* 10, 255–259.

Van Wees, S. C., Van der Ent, S., and Pieterse, C. M. (2008). Plant immune responses triggered by beneficial microbes. *Curr. Opin. Plant Biol.* 11, 443–448. doi: 10.1016/j.pbi.2008.05.005

Wang, B., Li, R., Ruan, Y., Ou, Y., Zhao, Y., and Shen, Q. (2015). Pineapple–banana rotation reduced the amount of *Fusarium oxysporum* more than maize–banana rotation mainly through modulating fungal communities. *Soil Biol. Biochem.* 86, 77–86. doi: 10.1016/j.soilbio.2015.02.021

Wang, W., Wang, Z., Yang, K., Wang, P., Wang, H., Guo, L., et al. (2020). Biochar application alleviated negative plant-soil feedback by modifying soil microbiome. *Front. Microbiol.* 11:799. doi: 10.3389/fmicb.2020.00799

Wei, X., Cao, P., Wang, G., and Han, J. (2020). Microbial inoculant and garbage enzyme reduced cadmium (Cd) uptake in *Salvia miltiorrhiza* (Bge.) under Cd stress. *Ecotoxicol. Environ. Saf.* 192:110311. doi: 10.1016/j.ecoenv.2020.110311

Wei, Z., Gu, Y., Friman, V. P., Kowalchuk, G. A., Xu, Y., Shen, Q., et al. (2019). Initial soil microbiome composition and functioning predetermine future plant health. *Sci. Adv.* 5:eaaw0759. doi: 10.1126/sciadv.aaw0759

Wei, Z., Hu, J., Gu, Y., Yin, S., Xu, Y., Jousset, A., et al. (2018). *Ralstonia solanacearum* pathogen disrupts bacterial rhizosphere microbiome during an invasion. *Soil Biol. Biochem.* 118, 8–17. doi: 10.1016/j.soilbio.2017.11.012

Wu, H., Qin, X., Wang, J., Wu, L., Chen, J., Fan, J., et al. (2019). Rhizosphere responses to environmental conditions in *Radix pseudostellariae* under continuous monoculture regimes. *Agric. Ecosyst. Environ.* 270-271, 19–31. doi: 10.1016/j.agee.2018.10.014

Xiong, W., Guo, S., Jousset, A., Zhao, Q., Wu, H., Li, R., et al. (2017). Bio-fertilizer application induces soil suppressiveness against *Fusarium* wilt disease by reshaping the soil microbiome. *Soil Biol. Biochem.* 114, 238–247. doi: 10.1016/j.soilbio.2017.07.016

Xiong, W., Zhao, Q., Xue, C., Xun, W., Zhao, J., Wu, H., et al. (2016). Comparison of fungal community in black pepper-vanilla and vanilla monoculture systems associated with vanilla *Fusarium* wilt disease. *Front. Microbiol.* 7:117. doi: 10.3389/fmicb.2016.00117

Xu, Z., Yang, Z., Zhu, T., Shu, W., and Geng, L. (2021). Ecological improvement of antimony and cadmium contaminated soil by earthworm *Eisenia fetida*: soil enzyme and microorganism diversity. *Chemosphere* 273:129496. doi: 10.1016/j.chemosphere.2020.129496

Yu, K., Liu, Y., Tichelaar, R., Savant, N., Lagendijk, E., van Kuijk, S. J. L., et al. (2019). Rhizosphere-associated *Pseudomonas* suppress local root immune responses by gluconic acid-mediated lowering of environmental pH. *Curr. Biol.* 29, 3913–3920. doi: 10.1016/j.cub.2019.09.015

Zhai, Y., Zhu, J. X., Tan, T. M., Xu, J. P., Shen, A. R., Yang, X. B., et al. (2021). Isolation and characterization of antagonistic *Paenibacillus polymyxa* HX-140 and its biocontrol potential against *Fusarium* wilt of cucumber seedlings. *BMC Microbiol.* 21:75. doi: 10.1186/s12866-021-02131-3

Zhang, Y., Gao, Y., Zheng, Z., Meng, X., Cai, Y., Liu, J., et al. (2020). A microbial ecosystem: agricultural Jiaosu achieves effective and lasting antifungal activity against *Botrytis cinerea*. *AMB Express* 10:216. doi: 10.21203/rs.3.rs-120269/v1

Zhao, M., Zhao, J., Yuan, J., Hale, L., Wen, T., Huang, Q., et al. (2021). Root exudates drive soil-microbe-nutrient feedbacks in response to plant growth. *Plant Cell Environ.* 44, 613–628. doi: 10.1111/pce.13928

Zhao, X., Liu, J., Liu, J., Yang, F., Zhu, W., Yuan, X., et al. (2017). Effect of ensiling and silage additives on biogas production and microbial community dynamics during anaerobic digestion of switchgrass. *Bioresour. Technol.* 241, 349–359. doi: 10.1016/j.biortech.2017.03.183

Zhou, X., and Wu, F. (2018). Vanillic acid changed cucumber (*Cucumis sativus* L.) seedling rhizosphere total bacterial, *Pseudomonas* and *Bacillus* spp. communities. *Sci. Rep.* 8:4929. doi: 10.1038/s41598-018-23406-2

Zhu, G., Cheng, D., Liu, X., Nie, P., Zuo, R., Zhang, H., et al. (2020). Effects of garbage enzyme on the heavy metal contents and the growth of castor under mine tailing. *IOP Conf. Ser. Earth Environ. Sci.* 474:022010. doi: 10.1088/1755-1315/474/2/022010

Conflict of Interest: The authors declare that the research was conducted in the absence of any commercial or financial relationships that could be construed as a potential conflict of interest.

Publisher's Note: All claims expressed in this article are solely those of the authors and do not necessarily represent those of their affiliated organizations, or those of the publisher, the editors and the reviewers. Any product that may be evaluated in this article, or claim that may be made by its manufacturer, is not guaranteed or endorsed by the publisher.

frontiers | Frontiers in Microbiology

REVIEW
published: 01 April 2022
doi: 10.3389/fmicb.2022.799345

Geminivirus-Derived Vectors as Tools for Functional Genomics

Bipasha Bhattacharjee[1,2] *and Vipin Hallan*[1,2]*

[1] Academy of Scientific and Innovative Research (AcSIR), Ghaziabad, India, [2] Plant Virology Laboratory, Division of Biotechnology, CSIR-Institute of Himalayan Bioresource Technology, Palampur, India

A persistent issue in the agricultural sector worldwide is the intensive damage caused to crops by the geminivirus family of viruses. The diverse types of viruses, rapid virus evolution rate, and broad host range make this group of viruses one of the most devastating in nature, leading to millions of dollars' worth of crop damage. Geminiviruses have a small genome and can be either monopartite or bipartite, with or without satellites. Their ability to independently replicate within the plant without integration into the host genome and the relatively easy handling make them excellent candidates for plant bioengineering. This aspect is of great importance as geminiviruses can act as natural nanoparticles in plants which can be utilized for a plethora of functions ranging from vaccine development systems to geminivirus-induced gene silencing (GIGS), through deconstructed viral vectors. Thus, the investigation of these plant viruses is pertinent to understanding their crucial roles in nature and subsequently utilizing them as beneficial tools in functional genomics. This review, therefore, highlights some of the characteristics of these viruses that can be deemed significant and the subsequent successful case studies for exploitation of these potentially significant pathogens for role mining in functional biology.

Keywords: geminivirus, silencing system, crop improvement, CRISPR/Cas9, biopharmaceuticals, viral vector, peptide expression systems

OPEN ACCESS

Edited by:
Christopher Rensing, Fujian Agriculture and Forestry University, China

Reviewed by:
Hernan Garcia-Ruiz, University of Nebraska-Lincoln, United States
Susheel Kumar, National Botanical Research Institute (CSIR), India

***Correspondence:**
Vipin Hallan
hallan@ihbt.res.in

Specialty section:
This article was submitted to Microbe and Virus Interactions with Plants, a section of the journal Frontiers in Microbiology

Received: *21 October 2021*
Accepted: *03 February 2022*
Published: *01 April 2022*

Citation:
Bhattacharjee B and Hallan V (2022) Geminivirus-Derived Vectors as Tools for Functional Genomics. Front. Microbiol. 13:799345. doi: 10.3389/fmicb.2022.799345

INTRODUCTION

The "geminate" morphology which is typically a twinned capsid type of shape is the primary backdrop for the "geminivirus" nomenclature. Geminiviral genomes are termed ambisense because they comprise a coding segment which has two oppositely aligned reading frames (Hefferon, 2014). These viruses cause serious damage to crops resulting in having a devastating effect to produce quality and quantity globally (Navas-Castillo et al., 2011). Geminiviruses are characterized by their relatively small-sized genome and an extensive host range and can replicate in infected cells to enormously large copy numbers (Timmermans et al., 1994). They are categorized as class II viruses according to the Baltimore classification. This is the largest family of ssDNA plant viruses known in the virus kingdom, with newer variants constantly being discovered. Each paired particle encapsulates a single circular, ssDNA molecule that ranges in size from 2.5 to 4 kb contingent on the virus (Carrillo-Tripp et al., 2006; Yang et al., 2016). In the nucleus of the host cell, the genomic ssDNA is replicated by a rolling-circle process using double-stranded DNA (dsDNA) intermediates in a manner like the ssDNA bacteriophages. The International Committee on Virus Taxonomy (ICTV) has characterized the *Geminiviridae* family into fourteen genera, *viz*., *Becurtovirus*, *Begomovirus*, *Capulavirus*, *Curtovirus*, *Eragrovirus*, *Grablovirus*, *Mastrevirus*,

Topocuvirus, *Turncurtovirus*, *Citlodavirus*, *Maldovirus*, *Mulcrilevirus*, *Opunvirus*, and *Topilevirus*, based on the vector (insect pest), host dissemination, genome organization, and pair sequence identities (Varsani et al., 2017; Zerbini et al., 2017; Fiallo-Olivé et al., 2021).

Understanding the distinct genomic components of geminiviruses is the primary step toward their genetic manipulation. The genome sequence typically contains a nonanucleotide "TAATATTAC" sequence, which is conserved, is in the form of a stem loop structure, and is important for the initiation of the rolling circle replication (RCR) (Stanley, 1995). The nonanucleotide is present in the DNA-A and DNA-B genomes of a bipartite geminivirus common region (CR) and a long intergenic region (LIR) for a monopartite geminivirus genome. Alpha and beta satellites are extra chromosomal small molecules which sometimes accompany certain old-world monopartite geminiviruses (Nawaz-ul-Rehman and Fauquet, 2009; Kumar et al., 2017; Gnanasekaran et al., 2019). A complete genome of a geminivirus would typically comprise CRs/IRs/SCRs (satellite-conserved regions) along with additional regulatory elements (Yang et al., 2016).

Insect vectors perform an imperative role in the introduction of these viruses within plant cells while keeping its primary target as differentiated cells (Kumar, 2019). Due to the non-existence of DNA replicase in these host insect cells, viral replication is seemingly improbable. Geminiviruses, therefore, instigate host cells to retrace the cell cycle from the dormant state to encourage recombination-dependent replication of the virus (Gutierrez, 1999). Insect vectors basically transmit geminiviruses through acquisition, retention, and ejection to host plant cells facilitating the entry of virions through the plant phloem sap. The interaction of the viral Rep protein with the whitefly's proliferative cell nuclear antigen and DNA polymerase allows the TYLCV genome to replicate within the insect salivary glands (Pakkianathan et al., 2015). It is tempting to guess whether it can disrupt the insect cell cycle and produce an endoreplication cycle in the same way that plants can, or whether the insect has evolved alternative techniques. Because not all begomoviruses appear to reproduce in the whitefly, more research is needed to figure out why only some virus species replicate in the insect. Some begomoviruses can have active viral gene transcription within the insect.

Co-replication of the plant genome and the virion is initiated by geminiviruses through cell cycle reprogramming in the infected cells in order to compensate for its inability to produce enzymes for host cell replication and autonomous movement (Ramesh et al., 2017). Consequently, patterns of gene expression of the host are disrupted, necrosis pathways may get altered, and cell signaling and intercellular trafficking of macromolecules are redirected, causing dramatic changes in the host inherent environment. Additionally, geminiviruses modify host DNA methylation and miRNA pathways by encoding numerous suppressors of silencing, often causing plant developmental aberrations by suppressing multiple constituents of transcriptional and posttranscriptional gene silencing (Raja et al., 2010; Hanley-Bowdoin et al., 2013; Gnanasekaran et al., 2019; Prasad et al., 2019).

Typical geminiviral infection symptoms often include leaf curling, mosaic patterns of variegated colors, occasional vein swelling, and enations, often leading to the confirmation that cellular homeostasis and plant growth have been affected, thereby reflecting transcriptional changes. Geminiviral infectivity primes cellular signaling which leads to the misregulation of plant miRNAs concomitant to developmental shifts and hormone signaling. Although geminiviruses and their interactions with insect hosts have not been well understood, the latest studies have indicated that virus-mediated changes in defense and signaling pathways tend to occur. Past reviews have majorly focused on the pathogenicity of these viruses, their recombination, and synergism biology; hence, in this review, it is deemed appropriate to delve into the detailed understanding of utilization of these viruses as natural plant bioengineers. We have considered the already available information on the geminiviral genetic makeup and protein functions as well as the geminivirus–plant–insect tri-partnership in genetic manipulation. In this review, we have also focused on various essential characteristics of geminiviruses and have also extensively discussed the putative use of these significant pathogens for aspects ranging from functional biology to biopharmaceuticals.

GEMINIVIRUSES ACT AS DECONSTRUCTED VECTORS FOR EFFICIENT GENE TRANSFER

Many geminiviruses, except for some begomoviruses, are usually not mechanically communicable as cloned DNA or virions (Inoue-Nagata et al., 2016). Certain *Agrobacterium* strains inhabit plant cells by transferring their T-DNA (transfer DNA) and cause proliferation and production of opine-like substances which the bacteria use as its carbon source (Moore et al., 1997). Initial studies conducted on *Agrobacterium tumefaciens* identified that the bacterium might be used for transferring infectious clones of *Cauliflower mosaic virus* (CaMV), and hence, the "agro-inoculation" or "agro-infection" technique was used as a sensitive assay to ascertain if transfer of DNA occurs during *Agrobacterium* inoculations of the geminivirus *Maize streak virus* (MSV) to a graminaceous plant, *Zea mays* (Howell et al., 1980; Grimsley et al., 1987). In fact, three *Mastrevirus* species have thoroughly contributed to replicon vectors, i.e., the monocot-infecting *Wheat dwarf virus* (WDV) and MSV and the dicot-infecting *Bean yellow dwarf virus* (BeYDV). Therefore, the first account of facile transmission of MSV was reported without involving leafhoppers to the maize crop. Despite the constant availability of newer isolates, *Mastreviruses* and *Begomoviruses* have remained the most popular taxa of the geminiviral replicon study (GVR) (Ellison et al., 2021). The study was considered a breakthrough of sorts as it confirmed that geminiviruses could be employed for development of transgenic cereals without the use of insect vectors, relying primarily on *Agrobacterium* transformation and their subsequent introduction to hosts (Grimsley et al., 1987). Biolistics and agroinfection have been commonly used to deliver engineered GVRs into plant cells, and many of these maintain mobility with plant tissue and insect cells allowing a transient

system of expression to function efficiently. Precision-editing methods that need homology-directed repair (HDR) from a donor template molecule to integrate precise alterations into the genome benefit greatly from GVRs. The last decade has been watershed in exploratory studies between plant–geminivirus–whiteflies, although very few have explored the interacting proteins involved. Interactions mediated by plants between the geminivirus and insect vectors are important influences in understanding the biology of vector insects and the epidemiology of geminiviral diseases (Wang et al., 2012; Prasad et al., 2020).

Efficacious transfer of the T-DNA to juvenile embryos of MSV-infected germinated plants inferred the role of MSV as a highly sensitive genetic marker in maize–*Agrobacterium* pathogen–host interaction studies (Schlappi and Hohn, 1992; Escudero et al., 1996). Similarly, multiple experiments on WDV in wheat and barley showed the benefit of using geminiviral replication to evaluate direct gene transmission which lies in the context that transient expression could not show if cells were alive at the time of transfer of the gene. The successful infection of WDV in viable cells through *Agrobacterium* and microprojectile bombardment was used as a marker which methodically proved the efficacy of geminiviruses (Creissen et al., 1990; Chen and Dale, 1992).

It was initially hypothesized that agroinfection with geminiviruses can potentially be used by random incorporation of viral DNA-carrying foreign genes into the plant chromosome to produce transgenic plants. This phenomenon is likely to occur rarely, as indicated by Bejarano et al. (1996) and Hanley-Bowdoin et al. (2013), which found proof of an ancient incorporation of geminiviruses into the *Nicotiana* genome. At that time, it was postulated that the geminiviruses usually did not get transmitted by seeds, which was indicative of certain mechanisms, which impedes them for germline invasion (Rosas-Díaz et al., 2017). However, very recent studies conducted had also reported accounts of seed transmission. TYLCV was the first detected begomovirus that was shown in tomato plantlets which had germinated from fruits produced by infected plants in 2013 and 2014 (Kil et al., 2016), in white soybean in 2016 (Kil et al., 2017), and in sweet pepper in 2018 (Kil et al., 2018). PCR studies revealed a complex relationship between the virus and seed tissues in this study; however, it could not be shown that the seed-accompanying virus causes tomato yellow leaf curl disease in plants grown from the infected seed. It is likely that plants infected with seed-borne inoculum have a lengthier dormant period, although this has yet to be experimentally verified. Furthermore, if TYLCV seed transmission is to a significant degree, there should ideally be more infected transplants grown in sheltered culture or in locations like in fields where the virus does not exist, particularly for hybrid seed-generated places where the virus does exist (e.g., China and Thailand). The intimate interaction of this virus with the seed during maturity was confirmed by the detection of TYLCV-IL replication in tomato and *N. benthamiana* flower reproductive organs. However, the considerable drop in TYLCV DNA load after surface disinfection of tomato seed implies that the virus is mostly found outside the seed coat as a contaminant (Pérez-Padilla et al., 2020), therefore laying to rest the debate as to whether the geminivirus is actually seed transmitted or not. Seed transmission of geminiviruses does not appear to be epidemiologically significant in the family so far. A more recent study has shown that this is a potentially significant attribute which can be relevant in the investigation for gene transfer systems as these viruses have a very broad-range host and are very pervasive in their infectivity. An exploration of geminivirus invasion in compromised plants showed that the virus did not infect the shoot apical meristem, apparently because of the high degree of cell division and the compounded lack of vasculature paths for the section (Lucy et al., 1996). This contrasted the study that had established that MSV could infect meristematic cells in the shoot apex by agro-inoculation (Grimsley et al., 1987). Past studies have proved that *Agrobacterium* transferred the T-DNA in the already preformed cells of the leaf primordia, hence clearing all doubts that geminiviruses indeed infected somatic tissues (Shen et al., 1992; Shen and Hohn, 1992, 1994). These findings laid down the foundation of understanding geminivirus infection and incursion that proved to be vital for the studies on manipulation of geminiviruses as vectors (**Figure 1**).

Efficient Transient Expression Vector Systems

The transient expression procedure is one of the most convenient tools in molecular biology, giving appropriate results for further downstream processing as compared to stable transgenic development, which is both effort and time intensive. The expression of an extrinsic gene is simplified in this technique due to the negation of the host regeneration step, which makes the viral-mediated transient system very convenient to use while achieving the desired results. Host genome modification does not occur, and the geminiviral vectors can generate copious coding sequences to plants, posing as a competent alternative to stable line generation and exogenous gene manifestation (Yang et al., 2017).

The first proposal to construct a plant DNA virus backbone expression vector dates four decades back to the year 1978 (Hull, 1978). The geminivirus genome is conserved and already available in a plethora of online resources, and hence developing vectors with a geminiviral backbone is well established, although, in early reports, stable transformation (*Agrobacterium* mediated) and the plant virus-based vector usage were well thought out to be contending technologies. Lately, the merging of the two schools of thought brought the implication forward that agroinfection was the most effectual technique of application of "deconstructed" vectors to the host plant. This led to the rise of many groups of viruses like geminivirus, potexvirus, comovirus, and tobamoviruses for deconstructed viral vector development for rapid, enhanced levels of production of proteins in plants which could be a huge boon for the pharmaceutical industry (Xu et al., 2019; **Figure 1**).

The geminiviral genome structure knowledge is imperative in the understanding of vector preparation. This technique is very time efficient and requires small amounts of starting material. With the help of the Rep protein, geminiviruses autonomously multiply (Akbar Behjatnia et al., 1998). For initiation of RCR, replication-associated protein (Rep) binds to its complex binding

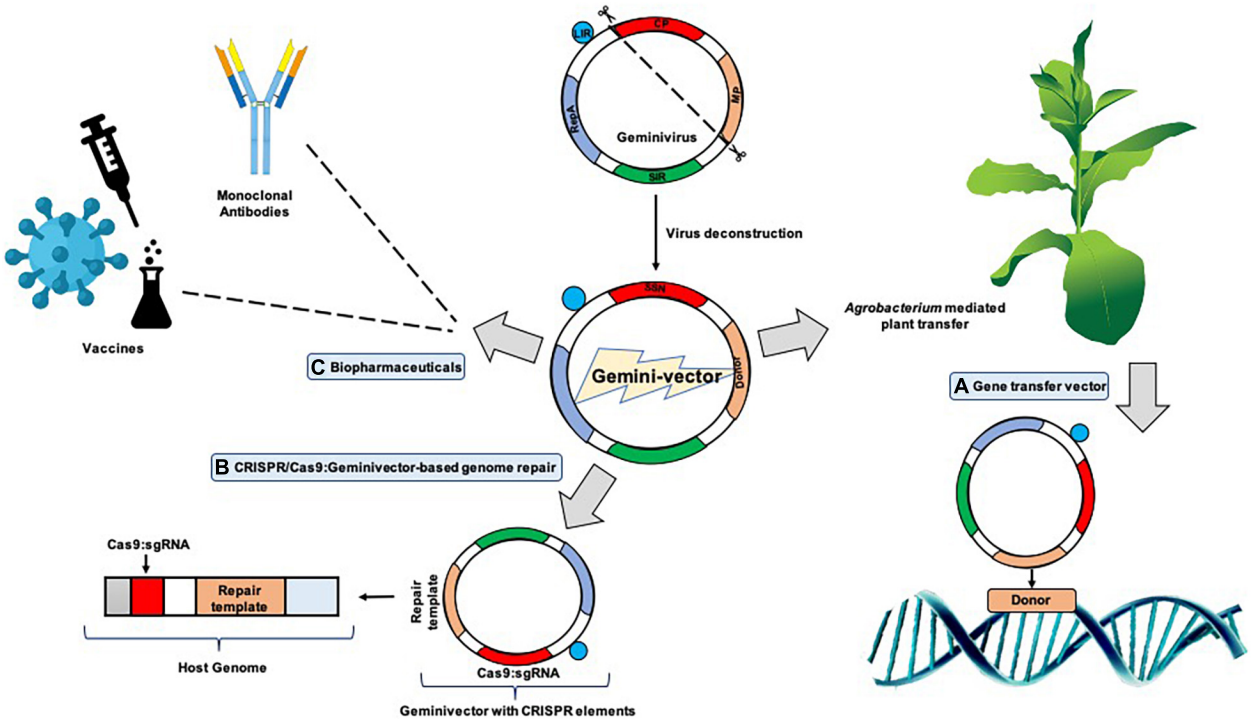

FIGURE 1 | Geminiviral vectors and their functional relevance. Virulence factors like the viral movement protein (MP) and coat protein (CP) are detached to be replaced with the donor DNA and specific nucleases which give rise to "geminivectors." These vectors have multidirectional functionalities in which they primarily act as **(A)** gene transfer vectors, where vectors are used for the transient expression of genes of interest, production of specific proteins, and participation and annotation of unknown gene characteristics, among others; **(B)** CRISPR/Cas9-based genome repair**:** where they are used for template repair in the host genome, while also essentially participating in genome editing; and **(C)** biopharmaceuticals: where production of important vaccines has been successfully conducted using geminivectors. Monoclonal antibodies have been prepared for the deadly *Ebola virus*, and antigen production for hepatitis B and HIV has been successful.

site comprising the nonanucleotide-repeated sequence flanked by the transcription start sites (TSS) and the conserved TATA box in the case of begomoviruses. On the other hand, mastreviruses follow a slightly different mode of adherence as the Rep complex seemingly has a binding region juxtaposed upstream of two deviating TATA boxes and a replication start site downstream and at the bottom of the stem-loop conserved region (Fontes et al., 1992; Laufs et al., 1995; Castellano et al., 1999; Fondong, 2013). Among the first cases of introduction of geminiviral genomes in plants, the *Potato yellow mosaic geminivirus* (PYMV) was introduced within the Ti plasmid of *Agrobacterium* and agro-infection of *Nicotiana benthamiana*, tomato, and potato was successfully conducted (Buragohain et al., 1994). The approach engaged was that the head-to-tail dimeric PYMV on introduction to the Ti plasmid recombined in the IR region to form an autonomously replicating circular viral genome. The IR/CR contains the conserved nonanucleotide 5′-TAATATTAC-3′ sequence and a conserved stem loop structure within its origin of replication. This efficient strategy therefore became a conveniently implemented geminivirus vector assembly method (Peyret and Lomonossoff, 2015; Xu et al., 2019; **Figure 1**).

In other references, it was inferred that the process of the short/long intergenic region (SIR/LIR, respectively) recircularization by the viral *Rep/Rep A* proteins formed the crux of "LSL" vector (LIR–SIR–LIR) deployment (Mor et al., 2003; **Figure 2**). The case study of BeYDV consisting of the "LSL" sequence could be delivered within plants with successful replicon formation after recircularization. The Rep protein could be provided in *trans* which permits better regulation of the gene of interest, which is constructed on the LSL replicon, also allowing toxicity control of Rep. This system was also suggested to be fit for stable transgenic generation, with the gene of interest expressed from circular replicons on Rep gene induction which was then proven (Zhang and Mason, 2006). An LSL system was designed for stable tobacco cell cultures and potato lines based on the *Norwalk virus* (NV). With the Rep being under impact of the *Aspergillus nidulans* ethanol-inducible promoter, the gene of interest is constitutively expressed at reduced levels in the absence of ethanol. However, in the presence of ethanol, NV coat protein increased up to 10-fold in the cell cultures of tobacco and green fluorescent protein (GFP) got augmented up to 8 times (Zhang and Mason, 2006). These promising results were somewhat marred by the fact that silencing of the system eventually took place 8 days after induction in the transgenic potato lines; however, it could be resolved on adding a suppressor of silencing and additions of enhancers which could increase the amount of mRNA produced on addition and optimization of the amount of ethanol.

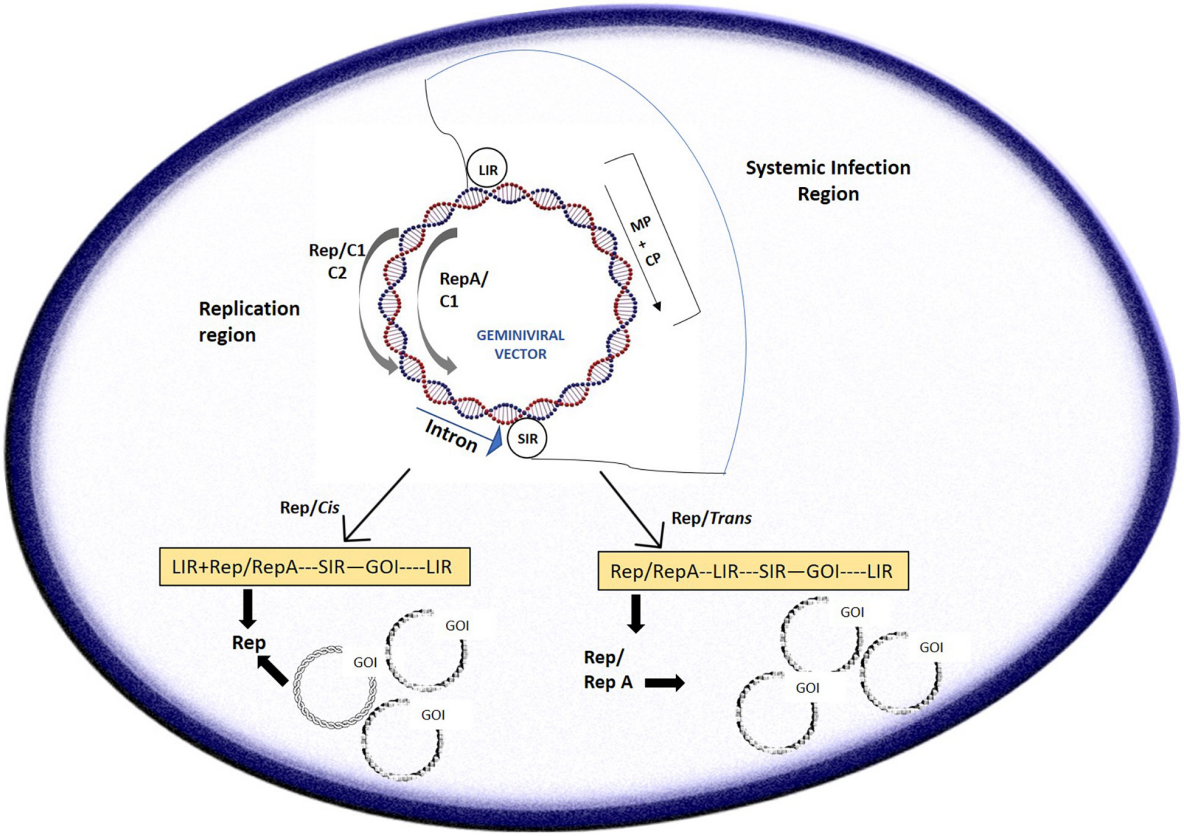

FIGURE 2 | A typical geminivirus deconstruction vector: the LIR (long intergenic region) region initiates transcription of the movement/coat protein (MP/CP) regions while the SIR (short intergenic region) terminates transcription. Geminivirus-derived vectors can be sent to cells in two different pathways: the *cis* or autonomous and *trans* or tethered route wherein *cis* employs the Rep in its native position to the LIR, driven by a C-sense promoter, and can give rise to thousands of copies of the replicons and *trans* employs persistent production of Rep protein through stable integration to drive production of the replicon.

In a further improvement of the same system, the placement of the transgene was tweaked by having the *Tobacco etch virus* (TEV) 5′ UTR and soybean vspB 3′ region flanking it, aiming at the enhanced translational efficacy of the LSL (Zhang and Mason, 2006). When the promoter activity was weak and Rep/Rep A was made available in *cis* within the LSL, the transgene activity was at its highest (genes for reference were GFP, HBcAG, and NV coat protein). When a suppressor of silencing, TBSV p19, was added, the yield was further increased as the silencing machinery was severely affected (Huang et al., 2010), co-expressing two transgenes with the same T-DNA from a dual LSL construct which form two detached circular replicons individually overexpressing one transgene. The breakthrough of this system was that it was employed to generate 0.5 mg/g of anti-Ebola virus monoclonal IgG 6D8 utilizing the *Nicotiana benthamiana* system. On addition of the p19 suppressor of silencing in *cis*, instead of *trans* as was done till then, the expression system was treated as more efficient and by substituting the TEV 5′ leader with the "hyper translatable" *Cowpea mosaic virus* (CPMV)-based CPMV-*HT* 5′ leader (Sainsbury and Lomonossoff, 2008). The user-friendly BeYDV vectors pBYR1 and pBYR2 were then developed containing an extra kanamycin cassette, and the pBYR1p19 and pBYR2p19 variants had the p19 cassette instead of kanamycin (Chen et al., 2011).

The BeYDV-based pRIC system is another improved geminiviral vector system (Regnard et al., 2010). It is based on the pTRAC system which employs the tobacco Rb7 gene scaffold attachment area (Maclean et al., 2007) for a heightened heterologous gene expression (Halweg et al., 2005). This system was used to overexpress the *Human papillomavirus* CP (HPV-CP) and HIV CPp24 at 0.55 mg/g FWT and 3.23 μg/g FWT, respectively. The system has reported a replication efficiency up to a 1,000-fold and a protein expression fold change up to 7 times, indicating that this is a robust system of overproduction of antibodies and vaccines (Maclean et al., 2007). The *Beet curly top virus* (BCTV) which comprises a *Cassava vein mosaic virus* promoter (CsVMV) has also been employed to synthesize vaccines like *Hepatitis A-virus* VP1 protein in modest levels in fusion with IgG (Kim et al., 2007; Chung et al., 2011). With unique techniques like precise target-based editing and exploration of current cas9 homologs (C2c1, C2c2, C2c3, and Cpf1) (Lu and Zhu, 2017; Nakade et al., 2017), geminivirus vectors stand a lot to gain and get developed further (Peyret and

Lomonossoff, 2015). Vectors were constructed using truncated regions of *Tomato leaf curl virus* (ToLCV), and it was deduced that a segment between CR and AC3 could replicate efficiently. Therefore, a viral vector was constructed which efficiently produced siRNAs, giving rise to a system that could be an efficient GIGS vector in a broad range of plants (Pandey et al., 2009).

Plant geminivirus-based replicating expression vectors have been widely employed in recent decades to improve the effectiveness of plant transient expression. The BeYDV-derived vectors have been successfully employed to explore the properties of phytohormones like α-naphthalene acetic acid, 6-benzyladenine, and gibberellins$_3$ on plant biomass and efficiency using the GIGS process of transient expression in *N. benthamiana* L. leaves (Li et al., 2021). The transient enhanced expression *in planta* may provide an understanding of how to exploit plant growth regulators (PGRs) to recover the production of recombinant protein using geminiviral vectors as the expression source of desired genes.

There is a major potential for human gene expression studies in plants to showcase the biological activity in a safer system with easier accessibility to experimental plants and tissues. A recent study where a human vascular endothelial growth factor (VEGF) was transiently expressed in *Nicotiana benthamiana* showed that VEGF could be expressed in high levels and did not exhibit any cytotoxic effect on HaCaT (human keratinocyte) cells, while also inducing cell migration *in vitro*. VEGF is a very important factor which is pro-angiogenic and important for wound healing. The recombinant clone of the VEGF gene was made using the geminiviral vector pBYR2e, which indicated that the functional VEGF protein could be made in plants that can possibly be exploited for their use in tissue engineering and dermo-cosmetics (Bulaon et al., 2020). Using *Agrobacterium*-mediated transformation, the capacity of the DNA geminiviral vector with Rep-mediated replication to produce recombinant proteins transiently in aquatic microalgal species was tested in *Chlamydomonas reinhardtii* and *Chlorella vulgaris*. Representative antigen and growth factor proteins, the SARS-CoV-2 receptor-binding domain (RBD) and basic fibroblast growth factor (bFGF), were cloned in a geminiviral vector and employed for rapid transformation to express the proteins in a transient manner in *C. reinhardtii* and *C. vulgaris*, respectively. The outcome demonstrated that the geminiviral vector could allow the expression of both the proteins in both the algal species, with yields of up to 1.14 g/g RBD and 1.61 ng/g FGF in *C. vulgaris* and 1.61 g/g RBD and 1.025 ng/g FGF in *C. reinhardtii* at 48 h post transformation. As a result, this study showed that DNA viral vectors could be used to produce recombinant proteins in a simple, quick, and effective manner, overcoming the challenges of genetic transformation in these unicellular green microalgae. This notion brings up the possibility of researching and optimizing green microalgae as a cost-effective platform for producing medicinal and industrially important recombinant proteins in shorter time frames with higher yields (Malla et al., 2021). Transient expression methods are ideal for swift and versatile development and production of vaccines against viruses like 2019-nCoV that exhibit abrupt and unpredictable outbreaks due to their rapid and high-level protein production potential. Plants have been offered as a viable, cost-effective, efficient, ethical, and sustainable expression system, despite the fact that many recombinant proteins are created by microbial or mammalian cell-based expression systems. The introduction and refinement of transient expression systems have resulted in a significant reduction in protein synthesis time and an increase in recombinant protein yield in plants (Nosaki et al., 2021). Such case studies are the need of the hour, and having results which can impact the human life indirectly and directly shows that the there is a huge unexplored territory of viral deconstruction and manipulation which should be researched upon. Geminiviruses have, therefore, tremendous potential to be utilized as vectors for gene transfer, protein expression, and mutagenesis studies due to its highly efficient ssDNA genome and ability to mold under any exogenous deconstruction (**Figure 1**).

Efficient Gene Silencing Vector Systems

The most common geminiviral silencing vectors initially developed were the begomoviral vectors derived from the following viruses: *African cassava mosaic virus* (ACMV), *Cabbage leaf curl virus* (CaLCuV), *Pepper huasteco yellow vein virus* (PHYVV), *Tomato golden mosaic virus* (TGMV), and *Tomato yellow leaf curl china virus* (TYLCCV) (**Table 1**). ACMV has been utilized to construct a functional reverse genetic tool by incorporating a partial *NtSu* gene (*Nicotiana tabacum sulfur gene*) which includes one unit of the magnesium chelate chloroplast enzyme (Fofana et al., 2004). This system was used for successful silencing of the orthologous gene of cassava resulting in the characteristic white and yellow dotted phenotype. Another gene of the same plant, *CYP79D2*, was cloned as a partial fragment in the ACMV vector which directly led to their downregulation, leading to a 76% lesser production of linamarin at 21 dpi, as the gene is one of the essential enzymes for the synthesis of linamarin in cassava. As the cassava transformation is a very laborious procedure, the ACMV-based gene silencing is very effective and can be used as a substitute to the stable transgenic approach (Fofana et al., 2004; **Table 1**). The bipartite CaLCuV opened new dimensions of silencing of singular or multiple endogenous genes in the entirely sequenced easy-to-handle model plant, *Arabidopsis thaliana*. The DNA A and B components have been utilized for vector development, resulting in extensive silencing patterns in the plants with the DNA A-modified vector. With the success of endogenous gene silencing or geminivirus-induced gene silencing (GIGS), this vector offers a distinct advantage of direct plant inoculation, bypassing the agro-transformation method, and could be used to augment phenotypes, for identification of redundant functions, and for understanding epistasis biology (Turnage et al., 2002).

Like CaLCuV, TGMV-derived vectors were also tested for DNA A/B efficacy, with DNA B showing better silencing efficiency. The TGMV B vector was specialized to use endogenous fragments <100 bp, thereby showing improved specificity which could also be tissue specific. Magnesium chelatase and proliferating cell nuclear antigen (PCNA) were downregulated all over meristematic tissues which showed that two different genes could be silenced simultaneously using the

same viral vector components, using the immune-localization technique (Peele et al., 2001; **Table 1**). The PHYVV-derived vector was used to silence three gene fragments of *Comt* (coding for a caffeic acid *O*-methyl transferase), p*Amt* (a possible aminotransferase), and *Kas* (a β-keto-acyl-[acyl-carrier-protein] synthase) genes, resulting in a non-pungent chili pepper and was confirmed by assessing the reduced mRNA levels of individual genes and because of the heightened siRNA presence (**Table 1**). A unique characteristic of silencing was that fruiting was normal, although PHYVV-p*Amt* infections were asymptomatic. Non-pungent chili peppers could be efficaciously produced using this technique (del Rosario Abraham-Juárez et al., 2008). The TYLCCV Y10 isolate has an accompanying β satellite which has a dependency on DNA A for replication and encapsulation and is indispensable for symptom development in host plants (Tao and Zhou, 2004). DNAβ was modified to DNAmβ by replacing its C1 ORF with an MCS, effectively transforming it into a silencing vector. This resulted in a symptomless virus invasion with clear demarcated transgene-specific symptoms visible for inference. Multiple plants like *N. glutinosa*, *N. tabacum*, and *Lycopersicon esculentum* were successfully tested with the vector with multiple endogenous gene downregulation like PCNA, phytoene desaturase synthase (PDS), and GFP.

The phytoene desaturase (PDS) gene was chosen as an efficient visual indication of VIGS and was used to improve the VIGS system in cabbage utilizing the *Tobacco rattle virus* (TRV)-based pTYs and CaLCuV-based gene-silencing vectors (PCVA/PCVB). In response to pTYs and CaLCuV, the latter came out to be a more efficient system in terms of operation costs and expense because the pTY mode of VIGS requires the particle bombardment mode of plants using expensive instrumentation. CaLCuV-based GIGS involved the use of *Agrobacterium* and was relatively inexpensive and had a higher batch efficiency target. This geminiviral vector system has also been said to be equally efficient in other *Brassica* species, *B. rapa,* and *B. nigra*, and therefore a potent functional genomic tool for crop plants (Xiao et al., 2020).

Geminiviruses have a compact genome that makes cloning and sequencing simple, and propagation is significantly easier than *in vitro* RNA synthesis (Abrahamian et al., 2020). Furthermore, DNA is much less labile than RNA and could be inoculated directly. Moreover, because DNA vectors lack an RNA intermediary and so are not susceptible to RNA degradation, they have demonstrated to be more stable than RNA vectors. As a result, even if the transcripts are suppressed, the replicons continue to increase and transport, albeit at a comparatively slower rate than wild-type counterparts. This, consequently, was modeled as a powerful tool for functional genomic approaches and gene discovery (**Table 1**).

Geminiviral Vectors and Genome Editing (GE)

Popular RNA vectors such as the *Potato virus X* (PVX) and TRV are commonly used for gene targeting and functional validation studies by transient silencing/overexpression of plant genes. Although effective, the insert size needs to be very small for RNA interference to occur (Dinesh-Kumar et al., 2003). The newer-generation genome-editing tools like CRISPR/Cas9 involve Cas9 delivery to plants, which is a large-sized protein and hence not appropriate for the RNA vector systems. Geminiviral replicons which are mutated to remove the infectivity have been developed to retain bigger-sized sequences like sequence-specific nucleases (SSNs) and DNA repair templates. BeYDV geminiviruses have been successfully proposed as CRISPR/CAS candidates for targeted genome editing and mutagenesis due to the zinc finger nucleases (Baltes et al., 2014). The advancement of viral modulation studies gave rise to the BeYDV deconstruction (Baltes et al., 2014) with it comprising the Rep/RepA-LIR-SIR components. The Rep A protein interacts with components of the cell cycle relating to replication while the Rep protein binds to the LIR region, starting a nick formation to initiate RCR, which is an important aspect for utilization for multi-copy generation of the donor and stimulate homologous recombination between donor and target. Being a very host-diverse system, BeYDV has been used (Čermák et al., 2015) to replace the endogenous anthocyanin constitutive promoter with a strong promoter, aiding as a marker for gene targeting at a very early calli stage in tomato, having an approximately 12-fold higher expression as compared to the routine *Agrobacterium*-T DNA delivery system. It was also used for creating targeted mutations in cassava as well as in potato (Butler et al., 2015, 2016; Hummel et al., 2018; **Table 1**). WDV and ToLCV are other geminiviruses which have been used for gene targeting in wheat by multiplying gene targeting (GT) efficiency manifold and achieving multifold targeted reporter gene integration in the hexaploid wheat genome (**Table 1**). WDV has also been successfully used in rice (Gil-Humanes et al., 2017; Wang et al., 2017). WDV was characterized and optimized by comparative replicon assessment to make it a suitable candidate for GT in cereal crops and for delivering CRISPR/Cas9 donor templates (**Figure 1**).

The above studies showed that GT could be successfully undertaken and had more reliability as compared to agro-transformation procedures but posed few challenges like low efficiency and high reliance on selectable or reporter exogenous markers like GFP and others. The CRISPR/Cas9-coupled geminiviral vector experimentations opened newer insights toward GT and editing (**Figure 1**). On BeYDV infection, *N. benthamiana* constitutively expressing Cas9 components showed relatively lower viral load and obstructed (or reduced) symptoms. BeYDV-based replicons were used for transient assays which detected Cas9 reagent-induced mutations within the virome, effectively reducing the virus copy number (Baltes et al., 2015). Ji et al. (2015) also worked out transient detections on *N. benthamiana* which comprised the Cas9-sgRNA construct which inhibited *Beet severe curly top virus* (BSCTV) accumulation and mutagenesis at targeted sequences, while overexpression of the same construct in transgenic *Arabidopsis* and *N. benthamiana* made the plants highly resistant to virus infection. Targeted coding sequence mutations in various geminiviruses caused the generation of viral variants adept in replication and systemic spread while noncoding IR mutations within geminiviruses provided viral intervention activity which limits significantly the replication and infectious variant generation, leading to

TABLE 1 | Examples of gemini vectors designed for expression/silencing and biopharmaceutical development.

Virus or satellite	Final outcome	Host	Gene target	References
African cassava mosaic virus	Silencing	*N. benthamiana, M. esculenta*	Su, PDS	Fofana et al., 2004
Cabbage leaf curl virus	Silencing	*A. thaliana*	Su, PDS	Muangsan and Robertson, 2004
Pepper huasteco yellow vein virus	Silencing	*C. annuum N. tabacum L. esculentum*	Su, Comt pAmt, Kas	Tao and Zhou, 2004
Tomato golden mosaic virus	Silencing	*N. benthamiana*	Su, PCNA	Kjemtrup et al., 1998; Peele et al., 2001
Tomato yellow leaf curl China virus DNA-β	Silencing	*N. glutinosa N. tabacum L. esculentum*	PCNA, PDS, Su	del Rosario Abraham-Juárez et al., 2008
Bean yellow dwarf virus	Expression/ Silencing/ Vaccine production/ Monoclonal antibodies	*S. lycopersicum S. tuberosum N. tabacum*	ANT1, NPTII ALS1, ALS2, SEB vaccine, Ebola, HPV Ab	Baltes et al., 2014; Butler et al., 2015, 2016; Čermák et al., 2015
Wheat dwarf virus	Gene transfer/Expression	*T. aestivum, O. sativa H. vulgare*	Ubi, MLO, GFP Gus	Gil-Humanes et al., 2017; Wang et al., 2017
Chili leaf curl virus	Phloem-specific silencing/expression	*N. benthamiana*	eGFP, PDS	Kushwaha and Chakraborty, 2017
Cotton leaf crumple virus	Silencing	*G. hirsutum*	ChlI, PDS	Tuttle et al., 2012
Bhendi yellow vein mosaic virus β DNA	Silencing	*N. benthamiana*	Su, PDS, PCNA, and AGO1	Jeyabharathy et al., 2015

The abbreviations are as such: Su, sulfur allele of magnesium chelatase complex; PDS, phytoene desaturase synthase; Kas, keto-acyl ACP synthase gene; pAmt, possible aminotransferase gene; Comt, caffeic acid O-methyltransferase gene; ALS1, acetolactate synthase 1; GFP, green fluorescent protein; NPTII, promoter of GUS and neomycin phosphotransferase; PCNA, proliferating cell nuclear antigen. These highlight the diverse roles of deconstructed vectors in functional genomics.

long-lasting crop protection strategies against plant viruses (Ali et al., 2016).

A novel insight toward the use of geminiviral vectors was presented as the virus-induced gene editing (VIGE) protocol which is basically a geminiviral-centered guide RNA delivery system for plant genetic engineering using CRISPR/Cas9 (Yin et al., 2001; Yin et al., 2015). Cas9 is overexpressed in model plants like *N. benthamiana*, and geminiviral vectors comprising single-guide RNA (sgRNA) are transiently expressed targeting the gene of interest. This model has been touted to be used for generation of knockout libraries and has the potential to revolutionize crop genetic engineering (GE) in future. Recently, geminiviral reporter vectors WDV-GFP and WDV-GUS were constructed to deliver profuse amount of DNA to rice cells to make a practical KI (knock-in) method by combining CRISPR/Cas9 to produce double-strand breaks, with a noticeable 19.4% increase in KI frequency (Wang et al., 2017). Similarly, a geminiviral replicon (GVR) was used to deploy SSNs targeting the potato ALS1 gene, which resulted in a significantly lowered herbicide susceptibility phenotype. This validated the geminivirus-based CRISPR/Cas9 delivery approach to plant species and a novel GT methodology for vegetative propagated species (Butler et al., 2016), along with the increase in efficiency of homology-directed repair (HDR) and the possibility of stable transgenic line generation. HDR using a donor template molecule is often used to accomplish precise GT, which includes site-specific sequence changes and targeted insertions. SSNs such as zinc-finger nucleases (ZFNs) (Townsend et al., 2009), TAL-effector nucleases (TALENs) (Zhang et al., 2013), and CRISPR/Cas nucleases have been employed to induce HDR and restore stable GT events because induction of double-stranded breaks (DSBs) considerably enhances the frequency of HDR in plant cells (Puchta et al., 1993). Mutagenesis is the most common result of SSN-mediated DSB induction, although GT events are generally an order of magnitude less common. This is due to the prevalence of alternative DNA repair mechanisms, including as microhomology-mediated end joining and quasi end joining, as well as the necessity for HDR that DSB induction be synchronized with the donor molecule.

The ability of GVRs to efficiently reproduce template DNA, providing an adequate supply of HDR templates, is an advantage of GVRs in GT. However, geminiviruses' reliance on the replication initiator protein (Rep) restricts their usage in gene editing because Reps are recognized to interact with a number of host cell proteins involved in the cell cycle, DNA replication and restoration, and DNA methylation (Maio et al., 2020; Kujur et al., 2021). Off-target genomic alterations are a serious problem linked with a constitutive overexpression of CRISPR/Cas9 systems. Ji et al. (2018) and Rato et al. (2021) created a virus-inducible method based on the promoter segments of the geminivirus BSCTV to overcome this limitation. The modified *Arabidopsis* producing virus-inducible Cas9 and gRNAs directly targeting the Rep gene were infected with BSCTV after validation in transient *N. benthamiana*. Plants had a very low virus load and displayed no symptoms. Crucially, there were no off-target genomic alterations in these plants (Ji et al., 2018). Another study described a Cas9 expression system controlled by a virus-inducible endogenous rgsCaM tomato promoter, which raised similar difficulties. Transient experiments validated the inducible expression of Cas9 in the *S. lycopersicum* when infected with the *Tomato yellow leaf curl virus* (TYLCV), as well as the decrease of Cas9 expression in tomato when infected with TYLCV (Ghorbani Faal et al., 2020). With viruses being highly mutating and failure of pest sprays in targeting viral infections and the

TABLE 2 | Therapeutic products and vaccines produced by geminiviral vectors.

Therapeutic protein	Viral vector	Host plant	Immunogenicity	References
SEB	BeYDV	*N. benthamiana*	+	Shen and Hohn, 1995
Norwalk virus VLPs	BeYDV	Tobacco, lettuce	+	Lai et al., 2012
WNV E protein Mab Ebola	BeYDV	*N. benthamiana*	–	Huang et al., 2009
Virus GP1 Mab	BeYDV	Tobacco, lettuce	+	Phoolcharoen et al., 2011
HPV-1 L1 HIV-1 type	BeYDV	Tobacco, lettuce	+	Phoolcharoen et al., 2011
C p24	BeYDV, mild	*N. benthamiana*	–	Regnard et al., 2010
HAV VP1	BeYDV, mild	*N. benthamiana*	–	Regnard et al., 2010
Vitronectin	BCTV	*N. benthamiana*	–	Chung et al., 2011
	TYDV	*N. benthamiana*	N/A	Dugdale et al., 2014

viruses' quick spread, genome editing has become a precision-based technology which could address the huge demand of targeted viral disease management in crop plants. GE is hence a critical tool for ensuring long-term food safety and security, as well as mitigating the problems faced by the world's expanding population and climate change.

GEMINIVIRUSES IN BIOPHARMACEUTICALS

Geminiviruses are used as a system which is under expansion for the manufacture of plant-derived biopharmaceuticals. Transgenic plants are cheap and effective platforms for bulk vaccine and enzyme production (Hefferon, 2012; **Figure 1**). Plant viral expression vectors provide a reliable alternative for high levels of protein production *in planta* by carrying in its construct the epitopes for vaccines and full therapeutic proteins within its tissues. This offers a good prospect for the biomanufacture of important vaccines through proper biocontainment for critical diseases and offers a candidate for urgent protein therapeutics development in case of pandemics.

The deconstructed vector of BeYDV has been used for *Staphylococcus* enterotoxin B (SEB) vaccine production, which is considered as a tentative bio-warfare agent. The viral genes for coat and movement proteins have been deleted, and an expression cassette for a protein of interest has been inserted into BeYDV-derived expression vectors. When the geminiviral vector is delivered to leaf cells through *Agrobacterium*, it creates a large amount of recombinant DNA that may be used as a transcription template, resulting in a large amount of mRNA for the protein of interest (Chen et al., 2011). Antigens derivative from the *Hepatitis B virus*, HIV, HPV, and *NV* have also been successfully made (Hefferon and Fan, 2004; Huang et al., 2009; Regnard et al., 2010; **Figure 1**). The deadly *Ebola virus*, which was a huge life-altering epidemic causing huge economic and socio-cultural disruption in Africa, was similarly combated by utilizing monoclonal antibodies prepared using this technique by eliminating the production of hetero-oligomeric proteins (Huang et al., 2010). From a single-vector replicon, monoclonal antibodies against the *Ebola virus* (EV) GP1 protein and the *West Nile Virus* (WNV) E protein were produced and accumulated at levels of 0.23 to 0.27 mg/g leaf fresh weight in lettuce plants. A curtovirus, namely, the BCTV, was deconstructed to develop an exogenous protein production system which worked efficiently on addition of a virus-based suppressor of RNA silencing plasmid (Kim et al., 2007). The *Cassava vein mosaic virus* (CsVMV) promoter was used instead of the CAMV 35S promoter to create this vector. When the P19 gene-silencing suppressor was added, reporter gene expression rose by 320% at the RNA level and by 240% at the protein level. In *N. benthamiana*, the capsid protein of the *Hepatitis A virus* (HAV VP1) was linked to an Fc antibody fragment and expressed. After intraperitoneal vaccination, recombinant HAV VP1-Fc isolated by affinity chromatography was able to induce a serum IgG response. IFN- and IL-4 levels were also shown to rise after vaccination. The TYDV system, which offered a fresh twist to the mastrevirus-based geminiviral vector system, is made up of two expression cassettes: one encodes Rep/RepA under the control of the AlcA:AlcR promoter, and the other includes the gene of interest activated under the control of an ethanol inducible promoter, which may be triggered by simply spraying an ethanol solution on it. The gene of interest is broken into two sections, separated by a synthetic intron, and put into the INPACT (In Plant Activation) cassette. In this method, the gene of interest could only be translated from replicons created during geminivirus sequence activation and applied to remove the intron (Dugdale et al., 2013). This method has proved to be adaptable to a variety of host plant species, giving it a distinct edge over many other plant virus expression systems now on the market. The therapeutic protein vitronectin was generated and easily isolated from leaves with this virus expression system and sprayed with 1% ethanol as a proof of concept. A list of vaccines derived from geminiviral vectors is shown in **Table 2**.

The easy scalability along with flexibility makes geminiviruses an attractive candidate for biomedical interventions in terms of vaccine production. This will provide innovative approaches ranging from developing modern, customized drugs to combating potential pandemics, and of course protecting the world's poor from preventable infectious diseases.

CONCLUDING PERSPECTIVES

Plant viruses are usually seen mainly as disease-causing agents, which is only one part of the story. Through the decades of

research, there has been an unraveling of a host of possibilities in the role elucidation of these pathogens. As we have extensively discussed in this review, geminiviruses and many other classes of viruses offer tremendous functional potential in genome editing, changing the way virus-induced agricultural havoc is generally tackled. Crops with a complex genome like wheat and recalcitrant crops like cassava and chili pepper have been successfully transformed using the aid of modified viruses, thereby opening immense prospects of engineering viral vectors for host genome improvements. Discovering new genes and their characteristics is also possible due to the rapid assays the transient GIGS procedures can present, making it a novel and pertinent molecular tool, bypassing the time taken for stable transformation protocols.

The past 30 years have been watershed for gemini-vector design, for applications in plant improvement. Geminiviral vectors have been used in multiple processes like ncDNA expression, vaccine and antibody production, gene silencing systems and expression systems, and CRISPR/Cas9 system construction for rapid assays, in the area of functional genomics. The biopharmaceutical industry has also realized the potential for gemini-vector utilization for vaccine development, where several vaccines are in clinical trials, and few have been approved in the past. The fluidity of geminiviral vectors into morphing successfully on any given "omics" aspect makes it a much-undervalued system of study in the current times, although apprehensions seem to arise due to possible geminiviral vector-linked environmental concerns, even though plant viruses have never posed any threat to human health as consumption of infected food has been done from centuries, albeit unknowingly.

An important perspective in genome manipulation is the identification of elements which could help in the development of geminiviral vectors for stable transgenics development. The current method extensively uses *Agrobacterium*-mediated delivery of the gene of interest cloned in non-viral vectors, which then involves a lengthy plant transformation procedure and subsequent generation of stable lines. As rapid development in sciences also deal with identification of shorter yet effective experimental strategies, geminiviruses can be exploited as a model virus for shorter infiltration strategy development which could be a prospective replacement to the *Agrobacterium* transformation stages with direct mechanical inoculation plant transformation. Therefore, gemini-vector construction–deconstruction with host genome integrative sequences should be exploited aggressively for mimicking *Agrobacterium*-mediated stable line generation.

Another significant concept that should be delved into is the overexpression and silencing of small RNAs through geminiviral vectors within the plant host genome. A notable disadvantage with geminiviral vectors is that it can only accommodate smaller sequences coding for size-restricted proteins as recombinant vectors with larger sequences are not stable. However, this can be advantageous in that it could serve as the backbone for delivering small RNAs in plants, thereby helping in modulation of regulatory processes in the DNA/RNA level, modulation of unwanted characters, and targeted overproduction of desirable traits in plants. Further, under the control of a suitable promoter, these vectors can be used as vehicles for overexpression of small peptides for many applications, such as peptide antibiotic nicin. Such viral vectors can be very useful for expressing venom peptides, having applications for developing anti-venoms, like mite allergens (Hsu et al., 2004; Kang et al., 2016). An in-depth investigation of roles is required to completely understand and realize the true potential of gemini vectors for the betterment of crop health and for bio-pharmaceutical role mining so that the middle- and low-income countries too can benefit from the end products.

AUTHOR CONTRIBUTIONS

BB and VH planned and designed the review. BB drafted the manuscript and prepared the table and figure. VH edited the manuscript. Both authors read and approved the final version of the manuscript.

ACKNOWLEDGMENTS

We are thankful to the Director of CSIR-IHBT for his support. BB would like to thank DST of Govt. of India for the INSPIRE fellowship and AcSIR for Ph.D. registration. We are grateful to Sourabh Soni, Harvard Medical School, United States, for his help in manuscript and figure editing. This is IHBT communication number 4639.

REFERENCES

Abrahamian, P., Hammond, R. W., and Hammond, J. (2020). Plant virus–derived vectors: applications in agricultural and medical biotechnology. *Annu. Rev. Virol.* 7, 513–535. doi: 10.1146/annurev-virology-010720-054958

Akbar Behjatnia, S. A., Dry, I. B., and Ali Rezaian, M. (1998). Identification of the replication-associated protein binding domain within the intergenic region of tomato leaf curl geminivirus. *Nucleic Acids Res.* 26, 925–931. doi: 10.1093/nar/26.4.925

Ali, Z., Ali, S., Tashkandi, M., Zaidi, S. S. E. A., and Mahfouz, M. M. (2016). CRISPR/Cas9-mediated immunity to geminiviruses: differential interference and evasion. *Sci. Rep.* 6, 1–13.

Baltes, N. J., Gil-Humanes, J., Cermak, T., Atkins, P. A., and Voytas, D. F. (2014). DNA replicons for plant genome engineering. *Plant Cell* 26, 151–163. doi: 10.1105/tpc.113.119792

Baltes, N. J., Hummel, A. W., Konecna, E., Cegan, R., Bruns, A. N., Bisaro, D. M., et al. (2015). Conferring resistance to geminiviruses with the CRISPR–Cas prokaryotic immune system. *Nat. Plants* 1:15145.

Bejarano, E. R., Khashoggi, A., Witty, M., and Lichtenstein, C. (1996). Integration of multiple repeats of geminiviral DNA into the nuclear genome of tobacco during evolution. *Proc. Natl. Acad. Sci.* 93, 759–764. doi: 10.1073/pnas.93.2.759

Bulaon, C. J. I., Shanmugaraj, B., Oo, Y., Rattanapisit, K., Chuanasa, T., Chaotham, C., et al. (2020). Rapid transient expression of functional human vascular endothelial growth factor in *Nicotiana benthamiana* and characterization of its biological activity. *Biotechnol. Rep.* 27:e00514. doi: 10.1016/j.btre.2020.e00514

Buragohain, A. K., Sung, Y. K., Coffn, R. S., and Coutts, R. H. (1994). The infectivity of dimeric potato yellow mosaic geminivirus clones in different hosts. *J. Gen. Virol.* 75, 2857–2861. doi: 10.1099/0022-1317-75-10-2857

Butler, N. M., Atkins, P. A., Voytas, D. F., and Douches, D. S. (2015). Generation and inheritance of targeted mutations in potato (*Solanum tuberosum* L.) using the CRISPR/Cas system. *PLoS One* 10:e0144591. doi: 10.1371/journal.pone.0144591

Butler, N. M., Baltes, N. J., Voytas, D. F., and Douches, D. S. (2016). Geminivirus mediated genome editing in potato (*Solanum tuberosum* L.) using sequence specific nucleases. *Front. Plant Sci.* 7:1045. doi: 10.3389/fpls.2016.01045 doi: 10.3389/fpls.2016.01045

Carrillo-Tripp, J., Shimada-Beltrán, H., and Rivera-Bustamante, R. (2006). Use of geminiviral vectors for functional genomics. *Curr. Opin. Plant Biol.* 9, 209–215.

Castellano, M. M., Sanz-Burgos, A. P., and Gutiérrez, C. (1999). Initiation of DNA replication in a eukaryotic rolling-circle replicon: identification of multiple DNA-protein complexes at the geminivirus origin. *J. Mol. Biol.* 290, 639–652. doi: 10.1006/jmbi.1999.2916

Čermák, T., Baltes, N. J., Čegan, R., Zhang, Y., and Voytas, D. F. (2015). High-frequency, precise modification of the tomato genome. *Genome Biol.* 16:232. doi: 10.1186/s13059-015-0796-9

Chen, D. F., and Dale, P. J. (1992). A comparison of methods for delivering DNA to wheat: the application of wheat dwarf virus DNA to seeds with exposed apical meristems. *Transgenic Res.* 1, 93–100.

Chen, Q., He, J., Phoolcharoen, W., and Mason, H. S. (2011). Geminiviral vectors based on bean yellow dwarf virus for production of vaccine antigens and monoclonal antibodies in plants. *Hum. Vaccin.* 7, 331–338. doi: 10.4161/hv.7.3.14262

Chung, H. Y., Lee, H. H., Kim, K. I., Chung, H. Y., Hwang-Bo, J., Park, J. H., et al. (2011). Expression of a recombinant chimeric protein of hepatitis A virus VP1-Fc using a replicating vector based on Beet curly top virus in tobacco leaves and its immunogenicity in mice. *Plant Cell Rep.* 30, 1513–1521. doi: 10.1007/s00299-011-1062-6

Creissen, G., Smith, C., Francis, R., Reynolds, H., and Mullineaux, P. (1990). Agrobacterium-and microprojectile-mediated viral DNA delivery into barley microspore-derived cultures. *Plant Cell Rep.* 8, 680–683. doi: 10.1007/BF00269992

del Rosario Abraham-Juárez, M., Rocha-Granados, M. del. C., López, M. G., Rivera-Bustamante, R. F., and Ochoa-Alejo, N. (2008). Virus-induced silencing of Comt, pAmt and Kas genes results in a reduction of capsaicinoid accumulation in chili pepper fruits. *Planta* 227, 681–695. doi: 10.1007/s00425-007-0651-7

Dinesh-Kumar, S. P., Anandalakshmi, R., Marathe, R., Schiff, M., and Liu, Y. (2003). Virus-induced gene silencing. *Methods Mol. Biol.* 236, 287–294.

Dugdale, B., Mortimer, C. L., Kato, M., James, T. A., Harding, R. M., and Dale, J. L. (2013). In plant activation: an inducible, hyperexpression platform for recombinant protein production in plants. *Plant Cell* 25, 2429–2443. doi: 10.1105/tpc.113.113944

Dugdale, B., Mortimer, C. L., Kato, M., James, T. A., Harding, R. M., and Dale, J. L. (2014). Design and construction of an in-plant activation cassette for transgene expression and recombinant protein production in plants. *Nat. Protoc.* 9, 1010–1027.

Ellison, E. E., Chamness, J. C., and Voytas, D. F. (2021). "Viruses as vectors for the delivery of gene editing reagents," in *Genome Editing for Precision Crop Breeding*, (Cambridge, MA: Burleigh Dodds Science Publishing), 97–122.

Escudero, J., Neuhaus, G., Schläppi, M., and Hohn, B. (1996). T-DNA transfer in meristematic cells of maize provided with intracellular Agrobacterium. *Plant J.* 10, 355–360.

Fiallo-Olivé, E., Lett, J. M., Martin, D. P., Roumagnac, P., Varsani, A., Zerbini, F. M., et al. (2021). ICTV virus taxonomy profile: geminiviridae 2021. *J. Gen. Virol.* 102:001696. doi: 10.1099/jgv.0.001696

Fofana, I. B., Sangaré, A., Collier, R., Taylor, C., and Fauquet, C. M. (2004). A geminivirus-induced gene silencing system for gene function validation in cassava. *Plant Mol. Biol.* 56, 613–624. doi: 10.1007/s11103-004-0161-y

Fondong, V. N. (2013). Geminivirus protein structure and function. *Mol. Plant Pathol.* 14, 635–649. doi: 10.1111/mpp.12032

Fontes, E. P., Luckow, V. A., and Hanley-Bowdoin, L. (1992). A geminivirus replication protein is a sequence-specific DNA binding protein. *Plant Cell* 4, 597–608. doi: 10.1105/tpc.4.5.597

Ghorbani Faal, P., Farsi, M., Seifi, A., and Mirshamsi Kakhki, A. (2020). Virus-induced CRISPR-Cas9 system improved resistance against tomato yellow leaf curl virus. *Mol. Biol. Rep.* 47, 3369–3376. doi: 10.1007/s11033-020-05409-3

Gil-Humanes, J., Wang, Y., Liang, Z., Shan, Q., Ozuna, C. V., Sánchez-León, S., et al. (2017). High-efficiency gene targeting in hexaploid wheat using DNA replicons and CRISPR/Cas9. *Plant J.* 89, 1251–1262. doi: 10.1111/tpj.13446

Gnanasekaran, P., KishoreKumar, R., Bhattacharyya, D., Vinoth Kumar, R., and Chakraborty, S. (2019). Multifaceted role of geminivirus associated betasatellite in pathogenesis. *Mol. Plant Pathol.* 20, 1019–1033.

Grimsley, N., Hohn, T., Davies, J. W., and Hohn, B. (1987). Agrobacterium-mediated delivery of infectious maize streak virus into maize plants. *Nature* 325, 177–179. doi: 10.1007/BF00017445

Gutierrez, C. (1999). Geminivirus DNA replication. *Cell. Mol. Life Sci.* 56, 313–329.

Halweg, C., Thompson, W. F., and Spiker, S. (2005). The Rb7 matrix attachment region increases the likelihood and magnitude of transgene expression in tobacco cells: a flow cytometric study. *Plant Cell* 17, 418–429. doi: 10.1105/tpc.104.028100

Hanley-Bowdoin, L., Bejarano, E. R., Robertson, D., and Mansoor, S. (2013). Geminiviruses: masters at redirecting and reprogramming plant processes. *Nat. Rev. Microbiol.* 11, 777–788. doi: 10.1038/nrmicro3117

Hefferon, K. L. (2012). Plant virus expression vectors set the stage as production platforms for biopharmaceutical proteins. *Virology* 433, 1–6. doi: 10.1016/j.virol.2012.06.012

Hefferon, K. L. (2014). DNA virus vectors for vaccine production in plants: spotlight on geminiviruses. *Vaccines* 2, 642–653. doi: 10.3390/vaccines2030642

Hefferon, K. L., and Fan, Y. (2004). Expression of a vaccine protein in a plant cell line using a geminivirus-based replicon system. *Vaccine* 23, 404–410. doi: 10.1016/j.vaccine.2004.04.038

Howell, S. H., Walker, L. L., and Dudley, R. K. (1980). Cloned cauliflower mosaic virus DNA infects turnips (*Brassica rapa*). *Science* 208, 1265–1267. doi: 10.1126/science.208.4449.1265

Hsu, C. H., Lin, S. S., Liu, F. L., Su, W. C., and Yeh, S. D. (2004). Oral administration of a mite allergen expressed by zucchini yellow mosaic virus in cucurbit species downregulates allergen-induced airway inflammation and IgE synthesis. *J. Allergy Clin. Immunol.* 113, 1079–1085. doi: 10.1016/j.jaci.2004.02.047

Huang, Z., Chen, Q., Hjelm, B., Arntzen, C., and Mason, H. (2009). A DNA replicon system for rapid high-level production of virus-like particles in plants. *Biotechnol. Bioeng.* 103, 706–714. doi: 10.1002/bit.22299

Huang, Z., Phoolcharoen, W., Lai, H., Piensook, K., Cardineau, G., Zeitlin, L., et al. (2010). High-level rapid production of full-size monoclonal antibodies in plants by a single-vector DNA replicon system. *Biotechnol. Bioeng.* 106, 9–17. doi: 10.1002/bit.22652

Hull, R. (1978). The possible use of plant viral DNAs in genetic manipulation in plants. *Trends Biochem. Sci.* 3, 254–256.

Hummel, A. W., Chauhan, R. D., Cermak, T., Mutka, A. M., Vijayaraghavan, A., Boyher, A., et al. (2018). Allele exchange at the EPSPS locus confers glyphosate tolerance in cassava. *Plant Biotechnol. J.* 16, 1275–1282. doi: 10.1111/pbi.12868

Inoue-Nagata, A. K., Lima, M. F., and Gilbertson, R. L. (2016). A review of geminivirus diseases in vegetables and other crops in Brazil: current status and approaches for management. *Horticult. Bras.* 34, 8–18.

Jeyabharathy, C., Shakila, H., and Usha, R. (2015). Development of a VIGS vector based on the β-satellite DNA associated with bhendi yellow vein mosaic virus. *Virus Res.* 195, 73–78. doi: 10.1016/j.virusres.2014.08.009

Ji, X., Si, X., Zhang, Y., Zhang, H., Zhang, F., and Gao, C. (2018). Conferring DNA virus resistance with high specificity in plants using virus-inducible genome-editing system. *Genome Biol.* 19:197. doi: 10.1186/s13059-018-1580-4

Ji, X., Zhang, H., Zhang, Y., Wang, Y., and Gao, C. (2015). Establishing a CRISPR–Cas–like immune system conferring DNA virus resistance in plants. *Nat. Plants* 1:15144. doi: 10.1038/nplants.2015.144

Kang, M., Seo, J. K., Choi, H., Choi, H. S., and Kim, K. H. (2016). Establishment of a simple and rapid gene delivery system for cucurbits by using engineered of Zucchini yellow mosaic virus. *Plant Pathol. J.* 32:70. doi: 10.5423/PPJ.NT.08.2015.0173

Kil, E. J., Kim, S., Lee, Y. J., Byun, H. S., Park, J., Seo, H., et al. (2016). Tomato yellow leaf curl virus (TYLCV-IL): a seed-transmissible geminivirus in tomatoes. *Sci. Rep.* 6, 1–10. doi: 10.1038/srep19013

Kil, E. J., Park, J., Choi, E. Y., Byun, H. S., Lee, K. Y., An, C. G., et al. (2018). Seed transmission of tomato yellow leaf curl virus in sweet pepper (Capsicum annuum). *Eur. J. Plant Pathol.* 150, 759–764.

Kil, E. J., Park, J., Choi, H. S., Kim, C. S., and Lee, S. (2017). Seed transmission of Tomato yellow leaf curl virus in white soybean (*Glycine max*). *Plant Pathol. J.* 33, 424.

Kim, K. I., Sunter, G., Bisaro, D. M., and Chung, I. S. (2007). Improved expression of recombinant GFP using a replicating vector based on Beet curly top virus in leaf-disks and infiltrated *Nicotiana benthamiana* leaves. *Plant Mol. Biol.* 64, 103–112. doi: 10.1007/s11103-007-9137-z

Kjemtrup, S., Sampson, K. S., Peele, C. G., Nguyen, L. V., Conkling, M. A., Thompson, W. F., et al. (1998). Gene silencing from plant DNA carried by a geminivirus. *Plant J.* 14, 91–100. doi: 10.1046/j.1365-313X.1998.00101.x

Kujur, S., Senthil-Kumar, M., and Kumar, R. (2021). Plant viral vectors: expanding the possibilities of precise gene editing in plant genomes. *Plant Cell Rep.* 40, 931–934. doi: 10.1007/s00299-021-02697-2

Kumar, R. V. (2019). Plant antiviral immunity against geminiviruses and viral counter-defense for survival. *Front. Microbiol.* 10:1460. doi: 10.3389/fmicb.2019.01460

Kumar, R. V., Singh, D., Singh, A. K., and Chakraborty, S. (2017). Molecular diversity, recombination and population structure of alphasatellites associated with begomovirus disease complexes. *Infect. Genet. Evol.* 49, 39–47. doi: 10.1016/j.meegid.2017.01.001

Kushwaha, N. K., and Chakraborty, S. (2017). Chilli leaf curl virus-based vector for phloem-specific silencing of endogenous genes and overexpression of foreign genes. *Appl. Microbiol. Biotechnol.* 101, 2121–2129.

Lai, H., He, J., Engle, M., Diamond, M. S., and Chen, Q. (2012). Robust production of virus-like particles and monoclonal antibodies with geminiviral replicon vectors in lettuce. *Plant Biotechnol. J.* 10, 95–104. doi: 10.1111/j.1467-7652.2011.00649.x

Laufs, J., Jupin, I., David, C., Schumacher, S., Heyraud-Nitschke, F., and Gronenborn, B. (1995). Geminivirus replication: genetic and biochemical characterization of Rep protein function, a review. *Biochimie* 77, 765–773. doi: 10.1016/0300-9084(96)88194-6

Li, Y., Sun, M., Wang, X., Zhang, Y. J., Da, X. W., Jia, L. Y., et al. (2021). Effects of plant growth regulators on transient expression of foreign gene in *Nicotiana benthamiana* L. leaves. *Bioresour. Bioprocess.* 8, 1–8.

Lu, Y., and Zhu, J. K. (2017). Precise editing of a target base in the rice genome using a modifed CRISPR/Cas9 system. *Mol. Plant* 10, 523–525. doi: 10.1016/j.molp.2016.11.013

Lucy, A. P., Boulton, M. I., Davies, J. W., and Maule, A. J. (1996). Tissue specificity of *Zea mays* infection by maize streak virus. *Mol. Plant Microbe Interact.* 9, 22–31.

Maclean, J., Koekemoer, M., Olivier, A. J., Stewart, D., Hitzeroth, I. I., Rademacher, T., et al. (2007). Optimization of human papillomavirus type 16 (HPV-16) L1 expression in plants: comparison of the suitability of different HPV-16 L1 gene variants and different cell-compartment localization. *J. Gen. Virol.* 88, 1460–1469. doi: 10.1099/vir.0.82718-0

Maio, F., Helderman, T. A., Arroyo-Mateos, M., van der Wolf, M., Boeren, S., Prins, M., et al. (2020). Identification of tomato proteins that interact with replication initiator protein (Rep) of the geminivirus TYLCV. *Front. Plant Sci.* 11:1069. doi: 10.3389/fpls.2020.01069

Malla, A., Rosales-Mendoza, S., Phoolcharoen, W., and Vimolmangkang, S. (2021). Efficient transient expression of recombinant proteins using DNA viral vectors in freshwater microalgal species. *Front. Plant Sci.* 12:650820. doi: 10.3389/fpls.2021.650820

Moore, L. W., Chilton, W. S., and Canfield, M. L. (1997). Diversity of opines and opine-catabolizing bacteria isolated from naturally occurring crown gall tumors. *Appl. Environ. Microbiol.* 63, 201–207. doi: 10.1128/aem.63.1.201-207.1997

Mor, T. S., Moon, Y. S., Palmer, K. E., and Mason, H. S. (2003). Geminivirus vectors for high-level expression of foreign proteins in plant cells. *Biotechnol. Bioeng.* 81, 430–437. doi: 10.1002/bit.10483

Muangsan, N., and Robertson, D. (2004). Geminivirus vectors for transient gene silencing in plants. *Methods Mol Biol.* 265, 101–115. doi: 10.1385/1-59259-775-0:101

Nakade, S., Yamamoto, T., and Sakuma, T. (2017). Cas9, Cpf1 and C2c1/2/3-What's next? *Bioengineered* 8, 265–273. doi: 10.1080/21655979.2017.1282018

Navas-Castillo, J., Fiallo-Olivé, E., and Sánchez-Campos, S. (2011). Emerging virus diseases transmitted by whiteflies. *Annu. Rev. Phytopathol.* 49, 219–248. doi: 10.1146/annurev-phyto-072910-095235

Nawaz-ul-Rehman, M. S., and Fauquet, C. M. (2009). Evolution of geminiviruses and their satellites. *FEBS Lett.* 583, 1825–1832. doi: 10.1016/j.febslet.2009.05.045

Nosaki, S., Hoshikawa, K., Ezura, H., and Miura, K. (2021). Transient protein expression systems in plants and their applications. *Plant Biotechnol.* 38, 297–304. doi: 10.5511/plantbiotechnology.21.0610a

Pakkianathan, B. C., Kontsedalov, S., Lebedev, G., Mahadav, A., Zeidan, M., Czosnek, H., et al. (2015). Replication of tomato yellow leaf curl virus in its whitefly vector, *Bemisia tabaci*. *J. Virol.* 89, 9791–9803. doi: 10.1128/JVI.00779-15

Pandey, P., Choudhury, N. R., and Mukherjee, S. K. (2009). A geminiviral amplicon (VA) derived from tomato leaf curl virus (ToLCV) can replicate in a wide variety of plant species and also acts as a VIGS vector. *Virol. J.* 6, 1–13. doi: 10.1186/1743-422X-6-152

Peele, C., Jordan, C. V., Muangsan, N., Turnage, M., Egelkrout, E., Eagle, P., et al. (2001). Silencing of a meristematic gene using geminivirus-derived vectors. *Plant J.* 27, 357–366. doi: 10.1046/j.1365-313x.2001.01080.x

Pérez-Padilla, V., Fortes, I. M., Romero-Rodríguez, B., Arroyo-Mateos, M., Castillo, A. G., Moyano, C., et al. (2020). Revisiting seed transmission of the type strain of tomato yellow leaf curl virus in tomato plants. *Phytopathology* 110, 121–129. doi: 10.1094/PHYTO-07-19-0232-FI

Peyret, H., and Lomonossoff, G. P. (2015). When plant virology met Agrobacterium: the rise of the deconstructed clones. *Plant Biotechnol. J.* 13, 1121–1135. doi: 10.1111/pbi.12412

Phoolcharoen, W., Bhoo, S. H., Lai, H., Ma, J., Arntzen, C. J., Chen, Q., et al. (2011). Expression of an immunogenic Ebola immune complex in Nicotiana benthamiana. *Plant Biotechnol. J.* 9, 807–816. doi: 10.1111/j.1467-7652.2011.00593.x

Prasad, A., Sharma, N., Hari-Gowthem, G., Muthamilarasan, M., and Prasad, M. (2020). Tomato yellow leaf curl virus: impact, challenges, and management. *Trends Plant Sci.* 25, 897–911. doi: 10.1016/j.tplants.2020.03.015

Prasad, A., Sharma, N., Muthamilarasan, M., Rana, S., and Prasad, M. (2019). Recent advances in small RNA mediated plant-virus interactions. *Crit. Rev. Biotechnol.* 39, 587–601. doi: 10.1080/07388551.2019.1597830

Puchta, H., Dujon, B., and Hohn, B. (1993). Homologous recombination in plant cells is enhanced by *in vivo* induction of double strand breaks into DNA by a site-specific endonuclease. *Nucleic Acids Res.* 21, 5034–5040. doi: 10.1093/nar/21.22.5034

Raja, P., Wolf, J. N., and Bisaro, D. M. (2010). RNA silencing directed against geminiviruses: post-transcriptional and epigenetic components. *Biochim. Biophys. Acta* 1799, 337–351. doi: 10.1016/j.bbagrm.2010.01.004

Ramesh, S. V., Sahu, P. P., Prasad, M., Praveen, S., and Pappu, H. R. (2017). Geminiviruses and plant hosts: a closer examination of the molecular arms race. *Viruses* 9:256. doi: 10.3390/v9090256

Rato, C., Carvalho, M. F., Azevedo, C., and Oblessuc, P. R. (2021). Genome editing for resistance against plant pests and pathogens. *Transgenic Res.* 30, 427–459. doi: 10.1007/s11248-021-00262-x

Regnard, G. L., Halley-Stott, R. P., Tanzer, F. L., Hitzeroth, I. I., and Rybicki, E. P. (2010). High level protein expression in plants through the use of a novel autonomously replicating geminivirus shuttle vector. *Plant Biotechnol. J.* 8, 38–46. doi: 10.1111/j.1467-7652.2009.00462.x

Rosas-Díaz, T., Zhang, D., and Lozano-Durán, R. (2017). No evidence of seed transmissibility of tomato yellow leaf curl virus in *Nicotiana benthamiana*. *J. Zhejiang Univ. Sci. B* 18, 437–440. doi: 10.1631/jzus.B1600463

Sainsbury, F., and Lomonossoff, G. P. (2008). Extremely high-level and rapid transient protein production in plants without the use of viral replication. *Plant Physiol.* 148, 1212–1218. doi: 10.1104/pp.108.126284

Schlappi, M., and Hohn, B. (1992). Competence of immature maize embryos for Agrobacterium-mediated gene transfer. *Plant Cell* 4, 7–16. doi: 10.1105/tpc.4.1.7

Shen, W. H., Das, S., and Hohn, B. (1992). Mechanism of Ds1 excision from the genome of maize streak virus. *Mol. Gen. Genet.* 233, 388–394. doi: 10.1007/BF00265435

Shen, W. H., and Hohn, B. (1992). Excision of a transposable element from a viral vector introduced into maize plants by agroinfection. *Plant J.* 2, 35–42.

Shen, W. H., and Hohn, B. (1994). Amplification and expression of the β-glucuronidase gene in maize plants by vectors based on maize streak virus. *Plant J.* 5, 227–236.

Shen, W. H., and Hohn, B. (1995). Vectors based on maize streak virus can replicate to high copy numbers in maize plants. *J. Gen. Virol.* 76, 965–969. doi: 10.1099/0022-1317-76-4-965

Stanley, J. (1995). Analysis of African cassava mosaic virus recombinants suggests strand nicking occurs within the conserved non-anucleotide motif during the initiation of rolling circle DNA replication. *Virology* 206, 707–712. doi: 10.1016/s0042-6822(95)80093-x

Tao, X., and Zhou, X. (2004). A modified viral satellite DNA that suppresses gene expression in plants. *Plant J.* 38, 850–860. doi: 10.1111/j.1365-313X.2004.02087.x

Timmermans, M. C., Das, O. P., and Messing, J. (1994). Geminiviruses and their uses as extrachromosomal replicons. *Annu. Rev. Plant Biol.* 45, 79–112.

Townsend, J. A., Wright, D. A., Winfrey, R. J., Fu, F., Maeder, M. L., Joung, J. K., et al. (2009). High-frequency modification of plant genes using engineered zinc-finger nucleases. *Nature* 459, 442–445. doi: 10.1038/nature07845

Turnage, M. A., Muangsan, N., Peele, C. G., and Robertson, D. (2002). Geminivirus-based vectors for gene silencing in *Arabidopsis*. *Plant J.* 30, 107–114.

Tuttle, J. R., Haigler, C. H., and Robertson, D. (2012). Method: low-cost delivery of the cotton leaf crumple virus-induced gene silencing system. *Plant Methods* 8:27. doi: 10.1186/1746-4811-8-27

Varsani, A., Roumagnac, P., Fuchs, M., Navas-Castillo, J., Moriones, E., Idris, A., et al. (2017). Capulavirus and Grablovirus: two new genera in the family Geminiviridae. *Arch. Virol.* 162, 1819–1831. doi: 10.1007/s00705-017-3268-6

Wang, J., Bing, X. L., Li, M., Ye, G. Y., and Liu, S. S. (2012). Infection of tobacco plants by a begomovirus improves nutritional assimilation by a whitefly. *Entomol. Exp. Appl.* 144, 191–201.

Wang, M., Lu, Y., Botella, J. R., Mao, Y., Hua, K., and Zhu, J. K. (2017). Gene targeting by homology-directed repair in rice using a geminivirus-based CRISPR/Cas9 system. *Mol. Plant* 10, 1007–1010. doi: 10.1016/j.molp.2017.03.002

Xiao, Z., Xing, M., Liu, X., Fang, Z., Yang, L., Zhang, Y., et al. (2020). An efficient virus-induced gene silencing (VIGS) system for functional genomics in Brassicas using a cabbage leaf curl virus (CaLCuV)-based vector. *Planta* 252:42. doi: 10.1007/s00425-020-03454-7

Xu, X., Qian, Y., Wang, Y., Li, Z., and Zhou, X. (2019). Iterons homologous to helper geminiviruses are essential for efficient replication of betasatellites. *J. Virol.* 93:e1532-18. doi: 10.1128/JVI.01532-18

Yang, Q., Yang, X., Ding, B., and Zhou, X. (2016). The application of geminiviruses in biotechnology. *Sci. Sin. Vitae* 46, 524–534.

Yang, Q. Y., Bo, D. I. N. G., and Zhou, X. P. (2017). Geminiviruses and their application in biotechnology. *J. Integr. Agric.* 16, 2761–2771. doi: 10.1016/s2095-3119(17)61702-7

Yin, K., Han, T., Liu, G., Chen, T., Wang, Y., Yu, A. Y., et al. (2015). A geminivirus based guide RNA delivery system for CRISPR/Cas9 mediated plant genome editing. *Sci. Rep.* 5:14926. doi: 10.1038/srep14926

Yin, Q., Yang, H., Gong, Q., Wang, H., Liu, Y., Hong, Y., et al. (2001). Tomato yellow leaf curl China virus: monopartite genome organization and agroinfection of plants. *Virus Res.* 81, 69–76. doi: 10.1016/s0168-1702(01)00363-x

Zerbini, F. M., Briddon, R. W., Idris, A., Martin, D. P., Moriones, E., Navas-Castillo, J., et al. (2017). ICTV virus taxonomy profile: geminiviridae. *J. Gen. Virol.* 98:131.

Zhang, X., and Mason, H. (2006). Bean Yellow Dwarf Virus replicons for high-level transgene expression in transgenic plants and cell cultures. *Biotechnol. Bioeng.* 93, 271–279. doi: 10.1002/bit.20695

Zhang, Y., Zhang, F., Li, X., Baller, J. A., Qi, Y., Starker, C. G., et al. (2013). Transcription activator-like effector nucleases enable efficient plant genome engineering. *Plant Physiol.* 161, 20–27. doi: 10.1104/pp.112.205179

Conflict of Interest: The authors declare that the research was conducted in the absence of any commercial or financial relationships that could be construed as a potential conflict of interest.

Publisher's Note: All claims expressed in this article are solely those of the authors and do not necessarily represent those of their affiliated organizations, or those of the publisher, the editors and the reviewers. Any product that may be evaluated in this article, or claim that may be made by its manufacturer, is not guaranteed or endorsed by the publisher.

frontiers | Frontiers in Microbiology

ORIGINAL RESEARCH
published: 25 April 2022
doi: 10.3389/fmicb.2022.793122

Isolation, Mutagenesis, and Organic Acid Secretion of a Highly Efficient Phosphate-Solubilizing Fungus

Tianyou Yang[1], Linbo Li[1], Baoshi Wang[1], Jing Tian[1], Fanghao Shi[2], Shishuang Zhang[1] and Zhongqi Wu[1]*

[1]School of Life Science and Technology, Henan Institute of Science and Technology, Xinxiang, China, [2]Sino-Danish Center, University of Chinese Academy of Sciences, Beijing, China

The highly effective phosphate-solubilizing microorganisms are significant for making full use of the potential phosphorus resources in the soil and alleviating the shortage of phosphorus resources. In this study, a phosphate-solubilizing fungus was isolated from wheat and cotton rhizosphere soils in the lower reaches of the Yellow River in China and was identified as *Penicillium oxalicum* by morphological and ITS sequencing analysis. In order to obtain a fungus with more efficient phosphorus solubilization ability, we tested three positive mutant strains (P1, P2, and P3) and three negative mutant strains (N1, N2, and N3) through low-energy nitrogen ion implantation mutagenesis. Compared with the parental strain, the phosphate-solubilizing capacity of P1, P2, and P3 was enhanced by 56.88%, 42.26%, and 32.15%, respectively, and that of N1, N2, and N3 was weakened by 47.53%, 35.27%, and 30.86%, respectively. Compared with the parental strain, the total amount of organic acids secreted significantly increased in the three positive mutant strains and decreased in the negative mutant strains; the pH of culture medium was significantly lower in the positive mutant strains and higher in the negative mutant strains. The capacity of phosphate-solubilizing fungus to secrete organic acids and reduce the growth-medium pH was closely related to its phosphate-solubilizing ability. The changes in the amount of organic acids secreted by mutants can alter their acidification and phosphate-solubilizing capacity. In conclusion, this study offers a theoretical basis and strain materials for the exploration and application of phosphate-solubilizing fungi.

Keywords: phosphate-solubilizing fungi, low-energy ion implantation mutagenesis, mutants, organic acids, sustainable agriculture

OPEN ACCESS

Edited by:
Ying Ma,
University of Coimbra, Portugal

Reviewed by:
Divjot Kour,
Eternal University, India
Yunpeng Qiu,
Nanjing Agricultural University, China
Anzhen Qin,
Farmland Irrigation Research Institute (CAAS), China

****Correspondence:***
Tianyou Yang
yangtianyou2004@163.com

Specialty section:
This article was submitted to Microbiotechnology, a section of the journal Frontiers in Microbiology

Received: *11 October 2021*
Accepted: *04 April 2022*
Published: *25 April 2022*

Citation:
Yang T, Li L, Wang B, Tian J, Shi F, Zhang S and Wu Z (2022) Isolation, Mutagenesis, and Organic Acid Secretion of a Highly Efficient Phosphate-Solubilizing Fungus. Front. Microbiol. 13:793122. doi: 10.3389/fmicb.2022.793122

INTRODUCTION

Phosphorus is an essential nutrient element for crop growth and development (Yongbin et al., 2020). There is little available inorganic phosphorus to be absorbed and utilized by crops in the soil, whereas the majority of phosphorus is in insoluble forms that crops cannot utilize (Busato et al., 2017). Given low phosphorus availability but abundant potential phosphorus sources in the soil, finding and characterizing phosphate-solubilizing microorganisms to make full use of potential phosphorus resources in the soil has profound strategic significance for alleviating the shortage of phosphorus resources and developing sustainable and efficient

agriculture (Sharma et al., 2013). At present, the research on phosphate-solubilizing microorganisms mostly focuses on isolation (Shi et al., 2014; Tomer et al., 2017), screening, and identification (Chakdar et al., 2018). There is a lack of highly efficient phosphate-solubilizing microorganisms, and the underlying phosphate-solubilizing mechanisms are poorly understood, thus restricting the utilization of phosphate-solubilizing microorganisms (Antoun, 2012). Using mutation to produce highly efficient phosphate-solubilizing microorganisms and characterization of phosphate-solubilizing mechanisms have always been important research topics in the field of soil microorganisms and biofertilizers (Gong et al., 2014). Both acid production and phosphate solubilization by phosphate-solubilizing microorganisms can be enhanced by radiation mutagenesis (Busato et al., 2017). Silva et al. (2014) induced mutation of *Aspergillus niger* by UV and found that the phosphate-solubilizing ability of mutant FS1-331 increased by up to 2.50 times compared with that of the original strain, with an increase in organic acid production being an important reason for improved phosphate-solubilizing ability. Moreover, Li et al. (2011b) studied the effect of microwave radiation on *Klebsiella pneumonia* RSN19 and showed that it could greatly enhance the nitrogen-fixing and phosphate-solubilizing capacities of the strain.

Since its application in biological mutation and genetic breeding in the 1980s, low-energy ion beam mutagenesis, characterized by a unique radiation effect, has been widely applied in microbial breeding (Li et al., 2013). In recent years, low-energy ion beam mutagenesis for phosphate-solubilizing microorganisms has been studied extensively. For example, You et al. (2009) mutated *Bacillus subtilis* P-1 using nitrogen ion beam implantation, and one phosphate-solubilizing mutant strain was obtained, with phosphate-solubilizing ability enhanced by 48%. Peng et al. (2020) adopted ion beam implantation technique in the breeding of phosphate-solubilizing mutant strain of *Bacillus subtilis* LA, resulting in the improved phosphate-solubilizing ability. Low-energy ion beam is a new type of mutation source (Semsang et al., 2018) with four mutagenic effects (energy exchange, energy deposition, mass deposition, and charge exchange), little induced damage, a wide spectrum of mutations, and a high mutation rate (Maekawa et al., 2003; Okamura et al., 2003; Yamaguchi et al., 2003; Li et al., 2007). Currently, the mutagenic materials in ion beam mutagenesis are mostly phosphate-solubilizing bacteria, and there are few studies on the ion beam mutagenesis in fungi (Nguyen and Bruns, 2015). Ion beam mutagenesis for phosphate-solubilizing fungi is expected to result in the formation of highly efficient phosphate-solubilizing fungal mutants (Semsang et al., 2018), which is of great significance for the breeding of phosphate-solubilizing strains and the characterization of the underlying phosphate-solubilizing mechanisms.

There are four main mechanisms involved in inorganic phosphate solubilization by microorganisms, including secretion of organic acids, hydrogen protons, proteins, and chelation (Khan et al., 2014). Gong et al. (2014) isolated one strain of *Penicillium* sp. PSM11-5 from an alum mine and its phosphate-solubilizing effect was closely related to the secretion of gluconic acid and citric acid. Ahuja et al. (2007) argued that the citric acid and oxalic acid produced by *Paecilomyces marquandii* AA1 were important in phosphate solubilization. Mendes et al. (2013) found that citric acid, gluconic acid, and oxalic acid secreted by *Penicillium canescens* were the main mechanisms for solubilizing calcium phosphate. In general, the organic acids found to be involved in phosphate solubilization include oxalic (Mendes et al., 2020), citric, lactic, acetic, oxaloacetic, etc. (Parsons and Fry, 2012; Della Monica et al., 2018).

In this study, phosphate-solubilizing fungi in the rhizospheric soil of crops were screened to obtain highly efficient phosphate-solubilizing mutants using ion beams, and the underlying phosphate-solubilizing mechanisms were explored from the perspective of secretion of organic acid, for example, lowering pH and chelating calcium ions to release phosphate. This study is aimed to provide biological materials and a theoretical basis for the development of highly efficient phosphate-solubilizing fungi and the characterization of phosphate-solubilizing mechanisms.

MATERIALS AND METHODS

Isolation and Screening of Phosphate-Solubilizing Fungi

The rhizospheric soil samples of wheat and cotton were collected from the Henan Institute of Science and Technology experimental field (longitude: 113.77° latitude: 35.46°) located at downstream region of the Yellow River of China. Five grams of rhizospheric soil was mixed evenly in 50 ml of sterile water using a shaker and then left to stand. The supernatant was collected and serially diluted (10^{-4}, 10^{-5}, and 10^{-6}). 0.20 ml of each fungi dilution was spread onto the solid PSFM and cultured at 28°C for 5 days, with five replicates in each treatment. Then, fungal colonies with obvious phosphate-solubilizing (clear) zones around them were selected, transferred to PDA slants, and stored at 4°C. The isolated phosphate-solubilizing fungi were cultured in the PSFM for 120 h, and the diameter of colonies (D_{colonies}) and the diameter of surrounding phosphate-solubilized zones ($D_{\text{solvent zones}}$) were measured. The fungal colonies with $D_{\text{solvent zones}}/D_{\text{colonies}} > 1.1$ were transferred to PDA slants and stored at 4°C. Then, spores from slants of phosphate-solubilizing fungi that had the above ratio > 2 were taken into 100 ml of PSFM and cultured on a shaker at 70 r·min^{-1} and 28°C for 5 days, with three olybdenum-stibium colorimetry method (Zhang et al., 2018), and the most efficient strains of phosphate-solubilizing fungi were selected as the test strains.

Identification of Phosphate-Solubilizing Fungi

The test strains were inoculated onto the PDA medium and cultured at 28°C for 2 days, and the colony morphology was observed. Potato dextrose agar (PDA) medium was composed of 200 g of potato, 20 g of sucrose, 20 g of agar, and 1,000 ml of distilled water (pH 7.00). The spores of *P. oxalicum* F9 were picked with a sterile toothpick and inoculated onto a

PDA plate. A 1 cm^2 metal sheet was inserted near the inoculation point, followed by culturing at 28°C. After the mycelia climbed on the metal sheet, they were observed under a Quanta 200 environmental scanning electron microscope (FEI Company, United States).

In the ITS sequence analysis, the *P. oxalicum* F9 was cultured on the PDA medium, and the mycelia on the surface of the dish were scraped off and ground in a mortar with liquid nitrogen. The genomic DNA was extracted from the ground mycelia using a Fungal DNA Extraction Kit (Sangon Biotech, Shanghai). The universal primers for the fungal ITS are: forward: ITS1 5'-TCCGTAGGTGAACCTGCGG-3′ and reverse: ITS4 5'-TCCTCCGCTTATTGATATGC-3′. The universal primers for fungal internal transcript space (ITS) sequence amplification were synthesized by TaKaRa Bioengineering (Dalian) Co., Ltd. The PCR products were sent to TaKaRa Bioengineering (Dalian) Co., Ltd., for sequencing, and the DNA sequences were obtained. Finally, the sequences were compared and analyzed through BLAST in GenBank, and the phylogenetic tree of *P. oxalicum* F9 was constructed using MEGA7.0 software.

Determination of pH of Phosphate-Solubilizing Fungal Culture Medium

PSFM liquid (1 ml) of phosphate-solubilizing fungi was taken and centrifuged at 8,000 r·min^{-1} for 5 min. The pH of supernatant was measured by pH meter. Phosphate-solubilizing fundamental medium (PSFM) was composed of 10 g of glucose, 0.30 g of NaCl, 0.30 g of KCl, 0.30 g of $MgSO_4{\cdot}7H_2O$, 0.03 g of $FeSO_4{\cdot}7H_2O$, 0.03 g of $MnSO_4{\cdot}4H_2O$, 0.50 g of $(NH_4)_2SO_4$, 5 g of $Ca_3(PO_4)_2$, and 1,000 ml of distilled water (pH 7.00–7.50). $Ca_3(PO_4)_2$ was added after being fully ground and sterilized. Solid PSFM was supplemented with 15 g·L^{-1} agar.

Ion Beam Mutagenesis for Phosphate-Solubilizing Fungus *Penicillium oxalicum* F9

Evenly mixed *P. oxalicum* F9 spore suspension (0.20 ml, 10^8 CFU·ml^{-1}) was spread in a clean and sterile Petri dish, placed on a super clean bench and blown dry with sterile air to prepare the *P. oxalicum* F9 spore membrane. The Petri dish was placed in a microbial target chamber of a Titan ion implanter, followed by radiation mutagenesis with low-energy nitrogen ions (20, 25, and 30 keV) at a radiation dose of 5×10^{14}, 1×10^{15}, 5×10^{15}, and 1×10^{16} ions·cm^{-2}, including the vacuum controls. After implantation, the bacterial membrane was rinsed with 1 ml of sterile water in a test tube, thoroughly dispersed and mixed, diluted to 10^{-3}, 10^{-4}, and 10^{-5}, and then spread onto a PSFM plate. The survival rate of *P. oxalicum* F9 was calculated as:

Penicillium oxalicum F9 was screened primarily based on $D_{\text{solvent zones}}/D_{\text{colonies}}$ and rescreened *via* PSFM culturing on a shaker at 28°C for 5 days. The phosphate-solubilizing ability of fungus strains was detected *via* molybdenum-antimony anti-colorimetry.

Determination of Organic Acids in Phosphate-Solubilizing Fungal Culture Medium

Penicillium oxalicum F9 culture medium (1 ml) was placed into a centrifuge tube and centrifuged at 8,000 r·min^{-1} for 5 min. The supernatant was filtered through a 0.22-μm filter membrane and injected by a 1 ml syringe into an ICS-2000 ion chromatograph (DIONEX, United States) for detection using a DIONEX IonPac®AS11-HC anion-exchange column (aqueous; sample flow rate: 1.20 ml·min^{-1}, column temperature: 30°C, injection volume: 0.50 ml). The chromatographic data were analyzed according to the instructions using a Chromeleon chromatographic working station.

Data Analysis

All tests and treatments were performed with three repetitions, and the values were expressed as the mean of them. Pearson correlation analysis was used to evaluate whether there was a significant relationship in phosphate-solubilizing ability of fungus and the culture medium pH. The significant data were compared using the LSD test of one-way ANOVA ($p < 0.05$).

RESULTS

Screening of Phosphate-Solubilizing Fungus

Nine strains (F1, F2, F3, F4, F5, F6, F7, F8, and F9) of phosphate-solubilizing fungi were isolated *via* the primary screening and rescreening based on the $D_{\text{solvent zones}}/D_{\text{colonies}}$ (**Figure 1**). All of them could grow on the PSFM plate with tricalcium phosphate as the only phosphorus source and could produce obvious halo zones. The $D_{\text{solvent zones}}/D_{\text{colonies}}$ of F1 was the lowest (1.18), and that of F9 was the highest (1.42). The

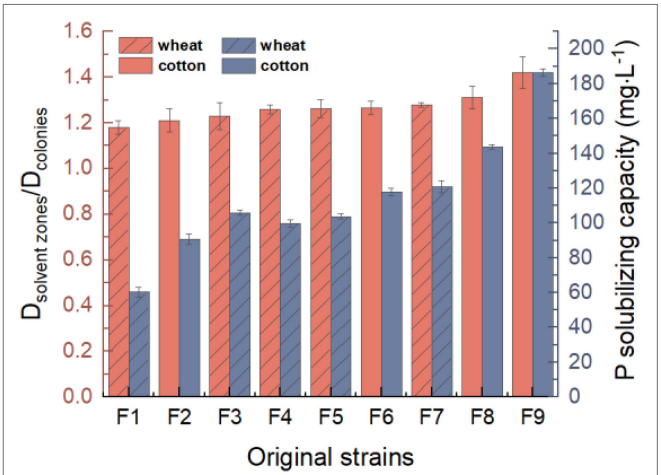

FIGURE 1 | Screening of phosphate solubilizing fungi from rhizospheric of crops. The red represents $D_{\text{solvent zones}}/D_{\text{colonies}}$ value, and the blue represents P-solubilizing capacity.

results of molybdenum-stibium colorimetry confirmed that eight strains could solubilize $Ca_3(PO_4)_2$. F9 had the strongest phosphate-solubilizing ability (186.41 mg·L^{-1}). Therefore, F9 was selected as a test strain for further research.

Identification of Phosphate-Solubilizing Fungus

Phosphate-solubilizing fungus F9 was inoculated onto the PDA medium and cultured at 28°C for 120 h, and the colony morphological characteristics are shown in **Figure 2A**. The F9 colonies on the PDA plate were white at first, gradually turned dark green and finally became grayish green, with white edges, were flat and floss-shaped, and conidia shed off easily. Obvious solubilized (halo) zones emerged on the PSFM plate (**Figure 2B**). The structure of phosphate-solubilizing fungus F9 observed under the electron microscope is shown in **Figure 2C**. The conidiophores of F9 were found in the substrate, and the penicillus was composed of verticillated sterigma of conidiophores, showing single verticillation. According to the contrast analysis in line with Fungal Identification Manual, fungus F9 conformed to the growth characteristics of *Penicillium*.

The molecular identification of F9 was performed using the ITS technique. The ITS sequence of F9 was obtained by PCR amplification, and the GenBank ID was KT351451. The results of BLAST analysis revealed that this sequence was 99% homologous to the ITS sequence of related *Penicillium* strains published. The phylogenetic tree based on the *Penicillium* rDNA-ITS sequence was constructed using MEGA7.0 software (**Figure 2D**). It was found that the evolutionary distance between phosphate-solubilizing fungus F9 and *P. oxalicum* SD123 KP639194.1 was the shortest. Combined with the morphological characteristics and the structural characteristics of conidia, the phosphate-solubilizing fungus F9 was preliminarily determined as *P. oxalicum*.

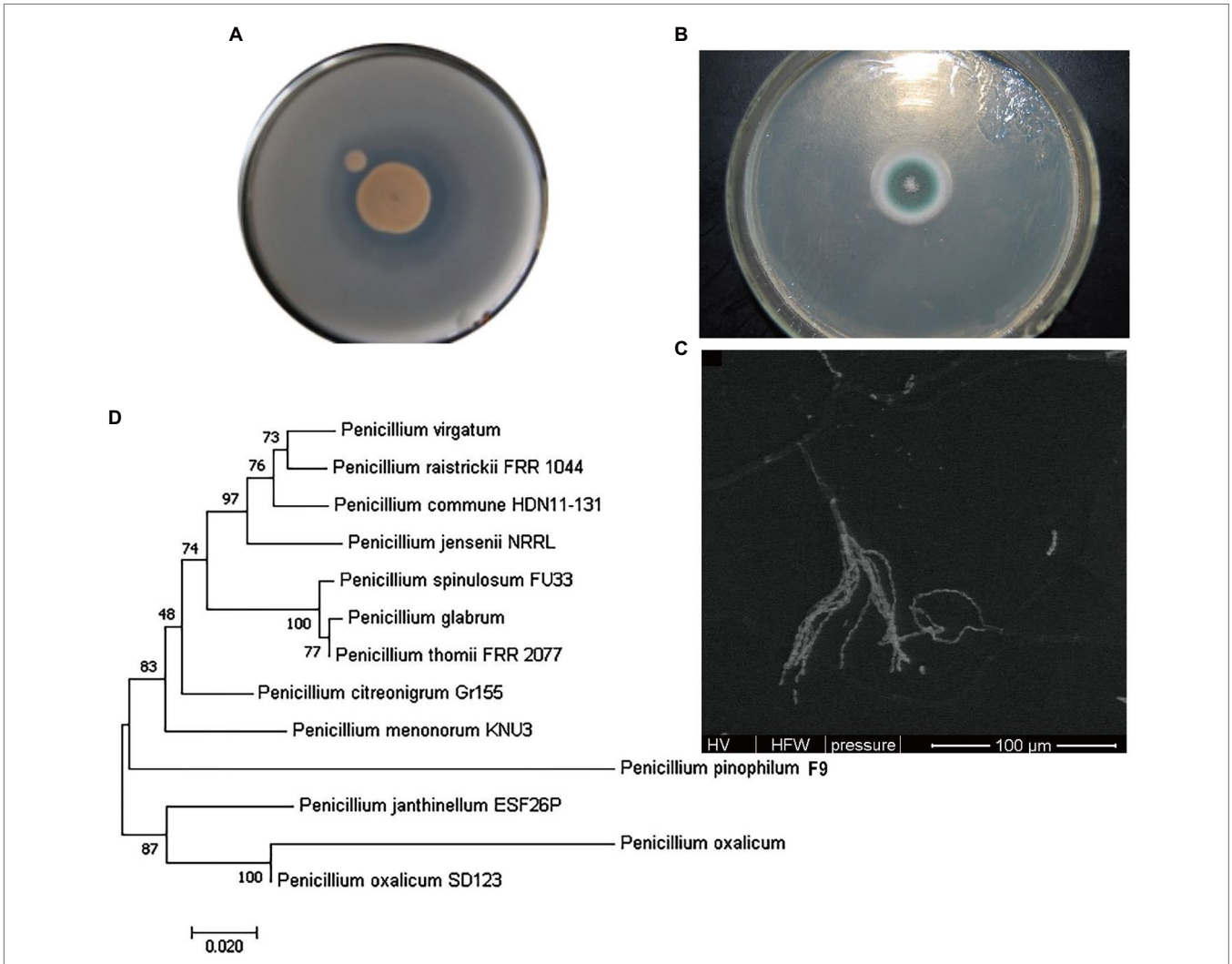

FIGURE 2 | Identification of phosphate-solubilizing fungus F9. **(A)** Colony of F9. **(B)** Solubilized (halo) zone of F9. **(C)** Electron micrograph of F9. **(D)** Phylogenetic tree of F9.

Analysis of Organic Acids in the Culture Medium of *Penicillium oxalicum* F9 During Growth

Ion chromatograms for the culture medium of phosphate-solubilizing *P. oxalicum* F9 cultured in the PSFM for 24, 72, 96, and 120 h are shown in **Figure 3E**. Obviously, it shows solubilization of calcium phosphate in the culture medium of *P. oxalicum* F9 at various time points during growth. There were four obvious absorption peaks (6.60, 7.30, 15.60, and 19.10 min of elution time) in the culture medium during solubilization of calcium phosphate by *P. oxalicum* F9. Furthermore, it was found that the retention times of the four peaks a, b, c, and d (**Figure 3E**) were the same as those of the single standard samples of lactic acid, acetic acid, oxalic acid, and phosphoric acid, respectively (**Figures 3A–D**). The absorption peaks of lactic acid, acetic acid, and oxalic acid were low after 24 h of growth and were gradually increased during additional growth. The absorption peaks of lactic acid and acetic acid were the highest after 96 h, whereas oxalic acid had the highest absorption peak after 120 h of growth. Lactic acid and acetic acid had higher absorption peaks than oxalic acid after 24, 72, and 96 h of growth, whereas oxalic acid had a remarkably higher absorption peak than lactic acid and acetic acid after 120 h of growth. The absorption peak (corresponding to phosphoric acid) was not detected on prophase, but the absorption peak increased gradually with the increase in fermentation time. The

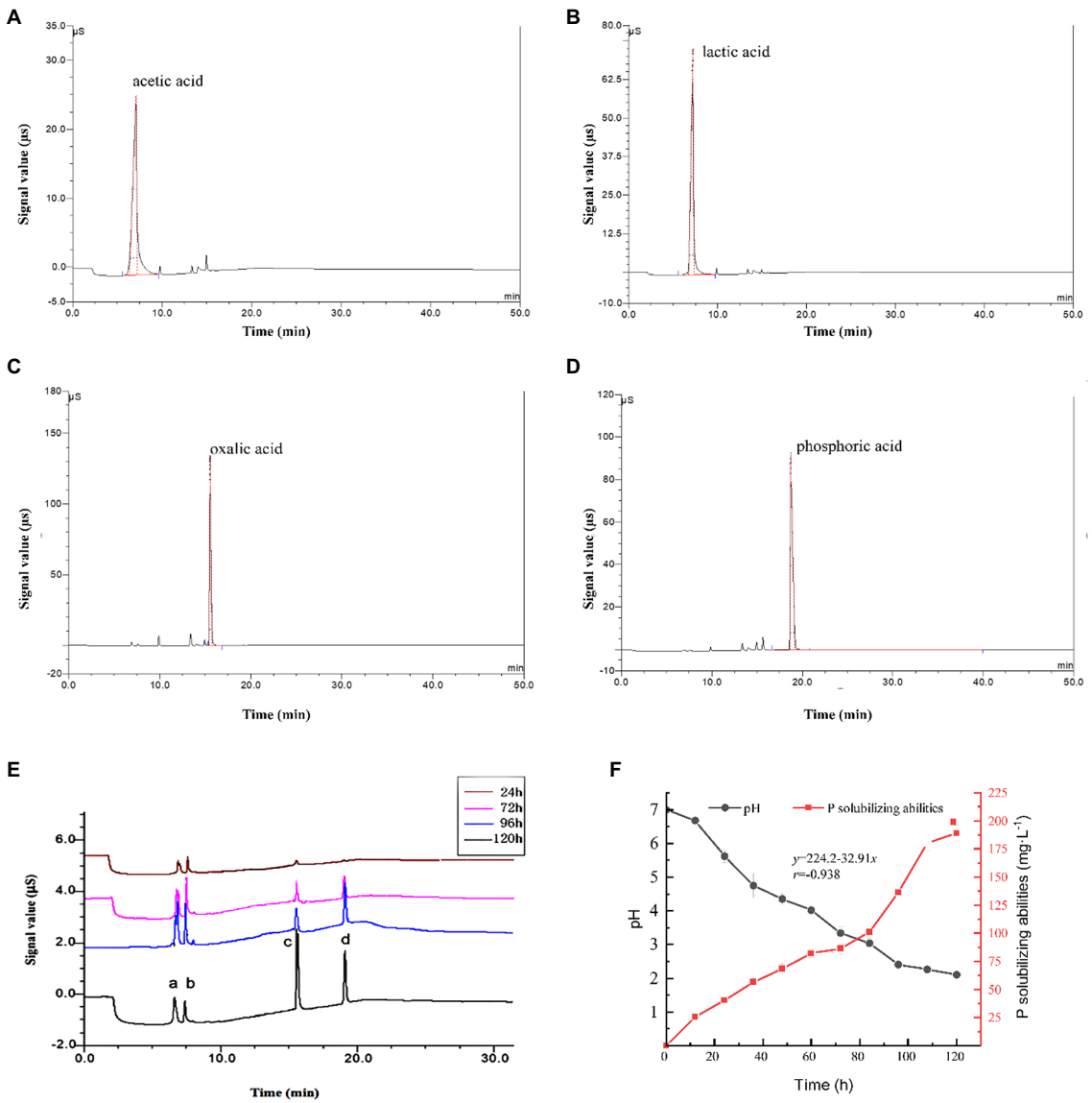

FIGURE 3 | *Penicillium oxalicum* F9 phosphorus-solubilizing ability. **(A–D)**. The ion chromatograms of lactic acid, acetic acid, oxalic acid, and phosphoric acid standard samples, respectively. **(E)** Ion chromatography of *P. oxalicum* F9 culture medium during growth, a, b, c, and d is lactic acid, acetic acid, oxalic acid, and phosphoric acid, respectively. **(F)** Culture medium pH and P-solubilizing capacity of *P. oxalicum* F9.

reason may be that the total amount of organic acids is low in the early stage and the ability of organic acids to dissolve insoluble calcium phosphate to release soluble phosphorus is limited. With the extension of culture time, the total amount of organic acids secreted by *P. oxalicum* F9 gradually increased, resulting in the increase in phosphate release. The content of organic acids in different stages is shown in **Table 1**.

During solubilization of calcium phosphate by *P. oxalicum* F9, the concentration of lactic, acetic, and oxalic acids, as well as total acids showed an increasing trend when incubation time was prolonged. After 24 h, the concentrations of lactic acid and acetic acid were 0.023 mmol·L^{-1} and 0.015 mmol·L^{-1}, respectively, whereas the concentration of oxalic acid (0.010 mmol·L^{-1}) was significantly lower than that of lactic acid and acetic acid ($p < 0.05$). With the increased culturing time, the concentration of lactic, acetic, and oxalic acids, as well as total acids displayed an upward trend. The concentration of lactic acid (0.054 mmol·L^{-1}) and acetic acid (0.054 mmol·L^{-1}) was highest after 96 h of culturing, and that of oxalic acid (0.064 mmol·L^{-1}) peaked after 120 h of culturing. Furthermore, the concentration of oxalic acid was higher than that of lactic acid (by 0.024 mmol·L^{-1}) and acetic acid (by 0.026 mmol·L^{-1}).

Meanwhile, the pH of the culture medium gradually declined with an increase in culturing time during solubilization of calcium phosphate by *P. oxalicum* F9 (**Figure 3F**). At 108 and 120 h, the pH tended to be stable and dropped to 2.40. The phosphate-solubilizing effect was enhanced with the prolonged culturing time. The phosphate-solubilizing ability of *P. oxalicum* F9 on calcium phosphate reached 180–190 mg·L^{-1} after 108 h. During solubilization of calcium phosphate by *P. oxalicum* F9, there was a correlation between the culture medium pH and phosphate-solubilizing ability. The lower the pH of the culture medium was, the stronger the phosphate-solubilizing effect would be, showing a negative correlation ($r = -0.938$).

Phosphate-Solubilizing Effect of *Penicillium oxalicum* F9 on the Different Phosphorus Sources

To evaluate the phosphate-solubilizing effect of *P. oxalicum* F9 on the different insoluble phosphorus sources, except for, the other insoluble phosphorus sources $AlPO_4$ and $FePO_4$ were utilized in our research (**Table 2**). The total acid concentration in medium was 0.143 mmol·L^{-1} for insoluble phosphorus sources $Ca_3(PO_4)_2$; however, the total acid concentrations for $AlPO_4$ and $FePO_4$ were 0.073 and 0.089 mmol·L^{-1}, lower than the insoluble phosphorus sources $Ca_3(PO_4)_2$. And the solubilizing ability of *P. oxalicum* F9 on $Ca_3(PO_4)_2$ was 189.10 mg·L^{-1} and significantly higher than the other two insoluble phosphorus sources $AlPO_4$, 40.83 mg·L^{-1}, and $FePO_4$, 72.11 mg·L^{-1} ($p < 0.05$). This result indicated that the phosphate-solubilizing ability of *P. oxalicum* F9 on $Ca_3(PO_4)_2$, as a phosphorus source, was greater than on $AlPO_4$ and $FePO_4$. Consequently, to better investigate the phosphorus solubilization ability of *P. oxalicum* F9 and its mutant strains, the following study used $Ca_3(PO_4)_2$, as a source of insoluble phosphorus.

Ion-Beam Mutagenesis of *Penicillium oxalicum* F9

The *P. oxalicum* F9 spores were subjected to the first round of mutagenesis *via* low-energy nitrogen ion radiation at the doses of 30 keV, 1×10^{15} ions·cm^{-2} and 25 keV, 1×10^{16} ions·cm^{-2}. The fungal strains were initially screened by assessing the solubilized (halo) zones (**Figure 4**) on the solid PSFM plates

TABLE 1 | Organic acids in the *Penicillium oxalicum* F9 culture medium.

Duration of growth	Organic acids (mmol·L^{-1})			
	Lactic acid	Acetic acid	Oxalic acid	Total acids
24 h	0.023 ± 0.003d	0.015 ± 0.003c	0.010 ± 0.001c	0.047 ± 0.008c
72 h	0.033 ± 0.001c	0.051 ± 0.004a	0.033 ± 0.005b	0.139 ± 0.013b
96 h	0.054 ± 0.002a	0.053 ± 0.003a	0.047 ± 0.009b	0.153 ± 0.014a
120 h	0.040 ± 0.001b	0.038 ± 0.003b	0.064 ± 0.004a	0.163 ± 0.003a

The significance letters in each column indicate significant differences in various stages of growth.

TABLE 2 | The phosphate-solubilizing ability of *Penicillium oxalicum* F9 in different phosphorus sources.

Phosphorus source	Organic acid (mmol·L^{-1})				P-solubilizing abilities (mg·L^{-1})
	Lactic acid	Acetic acid	Oxalic acid	Total acid	
$Ca_3(PO_4)_2$	0.040 ± 0.001a	0.038 ± 0.003a	0.064 ± 0.004a	0.143 ± 0.010a	189.10 ± 6.21a
$AlPO_4$	0.021 ± 0.002b	0.020 ± 0.004c	0.052 ± 0.005b	0.073 ± 0.010c	40.83 ± 4.30c
$FePO_4$	0.010 ± 0.010c	0.037 ± 0.008b	0.042 ± 0.002c	0.089 ± 0.008b	72.11 ± 3.92b

The significance letters in each column indicate significant differences in different phosphorus sources.

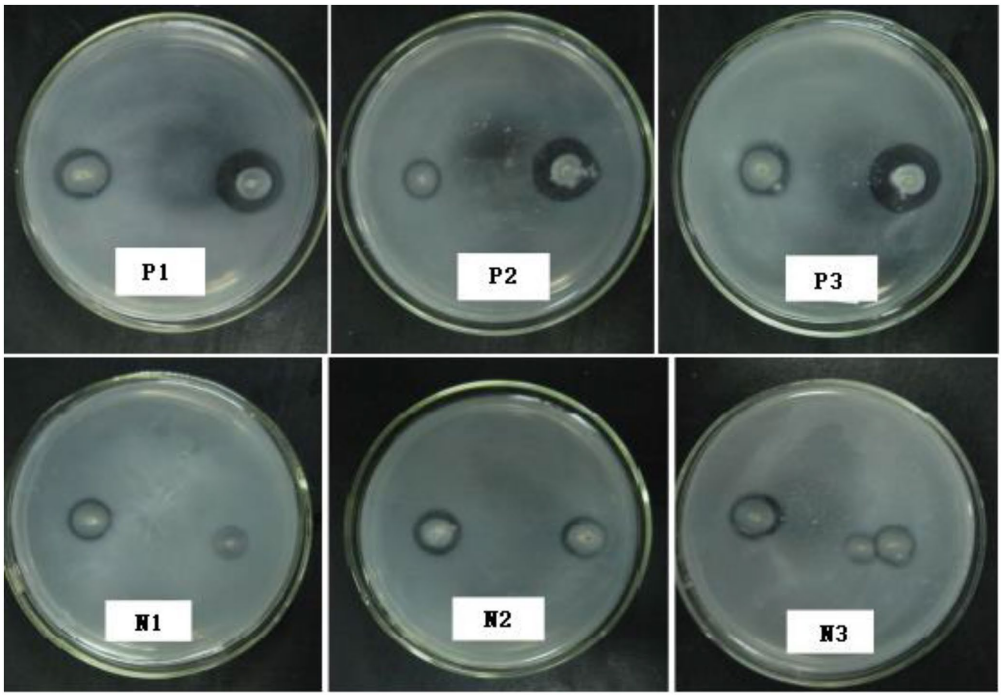

FIGURE 4 | Soluble (halo) zones of mutants after the second round of mutagenesis.

TABLE 3 | Positive and negative mutants of *Penicillium oxalicum* F9 obtained by low-energy ion beam mutagenesis.

Mutagenesis	Mutants	$D_{solvent\ zones}/D_{colonies}$	P-solubilizing capacity ($mg \cdot L^{-1}$)	Change in P-solubilizing capacity (%)
	F9	1.24 ± 0.05	186.41 ± 3.20	0
	p-1	1.66 ± 0.06	235.70 ± 3.59	+26.41 ± 1.93
	p-2	1.49 ± 0.06	228.20 ± 2.61	+22.41 ± 1.41
	p-3	1.45 ± 0.02	225.92 ± 4.88	+21.23 ± 2.62
	p-4	1.49 ± 0.04	225.01 ± 4.27	+20.71 ± 2.29
	p-5	1.48 ± 0.05	224.13 ± 4.43	+20.20 ± 2.38
	p-6	1.47 ± 0.08	223.91 ± 6.25	+20.12 ± 3.35
First round	n-1	1.04 ± 0.04	133.80 ± 3.13	−28.21 ± 1.68
	n-2	1.08 ± 0.03	141.92 ± 2.66	−23.92 ± 1.43
	n-3	1.12 ± 0.07	145.51 ± 4.60	−22.03 ± 2.47
	n-4	1.14 ± 0.05	147.31 ± 4.41	−21.01 ± 2.37
	n-5	1.12 ± 0.06	147.72 ± 2.88	−20.80 ± 1.54
	n-6	1.10 ± 0.02	148.40 ± 3.54	−20.41 ± 1.90
	n-7	1.12 ± 0.06	148.92 ± 3.15	−20.11 ± 1.69
	n-8	1.11 ± 0.07	149.21 ± 3.19	−20.03 ± 1.71
	n-9	1.10 ± 0.01	149.11 ± 1.39	−20.02 ± 0.75
	P1	2.02 ± 0.06	291.81 ± 5.50	+56.88 ± 2.96
	P2	1.92 ± 0.06	264.62 ± 10.21	+42.26 ± 5.48
Second round	P3	2.12 ± 0.04	245.80 ± 8.72	+32.15 ± 4.67
	N1	1.00 ± 0.04	97.61 ± 4.41	−47.53 ± 2.36
	N2	1.03 ± 0.02	120.40 ± 7.21	−35.27 ± 3.87
	N3	1.02 ± 0.03	128.60 ± 8.30	−30.86 ± 4.46

and rescreened *via* culturing in the liquid medium on a shaker for 120 h; as a result, we identified six phosphate-solubilizing *Penicillium* strains with more than 20% increased phosphate-solubilizing ability and nine strains with 20% decreased phosphate-solubilizing ability (**Table 3**). The phosphate-solubilizing ability of positive mutant strain p-1 was enhanced most significantly (235.70 $mg \cdot L^{-1}$), up by 26.40% compared with the control strain. The phosphate-solubilizing ability of negative mutant strain n-1 declined most significantly (133.80 $mg \cdot L^{-1}$), down by 28.20% compared with the control strain. The p-1 and n-1 strains were subjected to the second round of mutagenesis under the same radiation conditions. Six mutant strains varying in phosphate-solubilizing ability by more than 30% were obtained, including three positive (P1, P2, and P3) and three negative (N1, N2, and N3) mutant strains. The soluble (halo) zones of the six mutant strains are shown in **Figure 4** and **Table 3** displays the quantification of the phosphate-solubilizing ability. The soluble (halo) zones of positive mutant strains (P1, P2, and P3) of *Penicillium* strains were greater compared with those of the control strains, whereas the negative mutant strains (N1, N2, and N3) had substantially smaller soluble (halo) zones compared with the control strains (**Figure 4**). Compared with that of control strains, the phosphate-solubilizing ability of P1, P2, and P3 was enhanced by 56.88%, 42.26%, and 32.15%, and that of N1, N2, and N3 was weakened by 47.53%, 35.27%, and 30.86%, respectively.

Analysis of organic acids and pH of culture medium of mutant strains of phosphate-solubilizing *P. oxalicum* F9.

After the *P. oxalicum* F9 strain and the mutant strains (P1, P2, and P3 as well as N1, N2, and N3) were cultured in the PSFM for 120 h, the organic acid concentrations and pH of the culture medium were analyzed (**Figures 5, 6**).

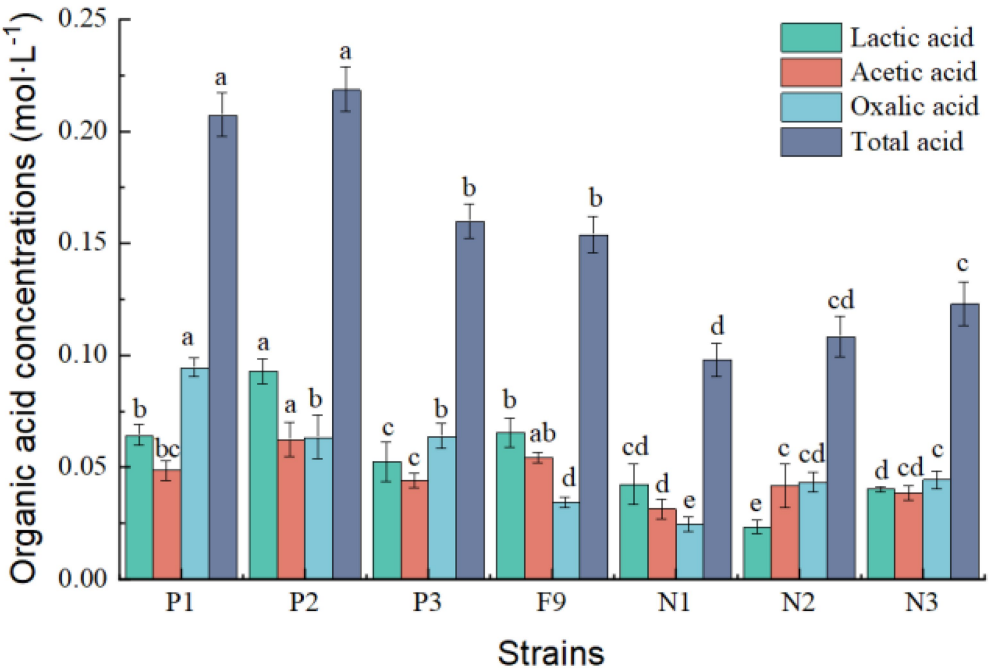

FIGURE 5 | Organic acid content in PSFM medium of *Penicillium oxalicum* F9 and mutants. a, b, c, d, and e indicate significant differences in various strains.

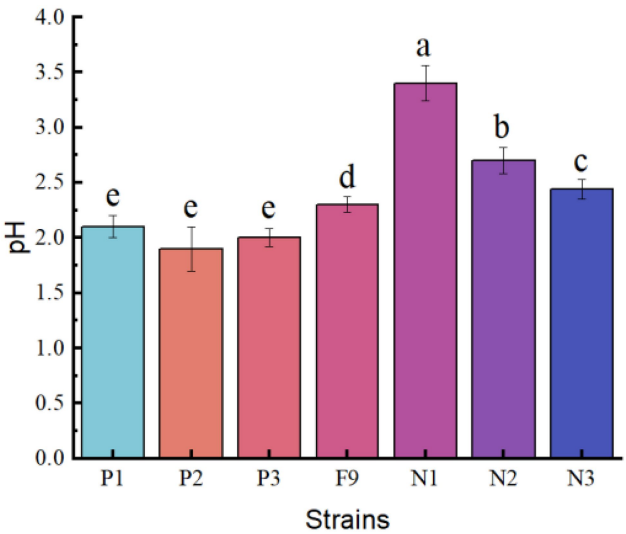

FIGURE 6 | The pH of the PSFM culture medium of *Penicillium oxalicum* F9 and mutants. a, b, c, d, and e indicate significant differences in various strains.

The total amounts of organic acids secreted by the three positive mutant strains P1, P2, and P3 were 0.207, 0.218, and 0.160 mmol·L^{-1}, respectively, representing increases of 68.73%, 77.85%, and 30.13%, respectively, compared with the original strain *P. oxalicum* F9 ($p < 0.05$). The total amounts of organic acids secreted by the three negative mutant strains N1, N2, and N3 were 0.098, 0.108, and 0.114 mmol·L^{-1}, respectively, representing decreases of 20.36%, 11.89%, and 7.41%, respectively, compared with the original *P. oxalicum* F9 strain ($p < 0.05$; **Figure 5**). The phosphate-solubilizing ability of positive mutant strains P1, P2, and P3 was enhanced by 56.88%, 42.26%, and 32.15%, whereas that of negative mutant strains N1, N2, and N3 was weakened by 47.53%, 35.27%, and 30.86%, respectively, compared with *P. oxalicum* F9 (**Table 2**). The larger the total amount of organic acids secreted by the strains, the stronger their phosphate-solubilizing ability would be.

The pH of the culture medium of the positive mutant strains P1, P2, and P3 was 2.10, 1.91, and 2.02, respectively, and there was no significant difference among the three ($p > 0.05$). However, the pH of the culture medium of the three mutant strains was significantly lower than that of the *P. oxalicum* F9 ($p < 0.05$). The capacity of the three mutant strains to acidify the growth medium was stronger than that of the *P. oxalicum* F9. The pH of the culture medium of inoculation strains N1, N2, and N3 was 3.42, 2.71, and 2.44, respectively. The pH of the culture medium of the three mutant strains was significantly higher than that of the original *P. oxalicum* F9 strain ($p < 0.05$). The capacity of the three mutant strains to acidify the growth medium was weaker than that of the *P. oxalicum* F9. The three positive mutant strains had lower pH, and the three negative mutant strains had higher pH than *P. oxalicum* F9. Based on the phosphate-solubilizing ability of *P. oxalicum* F9 and the mutant strains (**Table 2**), it can be inferred that the phosphate-solubilizing ability of phosphate-solubilizing *P. oxalicum* F9 had a negative correlation with the pH of the culture medium.

DISCUSSION

Currently, there have been about 60 types of phosphate-solubilizing fungi identified (Busato et al., 2017), and they mainly belong to *Alternaria*, *Aspergillus*, *Fusarium*, *Penicillium*, *Talaromyces*, and *Trichoderma* (Doilom et al., 2020). *Aspergillus* and *Penicillium* have widely reported fungi with a strong phosphate-solubilizing ability (Kucey, 1983; Hao et al., 2021). Lin et al. (2001) conducted a comparative study on the phosphate-solubilizing ability of some bacteria and fungi and found that the capacity of bacteria to dissolve phosphate rock powder ranged from 26.92 to 43.34 mg·L^{-1}, whereas the capacity of most fungi was 59.64–145.36 mg·L^{-1}; hence, fungi have a stronger capacity to dissolve phosphate rock powder than bacteria. Nath et al. (2012) found two strains of *Penicillium* with a strong phosphate-solubilizing ability (39.22 and 86.10 mg·L^{-1}). In the current study, nine strains of phosphate-solubilizing fungi were isolated from the rhizospheric soil of major crops wheat and cotton in the downstream region of the Yellow River. Among them, *P. oxalicum* F9 had the strongest phosphate-solubilizing ability, and it was identified by morphological and molecular characterization that the strain was *Penicillium oxalicum* with the high phosphate-solubilizing activity (186.41 mg·L^{-1}), higher than that of bacteria and fungi of the same type reported previously. The *P. oxalicum* F9 isolated in this study provides important material for the research on the phosphate-solubilizing mechanism and application of phosphate-solubilizing fungi.

Low-energy ion beam mutagenesis leads to single base substitution and DNA double-strand breakage (Thopan et al., 2017), and a large number of free radicals will be produced. Mutation breeding of highly efficient phosphate-solubilizing fungi microorganisms and characterization of the underlying phosphate-solubilizing mechanism has always been hot research topics in the field of soil microorganisms and biofertilizers (Guo et al., 2019). The phosphate-solubilizing effect of microorganisms can be enhanced by radiation mutagenesis. Silva et al. (2014) induced mutation of *Aspergillus niger via* UV and confirmed that the phosphate-solubilizing ability of mutant FS1-331 was increased by 1.70 times compared with that of wild strains. In recent years, low-energy ion beam mutagenesis for microorganisms has been extensively researched (You et al., 2009; Li et al., 2011a; Zhang et al., 2016; Semsang et al., 2018). Semsang et al. (2018) used low-energy N ion beam mutagenesis to acquire a mutant which had improved yields and seed quality. In this study, *P. oxalicum* F9 was subjected to two rounds of low-energy nitrogen ion mutagenesis. The three positive mutants (P1, P2, and P3) obtained by ion beam mutagenesis had significantly higher phosphorus solubilization abilities than the control strain (56.88%, 42.26%, and 32.15%); in contrast, the three negative mutants exhibited significantly lower phosphorus solubilization abilities than the control strain. In addition, the acidification and organic acid secretion by the positive mutant strains obtained by ion beam mutagenesis were markedly stronger than those of *P. oxalicum* F9, but they were weaker in the negative mutant strains than those of *P. oxalicum* F9 (**Figures 5, 6**). Ion beam mutagenesis can alter the acidification, organic acid-secreting, and phosphate-solubilizing capacities of *P. oxalicum* F9. In summary, numerous phosphate-solubilizing mutants were induced *via* low-energy ion implantation, which provided valuable test materials for breeding of highly efficient phosphate-solubilizing microorganisms and exploration of the underlying phosphate-solubilizing mechanism in *P. oxalicum* F9.

Secreting organic acids is a common phenomenon and also the main reason for the phosphate-solubilizing effect by phosphate-solubilizing microorganisms that can secrete organic acids to lower the growth medium pH, thereby solubilizing insoluble inorganic phosphorus (Alori et al., 2017; Tomer et al., 2017; Zhang et al., 2018). Most studies showed a significant correlation between the phosphate-solubilizing ability of phosphate-solubilizing bacteria and the pH of fermentation liquid. In this study, the capacity of *P. oxalicum* F9 to solubilize calcium phosphate in the PSFM was significantly and negatively correlated with the pH of the culture medium ($r = -0.938$). There was also a similar relation between the phosphate-solubilizing ability of mutant strains obtained by ion beam mutagenesis and the pH. The pH of the culture medium of the positive mutant strains (P1, P2, and P3) at 120 h (pH 2.40) was significantly lower than that of *P. oxalicum* F9 ($p < 0.05$), whereas the pH of the culture medium of the negative mutant strains (N1, N2, and N3) at 120 h was evidently higher than that of *P. oxalicum* F9. The phosphate-solubilizing ability of the mutant strains of phosphate-solubilizing *P. oxalicum* F9 was negatively correlated with the pH of their culture medium.

The organic acids secreted by phosphate-solubilizing *P. oxalicum* F9 form complexes or chelates with calcium ions of water-insoluble calcium phosphate so that the phosphate ions are released. During solubilization of calcium phosphate in the PSFM by *P. oxalicum* F9 and its mutants, the three types of organic acids (lactic acid, acetic acid, and oxalic acid) were secreted. It is speculated that these three types are the main organic acids involved in phosphate solubilization by *P. oxalicum* F9. During the growth of *P. oxalicum* F9 and solubilization of calcium phosphate, the total amount of organic acids secreted increased, and the phosphate-solubilizing effect also became more obvious with the increased duration of growth. In this study, the concentration of lactic acid and acetic acid in the culture medium was significantly higher than that of oxalic acid after 24 h of growth ($p < 0.05$), whereas the concentration of oxalic acid was significantly higher than that of lactic acid and acetic acid after 120 h of growth ($p < 0.05$). It is speculated that the phosphate-solubilizing effect of *P. oxalicum* F9 was dominated by lactic acid and acetic acid after 24 h of growth, but it is dominated by oxalic acid after 120 h of growth. The close relation between the total amount of organic acids secreted by *P. oxalicum* F9 and its phosphate-solubilizing effect was also confirmed in the mutant strains. The total amount of organic acids of the three positive mutant strains (P1, P2, and P3) was significantly larger than that of the *P. oxalicum* F9, whereas the three negative mutant strains (N1, N2, and N3) secreted significantly less organic acids than *P. oxalicum* F9. Consequently, a stronger capacity of *P. oxalicum* F9 to secrete organic acids will result in a greater capacity of it to solubilize phosphate.

CONCLUSION

In this study, a phosphorus-solubilizing fungus *P. oxalicum* F9 was isolated from the rhizospheric soil under wheat and cotton fields in the lower reaches of the Yellow River. *P. oxalicum* F9 dissolved water-insoluble calcium phosphate by secreting lactic acid, acetic acid, and oxalic acid. And the secretion of the above three organic acids gradually increased with the extension of the culture time with pH values of the medium decreased correspondingly. In addition, the organic acids formed complexes or chelates with calcium ions, so that the phosphate was released. Furthermore, compared with the original strain, the high-efficiency phosphorus-solubilizing mutant obtained by ion beam mutagenesis secreted more organic acids and had a stronger phosphorus-solubilizing effect. Overall, this study provides a theoretical basis and a new direction for the study and development of the phosphorus-solubilizing mechanism of phosphorus-solubilizing fungi.

DATA AVAILABILITY STATEMENT

The raw data supporting the conclusions of this article will be made available by the authors, without undue reservation.

AUTHOR CONTRIBUTIONS

TY, LL, BW, JT, SZ, and ZW designed and performed research study. TY, LL, SZ, and FS wrote the paper. All authors contributed to the article and approved the submitted version.

FUNDING

This research was supported by National Natural Science Foundation of China (11305047) and Science and Technology Program of Henan Province (222102110122).

REFERENCES

Ahuja, A., Ghosh, S. B., and D'souza, S. F. (2007). Isolation of a starch utilizing, phosphate solubilizing fungus on buffered medium and its characterization. *Bioresour. Technol.* 98, 3408–3411. doi: 10.1016/j.biortech.2006.10.041

Alori, E. T., Glick, B. R., and Babalola, O. O. (2017). Microbial phosphorus solubilization and its potential for use in sustainable agriculture. *Front. Microbiol.* 8, 971. doi: 10.3389/fmicb.2017.00971

Antoun, H. (2012). Beneficial microorganisms for the sustainable use of phosphates in agriculture. *Procedia Eng* 46, 62–67. doi: 10.1016/j.proeng.2012.09.446

Busato, J. G., Zandonadi, D. B., Mol, A. R., Souza, R. S., Aguiar, K. P., Junior, F. B., et al. (2017). Compost biofortification with diazotrophic and P-solubilizing bacteria improves maturation process and P availability. *J. Sci. Food Agric.* 97, 949–955. doi: 10.1002/jsfa.7819

Chakdar, H., Dastager, S. G., Khire, J. M., Rane, D., and Dharne, M. S. (2018). Characterization of mineral phosphate solubilizing and plant growth promoting bacteria from termite soil of arid region. *3. Biotech* 8:463. doi: 10.1007/s13205-018-1488-4

Della Monica, I. F., Godoy, M. S., Godeas, A. M., and Scervino, J. M. (2018). Fungal extracellular phosphatases: their role in P cycling under different pH and P sources availability. *J. Appl. Microbiol.* 124, 155–165. doi: 10.1111/jam.13620

Doilom, M., Guo, J. W., Phookamsak, R., Mortimer, P. E., Karunarathna, S. C., Dong, W., et al. (2020). Screening of phosphate-solubilizing fungi from air and soil in Yunnan, China: four novel species in Aspergillus, Gongronella, Penicillium, and Talaromyces. *Front. Microbiol.* 11:585215. doi: 10.3389/fmicb.2020.585215

Gong, M., Tang, C., and Zhu, C. (2014). Cloning and expression of delta-1-pyrroline-5-carboxylate dehydrogenase in Escherichia coli DH5α improves phosphate solubilization. *Can. J. Microbiol.* 60, 761–765. doi: 10.1139/cjm-2014-0412

Guo, X., Zhang, M., Gao, Y., Cao, G., Yang, Y., Lu, D., et al. (2019). A genome-wide view of mutations in respiration-deficient mutants of Saccharomyces cerevisiae selected following carbon ion beam irradiation. *Appl. Microbiol. Biotechnol.* 103, 1851–1864. doi: 10.1007/s00253-019-09626-0

Hao, S., Tian, J., Liu, X., Wang, P., Liu, Y., Deng, S., et al. (2021). Combined effects of Penicillium oxalicum and tricalcium phosphate on lead immobilization: performance, mechanisms and stabilities. *Ecotox Environ Safe* 227:112880. doi: 10.1016/j.ecoenv.2021.112880

Khan, M. S., Zaidi, A., and Ahmad, E. (2014). "Mechanism of phosphate solubilization and physiological functions of phosphate-solubilizing microorganisms," in *Phosphate Solubilizing Microorganisms*. eds. M. Khan, A. Zaidi and J. Musarrat (Cham: Springer), 34–35. doi: 10.1007/978-3-319-08216-5_2

Kucey, R. M. N. (1983). Phosphate-solubilizing bacteria and fungi in various cultivated and virgin Alberta soils. *Can. J. Soil Sci.* 63, 671–678. doi: 10.4141/cjss83-068

Li, F., Wang, T., Xu, S., Yuan, H., Bian, P., Wu, Y., et al. (2011a). Abscopal mutagenic effect of low-energy-ions in Arabidopsis thaliana seeds. *Int. J. Radiat. Biol.* 87, 984–992. doi: 10.3109/09553002.2011.574780

Li, S. C., Zhang, P. P., Gu, S. B., Liu, H. X., Liu, Y., and Liu, S. N. (2013). Screening of lipid high producing mutant from rhodotorula glutinis by low ion implantation and study on optimization of fermentation medium. *Indian J. Microbiol.* 53, 343–351. doi: 10.1007/s12088-013-0361-8

Li, J., Zhang, S., Shi, S., and Huo, P. (2011b). Mutational approach for N2-fixing and P-solubilizing mutant strains of Klebsiella pneumoniae RSN19 by microwave mutagenesis. *World J. Microbiol. Biotechnol.* 27, 1481–1489. doi: 10.1007/s11274-010-0600-7

Li, J., Zhang, Y., Yu, Z., Wang, Y., Yang, Y., Liu, Z., et al. (2007). Superior storage stability in low lipoxygenase maize varieties. *J. Stored Prod. Res.* 43, 530–534. doi: 10.1016/j.jspr.2006.09.005

Lin, Q., Wang, H., Zhao, X., and Zhao, Z. (2001). Capacity of some bacteria and fungi in dissolving phosphate rock. *Microbiology* 28, 26–30. doi: 10.13344/j.microbiol.china.2001.02.008

Maekawa, M., Hase, Y., Shikazono, N., and Tanaka, A. (2003). Induction of somatic instability in stable yellow leaf mutant of rice by ion beam irradiation. *Nucl Instrum Meth B* 206, 579–585. doi: 10.1016/s0168-583x(03)00839-5

Mendes, G. O., Dias, C. S., Silva, I. R., Junior, J. I., Pereira, O. L., and Costa, M. D. (2013). Fungal rock phosphate solubilization using sugarcane bagasse. *World J. Microbiol. Biotechnol.* 29, 43–50. doi: 10.1007/s11274-012-1156-5

Mendes, G. D., Murta, H. M., Valadares, R. V., Da Silveira, W. B., Da Silva, I. R., and Costa, M. D. (2020). Oxalic acid is more efficient than sulfuric acid for rock phosphate solubilization. *Miner. Eng.* 155:106458. doi: 10.1016/j.mineng.2020.106458

Nath, R., Sharma, G. D., and Barooah, M. (2012). Efficiency of tricalcium phosphate solubilization by two different endophytic Penicillium sp. isolated from tea (Camellia sinensis L.). *Euro J of Exper Biol* 2, 1354–1358.

Nguyen, N. H., and Bruns, T. D. (2015). The microbiome of Pinus muricata ectomycorrhizae: community assemblages, fungal species effects, and Burkholderia as important bacteria in multipartnered symbioses. *Microb. Ecol.* 69, 914–921. doi: 10.1007/s00248-015-0574-y

Okamura, M., Yasuno, N., Ohtsuka, M., Tanaka, A., Shikazono, N., and Hase, Y. (2003). Wide variety of flower-color and -shape mutants regenerated from leaf cultures irradiated with ion beams. *Nucl Instrum Meth B* 206, 574–578. doi: 10.1016/s0168-583x(03)00835-8

Parsons, H. T., and Fry, S. C. (2012). Oxidation of dehydroascorbic acid and 2, 3-diketogulonate under plant apoplastic conditions. *Phytochemistry* 75, 41–49. doi: 10.1016/j.phytochem.2011.12.005

Peng, Y., Gong, X., Zhu, Y., Li, B., Lu, D., Yang, H., et al. (2020). Breeding of a highly effective organophosphorus-degrading mutant bacteria obtained by ion beam irradiation. *J. Radiat. Res. Radiat Process* 38, 59–68. doi: 10.11889/j.1000-3436.2020.rrj.38.040401

Semsang, N., Techarang, J., Yu, L. D., and Phanchaisri, B. (2018). Low-energy N-ion beam biotechnology application in the induction of Thai jasmine rice mutant with improved seed storability. *Nucl. Instrum. Meth. B* 425, 32–37. doi: 10.1016/j.nimb.2018.04.007

Sharma, S. B., Sayyed, R. Z., Trivedi, M. H., and Gobi, T. A. (2013). Phosphate solubilizing microbes: sustainable approach for managing phosphorus deficiency in agricultural soils. *Springerplus* 2:587. doi: 10.1186/2193-1801-2-587

Shi, F., Yin, Z., Jiang, H., and Fan, B. (2014). Screening, identification of P-dissolving fungus P 83 strain and its effects on phosphate solubilization and plant growth promotion. *Acta Microbiol Sin.* 54, 1333–1343. doi: 10.13343/j.cnki.wsxb.2014.11.011

Silva, U. D., Mendes, G. D., Silva, N. M. R. M., Duarte, J. L., Silva, I. R., Totola, M. R., et al. (2014). Fluoride-tolerant mutants of Aspergillus Niger show enhanced phosphate solubilization capacity. *PLoS One* 9:e110246. doi: 10.1371/journal.pone.0110246

Thopan, P., Yu, L., Brown, I. G., and Tippawan, U. (2017). Low-energy ion-species-dependent induction of DNA double-strand breaks: ion energy and fluence thresholds. *Radiat. Res.* 188, 426–432. doi: 10.1667/RR14721.1

Tomer, S., Suyal, D. C., Shukla, A., Rajwar, J., Yadav, A., Shouche, Y., et al. (2017). Isolation and characterization of phosphate solubilizing bacteria from Western Indian Himalayan soils. *3. Biotech* 7:95. doi: 10.1007/s13205-017-0738-1

Yamaguchi, H., Nagatomi, S., Morishita, T., Degi, K., Tanaka, A., Shikazono, N., et al. (2003). Mutation induced with ion beam irradiation in rose. *Nucl. Instrum. Meth. B* 206, 561–564. doi: 10.1016/S0168-583X(03)00825-5

Yongbin, L., Qin, L., Guohua, G., and Sanfeng, C. (2020). Phosphate solubilizing bacteria stimulate wheat rhizosphere and endosphere biological nitrogen fixation by improving phosphorus content. *Peer J.* 8:e9062. doi: 10.7717/peerj.9062

You, Y. W., Wang, M., Jiang, L. H., Yue, S. S., and Liu, Z. H. (2009). Mutant breeding of high effective phosphate-solubilizing bacteria Bacillus subtilis P-1 by nitrogen ionic beam. *Southwest China J. Agric. Sci.* 22, 1020–1022. doi: 10.16213/j.cnki.scjas.2009.04.008

Zhang, Y., Chen, F. S., Wu, X. Q., Luan, F. G., Zhang, L. P., Fang, X. M., et al. (2018). Isolation and characterization of two phosphate-solubilizing fungi from rhizosphere soil of moso bamboo and their functional capacities when exposed to different phosphorus sources and pH environments. *PLoS One* 13:e0199625. doi: 10.1371/journal.pone.0199625

Zhang, L., Qi, W., Xu, H., Wang, L., and Jiao, Z. (2016). Effects of low-energy N(+)-beam implantation on root growth in Arabidopsis seedlings. *Ecotoxicol. Environ. Saf.* 124, 111–119. doi: 10.1016/j.ecoenv.2015.10.003

Conflict of Interest: The authors declare that the research was conducted in the absence of any commercial or financial relationships that could be construed as a potential conflict of interest.

Publisher's Note: All claims expressed in this article are solely those of the authors and do not necessarily represent those of their affiliated organizations, or those of the publisher, the editors and the reviewers. Any product that may be evaluated in this article, or claim that may be made by its manufacturer, is not guaranteed or endorsed by the publisher.

frontiers | Frontiers in Microbiology

ORIGINAL RESEARCH
published: 28 April 2022
doi: 10.3389/fmicb.2022.858546

The Potential of Pre-fermented Juice or *Lactobacillus* Inoculants to Improve the Fermentation Quality of Mixed Silage of Agro-Residue and Lucerne

*Lin Mu, Qinglan Wang, Xin Cao, Hui Li and Zhifei Zhang**

Department of Grassland Science, College of Agronomy, Hunan Agricultural University, Changsha, China

OPEN ACCESS

Edited by:
Christopher Rensing, Fujian Agriculture and Forestry University, China

Reviewed by:
Siran Wang, Nanjing Agricultural University, China
Xianjun Yuan, Nanjing Agricultural University, China

***Correspondence:**
Zhifei Zhang
zhangzf@hunau.edu.cn

Specialty section:
This article was submitted to Microbiotechnology, a section of the journal Frontiers in Microbiology

Received: *20 January 2022*
Accepted: *21 February 2022*
Published: *28 April 2022*

Citation:
Mu L, Wang Q, Cao X, Li H and Zhang Z (2022) The Potential of Pre-fermented Juice or Lactobacillus Inoculants to Improve the Fermentation Quality of Mixed Silage of Agro-Residue and Lucerne. Front. Microbiol. 13:858546. doi: 10.3389/fmicb.2022.858546

The objective of this study was to determine the effect of pre-fermented juice, *Lactobacillus plantarum*, and *L. buchneri* on chemical composition, fermentation, aerobic stability, dynamics of microbial community, and metabolic pathway of a mixture of lucerne, wheat bran (WB), and rice straw (RS). All mixtures were ensiled for 1, 3, 5, 7, 15, 30, and 45 days after treatment with uninoculated (control, C); *L. plantarum* [LP, 1×10^6 cfu/g of fresh weight (FW)]; *L. buchneri* (LB, 1×10^6 cfu/g of FW); LP + LB (LPB, 1×10^6 cfu/g of FW of each inoculant); and pre-fermented juice (J; 2×10^6 cfu/g of FW). Four lactic acid bacteria (LAB) species from three genera were cultured from the pre-fermented juice, with *W. cibaria* being dominant. The inoculants increased lactic acid (LA), decreased pH and ammonia nitrogen (AN) compared to C silage at earlier stages of ensiling, and high dry matter (DM) and water-soluble carbohydrate (WSC) content in inoculated silages. Adding LPB increased the abundance of *L. plantarum*, *L. paralimentarius,* and *L. nodensis,* resulting in the lowest pH. Pre-fermented juice enriched *W. cibaria*, *L. sakei*, *L. parabrevis*, *Pseudomonas putida,* and *Stenotrophomonas maltophilia*, mainly enhanced accumulation of acetic acid (AA) and LA, and decreased pH, crude protein losses, AN, and hemicellulose contents. *L. buchneri* and *L. brevis* had a high abundance in LB-treated and J silages, respectively, inhibited undesirable bacteria, and improved aerobic stability with more than 16 days. In addition, the metabolic pathways changed with time and *L. buchneri* inoculants promoted global metabolism. In conclusion, inoculations altered bacterial succession and metabolic pathways in silage; LB and pre-fermented juice enhanced ensiling by promoting pH reductions, enhancing concentrations of LA and AA, and extending aerobic stability more than 16 days.

Keywords: pre-fermented juice, bacterial inoculants, microbial community, agro-residue, mixed silage

INTRODUCTION

With livestock production and cultivation of lucerne both increasing in southern China, ensiled lucerne is becoming a common forage source. However, the humid and rainy climate makes it difficult to obtain optimal dry matter (DM) for silage. Fortunately, crop by-product, an important biomass resource in green, sustainable, and intensive agricultural production, is a promising adsorbent to reduce silage moisture. Ensiling lucerne with crop by-products would not only reduce moisture, but also reduce competition between humans and animals for the same food sources (Chen, 2016; Du et al., 2021a). Rice straw (RS) is an abundant agro-residue biomass in China, with most of it incinerated in fields, thereby precluding any use and causing environmental pollution. In addition, wheat bran (WB), a common byproduct of wheat production with abundant carbohydrates and high DM, is widely available for use as an animal feed (Chen, 2016). The addition of WB to paper mulberry silage enhanced fermentation quality and enabled *Lactobacillus plantarum* (LP) to become the dominant microbe. Furthermore, WB can also be combined with RS to produce high-nutrient silage by increasing DM recovery (Jian-Xin et al., 2001; Du et al., 2021b). Therefore, it is believed that mixing WB and RS in lucerne silage could effectively use large quantities of crop by-products and alleviate the feed shortage in tropical areas. However, adding RS and WB in lucerne silage absorbs moisture and increases DM, but concurrently decreases concentrations of lactic acid bacteria (LAB), as these products have a paucity of epiphytic LAB (Mu et al., 2020; Du et al., 2021a).

Various inoculants are used to promote fermentation, namely acid production rate and aerobic stability. The most common inoculants for silage are *L. plantarum* and *L. buchneri* to decrease pH and inhibit yeasts and molds (Guo et al., 2018). In addition, pre-fermented juice, cultured epiphytic microorganisms of crop materials, has been recommended to enhance silage fermentation, as it can be produced at low cost, is environmentally friendly, and an excellent biological source of LAB (Ohshima, 1997). Inoculating pre-fermented juice to alfalfa silage improved the quality of fermentation by decreasing pH through lactobacilli-driven LA production (Wang et al., 2009). Although many researchers have used LAB and pre-fermented juice as inoculants for silage production, results have varied, as microbial content of pre-fermented juice is usually complex and inconsistent (Adesogan, 2008). There are limited studies on the bacterial community in pre-fermented juice, and how pre-fermented juice affects bacterial community succession in lucerne-based silage is unclear. Thus, the objective was to determine whether pre-fermented juice and inoculations affected fermentation quality and microbiome, and microbial taxa of pre-fermented juice that influenced silage fermentation. We hypothesized that pre-fermented juice is constituted by complicated bacteria, which could successively play a role during the ensiling process.

MATERIALS AND METHODS

Silage Preparation

Both lucerne and rice were grown by Chang De, China (longitude 112°06′58″, latitude 29°06′27″, altitude 30 m), whereas WB was from Kangda Agricultural Products Co., Ltd. (Anhui, China). In May 2019, the second crop of lucerne at the 10% bloom stage was harvested (hand clippers) from three plots. The RS was procured after rice was harvested. Lucerne and RS were processed in a fodder cutter and reduced to an overall length of 1–2 cm. Lucerne, WB, and RS were combined in a ratio of 80:15:5, based on preliminary experiments. Additives used were commercial *L. plantarum* and *L. buchneri* inoculants (Yaxin Biotechnology Co., Ltd., Taiwan, China), and pre-fermented juice. The latter was prepared from lucerne that was chopped from three plots and used as replicates. For this, 200 g of chopped forage were mixed with 1 L of distilled water and macerated for 2 min in a blender, filtered (two layers of cheesecloth), and glucose (2 g/100 ml) was added, the solution was well mixed and placed in a sealed plastic container in an incubator at 30°C for 48 h (Tao et al., 2018).

A total of 158 silage mixtures (4 kg lucerne, 0.75 kg WB, and 0.25 kg RS) were prepared, with 105 randomly selected (5 treatments × 7 sampling days × 3 replicates/treatment), as follows: (1) uninoculated (control, C); (2) *L. plantarum* (LP; 1×10^6 cfu/g FW); (3) *L. buchneri* (LB; 1×10^6 cfu/g FW); (4) LP + LB (LPB; 1×10^6 cfu/g FW of each inoculant); (5) pre-fermented juice (J; 2×10^6 cfu/g FW, with 7.61 log cfu/ml and pH 4.16). Inoculants were added to deionized water, and with constant mixing, 20 ml/kg was sprayed as a fine mist on the material to be ensiled. Similarly, 20 ml/kg of fermented juice or distilled water (J and C treatments, respectively), were also applied. All samples (600 g of raw material) were ensiled in vacuum-heat sealed nylon-polyethylene standard barrier bags (200 × 300 mm; Huaguan Printing Co., Ltd., Zhejiang, China). Air was withdrawn from silos; they were sealed with a vacuum extractor (Dafeng Machinery Co., Ltd., Zhejiang, China) and kept at ∼30°C. On Days 1, 3, 5, 7, 15, 30, and 45, triplicate samples were collected to assess fermentation and composition. Assessment of the microbial community was done at Day 5, 15, and 45 of ensiling and for the fermented juice, after 48 h of incubation.

Chemical Composition and Fermentation Characteristics

A sample of silage (20 g) was put into 180 ml distilled water and processed in a blender for 1 min. The solution was filtered through 2 layers of cheesecloth and pH measured (SI400 pH meter, Spectrum, Aurora, IL). The filtrate was centrifuged (10,000 × g, 15 min, 4°C) and the supernatant was assessed for the following: volatile fatty acids (VFAs), with gas chromatography (GC7890A, Agilent Technologies, Santa Clara, CA), as described by Mu et al. (2020); lactic acid (LA), *via* an Agilent 1260 HPLC system with a UV detector and Acclaim TM organic acid column (Dionex Co., Ltd., Sunnyvale, CA) with 50 mmol/L NaH_2PO_4, 0.6 ml/min at 30°C; and ammonia nitrogen (AN) (Broderick and Kang, 1980). Samples were dried

at 65°C for 48 h in a forced-draft for DM analysis, ground in a knife mill with a 1-mm screen, and assessed for neutral and acid detergent fiber (NDF and ADF, respectively) (Van Soest et al., 1991), crude protein (CP) (Mu et al., 2020), and water-soluble carbohydrate (WSC) (Mu et al., 2020), with ADF subtracted from NDF to calculate hemi-cellulose (HC) content. The LAB in pre-fermented juice was cultured on MRS agar plates and enumerated (Cai et al., 1998).

Sequence Analyses of Bacterial Communities

Pre-fermented juice samples (50 ml) were centrifuged at 10,000 × g for 5 min, the supernatant removed, and the residue stored at −80°C. The DNA was isolated (DNA kit, DP812, Tiangen, Beijing, China) according to the manufacturer's instructions, from frozen-thawed samples of pre-fermented juice and silage. The DNA was quantified with a NanoDrop 2000 and quality determined with 1% agarose gels. Single-molecule real-time (SMRT) sequencing was done, with primers 27F and 1492R to detect 16S rRNA genes, and polymerase chain reaction (PCR) was done as described by Mu et al. (2021). All DNA assessments were done by Biomarker Technologies Corporation (Beijing, China). A PacBio Sequel (Pacific Biosciences, Menlo Park, CA) was used for analyses, with sequences determined as described by Mu et al. (2021). Alpha diversity used Shannon, Simpson's diversity, Chao1 and rarefaction estimators, principle component analysis (PCA), R heatmaps were prepared as described by Mu et al. (2020), and Venn diagrams (VennDiagram, Version 1.6.16) were used to compare bacterial communities. Microbial functions were determined based on the Kyoto Encyclopedia of Genes and Genomes (KEGG) database using Phylogenetic Investigation of Communities by Reconstruction of Unobserved States (PICRUSt). The BMK Cloud Platform[1] was used for data analysis.

Aerobic Stability

To determine aerobic stability, 90 piles of silage were prepared as described for silage, and 60 were randomly chosen and ensiled. After 45 days, bales were opened, mixed thoroughly, and loosely packed into 2-L sterile plastic boxes that were covered with two layers of gauze and held at 30–35°C. Every 2 h, temperatures of air and silage (middle of the bottle) were measured (Smowo MDL-1048A, Tianhe Automation Instrument Co., Ltd., Shanghai, China). Aerobic stability was defined as the interval for silage to become at least 2°C warmer than air. Effects of aerobic exposure on pH were determined after Day 0, 4, 8, 12, and 16 (three boxes per treatment).

Statistical Analyses

This experiment was conducted as a completely randomized design (5 treatments, with 7 durations of ensiling to assess fermentation and chemical compositions, and 5 durations of aerobic exposure). The GLM procedure (SAS 9.3, SAS Institute Inc., Cary, NC) was used to conduct two-way ANOVA, with fixed effects of treatment, ensiling day, and their interaction. Fixed effects of LP, LB, LPB, and pre-fermented juice were used to assess sequence, bacterial diversity, and succession of inoculations. For all analyses, $P < 0.05$ was considered significant and differences were located with Tukey's.

[1] http://www.biocloud.net/

RESULTS

The Chemical Composition of Fresh Forage

Contents of NDF, ADF, and DM were higher ($P < 0.05$) in RS than lucerne, whereas the CP content was lower ($P < 0.05$) in RS than lucerne. The WB had higher ($P < 0.05$) DM and HC contents, but lower ($P < 0.05$) NDF, ADF, and CP content than lucerne. However, the mixture had lower ($P < 0.05$) NDF, ADF, and CP and higher ($P < 0.05$) DM and HC compared to lucerne (**Table 2**).

Fermentation Products

There were effects of treatment group and ensiling days ($P < 0.01$) on pH, LA, AA, propionic acid (PA), butyric acid (BA), and AN, and there was an interaction between group and days for silage pH, LA, AA, propionic acid (PA), butyric acid (BA), and AN (**Table 2**). Across groups, pH decreased as ensiling progressed, with all groups having pH < 4.2 at 45 days. On Day 3 and 5, the pH in all inoculants was lower than in C silage. The pH of silage treated with pre-fermented juice had decreased ($P < 0.05$) after 3 days of ensiling and was lower than C silage at Day 45. After 15 days of ensiling, pH of LPB silage was always lower ($P < 0.05$) than in the other four groups.

There was rapid LA production in silage treated with pre-fermented juice, LP, LB, or LPB after 1 day of ensiling. The J silage had the highest ($P < 0.05$) LA concentration among all silages during the initial 7 days of ensiling, whereas the lower LA ($P < 0.05$) concentration in J silage than in C occurred at Day 15 and 30 of ensiling. The LA concentration of LB silage increased most slowly during 3 days of ensiling, and was significantly lower than all other groups at 45 days of ensiling. However, inoculated treatments with pre-fermented juice, LP, LB, or LPB had greater AA concentrations than the uninoculated C group at 45 days of ensiling. Concentration of AA was highest ($P < 0.05$) in J silage at both 3 and 15 days of ensiling. Furthermore, in LB and LPB silages, AA had the slowest ($P < 0.05$) increase in the first 5 days of ensiling, but AA in these two groups generally exceeded that in C silage until the end of the trial. The PA concentration was higher ($P < 0.05$) in J silage than LB silage only was observed after Day 5 of ensiling, and then it became lower ($P < 0.05$) than LB silage. Both LB and LPB silages had lower ($P < 0.05$) BA concentrations than other treatments after 45 days of ensiling. All inoculants reduced ($P < 0.05$) AN concentration relative to C silage after 1 day of ensiling. The addition of pre-fermented juice lowered AN concentration as compared to C silage over the entire ensiling, with LB silage having the opposite trend.

Chemical Composition

There were effects of group and time ($P < 0.01$) on DM, WSC, CP, NDF, and HC and an interaction for DM, WSC, CP, NDF,

TABLE 1 | Mean (SEM[1]) chemical composition before ensiling (n = 3 samples).

Item[2]	AF	RS	WB	F
DM (g/kg FW)	163 ± 4.63^{C}	924 ± 0.33^{A}	913 ± 1.73^{A}	364 ± 4.62^{B}
Crude protein (g/kg DM)	219.83 ± 0.01^{A}	30.16 ± 0.25^{D}	167.01 ± 0.17^{C}	172.37 ± 0.22^{B}
NDF (g/kg DM)	522.92 ± 1.29^{B}	680.16 ± 1.46^{A}	459.43 ± 3.34^{D}	489.05 ± 3.45^{C}
ADF (g/kg DM)	389.26 ± 5.75^{B}	538.14 ± 0.63^{A}	224.90 ± 2.89^{D}	321.65 ± 5.83^{C}
Hemicellulose (g/kg DM)	139.76 ± 3.52^{C}	142.02 ± 0.83^{C}	239.92 ± 3.11^{A}	167.41 ± 3.02^{B}
WSC (g/kg DM)	78.03 ± 0.98^{A}	34.51 ± 1.66^{B}	83.79 ± 0.89^{A}	79.85 ± 2.27^{A}

$^{A-D}$Within a row, means without a common superscript differed ($P < 0.05$).
[1]SEM, standard error of the mean.
[2]DM, dry matter; FW, fresh weight; WSC, water-soluble carbohydrates; NDF, neutral detergent fiber; ADF, acid detergent fiber. FW, fresh weight; DM, dry matter. AF, fresh lucerne; RS, rice straw; WB; wheat bran; F, mixture.

TABLE 2 | Effects of additives on fermentative characteristics of silages.

Item	Treatment[1]	Day of ensiling							SEM[2]	*P*-value[3]		
		1	3	5	7	15	30	45		T	D	T × D
pH	C	4.93^{A}	4.52^{AB}	4.23^{A}	4.20^{A}	4.20^{A}	4.16^{AB}	4.17^{A}	0.04	<0.001	<0.001	<0.001
	J	4.93^{A}	4.43^{B}	4.19^{BC}	4.17^{B}	4.20^{A}	4.17^{AB}	4.15^{BC}				
	LB	4.96^{A}	4.58^{A}	4.20^{BC}	4.14^{C}	4.19^{AB}	4.18^{A}	4.17^{A}				
	LP	4.91^{A}	4.49^{AB}	4.20^{B}	4.18^{B}	4.19^{A}	4.17^{AB}	4.16^{AB}				
	LPB	4.96^{A}	4.48^{AB}	4.18^{C}	4.18^{B}	4.17^{B}	4.15^{B}	4.14^{C}				
Lactic acid	C	8.29^{B}	19.20^{B}	30.34^{B}	35.46^{AB}	41.51^{AB}	41.86^{A}	40.16^{A}	1.49	<0.001	<0.001	<0.001
(g/kg DM)	J	9.74^{A}	26.84^{A}	35.02^{A}	37.40^{A}	39.90^{C}	40.26^{B}	40.07^{A}				
	LB	10.39^{A}	16.13^{C}	30.93^{AB}	35.35^{B}	40.86^{AB}	41.17^{AB}	39.08^{B}				
	LP	10.40^{A}	19.23^{B}	32.01^{AB}	35.09^{B}	40.75^{BC}	41.24^{AB}	39.80^{A}				
	LPB	10.01^{A}	20.41^{B}	30.76^{B}	35.59^{AB}	41.71^{A}	42.16^{A}	39.77^{A}				
Acetic acid	C	4.39^{A}	6.19^{C}	9.38^{A}	9.81^{B}	11.74^{AB}	12.35^{A}	11.72^{B}	0.57	<0.001	<0.001	<0.001
(g/kg DM)	J	4.26^{AB}	8.55^{A}	9.31^{A}	9.63^{BC}	12.01^{A}	14.08^{A}	12.77^{A}				
	LB	4.09^{B}	6.47^{C}	6.65^{C}	10.08^{A}	11.63^{AB}	12.73^{A}	12.73^{A}				
	LP	4.26^{AB}	7.77^{B}	9.26^{A}	9.61^{C}	11.24^{B}	12.50^{A}	12.77^{A}				
	LPB	4.18 ^{AB}	4.22^{D}	8.76^{B}	10.10^{A}	11.16^{B}	13.21^{A}	12.01^{B}				
Propionic acid	C	0.15^{AB}	0.17^{C}	0.32^{A}	0.52^{A}	0.71^{A}	0.76^{A}	0.86^{A}	0.10	<0.001	<0.001	<0.001
(g/kg DM)	J	0.14^{B}	0.30^{A}	0.34^{A}	0.42^{A}	0.68^{A}	0.78^{A}	0.70^{B}				
	LB	0.15^{A}	0.16^{D}	0.16^{B}	0.42^{A}	0.51^{A}	0.33^{B}	0.79^{A}				
	LP	0.15^{AB}	0.24^{B}	0.32^{A}	0.40^{A}	0.69^{A}	0.31^{B}	0.86^{A}				
	LPB	0.16^{A}	0.15^{E}	0.30^{A}	0.54^{A}	0.57^{A}	0.75^{A}	0.66^{B}				
Butyric acid	C	0.06^{B}	0.06^{A}	0.06^{C}	0.11^{BC}	0.11^{C}	0.11^{A}	0.12^{A}	0.00	<0.001	<0.001	<0.001
(g/kg DM)	J	0.06^{B}	0.06^{B}	0.11^{A}	0.11^{BC}	0.12^{A}	0.11^{A}	0.12^{A}				
	LB	0.06^{A}	0.06^{B}	0.06^{BC}	0.11^{B}	0.11^{AB}	0.10^{A}	0.11^{BC}				
	LP	0.06^{B}	0.06^{B}	0.06^{B}	0.11^{C}	0.11^{AB}	0.11^{A}	0.11^{AB}				
	LPB	0.06^{B}	0.06^{B}	0.06^{C}	0.11^{A}	0.11^{BC}	0.11^{A}	0.10^{C}				
Ammonia	C	22.58^{A}	35.35^{A}	38.14^{A}	49.21^{A}	70.25^{A}	74.59^{B}	95.13^{B}	2.68	<0.001	<0.001	<0.001
nitrogen	J	15.83^{B}	33.68^{AB}	36.88^{A}	42.78^{BC}	66.30^{A}	79.81^{AB}	88.30^{C}				
(g/kg TN)	LB	15.12^{B}	36.42^{A}	38.18^{A}	46.90^{AB}	66.63^{A}	82.27^{AB}	101.90^{A}				
	LP	16.73^{B}	33.50^{AB}	36.43^{A}	38.98^{C}	67.51^{A}	78.82^{AB}	92.86^{BC}				
	LPB	15.30^{B}	29.83^{B}	37.36^{A}	42.77^{BC}	67.69^{A}	88.32^{A}	99.07^{AB}				

$^{A-D}$Within a day of ensiling, groups without a common superscript differed ($P < 0.05$).
[1]C,control; J, pre-fermented juice-treated silage; LP, L. plantarum-treated silage; LB, L. buchneri-treated silage; LPB, L. plantarum + L. buchneri-treated silage.
[2]SEM,standard error of mean.
[3]treatments; D, ensiling days; T × D, interaction between treatments and ensiling days.

and HC. The C silage had lower DM after 45 days of ensiling and tended to have lower WSC contents than other treatments after 7 days of ensiling. The content of WSC in J silage was lowest in the first 5 days of ensiling, with J silage having higher CP and lower HC contents than other treatments after 45 days of ensiling. The contents of NDF and HC decreased markedly

TABLE 3 | Effects of additives on chemical compositions of silages.

Item[1]	Treatment[2]	Day of ensiling							SEM[3]	*P*-value[4]		
		1	3	5	7	15	30	45		T	D	T × D
DM	C	357^{A}	352^{AB}	345^{B}	346^{C}	347^{B}	346^{A}	344^{B}	0.80	<0.001	<0.001	<0.001
(g/kg FM)	J	361^{A}	356^{AB}	354^{A}	347^{BC}	348^{B}	350^{A}	348^{AB}				
	LB	368^{A}	349^{B}	352^{A}	347^{B}	348^{B}	347^{A}	349^{A}				
	LP	361^{A}	350^{B}	352^{A}	352^{AB}	345^{B}	347^{A}	348^{A}				
	LPB	360^{A}	362^{A}	354^{A}	358^{A}	358^{A}	348^{A}	346^{AB}				
WSC	C	60.35^{B}	60.24^{B}	60.16^{B}	56.89^{C}	57.46^{B}	56.37^{B}	52.88^{A}	1.11	<0.001	<0.001	<0.001
(g/kg DM)	J	60.12^{B}	59.24^{B}	51.02^{C}	62.51^{A}	62.92^{A}	59.91^{A}	55.51^{A}				
	LB	66.31^{A}	64.45^{A}	60.95^{B}	60.69^{A}	61.23^{A}	59.42^{A}	58.44^{A}				
	LP	65.28^{AB}	64.60^{A}	64.03^{A}	61.70^{A}	58.19^{B}	58.21^{AB}	55.02^{A}				
	LPB	63.64^{AB}	63.03^{A}	61.55^{B}	59.05^{AB}	61.45^{A}	58.96^{A}	59.51^{A}				
Crude protein	C	177.09^{AB}	178.80^{A}	175.10^{A}	175.78^{A}	175.95^{A}	175.07^{A}	172.32^{BC}	0.23	<0.001	<0.001	<0.001
(g/kg DM)	J	174.63^{B}	174.49^{C}	175.43^{A}	175.04^{A}	174.76^{A}	173.78^{B}	175.48^{A}				
	LB	177.54^{A}	176.47^{B}	174.54^{A}	175.35^{A}	175.85^{A}	175.00^{A}	172.50^{B}				
	LP	175.26^{AB}	176.91^{B}	173.74^{A}	175.95^{A}	174.69^{A}	173.95^{B}	172.04^{BC}				
	LPB	176.69^{AB}	176.33^{B}	172.87^{A}	176.52^{A}	174.47^{A}	173.74^{B}	171.82^{C}				
NDF	C	488.86^{A}	491.92^{A}	480.54^{A}	474.90^{A}	488.06^{A}	440.55^{AB}	438.09^{A}	3.03	<0.001	<0.001	<0.001
(g/kg DM)	J	483.39^{A}	463.54^{B}	466.72^{A}	468.79^{A}	458.00^{B}	430.13^{B}	442.82^{A}				
	LB	488.81^{A}	466.69^{B}	464.74^{A}	465.29^{A}	468.62^{B}	448.80^{A}	446.66^{A}				
	LP	470.76^{A}	478.87^{AB}	465.34^{A}	466.42^{A}	468.08^{B}	441.31^{AB}	448.66^{A}				
	LPB	472.91^{A}	475.93^{AB}	458.47^{A}	467.82^{A}	465.63^{B}	456.28^{A}	445.57^{A}				
ADF	C	317.35^{B}	341.06^{A}	338.47^{A}	315.28^{B}	325.03^{A}	316.01^{B}	322.03^{A}	1.60	0.025	<0.001	<0.001
(g/kg DM)	J	348.93^{A}	315.36^{B}	337.72^{A}	327.71^{AB}	321.47^{A}	312.19^{B}	334.51^{A}				
	LB	311.25^{B}	324.56^{AB}	316.33^{B}	337.24^{A}	317.88^{A}	324.04^{B}	327.26^{A}				
	LP	303.63^{B}	319.57^{AB}	316.69^{B}	328.13^{AB}	329.51^{A}	314.64^{B}	324.42^{A}				
	LPB	325.29^{B}	337.80^{AB}	312.50^{B}	344.93^{A}	335.82^{A}	350.29^{A}	324.61^{A}				
Hemicellulose	C	171.51^{A}	150.86^{A}	142.07^{A}	159.62^{A}	163.03^{A}	124.54^{A}	116.07^{AB}	2.72	<0.001	<0.001	<0.001
(g/kg DM)	J	134.46^{A}	148.18^{A}	129.00^{A}	141.08^{AB}	136.54^{A}	117.94^{AB}	108.31^{B}				
	LB	177.56^{A}	142.13^{A}	148.40^{A}	128.05^{AB}	150.74^{A}	124.76^{A}	119.40^{AB}				
	LP	167.12^{A}	159.30^{A}	148.65^{A}	138.30^{AB}	138.57^{A}	126.67^{A}	124.24^{A}				
	LPB	147.62^{A}	138.13^{A}	145.97^{A}	122.89^{B}	129.82^{A}	105.99^{B}	120.96^{AB}				

$^{A-C}$Within a day of ensiling, groups without a common superscript differed ($P < 0.05$).

[1]DM, dry matter; FW, fresh weight; WSC, water-soluble carbohydrates; NDF, neutral detergent fiber; ADF, acid detergent fiber.

[2]C, control; J, pre-fermented juice-treated silage; LP, L. plantarum-treated silage; LB, L. buchneri-treated silage; LPB, L. plantarum + L. buchneri-treated silage.

[3]SEM, standard error of mean.

[4]T, treatments; D, ensiling days; T × D, interaction between treatments and ensiling days.

in all groups at 45 days of ensiling with no differences in NDF and ADF content in inoculant treatments vs. control after 45 days of ensiling (**Table 3**).

Microbial Community

A total of 514,997 quality sequencing reads were generated by SMRT sequencing of the 16S rRNA gene (full-length) in 9 raw materials and 45 silages samples; based on 3% dissimilarity, there were 306 operational taxonomic units (OTUs). The Simpson, Shannon index, and Chao1 values in raw materials were greater than ($P < 0.05$) those of silage samples after 45 days of ensiling (**Table 4**). Inoculants decreased the Simpson, Shannon index, and Chao1 values relative to the C group, during 5 days of ensiling. However, at 5 and 15 days of ensiling, Simpson, Shannon index, and Chao1 were lowest in J silage, whereas after 45 days of ensiling, these indices were lowest in J, LB, and LPB. In principal component analysis (PCA; **Figure 1**), at 5 and 15 days of ensiling, all groups were clustered in the second and third quadrants, whereas after 45 days of ensiling, LP and LPB were in the third quadrant and the remainder were assigned to the fourth quadrant. Based on Venn analysis, overlapping OTUs (31) between fresh alfalfa and pre-fermented juice accounted for 81.6% of pre-fermented juice OTUs (**Figure 2A**). In addition, there were 3 specific OTUs in pre-fermented juice, whereas 31 bacterial OTUs were shared by pre-fermented juice and J silage at 5 and 15 days of ensiling. Furthermore, after 45 days of ensiling, fewer bacterial OTUs were shared by pre-fermented juice and J silage (**Figure 2B**).

Relative abundances of bacteria (genus and species levels) are shown in **Figures 3**, **4**, respectively. *Weissella*, *Acinetobacter,* and *Pseudomonas* were the main epiphytic bacteria of lucerne and mixture (**Figure 3**). Furthermore, *W. cibaria* (19.3 and 10.3%),

TABLE 4 | General information of sequence and bacterial diversity.

Day	Treatment	Item				
		Sequences	Shannon	Simpson	Chao 1	Good's coverage
	FJ	25,200	0.31^{G}	0.06^{H}	36.53^{E}	0.9986
	AF	28,782	5.30^{A}	0.94^{AB}	217.07^{A}	0.9982
	F	27,594	5.82^{A}	0.97^{A}	207.13^{AB}	0.9980
5 days	C	29,046	4.01^{BCD}	0.85^{ABCD}	190.93^{AB}	0.9957
	J	24,185	3.67^{BCDE}	0.83^{ABCD}	155.11^{ABC}	0.9958
	LB	26,077	3.87^{BCD}	0.84^{ABCD}	186.29^{AB}	0.9953
	LP	29,194	3.84^{BCD}	0.84^{ABCD}	177.71^{AB}	0.9966
	LPB	24,766	3.35^{CDE}	0.80^{BCD}	179.66^{AB}	0.9956
15 days	C	29,056	4.30^{B}	0.89^{ABC}	186.63^{AB}	0.9963
	J	28,633	3.13^{DE}	0.72^{CDE}	145.29^{BC}	0.9974
	LB	27,288	3.83^{BCD}	0.83^{ABCD}	181.41^{AB}	0.9964
	LP	28,675	4.10^{BC}	0.86^{ABC}	181.66^{AB}	0.9963
	LPB	28,658	3.58^{BCDE}	0.82^{ABCD}	178.27^{AB}	0.9951
45 days	C	31,814	2.85^{E}	0.69^{DEF}	98.04^{CDE}	0.9991
	J	33,682	1.66^{F}	0.56^{EFG}	63.44^{DE}	0.9992
	LB	32,309	1.45^{F}	0.49^{G}	50.23^{DE}	0.9983
	LP	29,640	3.21^{CDE}	0.80^{ABCD}	104.41^{CD}	0.9973
	LPB	30,398	1.73^{F}	0.55^{FG}	75.25^{DE}	0.9988

$^{A-H}$*Within a column, means without a common superscript differed ($P < 0.05$). AF, fresh lucerne; RS, rice straw; WB, wheat bran; F, mixture; C, control; FJ, pre-fermented juice; J, pre-fermented juice-treated silage; LP, L. plantarum-treated silage; LB, L. buchneri-treated silage; LPB, L. plantarum + L. buchneri-treated silage.*

Acinetobacter sp. (12.8 and 9.7%), *Sphingobacterium* sp. (5.2 and 4.8%), uncultured bacterium *Stenotrophomonas* (4.4 and 5%), *Pseudomonas putida* (2.8 and 4.7%), and *Pseudomonas fragi* (4.8 and 4.9%) were the major bacterial species in lucerne and mixture (**Figure 4**). In pre-fermented juice, there were six predominant genera: *Weissella* (97%), *Lactobacillus* (1.1%), *Pediococcus* (0.4%), *Pantoea* (0.4%), *Pseudomonas* (0.1%), and *Sphingomonas* (0.1%). The major microbiota species in pre-fermented juice were *W. cibaria* (96.9%), *L. brevis* (0.6%), *Pantoea agglomerans* (0.4%), *L. plantarum* (0.3%), *L. paralimentarius* (0.3%), and *Pseudomonas putida* (0.1%). After 5 and 15 days of ensiling, LA-producing bacteria (*Lactobacillus*, *Weissella*, and *Pediococcus*) were the dominant genera (64.1–84.3%) in all silage samples. Furthermore, for all groups, at 5 and 15 days of ensiling, dominant LAB species were *L. parabrevis*, *L. nodensis*, *W. cibaria*, *L. buchneri*, *L. plantarum*, *L. paralimentarius*, *L. brevis*, *W. hellenica*, *L. sakei,* and *L. paucivorans*. However, after 45 days of ensiling, *Pseudomonas putida* and *Stenotrophomonas maltophilia* sharply increased and remained predominant, followed by *L. buchneri* and *L. acetotolerans*.

Differences in microbial communities of silages during ensiling are shown (**Figures 3**–**6**). Relative abundances of LA-producing bacteria at the genus level in inoculant treatments were higher than C silage (69.8 vs. 64%), whereas there were greater abundances of LA-producing bacteria in J (81.9 and 86.4%) and LPB (83.6 and 84.3%) silages than that of other treatments at 5 and 15 days of ensiling (**Figure 3**). After 5 days of ensiling, except for J silage, *L. nodensis* was the most abundant species, whereas *L. parabrevis* remained predominant in J silage, followed by *L. nodensis*. Furthermore, compared to other treatments, J silage had more *W. cibaria* and *L. sakei* after 5 days of ensiling. *L. parabrevis* gradually replaced *L. nodensis* as the dominant species in all silage samples after 15 days of ensiling, whereas compared to C silage, relative abundance of *L. parabrevis* was increased by 23.8, 11.7, 5.8, and 10.3% in J, LB, LP, and LPB silages, respectively. For the J silage, there were more *W. cibaria*, whereas *L. paralimentarius* had the highest abundance in LPB silage after 15 days of ensiling. However, *Acinetobacter lwoffii* and *Acinetobacter* sp. were observed in C silage at Days 5 and 15 of ensiling, respectively, and Enterobacterales was identified in LP silage after 15 days of ensiling (**Figures 5A,B**).

Overall, during 45 days of ensiling, the dominant species in C and J silages were *Pseudomonas putida* and *Stenotrophomonas maltophilia,* whereas in LP and LPB, *L. buchneri* was the most abundant. *L. acetotolerans* was the dominant species in LP and was also present in J and LB after 45 days of ensiling. There was greater relative abundance of *Psychrobacillus soli*, *Sporosarcina globispora*, *Carnobacterium inhibents*, *Paenibacillus hispanicus*, and *Acinetobacter* sp. in C silage compared to other treatments during 45 days of ensiling (**Figure 5C**). Heatmaps (species level) of main bacterial communities in mixed silage are shown (**Figure 6**). There was a positive correlation with C silage and *Acinetobacter* sp., *Erwinia* sp., *Ewingella americana*, *Paenibacillus* sp., and uncultured *Stenotrophomonas*. In addition, there were positive correlations between J silage and *L. parabrevis*, *L. brevis*, *Pseudomonas putida,* and *Stenotrophomonas maltophilia*, whereas there were negative correlations between LB silage and *Pseudomonas putida*, *Stenotrophomonas maltophilia,* and *Paenibacillus* sp., whereas LP silage was positively correlated with *W. cibaria*, *Erwinia* sp., *Ewingella americana*, *Paenibacillus* sp., and *L. acetotolerans*. In addition, LPB silage was positively correlated with *L. plantarum*, *L. paralimentarius*, *L. buchneri,* and *L. nodensis*, but had negative correlations with *Erwinia* sp., *Ewingella americana,* and *L. acetotolerans*.

The succession of inoculations in the silage environment is shown in **Table 5**. As *W. cibaria* was dominant in pre-fermented juice, we focused on *W. cibaria* succession in J silage. The addition of pre-fermented juice tended to cause greater abundances of *W. cibaria* in J vs. C silages after 5 days of ensiling, and higher ($P < 0.01$) relative abundances of *W. cibaria* (relative to other inoculated silages) after 15 days of ensiling. Furthermore, inoculation with *L. plantarum* had no obvious effect on increasing relative abundance of *L. plantarum* at 5, 15, or 45 days of ensiling. Relative abundance of *L. buchneri* in silages not inoculated with this bacterium was very limited (<1%) over the entire ensiling period, whereas inoculation with *L. buchneri* strains increased its relative abundance, with a sharp increase in LB and LPB silages after 45 days of ensiling.

A heatmap of KEGG metabolic pathways during the ensiling process is shown in **Figure 7**. Metabolic pathways changed with ensiling days, with carbohydrate metabolism and cofactors and vitamins positively correlated with silage samples after 5 and 15 days, but negatively correlated with silage samples after 45 days. However, silage samples were negatively correlated with amino acid metabolism and nucleotides after 5 and 15 days, whereas the

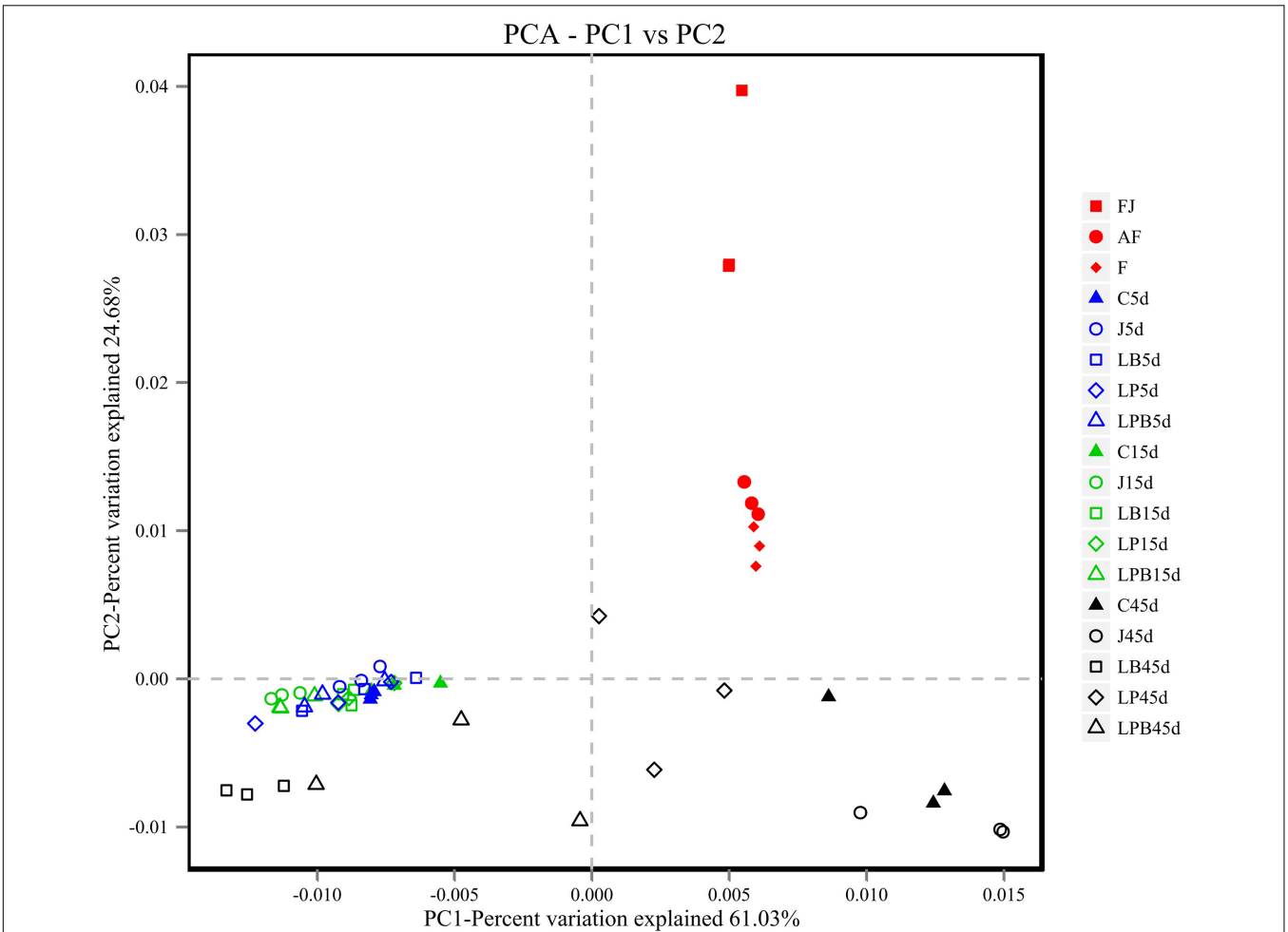

FIGURE 1 | Principal coordinate analysis of the bacterial community in mixed silage. AF, fresh lucerne; RS, rice straw; WB; wheat bran; F, mixture; C, control; J, pre-fermented juice-treated silage; LP, *L. plantarum*-treated silage; LB, *L. buchneri* treated silage; LPB, *L. plantarum* + *L. buchneri*-treated silage.

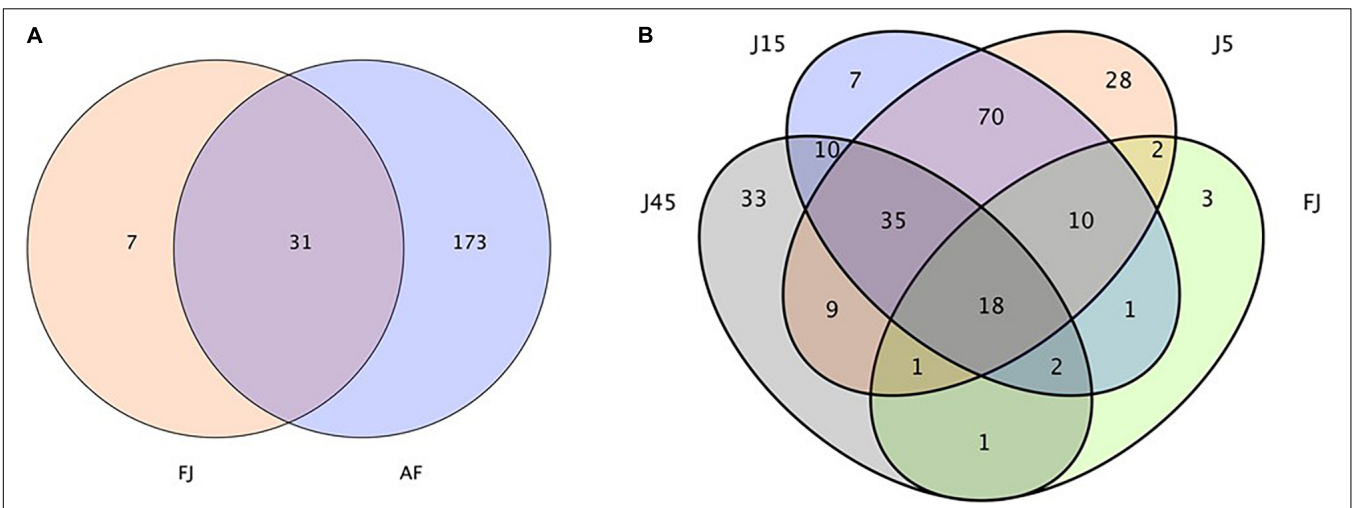

FIGURE 2 | (A) Diagram of the operational taxonomic units between the AF, fresh lucerne and FJ, pre-fermented juice. **(B)** Venn analysis for operational taxonomic units FJ and J, pre-fermented juice-treated silage.

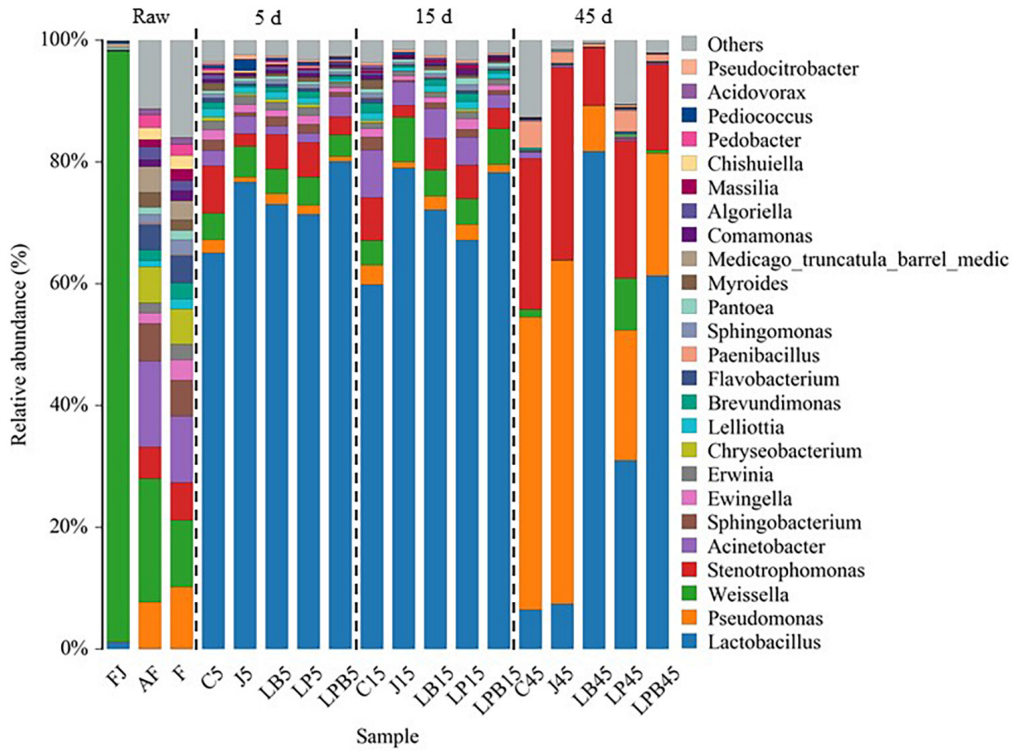

FIGURE 3 | Bacterial community (genus level) of mixed silage. AF, fresh lucerne; FJ, pre-fermented juice; F, mixture; C, control; J, pre-fermented juice-treated silage; LP, *L. plantarum*-treated silage; LB, *L. buchneri*-treated silage; LPB, *L. plantarum* + *L. buchneri*-treated silage.

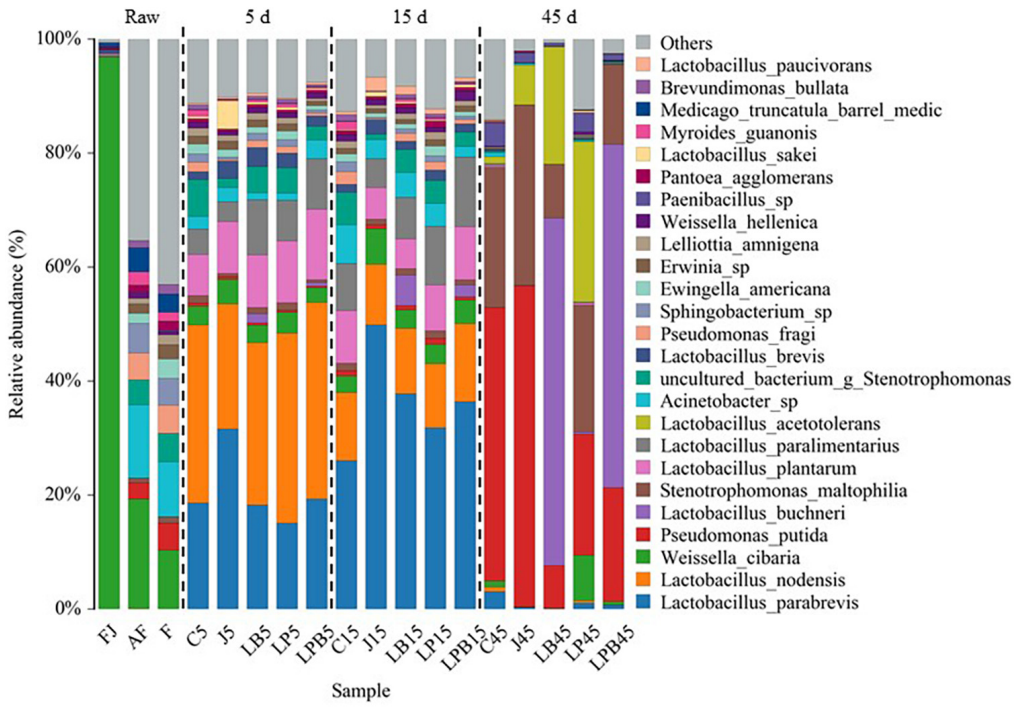

FIGURE 4 | Bacterial community (species level) of mixed silage. AF, fresh lucerne; FJ, pre-fermented juice; F, mixture; C, control; J, pre-fermented juice-treated silage; LP, *L. plantarum*-treated silage; LB, *L. buchneri*-treated silage; LPB, *L. plantarum L. buchneri*-treated silage.

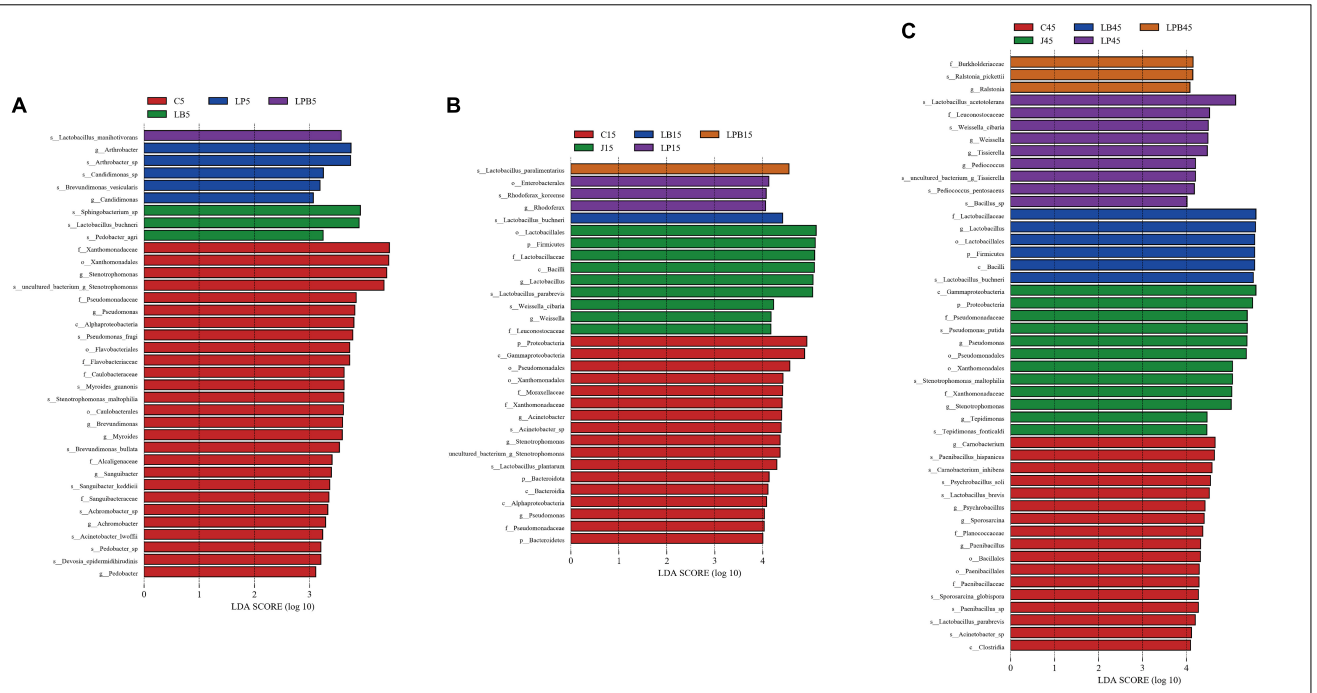

FIGURE 5 | Comparison of microbial variations during the ensiling using the Latent Dirichlet allocation effect size (LEfSe) analysis using the Kruskal-Wallis test ($P < 0.05$) with linear discriminant analysis (LDA) score > 3.0. 5 days **(A)**, 15 days **(B)**, and 45 days **(C)** of ensiling. C, control; J, pre-fermented juice-treated silage; LP, *L. plantarum*-treated silage; LB, *L. buchneri*-treated silage; LPB, *L. plantarum* + *L. buchneri*-treated silage.

opposite trend was observed after 45 days of ensiling. *L. buchneri* inoculants increased abundances of global and overview maps compared to other treatments.

Aerobic Stability

The aerobic stability of silage treated with *L. buchneri* and pre-fermented juice improved significantly, relative to C and LP silage, with LB, LPB, and J silages stable for > 384 h. The pH of aerobic stability was affected ($P < 0.01$) by inoculant, ensiling days, and their interaction (**Figures 8A,B**). For C and LP silages, there was a sharp rise in pH after 12 days of aerobic exposure.

DISCUSSION

Characteristics of Fresh Material and Pre-fermented Juice

The LAB count and pH in pre-fermented juice before ensiling were 7.61 log cfu/ml and 4.16, consistent with the previous studies (Sun et al., 2021). When 80% lucerne was mixed with RS and WB, the adjusted DM content was > 360 g/kg, which met requirements for ideal DM (range of 300–400 g/kg for quality silage; McDonald et al., 1991).

Effect of Pre-fermented Juice and Inoculants Ensiling on Silage Quality

Adding LAB inoculants could accelerate the decline of silage pH by enhancing LA- fermentation and inhibiting undesirable bacteria (Adesogan, 2008). In the study, we also observed higher LA concentration, lower pH and AN concentration at earlier stages of ensiling in all inoculants treated silages than C silage. Applying a combination of homofermentative LAB and heterofermentative LAB captured the benefits of both types of bacteria while overcoming their drawbacks (Adesogan, 2008). In this study, LPB silage had the lowest pH over the ensiling period. Similarly, there was rapid and substantial LA production and the initial rate of acidification was also increased in LP and LB-inoculated low-DM corn and sorghum silages (Filya, 2003). In the current study, inoculation with pre-fermented juice increased LA, AA, and PA concentrations and decreased pH rapidly after 3 days of ensiling. Wang et al. (2009) reported that addition of pre-fermented juice accelerated the early decline of pH to a lower level than control alfalfa silage, due to faster accumulation of LA at the start of ensiling. The number of bacterial OTUs shared by pre-fermented juice and J silage was higher at 5 or 15 days than at 45 days. Addition of pre-fermented juice had more obvious effects on microorganisms in the early stages of ensiling. Furthermore, inoculation with pre-fermented juice decreased silage AN concentration over the entire ensiling interval. Similar to that of Sun et al. (2021), who added pre-fermented juice to lucerne silage and found that pre-fermented juice efficacity decreased pH and AN and increased LA content. The possible reason was as follows: first, exogenous microbiota prepared from epiphytic LAB of lucerne were more likely to adapt and reconstitute in lucerne compared to LAB derived from other crops during ensiling; second, inoculation with pre-fermented juice could stimulate LAB to use fermentable substances at the

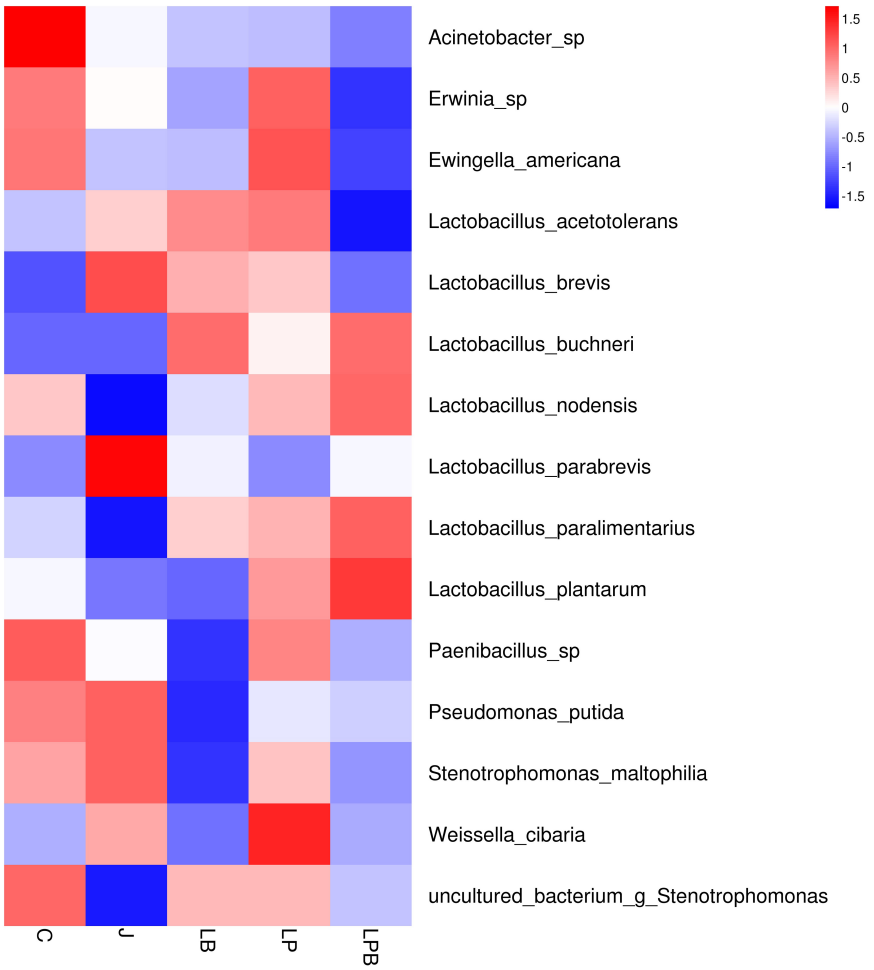

FIGURE 6 | Heatmap of prominent bacterial species (15 most abundant genera) for alfalfa mixed silage. C, control; J, pre-fermented juice-treated silage; LP, *L. plantarum*-treated silage; LB, *L. buchneri*-treated silage; LPB, *L. plantarum L. buchneri*-treated silage.

onset of ensiling (Ohshima, 1997; Shao et al., 2007). In addition, Ali et al. (2020) reported extracted epiphytic microbiota from red clover inoculation more rapidly decreased pH in sterile red clover at earlier stages of ensiling than extracted epiphytic microbiota from maize and sorghum. In addition, higher AA concentration for pre-fermented juice treatments suggested some heterofermentative pathways were promoted during ensiling (Ohshima, 1997). In addition, these results supported the notion that inoculation of lucerne with pre-fermented juice derived from barley, wheat, and grass herbages increased silage AA after 45 days of ensiling (Denek et al., 2011), as our results had a similar tendency. In the current study, concentrations of LA and AA increased most slowly during the preliminary stages of ensiling with *L. buchneri* inoculants, whereas AA concentrations were higher in LB vs. C silage after 45 days of ensiling. *L. buchneri* usually became active after 45 days of ensiling (Muck, 2010). Inoculating with LB resulted in the greatest AN after 45 days of ensiling, perhaps due to the slower LA, AA production, and pH decline in LB silage during 5 days of ensiling. This agrees with previous reports that increased AN with *L. buchneri* inoculants in corn silage was associated with the increased potential for pH during the ensiling (Driehuis et al., 2001). Others also observed increased AN concentration in corn and sorghum silages treated with LB (Filya, 2003).

Effect of Pre-fermented Juice and Inoculants on Silage Chemical Composition

Lower residual WSC content of silage indicated higher DM losses during ensiling, producing worse silage quality (Weinberg et al., 1993). That the C silage had less DM and WSC after 7 days of ensiling was attributed to proliferation of undesirable bacteria increasing nutrient losses. In addition, the WSC content of J silage decreased more rapidly compared to that of other treatments during 5 days of ensiling, perhaps due to this silage having more LA and AA. Similarly, lower WSC in calcium propionate-treated silage after 45 days of ensiling was attributed to higher LA and AA (Mu et al., 2021). Concentration of CP was higher in J silage than C silage on Day 45. This agrees with previous reports of

TABLE 5 | The succession of inoculations in a silage environment.

Day	Treatment	*Weissella cibaria* (%)	*L. plantarum* (%)	*L. buchneri* (%)
5 days	C	3.24^{A}	7.31^{A}	<0.01^{B}
	J	4.35^{A}	9.03^{A}	<0.01^{B}
	LB	3.07^{A}	9.14^{A}	1.59^{A}
	LP	3.68^{A}	10.78^{A}	0.00^{B}
	LPB	2.57^{A}	12.23^{A}	0.56^{B}
SEM		0.23	0.77	0.17
15 days	C	2.95^{B}	9.36^{A}	<0.01^{C}
	J	6.17^{A}	5.50^{A}	<0.01^{C}
	LB	3.24^{B}	5.17^{A}	5.33^{A}
	LP	3.41^{B}	8.05^{A}	<0.01^{C}
	LPB	4.16^{AB}	9.28^{A}	2.13^{B}
SEM		0.36	0.61	0.56
45 days	C	1.09^{A}	0.32^{A}	0.01^{B}
	J	0.09^{A}	0.04^{A}	0.01^{B}
	LB	0.05^{A}	0.01^{A}	61.00^{A}
	LP	7.30^{A}	0.36^{A}	0.31^{B}
	LPB	0.54^{A}	0.07^{A}	60.64^{A}
SEM		1.28	0.06	8.38

$^{A-C}$Within a column and sampling day, means without a common superscript differed ($P < 0.05$).
AF, fresh lucerne; RS, rice straw; WB; wheat bran; F, mixture; C, control; J, pre-fermented juice-treated silage; LP, L. plantarum-treated silage; LB, L. buchneri-treated silage; LPB, L. plantarum + L. buchneri-treated silage.

higher CP content in pre-fermented juice-treated silage than un-treated silage in total mixed ration silage (Yanti et al., 2019). In addition, pre-fermented juice was better than LAB for inhibiting proteolysis, based on non-protein N concentrations in alfalfa silage (Wang et al., 2009). The contents of NDF and HC decreased markedly among all silages at 45 days of ensiling, whereas J silage had the lowest HC content at 45 days of ensiling. This may be related to the structural carbohydrates, which could be hydrolysis by organic acids after a long fermentation (Wang et al., 2018). The decline of NDF and HC contents during ensiling of corn silage could possibly be due to the acid hydrolysis of the cell wall fraction (Huisden et al., 2009). Hence, greater concentration of LA and AA in J silage could explain the lowest HC in J silage after 45 days of ensiling. However, there were no significant differences in NDF and ADF contents in inoculant treatments vs. C silage after 45 days of ensiling. This is similar to that of Wang et al. (2009), who reported that applying pre-fermented juice as an additive did not affect NDF and ADF contents of alfalfa silage. This contradicts Denek et al. (2012) who reported that inoculation contributed to lower NDF and ADF contents in alfalfa silage because some bacteria are able to breakdown cellulose and HC.

Effect of Pre-fermented Juice and Inoculants Ensiling on Silage Bacterial Community

Greater bacterial diversity and richness in raw materials than those of silage were due to the unviability of some epiphytic microbes under the aerobic and acerbic environment. Yuan et al. (2019) reported that the bacterial diversity index was greater in fresh materials than Napier grass silages. The addition of inoculants decreased the Simpson, Shannon index, and Chao1 values as compared to C silage after 5 days of ensiling, whereas J silage had the lowest bacterial diversity and richness after Day 5 of ensiling, attributed to the sharp initial decline in pH. Inoculating LAB could decrease silage pH, which inhibited the growth of undesirable microbes with lower microbial diversity compared to untreated alfalfa silage (Yang et al., 2019). After 45 days of ensiling, the higher Simpson, Shannon index, and Chao1 values in C and LP silages vs. other groups may have been due to more undesirable microbes (**Figure 6**).

Tao et al. (2018) observed the *Lactobacillus* and *Pediococcus* in pre-fermented juice prepared from lucerne using agar media-based culturing method, while seven common LAB species were identified in lucerne pre-fermented juice using 16S rRNA gene sequencing techniques (Sun et al., 2021). However, in this study four species (*W. cibaria*, *L. brevis*, *L. plantarum*, and *L. paralimentarius*) of LAB in three genera were present in pre-fermented juice, with *W. cibaria* (96.9%) being dominant. Sun et al. (2021) also found that *W. cibaria* was identified in the pre-fermented juice prepared from lucerne. Preparation of pre-fermented juice involved culturing microbes on the crop surface. That 81.6% of microorganisms in pre-fermented juice were also present in fresh lucerne confirmed that epiphytic microorganisms affected the composition of the microbial community in pre-fermented juice. Furthermore, *Weissella*, *Lactobacilli,* and *Cocci* species were reported as major components in various crops (Cai et al., 1998).

The addition of exogenous microbial inoculant enriched LA-producing bacteria after 5 and 15 days of ensiling, whereas adding LP enriched *Lactobacillus* and *Weissella* of cauliflower leaf silages at 30 days of ensiling (Ren et al., 2020). There were greater abundances of *Lactobacillus*, *Weissella*, and *Pediococcus* in J and LPB silages at Days 5 and 15 of ensiling, which may have promoted rapid and efficient LA fermentation and faster pH reduction early in ensiling. Similarly, silages treated with pre-fermented juice had higher LAB counts and LA contents, but lower pH than untreated lucerne silage (Sun et al., 2021). In the current study, *L. nodensis* and *L. parabrevis* were the predominant bacteria in all groups on Days 5 and 15 of ensiling. Kashiwagi et al. (2009) isolated *L. nodensis* from rice bran; however, there is limited information about this species in silage. Perhaps the presence of *L. nodensis* was associated with a rapid increase in LA and decline in pH during 5 days of ensiling. Pre-fermented juice has the potential to promote the shift of *L. nodensis* to *L. parabrevis* during15 days of ensiling, and *L. parabrevis* had a greater abundance in J silage than other treatments at Days 5 and 15 of ensiling. Xu et al. (2021) observed that *L. parabrevis* was enriched in all treatments of whole crop corn silage after 7 days of ensiling. Wu et al. (2020) reported that LP-treated silage increased the abundance of *L. parabrevis* in high-moisture sweet corn kernel silage. In addition, more *W. cibaria* and *L. sakei* were observed in J silage than other treatments after 5 and 15 days of ensiling. Bai C. et al. (2021) speculated that *W. cibaria* maintained a high relative abundance in alfalfa silage because

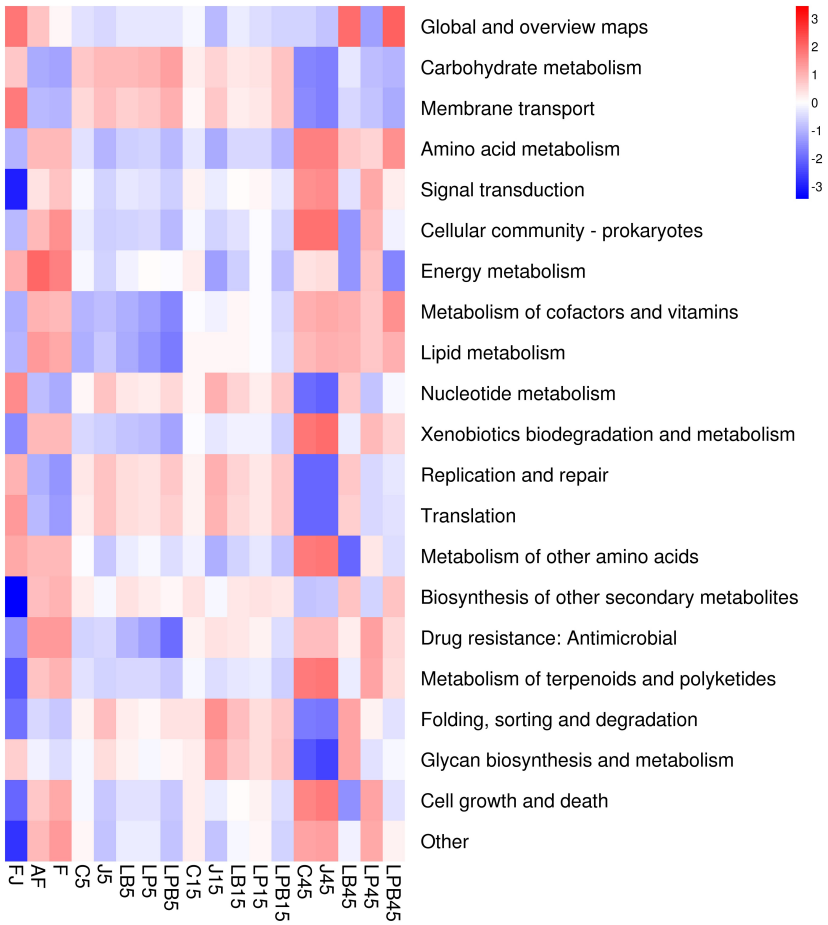

FIGURE 7 | Heatmap of KEGG pathway, the second level of the predicted functional shift is shown with respect to the fermentation processes and inoculant treatments. AF, fresh alfalfa; FJ, pre-fermented juice; F, mixture; C, control; J, pre-fermented juice-treated silage; LP, *L. plantarum*-treated silage; LB, *L. buchneri*-treated silage; LPB, *L. plantarum* + *L. buchneri*-treated silage.

of their stronger vitality and competitiveness. That *W. cibaria* was the dominant species in pre-fermented juice accounted for its competitiveness in J silage. *L. sakei* had a significant role in fermentation of grass, with concentrations of LA and AA positively correlated with this bacterium (Ding et al., 2020). In the present study, the LPB silage had the highest abundance of *L. paralimentarius* after 15 days of ensiling. Similarly, inoculation of ensiled corn with LB and LP increased relative abundances of *L. paralimentarius* (Xu et al., 2021). After 45 days of ensiling, *Pseudomonas putida* and *Stenotrophomonas maltophilia* in C and J silages reached the highest relative abundance. Some species of *Pseudomonas* are usually associated with decreases in AN concentration and yeast count, and they also have been reported in other silages such as mulberry leaf and sweet sorghum (Wang et al., 2019; Ren et al., 2021). In the current study, J silage tended to have lower AN concentration, attributed to a greater abundance of *Pseudomonas putida*. Dong et al. (2020) assessed the microbial communities of ryegrass silage and reported a positive correlation between *Stenotrophomonas* and LA concentrations. *Stenotrophomonas maltophilia* was also isolated from fermented high-moisture sweet corn kernel (Wu et al., 2020). In this study, there was a high abundance of spoilage-producing organisms, including *Acinetobacter* sp., *Erwinia* sp., *Paenibacillus* sp., *Paenibacillus hispanicus*, *Psychrobacillus soli,* and *Carnobacterium inhibents* in C silage, and Enterobacterales, *Paenibacillus* sp., and *Erwinia* sp., in LP silage. However, inoculating with *L. buchneri* inoculants could inhibit *Erwinia* sp. and *Paenibacillus* sp. Considerable abundance of *Acinetobacter* was detected in *Neolamarckia cadamba* leaf, which can use AA as substrates and decrease silage quality under anaerobic conditions (He et al., 2020). A lower relative abundance of *Erwinia* in total mixed ration silage was associated with the improved silage quality (Jiang et al., 2020), as this genus belongs to *Enterobacteria,* which can compete with LAB for substrate. Both *Paenibacillus* and *Psychrobacillus* may promote growth of less acid-tolerant spoilage microorganisms; they were detected in Napier grass silage and mixed corn and soybean silage (Zeng et al., 2020; Yin et al., 2021). Furthermore, *Carnobacterium* apparently decreased fermentation quality of Italian ryegrass silage (Yan et al., 2019).

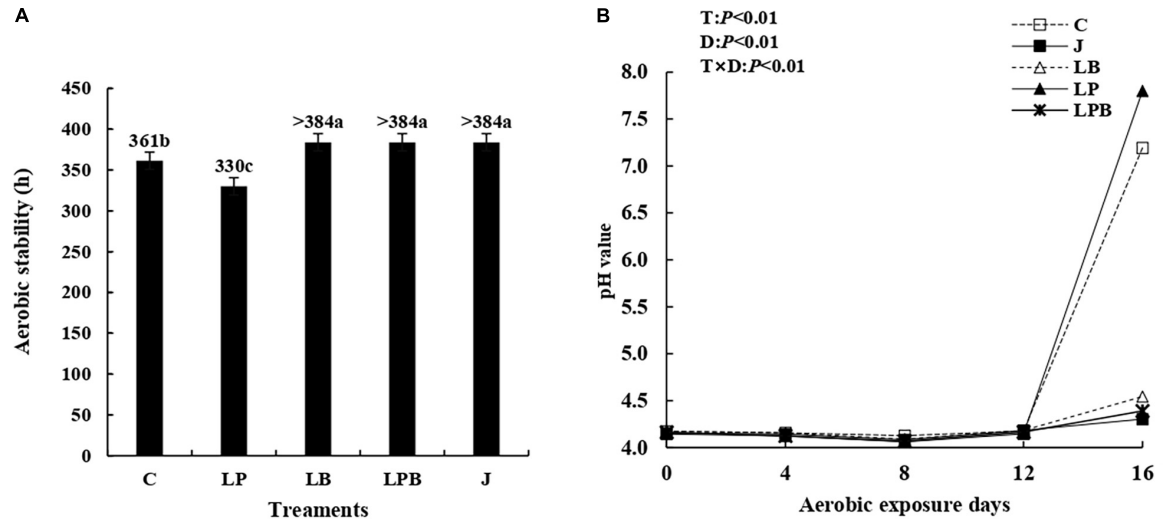

FIGURE 8 | Aerobic stability **(A)** and dynamics of pH **(B)** during aerobic exposure days. C, control; J, pre-fermented juice-treated silage; LP, *L. plantarum*-treated silage; LB, *L. buchneri*-treated silage; LPB, *L. plantarum* + *L. buchneri*-treated silage. D, ensilage days; T, treatments; T × D, the interaction between treatment and ensiling days.

The Succession of Three Inoculants Over Ensiling

In most studies, regardless of whether *Weissella* was present in fresh forage or silage, eventually, *Lactobacilli* became dominant during terminal fermentation (Cai et al., 1998; Mu et al., 2021). *W. cibaria* initiated lactate fermentation in silage, creating an aerobic environment suitable for development of *Lactobacilli*, although they grew vigorously only during the early stage of ensiling. Inoculants may have undesirable effects due to a lack of compatibility between the additive and plant material (Koc et al., 2017). In this study, adding *L. plantarum* treatments did not obviously increase the relative abundance of this bacterium, with more spoilage-inducing organisms present in LP silage. In previous studies with *L. buchneri*, a longer conservation period (from 45 to 90 days) was needed to be efficacious (Arriola et al., 2021b). Likewise, in this study, a dramatic shift in microbial composition occurred in LB and LPB silages after 45 days of ensiling, with massive amounts of *L. buchneri* as assessed with SMRT.

Effect of Kyoto Encyclopedia of Genes and Genomes Metabolism Pathways in Raw Material and Silages

Functional predictions of bacterial communities facilitate assessment of effects of bacterial communities on changes in metabolic pathways underlying silage formation (Bai J. et al., 2021). In the present study, the metabolic pathways changed with time. There was a high incidence of carbohydrate metabolism in silages from 5 to 15 days of ensiling, whereas metabolism of cofactors and vitamins, and amino acid metabolism had a high incidence only after 45 days of ensiling. Expression of the carbohydrate metabolism pathway may be related to active LAB metabolism during early ensiling, with accumulation of much LA and VFA during 15 days of ensiling. Similarly, Bai J. et al. (2021) reported higher relative abundances of carbohydrate metabolism during the early stage of ensiling alfalfa treated with *L. plantarum* and *P. pentosaceus*. Higher amino-acid metabolism at the end of ensiling was caused by undesirable microbes that increased AN concentration at 45 days of ensiling; conversely, high amino-acid metabolism may be an attempt to degrade macromolecular proteins into readily absorbable amino acids or peptides (Bai J. et al., 2021; Du et al., 2021b). In addition, *L. buchneri* inoculants promoted global metabolism, perhaps due to this bacterium suppressing harmful microorganisms in LB and LPB silages. Du et al. (2021a) also reported that superior global metabolism in woody plant mixed silage was due to inhibition of harmful microorganisms by extensive LA-fermentation.

Effect of Inoculants Ensiling on Aerobic Stability

Aerobic stability was improved with LB-treated silages, which is not only due to more AA accumulation after 45 days of ensiling but also some antimicrobial substances like bacteriocin produced by *L. buchneri* (Arriola et al., 2021a). The recent meta-analysis also reported that *L. buchneri* -based inoculants improved aerobic stability by increased AA concentration and reduced yeast counts (Arriola et al., 2021a). According to Tao et al. (2017), the pre-fermented juice application prolonged aerobic stability by 17 h in comparison to the control. Similarly, in this study, pre-fermented juice significantly improved the aerobic stability of silage, which is likely due to the increased relative abundance of *L. brevis*. *L. brevis* is known as a hetero-fermentative strain belonging to the *L. buchneri* group of lactobacilli, which showed antibacterial and probiotic properties (Soundharrajan et al., 2019).

CONCLUSION

In this study, four species of LAB from three genera were detected in pre-fermented juice, with *W. cibaria* dominating. Adding LPB increased abundance of *L. plantarum*, *L. paralimentarius,* and *L. nodensis* and resulted in the lowest pH. Pre-fermented juice enriched abundance of *W. cibaria*, *L. sakei*, *L. parabrevis*, *Pseudomonas putida,* and *Stenotrophomonas maltophilia*, enhanced accumulation of AA and LA, rapidly decreased pH, and reduced CP losses, AN, and HC. Aerobic stability was prolonged (>384 h) by inoculating with LB, LPB, or pre-fermented juice; the latter is a promising biological source of LAB for cleaner production to improve silage quality.

DATA AVAILABILITY STATEMENT

Publicly available datasets were analyzed in this study. This data can be found here: The sequencing data were submitted to the NCBI Sequence Read Archive database (accession number: PRJNA798538). https://www.ncbi.nlm.nih.gov/bioproject/PRJNA798538.

AUTHOR CONTRIBUTIONS

LM: conceptualization, methodology, and writing—review and editing. QW: resources and formal analysis. XC: investigation and data curation. HL: methodology and investigation. ZZ: validation and supervision. All authors contributed to the article and approved the submitted version.

FUNDING

This work was funded by the Hunan Science and Technology Planning Project (Grant No. 2020NK3008) and Key R&D Program of Hunan Province (Grant No. 2020NK2061).

REFERENCES

Adesogan, A. T. (2008). "Recent advances in bacterial silage inoculant technology," in *Proceedings of the Florida Ruminant Nutrition Symposium* (Gainesville, FL: Best Western Gateway Grand).

Ali, N., Wang, S., Zhao, J., Dong, Z., Li, J., Nazar, M., et al. (2020). Microbial diversity and fermentation profile of red clover silage inoculated with reconstituted indigenous and exogenous epiphytic microbiota. *Bioresour. Technol.* 314:123606. doi: 10.1016/j.biortech.2020.123606

Arriola, K. G., Oliveira, A. S., Jiang, Y., Kim, D., Silva, H. M., Kim, S. C., et al. (2021a). Meta-analysis of effects of inoculation with *Lactobacillus buchneri*, with or without other bacteria, on silage fermentation, aerobic stability, and performance of dairy cows. *J. Dairy Sci.* 104, 7653–7670. doi: 10.3168/jds.2020-19647

Arriola, K. G., Vyas, D., Kim, D., Agarussi, M. C. N., Silva, V. P., Flores, M., et al. (2021b). Effect of *Lactobacillus hilgardii*, *Lactobacillus buchneri*, or their combination on the fermentation and nutritive value of sorghum silage and corn silage. *J. Dairy Sci.* 104, 9664–9675. doi: 10.3168/jds.2020-19512

Bai, C., Wang, C., Sun, L., Xu, H., Jiang, Y., Na, N., et al. (2021). Dynamics of bacterial and fungal communities and metabolites during aerobic exposure in whole-plant corn silages with two different moisture levels. *Front. Microbiol.* 12:663895. doi: 10.3389/fmicb.2021.663895

Bai, J., Ding, Z., Ke, W., Xu, D., Wang, M., Huang, W., et al. (2021). Different lactic acid bacteria and their combinations regulated the fermentation process of ensiled alfalfa: ensiling characteristics, dynamics of bacterial community and their functional shifts. *Microb. Biotechnol.* 14, 1171–1182. doi: 10.1111/1751-7915.13785

Broderick, G. A., and Kang, J. H. (1980). Automated simultaneous determination of ammonia and total amino acids in ruminal fluid and *in vitro* media. *J. Dairy Sci.* 63, 64–75. doi: 10.3168/jds.S0022-0302(80)82888-8

Cai, Y., Benno, Y., Ogawa, M., Ohmomo, S., Kumai, S., and Nakase, T. (1998). Influence of *Lactobacillus* spp. from an inoculant and of *Weissella* and *Leuconostoc* spp. from forage crops on silage fermentation. *Appl. Environ. Microbiol.* 64, 2982–2987. doi: 10.1128/AEM.64.8.2982-2987.1998

Chen, X. (2016). Economic potential of biomass supply from crop residues in China. *Appl. Energy* 166, 141–149. doi: 10.1016/j.scitotenv.2020.136915

Denek, N., Can, A., Avci, M., and Aksu, T. (2012). The effect of fresh and frozen pre-fermented juice on the fermentation quality of alfalfa silage. *Kafkas Univ. Vet. Fak. Derg.* 18, 785–790.

Denek, N., Can, A., Avci, M., Aksu, T., and Durmaz, H. (2011). The effect of molasses-based pre-fermented juice on the fermentation quality of first-cut lucerne silage. *Grass Forage Sci.* 66, 243–250. doi: 10.1111/j.1365-2494.2011.00783.x

Ding, Z., Bai, J., Xu, D., Li, F., Zhang, Y., and Guo, X. (2020). Microbial community dynamics and natural fermentation profiles of ensiled alpine grass *Elymus nutans* prepared from different regions of the Qinghai-Tibetan Plateau. *Front. Microbiol.* 11:855. doi: 10.3389/fmicb.2020.00855

Dong, L., Zhang, H., Gao, Y., and Diao, Q. (2020). Dynamic profiles of fermentation characteristics and bacterial community composition of *Broussonetia papyrifera* ensiled with perennial ryegrass. *Bioresour. Technol.* 310:123396. doi: 10.1016/j.biortech.2020.123396

Driehuis, F., Oude Elferink, S., and Van Wikselaar, P. (2001). Fermentation characteristics and aerobic stability of grass silage inoculated with *Lactobacillus buchneri*, with or without homofermentative lactic acid bacteria. *Grass Forage Sci.* 56, 330–343. doi: 10.1046/j.1365-2494.2001.00282.x

Du, Z., Lin, Y., Sun, L., Yang, F., and Cai, Y. (2021a). Microbial community structure, co-occurrence network and fermentation characteristics of woody plant silage. *J. Sci. Food Agric.* 102, 1193–1204. doi: 10.1002/jsfa.11457

Du, Z., Sun, L., Chen, C., Lin, J., Yang, F., and Cai, Y. (2021b). Exploring microbial community structure and metabolic gene clusters during silage fermentation of paper mulberry, a high-protein woody plant. *Anim. Feed Sci. Technol.* 275:114766. doi: 10.1016/j.anifeedsci.2020.114766

Filya, I. (2003). The effect of *Lactobacillus buchneri* and *Lactobacillus plantarum* on the fermentation, aerobic stability, and ruminal degradability of low dry matter corn and sorghum silages. *J. Dairy Sci.* 86, 3575–3581. doi: 10.3168/jds.S0022-0302(03)73963-0

Guo, X. S., Ke, W. C., Ding, W. R., Ding, L. M., Xu, D. M., Wang, W. W., et al. (2018). Profiling of metabolome and bacterial community dynamics in ensiled *Medicago sativa* inoculated without or with *Lactobacillus plantarum* or *Lactobacillus buchneri*. *Sci. Rep.* 8:357. doi: 10.1038/s41598-017-18348-0

He, L., Lv, H., Xing, Y., Chen, X., and Zhang, Q. (2020). Intrinsic tannins affect ensiling characteristics and proteolysis of *Neolamarckia cadamba* leaf silage by largely altering bacterial community. *Bioresour. Technol.* 311:123496. doi: 10.1016/j.biortech.2020.123496

Huisden, C. M., Adesogan, A. T., Kim, S. C., and Ososanya, T. (2009). Effect of applying molasses or inoculants containing homofermentative or heterofermentative bacteria at two rates on the fermentation and aerobic stability of corn silage. *J. Dairy Sci.* 92, 690–697. doi: 10.3168/jds.2008-1546

Jiang, D., Li, B., Zheng, M., Niu, D., Zuo, S., and Xu, C. (2020). Effects of *Pediococcus pentosaceus* on fermentation, aerobic stability and microbial communities during ensiling and aerobic spoilage of total mixed ration silage containing alfalfa (*Medicago sativa* L.). *Grassl. Sci.* 66, 215–224. doi: 10.1111/grs.12272

Jian-Xin, L., Wang, X., and Shi, Z. (2001). Addition of rice straw or/and wheat bran on composition, ruminal degradability and voluntary intake of bamboo shoot shells silage fed to sheep. *Anim. Feed Sci. Technol.* 91, 129–138. doi: 10.1016/s0377-8401(01)00238-3

Kashiwagi, T., Suzuki, T., and Kamakura, T. (2009). *Lactobacillus nodensis* sp. nov., isolated from rice bran. *Int. J. Syst. Evol. Microbiol.* 59, 83–86. doi: 10.1099/ijs.0.65772-0

Koc, F., Aksoy, S. O., Okur, A. A., Celikyurt, G., Korucu, D., and Ozduven, M. (2017). Effect of pre-fermented juice, *Lactobacillus plantarum* and *Lactobacillus buchneri* on the fermentation characteristics and aerobic stability of high dry matter alfalfa bale silage. *J. Anim. Plant Sci.* 27, 1766–1773.

McDonald, P., Henderson, A., and Heron, S. (1991). *The Biochemistry of Silage*. Marlow: Chalcombe publications.

Mu, L., Wang, Q., Cao, X., and Zhang, Z. (2021). Effects of fatty acid salts on fermentation characteristics, bacterial diversity and aerobic stability of mixed silage prepared with alfalfa, rice straw and wheat bran. *J. Sci. Food Agric.* 102, 1475–1487. doi: 10.1002/jsfa.11482

Mu, L., Xie, Z., Hu, L., Chen, G., and Zhang, Z. (2020). Cellulase interacts with *Lactobacillus plantarum* to affect chemical composition, bacterial communities, and aerobic stability in mixed silage of high-moisture amaranth and rice straw. *Bioresour. Technol.* 315:123772. doi: 10.1016/j.biortech.2020.123772

Muck, R. E. (2010). Silage microbiology and its control through additives. *Rev. Bras. Zootec.* 39, 183–191. doi: 10.1590/s1516-35982010001300021

Ohshima, M. (1997). Fermentation quality of alfalfa and Italian ryegrass silages treated with previously fermented juices prepared from both the herbages. *Anim. Sci. Technol.* 68, 41–44. doi: 10.2508/chikusan.68.41

Ren, H., Feng, Y., Pei, J., Li, J., Wang, Z., Fu, S., et al. (2020). Effects of *Lactobacillus plantarum* additive and temperature on the ensiling quality and microbial community dynamics of cauliflower leaf silages. *Bioresour. Technol.* 307:123238. doi: 10.1016/j.biortech.2020.123238

Ren, H., Sun, W., Yan, Z., Zhang, Y., Wang, Z., Song, B., et al. (2021). Bioaugmentation of sweet sorghum ensiling with rumen fluid: fermentation characteristics, chemical composition, microbial community, and enzymatic digestibility of silages. *J. Clean. Prod.* 294:126308. doi: 10.1016/j.jclepro.2021.126308

Shao, T., Zhanga, L., Shimojo, M., and Masuda, Y. (2007). Fermentation quality of Italian ryegrass (*Lolium multiflorum* Lam.) silages treated with encapsulated-glucose, glucose, sorbic acid and pre-fermented juices. *Asian Australas. J. Anim. Sci.* 20, 1699–1704. doi: 10.5713/ajas.2007.1699

Soundharrajan, I., Kim, D., Kuppusamy, P., Muthusamy, K., Lee, H. J., and Choi, K. C. (2019). Probiotic and *Triticale* silage fermentation potential of *Pediococcus pentosaceus* and *Lactobacillus brevis* and their Impacts on pathogenic bacteria. *Microorganisms* 7:318. doi: 10.3390/microorganisms7090318

Sun, L., Jiang, Y., Ling, Q., Na, N., Xu, H., Vyas, D., et al. (2021). Effects of adding pre-fermented fluid prepared from red clover or lucerne on fermentation quality and *in vitro* digestibility of red clover and lucerne silages. *Agriculture* 11:454. doi: 10.3390/agriculture11050454

Tao, L., Zhou, H., Zhang, N., Si, B., Tu, Y., Ma, T., et al. (2017). Effects of different source additives and wilt conditions on the pH value, aerobic stability, and carbohydrate and protein fractions of alfalfa silage. *Anim. Sci. J.* 88, 99–106. doi: 10.1111/asj.12599

Tao, L., Zhou, H., Zhang, N. F., Si, B. W., Tu, Y., Ma, T., et al. (2018). Changes in carbohydrate and protein fractions during ensiling of alfalfa treated with previously fermented alfalfa juice or lactic acid bacteria inoculants. *Anim. Prod. Sci.* 58, 577–584. doi: 10.1071/an15067

Van Soest, P. V., Robertson, J., and Lewis, B. (1991). Methods for dietary fiber, neutral detergent fiber, and nonstarch polysaccharides in relation to animal nutrition. *J. Dairy Sci.* 74, 3583–3597. doi: 10.3168/jds.S0022-0302(91)78551-2

Wang, J., Wang, J. Q., Zhou, H., and Feng, T. (2009). Effects of addition of previously fermented juice prepared from alfalfa on fermentation quality and protein degradation of alfalfa silage. *Anim. Feed Sci. Technol.* 151, 280–290. doi: 10.1016/j.anifeedsci.2009.03.001

Wang, S., Guo, G., Li, J., Chen, L., Dong, Z., and Shao, T. (2018). Improvement of fermentation profile and structural carbohydrate compositions in mixed silages ensiled with fibrolytic enzymes, molasses and *Lactobacillus plantarum* MTD-1. *Ital. J. Anim. Sci.* 18, 328–335. doi: 10.1080/1828051x.2018.1528899

Wang, Y., Chen, X., Wang, C., He, L., Zhou, W., Yang, F., et al. (2019). The bacterial community and fermentation quality of mulberry (*Morus alba*) leaf silage with or without *Lactobacillus casei* and sucrose. *Bioresour. Technol.* 293:122059. doi: 10.1016/j.biortech.2019.122059

Weinberg, Z., Ashbell, G., Hen, Y., and Azrieli, A. (1993). The effect of applying lactic acid bacteria at ensiling on the aerobic stability of silages. *J. Appl. Bacteriol.* 75, 512–518. doi: 10.1111/j.1365-2672.1993.tb01588.x

Wu, Z., Luo, Y., Bao, J., Luo, Y., and Yu, Z. (2020). Additives affect the distribution of metabolic profile, microbial communities and antibiotic resistance genes in high-moisture sweet corn kernel silage. *Bioresour. Technol.* 315:123821. doi: 10.1016/j.biortech.2020.123821

Xu, D., Wang, N., Rinne, M., Ke, W., Weinberg, Z. G., Da, M., et al. (2021). The bacterial community and metabolome dynamics and their interactions modulate fermentation process of whole crop corn silage prepared with or without inoculants. *Microb. Biotechnol.* 14, 561–576. doi: 10.1111/1751-7915.13623

Yan, Y., Li, X., Guan, H., Huang, L., Ma, X., Peng, Y., et al. (2019). Microbial community and fermentation characteristic of Italian ryegrass silage prepared with corn stover and lactic acid bacteria. *Bioresour. Technol.* 279, 166–173. doi: 10.1016/j.biortech.2019.01.107

Yang, L., Yuan, X., Li, J., Dong, Z., and Shao, T. (2019). Dynamics of microbial community and fermentation quality during ensiling of sterile and nonsterile alfalfa with or without *Lactobacillus plantarum* inoculant. *Bioresour. Technol.* 275, 280–287. doi: 10.1016/j.biortech.2018.12.067

Yanti, Y., Kawai, S., and Yayota, M. (2019). Effect of total mixed ration silage containing agricultural by-products with the fermented juice of epiphytic lactic acid bacteria on rumen fermentation and nitrogen balance in ewes. *Trop. Anim. Health Prod.* 51, 1141–1149. doi: 10.1007/s11250-019-01798-1

Yin, X., Tian, J., and Zhang, J. (2021). Effects of re-ensiling on the fermentation quality and microbial community of Napier grass (*Pennisetum purpureum*) silage. *J. Sci. Food Agric.* 101, 5028–5037. doi: 10.1002/jsfa.11147

Yuan, X., Dong, Z., Li, J., and Shao, T. (2019). Microbial community dynamics and their contributions to organic acid production during the early stage of the ensiling of Napier grass (*Pennisetum purpureum*). *Grass Forage Sci.* 75, 37–44. doi: 10.1111/gfs.12455

Zeng, T., Li, X., Guan, H., Yang, W., Liu, W., Liu, J., et al. (2020). Dynamic microbial diversity and fermentation quality of the mixed silage of corn and soybean grown in strip intercropping system. *Bioresour. Technol.* 313:123655. doi: 10.1016/j.biortech.2020.123655

Conflict of Interest: The authors declare that the research was conducted in the absence of any commercial or financial relationships that could be construed as a potential conflict of interest.

Publisher's Note: All claims expressed in this article are solely those of the authors and do not necessarily represent those of their affiliated organizations, or those of the publisher, the editors and the reviewers. Any product that may be evaluated in this article, or claim that may be made by its manufacturer, is not guaranteed or endorsed by the publisher.

frontiers | Frontiers in Microbiology

ORIGINAL RESEARCH
published: 04 May 2022
doi: 10.3389/fmicb.2022.864963

A Fluorescent Reporter-Based Evaluation Assay for Antibacterial Components Against *Xanthomonas citri* subsp. *citri*

Yunfei Long[1†], Ruifang Luo[1†], Zhou Xu[1], Shuyuan Cheng[1], Ling Li[1], Haijie Ma[2], Minli Bao[1], Min Li[1], Zhigang Ouyang[1], Nian Wang[3] and Shuo Duan[1†]*

[1] China-USA Citrus Huanglongbing Joint Laboratory, National Navel Orange Engineering Research Center, Gannan Normal University, Ganzhou, China, [2] College of Agricultural and Food Sciences, Zhejiang A&F University, Hangzhou, China, [3] Department of Microbiology and Cell Science, Citrus Research and Education Center, University of Florida, Lake Alfred, FL, United States

OPEN ACCESS

Edited by:
Christopher Rensing,
Fujian Agriculture and Forestry University, China

Reviewed by:
Yunzeng Zhang,
Yangzhou University, China
Betiana Soledad Garavaglia,
Instituto de Biología Molecular y Celular de Rosario (IBR-CONICET), Argentina

***Correspondence:**
Shuo Duan
duansure@163.om

[†] These authors have contributed equally to this work

Specialty section:
This article was submitted to Microbiotechnology, a section of the journal Frontiers in Microbiology

Received: 29 January 2022
Accepted: 05 April 2022
Published: 04 May 2022

Citation:
Long Y, Luo R, Xu Z, Cheng S, Li L, Ma H, Bao M, Li M, Ouyang Z, Wang N and Duan S (2022) A Fluorescent Reporter-Based Evaluation Assay for Antibacterial Components Against Xanthomonas citri subsp. citri. Front. Microbiol. 13:864963. doi: 10.3389/fmicb.2022.864963

Xanthomonas citri subsp. *citri* (*Xcc*) is the agent of citrus bacterial canker (CBC) disease, which has significantly reduced citrus quantity and quality in many producing areas worldwide. Copper-based bactericides are the primary products for CBC control and management, but the problems derived from copper-resistant and environmental contamination have become issues of anxiety. Thus, there is a need to find alternative antibacterial products instead of relying on a single type of agent. This study developed a method to evaluate the inhibition of antibacterial agents using the fluorescence-labeled recombinant *Xcc* strain (*Xcc-eYFP*). The optimization of timelines and parameters for the evaluation of antibacterial agents involved the use of a Spark^{TM} multimode microplate reader. This evaluation and screening method can be applied to bactericides, cocktail-mixture formulations, antagonistic bacteria, and derived metabolites. The results showed that the minimum inhibitory concentration (MIC) of commercial bactericides determined by fluorescence agrees with the MIC values determined by the conventional method. A screened cocktail-mixture bactericide presents more activity than the individual agents during the protective effects. Notably, this method has been further developed in the screening of *Xcc*-antagonistic bacterial strains. In summary, we provide a validated strategy for screening and evaluation of different antibacterial components for inhibition against *Xcc* for CBC control and management.

Keywords: antagonistic, *Xanthomonas citri*, evaluation and screening, citrus canker, reporter-based

INTRODUCTION

Citrus is one of the essential fruit tree crops worldwide concerning total production and economic value (Sangiorgio et al., 2020). Citrus bacterial canker (CBC) disease is one of the most severe bacterial diseases harming the citrus industry (Li and Wang, 2011a; Rabbee et al., 2019). The causal agent is composed of strains that have been designated as *Xcc*A, *Xcc*A^{w}, *Xcc*A*, *Xcc*B, and *Xcc*C according to host range and ability to elicit a hypersensitive response (HR) in different citrus

varieties (Leduc et al., 2011; Ference et al., 2018). The *Xanthomonas citri* subsp. *citri* Asiatic strain *Xcc*A was distributed in many citrus-producing countries with high pathogenicity and a broad host range. *Xcc*A invades citrus leaves, stems, and fruit *via* natural openings such as stomata and wounds, further reducing citrus quality and productivity by causing severe defoliation, blemished fruit, and premature fruit drop. Theoretically, *Xcc*A causes hypertrophy and hyperplasia symptoms by secreting PthA4 and functional homologs, which are transcriptional activator-like effectors, *via* the type III secretion system (T3SS) into the nucleus of plant cells to induce the expression of the canker susceptibility gene *CsLOB*1 (Yan et al., 2012; Hu et al., 2014, 2016; Duan et al., 2018). In addition to T3SS and T3SS effectors, virulence factors involved in biofilm (Rigano et al., 2007; Li and Wang, 2011a), xanthan gum (Li and Wang, 2012), lipopolysaccharides (Li and Wang, 2011b; Yan and Wang, 2011; Petrocelli et al., 2012; Yan et al., 2012), and epiphytic fitness (Rigano et al., 2007) also play essential roles in the infection of *Xcc*.

In endemic canker regions, the primary control strategy is the application of copper-based bactericides to prevent *Xcc* infection (Narciso et al., 2012; Scapin et al., 2015; Gochez et al., 2018; Behlau et al., 2021b). Copper-based bactericides, in the presence of water and low pH, release copper ions to bind to proteins of pathogenic bacteria, leading to protein misfunction, proteins and nucleic acid damage, and ultimately the death of pathogens (Behlau et al., 2011). Even though the application of copper is not practical for protecting young, susceptible citrus foliage against *Xcc* infection, copper sprays still showed the highest contribution to canker control by reducing disease incidence and crop losses (Behlau et al., 2017; Heydarpanah et al., 2020; Machado et al., 2021). In contrast, the extensive use of copper-based bactericides has led to soil and water contamination that directly harms humans and surrounding ecosystems (Zhang et al., 2003). Copper accumulation has been reported to reduce microbial biomass and diversity in copper-affected soils (Zhou et al., 2011). Moreover, long-term use of copper-based bactericides has led to the development of copper-resistant strains in many phytopathogenic bacteria, including *Xcc*, resulting in a reduction of disease control (Behlau et al., 2011, 2012a). Even though the copper-resistant *Xcc* strain was only reported in Argentina and Reunion Island (Behlau et al., 2012b; Richard et al., 2017), it could appear under reliance on the extensive use of copper-based bactericides for disease management.

Disease-resistant crop varieties are efficient and environmentally friendly approaches to disease management (de Carvalho et al., 2015; Fu et al., 2020). Citrus-producing regions without CBC rely mainly on quarantine measures to keep the groves free of *Xcc*. Windbreaks also have a positive control effect on CBC by reducing wounds (Behlau et al., 2021a). Diverse and integrated disease control can reduce the risk of the application of copper-based bactericides during CBC control and management, but chemical control is still the primary method for preventing *Xcc* worldwide. Some substitutes for copper-based bactericides have been applied to CBC control. For example, imidacloprid and systemic acquired resistance-inducing compounds applied to soil (Graham and Myers, 2011); exogenous application of nicotinamide adenine dinucleotide by soil drenches or leaf infiltration (Alferez et al., 2018); foliar spraying of nanoformulated zinc oxide (Graham and Myers, 2016); and biofilm inhibitors (Li and Wang, 2014) and the root application of rhizobacteria (Riera et al., 2018) have positive control effects on CBC.

The application of new or mixed antibacterial components is a substitute strategy for copper-based bactericides, which can reduce the side effects of extensive use of copper-based bactericides separately (Ibrahim et al., 2017). Field protection revealed that the combination of bactericides presents a better performance effect than a single agent. However, the combination ratio of bactericides derived a significant number of combinations. Picking out the well-performance ratio from combinations requires an efficient approach instead of conventional methods because these are usually time-consuming, laborious, and less accurate. Minimum inhibitory concentration (MIC) is conventionally based on the absorption value and plate colony count, which is time-consuming and laborious. The inhibition zone method is commonly used for antagonism to evaluate bactericides against bacteria, based on the scope of the inhibition zone on the plate and the parameter MIC, which is affected by the nurturing plate and environment. Here, we firstly developed a rapid evaluation method based on eYFP labeling of *Xcc* strains. This study evaluated the inhibition rates of commercial bactericides, corresponding mixed formulations, *Xcc*-antagonistic bacterial strains, and derived products using a reporter-based assay. Subsequently, this method was evaluated for the indoor inhibition activity and field protective effect of bactericides.

MATERIALS AND METHODS

Bacterial Strains, Plants, and Growth Conditions

Xcc strains were isolated from the Jiangxi province, China. All bacterial strains were maintained in 15% glycerol and preserved in a freezer at −80°C. *Escherichia coli* cells were cultured in the Luria–Bertani (LB) medium (tryptone 10 g/L, yeast extract 5 g/L, and NaCl 10 g/L) at 37°C. *Xcc* strains were recovered and cultured on nutrient broth (NB) medium (beef extract 3 g/L and peptone 5 g/L) and on nutrient agar (NA) medium (beef extract 3 g/L, peptone 5 g/L, and agar 12 g/L) plates at 28°C. When required, growth media were supplemented with gentamicin (20 μg/ml) and kanamycin (50 μg/ml).

Hamlin sweet orange [*Citrus sinensis* (L.) Osbeck] was grown in a greenhouse with a 16-h light and 8-h dark photoperiod, a 28/26°C temperature cycle, and 80% humidity. Fully expanded young leaves of approximately 1-month old were used.

Construction of eYFP Plasmid

The plasmid was constructed as described in previous research (Duan et al., 2021). The plasmid DNA concentration was measured with the NanoDrop® ND-1000 (NanoDrop, United States). Briefly, the broad-host-range vector pBBR1-eYFP was constructed by cloning the *eYFP* coding region into

pBBR1-MCS5. The construct for pBBR1-eYFP was introduced into an *E. coli* DH5α competent cell and then selected on LB plates containing 20 μg/ml of gentamycin. Plasmid DNA extracted from *E. coli* transformants was reintroduced into *Xcc* competent cells using electroporation of the Gene Pulser Xcell system (Bio-Rad, United States) under the following conditions: 1 mm cuvette, voltage of 2,400 V; capacitance of 25 μF. The reconstructed *Xcc* strains were spread on NA plates containing 20 μg/ml of gentamycin. Polymerase chain reaction (PCR) and restricted enzymatic digestion were applied for the confirmation of plasmids. Meanwhile, the *Xcc-eYFP* strain can represent the fluorescent signal (excitation/emission at 514/527 nm) at 24-h post-transformation. The bacterial cell, clones, and suspension of *Xcc-eYFP* can be observed under a handheld lamp (#LUYOR-3260CY, LUYOR, China) and a fluorescent microscope (Leica, Germany) with corresponding filters.

Xanthomonas citri subsp. *citri* Strain Susceptibility to Solvents

The susceptibility of *Xcc-eYFP* strains to solvents were examined under laboratory conditions: 10 mM $MgCl_2$, liquid medium NB, dimethyl sulfoxide (DMSO), dimethylformamide (DMF), and acetone. A logarithmic culture of *Xcc-eYFP* was diluted into OD_{600} of 0.3 [about 5×10^8 colony-forming units/ml (CFU/ml)] and suspended in a range of solvent concentration from 0 to 100% (20% of the interval). Plates were incubated at room temperature, and the luminescence of *Xcc-eYFP* was read at 0, 6, 12, 24, and 48 h using a Spark^{TM} multimode microplate reader (TECAN, Switzerland) for fluorescent signal detection. Susceptibility to solvents was calculated as percentage inhibition using the formula [(negative control signal – sample signal)/negative control signal × 100].

Bactericide Treatments and Pathogenicity Test

Commercial bactericides: 33% kasugamycin xine-copper (SC), 1.2% xinjunan acetate (AS), 30% copper oxychloride (SC), and 20% resin acid copper (EW) were diluted to the corresponding concentrations and mixed in a series of synergistic ratios with the corresponding solvent (**Supplementary Tables 1, 2**). The control effect of four individual bactericides (2 mg/ml) and three mixture formulations of bactericides were investigated. Briefly, Hamlin sweet orange leaves (2–3 weeks after leaf emergence) of 3–4-year-old citrus plants were punctured with five pins at six inoculation sites. Then, we sprayed these leaves with a bactericide or mock treatment. Twelve hours later, *Xcc-eYFP* suspensions were sprayed at the concentration of 5×10^8 CFU/ml on the same inoculation sites. The treated leaves were cultured at a greenhouse at 28°C, with 80% relative humidity and a 16/8 h light/dark photocycle. Eight days post-spray treatment, the symptoms of the inoculated leaves were observed and photographed with a digital Canon-EOS 200D camera (Canon, Japan). The measurement process of the bacterial *Xcc-eYFP* population is described as follows: a 6-mm-diameter leaf disc, containing only a single puncture site, was excised from inoculated leaves 8 days after inoculation using a punch. Three biological repeats were collected and homogenized in 0.2 ml of double-distilled water (ddH_2O) in 1.5-ml Eppendorf tubes. The homogenized solution was centrifuged at 1,000 rpm for 5 s to precipitate the debris. The upper phase with *Xcc-eYFP* was collected, and 10 μl of the solution was loaded into a Helber counting chamber (Auvon, United Kingdom) to be observed under a Leica DM3000 fluorescence microscope (Leica, Germany). The number of fluorescence spots in the square of the Helber counting chamber was counted. This procedure was repeated to collect the average for bacterial population calculation and then calculated following the formula in the Helber counting chamber instructions. Each experiment was repeated three times.

Reporter-Based Determination of Minimum Inhibitory Concentrations

The MIC, defined as the lowest drug concentration at which more than 99% of bacterial growth is inhibited, was calculated from the fitted curve compared to the untreated control. Two methods were tested in this study. The first conventional method: *Xcc* and *Xcc-eYFP* strain, was grown in NB at 28°C with shaking at 200 rpm for 8 h. The cultures were standardized to an OD_{600} of 0.03 (about 5×10^6 CFU/ml) in NB and then aliquoted 190 μl into wells of a 96-well plate. Initial test concentrations of the compounds were diluted (1:20) in culture (10 μl of the compound in 190 μl of culture) and incubated at 28°C. Cultures were monitored at 24 and 48 h at OD_{600}, and the lowest concentration resulting in no growth after 48 h compared with control samples was defined as the MIC for *Xcc* or *Xcc-eYFP*. All determinations were conducted in eight replicate wells and repeated three times. The second fluorescent-based method: *Xcc* and *Xcc-eYFP* cultures were diluted from a logarithmic phase culture in NB liquid medium and added to the appropriate 96 wells microtiter plates at a final OD_{600} of 0.03 (about 5×10^6 CFU/ml). And, 190 μl were aliquoted into the wells of a 96-well plate. The initial test concentrations of the compounds were diluted (1:20) in the culture (10 μl of the compound in 190 μl of culture). The plates were incubated at 28°C, and luminescence and fluorescence were read at 0, 6, 12, 24, and 48 h. A Gompertz model was used to fit the data and generate dose–response curves using GraphPad Prism (GraphPad Software, United States).

The Inhibition Zone Method

A certain amount of *Xcc-eYFP* suspension was poured into the NA medium that had been cooled to about 50°C, mixed evenly, poured into the 80-mm plate (about 80 ml/plate), and let it stand horizontally for use after solidification. The bactericides were diluted stepwise and 11 concentration gradients were prepared for testing. Holes were punched in the test plate with a sterilized steel pipe, small pieces of medium were carefully picked out to make round holes, 80 μl of bactericides were injected into the holes and incubated at 28°C for 48 h. A Vernier caliper was applied to measure the zone of inhibition around the specimens in centimeters. The inhibition activity of bactericide can be preliminarily determined according to the diameter of the inhibition zone. The inhibition ratios were calculated: Inhibition rate (%) = $(R_t\text{-}R_o)/R_o \times 100\%$, where R_t is the average diameter of

the treatment group, and R_o is the average diameter of the control group. The experiments were performed in triplicate.

Plant Tested Bactericide Mixture Formulation Using the Outdoor Spray Method

The control effect of a selected 1:1 mixture formulation of bactericides was investigated using a greenhouse with 20-week-old potted citrus lemon [*Citrus limon* (L.) Burm. f.] plants. The bacterial inoculum was prepared and suspended in ddH_2O, and the concentration was adjusted to approximately OD_{600} = 0.3 (5×10^8 CFU/ml). The treatment was performed using a spray method as previously described (Duan et al., 2021). Briefly, the abaxial surfaces of flush leaves (2–3 weeks after leaf emergence) and immature leaves were sprayed with the following treatments: *Xcc* and *Xcc-eYFP* strain combined with three 1:1 synergistic bactericides of 1.2% xinjunan acetate (AS) (0.5 mg/ml) mix 33% kasugamycin xine-copper (SC) (0.25 mg/ml), 1.2% xinjunan acetate (AS) (0.5 mg/ml) mix 20% resin acid copper (EW) (0.03 mg/ml), and 1.2% xinjunan acetate (AS) (0.5 mg/ml) mix 30% copper oxychloride (SC) (0.03 mg/ml). These mixed formulations were added to each treatment at a final concentration of 0.03% (vol/vol). *Xcc* strain and *Xcc-eYFP* strain combined with ddH_2O were used as controls. At 28 days post-spray treatment, leaf symptoms were observed and photographed with a digital camera.

For bacterial population assays, the leaves of citrus lemon plants were inoculated as described above. Two randomly selected leaf discs were cut from three inoculated leaves with a cork borer (6 mm of diameter). The bacterial population of the *Xcc-eYFP* strain was measured by the method described above. For the *Xcc* strain bacterial population, the leaf discs were ground in 1 ml of ddH_2O. Suspensions were serially diluted and plated on NA plates. After incubation at 28°C for 48 h, bacterial colonies were counted, and the number of CFU/cm^2 of the leaf tissue was calculated. The assays were repeated three times independently.

Evaluation of Reporter-Based Bactericides

Xcc and *Xcc-eYFP* strains were collected on the corresponding plate, rinsed with ddH_2O three times, and finally diluted in 10 mM $MgCl_2$ at a density (OD_{600} = 0.6). 96-well plates were designed for screening treatment with the corresponding control. Bactericides or mixture formulations were dissolved in the corresponding buffer with the designed synergistic ratios. Then, they were proportioned with related bacterial suspension (OD_{600} = 0.6) of *Xcc-eYFP*, *Xcc* and the mock treatment into 96-well plates (Black 96-well microplate, flat bottom, Falcon). A total of 200 μl of the solution, including bacterial suspension, bactericides, or mock treatment, was pipetted into the well and incubated at 28°C for 6 h. Next, for *Xcc* strain, the suspension from the wells was determined by plating 10 μl of 10-fold serial dilutions on the NA plate and counting the resulting colonies. To *Xcc-eYFP* strain, 10 μl of the suspension from the wells was diffused into a Helber counting chamber for fluorescent spot counting using a Leica DM3000 fluorescence microscope (Leica Microsystems, Wetzlar, Germany). The number of fluorescent spots in the square of the Helber counting chamber was counted. This procedure was repeated to determine the average for bacterial population calculation. The bacterial population was calculated following the formulas in the instructions provided by the manufacturers of the Helber counting chamber A30000 (Auvon, Tonbridge, United Kingdom).

Calculation of Reporter-Based Inhibition Rate

Wild-type *Xcc* and *Xcc-eYFP* without bactericides were applied as a control and three replicates for each treatment postincubation at 28°C for 6 h. The fluorescence intensity at an excitation/emission wavelength of 485/535 nm was measured using the Spark™ Multimode Microplate reader. Inhibition rates were calculated as percentage inhibition using the formula [(negative control signal - sample signal)/negative control signal × 100].

Evaluation of *Xanthomonas citri* subsp. *citri*-Antagonistic Bacterial Strains

Bacterial strains were cultured in the LB or NB medium. Bacteria stock 15% glycerol was streak cultured on NA plates at 28°C for 2 days and then re-cultured in the corresponding medium. The potential antagonistic metabolites of bacteria were induced in liquid LB/NB medium at 28°C and 150 rpm in a shaking culture machine. The supernatant of culture suspension was then collected by centrifugation at 4,000 rpm. The supernatant containing potential antibacterial compounds was processed following the experiment of antagonistic strain screening. About 10 μl of *Xcc-eYFP* bacterial suspension (OD_{600} = 0.6) was added to 1 ml of fresh LB/NB medium with gentamycin (20 mg/ml) in a sterile 2-ml Eppendorf tube. The above supernatant was mixed proportionately into the tube and then cultured on a 28°C incubation shaker at 200 rpm for 12 h. *Xcc-eYFP* was precipitated at 13,000 rpm for 5 min and then resuspended by 200 μl of $MgCl_2$ (10 mM). The resuspended bacterial suspensions were loaded on designed 96-well plates with controls, which were further delivered into the Spark™ multimode microplate reader (TECAN, Switzerland) for fluorescent signal detection. The collected data will be processed into the visual quantification below.

Extraction and Evaluation of Antibacterial Components

Metabolites were extracted according to the following steps: ethyl acetate was selected for the metabolite extraction process because of its low boiling point and moderate polarity. Seed liquid cultures (5 ml NB) were re-cultured to 200 ml of NB in 0.5-L Erlenmeyer flasks at 28°C with 180 rpm for 36 h until the OD_{600} reached 1. An equal volume of ethyl acetate was added to the bacterial cultures, and the flasks were sonicated for 5 min and maintained overnight with vigorous shaking. Then, the culture broth was centrifuged at 3,500 rpm for 15 min at 4°C, and the supernatant was collected and dried on a rotary evaporator (Eppendorf, Hamburg, Germany) at 50°C. The residues were

dissolved in 0.5 ml of high-performance liquid chromatography-(HPLC-) grade methanol, collected in tubular glass vials, and air-dried under a chemical hood. An antibiotic assay was performed by dissolving the extracts in methanol to a concentration of 60 mg/ml, and 30 μl of the solution was used for an agar well diffusion assay. The antagonistic activities of the isolates against the *Xcc* and *Xcc-eYFP* strains were determined using the diameter of the inhibition zone. The MIC of streptomycin and ethyl acetate extracts was determined. For minimum bactericidal concentration (MBC) determination, 10 μl of MIC cultures were transferred from the microtiter plates to NA plates and incubated at 28°C for 24 h. The lowest concentrations of the ethyl acetate extract that prevented visible growth of bacteria on NA plates were indicated as the MBCs. Both MIC and MBC were denominated in μg/ml.

Statistics and Reproducibility

Numeric data are presented as mean ± standard deviation (SD) unless otherwise specified in the figures. Statistical analysis was performed with the software Prism 9. *P*-values and statistical analysis methods are indicated. The correlations of *Xcc-eYFP* and *Xcc* and the correlations of two methods in the bactericide inhibition rates from the plaque neutralization assay were analyzed using a linear regression model, Pearson's correlation coefficient, and two-tailed *p*-value. One-/two-way ANOVA analyses with the following corresponding multiple comparisons were processed to meet the data analysis requirement with the Tukey's test [95% confidence interval (CI)] using the software of GraphPad Prism 9 (**$p < 0.05$, ***$p < 0.001$, ****$p < 0.0001$, *nsP*>0.05).

RESULTS

Determination of Buffer and Incubation Time

The *Xcc-eYFP* suspension was suspended with ddH_2O into a final concentration with OD_{600} = 1 (the optical density at 600 nm is equal to 1). The bacterial suspension was pipetted into the black 96-well plate. Then, the optimal excitation/emission wavelength measured by the Spark™ multimode microplate reader (TECAN, Switzerland) has arisen at 485/535 nm. We used four bacterial suspension buffers to reduce the noise signal, including NB, LB, ddH_2O, and 10 mM $MgCl_2$. Those buffers were processed into fluorescence intensity tests using the screened optimal excitation/emission wavelength. The results showed that the autofluorescence intensity of NB is 11,513.67 ± 85.70, and that of LB is 10,632.00 ± 195.85. 10 mM $MgCl_2$ and ddH_2O are 56.67 ± 1.53 and 57.16 ± 1.16, respectively. 10 mM $MgCl_2$ and ddH_2O had the minimum noise signal during detection

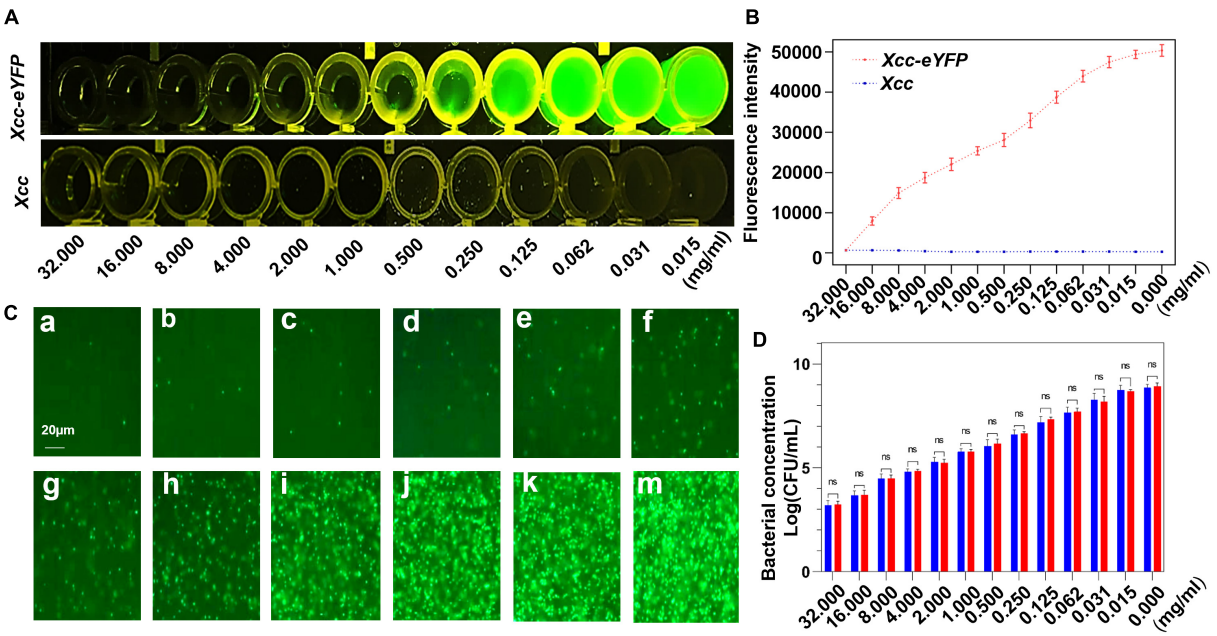

FIGURE 1 | The correlation between fluorescence reading and the alive bacterial population of *Xcc-eYFP*. **(A)** After 6 h of incubation, *Xanthomonas citri* subsp. *citri* (*Xcc*) and *Xcc-eYFP* express fluorescence signals, at 12 concentrations of 30% copper oxychloride (SC), were captured under LUYOR-3145RG irradiation. **(B)** After 6 h of incubation, *Xcc* and *Xcc-eYFP* express fluorescence intensity, at 12 concentrations of 30% copper oxychloride (SC), were captured under the Spark™ multimode microplate reader (TECAN, Switzerland). Means and SDs of five replicates of a representative result are shown. Vertical bars represent the SD of the means. **(C)** *Xcc-eYFP* suspension (OD = 1) was co-incubated with a series of 30% copper oxychloride (SC) concentrations of *a* = 32, *b* = 16, *c* = 8, *d* = 4, *e* = 2, *f* = 1, *g* = 0.5, *h* = 0.25, *i* = 0.125, *j* = 0.062, *k* = 0.031, *m* = 0.015 mg/ml, after 6 h of incubation, The fluorescence of *Xcc-eYFP* footprint was captured through a transmission fluorescence microscope. **(D)** Alive bacterial concentrations of *Xcc* and *Xcc-eYFP* were counted by the plate colony counting method and fluorescent spots counting method. Means and SDs of the three replicates of a representative result are shown. Error bars are representative of the SD from the mean. Statistical analysis was studied with the Tukey's test (95% confidence interval (CI), *nsP*>0.05). ddH_2O, double-distilled water.

among the four buffers. Next, *Xcc-eYFP* bacterial suspensions were incubated in different buffer concentrations (OD_{600} = 0.3) for 0, 6, 12, 24, 30, and 36 h (**Supplementary Figure 1**). The result showed that the fluorescence of *Xcc-eYFP* in the 10 mM $MgCl_2$ buffer presented more stable than the other treatments. In addition, we examined the tolerance of *Xcc-eYFP* reporter strains to organic solvents commonly used to dissolve compounds in most drug libraries. We exposed *Xcc-eYFP* suspensions at a concentration of 5×10^8 (CFU/ml) to DMSO, DMF, NB, 10 mM $MgCl_2$, and acetone at concentrations ranging from 0 to 100% for 36 h. We found that *Xcc-eYFP* in 10 mM $MgCl_2$ and DMSO solvents presented a lower inhibition effect than the other solvents (**Supplementary Figure 2**). This information is critical to guide decisions regarding the choice of solvents and appropriate concentrations to use in drug screening assays without compromising the vitality of *Xcc-eYFP* reporter strains.

For incubation time determination, we mixed 190 μl *Xcc-eYFP* (suspended in the corresponding solvent as the same as bactericides) with 10 μl of different bactericides in 96-well plates to monitor the bacterial vitality *Xcc-eYFP* dynamically. The plate was incubated at 28°C for a series of time points and then delivered for fluorescent signal detection. The results showed a dynamic fluorescent quenching phenomenon during incubation at different time points. Constant fluorescence intensity of *Xcc-eYFP* was observed at 6 h in all treatments (**Supplementary Figure 3**). The optimal incubation time for the following experiments is defined as 6 h postinoculation.

The Correlation Between the Fluorescence Intensity of *Xanthomonas citri* subsp. *citri* Strain and the Alive Bacterial Population

The counting of colony-forming units based on dilution series of plates on agar media is a common approach to measure bacterial growth from the treatment, but this is time-consuming and laborious. We aimed to simplify and expedite the quantification of *Xcc* by counting fluorescent *Xcc-eYFP* under a fluorescent microscope, and then the correlation between fluorescence intensity and the bacterial population was calculated. To further match the correlation in this study, copper oxychloride was used for evaluation to fit the linear equation. The fluorescence quenching of *Xcc-eYFP* was observed at different concentrations of 30% copper oxychloride (SC). The fluorescence intensity of *Xcc-eYFP* gradually decreased along with increasing bactericide concentration when the wild-type *Xcc* was used as a negative control (**Figures 1A,B**). The bacterial population of *Xcc-eYFP* stains at different bactericide concentrations was calculated by counting the fluorescent spots under fluorescent microscopy, as previously described (Duan et al., 2021; **Figure 1C**). The bacterial population of the *Xcc-eYFP* strain calculated by both methods showed high consistency in different groups (**Figure 1D**). The result showed a typical linear matched relationship among the treatments, changes in the bacterial population of the *Xcc-eYFP* and *Xcc* strains, which calculated the correlation coefficient as 0.998. These data indicate that the fluorescence intensity of *Xcc-eYFP* measured by the Spark™ multimode microplate reader (TECAN, Switzerland) can be used to quantify the bacterial population.

Comparison of the Conventional Method and the *Xanthomonas citri* subsp. *citri* Strain-Based Assay for the Determination of Bactericide Inhibition

The inhibition zone method is commonly used to evaluate the antagonism of bactericides against bacteria, but we aimed to simplify and expedite the determination of the bactericide inhibition rate by reading the fluorescence of *Xcc-eYFP*. The inhibition rate of 30% copper oxychloride (SC) was determined by the inhibition zone method (**Figure 2A**). As the concentration gradually decreased, the diameter of the inhibition zone also gradually decreased (**Figure 2B**). The inhibition rates calculated by both inhibition zone and reporter-based methods were significantly consistent and met a typical linear matched relationship with a correlation coefficient of 0.953 (**Figure 2D**). However, it is worth noting that the inhibition threshold value calculated by a reporter-based assay is higher than that calculated by the inhibition zone method (**Figure 2C**), which indicates that this assay presents more accuracy and can afford the duty of inhibition rate calculation the same as conventional ways.

Evaluation of the Activity of Different Bactericides

The fluorescence intensity of *Xcc-eYFP* suspended in four bactericides at different concentrations was measured. According to the fluorescence curve, it is found that the minimum concentration of 1.2% xinjunan acetate (AS) for complete fluorescence quenching is 128 mg/ml, 33% kasugamycin xine-copper (SC) is 16 mg/ml, 30% copper oxychloride (SC) is 32 mg/ml, and 20% resin acid copper (EW) is 2 mg/ml (**Supplementary Figure 4**). We used a pinprick-inoculation method to verify CBC disease development on Hamlin sweet orange leaves. The result showed that mock-treated leaves have significant symptoms compared with those of bactericidal treatment (**Figure 3A**). According to the bacterial growth curve result (**Figure 3B**), the antimicrobial activity of the four bactericides is ranked as 20% resin acid copper (EW) > 33% kasugamycin xine-copper (SC) > 30% copper oxychloride (SC) > 1.2% xinjunan acetate (AS). The MIC result determined by the conventional method is consistent with the fluorescence intensity change monitored by the Spark™ multimode microplate reader (**Supplementary Table 3**).

The Reporter-Based Evaluation of Different Mixture Formulation Bactericides

To screen the optimal ratio of cocktail combination bactericides, we mixed the formulations of 1.2% xinjunan acetate (AC) (0.5 mg/ml) with three copper bactericides of 33% kasugamycin xine-copper (SC) (0.03 mg/ml), 20% resin acid copper (EW) (0.03 mg/ml), and 20% resin acid copper (EW) (0.25 mg/ml). The dynamic fluorescence intensity of *Xcc-eYFP* co-incubated with

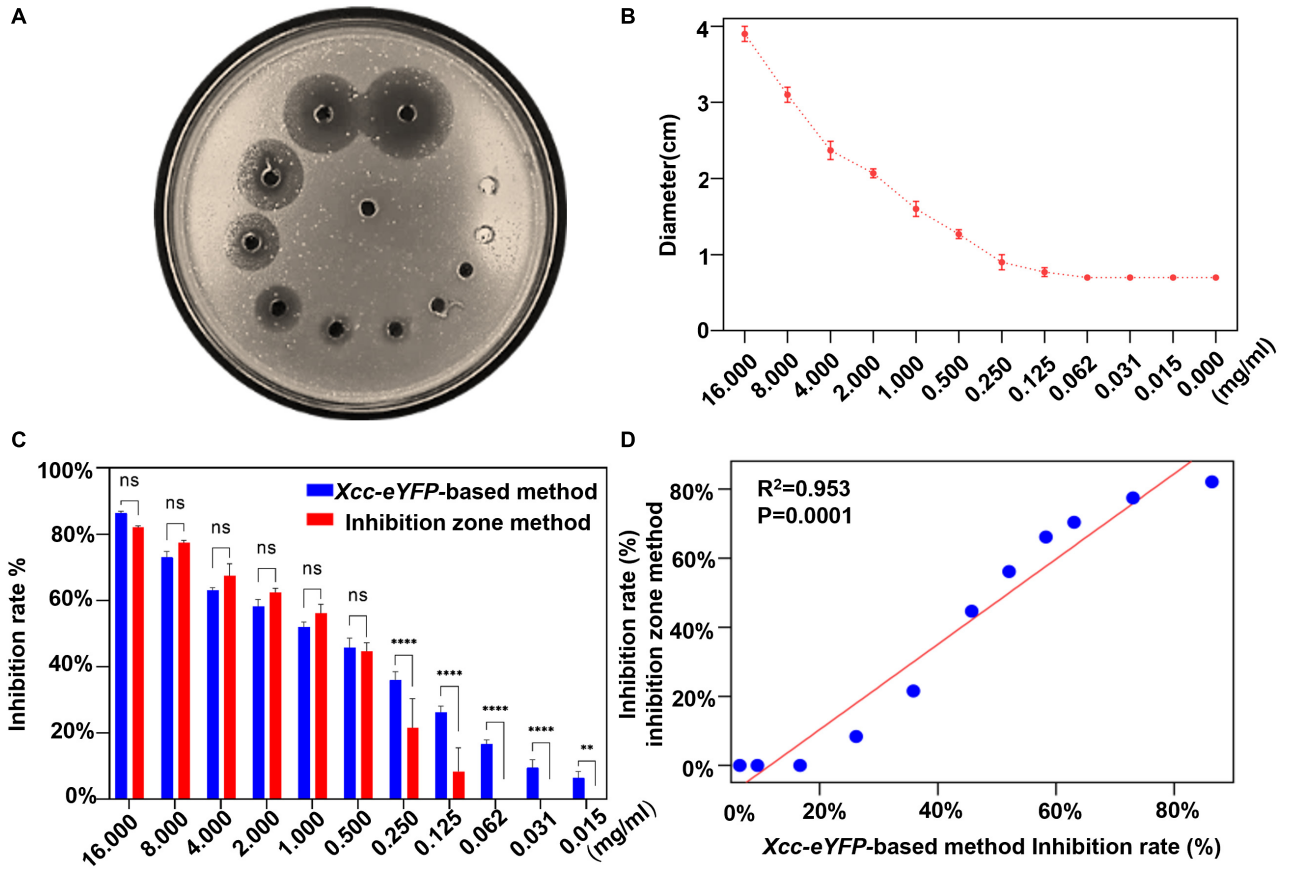

FIGURE 2 | Comparison of bactericidal inhibition rates between reporter-based and conventional inhibition zone methods. **(A)** The image of inhibition zones on an *Xcc-eYFP* plate treated with different 11 concentrations of 30% copper oxychloride (SC) by the inhibition zone method. **(B)** The inhibition zone diameters were caused by 11 concentrations of 30% copper oxychloride (SC) and the control group. Means and SDs of three replicates of a representative result are shown. The vertical bars represent the SD of the means. **(C)** The accuracy comparison between the reporter-based assay and the inhibition zone method to calculate the inhibition rate at a series of 30% copper oxychloride (SC) concentrations. Means and SDs of three replicates of a representative result are shown. Statistical analysis was processed by two-way ANOVA following multiple comparisons with the Tukey's test (95% CI) using GraphPad Prism 9 (**$p < 0.05$, ****$p < 0.0001$, and ns > 0.05).

different bactericides was monitored (**Figure 4A**). With a gradual increase in the volume ratios of three mixture formulation bactericides, the fluorescence intensity in the combination of 1.2% xinjunan acetate (AC) (0.5 mg/ml) and 30% copper oxychloride (SC) (0.03 mg/ml) changed obviously and in the other two compounds was relatively stable. According to the computational formula of inhibition rate, the synergistic effect of 1.2% xinjunan acetate (AC) (0.5 mg/ml) and 30% copper oxychloride (SC) (0.03 mg/ml) reaches the peak when the volume ratio was 1:1. It is worth noting that when 20% resin acid copper (EW) (0.03 mg/ml), 33% kasugamycin xine-copper (SC) (0.25 mg/ml) and 1.2% xinjunan acetate (AC) (0.5 mg/ml) are compounded, the synergistic effect does not become robust as the volume ratio varies (**Figure 4B**). When the volume ratio of 1.2% xinjunan acetate (AC) (0.5 mg/ml) and 30% copper oxychloride (SC) (0.03 mg/ml) is 1:1, the inhibition rate of the compound bactericide is 67.75% overtop the 1.50 and 1.24% of the two individual bactericides (**Supplementary Figure 4A**). Therefore, the amount of copper-based bactericides used can be reduced to 55.8% under the same inhibition level. In addition, the alive *Xcc-eYFP* and *Xcc* population co-incubated with 11 synergistic rates was calculated. With the different synergistic proportion of 1.2% xinjunan acetate (AC) (0.5 mg/ml) and 30% copper oxychloride (SC) (0.03 mg/ml), the inhibition rates and alive *Xcc-eYFP* and *Xcc* strain population were dramatically altered, but with totally opposite change trend (**Supplementary Figure 4B**). The inhibition rate calculated here is consistent with the MIC determination that the results showed that the 1:1 synergistic bactericide of 2% xinjunan acetate (AC) (0.5 mg/ml) and 30% copper oxychloride (SC) (0.03 mg/ml) had the lowest MICs of 1 mg/ml for *Xcc* and *Xcc-eYFP* strains (**Supplementary Table 3**).

The pinprick-inoculation method was used to evaluate the indoor protective effect of bactericides (**Figure 5A**). The results showed that the synergistic bactericide of 1.2% xinjunan acetate (AC) (0.5 mg/ml) and 30% copper oxychloride (SC) (0.03 mg/ml) at 1:1 has significant protective effects of inhibiting the bacterial growth of *Xcc* compared with those of the other two treatments and mock-treated (**Figure 5B**). The result of the outdoor

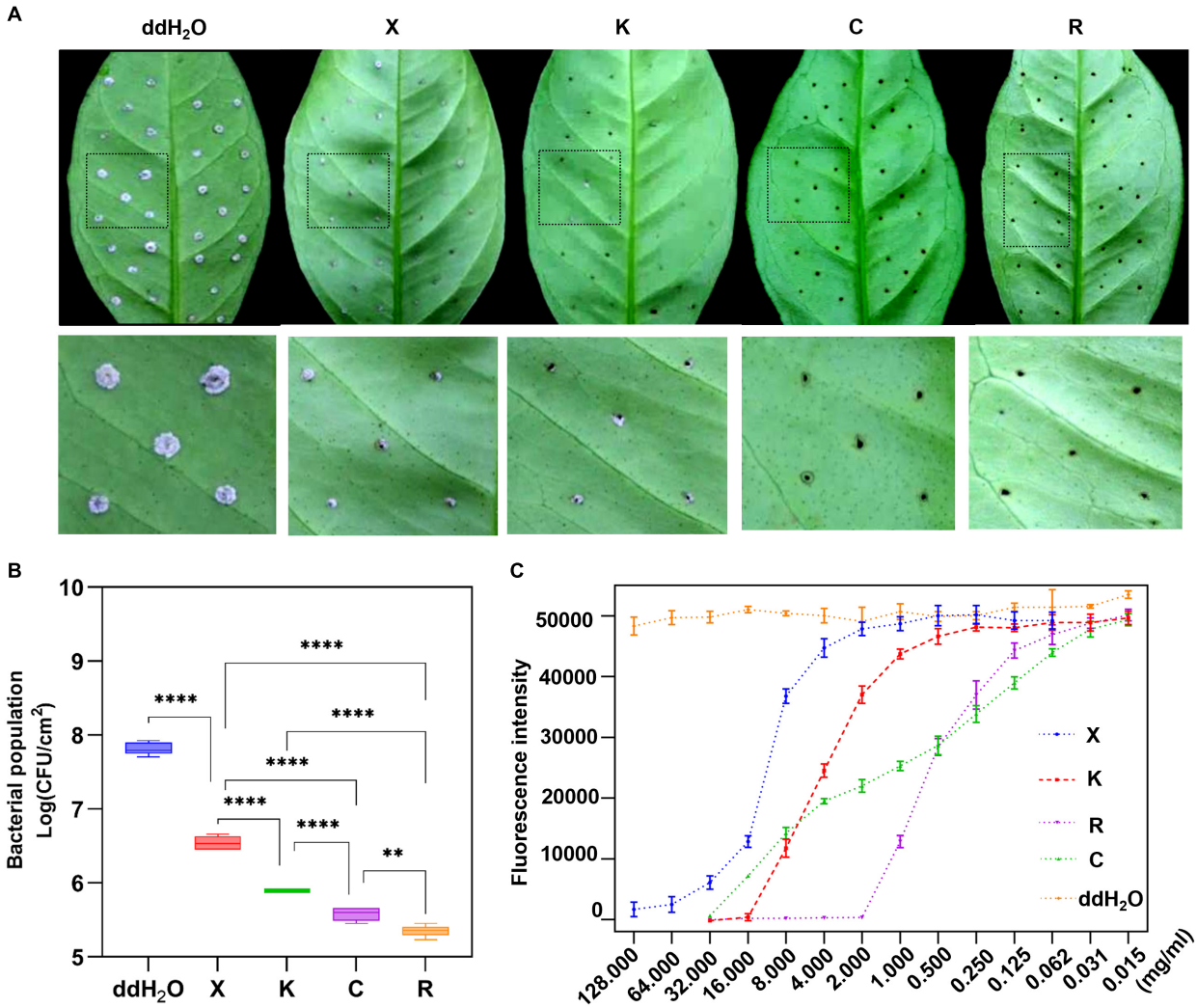

FIGURE 3 | Prevention effect and determination of minimum inhibitory concentrations (MICs) of four individual bactericides with the reporter-based assay. **(A)** After 7 days, the development of citrus bacterial canker (CBC) disease on citrus leaves pretreated with different bactericides was processed in the evaluation of the inhibition rate using the pinprick-inoculation method. **(B)** The result represents the bacterial population among different treatments using the fluorescence spot counting method to calculate the bacterial population of *Xcc-eYFP* at 7 days postinoculation. Experiments were repeated three times with similar results. Error bars are representative of the SD of the mean of five replicates. Statistical analysis was processed by two-way ANOVA following multiple comparisons with the Tukey's test (95% CI) using GraphPad Prism 9 (**$p < 0.05$, ****$p < 0.0001$, *nsP*>0.05). X:1.2% xinjunan acetate (AS); K:33% kasugamycin xine-copper (SC); C:30% copper oxychloride (SC); R: 20% resin acid copper (EW); ddH$_2$O: double-distilled water. K:33% kasugamycin xine-copper (SC); X:1.2% xinjunan acetate (AS); C:30% copper oxychloride (SC); R: 20% resin acid copper (EW); ddH$_2$O: water. **(C)** After 6 h of incubation, the *Xcc-eYFP* expressing fluorescence intensity in four individual bactericides was captured under the Spark^{TM} Multimode Microplate reader. The *x*-axis represents the concentration of the bactericides. The *y*-axis represents the fluorescence intensity. Means and SDs of nine replicates of a representative result are shown.

protective effect showed that the 1:1 combination of 1.2% xinjunan acetate (AC) (0.5 mg/ml) and 30% copper oxychloride (SC) (0.25 mg/ml) was able to reduce the development of canker symptoms on lemon leaves, as evidenced by the decrease in the number of lesions compared with the positive control (**Figure 6A**). Treatment of the lemon leaves with a 1:1 combination of 1.2% xinjunan acetate (AC) (0.5 mg/ml) and 30% copper oxychloride (SC) (0.25 mg/ml) resulted in an approximate 2.0 log reduction in the bacterial population compared with the untreated control. However, the treatment of lemon leaves with two 1:1 combination of 1.2% xinjunan acetate (AC) (0.5 mg/ml) compound 33% kasugamycin xine-copper (SC) (0.25 mg/ml), and 20% resin acid copper (EW) (0.03 mg/ml) did not reduce in the number of CFU compared with the untreated control (**Figure 6B**).

Screening and Evaluation of Antagonistic Bacterial Strains Against *Xanthomonas citri* subsp. *citri*

Microbes can secrete antibacterial components to restrain bacterial growth. Here, we establish a timeline and processes for

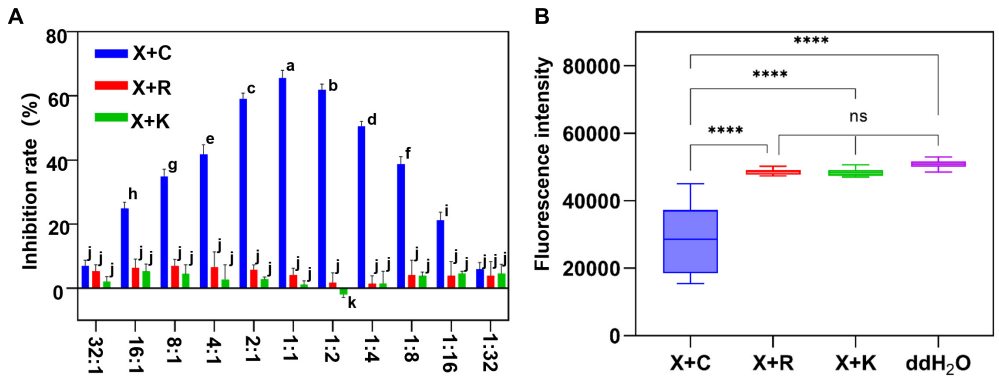

FIGURE 4 | The inhibition evaluation and screening of mixture formulation bactericides. **(A)** The inhibition rate of three different mixture formulations of bactericides was evaluated. The *y*-axis represents the inhibition rate, and the *x*-axis represents the synergistic ratio of bactericides. Statistical analysis was studied by two-way ANOVA following multiple comparisons with the Tukey's test (95% CI) using GraphPad Prism 9. Different letters in the bars indicate significant differences among the treatments. **(B)** *Xcc-eYFP* expressing fluorescence intensity in three mixture formulations of bactericides was captured under the Spark^{TM} Multimode Microplate reader at 6 h postincubation. The *x*-axis represents three synergetic bactericides, ddH_2O: double-distilled water, the *y*-axis represents the fluorescence intensity. Statistical analysis was studied by one-way ANOVA following multiple comparisons with the Tukey's test (95% CI) using GraphPad Prism 9. (****$p < 0.0001$, *nsP*>0.05). X + C:1:1 mixture formulation of 1.2% xinjunan acetate (AS) and 30% copper oxychloride (SC); X + R:1:1 mixture formulation of 1.2% xinjunan acetate (AS), and 20% resin acid copper (EW). X + K: 1:1 mixture formulation of 1.2% xinjunan acetate (AS) and 33% kasugamycin xine-copper (SC).

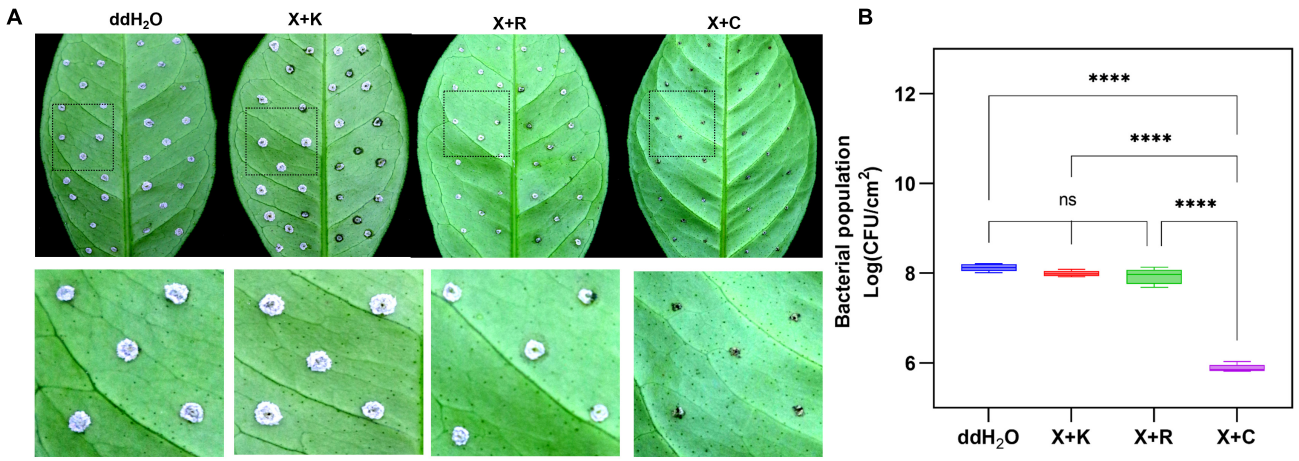

FIGURE 5 | Indoor prevention effect of different mixture combinations of bactericides. **(A)** After 7 days, CBC development on citrus leaves was pretreated with three different 1:1 synergistic bactericides using the pinprick-inoculation method. The experiments were repeated three times with similar results. **(B)** The result represents the bacterial population among the different treatments using the fluorescence spot counting method at 7 days postinoculation. The bar value shown is the mean of three independent experiments. The vertical bars represent the SD of the means. Statistical analysis was studied by one-way ANOVA following multiple comparisons with the Tukey's test (95% CI) using GraphPad Prism 9 (****$p < 0.0001$, *nsP*>0.05). X + C:1:1 mixture formulation of 1.2% xinjunan acetate (AS) and 30% copper oxychloride (SC); X + R:1:1 mixture formulation of 1.2% xinjunan acetate (AS), and 20% resin acid copper (EW). X + K: 1:1 mixture formulation of 1.2% xinjunan acetate (AS) and 33% kasugamycin xine-copper (SC); ddH_2O: double-distilled water.

Xcc-antagonistic bacteria and agents screening and evaluation (**Figure 7A**). In this study, an *Xcc*-antagonistic *Burkholderia* bacterial strain-1440 (Hereafter named *Burkholderia* strain-1440) was screened and applied for antagonism evaluation. *Burkholderia* strain-1440 (GenBank: OM943749) affiliated with *Burkholderia stabilis,* based on the result of 16S rDNA analysis, showed high inhibition against *Xcc*. In the conventional inhibition zone method, the *Burkholderia* strain-1440 derivative, secondary metabolites have high performance against *Xcc*/*Xcc-eYFP* (**Figure 7B**). Ethyl acetate extraction of *Burkholderia* strain-1440 (24 h at 28°C in the LB medium) exhibited stable thermostability (incubated at 60°C for 4 h) and inhibition activity, with an inhibition zone ranging from 22.49 ± 1.36 to 24.35 ± 1.36 mm. The extraction of *Burkholderia* strain-1440 was processed for metabolomics analysis by the UPLC-MS/MS. The result reveals that several potential antibacterial secondary metabolites were hatched from the extract of *Burkholderia* strain-1440 (**Supplementary Data Sheet 1**). The results of the outdoor protective effect showed that *Burkholderia* strain-1440 significantly inhibits the CBC symptom development and

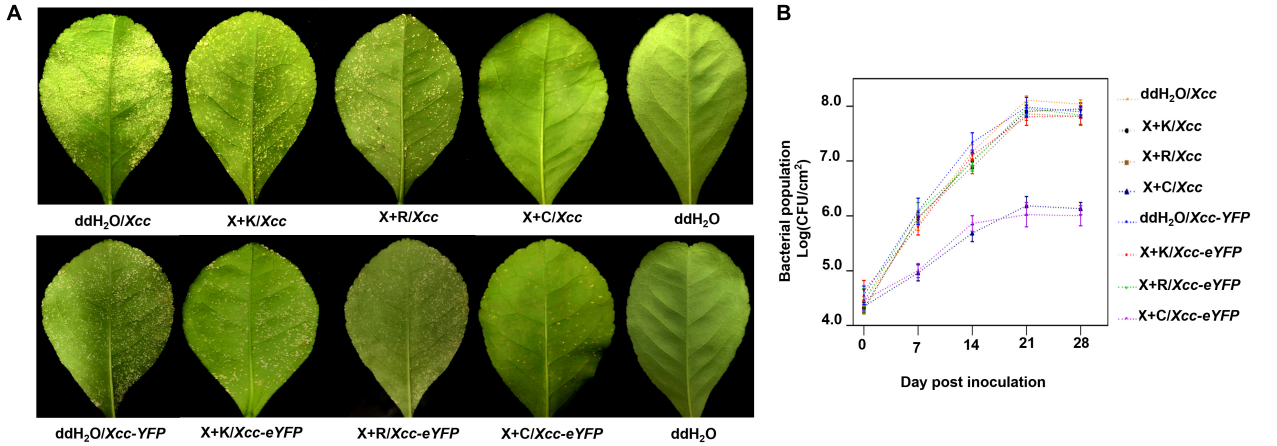

FIGURE 6 | Outdoor prevention effect of the mixture formulation of bactericides against CBC. **(A)** Images represent the development of citrus canker symptoms spray-inoculated by *Xcc* and *Xcc-eYFP* [about 5 × 10^8 colony-forming units/ml (CFU/ml)] and the corresponding bactericides 28 days postinoculation. **(B)** The bacterial growth curve of *Xcc* and *Xcc-eYFP* strain populations on Lemon leaves above. *Xcc* and *Xcc-eYFP* bacterial cells were extracted from the leaves at different time points after inoculation and quantified using the bacterial counting plate method and bacterial fluorescence spot counting method. The values shown are the means of five repeats and SDs. All assays were repeated three times with similar results. X + C: 1:1 mixture formulation of 1.2% xinjunan acetate (AS) and 30% copper oxychloride (SC); X + K: 1:1 mixture formulation of 1.2% xinjunan acetate (AS) and 33% kasugamycin xine-copper (SC); X + R:1:1 mixture formulation of 1.2% xinjunan acetate (AS) and 20% resin acid copper (EW); ddH_2O: double-distilled water.

bacterial growth obviously (**Figures 8A,B**). Spraying treatment of leaves with a 1:1 combination of *Burkholderia* strain-1440 and *Xcc/Xcc-eYFP* strain resulted in an approximate 2.0 log reduction in the number of CFU compared with the untreated control. Treatment with a 1:10 combination resulted in an approximately 1.0 log reduction in the number of CFU/square centimeter, while treatment with a 1:100 combination resulted in no reduction compared with the untreated control postinoculation. The inhibition result reveals that *Burkholderia* strain-1440 strain and secondary derived metabolites can be applied for CBC control and management *via* the protective and therapeutic application.

DISCUSSION

Fluorescent reporters have been applied to evaluate the antimicrobial activity of antimicrobial components against pathogenic microorganisms (Cooksey et al., 1995; Arain et al., 1996; Shawar et al., 1997; Gupta et al., 2017) to meet the high-throughput screening purpose, but surprisingly for *Xcc*. Even though the screening of antibacterial components for *Xanthomonas* has been reported (Jiang et al., 2020; Le et al., 2021), methods applied in those studies are conventional ways, such as antimicrobial spectrum experiments or the inhibition zone method. The need for new antimicrobial components to reduce the anxious issues of copper-resistant and environment contamination requires robust methods for screening and evaluation. So we developed a rapid evaluation method for antimicrobial components screening and evaluation to *Xcc* by using a fluorescent protein-labeled *Xcc-eYFP*, which can footprint the vitality of *Xcc* during antibacterial component screening with the Spark^{TM} multimode microplate reader. Notably, a previous study (Duan et al., 2021) proved that the eYFP protein does not affect the growth and virulence of *Xcc*. The MIC calculation results in the conventional method are notably equated to the corresponding base value in a reporter-based assay. It is more robust than the conventional inhibition zone and colony counting method *via* eliminating the need for plating on agar media, reducing labor and time-cost. Meanwhile, this method highly showed accuracy during inhibition evaluation to meet the low threshold of bactericide inhibition rate using the Spark^{TM} multimode microplate reader (TECAN, Switzerland).

In this study, one alkyl polyamine-type bactericide: 33% kasugamycin xine-copper (SC), and three copper-based bactericides: 1.2% xinjunan acetate (AS), C:30% copper oxychloride (SC), and 20% resin acid copper (EW) were processed in the construction and evaluation of the method. We calculated the inhibition activity of bactericides and ranked them in the following order: 20% resin acid copper (EW) > 33% kasugamycin xine-copper (SC) > 30% copper oxychloride (SC) > 1.2% xinjunan acetate (AS). The test of preventive effect by the outdoor spray method is consistent with the evaluation results. On the other hand, based on the evaluation of the combination with a different ratio, we screened out a well-performance combination ratio 1:1 combination of 1.2% xinjunan acetate (AC) (0.5 mg/ml) and 30% copper oxychloride (SC) (0.25 mg/ml). The combination bactericide can reduce up to 55.8% of copper component application dosage with the same protective effect as an individual bactericide, reducing the development of canker symptoms compared with the positive control. Usually, partial cocktail bactericide combinations present better performance in the filed application than the signal agent, but the ratio based on the experientialism cannot reach the optimal synergistic effect. The optimal ratio of bactericides formulation will enhance the prevention effect. Meanwhile, the application

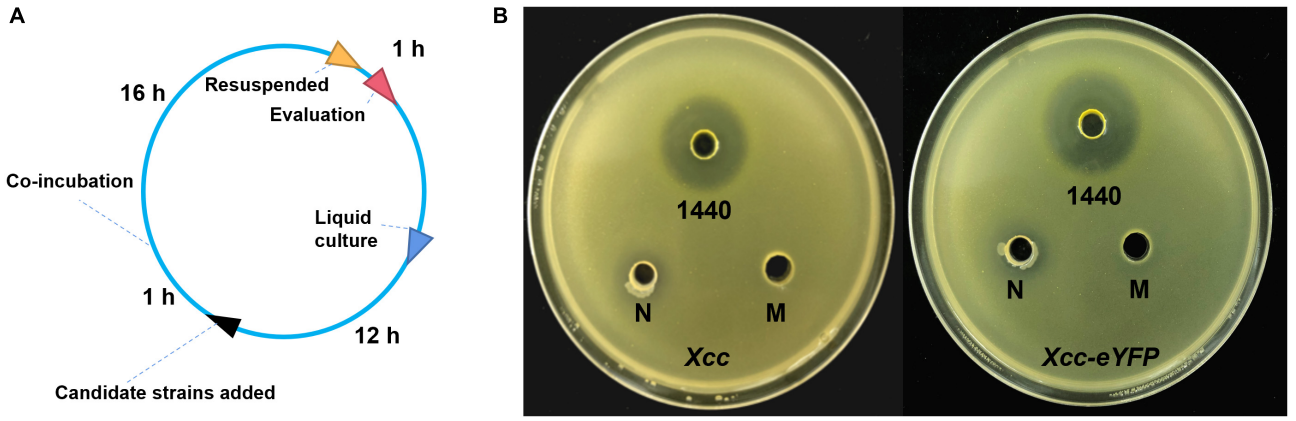

FIGURE 7 | The screening and evaluation process of *Xcc*-antagonistic bacterial strain. **(A)** Timelines of screening and evaluation processes of *Xcc*-antagonistic bacterial strains. **(B)** The antibacterial activity of the extraction was measured using the agar well diffusion assay. M, methanol control; 1440, ethyl acetate extract of antagonistic bacteria 1440. N: Negative control, ethyl acetate extract of *Agrobacterium* strain EHA105. All assays were repeated three times with similar results.

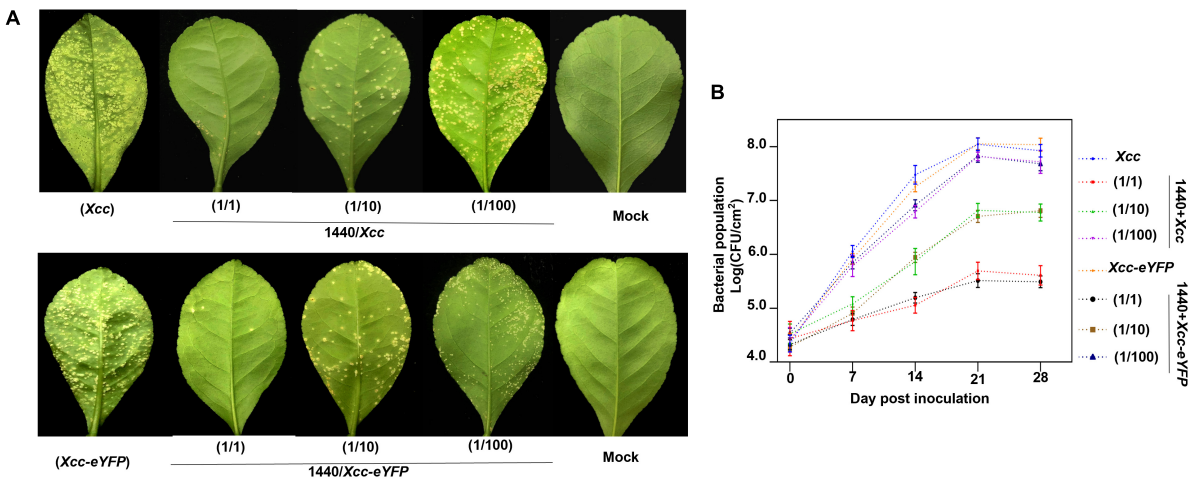

FIGURE 8 | Evaluation of outdoor protective effect of *Burkholderia* strain-1440 against CBC. **(A)** CBC symptom development on lemon leaves co-sprayed with *Xcc* and *Xcc-eYFP* and *Burkholderia* strain-1440. Images are representative of four independent replicates at 28 days postinoculation. **(B)** The bacterial growth curve of *Xcc* and *Xcc-eYFP* on the abovementioned leaves using the bacterial counting plate method and fluorescence spot counting method. The values shown are the means of five repeats and SDs. All assays were repeated three times with similar results. *Xcc*: strain *Xcc* alone; 1440/*Xcc*: (1/1): *Burkholderia* strain-1440 inoculated simultaneously with *Xcc* at the ratio of 1–1; (1/10): *Burkholderia* strain-1440 spray-inoculated simultaneously with *Xcc* at the ratio of 1–10; (1/100): *Burkholderia* strain-1440 spray-inoculated simultaneously with *Xcc* at the ratio of 1–100. *Xcc-eYFP*: *Xcc-eYFP* spray-inoculated alone; 1440/*Xcc-eYFP*: (1/1): *Burkholderia* strain-1440 inoculated simultaneously with *Xcc-eYFP* at the ratio of 1–1; (1/10): *Burkholderia* strain-1440 inoculated simultaneously with *Xcc-eYFP* at the ratio of 1–10; (1/100): *Burkholderia* strain-1440 inoculated simultaneously with *Xcc-eYFP* at the ratio of 1–100; Mock: ddH_2O.

of *Xcc*-antagonistic bacterial strain and derived metabolites will significantly reduce the application dosage of copper-based bactericides, further relieving the anxiety problems of copper-resistant and environmental contamination. Our study will accelerate the screening and evaluation process of new antibacterial ingredients to meet the requirements of CBC control and management.

However, some tips need more attention during screening and evaluation. Firstly, partial solvents/buffers/bactericides generate an autofluorescence that will disturb the honest signal value reading by the spark multimode microplate reader. In this case, we suggest increasing the dilution, setting up multiple controls, or changing the solvent. Secondly, the inhibition rate evaluated from the indoor inhibition rate test is appropriately different from the result calculated from the field application because factors such as the field climate, the attachment, and penetration capacity of the drug may be different from the actual application of antibacterial products in the field. However, whether the antibacterial compound has an anticipated preventive effect in the field, the indoor inhibition rate results obtained by the *Xcc-eYFP* assay can provide essential reference data for field medication. Some components remained valid hits with inhibition above the 50% threshold in the reporter-based assay, but failed in the oxford-cup inhibition zone method. Despite the

apparent inhibition of *Xcc* growth by the luminescence readout could be the result of different growth conditions or bacteriostatic mode that would dampen the increase in luminescence but not the decrease in the inhibition zone method. Some candidates do not appear rapid bactericidal activity as evident at low inhibition by the reporter-based assay, which could be due to a long duration of the fluorescent reporter signal post-treatment.

In summary, we have developed a new method to evaluate and screen antibacterial components against *Xcc*. This method has been successfully used to rank the inhibition rates of commercial bactericides, combination bactericides and *Xcc*-antagonistic bacterial strains. A well-performance *Xcc*-prevented combination of bactericide and a antagonistic bacterial strain was screened. This method can be applied for, in particular, a significant number of candidates, screening and evaluation of new/combination bactericides. The application dosage of copper-based bactericides can be reduced by new/combination bactericides, which will prevent the occurrence of ecosystem contamination and copper-resistant bacterial strains during the control and management of CBC.

DATA AVAILABILITY STATEMENT

The original contributions presented in the study are included in the article/**Supplementary Material**, further inquiries can be directed to the corresponding author/s.

AUTHOR CONTRIBUTIONS

SD contributed to the conception and design of the study and wrote the first draft of the manuscript. YL, ZX, RL, and SC organized the database. MB and ML performed the statistical analysis. LL kept plant maintenance. YL and HM wrote sections of the manuscript. All authors contributed to manuscript revision, read, and approved the submitted version.

FUNDING

This work was financially supported by the Major Science and Technology R&D Program of Jiangxi Province (20194ABC28007), the National Key R&D Program of China (2018YFD0201504), the Key R&D Projects of Jiangxi (20171ACF60022), the National Natural Science Foundation of China (32002021), and Projects of Jiangxi Education Department (GJJ201449).

SUPPLEMENTARY MATERIAL

The Supplementary Material for this article can be found online at: https://www.frontiersin.org/articles/10.3389/fmicb.2022.864963/full#supplementary-material

REFERENCES

Alferez, F. M., Gerberich, K. M., Li, J. L., Zhang, Y., Graham, J. H., and Mou, Z. (2018). Exogenous nicotinamide adenine dinucleotide induces resistance to citrus canker in citrus. *Front. Plant Sci*. 9:1472. doi: 10.3389/fpls.2018.01472

Arain, T. M., Resconi, A. E., Hickey, M. J., and Stover, C. K. (1996). Bioluminescence screening in vitro (Bio-Siv) assays for high-volume antimycobacterial drug discovery. *Antimicrob. Agents Chemother.* 40, 1536–1541. doi: 10.1128/AAC.40.6.1536

Behlau, F., Jones, J. B., Myers, M. E., and Graham, J. H. (2012b). Monitoring for resistant populations of *Xanthomonas citri* subsp. *citri* and epiphytic bacteria on citrus trees treated with copper or streptomycin using a new semi-selective medium. *Eur. J. Plant Pathol*. 132, 259–270. doi: 10.1094/PDIS-01-13-0062-PDN

Behlau, F., Canteros, B. I., Jones, J. B., and Graham, J. H. (2012a). Copper resistance genes from different *xanthomonads* and citrus epiphytic bacteria confer resistance to *Xanthomonas citri* subsp. *citri*. *Eur. J. Plant Pathol*. 133, 949–963. doi: 10.1007/s10658-012-9966-8

Behlau, F., Canteros, B. I., Minsavage, G. V., Jones, J. B., and Graham, J. H. (2011). Molecular characterization of copper resistance genes from *Xanthomonas citri* subsp. *citri* and *Xanthomonas alfalfae* subsp. *citrumelonis*. *Appl. Env. Microb*. 77, 4089–4096. doi: 10.1128/aem.03043-10

Behlau, F., Scandelai, L. H. M., da Silva, Junior, G. J., and Lanza, F. E. (2017). Soluble and insoluble copper formulations and metallic copper rate for control of citrus canker on sweet orange trees. *Crop Prot*. 94, 185–191. doi: 10.1016/j.cropro.2017.01.003

Behlau, F., Belasque, J. Jr., Leite, R. P. Jr., Filho, A. B., Gottwald, T. R., Graham, J. H., et al. (2021a). Relative Contribution of Windbreak, Copper Sprays, and Leafminer Control for Citrus Canker Management and Prevention of Crop Loss in Sweet Orange Trees. *Plant Dis*. 105, 2097–2105. doi: 10.1094/PDIS-10-20-2153-RE

Behlau, F., Lanza, F. E., da Silva, Scapin, M., Scandelai, L. H. M., and Silva Junior, G. J. (2021b). Spray volume and rate based on the tree row volume for a sustainable use of copper in the control of citrus canker. *Plant Dis*. 105, 183–192. doi: 10.1094/PDIS-12-19-2673-RE

Cooksey, R. C., Morlock, G. P., Beggs, M., and Crawford, J. T. (1995). Bioluminescence method to evaluate antimicrobial agents against *Mycobacterium-avium*. *Antimicrob. Agents Chemother.* 39, 754–756. doi: 10.1128/AAC.39.3.754

de Carvalho, S. A., de Carvalho Nunes, W. M., Belasque, J. Jr., Machado, M. A., Croce-Filho, J., Bock, C. H., et al. (2015). Comparison of resistance to asiatic citrus canker among different genotypes of citrus in a long-term canker-resistance field screening experiment in Brazil. *Plant Dis*. 99, 207–218. doi: 10.1094/PDIS-04-14-0384-RE

Duan, S., Jia, H., Pang, Z., Teper, D., White, F., Jones, J., et al. (2018). Functional characterization of the citrus canker susceptibility gene *CsLOB1*. *Mole. Plant Pathol*. 19, 1908–1916. doi: 10.1111/mpp.12667

Duan, S., Long, Y., Cheng, S., Li, J., Ouyang, Z., and Wang, N. (2021). Rapid evaluation of the resistance of citrus germplasms against *Xanthomonas citri* subsp. *citri*. *Phytopathology* 2021:175. doi: 10.1094/PHYTO-04-21-0175-R

Ference, C. M., Gochez, A. M., Behlau, F., Wang, N., Graham, J. H., and Jones, J. B. (2018). Recent advances in the understanding of *Xanthomonas citri* ssp. *citri* pathogenesis and citrus canker disease management. *Mole. Plant Pathol*. 19, 1302–1318. doi: 10.1111/mpp.12638

Fu, H., Zhao, M., Xu, J., Tan, L., Han, J., Li, D., et al. (2020). *Citron C-05* inhibits both the penetration and colonization of *Xanthomonas citri* subsp. *citri* to achieve resistance to citrus canker disease. *Horticult. Res*. 7, 1–12. doi: 10.1038/s41438-020-0278-4

Gochez, A. M., Huguet-Tapia, J. C., Minsavage, G. V., Shantaraj, D., Jalan, N., Straub, A., et al. (2018). Pacbio sequencing of copper-tolerant *Xanthomonas* citri reveals presence of a chimeric plasmid structure and provides insights into reassortment and shuffling of transcription activator-like effectors among *Xanthomonas. citri* strains. *BMC Gen.* 19:16. doi: 10.1186/s12864-017-4408-9

Graham, J. H., and Myers, M. E. (2011). Soil application of SAR inducers imidacloprid, thiamethoxam, and acibenzolar-S-methyl for citrus canker

control in young grapefruit trees. *Plant Dis.* 95, 725–728. doi: 10.1094/PDIS-09-10-0653

Graham, J. H., and Myers, M. E. (2016). Evaluation of soil applied systemic acquired resistance inducers integrated with copper bactericide sprays for control of citrus canker on bearing grapefruit trees. *Crop Prot.* 90, 157–162. doi: 10.1016/j.cropro.2016.09.002

Gupta, R., Netherton, M., Byrd, T. F., and Rohde, K. H. (2017). Reporter-Based Assays for High-Throughput Drug Screening against *Mycobacterium abscessus*. *Front. Microb.* 8:2204. doi: 10.3389/fmicb.2017.02204

Heydarpanah, S., Rezaei, R., Taghavi, S. M., and Charehgani, H. (2020). Efficacy of different copper compounds in the control of *Xanthomonas citri* subsp. *citri* pathotypes A and A. *J. Phytopathol.* 168, 73–80. doi: 10.1111/jph.12869

Hu, Y., Duan, S., Zhang, Y., Shantharaj, D., Jones, J. B., and Wang, N. (2016). Temporal transcription profiling of sweet orange in response to PthA4-mediated *Xanthomonas citri* subsp. *citri* infection. *Phytopathology* 106, 442–451. doi: 10.1094/PHYTO-09-15-0201-R

Hu, Y., Zhang, J., Jia, H., Sosso, D., Li, T., Frommer, W. B., et al. (2014). Lateral organ boundaries 1 is a disease susceptibility gene for citrus bacterial canker disease. *Proc. Natl. Acad. Sci.* 111, E521–E529. doi: 10.1073/pnas.1313271111

Ibrahim, Y. E., Saleh, A. A., and Al-Saleh, M. A. (2017). Management of asiatic citrus canker under field conditions in Saudi Arabia using bacteriophages and acibenzolar-S-methyl. *Plant Dis.* 101, 761–765. doi: 10.1094/PDIS-08-16-1213-RE

Jiang, S., Tang, X., Chen, M., He, J., Su, S., Liu, L., et al. (2020). Design, synthesis and antibacterial activities against *Xanthomonas oryzae* pv. *oryzae*, *Xanthomonas axonopodis* pv. *citri* and *Ralstonia solanacearum* of novel myricetin derivatives containing sulfonamide moiety. *Pest Manage. Sci.* 76, 853–860. doi: 10.1002/ps.5587

Le, N. T. M., Cuong, D. X., Thinh, P. V., Minh, T. N., Manh, T. D., Duong, T. H., et al. (2021). Phytochemical screening and evaluation of antioxidant properties and antimicrobial activity against *Xanthomonas axonopodis* of *Euphorbia tirucalli* extracts in Binh Thuan province, Vietnam. *Molecules* 26:941. doi: 10.3390/molecules26040941

Leduc, A., Vernière, C., Boyer, C., Vital, K., Pruvost, O., Niang, Y., et al. (2011). First report of *Xanthomonas citri* pv. *citri* pathotype A causing Asiatic citrus canker on grapefruit and Mexican lime in Senegal. *Plant Dis.* 95, 1311–1311. doi: 10.1094/PDIS-03-11-0217

Li, J., and Wang, N. (2011a). Genome-wide mutagenesis of *Xanthomonas axonopodis* pv. *citri* reveals novel genetic determinants and regulation mechanisms of biofilm formation. *Public Lib. Sci.* 6:e21804. doi: 10.1371/journal.pone.0021804

Li, J., and Wang, N. (2011b). The *wxacO* gene of *Xanthomonas citri* ssp. *citri* encodes a protein with a role in lipopolysaccharide biosynthesis, biofilm formation, stress tolerance and virulence. *Mole. Plant Pathol.* 12, 381–396. doi: 10.1111/j.1364-3703.2010.00681.x

Li, J., and Wang, N. (2012). The *gpsX* gene encoding a glycosyltransferase is important for polysaccharide production and required for full virulence in *Xanthomonas citri* subsp. *citri*. *BMC Microbiol.* 12, 1–16. doi: 10.1186/1471-2180-12-31

Li, J., and Wang, N. (2014). Biofilm formation in *Xanthomonas citri* subsp *citri* and potential of biofilm inhibitors to control citrus canker disease. *Phytopathology* 104, 69–69.

Machado, F. J., da Silva, Marin, T. G., Canˆoas, F., da Silva, Junior, G. J., et al. (2021). Timing of copper sprays to protect mechanical wounds against infection by *Xanthomonas citri* subsp. *citri*, causal agent of citrus canker. *Eur. J. Plant Pathol.* 160, 683–692. doi: 10.1007/s10658-021-02276-x

Narciso, J. A., Ference, C. M., Ritenour, M. A., and Widmer, W. W. (2012). Effect of copper hydroxide sprays for citrus canker control on wild-type *Escherichia coli*. *Lett. Appl. Microb.* 54, 108–111. doi: 10.1111/j.1472-765X.2011.03179.x

Petrocelli, S., Tondo, M. L., Daurelio, L. D., and Orellano, E. G. (2012). Modifications of *Xanthomonas axonopodis* pv. *citri* lipopolysaccharide affect the basal response and the virulence process during citrus canker. *Public Lib. Sci.* 7:e40051. doi: 10.1371/journal.pone.0040051

Rabbee, M. F., Ali, M., and Baek, K. H. (2019). Endophyte *Bacillus velezensis* Isolated from *citrus spp.* controls streptomycin resistant *Xanthomonas citri* subsp. *citri* that causes citrus bacterial canker. *Agronomy* 9:470. doi: 10.3390/agronomy9080470

Richard, D., Tribot, N., Boyer, C., Terville, M., Boyer, K., Javegny, S., et al. (2017). First report of copper resistant *Xanthomonas citri* pv. *citri* pathotype A causing Asiatic citrus canker in Réunion. *France. Plant Dis.* 101:503. doi: 10.1094/pdis-09-16-1387-pdn

Riera, N., Wang, H., Li, Y., Li, J., Pelz-Stelinski, K., and Wang, N. (2018). Induced systemic resistance against citrus canker disease by *rhizobacteria*. *Phytopathology* 108, 1038–1045. doi: 10.1094/PHYTO-07-17-0244-R

Rigano, L. A., Siciliano, F., Enrique, R., Sendín, L., Filippone, P., Torres, P. S., et al. (2007). Biofilm formation, epiphytic fitness, and canker development in *Xanthomonas axonopodis* pv. *citri*. *Mole. Plant-Microb. Interact.* 20, 1222–1230. doi: 10.1094/MPMI-20-10-1222

Sangiorgio, P., Verardi, A., Spagnoletta, A., Balducchi, R., Leone, G. P., Pizzichini, D., et al. (2020). Citrus as a multifunctional crop to promote new bio-products and valorize the supply chain. *Env. Eng. Manag. J.* 19, 1869–1889. doi: 10.30638/eemj.2020.179

Scapin, M. D, Behlau, F., Scandelai, L. H. M., Fernandes, R. S., Junior, G. J. S., et al. (2015). Tree-row-volume-based sprays of copper bactericide for control of citrus canker. *Crop Prot.* 77, 119–126. doi: 10.1016/j.cropro.2015.07.007

Shawar, R. M., Humble, D. J., vanDalfsen, J. M., Stover, C. K., Hickey, M. J., Steele, S., et al. (1997). Rapid screening of natural products for antimycobacterial activity by using luciferase-expressing strains of *Mycobacterium bovis* BCG and *Mycobacterium intracellulare*. *Antimicrob. Agents Chemother.* 41, 570–574. doi: 10.1128/AAC.41.3.570

Yan, Q., Hu, X., and Wang, N. (2012). The novel virulence-related gene *nlxA* in the lipopolysaccharide cluster of *Xanthomonas citri* ssp. *citri* is involved in the production of lipopolysaccharide and extracellular polysaccharide, motility, biofilm formation and stress resistance. *Mole. Plant Pathol.* 13, 923–934. doi: 10.1111/j.1364-3703.2012.00800.x

Yan, Q., and Wang, N. (2011). The *ColR/ColS* two-component system plays multiple roles in the pathogenicity of the citrus canker pathogen *Xanthomonas citri* subsp. *citri*. *J. Bacteriol.* 193, 1590–1599. doi: 10.1128/JB.01415-10

Zhang, M., He, Z., Calvert, D. V., Stoffella, P. J., and Yang, X. (2003). Surface runoff losses of copper and zinc in sandy soils. *J. Env. Qual.* 32, 909–915. doi: 10.2134/jeq2003.9090

Zhou, X., He, Z., Liang, Z., Stoffella, P. J., Fan, J., Yang, Y., et al. (2011). Long-term use of copper-containing fungicide affects microbial properties of citrus grove soils. *Soil Sci. Soc. Am. J.* 75, 898–906. doi: 10.2136/sssaj2010.0321

Conflict of Interest: The authors declare that the research was conducted in the absence of any commercial or financial relationships that could be construed as a potential conflict of interest.

Publisher's Note: All claims expressed in this article are solely those of the authors and do not necessarily represent those of their affiliated organizations, or those of the publisher, the editors and the reviewers. Any product that may be evaluated in this article, or claim that may be made by its manufacturer, is not guaranteed or endorsed by the publisher.

frontiers | Frontiers in Microbiology

ORIGINAL RESEARCH
published: 09 May 2022
doi: 10.3389/fmicb.2022.870413

A Potential Biofertilizer—Siderophilic Bacteria Isolated From the Rhizosphere of *Paris polyphylla* var. *yunnanensis*

Yihan Wang[1], Gongyou Zhang[1], Ya Huang[1], Min Guo[1], Juhui Song[1], Tingting Zhang[1,2], Yaohang Long[1,2], Bing Wang[1,2] and Hongmei Liu[1,2,3]**

[1] Engineering Research Center of Medical Biotechnology, School of Biology and Engineering, Guizhou Medical University, Guiyang, China, [2] Key Laboratory of Biology and Medical Engineering, Immune Cells and Antibody Engineering Research Center of Guizhou Province, School of Biology and Engineering, Guizhou Medical University, Guiyang, China, [3] School of Basic Medicine Science, Guizhou Medical University, Guiyang, China

The increasing demands for crop production have become a great challenge while people also realizing the significance of reductions in synthetic chemical fertilizer use. Plant growth-promoting rhizobacteria (PGPR) are proven biofertilizers for increasing crop yields by promoting plant growth *via* various direct or indirect mechanisms. Siderophilic bacteria, as an important type of PGPR, can secrete siderophores to chelate unusable Fe^{3+} in the soil for plant growth. Siderophilic bacteria have been shown to play vital roles in preventing diseases and enhancing the growth of plants. *Paris polyphylla* var. *yunnanensis* (*PPVY*) is an important traditional Chinese herb. However, reports about its siderophilic bacteria are still rare. This study firstly isolated siderophilic bacteria from the rhizosphere soil of *PPVY*, identified by morphological and physio-biochemical characteristics as well as 16S rRNA sequence analysis. The dominant genus in the rhizobacteria of *PPVY* was *Bacillus*. Among 22 isolates, 21 isolates produced siderophores. The relative amount of siderophores ranged from 4 to 41%. Most of the isolates produced hydroxamate siderophores and some produced catechol. Four isolates belonging to *Enterobacter* produced the catechol type, and none of them produced carboxylate siderophores. Intriguingly, 16 strains could produce substances that have inhibitory activity against *Candida albicans* only in an iron-limited medium (SA medium). The effects of different concentrations of Fe^{3+} and three types of synthetic chemical fertilizers on AS19 growth, siderophore production, and swimming motility were first evaluated from multiple aspects. The study also found that the cell-free supernatant (CFS) with high siderophore units (SUs) of AS19 strain could significantly promote the germination of pepper and maize seeds and the development of the shoots and leaves of *Gynura divaricata* (Linn.). The bacterial solution of AS19 strain could significantly promote the elongation of the roots of *G. divaricata* (Linn.). Due to its combined traits promoting plant growth and seed germination, the AS19 has the potential to become a bioinoculant. This study will broaden the application prospects of the siderophilic bacteria-AS19 as biofertilizers for future sustainable agriculture.

Keywords: plant growth promoting rhizobacteria (PGPR), siderophore, iron, *Paris polyphylla* var. *yunnanensis* (*PPVY*), biofertilizers

OPEN ACCESS

Edited by:
Christopher Rensing, Fujian Agriculture and Forestry University, China

Reviewed by:
Sumera Yasmin, National Institute for Biotechnology and Genetic Engineering, Pakistan
Pratiksha Singh, Guangxi University for Nationalities, China

****Correspondence:***
Bing Wang
wangbing_gmu_edu@163.com
Hongmei Liu
hmliu@gmc.edu.cn

Specialty section:
This article was submitted to Terrestrial Microbiology, a section of the journal Frontiers in Microbiology

Received: *06 February 2022*
Accepted: *28 March 2022*
Published: *09 May 2022*

Citation:
Wang Y, Zhang G, Huang Y, Guo M, Song J, Zhang T, Long Y, Wang B and Liu H (2022) A Potential Biofertilizer—Siderophilic Bacteria Isolated From the Rhizosphere of Paris polyphylla var. yunnanensis. Front. Microbiol. 13:870413. doi: 10.3389/fmicb.2022.870413

INTRODUCTION

Microorganisms (bacteria and fungi) present in the rhizosphere soil of plants play a significant role in the whole plant growth process (Bukhat et al., 2020). Among these, plant growth-promoting rhizobacteria (PGPR) can promote the plant growth by various direct or indirect mechanisms, such as nitrogen fixation (Raza et al., 2021), phosphate solubilization (Sahu et al., 2022), siderophore production (Braud et al., 2009; Ghazy and El-Nahrawy, 2021), heavy metal resistance (Ma et al., 2016; Bennis et al., 2022), indole compound production (Zahir et al., 2010), biocontrol (Hosseini et al., 2021), and stress responses, including 1-aminocyclopropane-1-carboxylate (ACC) deaminase production (Gupta et al., 2021), drought tolerance (Mansour et al., 2021), and halotolerance (Wang et al., 2022). In the past few decades, many studies on the screening and identification of these bacteria have been reported. Moreover, there is a rich diversity of plant PGPR (Gange and Gadhave, 2018; Yang et al., 2021). Many genera of PGPR have been identified, such as *Bacillus, Brevibacillus, Pseudomonas, Agrobacterium, Burkholderia, Streptomyces,* and *Thiobacillu* (Guo et al., 2020). As reported, the main genera were *norank_c__Cyanobacteria* (53.47%), *Rhizobium* (4.04%), *Flavobacterium* (3.14%), *norank_f__Mitochondria* (2.81%), and *Sphingobium* (2.27%) present in the roots of *PPVY* (Liu et al., 2020).

Iron is an essential element to sustain life activities. It mainly exists in the soil in the form of insoluble ferric Fe(III), and its bioavailability is low (Colombo et al., 2014; Gu et al., 2020). In the environment, Fe(III) forms ferric oxide hydrate complexes ($Fe_2O_3 \times nH_2O$), leading to a free Fe(III) concentration from 10^{-9} to 10^{-18} M. Thus, a plethora of microorganisms, including important human and animal pathogens, are severely restricted in iron acquisition (Miethke and Marahiel, 2007). The uptake of iron by the microorganisms mainly includes direct and indirect mechanisms. Direct mechanisms comprise the uptake of iron sources, including various lactoferrin, transferrin, ferritin, heme, and/or haemoproteins (Wandersman and Delepelaire, 2004). The indirect strategies of iron acquisition are quite diverse. One of these includes exploiting all available iron sources independent of their nature. This makes it the most widespread and successful mechanism of high-affinity iron acquisition in the microbial world (Miethke and Marahiel, 2007). Siderophores are high-affinity ferric ion-specific chelators with a low molecular weight of less than 1.5 kDa that are excreted under iron starvation by various organisms, including bacteria, fungi, and even some plants (Hider and Kong, 2010; Ellermann and Arthur, 2017; Khan et al., 2018). PGPR facilitates plant nutrient uptake from surrounding environments by producing siderophores to sequester iron (Kramer et al., 2020). More than 500 siderophores have been isolated, the majority of which possess either catecholate or hydroxamate functional groups, all of which form Fe(III) complexes with an exceptional stability (Powell et al., 1980).

Plant growth-promoting rhizobacteria that produce siderophores are also called siderophilic bacteria. They are major assets to plants by providing the required amount of iron (Khan et al., 2018). Beneduzi et al. (2012) reported that a potent siderophore plays an important role in the iron uptake by plants in the presence of other metals, such as nickel and cadmium. Gu et al. (2020) indicated that rhizosphere microbiome members with growth-inhibitory siderophores often suppress pathogens *in vitro*, such as in the natural and greenhouse soils (Gu et al., 2020). It has been proven that different kinds of siderophores produced by *Bacillus* spp. play an important role in maintaining the ionic balance and inhibiting the growth of pathogenic microbes (Radhakrishnan et al., 2017). In addition, pathogenic bacteria, such as *Mycobacterium tuberculosis*, continuously chelate their host's iron by secreting siderophores, causing extensive tissue damage and airway bleeding (Xu et al., 2020). Siderophore-mediated competition for iron drives eco-evolutionary dynamics in natural and infectious settings (Andrews et al., 2003; Cordero et al., 2012).

Siderophores are among the secondary metabolites of PGPR. The rich diversity of secondary metabolites produced by soil bacteria has been recognized for over a century. Screening of microbial extracts reveals the high structural diversity of natural compounds with broad biological activities, such as antimicrobial (Zhanel et al., 2019; Chakraborty et al., 2022), antiviral (Jakubiec-Krzesniak et al., 2018), immunosuppressive (Duan et al., 2020), pesticide (Keswani et al., 2020), biodeterioration (David et al., 2021), and antitumor activities (Wang and Ding, 2018), enabling the bacteria to survive in its natural environment. The lipopeptide produced by *Bacillus amyloliquefaciens* YN201732, mainly bacillomycin D, showed great biocontrol activity against the fungal pathogen, *Fusarium solani* (Jiao et al., 2021). Therefore, it is of great value and significance to study siderophilic bacteria and their secondary metabolite activity.

Paris polyphylla var. *yunnanensis (PPVY)* is one of the most important traditional Chinese herbs. The rhizomes of *PPVY* have become important medicinal materials due to their extensive pharmacological activities, including hemostatic, detoxification, detumescence, analgesic, immune regulating, and antibacterial, anti-inflammatory, and antitumor functions (Yun et al., 2007; Chan et al., 2011; Negi et al., 2014; Qin et al., 2016; Guo et al., 2018). However, the siderophilic bacteria in the rhizosphere of *PPVY* have not been studied systematically. Here, we report the diversity of siderophilic bacteria isolated from the rhizosphere of *PPVY* and the types and relative amounts of siderophores produced by the siderophilic bacteria. We found that the AS19 strain has the potential to be used as a biofertilizer. In addition, the antimicrobial activity of secondary metabolites of siderophilic bacteria was screened, and the influence of synthetic chemical fertilizers on siderophilic bacterial growth and siderophore production was investigated. Seed germination and plant growth promotion experiments were also carried out. These data provide a basis for the study of efficient bioinoculants and the development of green agriculture.

MATERIALS AND METHODS

Rhizosphere Soil Sampling

Samples of rhizosphere soil of *P. polyphylla* var. *yunnanensis* were collected from Yanla township (105.968°E, 26.041°N) Xi Xiu district, An shun city, Guizhou Province, China. The excess soil was first gently shaken from the roots, and the remaining soil attached to the tubers of *P. polyphylla var. yunnanensis* was considered the rhizosphere soil.

Isolation of Rhizobacteria

To isolate bacteria, 10 g of rhizosphere soil was mixed with 90 mL of sterile distilled water in a rotary shaker at 180 rpm for 30 min at 30°C. After serial dilution in sterile distilled water, 100 μl volumes of the diluted soil suspensions were plated on Luria–Bertani (LB) medium plates (peptone 10 g/L, yeast extract 5 g/L, sodium chloride 10 g/L, and agar 1.5 g/L). After a 24-h incubation at 37°C, colonies with clear morphological characteristics were selected, purified, and preserved in liquid LB medium. To avoid potential fungal contamination, only highly diluted samples were used for isolation. The isolates were then restreaked on LB plates for colony purification. The final collection consisted of 22 bacterial isolates from rhizosphere soil samples. All purified isolates were cultured in 5 ml of LB medium at 37°C with shaking (rotary shaker at 180 rpm) for 12 h before being frozen and stored at −80°C with 15% glycerol.

Identification of Rhizobacteria

Morphology

The purified bacteria were streaked on LB agar medium and incubated at 37°C for 12 h. The morphology, color, edge, and the shape of the bacterial colonies were observed with reference to Bergey's Manual of Systematic Bacteriology (Whitman, 2015). Moreover, Gram staining was examined with reference to Hans Christian Gram's method conducted in 1884.

Physiology and Biochemistry

Starch hydrolysis, gelatine liquefaction, sugar fermentation, methyl red (MR), indole, Voges- Proskauer reaction, citrate, and hydrogen sulfide tests were performed to determine the physiological and biochemical characteristics of the pure strains.

16S Ribosomal RNA Gene Sequencing and Phylogenetic Analysis of Rhizobacteria

Total genomic DNA was extracted from overnight cultures of the individual bacterial isolates, which were cultured in LB medium at 37°C with shaking (200 rpm.), using the Bacterial Genomic DNA Extraction Kit (TianGen CAT# dp302-02) according to the manufacturer's protocol. The 16S rRNA gene was amplified by PCR using the universal primers, 27F (5′-AGAGTTTGATCMTGGCTCAG-3′) and 1492R (5′-TACGGTTACCTTGTTACGACTT-3′). The PCR amplification was carried out on A600 Super Gradient (LongGene) in a mixture (50 μL) containing 10 × PCR buffer (5 μL), DNA (2 μL), dNTPs (4 μL), primer (1 μL), Taq polymerase (0.5 μL, TaKaRa), and double distilled water (36.5 μL) with 30 cycles as follows: denaturation at 94°C for 1 min, annealing at 56°C for 1 min, and elongation at 72°C for 1.5 min. Predenaturation was carried out at 95°C for 5 min, and final elongation was performed at 72°C for 10 min. The PCR products were detected by agarose gel electrophoresis and sequenced (supported by Sangon Biotech, Shanghai, China).

The 16S rRNA sequences of 22 isolates were analysed for alignment with sequences in the NCBI database using the Blastn method.[1] The phylogenetic trees were constructed using the neighbor-joining (NJ) algorithm with MEGA 7.0 (Kumar et al., 2018). The strengths of the internal branches of the resulting trees were statistically evaluated by bootstrap analysis with 1,000 bootstrap replications.

Detection of Siderophore Production in Rhizobacteria

To quantify the siderophore production, the isolates were inoculated into LB medium. One hundred microliters of bacteria culture was spread on an SA-CAS plate (1/2 SA medium + 1/2 CAS medium) and incubated at 30°C for 48 h. Siderophore production was analysed using a modified version of the universal chemical assay developed by Schwyn and Neilands (1987) and Silva-Bailao et al. (2014).

The liquid CAS assay was used to quantify the concentrations of siderophores. Specifically, we harvested the cell-free supernatant (CFS) from 1 mL of SA bacterial cultures by centrifugation (12,000 rpm, 10 min at 4°C) and filtration (using a 0.22 μm filter). Then, 100 μl of CFS (three biological replicates for all 22 soil isolates) and SA medium as a control reference were added to 100 μl of CAS assay solution in a 96-well plate. After 0.5–1 h of static incubation at room temperature, the OD_{630} of the CFSs (As) and SA medium controls (Ar) were then measured using a microplate reader (Elx800 microplate reader, BioTek) at room temperature. Siderophores induce a color change in the CAS medium, which lowers the OD_{630} measurements, and siderophore production can be quantified using the following formula (Guo et al., 2016):

$$Siderophore\ Unit\ (SU) = \frac{Ar - As}{Ar} \times 100\%$$

Ar–the absorbance of the reference (SA medium) at 630 nm. As–the absorbance of the sample (CFS/bacterial cultures) at 630 nm.

Determining the Type of Siderophores Produced by Rhizobacteria

Each isolate was cultured in 15 mL of LB medium at 37°C and 200 rpm for 12 h. Then, 1.5 mL of bacterial solution was inoculated into 50 mL of SA medium. Cells were grown for 48 h at 30°C and 200 rpm. Then, 1 mL of bacterial culture was centrifuged at 12,000 rpm for 10 min to obtain CFS for subsequent experiments.

Hydroxamates

The *$FeCl_3$ test* (Schwyn and Neilands, 1987) was used to detect hydroxamate-type siderophores. Then, 0.5–1 mL of 2%

[1] https://blast.ncbi.nlm.nih.gov/Blast.cgi

$FeCl_3$ solution was added to 0.5 mL of SA fermentation supernatants. The formation of red or purple colors indicated the presence of hydroxamate siderophores. An absorption peak between 420–450 nm indicated a hydroxamate nature. Peaks were noted on a UV–visible spectrophotometer (2802 UV/VIS SPECTROPHOTOMETER, UNICO).

Catecholates

Arnow's test (Arnow, 1937; Sheng et al., 2020) was used to detect catecholate-type siderophores. First, 0.5 mL of SA fermentation supernatant was added to 0.5 mL of 0.5 M HCl and 0.5 mL of reagent containing 10 g each of $NaNO_2$ and $Na_2MoO_4{\cdot}2H_2O$ in 100 ml water. When 0.5 mL of 1 M NaOH was added, the color of the solution turned from yellow to red. Absorbance was measured at 515 nm to indicate the presence of catecholic siderophores (2802 UV/VIS PECTROPHOTOMETER, UNICO).

Carboxylates

Shenker's test (Shenker et al., 2008) was used to detect carboxylate-type siderophores. First, 0.5 mL of 250 μM $CuSO_4$ and 1 mL of acetate buffer (pH = 4) were added to 0.5 mL of SA fermentation filtrate. The copper complex formed was observed between 190 and 280 nm to determine the maximum absorption. There is no specific wavelength at which the copper complex is absorbed. The entire wavelength from 190–280 nm was scanned to observe the peaks of siderophore absorption (2802 UV/VIS PECTROPHOTOMETER, UNICO).

Antimicrobial Activity of Rhizobacteria

To determine whether the CFS of SA or LB culture fermentation for 22 rhizobacteria isolates had an antimicrobial effect, gram-positive *Staphylococcus aureus,* gram-negative *Escherichia coli*, and the fungus *Candida albicans* were selected as indicator microbes. In this study, the agar diffusion method (the punch method) was used to investigate the antimicrobial activity of the siderophore solution. Each rhizobacterial isolate was inoculated in SA and LB medium at 30°C and 200 rpm for 48 h, respectively. The CFS of bacterial culture from SA and LB medium were prepared by centrifugation (12,000 rpm, 10 min at 4°C) and filtration (using a 0.22 μm filter). *Escherichia coli* and *Staphylococcus aureus* were cultured on LB agar medium at 37°C for 12–14 h. *Candida albicans* was cultured on PDA at 30°C for 14–16 h. Wells approximately 8 mm in diameter and 2 mm deep were made on the surface of the agar medium using a sterile borer. Each well was subsequently filled with 100 μL of test sample and labeled with a marker. The same amount of sterile SA medium was used as a negative control, while amphotericin and cephalosporin were used as positive controls. The size of the bacteriostatic zone was observed after overnight culture.

Effect of Different Concentrations of Iron on the Growth and Siderophore Production of the AS19 Strain

$FeCl_3$ was added to 150 mL of SA medium at a final concentration of 0, 100, 200, 400, 600, 800, 1,000, and 2,000 μM Fe^{3+}, 3–5 ml of bacterial culture was collected every 6 h. The bacterial growth was quantified spectrophotometrically by measuring the optical density at 600 nm. One milliliter of bacterial culture was centrifuged at 12,000 rpm for 10 min at the indicated time points. As described above, the CFS was detected by CAS assay and the siderophores units (SUs) were calculated quantitatively to evaluate the effects of different iron concentrations on the growth and the synthesis of siderophores of AS19 strain.

Evaluation of the Antimicrobial Activity of AS19 at Different Fe^{3+} Concentrations

AS19 strain was inoculated in 150 mL of SA medium with final concentrations of 0, 100, 200, 400, 600, 800, 1,000, and 2,000 μM Fe^{3+} and cultured at 30°C for 48 h. One milliliter of the bacterial culture was collected and centrifuged at 12,000 rpm for 10 min. The antimicrobial experiment was performed as described above.

Effects of Urea, KH_2PO_4, and Nitrogen, Phosphorus, and Potassium on the Growth and Siderophore Production of AS19

Urea, KH_2PO_4 was added to 150 mL of SA medium, and the final concentration was 10, 50, 90 mg/mL. Nitrogen, phosphorus, and potassium (NPK) synthetic chemical fertilizers (N:P:K = 15:15:15) was also added to 150 mL of SA medium, and the final concentration was 5, 20, 30, and 50 mg/mL. AS19 bacterial broth was inoculated in SA medium containing different concentration of urea, KH_2PO_4 and NPK at 30°C, 200 rpm. Bacterial growth (OD_{600}) and SUs were measured at some point in time. The calculation of the siderophore units was performed as described above.

Effects of Different Concentrations of Fe^{3+} on the Motility of AS19

The swimming motility of AS19 strain was analysed using solid LB medium with 0.3% of agar by adding different concentrations of Fe^{3+}, following a method published previously with some modifications (Chen et al., 2012; Gao et al., 2020). The addition of 100 μM 2,2-bipyridine was performed to establish to an iron-free environment. A single colony of AS19 was inoculated in 0.3% of agar medium and cultured at 30°C for swarming assays. Motility diameter was measured 16–24 h after inoculation.

Assessment of Growth-Promoting Traits *in vitro*

Indole-3-Acetic Acid Production

Indole-3-acetic acid (IAA) production by the isolate *Bacillus altitudinis* strain AS19 was determined according to the methodology described by Bric et al. (1991). The amount of IAA produced by AS19 was determined in a multimode reader (Cytation 5, BioTek) at 530 nm. The concentration of IAA produced by the bacterial isolate AS19 was calculated from the

standard curve of commercial IAA (Sigma, United States) in the range of 10–100 μg/mL.

Qualitative Estimation of Ammonia Production

Ammonia production by the bacterial isolate AS19 was determined by following the methodology of Cappuccino and Sherman (1992).

Solubilization of Phosphate

The phosphate solubilization ability of the bacterial isolate AS19 was determined in Pikovskaya agar medium according to Pikovskaya, R.I.'s method (Pikovskaya, 1948) with the solubilization index calculated as follows:

$$Solubilization\ Index(SI) = \frac{Colony\ diameter(mm) + Halozone\ diameter(mm)}{Colony\ diameter(mm)}$$

Organic Acid Production

AS19 was spot inoculated on M9 agar medium with methyl red as a pH indicator dye. Plates were incubated for three days at 28 ± 2°C (Sambrook and Russell, 2001).

Antagonism Experiment

Soilborne pathogenic fungi and bacteria including *Fusarium oxysporum*, *Fusarium solanum,* and *Pectobacterium carotovorum* were as indicator microbes to observe the inhibition zone in antagonism experiments.

Seed Germination Assay

Hot pepper and maize seeds were purchased at random and soaked in a dishwashing liquid, washed in running water for 30 min, and disinfected with 75% alcohol for 30 s. Then, the seeds were washed with sterile water 3–5 times, sterilized with 3% of sodium hypochlorite for 10 min, and rewashed with sterile water 4–5 times. The seeds were placed on presterilized filter paper in separate Petri plates (three replicates). First, 20 ml of CFS, bacterial solution, and SA medium were applied to each group. Seeds were kept damp by spraying 5 ml of the above active components on filter paper every 5 days. Plates with the hot pepper and maize seeds were incubated at 25 ± 1°C, and any physiological changes in each group of seeds were recorded. The experiment was carried out in a completely randomized design under controlled conditions. The experiment was performed in triplicate.

Evaluation of Plant Growth Promotion by AS19

Gynura divaricata (Linn.) was used to verify whether strain AS19 can promote plant growth. The seedlings were cultured in MS medium (with 0.02 mg/L NAA, 3% sucrose, 0.7% agar) for 15–18 days, and then experiments were carried out. The inoculated seedlings with uniform growth were selected, and the sealing film was removed to allow the seedlings to adapt to the external environment for 3 days. Then, the terminal buds, lateral leaves, and lateral roots were cut off. The remaining 5–6 primary roots were kept in the same initial state as the seedlings. The seedlings were transplanted into the same sized sterilized pot (9.5 cm high, 9 cm diameter) with a mixture of sterile sand and soil in the ratio of 3:1. The disinfection of the pots was carried out using 75% ethanol and washed with sterile water several times to remove chemicals. The soil was mixed thoroughly and then added to the pots for the control and treated seedlings. This step ensured that all the plants obtained the same nutrients. After transplantation, the plants were irrigated with 100 ml of water for the first time. After 5 days, the plants were randomly divided into three groups: the supernatant group, bacterial solution group, and SA medium group, with five pots in each group. Different nutrients of the experimental group and control group were added to the plants regularly, 20 ml each time, once every 4 days. Day and night were simulated by incandescent light. The temperature was maintained at 25 ± 3°C. After 40 days, the growth parameters of the plants were recorded and compared with those of the control plants. The parameters considered were the number of leaves, number of shoots, shoot length, root length, and stem length.

Toxicity Test of *Hermetia illucens* L. Larvae

The CFS of AS19 was lyophilized and dissolved with saline. *Hermetia illucens* L. larvae were fed wheat bran and housed in an environmentally controlled breeding room (temperature: 28–30°C; humidity: 60 ± 5%, 12 h dark/light cycle). The *H. illucens* L. larvae were divided into 5 groups ($n = 50$ larvae/group). The natural growth group was only punctured. The control group was injected with 2.5 μL of sterile saline. The experimental group was injected with 2.5 μL of CFS (30 mg/kg, 40 mg/kg, 1 g/kg). The survival rate and changes in body weight were observed and recorded every 24 h for 7 days.

Reproducibility of the Results and Statistical Analysis

The assays were repeated independently three times. In each assay, the values obtained at each time point were further measured in triplicate. The results are presented as an average of the total determination. The standard deviations associated with each average value were represented in the form of error bars. The mean values were further subjected to one-way ANOVA followed by the Tukey–Kramer multiple comparison method; *P*-values less than 0.05 were considered statistically significant.

Nucleotide Sequence Accession Numbers

The sequences of the 16S rRNA gene of the 22 isolates identified in this study have been deposited in the National Center for Biotechnology Information (NCBI) Nucleotide database. The accession numbers were shown in **Supplementary Table 1**.

RESULTS

Isolation and Identification the Rhizobacteria of *Paris polyphylla* var. *yunnanensis*

In our study, 22 strains of bacteria were isolated and used in the following experiments.

Morphological Characteristics

Morphologically distinct bacterial isolates were selected and studied for their colony characteristics. The size, shape, edge, transparency, and color of the isolates are described in **Supplementary Table 2**. The plates are shown in **Figure 1A**. Some isolates had similar morphological characteristics, such as AS3 and AS22. Gram staining results showed that AS1, AS5, AS6, AS7, and AS9 were gram-negative bacteria, while the others were gram-positive (**Figure 1B**).

Physiological and Biochemical Characteristics

The physiological and biochemical characteristics of these 22 strains are shown in **Supplementary Table 3**. Although AS3 and AS22 had similar morphological characteristics, the results of starch hydrolysis, gelatine liquefaction, citrate, and hydrogen sulfide tests of AS22 were positive, while those of AS3 were negative. Similarly, although AS5, AS6, and AS7 had similar morphological characteristics, the Voges–Proskauer reaction of AS6 showed positive results, which was different from AS5 and AS7.

Molecular Identification

The PCR products were observed as a single band with a size of approximately 1,500 bp (**Figure 1C**). The NJ tree based on 16S rRNA sequences showed that the 22 isolates were grouped into 3 different genera: *Bacillus*, *Enterobacter,* and *Stenotrophomonas* (**Figure 1D**). The *Bacillus* group contained 17 isolates, while the small group belonging to the *Stenotrophomonas* genus included only one isolate. The results suggested that the dominant genus in the rhizosphere of *PPVY* was *Bacillus*. Interestingly, 70.59% (12/17) of the isolates belonged to the *Bacillus pumilus* group but had different physiological and biochemical characteristics.

Siderophore Synthesis Validated in Rhizobacteria

Combined with CAS plate and liquid assays, we found that 21 isolates could secrete siderophores. Among them, nine isolates named AS2, AS3, AS4, AS5, AS6, AS7, AS9, AS13, and AS21 turned the blue color of the agar to pink in CAS liquid assays (**Figure 2A**). Another 12 isolates, including AS8,

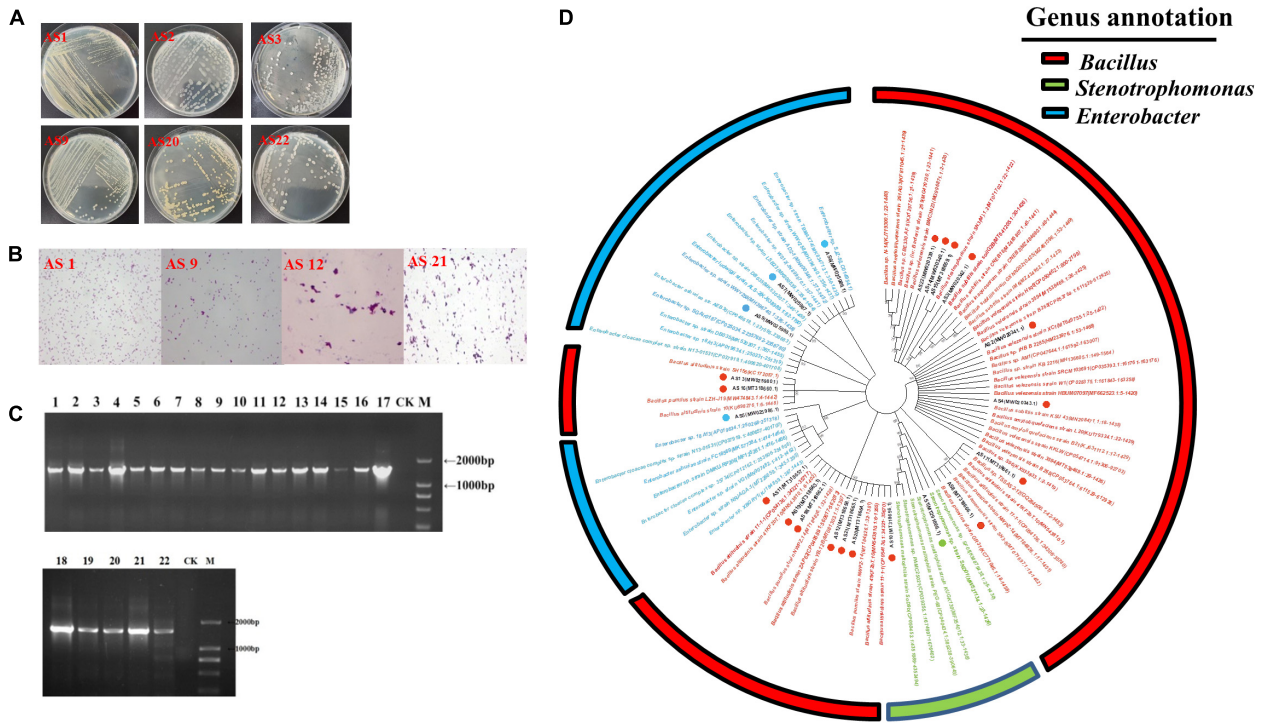

FIGURE 1 | Screening and identification of rhizosphere bacteria. **(A)** Representative colony morphology. After repeated isolation, monoclones were selected and cultured in LB liquid medium for 12–14 h at 37°C. The purified strain was streaked onto LB agar medium by the streak plate method, and the colony morphology was observed. **(B)** Gram staining. AS1 and AS9 represent gram-negative bacteria, and AS12 and AS21 represent gram-positive bacteria. **(C)** PCR results for 16S rRNA sequencing amplification of the 22 bacterial isolates. M: DL2000 DNA marker, CK: blank, the numbers 1–17 represent the bacterial isolates AS1, AS2, AS3, AS4, AS5, AS6, AS7, AS8, AS9, AS10, AS11, AS12, AS13, AS14, AS15, AS16, and AS17, and the numbers 18–22 represent the bacterial isolates AS18, AS19, AS20, AS21, and AS22, respectively. **(D)** Phylogenetic trees of the 22 bacterial isolates based on their 16S rRNA sequences.

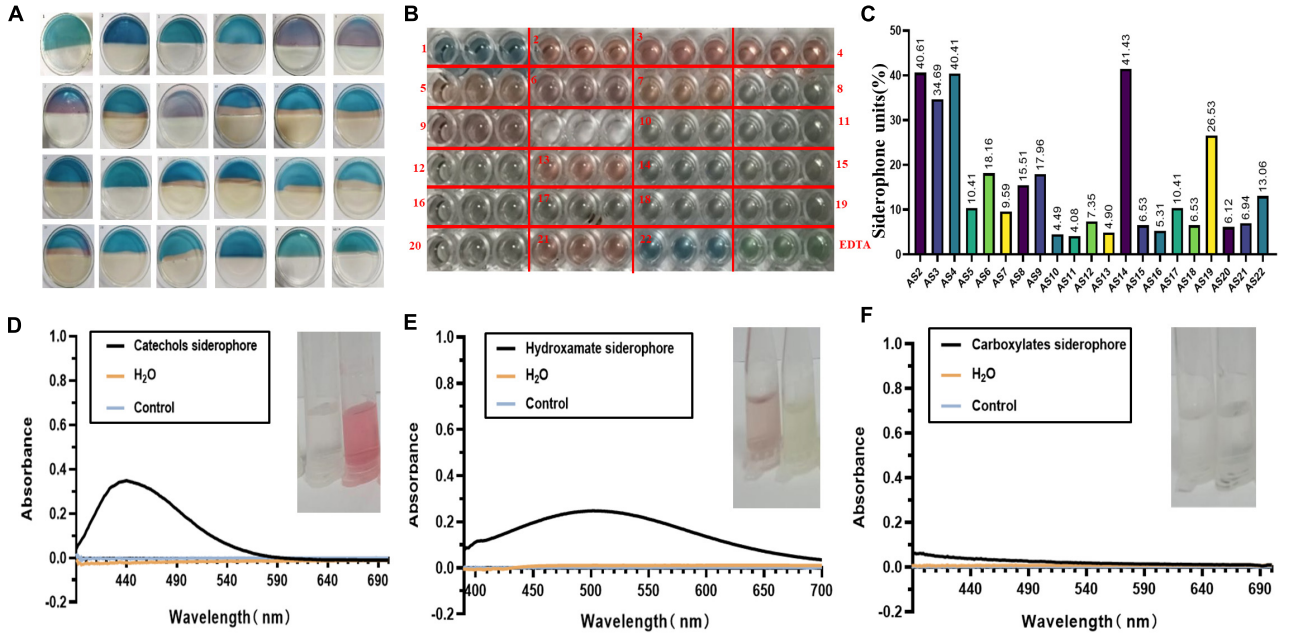

FIGURE 2 | The units and type of siderophores produced by 22 isolates. **(A)** SA-CAS agar plate assay. Isolates were cultured on SA-CAS agar plates, and the blue color changed to pink or yellow. **(B)** CAS liquid testing was performed in a 96-well plate. **(C)** The units of siderophores produced by 21 isolates calculated according to SU = (Ar − As)/Ar*100%. The absorbance was measured at 630 nm. **(D)** Catecholate-type siderophore. AS2, AS3, AS4, AS5, AS6, AS7, AS9, AS14, and AS22 absorption peaks were detected at 440 nm. **(E)** Hydroxamate-type siderophore. The absorption peaks of AS8, AS10, AS11, AS12, AS13, AS15, AS16, AS17, AS18, AS19, AS20, and AS21 were detected at 505 nm. **(F)** Carboxylate-type siderophore. No absorption peak was detected in any of the samples at 190–280 nm.

AS10, AS11, AS12, AS14, AS15, AS16, AS17, AS18, AS19, AS20, and AS22, produced a color change from blue to yellow (**Figure 2A**).

Different Types of Siderophores Produced by Rhizobacteria

We found that the SUs of each isolate were between 4 and 41% (**Figures 2B,C**). The maximum amount of siderophore production, 41.40%, was observed from the AS14 isolate. With the Arnow method, when NaOH was added to the SA fermentation supernatant, the AS2, AS3, AS4, AS5, AS6, AS7, AS9, AS14, and AS22 solutions immediately turned red, and absorption peaks were also detected at 440 nm by full wavelength scanning. The siderophore produced by these nine strains was identified as the catecholate type (**Figure 2D**). The hydroxamate type was identified by the $FeCl_3$ method. When 2% of $FeCl_3$ was added, the solutions of AS8, AS10, AS11, AS12, AS13, AS15, AS16, AS17, AS18, AS19, AS20, and AS21 turned red. After full wavelength scanning, absorption peaks were detected at 505 nm (**Figure 2E**). The siderophores produced by these 12 strains were identified as the hydroxamate type. In Shenker's method, the maximum absorption peak of the sample was not detected at 190–280 nm. The carboxylic type of siderophore was not found in this study (**Figure 2F**).

Antimicrobial Activity of Rhizobacteria

Among the 22 rhizobacteria isolated from *PPVY*, only the SA medium CFS of 16 strains, AS2, AS3, AS8, AS10, AS11, AS12, AS13, AS14, AS15, AS16, AS17, AS18, AS19, AS20, AS21, and AS22, could significantly inhibit the growth of *Candida albicans* (**Table 1** and **Figure 3C**). The inhibition zones of AS3, AS17, and AS21 were larger than those of the positive control (3 mg/ml, amphotericin). The inhibition zone diameters are shown in **Figure 3D**. However, no inhibition zone was observed near the sample wells on the *Staphylococcus aureus* and *Escherichia coli* plates (**Figures 3A,B**). In addition, the CFS of LB medium did not show antimicrobial activity against any of the three indicator microbes (**Table 1** and **Supplementary Figure 1**). These results demonstrated that the metabolites of 16 strains of siderophilic bacteria contain active substances that have a strong inhibitory effect on fungi. SA medium is a low-iron medium and is often used to induce siderophore production. Based on this, we speculated that the antimicrobial substance may be siderophore related.

Effect of Different Concentrations of Fe^{3+} on AS19 Siderophore Production

The AS19 strain was chosen for further study since it shows the largest inhibition zone and higher siderophore production units. Studies have shown that siderophore production is inhibited in the presence of excess iron. SA medium containing different concentrations of Fe^{3+} was used to determine the siderophore units produced by AS19 in different time periods. As shown in **Figure 4B**, the presence of an appropriate amount of Fe^{3+} could promote the growth of AS19, but when the Fe^{3+} concentration was more than 1,000 μM, AS19 stopped growing.

TABLE 1 | *In vitro* antimicrobial activity of cell-free supernatant (CFS) of bacterial strains.

Indicator bacteria	*Staphylococcus aureus*		*Escherichia coli*		*Candida albicans*	
Cell-free supernatant	LB	SA	LB	SA	LB	SA
AS1						
AS2						++
AS3						+++
AS4						–
AS5						–
AS6						–
AS7						–
AS8						++
AS9						–
AS10						+
AS11	–	–	–	–	–	+
AS12						+
AS13						++
AS14						+
AS15						+
AS16						+
AS17						+++
AS18						++
AS19						++
AS20						+
AS21						+++
AS22						+

–, no inhibition; +, inhibition;++, clear inhibition; +++, very clear inhibition.

When the concentration of Fe^{3+} was more than 100 μM, AS19 produced very little or no siderophores (**Figure 4A**), suggesting that the addition of Fe^{3+} inhibited the secretion of siderophores.

Antimicrobial Activity of AS19 Cell-Free Supernatant at Different Fe^{3+} Concentrations

To explore the effect of Fe^{3+} on the antimicrobial activity of AS19, CFS after 48 h of fermentation in SA medium with different concentrations of Fe^{3+} was utilized. The results showed that when the Fe^{3+} concentration was over 1,000 μM, the AS19 strain no longer grew, and the antimicrobial activity of the CFS was also lost (**Figures 4C,D**). As soon as the concentration of Fe^{3+} was over 100 μM, the siderophore production of AS19 was inhibited, but its antimicrobial activity was not affected. SA medium with different concentrations of Fe^{3+} was used as a negative control, and no inhibition zone was produced (**Supplementary Figure 2**). Therefore, we suspected that there were no siderophores produced by AS19 but other secondary metabolites or a combination of various substances that exerted antimicrobial activity on *Candida albicans*.

Effects of Synthetic Chemical Fertilizers on AS19 Growth and Siderophore Production

To further investigate the effect of fertilizers frequently used in farming on siderophore synthesis in AS19, a series of experiments were performed with urea, KH_2PO_4, and NPK fertilizers. As shown in **Figure 5B**, with increasing urea concentration, the growth of AS19 was inhibited. When the urea concentration was above 90 g/L, AS19 basically stopped growing. Similarly, a high concentration of KH_2PO_4 inhibited the growth of AS19 (**Figure 5D**). At the same time, when the concentration was 100 g/L, the biomass of AS19 could only reach half of that under normal conditions. The growth of AS19 was first inhibited and then promoted by the addition of NPK fertilizer. An appropriate amount of NPK fertilizer (≤30 g/L) was conducive to the growth of AS19, but excessive use of NPK fertilizer (≥50 g/L) could inhibit or even stop the growth of AS19 (**Figure 5F**). Overall, there was a phenomenon of promotion at low concentrations and inhibition at high concentrations.

On this basis, we detected the synthesis of siderophores by AS19. The addition of urea and NPK fertilizer inhibited the synthesis of siderophores overall (**Figures 5A,E**). The addition of KH_2PO_4 caused AS19 to produce siderophores no longer in the case of normal growth (**Figure 5C**). In conclusion, excess urea and KH_2PO_4 were not conducive to the growth and siderophore production of the AS19 strain. At low concentrations, NPK fertilizer slightly promoted the growth of AS19 but inhibited the secretion of siderophores. Therefore, the use of various synthetic chemical fertilizers limited the role of AS19 as a PGPR.

Effects of Different Concentrations of Fe^{3+} on the Swimming Motility of AS19

Motility is one of the most important traits for efficient rhizosphere colonization. In this study, the growth of AS19 was not affected by different concentrations of Fe^{3+}, but the swimming ability showed a different trend (**Figures 6A,B**). When the concentration was between 100 and 400 μM, the motility was strong and could extend to the edge of the plate. As the concentration reached 600 μM or above, the swimming ability declined, and the motility diameter decreased. Overall, low concentrations of iron promoted the swimming motility of the AS19 strain, while high concentrations inhibited swimming motility.

Plant Growth Promoting and Antagonism Traits of AS19

The AS19 isolates showed negative results for organic acid (**Figure 6C**) and IAA production (**Figure 6D**). In phosphate solubilization, a slightly transparent circle appeared on the inorganic phosphorus plate, while this was not observed in organic phosphorus, suggesting that it had a slight effect on phosphate solubilization (**Figure 6E**). The sample turned red to indicate ammonia production, proving that AS19 could produce ammonia (**Figure 6G**). Furthermore, AS19 can produce the hydroxamate type of siderophore, which is an important bioactive substance. Thus, AS19 could be considered

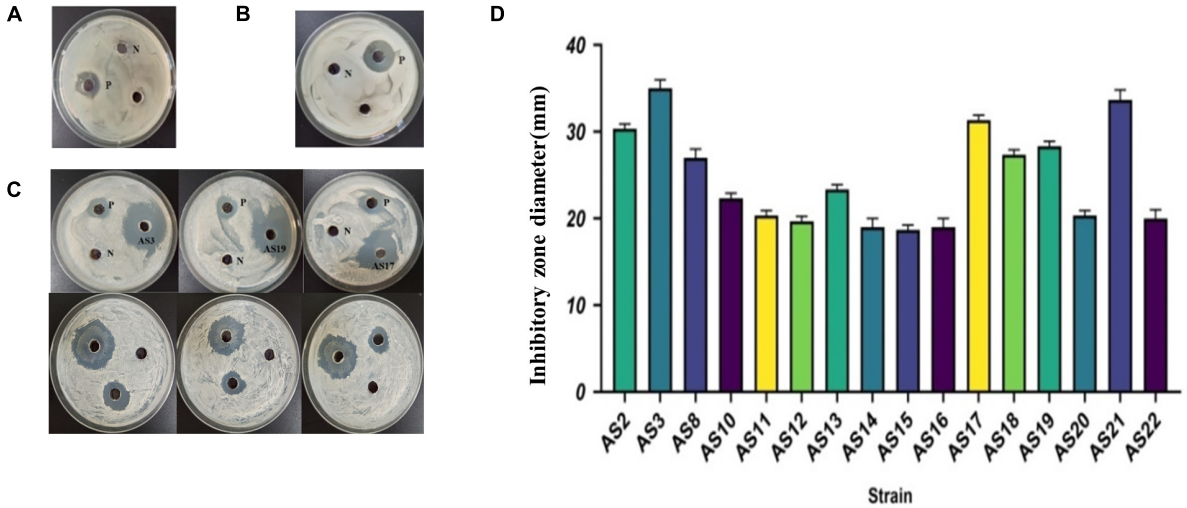

FIGURE 3 | The antimicrobial activity of CFSs of 22 isolates grown on SA. **(A)** Antimicrobial experiment with SA CFS against *Escherichia coli* N: SA medium negative control, P: Cephalosporin positive control. **(B)** Antimicrobial experiment with SA CFS against *Staphylococcus aureus.* N: SA medium negative control, P: cephalosporin positive control. **(C)** Antimicrobial experiment with SA CFS against *C. albicans.* N: SA medium negative control, P: Amphotericin positive control. **(D)** The inhibitory zone of 16 strains against *C. albicans*. Represented by individual plate experiments, the data statistics are shown in **Table 1**.

a PGPR to some extent. However, AS19 could not antagonize *F. oxysporum*, *F. solanum,* or *P. carotovorum* in the antagonism assays (**Figure 6F**).

Effects of AS19 on Seed Germination

To further understand the biofertilization potential of AS19, the effect on germination was observed and recorded. The final germination rate of pepper seed in CFS group was stable at 71% (5/7), which was nearly 10 times higher than that of the bacterial solution group (7.1%), but no seeds germinated in the medium group (**Figure 6I**). Furthermore, we found that pepper seeds in the supernatant group began to germinate on the 8th day, and seeds in the solution group only began to germinate on the 13th day (**Figure 6H**). Similarly, the CFS also promoted the germination of maize seeds, and the germination rate was up to 85.71% (6/7), which was six times higher than the SA medium group (**Figures 8B,C**). Our experiments indicated that the secondary metabolites of AS19 could promote the germination of pepper and maize seeds.

Plant Growth Promotion of *Gynura divaricata* (Linn.) by AS19

The growth parameters of the SA medium group and CFS and bacterized *Gynura divaricata* (Linn.) seedlings were compared, and the results are presented in **Figure 7A**. Treatment with AS19 CFS increased the germination number and leaf number of *Gynura divaricata* (Linn.) plants by up to 1.45 times (**Figure 7B**) and 1.57 times (**Figure 7C**), respectively, compared to the control group. Root elongation was significantly promoted by the bacterial solution by 1.19 times (**Figure 7F**). However, there was no significant difference in the length of germination and stems, and the supernatant group and the bacterial solution group had slightly higher values than the SA medium group (**Figures 7D,E**).

Prediction of Gene Clusters for Siderophore Synthesis

The siderophore synthesis genes of AS19 strain was preliminarily analysed and the pattern was mapped (**Figure 8A**). The siderophore synthesis gene cluster, including six core synthesis genes (*AS19_03748, AS19_03749, AS19_03750, AS19_03751, AS19_03752,* and *AS19_03753*). The analysis by the software, Hmmscan showed that the main genes of siderophore synthesis were *AS19_03750* and *AS19_03753*. One transcriptional regulatory gene *AS19_03744* located at the upstream of the siderophore synthesis gene cluster, was similar to *AlcR* in *Bordetella pertussis* (Accession no. AF018255.1), *AraC* in *Escherichia coli* (Accession no. V00259.1), and this transcriptional activator could positively regulate the production and transport of siderophore. It was also found that there were short base overlaps among six siderophore synthesis genes (**Figure 8A**).

Evaluation of the Biosafety of AS19 as a Biofertilizer

In order to evaluate the biosafety of AS19 as a biological fertilizer, *H. illucens* L. larvae was used as a test subject. The results of survival curve showed that the dosage of 30 mg/mL, 40 mg/mL, and 1 g/kg had no effect on the survival of *H. illucens* L. larvae (**Figure 8D**). These results implicated the safety of the CFS of AS19 fermentation liquid in organisms.

DISCUSSION

Siderophilic bacteria, a kind of plant growth-promoting bacteria, have attracted much attention and been investigated for decades. These bacteria can promote plant growth and regulate the

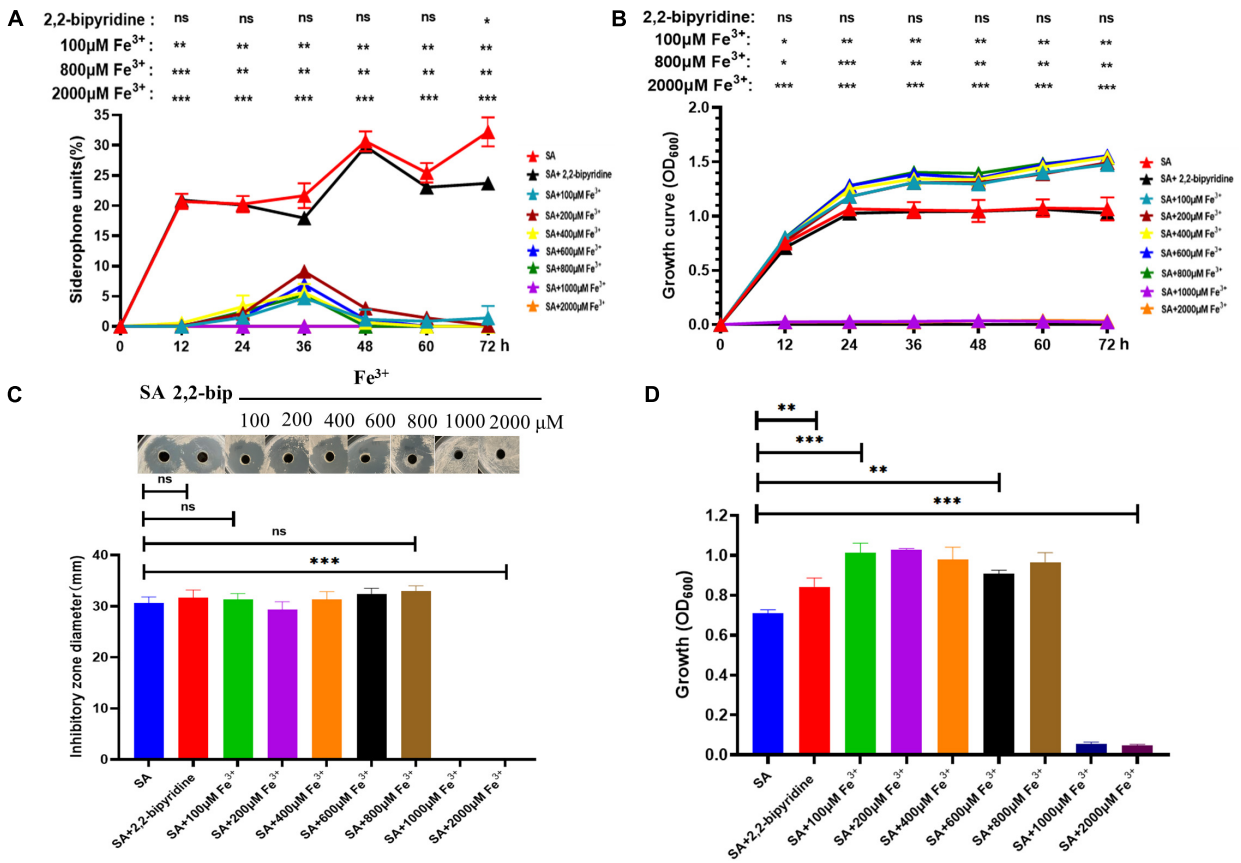

FIGURE 4 | Growth curve, siderophore production, and bacteriostasis of AS19 at different Fe^{3+} concentrations. **(A)** Effect of different concentrations of Fe^{3+} on AS19 siderophore production. AS19 was cultured in SA medium containing different concentrations of Fe^{3+} at 30°C and 200 rpm. **(B)** Effect of different concentrations of Fe^{3+} on AS19 growth. AS19 was inoculated into SA medium containing different concentrations of Fe^{3+} at 30°C and 200 rpm. **(C)** Effect of different concentrations of Fe^{3+} on AS19 bacteriostatic activity. AS19 was inoculated into SA medium containing different concentrations of Fe^{3+} at 30°C and 200 rpm for 48 h. One milliliters of bacterial solution were centrifuged at 12,000 rpm for 10 min. The CFS was used for the plate bacteriostasis test. **(D)** Effect of different concentrations of Fe^{3+} on AS19 growth at 48 h. (ns, no significant difference, $^{*}p < 0.05$, $^{**}p < 0.01$, $^{***}p < 0.001$).

soil microenvironment by secreting siderophores (Powell et al., 1980; Ellermann and Arthur, 2017; Khan et al., 2018; Kramer et al., 2020). In our study, 22 strains were isolated from the rhizosphere soil of *P. polyphylla* var. *yunnanensis* and divided into three groups, including the species of *Bacillus, Enterobacter,* and *Stenotrophomonas* (**Figure 1D**). The small group belonging to the *Stenotrophomonas* genus contained only one isolate. The dominant genus, *Bacillus*, contained 17 isolates. Twelve isolates with different physio-biochemical characteristics were identified as the *B. pumilus* group by 16S rRNA gene sequence analysis. The *B. pumilus* group contains five species, *B. pumilus*, Bacillus *safensis*, *Bacillus stratosphericus*, *Bacillus altitudinis*, and *Bacillus aerophilus*. Apart from the AS1 strain belonging to *Stenotrophomonas*, 95.45% (21/22) of isolates could secrete siderophores (**Figure 2B**). These results showed that siderophilic bacteria were abundant in the rhizosphere soil of *PPVY*. The *B. pumilus* group corresponded to the dominant siderophilic bacteria.

Studies have indicated that rhizosphere microorganisms of plants secrete one or more siderophores to prevent plant diseases (Zhou et al., 2019). To evaluate the siderophore production of 22 isolates, a CAS assay was performed. The AS14 strain showed the highest production of siderophores, which was 41.40% (**Figure 2C**). Two types of siderophores, catecholates and hydroxamates, were found in our experiment. We also found that *Enterobacter* mainly produced catecholic-type siderophores, which is consistent with the report of Neilands (1981). Habibi et al. (2019) reported that *Pseudomonas* species were more active in terms of siderophore production than species of other genera. It is interesting to note that no *Pseudomonas* isolate was identified in our study. The different results may have been due to the bacterial species varying with the rhizospheres of different plants and different locations.

The secondary metabolites produced by these isolated strains in our work had a significant inhibitory effect on *C. albicans* but there was no inhibitory effect on G^{-} *E. coli* and G^{+} *S. aureus* (**Figure 3**). When the 16 strains were cultured in LB or SA media, we found that only the fermentation filtrate in the low-iron SA medium showed strong antimicrobial activity against *C. albicans* (**Table 1**). It has been reported that siderophores are

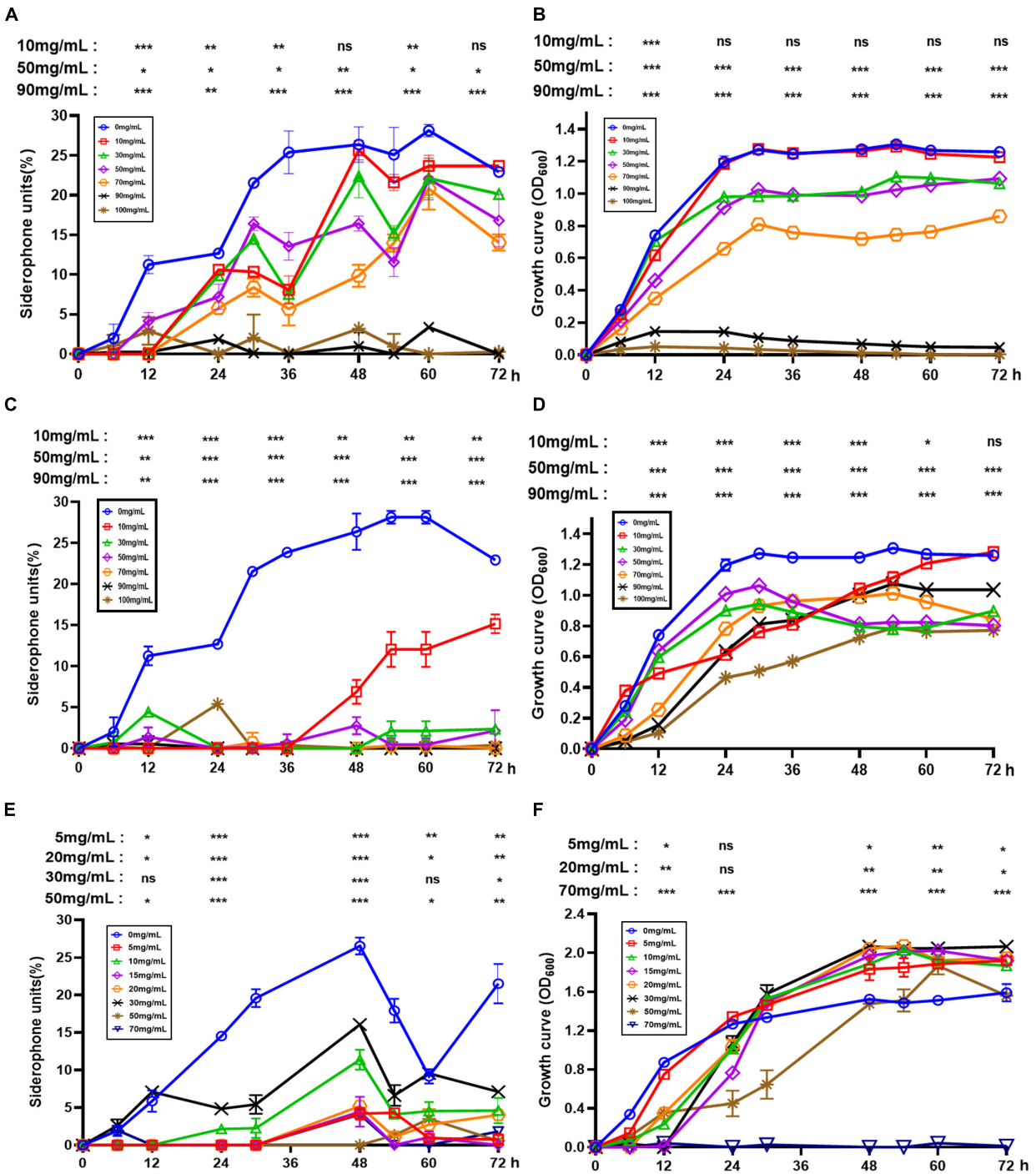

FIGURE 5 | Effects of urea, KH_2PO_4 and NPK on the growth and siderophore production of AS19. **(A)** Siderophore production at different concentrations of urea. **(B)** The growth curve at different concentrations of urea. **(C)** Siderophore production at different concentrations of KH_2PO_4. **(D)** The growth curve at different concentrations of KH_2PO_4. **(E)** Siderophore production at different concentrations of NPK compound fertilizer. **(F)** The growth curve at different concentrations of NPK compound fertilizer (ns, no significant difference, $^*p < 0.05$, $^{**}p < 0.01$, $^{***}p < 0.001$).

widely used not only in plant pest control (Hosseini et al., 2021), heavy metal pollution remediation (Yi et al., 2022), and fertilizer supplementation (Orr et al., 2020) but also in combination with antifungal drugs for the initial treatment of fungal infections, such as *Cryptococcus* (Chayakulkeeree et al., 2020; Sheng et al., 2020). The hydroxamate siderophore desferrioxamine B has been included in the World Health Organization (WHO) demonstration list of essential drugs for the treatment of iron load

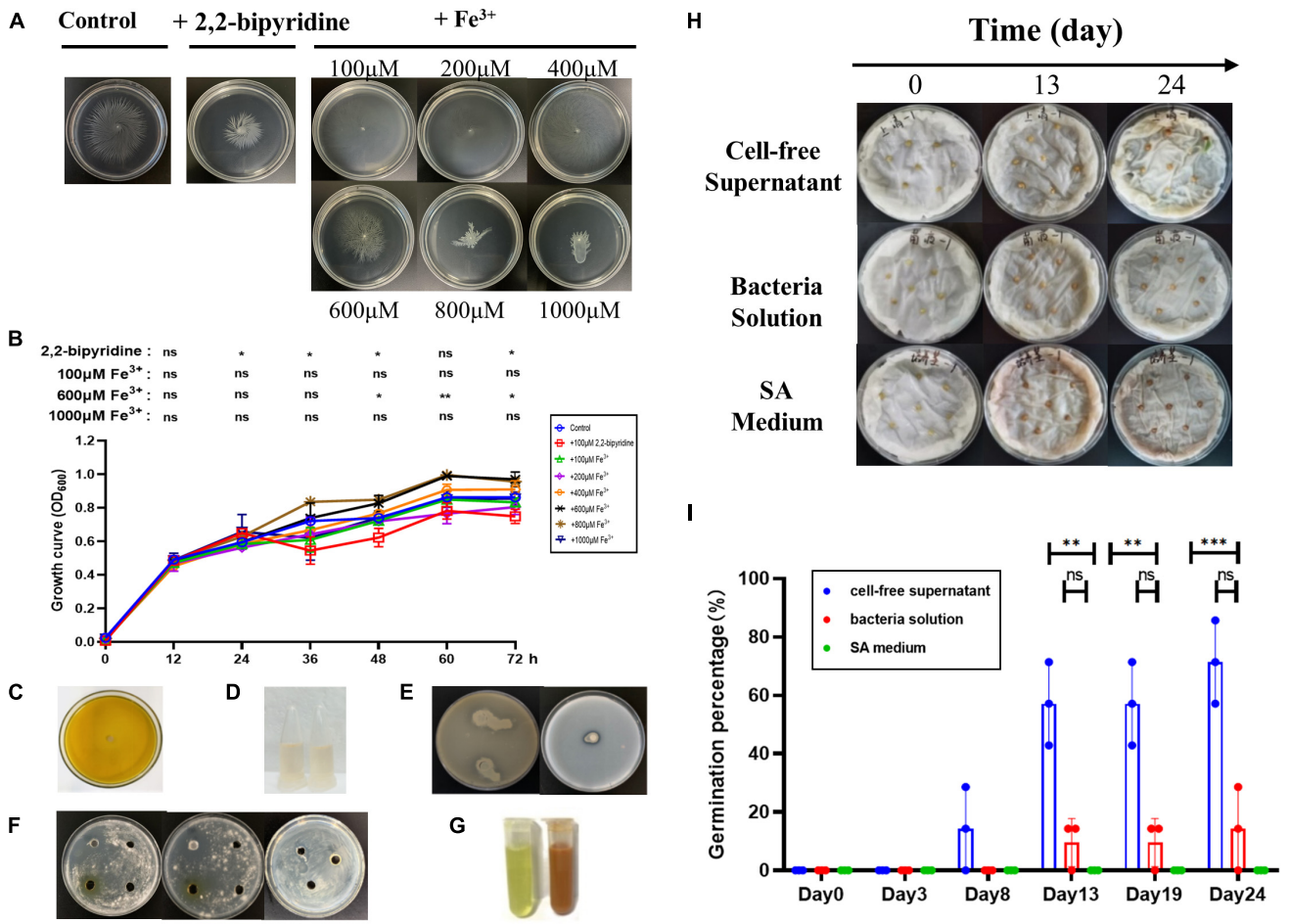

FIGURE 6 | Swimming motility, growth-promoting and seed-germination assays. **(A)** The swimming of AS19 in solid LB medium with 0.3% agar under different concentrations of Fe^{3+}. **(B)** Effect of different concentrations of Fe^{3+} on the growth of AS19. **(C)** Production of organic acids. **(D)** Production of IAA. **(E)** Decomposition of phosphate. **(F)** Antagonism experiment. **(G)** Production of ammonia. **(H)** The germination of pepper seeds treated with CFS and bacterial solution of AS19. The SA medium group was the control group. **(I)** The germination percentage of pepper seeds (a total of seven in each group). The experiment was repeated three times. Three dots represent the germination percentage of three experiments (ns, no significant difference, $*p < 0.05$, $**p < 0.01$, $***p < 0.001$).

in patients with thalassaemia (Aydinok et al., 2015). These results implied that the siderophores secreted by the 16 isolated strains have antimicrobial activity against *C. albicans*.

To further explore the effect of Fe^{3+} on siderophores, the *B. altitudinis* strain AS19, which had the best bacteriostatic activity and high siderophore units, was selected. The presence of a high concentration of Fe^{3+} significantly inhibited the growth of AS19. Concentrations exceeding 1,000 μM Fe^{3+} were toxic to the bacteria. However, the presence of 100 μM Fe^{3+} greatly reduced the production of siderophores, which could not be detected under these conditions. To investigate whether the antifungal activity of AS19 was related to the production of siderophores, we investigated the influence of the presence of Fe^{3+} on its antimicrobial activity. The results showed that the presence of Fe^{3+} at low concentrations did not affect the inhibition of *C. albicans* (**Figure 4C**). We speculated that the bacteriostatic activity might not mainly be caused by the siderophore or that there were other active components, such as bacteriocin, non-ribosomal peptides, dihydro-iso-coumarins, cyclic lipodepsipeptides, and linear lipodepsipeptides with antimicrobial properties in the metabolites of *Bacillus*, which played a bacteriostatic role together with the siderophore (Wang and Ding, 2018; Kaspar et al., 2019).

To further explore the biofertilizer potential of AS19, the effects of different chemical fertilizers on the growth and siderophore production of AS19 were creatively assessed. Urea and K_2HPO_4 significantly inhibited the growth of AS19 and reduced its siderophore production. Although the low concentration of NPK fertilizer had the tendency to promote the growth of AS19, it still inhibited the production of siderophores. This is consistent with the results of recent reports on the soil toxicity of chemical fertilizers and the destruction of the microbial ecological environment (Rahman et al., 2020). Long-term intensive fertilization may increase the risk of soil degradation due to the sensational modifications in soil microbial diversity (Sun et al., 2019; Tang et al., 2021). In addition, excessive

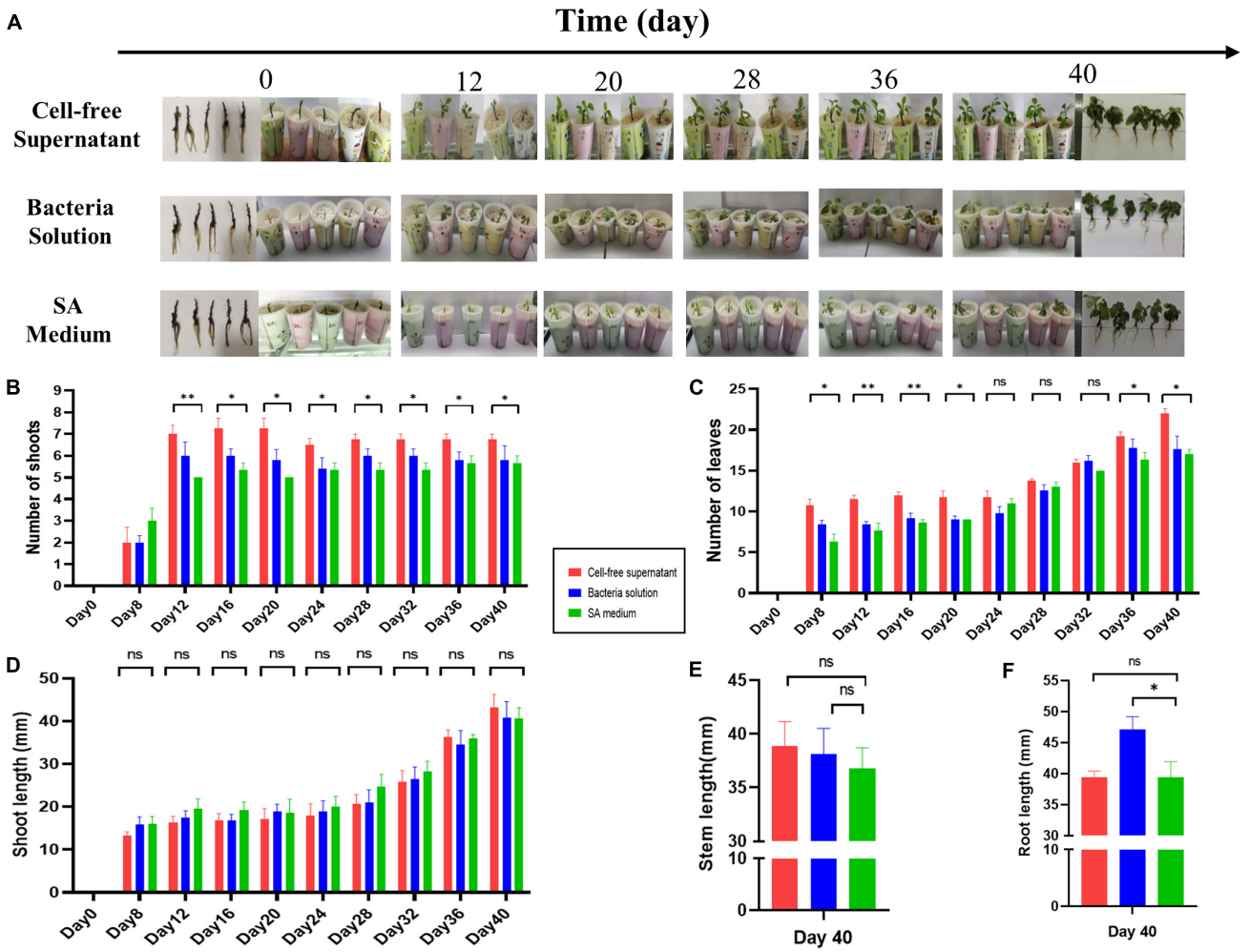

FIGURE 7 | Plant growth promoting effects of AS19. **(A)** Evaluation of the growth parameters of *Gynura divaricata* (*Linn.*) treated with CFS and bacterial solution of AS19. The SA medium group was the control group. **(B)** Number of shoots. **(C)** Number of leaves. **(D)** Shoot length. **(E)** Stem length. **(F)** Root length (ns, no significant difference, $*p < 0.05$, $**p < 0.01$).

use of chemical fertilizer harms the soil environment, leading to problems, such as soil acidification (Barak et al., 1997; Liu et al., 2010), soil compaction (Pagliai et al., 2004), and NP runoff loss (Baffaut et al., 2019). Cumulatively, these problems can easily lead to water eutrophication and the destruction of the steady state of affected aquatic ecosystems (Cui et al., 2018). Soil microorganisms have limited tolerance to fertilizers. Fertilizers could affect the growth and the traits of PGPR (**Figure 5**). Studies have shown that an appropriate reduction in fertilization is beneficial to achieve a win–win situation of environmental and economic benefits (Wang et al., 2020). Thus, it is necessary to use chemical fertilizers as little as possible in agricultural plantings. Moreover, an increasing number of biofertilizers and new potential PGPRs need to be utilized in future agriculture.

Swimming motility is important for PGPR distribution in soil. Interestingly, we found that a low concentration of Fe^{3+} promoted the swimming ability of the AS19 strain, while excessive Fe^{3+} inhibited its swimming ability (**Figure 6A**). It has not been reported that genes related to swimming motility in *Bacillus* are regulated by Fe^{3+}. As a siderophore bacteria isolated from the rhizosphere of *PPVY*, the properties of AS19 as a plant-growth promoter in the rhizosphere of plants was explored. It was found that AS19 could produce siderophores, ammonia, and phosphorus (**Figure 6G**) but not inhibit the growth of the soil pathogens *F. oxysporum*, *F. solanum*, and *P. carotovorum* (**Figure 6F**). Further, seed germination and plant growth promotion experiments showed that the CFS with high SUs and a variety of bioactive substances in its metabolites, could promote the germination of pepper and maize seeds (**Figures 6H,I**), and the development of the shoots and leaves of *G. divaricata* (Linn.) (**Figures 7B,C**). Chloroplasts are important organs for buds and leaves, and iron ions are important for chloroplasts. The CFS of AS19, with high SUs, could promote the transport of unavailable Fe^{3+} in the environment into plant cells. It was speculated that the shoots and leaves developed

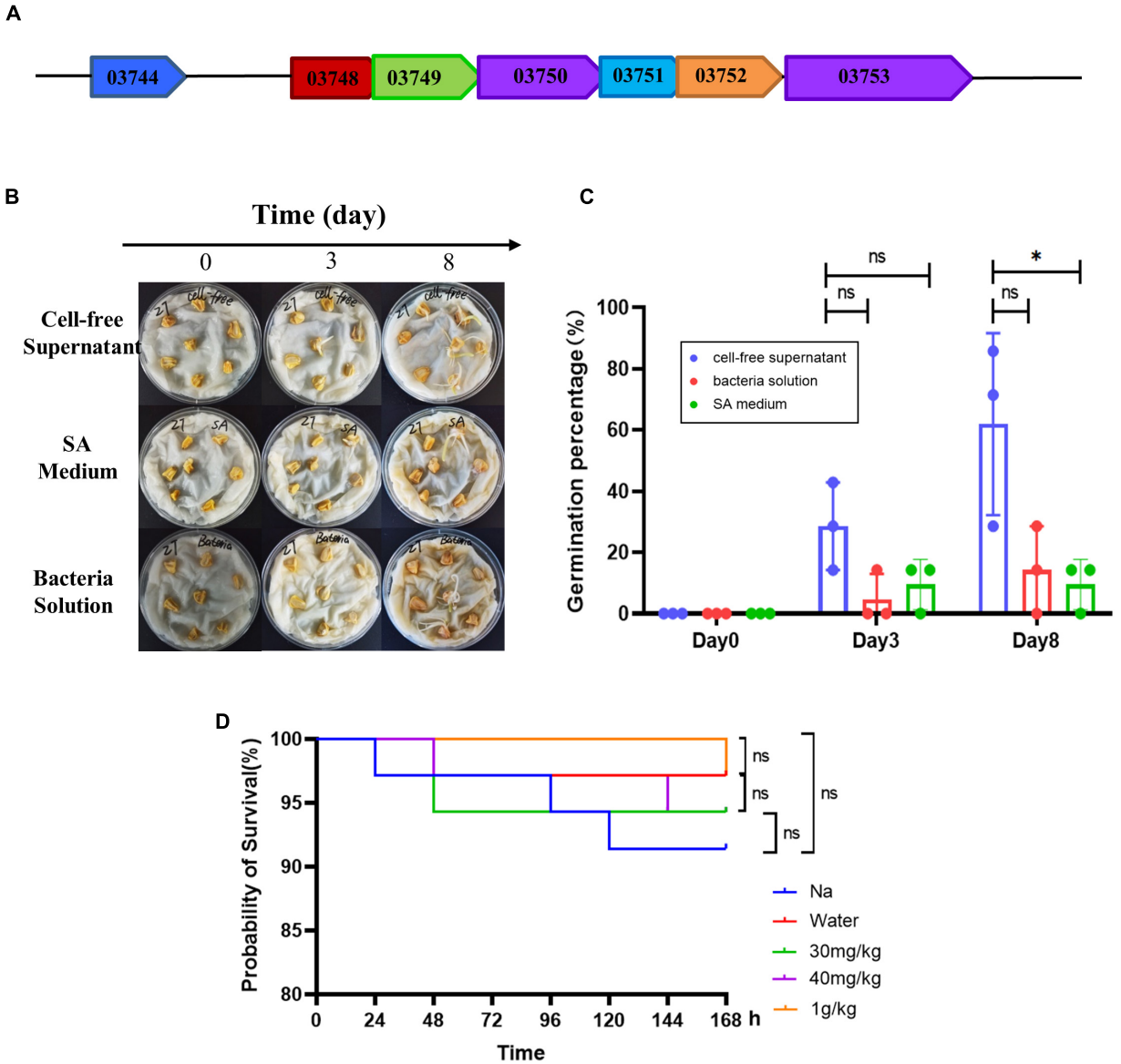

FIGURE 8 | Gene prediction, maize germination, and toxicity assessment. **(A)** Prediction of genes related to siderophore synthesis in AS19. The arrow direction indicates the direction of transcription. The overlapped of arrows indicates the base sequence of overlap. **(B)** The germination of maize seeds treated with CFS and the bacterial solution of AS19. The SA medium group was the control group. **(C)** The germination percentage of maize seeds (a total of seven in each group). The experiment was repeated three times. Three dots represent the germination percentage of three experiments (ns, no significant difference, $^*p < 0.05$). **(D)** Toxicity test of *Hermetia illucens* L. larvae. Improved survival rate of *H. illucens* L. larvae with CFS. *H. illucens* L. larvae were randomly divided into five groups. The natural growth (NG) group was only punctured. The control (Control) group was injected with 2.5 μL of sterile saline. The experimental group was injected with 2.5 μL of CFS (30 mg/kg, 40 mg/kg, and 1 g/kg). The number of surviving larvae was observed every 24 h, for 7 days. The survival rates were calculated, and the graph was drawn with GraphPad Prism 8.4 software (ns, no significant difference, $^*p < 0.05$, $n = 50$).

well because of the abundance of siderophore and nutrients in AS19 fermentation CFS. The reason why the bacterial solution could significantly promote the root elongation (**Figure 7F**) was that the siderophilic bacteria, AS19 had good motility (**Figure 6**) and could colonize in the roots of *G. divaricata* (Linn.) to promote elongation.

The siderophore synthesis gene clusters of AS19 were preliminarily predicted (**Figure 8A**), *AS19_03750* and *AS19_03753* as the two main synthetic gene, and *AS19_03744* as the upstream transcriptional regulation factor should be further studied. In addition, the germination experiment of maize also confirmed the growth promoting effect of CFS with 26.53% of the SUs (**Figures 8B,C**). The biotoxicity of *H. illucens* L. larvae was evaluated as having no toxicity (**Figure 8D**). Furthermore, even more species need to be involved in biosafety assessment, but the existing results indicate the growth-promoting role

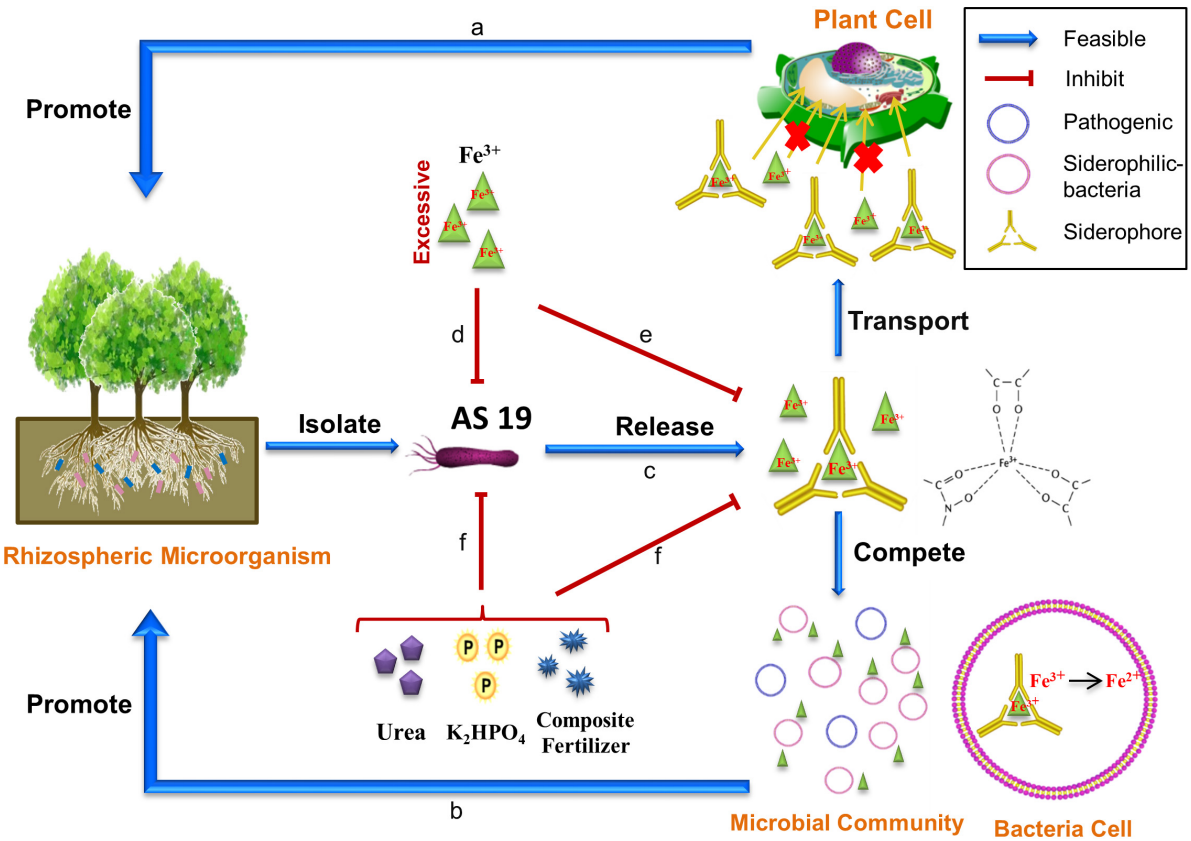

FIGURE 9 | Schematic of the possible plant growth promoting pathway by AS19. **(a)** Fe^{3+} cannot enter plant cells directly, but the complex is transported across the membrane into the plant to help it absorb nutrients. **(b)** Siderophores alter the microbial community. Pathogenic microbes do not grow due to a lack of bioavailable iron. **(c)** AS19 secretes siderophores. **(d)** In LB medium with 0.3% agar, the addition of iron had no effect on the growth of AS19, but a low concentration of Fe^{3+} promoted motility, and excessive Fe^{3+} inhibited motility. **(e)** In a low-iron environment, excessive Fe^{3+} significantly inhibited the growth of AS19 and the production of siderophores. **(f)** In a low-iron environment, chemical fertilizer inhibited the growth of AS19 and the secretion of siderophores to varying degrees. Interestingly, the addition of low-dose compound fertilizer slightly increased the bacterial growth but still inhibited the siderophore production.

of siderophore and the potential application prospects of siderophilic bacteria, AS19 as a biofertilizer.

In general, the role of AS19 as a growth promoter might be mediated by siderophores (**Figure 9**). The AS19 facilitates the absorption of Fe^{3+} by seeds and plants or competes with pathogenic microorganisms for iron resources through the secretion of siderophores. Different types of siderophores promote the growth of several plant species and increase their yield by enhancing Fe uptake by plants. The activities of siderophores as iron chelators have been shown in different studies, such as siderophores from *Chryseobacterium* spp. C138, which were effective in the supply of iron in tomato plants when delivered to the roots (Saha et al., 2016). Another case was seen in the supplementation of *Pseudomonas* strains, which showed a significant increase in germination and plant growth (Sharma and Johri, 2003).

The present investigation isolated and identified 22 strains of rhizosphere bacteria of *PPVY* and analysed the abundance of siderophilic bacteria. The metabolites of 16 strains with inhibitory effects on *C. albicans* were screened. Meanwhile, the effects of Fe^{3+} and different fertilizers on PGPR AS19 were further explored. This study establishes the promoting effect of the AS19 strain on seed germination and plant growth as a PGPR. This study paves the way for the further discovery of new compounds of anti-*Candida albicans* and the development of environmentally friendly biofertilizers, PGPR, for future sustainable agricultural development.

DATA AVAILABILITY STATEMENT

The datasets presented in this study can be found in online repositories. The names of the repository/repositories and accession number(s) can be found in the article/**Supplementary Material**.

AUTHOR CONTRIBUTIONS

YW contributed to the design and implementation of this study as well as preparation and drafting of the manuscript. GZ, YH, JS, MG, TZ, and YL coordinated and participated in the data

analysis and contributed to the discussion of the manuscript. BW and HL contributed to the design and implementation of the research work and revised the manuscript. All authors analysed and discussed the data and reviewed and approved the manuscript.

FUNDING

This work was supported by grants from the National Natural Science Foundation of China (32160668 and 31760250), the Science and Technology Program of Guizhou Province (2017)2833, the Academic New Seedling Cultivation and Innovation Exploration Project [Guizhou Science and Technology Platform Talents Fund (2018)5779-53], the Science and Technology Foundation of Health Commission of Guizhou Province (gzwkj2021-510), and the National Natural Science Foundation of Guizhou Medical University (20NSP055).

ACKNOWLEDGMENTS

We thank the Medical Biotechnology Engineering Research Center of Guizhou Medical University, Immune Cells and Antibody Engineering Research Center of Guizhou Province, and the Key Laboratory of Biology and Medical Engineering.

SUPPLEMENTARY MATERIAL

The Supplementary Material for this article can be found online at: https://www.frontiersin.org/articles/10.3389/fmicb.2022.870413/full#supplementary-material

REFERENCES

Andrews, S. C., Robinson, A. K., and Rodríguez-Quiñones, F. (2003). Bacterial iron homeostasis. *FEMS Microbiol. Rev.* 27, 215–237. doi: 10.1016/s0168-6445(03)00055-x

Arnow, L. E. (1937). Colorimetric determination of the components of 3,4-dihydroxyphenylalanine-tyrosine mixtures. *J. Biol. Chem.* 118, 531–537. doi: 10.1016/s0021-9258(18)74509-2

Aydinok, Y., Kattamis, A., Cappellini, M. D., El-Beshlawy, A., Origa, R., Elalfy, M., et al. (2015). Effects of deferasirox-deferoxamine on myocardial and liver iron in patients with severe transfusional iron overload. *Blood* 125, 3868–3877. doi: 10.1182/blood-2014-07-586677

Baffaut, C., Ghidey, F., Lerch, R. N., Kitchen, N. R., Sudduth, K. A., and Sadler, E. J. (2019). Long-term simulated runoff and water quality from grain cropping systems on restrictive layer soils. *Agric. Water Manag.* 213, 36–48. doi: 10.1016/j.agwat.2018.09.032

Barak, P., Jobe, B. O., Krueger, A. R., Peterson, L. A., and Laird, D. A. (1997). Effects of long-term soil acidification due to nitrogen fertilizer inputs in Wisconsin. *Plant Soil* 197, 61–69.

Beneduzi, A., Ambrosini, A., and Passaglia, L. M. P. (2012). Plant growth-promoting rhizobacteria (PGPR): their potential as antagonists and biocontrol agents. *Genet. Mol. Biol.* 35, 1044–1051. doi: 10.1590/s1415-47572012000600020

Bennis, M., Perez-Tapia, V., Alami, S., Bouhnik, O., Lamin, H., Abdelmoumen, H., et al. (2022). Characterization of plant growth-promoting bacteria isolated from the rhizosphere of *Robinia pseudoacacia* growing in metal-contaminated mine tailings in eastern Morocco. *J. Environ. Manage.* 304:114321. doi: 10.1016/j.jenvman.2021.114321

Braud, A., Jézéquel, K., Bazot, S., and Lebeau, T. (2009). Enhanced phytoextraction of an agricultural Cr- and Pb-contaminated soil by bioaugmentation with siderophore-producing bacteria. *Chemosphere* 74, 280–286. doi: 10.1016/j.chemosphere.2008.09.013

Bric, J. M., Bostock, R. M., and Silverstone, S. E. (1991). Rapid in situ assay for indoleacetic acid production by bacteria immobilized on a nitrocellulose membrane. *Appl. Environ. Microbiol.* 57, 535–538. doi: 10.1128/aem.57.2.535-538.1991

Bukhat, S., Imran, A., Javaid, S., Shahid, M., Majeed, A., and Naqqash, T. (2020). Communication of plants with microbial world: exploring the regulatory networks for PGPR mediated defense signaling. *Microbiol. Res.* 238:126486. doi: 10.1016/j.micres.2020.126486

Cappuccino, J. G., and Sherman, N. (1992). *Microbiology: a Laboratory Manual*. New York, NY: Pearson.

Chakraborty, K., Kizhakkekalam, V. K., Joy, M., and Chakraborty, R. D. (2022). Bacillibactin class of siderophore antibiotics from a marine symbiotic *Bacillus* as promising antibacterial agents. *Appl. Microbiol. Biotechnol.* 106, 329–340. doi: 10.1007/s00253-021-11632-0

Chan, J. Y., Koon, J. C., Liu, X., Detmar, M., Yu, B., Kong, S. K., et al. (2011). Polyphyllin D, a steroidal saponin from *Paris polyphylla*, inhibits endothelial cell functions in vitro and angiogenesis in zebrafish embryos in vivo. *J. Ethnopharmacol.* 137, 64–69. doi: 10.1016/j.jep.2011.04.021

Chayakulkeeree, M., Tangkoskul, T., Waywa, D., Tiengrim, S., Pati, N., and Thamlikitkul, V. (2020). Impact of iron chelators on growth and expression of iron-related genes of *Cryptococcus* species. *J. Mycol. Med.* 30:100905. doi: 10.1016/j.mycmed.2019.100905

Chen, Y., Chai, Y., Guo, J. H., and Losick, R. (2012). Evidence for cyclic Di-GMP-mediated signaling in *Bacillus subtilis*. *J. Bacteriol.* 194, 5080–5090. doi: 10.1128/JB.01092-12

Colombo, C., Palumbo, G., He, J.-Z., Pinton, R., and Cesco, S. (2014). Review on iron availability in soil: interaction of Fe minerals, plants, and microbes. *J. Soils Sediments* 14, 538–548. doi: 10.1007/s11368-013-0814-z

Cordero, O. X., Ventouras, L. A., Delong, E. F., and Polz, M. F. (2012). Public good dynamics drive evolution of iron acquisition strategies in natural bacterioplankton populations. *Proc. Natl. Acad. Sci. U.S.A.* 109, 20059–20064. doi: 10.1073/pnas.1213344109

Cui, Z., Zhang, H., Chen, X., Zhang, C., Ma, W., Huang, C., et al. (2018). Pursuing sustainable productivity with millions of smallholder farmers. *Nature* 555, 363–366. doi: 10.1038/nature25785

David, S. R., Jaouen, A., Ihiawakrim, D., and Geoffroy, V. A. (2021). Biodeterioration of asbestos cement by siderophore-producing *Pseudomonas*. *J. Hazard. Mater.* 403:123699. doi: 10.1016/j.jhazmat.2020.123699

Duan, X., Tan, X., Gu, L., Liu, J., Hao, X., Tao, L., et al. (2020). New secondary metabolites with immunosuppressive activity from the phytopathogenic fungus *Bipolaris maydis*. *Bioorg. Chem.* 99:103816. doi: 10.1016/j.bioorg.2020.103816

Ellermann, M., and Arthur, J. C. (2017). Siderophore-mediated iron acquisition and modulation of host-bacterial interactions. *Free Radic. Biol. Med.* 105, 68–78. doi: 10.1016/j.freeradbiomed.2016.10.489

Gange, A. C., and Gadhave, K. R. (2018). Plant growth-promoting rhizobacteria promote plant size inequality. *Sci. Rep.* 8:13828. doi: 10.1038/s41598-018-32111-z

Gao, T., Ding, M., and Wang, Q. (2020). The recA gene is crucial to mediate colonization of *Bacillus cereus* 905 on wheat roots. *Appl. Microbiol. Biotechnol.* 104, 9251–9265. doi: 10.1007/s00253-020-10915-2

Ghazy, N., and El-Nahrawy, S. (2021). Siderophore production by *Bacillus subtilis* MF497446 and *Pseudomonas koreensis* MG209738 and their efficacy in controlling *Cephalosporium maydis* in maize plant. *Arch. Microbiol.* 203, 1195–1209. doi: 10.1007/s00203-020-02113-5

Gu, S., Wei, Z., Shao, Z., Friman, V. P., Cao, K., Yang, T., et al. (2020). Competition for iron drives phytopathogen control by natural rhizosphere microbiomes. *Nat. Microbiol.* 5, 1002–1010. doi: 10.1038/s41564-020-0719-8

Guo, H., Yang, Y., Liu, K., Xu, W., Gao, J., Duan, H., et al. (2016). Comparative genomic analysis of *Delftia tsuruhatensis* MTQ3 and the identification

of functional NRPS genes for siderophore production. *Biomed Res. Int.* 2016:3687619. doi: 10.1155/2016/3687619

Guo, Y., Liu, Z., Li, K., Cao, G., Sun, C., Cheng, G., et al. (2018). *Paris Polyphylla*-derived saponins inhibit growth of bladder cancer cells by inducing mutant P53 degradation while up-regulating CDKN1A expression. *Curr. Urol.* 11, 131–138. doi: 10.1159/000447207

Guo, Y., Ren, C., Yi, J., Doughty, R., and Zhao, F. (2020). Contrasting responses of rhizosphere bacteria, fungi and arbuscular mycorrhizal fungi along an elevational gradient in a temperate montane forest of China. *Front. Microbiol.* 11:2042. doi: 10.3389/fmicb.2020.02042

Gupta, A., Bano, A., Rai, S., Kumar, M., Ali, J., Sharma, S., et al. (2021). ACC deaminase producing plant growth promoting rhizobacteria enhance salinity stress tolerance in *Pisum sativum*. *3 Biotech* 11:514. doi: 10.1007/s13205-021-03047-5

Habibi, S., Djedidi, S., Ohkama-Ohtsu, N., Sarhadi, W. A., Kojima, K., Rallos, R. V., et al. (2019). Isolation and screening of indigenous plant growth-promoting rhizobacteria from different rice cultivars in afghanistan soils. *Microbes Environ.* 34, 347–355. doi: 10.1264/jsme2.ME18168

Hider, R. C., and Kong, X. (2010). Chemistry and biology of siderophores. *Nat. Prod. Rep.* 27, 637–657. doi: 10.1039/b906679a

Hosseini, A., Hosseini, M., and Schausberger, P. (2021). Plant growth-promoting rhizobacteria enhance defense of strawberry plants against spider mites. *Front. Plant Sci.* 12:783578. doi: 10.3389/fpls.2021.783578

Jakubiec-Krzesniak, K., Rajnisz-Mateusiak, A., Guspiel, A., Ziemska, J., and Solecka, J. (2018). Secondary metabolites of actinomycetes and their antibacterial, antifungal and antiviral properties. *Pol. J. Microbiol.* 67, 259–272. doi: 10.21307/pjm-2018-048

Jiao, R., Cai, Y., He, P., Munir, S., Li, X., Wu, Y., et al. (2021). *Bacillus amyloliquefaciens* YN201732 produces lipopeptides with promising biocontrol activity against fungal pathogen *Erysiphe cichoracearum*. *Front. Cell. Infect. Microbiol.* 11:598999. doi: 10.3389/fcimb.2021.598999

Kaspar, F., Neubauer, P., and Gimpel, M. (2019). Bioactive secondary metabolites from *Bacillus subtilis*: a comprehensive review. *J. Nat. Prod.* 82, 2038–2053. doi: 10.1021/acs.jnatprod.9b00110

Keswani, C., Singh, H. B., Garcia-Estrada, C., Caradus, J., He, Y. W., Mezaache-Aichour, S., et al. (2020). Antimicrobial secondary metabolites from agriculturally important bacteria as next-generation pesticides. *Appl. Microbiol. Biotechnol.* 104, 1013–1034. doi: 10.1007/s00253-019-10300-8

Khan, A., Singh, P., and Srivastava, A. (2018). Synthesis, nature and utility of universal iron chelator - Siderophore: a review. *Microbiol. Res.* 212-213, 103–111. doi: 10.1016/j.micres.2017.10.012

Kramer, J., Ozkaya, O., and Kummerli, R. (2020). Bacterial siderophores in community and host interactions. *Nat. Rev. Microbiol.* 18, 152–163. doi: 10.1038/s41579-019-0284-4

Kumar, S., Stecher, G., Li, M., Knyaz, C., and Tamura, K. (2018). MEGA X: molecular evolutionary genetics analysis across computing platforms. *Mol. Biol. Evol.* 35, 1547–1549. doi: 10.1093/molbev/msy096

Liu, E., Yan, C., Mei, X., He, W., Bing, S. H., Ding, L., et al. (2010). Long-term effect of chemical fertilizer, straw, and manure on soil chemical and biological properties in northwest China. *Geoderma* 158, 173–180. doi: 10.1016/j.geoderma.2010.04.029

Liu, T. H., Zhou, Y., Tao, W. C., Liu, Y., Zhang, X. M., and Tian, S. Z. (2020). Bacterial diversity in roots, stems, and leaves of chinese medicinal plant *Paris polyphylla* var. *yunnanensis*. *Pol. J. Microbiol.* 69, 91–97. doi: 10.33073/pjm-2020-012

Ma, Y., Oliveira, R. S., Freitas, H., and Zhang, C. (2016). Biochemical and molecular mechanisms of plant-microbe-metal interactions: relevance for phytoremediation. *Front. Plant Sci.* 7:918. doi: 10.3389/fpls.2016.00918

Mansour, E., Mahgoub, H. A. M., Mahgoub, S. A., El-Sobky, E. E. A., Abdul-Hamid, M. I., Kamara, M. M., et al. (2021). Enhancement of drought tolerance in diverse *Vicia faba* cultivars by inoculation with plant growth-promoting rhizobacteria under newly reclaimed soil conditions. *Sci. Rep.* 11:24142. doi: 10.1038/s41598-021-02847-2

Miethke, M., and Marahiel, M. A. (2007). Siderophore-based iron acquisition and pathogen control. *Microbiol. Mol. Biol. Rev.* 71, 413–451. doi: 10.1128/MMBR.00012-07

Negi, J. S., Bisht, V. K., Bhandari, A. K., Bhatt, V. P., Singh, P., and Singh, N. (2014). *Paris polyphylla*: chemical and biological prospectives. *Anticancer Agents Med. Chem.* 14, 833–839. doi: 10.2174/1871520614666140611101040

Neilands, J. B. (1981). Microbial iron compounds. *Ann. Rev. Biochem.* 50, 715–731. doi: 10.1146/annurev.bi.50.070181.003435

Orr, R., Hocking, R. K., Pattison, A., and Nelson, P. N. (2020). Extraction of metals from mildly acidic tropical soils: interactions between chelating ligand, pH and soil type. *Chemosphere* 248:126060. doi: 10.1016/j.chemosphere.2020.126060

Pagliai, M., Vignozzi, N., and Pellegrini, S. (2004). Soil structure and the effect of management practices. *Soil Tillage Res.* 79, 131–143. doi: 10.1016/j.still.2004.07.002

Pikovskaya, R. I. (1948). Mobilization of phosphorus in soil connection with the vital activity of some microbial species. *Mikrobiologiya* 17, 362–370.

Powell, P. E., Cline, G. R., Rcidt, C. P. P., and Szaniszlo, P. J. (1980). Occurrence of hydroxamate siderophore iron chelators in soils. *Nature* 287, 833–834. doi: 10.1038/287833a0

Qin, X. J., Yu, M. Y., Ni, W., Yan, H., Chen, C. X., Cheng, Y. C., et al. (2016). Steroidal saponins from stems and leaves of *Paris polyphylla* var. *yunnanensis*. *Phytochemistry* 121, 20–29. doi: 10.1016/j.phytochem.2015.10.008

Radhakrishnan, R., Hashem, A., and Abd Allah, E. F. (2017). *Bacillus*: a biological tool for crop improvement through bio-molecular changes in adverse environments. *Front. Physiol.* 8:667. doi: 10.3389/fphys.2017.00667

Rahman, M. M., Nahar, K., Ali, M. M., Sultana, N., Karim, M. M., Adhikari, U. K., et al. (2020). Effect of long-term pesticides and chemical fertilizers application on the microbial community specifically anammox and denitrifying bacteria in rice field soil of jhenaidah and kushtia district, Bangladesh. *Bull. Environ. Contam. Toxicol.* 104, 828–833. doi: 10.1007/s00128-020-02870-5

Raza, A., Ejaz, S., Saleem, M. S., Hejnak, V., Ahmad, F., Ahmed, M. A. A., et al. (2021). Plant growth promoting rhizobacteria improve growth and yield related attributes of chili under low nitrogen availability. *PLoS One* 16:e0261468. doi: 10.1371/journal.pone.0261468

Saha, M., Sarkar, S., Sarkar, B., Sharma, B. K., Bhattacharjee, S., and Tribedi, P. (2016). Microbial siderophores and their potential applications: a review. *Environ. Sci. Pollut. Res. Int.* 23, 3984–3999. doi: 10.1007/s11356-015-4294-0

Sahu, S., Rajbonshi, M. P., Gujre, N., Gupta, M. K., Shelke, R. G., Ghose, A., et al. (2022). Bacterial strains found in the soils of a municipal solid waste dumping site facilitated phosphate solubilization along with cadmium remediation. *Chemosphere* 287:132320. doi: 10.1016/j.chemosphere.2021.132320

Sambrook, J., and Russell, D. (2001). *Molecular Cloning: A Laboratory Manual*, 3rd Edn. Cold Spring Harbor, NY: Cold Spring Harbor Laboratory Press.

Schwyn, B., and Neilands, J. B. (1987). Universal chemical assay for the detection and determination of siderophores. *Anal. Biochem.* 160, 47–56. doi: 10.1016/0003-2697(87)90612-9

Sharma, A., and Johri, B. N. (2003). Growth promoting influence of siderophore-producing *Pseudomonas* strains GRP3A and PRS9 in maize (*Zea mays* L.) under iron limiting conditions. *Microbiol. Res.* 158, 243–248. doi: 10.1078/0944-5013-00197

Sheng, M. M., Jia, H. K., Zhang, G. Y., Zeng, L. N., Zhang, T. T., Long, Y. H., et al. (2020). Siderophore production by rhizosphere biological control bacteria *Brevibacillus brevis* GZDF3 of pinellia ternata and its antifungal effects on *Candida albicans*. *J. Microbiol. Biotechnol.* 30, 689–699. doi: 10.4014/jmb.1910.10066

Shenker, M., Oliver, I., Helmann, M., Hadar, Y., and Chen, Y. (2008). Utilization by tomatoes of iron mediated by a siderophore produced byRhizopus arrhizus. *J. Plant Nutr.* 15, 2173–2182. doi: 10.1080/01904169209364466

Silva-Bailao, M. G., Bailao, E. F., Lechner, B. E., Gauthier, G. M., Lindner, H., Bailao, A. M., et al. (2014). Hydroxamate production as a high affinity iron acquisition mechanism in *Paracoccidioides* spp. *PLoS One* 9:e105805. doi: 10.1371/journal.pone.0105805

Sun, R., Li, W., Hu, C., and Liu, B. (2019). Long-term urea fertilization alters the composition and increases the abundance of soil ureolytic bacterial communities in an upland soil. *FEMS Microbiol. Ecol.* 95:fiz044. doi: 10.1093/femsec/fiz044

Tang, H., Li, C., Shi, L., Xiao, X., Cheng, K., Wen, L., et al. (2021). Effect of different long-term fertilizer managements on soil nitrogen fixing bacteria community in a double-cropping rice paddy field of southern China. *PLoS One* 16:e0256754. doi: 10.1371/journal.pone.0256754

Wandersman, C., and Delepelaire, P. (2004). Bacterial iron sources: from siderophores to hemophores. *Annu. Rev. Microbiol.* 58, 611–647. doi: 10.1146/annurev.micro.58.030603.123811

Wang, G., Li, B., Peng, D., Zhao, H., Lu, M., Zhang, L., et al. (2022). Combined application of H2S and a plant growth promoting strain JIL321 regulates photosynthetic efficacy, soil enzyme activity and growth-promotion in rice under salt stress. *Microbiol. Res.* 256:126943. doi: 10.1016/j.micres.2021.126943

Wang, K. W., and Ding, P. (2018). New bioactive metabolites from the marine-derived fungi aspergillus. *Mini Rev. Med. Chem.* 18, 1072–1094. doi: 10.2174/1389557518666180305160856

Wang, Z., Geng, Y., and Liang, T. (2020). Optimization of reduced chemical fertilizer use in tea gardens based on the assessment of related environmental and economic benefits. *Sci. Total Environ.* 713:136439. doi: 10.1016/j.scitotenv.2019.136439

Whitman, W. B. (2015). *Bergey's Manual of Systematics of Archaea and Bacteria*. Hoboken, NJ: Wiley.

Xu, Z., Wu, Y., Song, L., Chinnathambi, A., Ali Alharbi, S., and Fang, L. (2020). Anticarcinogenic effect of zinc oxide nanoparticles synthesized from *Rhizoma paridis* saponins on Molt-4 leukemia cells. *J. King Saud Univ. Sci.* 32, 1865–1871. doi: 10.1016/j.jksus.2020.01.023

Yang, D., Wang, L., Wang, T., Zhang, Y., Zhang, S., and Luo, Y. (2021). Plant growth-promoting rhizobacteria hn6 induced the change and reorganization of *Fusarium* microflora in the rhizosphere of banana seedlings to construct a healthy banana microflora. *Front. Microbiol.* 12:685408. doi: 10.3389/fmicb.2021.685408

Yi, S., Li, F., Wu, C., Wei, M., Tian, J., and Ge, F. (2022). Synergistic leaching of heavy metal-polycyclic aromatic hydrocarbon in co-contaminated soil by hydroxamate siderophore: role of cation-pi and chelation. *J. Hazard. Mater.* 424:127514. doi: 10.1016/j.jhazmat.2021.127514

Yun, H., Lijian, C., Wenhong, Z., Yuhong, D., Yongli, W., Qiang, W., et al. (2007). Separation and identification of steroidal compounds with cytotoxic activity against human gastric cancer cell lines *in vitro* from the rhizomes of *Paris polyphylla* var. *chinensis*. *Chem. Nat. Compd.* 43, 672–677. doi: 10.1007/s10600-007-0225-8

Zahir, Z. A., Shah, M. K., Naveed, M., and Akhter, M. J. (2010). Substrate-dependent auxin production by *Rhizobium phaseoli* improves the growth and yield of *Vigna radiata* L. under salt stress conditions. *J. Microbiol. Biotechnol.* 20, 1288–1294. doi: 10.4014/jmb.1002.02010

Zhanel, G. G., Golden, A. R., Zelenitsky, S., Wiebe, K., Lawrence, C. K., Adam, H. J., et al. (2019). Cefiderocol: a siderophore cephalosporin with activity against carbapenem-resistant and multidrug-resistant gram-negative bacilli. *Drugs* 79, 271–289. doi: 10.1007/s40265-019-1055-2

Zhou, H. Y., Han, Y., Shi, Q., and Chen, C. F. (2019). Directional transportation of a helic[6]arene along a nonsymmetric molecular axle. *J. Org. Chem.* 84, 5872–5876 doi: 10.1021/acs.joc.9b00229

Conflict of Interest: The authors declare that the research was conducted in the absence of any commercial or financial relationships that could be construed as a potential conflict of interest.

Publisher's Note: All claims expressed in this article are solely those of the authors and do not necessarily represent those of their affiliated organizations, or those of the publisher, the editors and the reviewers. Any product that may be evaluated in this article, or claim that may be made by its manufacturer, is not guaranteed or endorsed by the publisher.

frontiers | Frontiers in Microbiology

REVIEW
published: 12 May 2022
doi: 10.3389/fmicb.2022.861235

Endophytism: A Multidimensional Approach to Plant–Prokaryotic Microbe Interaction

*Simran Rani[1], Pradeep Kumar[1], Priyanka Dahiya[1], Rajat Maheshwari[1], Amita Suneja Dang[2] and Pooja Suneja[1]**

[1] Plant Microbe Interaction Laboratory, Department of Microbiology, Maharshi Dayanand University, Rohtak, India, [2] Centre for Medical Biotechnology, Maharshi Dayanand University, Rohtak, India

Plant growth and development are positively regulated by the endophytic microbiome *via* both direct and indirect perspectives. Endophytes use phytohormone production to promote plant health along with other added benefits such as nutrient acquisition, nitrogen fixation, and survival under abiotic and biotic stress conditions. The ability of endophytes to penetrate the plant tissues, reside and interact with the host in multiple ways makes them unique. The common assumption that these endophytes interact with plants in a similar manner as the rhizospheric bacteria is a deterring factor to go deeper into their study, and more focus was on symbiotic associations and plant–pathogen reactions. The current focus has shifted on the complexity of relationships between host plants and their endophytic counterparts. It would be gripping to inspect how endophytes influence host gene expression and can be utilized to climb the ladder of "Sustainable agriculture." Advancements in various molecular techniques have provided an impetus to elucidate the complexity of endophytic microbiome. The present review is focused on canvassing different aspects concerned with the multidimensional interaction of endophytes with plants along with their application.

Keywords: abiotic stress, biocontrol, detection of PGPEB, endophytism, sustainable agriculture

OPEN ACCESS

Edited by:
Ying Ma,
University of Coimbra, Portugal

Reviewed by:
Rupali Gupta,
Institute of Plant Protection, Agricultural Research Organization, Volcani Center, Israel
Divjot Kour,
Eternal University, India

****Correspondence:***
Pooja Suneja
poojapavit@gmail.com

Specialty section:
This article was submitted to Microbe and Virus Interactions with Plants, a section of the journal Frontiers in Microbiology

Received: *24 January 2022*
Accepted: *11 March 2022*
Published: *12 May 2022*

Citation:
Rani S, Kumar P, Dahiya P, Maheshwari R, Dang AS and Suneja P (2022) Endophytism: A Multidimensional Approach to Plant–Prokaryotic Microbe Interaction. Front. Microbiol. 13:861235. doi: 10.3389/fmicb.2022.861235

INTRODUCTION

Earth has been kneeling under the pressure of a rapidly increasing population which has exerted a lot of stress on the stakeholders, namely, farmers, scientists, and other intermediaries alike. What the world needs right now is extensive, yet a nature-friendly system of agriculture using modern tools along with systems sans application of chemical fertilizers (Lareen et al., 2016). The current system of agriculture is based on the application of chemical fertilizers and other inputs to enhance productivity, thereby leading to destruction of soil nutrients, groundwater contamination, eutrophication, and production of greenhouse gasses, thereby, impacting the overall environment and playing havoc to the health of consumers both humans and animals alike. To overcome this, microbes with plant growth promoting (PGP) traits are being explored to develop potential bioinoculants for sustainable and eco-friendly agriculture.

The plants and microorganisms are well known to interact by various natural amalgams that serve as signaling and nutritive substances for microbes to act upon and influence the nature of the plant microbiome. Plants are naturally associated with microorganisms in rhizosphere,

phyllosphere, and endosphere (Dong et al., 2019). The rhizosphere is the tapered region of soil regulated by plant root secretions and associated microbial community termed as root microbiome (Turner et al., 2013; Suneja et al., 2016). Phyllosphere is the microbial habitat on the exterior of above-ground plant organs and the most abundant microbial ecosystem on earth (Vorholt, 2012). Microorganisms living and growing within their host plants are termed endophytes, constituting the plant endosphere. Endophytic bacteria usually complete their life cycle inside host plants without causing any harm to them (Dudeja et al., 2012). However, these bacteria flourish copiously in the rhizosphere due to sufficient nutrition supply by plant root exudates (Canarini et al., 2019).

The abundance of microorganisms in the rhizosphere is known since the beginning of the 20th Century but the endosphere region has not been explored much (Sessitsch et al., 2011). Earlier, the endosphere was known mainly for the fungal group and as a result, our preliminary information about bacterial endophytes remained circumscribed. Various other factors restricted our understanding regarding the action of bacterial endophytes, which includes culturing hitches and lack of pioneering identification techniques. However, endophytic bacteria have attracted a lot of attention since the last two decades owing to recognition of their ability to promote plant growth and their biocontrol potential (Vasileva et al., 2019). This review discusses the PGP endophytic bacteria, their interaction with host plants leading to variations in colonization patterns and diversity, mechanisms of plant growth promotion under normal as well as stress conditions along with omics-led revolution in the field of exploring their bioactive metabolites.

PLANT GROWTH-PROMOTING ENDOPHYTIC BACTERIA–HOST PLANT: INTERACTION AND COLONIZATION

Endophytes (either bacteria or fungi) are defined as colonizers of the internal plant tissues without causing any disease or hostile symptoms and obtained from surface-sterilized tissue of plant (Santoyo et al., 2016; Afzal et al., 2019). Bacterial endophytes are known to be present in every plant part, namely, seeds, rhizomes, roots, nodules, stems, and leaves (Alibrandi et al., 2018). It has been anticipated that endophytic bacteria referred to as the subclass of rhizospheric bacteria or seed-borne bacterial communities, commonly termed as PGP rhizobacteria, established the ability to enter into the host plant (Khare et al., 2018). They possess all vital PGP traits as present in rhizobacteria, but their effect on host plants is typically more significant than rhizobacteria owing to the better adaptation during stress conditions resulting in augmentation of plant growth (Hardoim et al., 2008; Afzal et al., 2019).

The rhizosphere is the interaction point between roots and soil microorganisms (Bulgarelli et al., 2012). Plants release exudates such as organic acids, amino acids, and proteins from their roots, which serve as pre-communication signals between bacterial endophytes and host plants (Kawasaki et al., 2016). Colonization of bacteria into roots occurs through root hairs and, to some extent, through the stem and leaves (Maela, 2019). Some studies have reported that endophytes also colonize through flowers and fruits of the anthosphere and carposphere (Frank et al., 2017). A few regular hotspots have been observed for bacterial colonization such as emergence sites of lateral roots, outer layers of cells, and root cortex (dos Santos et al., 2018). Endophytic bacterial colonization is a multi-stage process that involves (a) chemotactic movement toward roots, (b) root surface attachment, (c) entry inside the root, and (d) movement and localization (Gupta et al., 2012; Kandel et al., 2017a). **Table 1** cites various genes involved in the colonization of endophytes.

Bacteria, in the vicinity of the roots, receive chemical signals from root exudates and move toward them. Saleh et al. (2020) reported that citric acid, a root exudate of *Brachypodium distachyon*, acting as a strong chemoattractant for PGP bacterial strains. The hypothesis of Streptomyces species being attracted by the root exudates was tested and confirmed by Worsley et al. (2021) on the root exudates of *Arabidopsis thaliana*. The study demonstrated that phytohormone, salicylate, plays a specific role in this process. The genes for proteins encoding motility, chemotaxis, and adhesion are upregulated in response to root exudates, indicating a two-way interaction between the endophyte and its host plant (Jha et al., 2018). Chemotaxis is a significant event in the rhizosphere and the interior parts of roots, for both movement and colonization (Kawasaki et al., 2016). Mutant strains of *Azorhizobium caulinodans* lacking chemotaxis gene cluster (che) were reported to undergo defective colonization owing to its significant role in biofilm formation and exopolysaccharides (EPSs) production (Liu X. et al., 2018; Liu W. et al., 2018, **Table 1**). Bacterial endophytes primarily bind to the root surface (rhizoplane) and detect the possible entry sites for accessing internal plant tissues (Kandel et al., 2017a). The entry points used by endophytes to reach the host plant are the gaps present in the roots where root hairs or lateral roots arise, as well as the holes in the shoots, wounds, stomata, and hydathodes (Hardoim et al., 2015). **Figure 1** illustrates distinct steps of colonization.

Many researchers have stated that extensive bacterial endophyte colonization occurs at the secondary root emergence site. It is because of rapid endophytic penetration at epidermal breakage-point, colonizing at the cortex and subsequent spreading through the endodermis to the vascular tissue (Mahaffee, 1994; Lodewyckx et al., 2002). Endophytes release the cell wall–degrading enzymes such as pectinases, xylanases, cellulases, and endoglucanases before colonizing the roots (Naveed et al., 2013; Maela, 2019). This phenomenon facilitates the entry of bacteria within plant tissues (Kandel et al., 2017a). Various gene sequences have been deduced by comparative genomics, engaged in biofilm formation, adhesion, and motility, leading to plant colonization and maintaining healthy plant–microbe interaction. Bacterial cells synthesize EPSs during the early colonization phase which help the cells to adhere to the root surface. The endophytic strain *Gluconacetobacter diazotrophicus* produces EPS that serves as a critical factor for adhesion and colonization in rice roots (Meneses et al., 2011). The study showed that EPS production by *G. diazotrophicus* shielded the bacterial cells from oxidative damage, and also decreased the

TABLE 1 | Genes involved in colonization of endophytes.

Category	Genes	Function	References
Chemotaxis and motility	fliC3	Encodes flagellin	Buschart et al., 2012
	MglB	Galactose chemotaxis	Neumann et al., 2012
	pilX	Type IV fimbrial biogenesis protein PilX	Shidore et al., 2012
	FliI	Flagellar apparatus	Bai et al., 2014; Minamino et al., 2016
	Hsero3720	Methyl accepting chemotaxis transducer transmembrane protein	Balsanelli et al., 2016
	Aer	Aerotaxis	Samanta et al., 2016
	RbsB	Ribose chemotaxis	Reimer et al., 2017
	CheZ	Response regulator	Liu X. et al., 2018; Liu W. et al., 2018
Attachment	lapF gene	Determines biofilm architecture	Martínez-Gil et al., 2010
	gumD	EPS biosynthesis	Meneses et al., 2011
	wssD gene	Cellulose production mutation	Monteiro et al., 2012
	waaL	O-antigen ligase (LPS biosynthesis)	Balsanelli et al., 2013
	eps and tasA	Biofilm formation	Beauregard et al., 2013
	PoaA, PoaB, and PoaC	Lipopeptide	Zachow et al., 2015
	Hsero1294 and fhaB	Filamentous hemagglutinin proteins	Pankievicz et al., 2016
	blr2358	EPS biosynthesis	Xu et al., 2021
Colonization	IacC	IAA degradation necessary for efficient rhizosphere colonization	Zúñiga et al., 2013
	N-acyl homoserine lactone Synthase	Quorum Sensing necessary for cell-to-cell communication in efficient colonization	
	EglS	Endo-β-1,4-glucanase (Plant cell wall modification)	Fan et al., 2016

EPS, exopolysaccharide; LPS, lipopolysaccharide; IAA, indole-3-acetic acid.

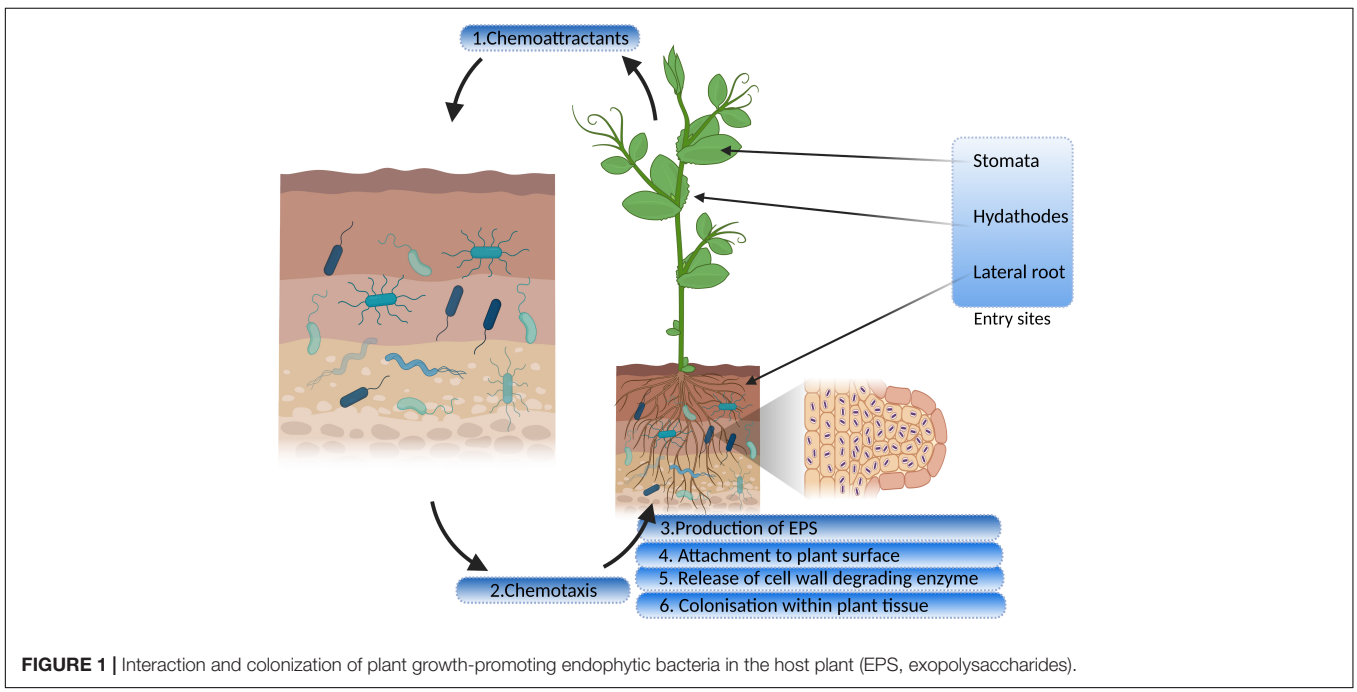

FIGURE 1 | Interaction and colonization of plant growth-promoting endophytic bacteria in the host plant (EPS, exopolysaccharides).

concentrations of free radicals. Colonization was found to be reduced in the case of EPS knockout strain of *G. diazotrophicus*, further rescued by the application of wild-type strain (Meneses et al., 2017). Fernández-Llamosas et al. (2021) used homologous recombination for insertional disruption of epsF genes in the genome of *Azoarcus* sp. CIB depicting their role in the efficient colonization of rice roots. Xu et al. (2021) identified EPS biosynthesis gene, blr2358, in *Bradyrhizobium diazoefficiens* USDA110, the mutant of which resulted in a reduced capacity to induce nodules. Other than playing a significant role in

plant–endophyte interactions, they exhibit antioxidant, anti-inflammatory, anti-tumor, and prebiotic activities (Liu W. et al., 2018). Lipopolysaccharide machinery is involved in the attachment and proliferation of endophyte colonization that includes the development of flagella and pili, quorum sensing, and movement of bacteria within the host plants (Rocío Suaìrez-Moreno et al., 2010; Scharf et al., 2016). The role of cell wall degrading enzymes in entering and spreading within the host tissue is also very well established. Fan et al. (2016) highlighted the importance of endo-β-1, 4-glucanase in penetration of *Bacillus amyloliquefaciens* into the host tissue. The disruption mutant of eglS gene encoding this enzyme halted colonization; however, overexpression of the same resulted in a substantial increase in the endophyte population. Mechanism of bacterial endophyte attachment with plant surface, entry, survival, is mediated by the cross-talk between host and microorganism, and a lot is to be studied in this regard.

ENDOPHYTISM VS. PATHOGENICITY: THIN LINE BETWEEN TWO LIFESTYLES

The prevalence of endophytes is decided by chance and genetic indicators of bacteria that promote intermodulation between bacteria and plants, contributing to an active colonization (Dong et al., 2019). Endophytes maintain a smaller cell density to prevent a systemic reaction in comparison to pathogens (Zinniel et al., 2002). They also produce lesser quantities of cell wall degrading enzymes as compared to the phytopathogens that secrete deleteriously large amounts of these enzymes, thereby, preventing the trigger of plant defense systems (Elbeltagy et al., 2000; Afzal et al., 2019). Anabolism-related genes are found to be more diverse and in abundance among the endophytes unlike the phytopathogens having catabolism genes prominently (Hardoim et al., 2015). Endophytes undergo several mechanisms to protect themselves from the plant defense system. Microbe-/pathogen-associated molecular patterns (MAMPs/PAMPs) are the characteristics of microbes recognized by pattern recognition receptors (PRRs) present on the surface of plant cells (Newman et al., 2013). Endophytic bacteria produce MAMPs which either remain unrecognized by plant's PRRs or induce only a weak reaction as a response in comparison to the pathogenic interactions (Vandenkoornhuyse et al., 2015). They produce enzymes of antioxidant machinery such as superoxide dismutase (SOD), catalase (CAT), peroxidase (POD), glutathione *S*-transferases (GSTs), and alkyl-hydroperoxide reductase C (AhpC), to mitigate the oxidative burst (Zeidler et al., 2004). Bacterial virulence factors are delivered in the extracellular environment or directly into the host by the secretion system (Depluverez et al., 2016). Type-III and Type-VI protein secretion systems, necessary to deliver effector proteins into the plant by pathogens, are altogether absent or present scarcely in endophytic bacteria (Liu W. et al., 2018). Endophytes have been found to undergo a reduction in genome size, which is associated with differences in niche specialization (Lòpez-Fernàndez et al., 2015; Zin et al., 2021). Some bacterial endophytes also downregulate flagella biosynthesis and upregulate functions related to flagellar motor rotation to mask up their flagellin PAMPs and move fast within plants during colonization.

Endophytes have been reported to undergo a change in their lifestyles from endophytes to pathogenic as a result of any imbalance in the host–microbe interaction (Mengistu, 2020). Strategies employed by the plants to distinguish endophytes from pathogens are still a matter of active research. Plett and Martin (2018) have indicated that LysM receptor-like kinases (LysM-RLKs) can differentiate pathogenic signals from those secreted by the mutualistic microbes. It has been suggested that different groups of genes are regulated during colonization in the plants to facilitate the same. The majority of pathways targeted by miRNAs of plant defense system are turned off. These microRNAs otherwise remain stable and can be used as a pathogenicity signal by the plants (Wang et al., 2017). Plants undergo nutrient monitoring to identify parasites and manipulate the ratio of MAMP/DAMP signals to identify the mutualistic signals. However, there are many such receptor/perceptor systems present throughout the plant kingdom that are yet to be studied (Plett and Martin, 2018). Many studies have pointed toward downregulation of plant defense during colonization by mutualistic partners (Khare et al., 2018). In the recruitment of an endophytic companion, the plant host often plays a pivotal role, where the release of specific root exudates and a selective host plant defense response are considered as crucial factors in choosing individual endophytes (Kumar A. et al., 2020).

APPREHENDING THE ENDOPHYTES

Enormous benefits provided by endophytes have led to robust research in this field world over. Harnessing their potential to the fullest and large scale application requires a more clear and better understanding of endophytes. It is no less than a challenge as the methods available for detection, isolation, and identification are not sufficient to provide the entire picture of the host–parasite interaction. Cultivation-based studies omit several microbes because it is not possible to reproduce and maintain the optimal conditions required for the growth of most of the microbes (Santoyo et al., 2016). However, the study of endophytes has come a long way from the typical isolation and cultivation methods to more sophisticated ones such as advanced microscopic techniques and "omics"-based studies (**Table 2**). The amalgamation of two or more techniques helps to significantly increase the discriminatory power of the analysis and a better overview of diversity. Therefore, a combination of techniques is employed to complement each other and to enrich our understanding of the detection and patterns of colonization as shown in **Figure 2**.

Microscopy is the sole direct method to observe the endophytes, which helps in understanding the mode of infection, tissue-specific concentration, and the extent of colonization along with the plant response (Johnston et al., 2006). Both light and electron microscopy can reveal the exact location of endophytes within the plant tissue (Kuldau and Yates, 2000). Electron microscopy provides us with the ultrastructural analysis of the

TABLE 2 | Detection of endophytism.

Technique employed	Endophytes detected	Plant	References
CLSM	*Azotobacter chroococcum* 67B, *Azotobacter chroococcum* 76A	*Solanum lycopersicon*	Viscardi et al., 2016
	Ralstonia sp. M1, *Ralstonia* sp. MS1, *Rhizobium* sp. W3, *Rhizobium* sp. SS2, *Rhizobium* sp. R2, *Acinetobacter* sp. M5, *Pantoea* sp. MS3, *Brevundimonas* sp. R3, *Achromobacter* sp. RS1, RS3, RS4, RS5, RS8	*Triticum aestivum*	Patel and Archana, 2017
	Bacillus cereus strain XB177	*Solanum melongena*	Achari and Ramesh, 2019
	Bacillus subtilis strain 1-L-29	*Camellia oleifera*, *Arabidopsis thaliana*	Xu et al., 2020
	Streptomyces sp. strain SA51	*Solanum lycopersicum*	Vurukonda et al., 2021
	Bacillus siamensis	*Cicer arietinum* L.	Gorai et al., 2021
GFP-CLSM-SEM	*Musa*	*Methylobacteriumsalsuginis*	Senthilkumar et al., 2021
FISH	*Arthrobacter agilis* UMCV2 *Bacillus methylotrophicus* M4-96	*Fragaria ananassa*	Hernández-Soberano et al., 2020
FISH-CLSM	*Burkholderia graminis* G2Bd5	*Lolium multiflorum*	Castanheira et al., 2016
	Gordonia KMP456-M40, *Enterococcus* KMP789-M107, *Micrococcus* KMP789-MA53, *Staphylococcus* KMP123-MS2, *Staphylococcus* KMP123-MS3, *Acinetobacter* KMP123-MA14, *Bacillus* KMP123-MS1	Mangroves	Soldan et al., 2019
	Firmicutes, Gammaproteobacteria	*Citrus limon*	Faddetta et al., 2021
DOPE-FISH-CLSM	*Streptomyces mutabilis*	*Triticum aestivum*	Toumatia et al., 2016
FISH-GFP-CLSM	*Pseudomonas* G1Dc10, *Paenibacillus* G3Ac9, *Sphingomonas azotifigens* DSMZ 18530	*Lolium multiflorum*	Castanheira et al., 2017
DOPE-FISH-CLSM-SEM	Alphaproteobacteria, Betaproteobacteria, Gammaproteobacteria, Firmicutes, and Actinobacteria	*Cucumis melo reticulates group* cv. 'Dulce'	Glassner et al., 2018
Fluorescence microscopy	Diazotrophic endophytes	*Oryza sativa*	Kandel et al., 2015
ROS staining combined with Light microscopy	*Burkholderia gladioli*	*Panicum virgatum*	White et al., 2014
	Enterobacter cloacae	*Agave tequilana*	Lima et al., 2018
	B. amyloliquefaciens	*Gossypium*	Irizarry and White, 2018
	LMT2b (*Microbacterium* sp.), LMY1a (*Pseudomonas baetica*), LTE3 (*Pantoea hericii*), LTE8 (*Paenibacillus* sp.), LYE4a (*Pseudomonas oryzihabitans*), LYY2b (*Pantoea vagans*), LLE3a (*P. agglomerans*)	*Oryza sativa* L., *Cynodon dactylon* L.	Verma et al., 2018
	Pseudomonas sp., *Bacillus* sp., *Paenibacillus* sp., *Microbacterium* sp., *Exiguobacterium* sp.	*Triticum aestivum*	Patel et al., 2021
SEM	*Azospirillum* spp., *Azoarcus* spp., *Azorhizobium* spp.	*Triticum aestivum* L.	Dal Cortivo et al., 2017
TEM	*Azotobacter chroococcum*	*Arnebia hispidissima*	Singh and Sharma, 2016
	Bacillus subtilis and *Serratia marcescens*	*Centella asiatica*	War Nongkhlaw and Joshi, 2017
	Bacillus methylotrophicus	*Potentilla fulgens*	
	Bacillus sp.	*Houttuynia cordata*	
SEM TEM	*Enterobacter hormaeche* RCE1, *Enterobacter asberiae* RCE2, *Enterobacter ludwigii* RCE5, *Klebsiella pneumoniae* RCE7	*Citrus reticulate*	Thokchom et al., 2017
GFP-SEM-TEM-Real Time RT-PCR	*Bacillus amyloliquefaciens*	*Zea mays, Arabidopsis thaliana* and *Lemna minor*	Fan et al., 2011
PCR-DGGE	*Burkholderia* sp. J62 *Pseudomonas thivervalensis* Y-1-3-9	Rape plants	Chen et al., 2013
FRET	*A. chroococcum* Avi2 strain	*Oryza sativa*	Banik et al., 2016
Serial dilution plating-CLSM-Bio-PCR	*Pseudomonas putida* BP25 (PpBP25)	*Arabidopsis thaliana*	Sheoran et al., 2016

(Continued)

TABLE 2 | (Continued)

Technique employed	Endophytes detected	Plant	References
Light microscopy-TEM-SEM-Qpcr	*Shinella* sp. UYSO24 and *Enterobacter* sp. UYSO10	*Saccharum officinarum*	Taulé et al., 2016
Real Time PCR	*Pseudomonas putida*	*Piper nigrum* L.	Agisha et al., 2017

GFP, green fluorescent protein; CLSM, confocal laser scanning microscopy; SEM, scanning electron microscopy; FISH, fluorescence in situ hybridization; DOPE-FISH, double labeling of oligonucleotide probes for FISH; ROS, reactive oxygen species; TEM, transmission electron microscopy; Real time RT-PCR, real time reverse transcriptase polymerase chain reaction; PCR-DGGE, polymerase chain reaction denaturing gradient gel electrophoresis; FRET, fluorescence resonance energy transfer.

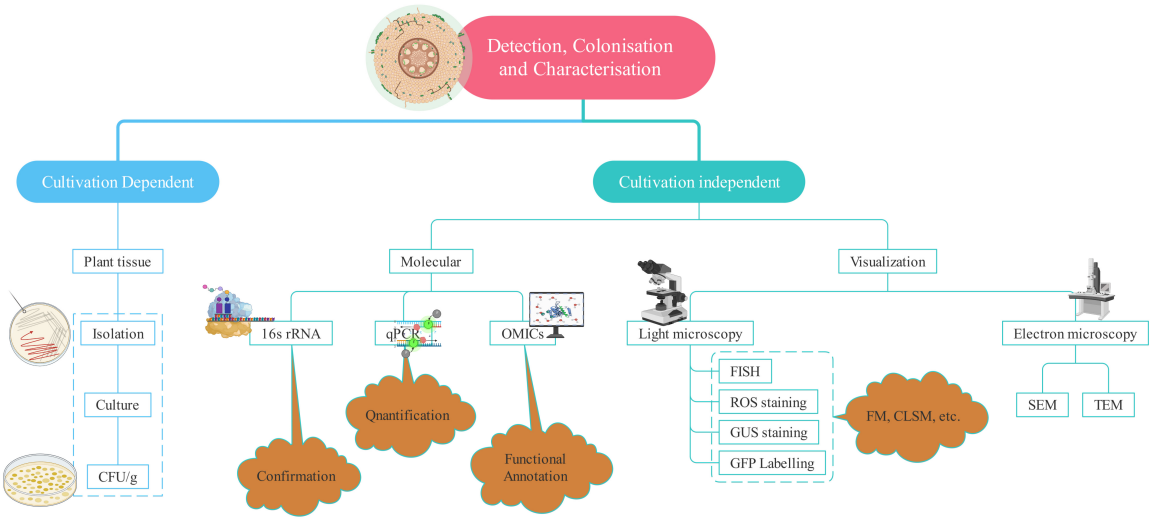

FIGURE 2 | Techniques used for the detection of endophytism.

endophytes (Pimentel Esposito-Polesi et al., 2017). Transmission electron microscopy (TEM) and scanning electron microscopy (SEM) yield valuable information about the inner structure and surface of the sample, respectively (Ramanujam et al., 2016). Electron microscopy has provided a lot of assistance in the detection of endophytes, the extent of colonization, interaction with the host, and establishment within the plant environment (War Nongkhlaw and Joshi, 2017). Fluorescence *in situ* hybridization is a powerful technique to analyze the microorganisms and screen various microbial communities employing group-specific probes. It involves targeting 16S rRNA gene's conserved region or species-specific probe to observe the individual cells of endophytic bacteria (Castanheira et al., 2017). Green fluorescent protein (GFP) tagging and β-glucuronidase (GUS) staining rely on the broad host plasmids containing constitutively expressed GUS or GFP genes for tracking bacteria within the endosphere (Robertson-Albertyn et al., 2017). GFP-tagged endophytes fluoresce in the presence of UV or blue light and oxygen thus unfolding the information concerned with the success of colonization as well as the sites of entry (Reinhold-Hurek and Hurek, 2011).

Reactive oxygen species (ROS) staining is a more convenient and cost-effective method than the visualization techniques, for instance, TEM and Fluorescent microscopy. Similar to ROS, hydrogen peroxide (H_2O_2) and superoxide (O_2^-) radicals associated with the microbial invasion of eukaryotic cells are stained by 3,3′-diaminobenzidine tetrachloride (DAB) and nitroblue tetrazolium (NBT), respectively. DAB results in brown coloration, indicating the presence of endophytes in tissues (White et al., 2014). NBT stains superoxide radicals, which reduce NBT and it results in dark blue and water-insoluble formazan (Shinogi et al., 2003). It is used to detect endophytes in different plant tissues unlike DAB, which is not able to detect endophytes in shoot tissues because of the inability of DAB to penetrate the same.

Genomics-based studies such as next-generation sequencing and continued development in bioinformatics have allowed a significant improvement in our understanding of plant–endophyte interactions. Metagenomics and transcriptomics in particular are proving to be extremely useful for analyzing the functional characteristics of endophyte species (Kaul et al., 2016). Molecular methods are being readily employed to cultivate bacteria for their identification and enable to distinguish the bacterial populations in plant tissues (Afzal et al., 2019). These have allowed a more rigorous analysis of endophytic bacteria's abundance and community composition (Santoyo et al., 2016). Different molecular methods used to characterize the endophytic bacteria include 16S rDNA sequencing, randomly amplified polymorphic DNA (RAPD), BOX-A_1R-based repetitive extragenic palindromic PCR, amplified ribosomal DNA

restriction analysis, enterobacterial repetitive intergeneric consensus, denaturing gradient gel electrophoresis (PCR-DGGE) and repetitive extra-genic palindromic sequence.

Ten bacterial endophytes were isolated and identified from three different cereals, *Triticum aestivum, Oryza sativa*, and *Zea mays* (Liu et al., 2017a). These isolates were classified by 879F-RAPD and 16S rDNA sequencing followed by clustering into seven groups signifying a clonal origin and assigned into four genera, *Paenibacillus, Enterobacter, Pantoea,* and *Klebsiella*. Recently, Zheng et al. (2020) identified root nodule endophytes from *Sesbania cannabina* and *Glycine soja* using PacBio's circular consensus sequencing of full-length 16S rDNA gene for more accurate taxonomic information. These nodule isolates were assigned to 18 genera and 55 species, *Ensifer* being the predominant genera. PacBio technology helps in less ambiguous classification and provides finer taxonomic details. This technique has also recently been used to explore microbial communities in different samples (Singer et al., 2016; Motooka et al., 2017; Pootakham et al., 2017). Lastochkina et al. (2020) performed RAPD-PCR analysis to confirm the identity of *Bacillus subtilis* within the internal tissues of *T. aestivum* L. The endophytic diversity and detailed analysis of endophytic bacterial composition from the commercial crop (*Paullinia cupana*) of Brazil using PCR-DGGE were studied. The study disclosed the presence of phyla Firmicutes, Proteobacteria, Actinobacteria, Bacteroidetes, and Acidobacteria, Firmicutes being the predominant phylum (Bogas et al., 2015). The endophytic community of *Distichlis spicata*, *Plucheaab sinthiodes*, *Gaultheria mucronate,* and *Hieracium pilosella* growing in extreme environments of Chile (Atacama desert and Patagonia) was studied. The composition and diversity were analyzed using quantitative PCR and high-throughput gene sequencing of 16S rDNA. The endophytes from both the regions were categorized into phylum Proteobacteria, Firmicutes, Actinobacteria, and Bacteroidetes (Zhang et al., 2019). Upon extensive data mining of endophytic diversity from various plants, it has been observed that the members of phylum Proteobacteria, Actinobacteria, and Firmicutes were the most dominant (Rana et al., 2020; Bhutani et al., 2021).

PLANT GROWTH PROMOTING ENDOPHYTIC BACTERIA: THE BASE OF "SUSTAINABLE AGROECOSYSTEM"

Plant growth promoting endophytic bacteria (PGPEB) are well known to enhance the growth of plants directly and indirectly. They benefit directly to host by the concerted activity of biological nitrogen fixation, phytohormones production, phosphate solubilization, and modulation of 1-aminocyclopropane-1-carboxylic acid (ACC) deaminase expression for better growth under normal and stress conditions. Endophytes being in direct association with plants provide nitrogen in the functional form to their host either by fixing atmospheric nitrogen or by producing ammonia (Marques et al., 2010; Brígido et al., 2019). The frequent usage of nitrogen in the form of chemical fertilizers predominantly increases the cost of crop production. Hence, ammonia production by bacterial endophytes is an essential attribute for the selection of desirable bioinoculants (Li et al., 2017).

Solubilization and mineralization of phosphate are accomplished by bacterial endophytes, which assist in lowering the pH by releasing various organic acids that break Ca-bonded phosphorus in the bound form of soil (Sharma et al., 2013). Members of several genera have been reported as efficient phosphate solubilizers, such as *Rhizobium, Bacillus, Serratia, Arthrobacter, Burkholderia, Pseudomonas, Erwinia,* and *Microbacterium* (Oteino et al., 2015; Li et al., 2017; Srinivasan et al., 2018). The production of phytohormones by PGPEB is another mechanism that significantly boosts the growth of plants and alters the plant morphology (de Souza et al., 2015). IAA is a commonly produced auxin by endophytic bacteria that controls various growth processes in plants, including cell division, elongation, differentiation, gravity, and light responses (Bhutani et al., 2018a). Thus, it aids the host plant in nutrient absorption (Dhungana and Itoh, 2019). There have been numerous studies documenting IAA-producing endophytic bacteria in addition to endogenous IAA in plants (Khan and Doty, 2009; Mohite, 2013; Etesami et al., 2015; Bhutani et al., 2018b; Maheshwari et al., 2021). The application of IAA-producing bacteria to plants has demonstrated substantial upsurge in growth and yield. In addition to this, microbial IAA has been reported as a signaling molecule in several interactions between plants and microbes (Duca et al., 2014).

Gaseous phytohormone, ethylene and its precursor 1-aminocyclopropane 1-carboxylic acid (ACC), play a significant role in response to a wide range of stresses (Glick, 2014). Symbiotic bacteria ease the negative impact of ethylene on plants by expressing the ACC deaminase (ACCD). A variety of endophytic bacteria such as *Azospirillum, Ralstonia, Pseudomonas, Rhizobium, Agrobacterium, Enterobacter, Achromobacter,* and *Bacillus mojavensis* possess ACC deaminase gene and are characterized for ACCD activity (Blaha et al., 2006; Glick et al., 2007; Maheshwari et al., 2020). Transgenic varieties of plants have been developed which, by expressing the bacterial ACCD gene, have improved stress tolerance mechanisms (Stearns and Glick, 2003; Singh et al., 2015). But the addition of ACCD-producing endophytic bacteria could be more cost-effective, readily available, and environmentally sustainable, with higher acceptability compared to transgenics (Glick, 2012; Barnawal et al., 2016).

Plant growth-promoting endophytic bacteria–based biofertilizers can be envisioned as the future nutrient delivery system for plants. This approach, if carried out effectively, can bring about "real" green revolution, which will be more sustainable and reliable (Lugtenberg and Kamilova, 2009; Liu et al., 2017b). To develop these endophytes as microbial inoculants in agriculture, their functional characterization based on PGP traits and *in vivo* evaluation to check their efficacy should be the first prerequisite (de Souza et al., 2015; Alori and Babalola, 2018). Ferchichi et al. (2019) evaluated *in vitro* and *in vivo* efficacy of bacterial endophytes from three species of *Lupinus*. Two endophytes *Paenibacillus glycanilyticus* and *Pseudomonas brenneri* possessed desired functional characters and promoted

plant growth *in vivo* and *in vitro* that can be developed as eco-friendly biofertilizers to boost up *Lupinus* productivity. Recently, the multifunctional potential of *Paenibacillus polymyxa* isolated from bulbs of *Lilium lancifolium* was assessed (Khan M. S. et al., 2020). The bacterial isolate possessed various PGP traits, including the production of IAA, siderophores, ACCD, fixation of nitrogen, and solubilization of phosphate. It also promoted the plant growth of different *Lilium* varieties under greenhouse conditions. The study demonstrated that the potential of *P. polymyxa* can be evaluated as an effective bioinoculant. Before any *ex-planta* application for the agricultural crop, some pre-requisites need to be fulfilled for selection as an inoculant. These factors include colonization ability in plant roots, competition with other microflora and their survival in soil, upsurge exudate production which acts as a bridge between plant and bacteria, and improvement of soil health (Beauregard et al., 2013; Carvalhais et al., 2013; Ríos-Ruiz et al., 2019). Seven bacterial endophytes were isolated from different legume crops, namely, *Glycine max, Vigna unguiculata, Vigna mungo, Vigna radiata*, and *Arachis hypogaea* and categorized on the basis of PGP traits. These isolates were used to bacterize the seeds of *A. hypogaea* for plant growth stimulation experiments using gnotobiotic systems and in pots. The results depicted a positive influence on *A. hypogaea* growth. Additional treatment given along with chemical fertilizer at 50% recommended dose, positively affected *A. hypogaea* growth, but the negative effect was seen over the bacterial population when the dose of fertilizers exceeded more than 50%. Their results suggested that root nodules harbor the endophytic population, which augments the growth of a plant, and the addition of fertilizers adversely affects their population and activity (Dhole et al., 2016). The 28 bacterial endophytes were isolated from dry and germinating seeds of *Cicer arietinum* and characterized for PGP attributes. Molecular identification analysis showed that these endophytes belong to *Pseudomonas* sp., *Enterobacter* sp., *Bacillus* sp., *Mixta* sp., and *Pantoea* sp. These were applied to *C. arietinum* roots and led to an increase in plant length, biomass, and chlorophyll content along with biocontrol activity against *Fusarium oxysporum* (Mukherjee et al., 2020). Maheshwari et al. (2019a) isolated and investigated endophytic bacteria from *C. arietinum* and *Pisum sativum* for PGP attributes. Most efficient isolates were identified as *Pantoea agglomerans*, *Bacillus cereus*, *Bacillus sonorensis*, *Bacillus subtilis*, *Pseudomonas chlororaphis*, *Ornithibacillus* sp., and *Ochrobactrum* sp. These studies convey direct evidence for the occurrence of valuable endophytes, which can be further harnessed as bioinoculants for improving plant health.

INDUCING CLIMATE CHANGE RESILIENCE IN FLORA

Plant community throughout the world is suffering in terms of growth, development, and yield as a result of climate change–induced environmental stress manifested in the form of drought, flood, temperature extremes, salinity, heavy metal toxicity combined with biotic stresses caused due to herbivores, pathogens, and so on. Enough studies have reported the significant role played by endophytes in mitigating abiotic and biotic stress (Rani et al., 2021). Different mechanisms have been deciphered revealing the complex regulation involved in the stress tolerance conferred by the endophytes to the host plants. Drought, salinity, and temperature extremes have been reported as the most devastating abiotic stresses for crops as far as the yield is concerned. Plants respond to drought and salinity *via* stomatal closure, reduced turgidity, osmotic stress, ultimately reducing growth and yield (Van Zelm et al., 2020). Increased evaporation induced by high temperature leads to water loss resulting in the formation of protein aggregates as a result of protein folding inhibition, whereas low temperature leads to the formation of ice crystals causing permanent damage to cells (Lamers et al., 2020). Extreme temperature alters membrane fluidity (Nicolson, 2014).

Endophytes alleviate these stresses by upregulating aquaporins, improving the level of abscisic acid, ACCD activity, enhancing enzymatic and non-enzymatic ROS scavenging machinery and osmolytes, higher expression of ion channels KAT1 and KAT2 resulting in decreased Na^+/K^+, adjusting gene expression, and reducing malondialdehyde (MDA) content (Cohen et al., 2015; Gond et al., 2015; Barnawal et al., 2016; Abdelaziz et al., 2017; Xu et al., 2017; Zhang et al., 2017; Sapre et al., 2018; Wang et al., 2018). Likewise, toxic metal ions evoke oxidative stress by generating ROS which promote DNA damage/impairment of DNA repair mechanisms, membrane functional integrity, nutrient homeostasis, and perturb protein function and activity (Tamás et al., 2014). Endophytes induce heavy metal tolerance to their hosts by reducing the mobility of heavy metals by chelation or intracellular sequestration and limiting the translocation of heavy metal ions from roots to shoots (Leonhardt et al., 2014). **Table 3** describes various endophytes conferring abiotic stress protection to their hosts by different mechanisms.

PLANT GROWTH PROMOTING ENDOPHYTIC BACTERIA-ASSISTED BIOCONTROL OF PHYTOPATHOGENS

Several microbes (viruses, bacteria, and fungi), nematodes, and insects are responsible for infecting plants leading to biotic stress. Physical barriers such as cuticle, wax, trichomes, etc., form first line of defense for the plants (Iqbal et al., 2021). Promoting the availability and absorption of nutrients, augmentation of stress tolerance and disease resistance of disease are the key means of plant disease control by endophytic bacteria (Hamilton et al., 2012). The most commonly reported bacterial genera with biocontrol activity are *Bacillus, Actinobacteria, Enterobacter, Pseudomonas, Paenibacillus,* and *Serratia* (Ek-Ramos et al., 2019). These mechanisms can be broadly grouped into direct and indirect biocontrol activities (**Figure 3**).

Direct biocontrol involves the production of growth-inhibiting compounds such as siderophores, hydrogen cyanide, cell wall–degrading enzymes, and quorum-sensing inhibitors. Siderophore complex provides Fe to plants during the scarcity and assists them in iron acquisition (Dimkpa, 2016). A lot of work has been done to screen siderophore-producing endophytic

TABLE 3 | Endophytes inducing abiotic stress tolerance in host plants.

Stress tolerance	Host	Endophytes	Mechanism of action	References
Drought	*Arabidopsis thaliana*	*Azospirillum brasilense*	Enhancement of ABA	Cohen et al., 2015
	Populus deltoids	*Rhodotorula graminis, Burkholderia vietnamiensis*, and *Rhizobium tropici*	Host plant damage reduced by ROS scavenging machinery	Khan A. et al., 2016
	Oryza sativa	*Piriformospora indica*	Regulation of miR159/miR396 that target MYB and GRF transcription factors involved in regulation of growth and hyposensitivity response	Fard et al., 2017
	Zea mays L.	*Piriformospora indica*	Enhanced antioxidant enzyme activity, proline accumulation, and expression of drought-related genes and lowered membrane damage	Xu et al., 2017
	Elymus dahuricus and *Triticum aestivum*	*Alternaria alternata* LQ1230	IAA secretion contributes to the growth and upregulation of antioxidant enzymes activities and osmoregulatory substances	Qiang et al., 2019
	Hordeum vulgare	*Piriformospora indica*	Resources in host redistributed to reduce negative impact of stress and presence of aquaporin water channels sustained	Ghaffari et al., 2019
Salinity	*Lycopersicon esculentum*	*Pseudomonas fluorescens* and *Pseudomonas migulae*	ACC deaminase activity	Ali et al., 2014
	Chlorophytum borivilianum	*Brachybacterium paraconglomeratum* strain SMR20	Potential deamination of ACC in the host roots leading to decreased production of stress ethylene, delayed chlorosis and senescence that resulted in improved yield of plants	Barnawal et al., 2016
	Triticum aestivum	*Dietzia natronolimnaea*	Enhanced expression of TaST, a salt stress-induced gene	Bharti et al., 2016
	Oryza sativa	*Bacillus pumilus*	Effective salt tolerance, survivability, root colonization and multifarious PGP trait, significant reduction in antioxidant enzyme activities and MDA content	Khan Z. et al., 2016
	Zea mays	*Pseudomonas fluorescens* 002	Release of IAA and protection of plants against the inhibitory effects of NaCl	Zerrouk et al., 2016
	Triticum aestivum	*Arthrobacter protophormiae* SA3, *Dietzia natronolimnaea* STR1, and *Bacillus subtilis* LDR2	IAA content of wheat increased under salt and drought stress conditions. SA3 and LDR2 inoculation counteracted increase of ABA and ACC	Barnawal et al., 2017
	Triticum aestivum	*Chryseobacterium gleum* sp. SUK	Improved root-shoot length, fresh-dry weight, chlorophyll, proteins, amino acids, phenolics, flavonoids content and decreased level of proline, Na^+ uptake, increase in K^+ uptake	Bhise et al., 2017
	Cicer arietinum	*Mesorhizobium ciceri* and *Bacillus subtilis*	Decreased H_2O_2 concentration and improved proline contents.	Egamberdieva et al., 2017
	Avena sativa	*Klebsiella* sp.	Biochemical parameters such as proline content, electrolyte leakage, MDA content and antioxidant enzyme activities analyzed and found to be notably lesser in IG3 inoculated plants	Sapre et al., 2018
	Oryza sativa	*Burkholderia* strain P50	ACC deaminase activity and united PGP traits of P50 successfully alleviate salt stress in rice seedlings by improving morphological and biochemical parameters and decreasing ROS scavenging antioxidant enzymes, osmolytes and stress ethylene	Sarkar et al., 2018
	Capsicum annuum L.	*Bacillus* sp.	Induced high levels of proline production and antioxidant enzyme activities	Wang et al., 2018

(Continued)

TABLE 3 | (Continued)

Stress tolerance	Host	Endophytes	Mechanism of action	References
	Oryza sativa	*Curtobacterium albidum* strain SRV4	SRV4 expressed positive attribute for nitrogen fixation, EPS, HCN, IAA, and ACCD activity leading to improvement in plant growth parameters, photosynthetic efficiency, membrane stabilization index and proline content, antioxidative enzymatic activities and K^+ uptake	Vimal et al., 2019
Heat	*Lycopersicon esculentum* Mill	*Paraburkholderia phytofirmans*	Accumulation of sugars, total amino acids, proline, and malate, promotion of gas exchange	Issa et al., 2018
	Glycine max	*Bacillus cereus* SA1	Induction in the endogenous levels of several phytohormones (ABA and SA), essential amino acids	Khan M. A. et al., 2020
Cold	*Arabidopsis thaliana*	*Burkholderia phytofirmans* strain PsJN	Significant changes in PS-II activity, differential accumulation of pigments	Su et al., 2015
	Solanum lycopersicum Mill.	*Pseudomonas vancouverensis* and *P. frederiksbergensis*	Improved reactive oxygen species levels and reduced membrane damage and high expression of cold acclimation genes LeCBF1 and LeCBF3	Subramanian et al., 2015
	Lycopersicon esculentum	*Bacillus cereus; Bacillus subtilis; Serratia* sp.	Promoting soluble sugar, proline, and osmotin accumulation, enhancing antioxidant defense system	Wang et al., 2016
Heavy metal	*Miscanthus sinensis*	*Pseudomonas koreensis* AGB-1	High tolerance to Zn, Cd, As, and Pb by extracellular sequestration, increased CAT and SOD activities	Babu et al., 2015
	Solanum nigrum	*Pseudomonas aeruginosa*	Enhanced Cd stress tolerance	Shi et al., 2016
	Panicum virgatum L.	*Pseudomonas putida* Bj05, *Pseudomonas fluorescens* Ps14, *Enterobacter* spp. Le14, So02, and Bo03	Plants protected from inhibitory effects of Cd, plant growth improved and Cd concentration decreased	Afzal S. et al., 2017
	Zea mays L.	*Gaeumannomyces cylindrosporus*	Height, basal diameter, root length, and biomass of maize seedlings increased significantly under Pb stress	Ban et al., 2017
	Glycine max L.	*Sphingomonas* sp.	Reduced Cr translocation to roots, shoot, and leaves and oxidative stress was significantly reduced regulating reduced GSH and enzymatic antioxidant CAT	Bilal et al., 2018
	Oryza sativa	*Enterobacter ludwigii* SAK5, *Exiguobacterium indicum* SA22	Protection against heavy metal Cd and Ni hyperaccumulation by enhanced detoxification mechanisms	Jan et al., 2019
	Brassica juncea	*Serratia* sp., *Enterobacter* sp.	Phytohormone production, phosphate solubilization, and antioxidative support responsible for Cd resistance	Ullah et al., 2019
	Saccharum officinarum	*Pseudomonas fluorescens*, *Kosakonia radicincitans*, *Paraburkholderia tropica*, and *Herbaspirillum frisingense*	Alleviating Al stress	Labanca et al., 2020
	Brassica napus L.	*Serratia* sp. IU01	Minimized the magnitude of the oxidative damage and advantages in terms of growth promotion and alleviating Cd toxicity	Shah et al., 2020

ABA, abscisic acid; MYB, myeloblastosis family; GRF, growth-regulating factors; ACCD, 1-aminocyclopropane-1-carboxylic acid deaminase; MDA, malondialdehyde; HCN, hydrogen cyanide; SA, salicylic acid; CAT, catalase; SOD, superoxide dismutase; GSH, glutathione.

bacteria–mediated improvement in plant growth along with biocontrol of phytopathogens (Lacava et al., 2008; Pandey et al., 2015; Passari et al., 2016; Walitang et al., 2017; Yan et al., 2018; Maheshwari et al., 2019b). A number of studies have demonstrated that siderophore-producing bacteria support the plants to endure both biotic and abiotic stresses. In a study by Ruiz et al. (2015), *Pseudomonas protegens* strain survived in the presence of Fusaric acid (mycotoxin)-producing *Fusarium* strains by producing metal scavenging siderophores (pyoverdine and pyochelin). Recently, Butaite et al. (2017) found that non- and low-pyoverdine siderophore producers coexist in various natural populations. The non-siderophore producers with

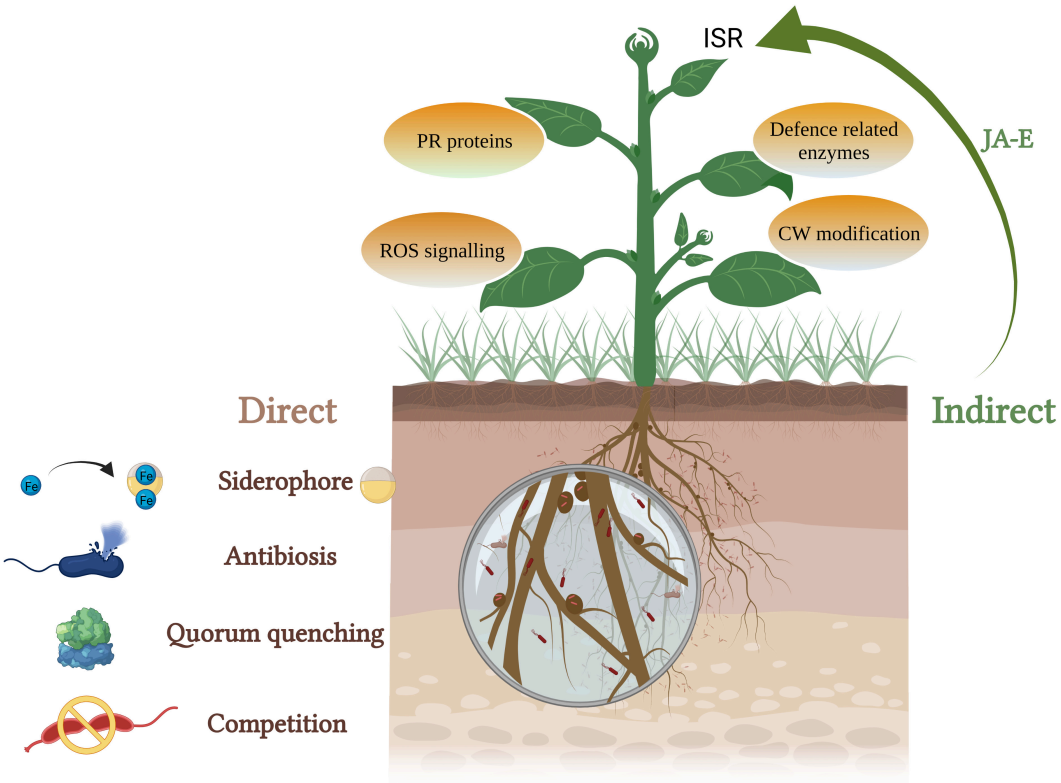

FIGURE 3 | PGPEB-mediated direct and indirect biocontrol of phytopathogens (JA, jasmonic acid; E, ethylene; ISR, induced systemic resistance; PR, pathogenesis related; ROS, reactive oxygen species; CW, cell wall).

suitable siderophore receptors can utilize external siderophores. The producers are different in the types of pyoverdine they secrete and offer protection against exploitation by non-producers and acquisition of iron unaccessible to opposing strains lacking the proper receptors.

Hydrogen cyanide (HCN) production leads to the growth inhibition of pathogens due to biogenic cyanogenesis. Cyanide, a metabolic inhibitor, inhibits the cytochrome C oxidase and the other metalloenzymes of the pathogen and thus helps the plant to combat against soil-borne diseases (Voisard et al., 1989; Blumer and Haas, 2000; Dheeman et al., 2019; Maheshwari et al., 2019a; Swarnalakshmi et al., 2019). Dubey et al. (2014) reported *Bacillus subtilis* strain producing HCN and other metabolites that inhibit the growth of phytopathogen *Fusarium oxysporum*. HCN-producing endophytes isolated from *Glycine max* exhibited *in vitro* antagonism against a wide range of phytopathogens, namely, *Sclerotium rolfsii, Rhizoctonia solani, Alternaria alternata, F. oxysporum, Macrophomina phaseolina*, and *Colletotrichum truncatum* (Dalal et al., 2015). The bacterial endophytes obtained from the medicinal plant *Clerodendrum colebrookianum* Walp possessed *in vitro* PGP activities including HCN production. These endophytes exhibited *in vitro* and *in vivo* biocontrol activity against various phytopathogenic fungi (Passari et al., 2016). Quorum sensing is mediated by small diffusible signaling molecules called autoinducers which mediate the regulation of diverse functions such as virulence and biofilm formation. Endophytic bacteria can interfere in quorum sensing using quorum sensing inhibitors and quorum quenching enzymes to control bacterial infections as a result of suppressing the formation of biofilm (Zhou et al., 2020). Many endophytic bacteria have been reported to produce lactonases and acylases which results in quorum quenching by the inactivation/degradation of major signaling molecules involved in quorum sensing, *N*-acyl homoserine lactones (Rashid et al., 2012).

Indirectly, endophytic bacteria are known to trigger jasmonic acid and ethylene-mediated induced systemic resistance which induces a defense mechanism and protects the plants from future attacks of plant pathogens (Miliute et al., 2015). It leads to the production of pathogenesis-related proteins, phytoalexins, defense-related enzymes such as polyphenol oxidase (PPO) and phenylalanine ammonia lyase, formation of physical barriers such as cuticles and modification of cell wall (Wiesel et al., 2014). Mao et al. (2019) demonstrated endophytic bacterial strain REB01 to induce disease resistance against rice sheath blight caused by *R. solani via* enhancing the activity of PPO, POD enzymes, and reducing the MDA content. Kim et al. (2019) isolated and selected pine endophytic bacteria on the basis of the relative expression of defense-related genes, *Pseudomonas putida* 16 YSM-E48, *Curtobacterium pusillum* 16YSM-P180,

and *Stenotrophomonas rhizophila* 16YSM-P3G, effective against *Bursaphelenchus xylophilus* (pinewood nematode) causing pine wilt disease. Asghari et al. (2020) reported induction of systemic resistance in *Vitis vinifera*, by *Pseudomonas* sp. Sn48 and *Pantoea* sp. Sa14 against *Agrobacterium tumefaciens* through improvement in the levels of PR1, PR2, and PR4 gene expression levels of plantlets.

Some of the endophytic bacteria undergo rhizophagy, biphasic cycle of alternation between the root intracellular phase (nutrients extracted by plants) and a free-living soil phase (acquisition of nutrients by bacteria) (Dudeja et al., 2021). "Endobiome interference" is the term used to describe the phenomenon in which other endophytes interfere with rhizophagy and extract the nutrients from native microbes post-colonization. Although the mechanism behind this remains poorly understood, it has been hypothesized that the oxidative resistance of microbes reduces the capacity of host cells to control the intracellular microbes using ROS produced by NOX enzymes on the root cell plasma membranes. They can be explored to develop bioherbicides to target competitive weeds (White et al., 2019). This way they enhance stress in the host and inhibit their growth leading to an eco-friendly biocontrol option (Verma et al., 2021). Kowalski et al. (2018) explored endobiome interference by the application of a bacterial endophyte, *Micrococcus luteus*, isolated from the seedling root hairs of *Lycopersicon esculentum*, to arrest the growth of a weedy plant sp., *Phragmites australis*, by targeting its growth promotional native microbiome. It also illustrates a vital precaution to be taken before applying any exogenous endophytes, that is, to analyze the interactions between the endophytes being applied and the native microflora (Verma et al., 2021). **Table 4** describes numerous studies depicting the biocontrol potential of the bacterial endophytes.

HARNESSING "OMICS" FOR ENHANCING THE BIOACTIVE METABOLITES

Bioactive compounds are mostly secondary metabolites produced by the microbes in an active culture cultivation process. Their unique properties have led to lots of research regarding their applications in healthcare as feed supplements, pharmaceuticals, and so on (Singh nee' Nigam, 2009). Endophytes have been reported to produce many secondary metabolites similar to their host under *in vitro* systems. This ability can lessen our dependency on endangered plants for the extraction of metabolites (Sharma et al., 2021). Several approaches have been employed to harness novel metabolites or to enhance the production of already known ones to support and flourish their large scale application (Du and van Wezel, 2018). Co-culture engineering by culturing more than one type of endophyte together can make us exploit the intermicrobial communications for the enhanced production of bioactive metabolites. A number of studies have reported the production of new metabolites by this method (Stierle et al., 2017; Arora et al., 2018; Gautam et al., 2019). The associated disadvantages such as compatibility issues, competition for substrates, and data acquisition problems pose remarkable challenges (Padmaperuma et al., 2017; Jawed et al., 2019). A number of reports have demonstrated the precise effects of endophytes on the production of secondary metabolites of the host (Khare et al., 2018). **Table 5** sums up recent studies dealing with the enhancement of bioactive compounds of the host owing to the endophytes. Other than enhancing the bioactive compounds of the host, endophytes serve as a great treasure of new metabolites which remains largely unexplored looking at the vast diversity of endophytic flora.

Some approaches have been developed in the recent past to trigger the expression of Biosynthetic gene clusters (BGCs) present in the genome of microbes (endophytes) that can yield some valuable secondary metabolites but remain either silent or poorly expressed. In most cases, BGCs remain silent under laboratory conditions due to complex regulation involved at transcriptional, translational, and post-translational levels. Therefore, the study of changes in gene expression at various levels needs to be done. Recent progress made in bioinformatics, especially genome mining tools have pushed the boundaries of "omics" technologies toward new horizons. It has revolutionized our understanding of the pathways controlling the expression of BGCs.

Genome mining is a powerful approach that can estimate the genetic potential of microbial strain by scanning genomes of interest and identifying the metabolites encoded by BGCs (Ziemert et al., 2016). Whole-genome sequencing and its comparative analysis yield the reconstruction of primary and secondary metabolic pathways that help in suggesting the key metabolic genes to be utilized for metabolic engineering (Palazzotto and Weber, 2018). Metabolic and genetic engineering involves the modulation of biosynthetic enzymes at cellular level/upregulation and downregulation of transcription and translation genes/knock-out and knock-in of desired genes and have been effective in enhancing the production of specific metabolites (Stephens et al., 2015). Mining tools such as antibodies and secondary metabolites analysis shell) (antiSMASH), generalized retro-biosynthetic assembly prediction engine (GRAPE), prediction informatics for secondary metabolomes (PRISM3) have been successful in overcoming the drawbacks associated with manual analyses to some extent. A number of natural products encoded by BGCs remain uncharacterized owing to the complicated regulations occurring at transcriptional, translational, and post-translational levels.

Transcriptome-based studies provide a comparative profile of gene expression and help to assess the key regulators which are in turn used for manifesting the designer strains having the ability to overproduce secondary metabolites (Chaudhary et al., 2013). Proteomics complements other two omics approaches, namely, transcriptomics and genomics, yielding information on differential pathways regulation highlighting key players in the biosynthesis of natural products, which can be used to target for rational engineering (Palazzotto and Weber, 2018). Comparative transcriptomics and proteomics are used to identify the alterations in gene expression associated with the overproduction which are subsequently re-engineered into

TABLE 4 | Biocontrol of phytopathogens using bacterial endophytes.

Host Plant	Endophytes	Disease	Causing agent	Mechanism	References
Diseases caused by fungi					
Zea mays L.	*Bacillus amyloliquefaciens* subsp. *subtilis*	Ear rot and stalk rot	*Fusarium moniliforme*	PR-1, PR-10 genes highly induced	Gond et al., 2015
Nicotiana glauca	*Alcaligenes faecalis* S18, *Bacillus cereus* S42	Fusarium wilt	*Fusarium oxysporum* f. sp. *lycopersici*	Proteolytic and chitinolytic activity, HCN production	Aydi Ben Abdallah et al., 2016
Salicaceae plants	*Burkholderia* strains WP40 and WP42	Root rot, Ear blight or scab, Take all, Seed blight or rot	*Rhizoctonia solani* AG-8, *Fusarium culmorum, Gaeumannomyces graminis* var. *tritici, Pythium ultimum*	Production of HCN and antifungal metabolite, occidofungin	Kandel et al., 2017b
Dodonaea viscosa L.	*Bacillus, Pseudomonas, and Streptomyces*	Black mold, Fusarium wilt	*Aspergillus niger, Fusarium oxysporum*	Chitinase, protease and antifungal activity	Afzal I. et al., 2017
Fragaria × *ananassa* (Duch.)	*Staphylococcus sciuri* MarR44	Celery stunt anthracn-ose	*Colletotrichum nymphaeae*	Production of antifungal metabolites (VOCs)	Alijani et al., 2019
Saccharum officinarum	*Bacillus subtilis*	Fusarium wilt	*Fusarium* strains	Production of surfactin	Hazarika et al., 2019
Pisum sativum	*Pseudomonas chlororaphis*	Black mold, Fusarium wilt	*Aspergillus niger* and *Fusarium oxysporum*	HCN production	Maheshwari et al., 2019a
Oryza sativa L.	*Bacillus subtilis*	Bacterial blight of rice, stalk and ear rot, and root rot	*Xanthomonas oryzae, Fusarium verticillioides, Rhizoctonia solani,* and *Sclerotium rolfsii*	Lipopeptide genes encoding surfactin, iturin D, bacillomycin D having antagonistic activities	Kumar V. et al., 2020
Lilium lancifolium	*Paenibacillus polymyxa*	Fusarium wilt, gray mold and cankers	*Botryosphaeria dothidea, Fusarium oxysporum, Botrytis cinerea*, and *Fusarium fujikuroi*	Production of antibiotic secondary metabolites	Khan M. S. et al., 2020
Pennisetum glaucum	*Bacillus subtilis*	Downy mildew	*Sclerospora graminicola*	Production of siderophore, HCN and ACC deaminase activity.	Sangwan et al., 2021
Glycine max	*Bacillus cereus* and *Pseudomonas* sp.	Fusarium wilt	*Fusarium oxysporum, Macrophomina phaseolina*, and *Alternaria alternata*	Production of cellulase, chitinase, and HCN	Dubey et al., 2021
Helianthus annuus	*Priestia koreensis*	Fusarium wilt	*Fusarium oxysporum*	Production of essential secondary metabolites and hydrolytic enzymes	Bashir et al., 2021
Disease caused by bacteria					
Pistacia atlantica L.	*Pseudomonas protegens*	Bacterial canker	*Pseudomonas syringae* pv. *syringae* Pss20 and *Pseudomonas tolaasii* Pt18	Production of siderophore and protease	Tashi-Oshnoei et al., 2017
Pyrus communis L.	Fluorescent *Pseudomonas* sp.	Fire blight disease	*Erwinia amylovora*	Production of antibiotic, PCA, DAPG, pyrrolnitrin and pyoluteorin.	Sharifazizi et al., 2017
Ventilago madraspatana	*Enterobacter* sp. CS66	Soft rot and black leg disease	*Pectobacterium atrosepticum*	Quorum quenching	Shastry et al., 2018
Citrus sinensis	*Bacillus cereus* Si-Ps1, *Pseudomonas azotoformans* La-Pot3-3	Bacterial apical necrosis	*Pseudomonas syringae* pv. *syringae* (Pss) B7289 and Pss3289	Quorum quenching	Akbari Kiarood et al., 2020
Disease caused by nematode					
Musa	*Streptomyces* sp.	Wilting leaves, gall formation	*Meloidogyne javanica*	Higher abundance of bacterivores	Su et al., 2017
P. densiflora, P. koraiensis, P. thunbergia, P. rigida	*Stenotrophomonas* and *Bacillus* sp.	Drying out	*Bursaphelenchus xylophilus*	Production of amocarzine, mebendazole and flubendazole compounds	Shanmugam et al., 2018; Ponpandian et al., 2019
Fragaria ananassa	*Bacillus cereus* BCM2	Root-knot disease	*Meloidogyne incognita*	Production of chitosanase, alkaline serine protease, and neutral protease	Hu et al., 2020

PR, pathogenesis related; VOC, volatile organic compounds; PCA, phenazine-1-carboxylic acid, DAPG: 2,4-diacetyl phloroglucinol.

TABLE 5 | Bioactive compounds enhancement in host plants by endophytes.

Host plant	Endophytes	Bioactive compound	Applications	References
Papaver somniferum	*Stenotrophomonas maltophilia*	Morphine, Thebaine, Codeine, and Oripavine	Used as analgesics, antitussives and anti- spasmodic	Liscombe and Facchini, 2008; Bonilla et al., 2014
Aristolochia elegans	*Piriformospora indica*	Aristolochic acid	Antimicrobial properties	Bagde et al., 2014
Curcuma longa	*Azotobacter chroococcum* CL13	Curcumin	Anti-inflammatory, antioxidative, antimalarial activities	Kumar et al., 2016
Putterlickia verrucosa; Putterlickia retrospinosa	*Hamigera avellanea*	Maytansine	Cancer chemotherapy	Kusari et al., 2014
Salvia miltiorrhiza	*Paecilomyces* sp.	Salvianolic acid	Antioxidative activities	Tang et al., 2014
Chamomilla recutita L. Rauschert	*Bacillus subtilis* Co1-6, *Paenibacillus polymyxa* Mc5Re-14	Apigenin-7-*O*-glucoside	Anti-inflammatory capacity	Schmidt et al., 2014
Panax ginseng	*Paenibacillus polymyxa.*	Ginsenosides	Anticancerous properties	Gao et al., 2015
Artemisia annua L.	*Piriformospora indica* DSM 11827, *Azotobacter chroococcum* W-5	Artemisinin	Artemisinin combination therapies (ACTs) to control malaria	Arora et al., 2016
Aloe vera	*Piriformospora indica*	Aloin	Numerous therapeutic applications	Sharma et al., 2014
Stevia rebaudiana	*Piriformospora indica*	Enhanced production of Steviol glycosides	High potency sweeteners	Kilam et al., 2017
Crocus sativus L.	*Mortierella alpine* CS10E4	Crocin, Picrocrocin, and Safranal	Anti-tumor activities	Wani et al., 2017
Kadsura angustifolia	*Umbelopsis dimorpha* SWUKD3.1410	Schitriterpenoids/ schinortriterpenoids.	Antihepatitis, antitumor and anti-HIV activities	Qin et al., 2018
Salvia miltiorrhiza	*Chaetomium globosum* D38	Phenylpropionic acids and tanshinones	Flavoring agents used in spices (Phenylpropionic acids); Cardiovascular and cerebrovascular protective actions (Tanshinones)	Zhai et al., 2018
Coleus forskohlii	*Phialemoniopsis cornearis* SF1, *Macrophomina pseudophaseolina* SF2, *Fusarium redolens* RF1	Davanone, Ethyl cinnamate	Perfumery products, flavoring agents	Mastan et al., 2019

the organism of interest by considering key genes involved in complex mechanisms. However, its success depends on the reproducibility of the overproducing mechanism in the new target strains (Chaudhary et al., 2013). One of the most important tools of system biology toolbox is metabolomics which catalogs all small metabolites in a biological sample. NMR- and MS-based metabolomic analysis facilitates measurement of low–molecular weight metabolites allowing the metabolic comparison of various biological samples leading to the identification of secondary metabolites from orphan BGCs. A comprehensive picture of metabolic networks helps to engineer the primary metabolism *via* cofactors and precursors for the biosynthesis of any secondary metabolite (Nguyen et al., 2012). Metagenomics is the most commonly used approach to study the chemistry of uncultivated bacteria. It provides a culture-independent approach to exploring the hidden potential of microorganisms.

Omics analysis in isolation is unable to completely unfurl the complexities involved in microbial metabolism associated with the production of secondary metabolites. Therefore, it is necessary to undertake their integration to get better insights into the same (Chaudhary et al., 2013). The combined use of multi-meta-omics approaches such as metabologenomics involves a combination of genome sequencing and automated gene clusters prediction with MS-based metabolomics. It provides us a complete picture of microbial metabolism shedding light on the silent BGCs and the role of natural products (Palazzotto and Weber, 2018). Precision engineering is another modern approach that integrates information from different sources, transcriptome profiling (DNA microarrays), proteome profiling (2D gel electrophoresis), and metabolic profiling (HPLC), thus enabling a more precise identification of key genetic targets and pathways engineered for strain improvement (Gao et al., 2010). Many microbes engineered by metabolic engineering are being used in industrial-scale processes; however, it is associated with challenges such as titers, yields, and productivities required for commercial viability. Different aspects of microbial physiology can also create obstacles for metabolic engineering (Montaño López et al., 2022).

LIMITATIONS AND CHALLENGES

Word "endophyte" searched on Google scholar (January 05, 2022) showed 80,100 results indicating extensive research happening in this arena. However, some lacunae need to be filled with regard to the research on endophytes. A sufficient number of studies have not been conducted to study the variations such as plant–microbe interactions on the field induced by a range of environmental and physiological conditions unlike *in vitro*. Information about the synergistic interaction between different microbial taxa such as bacteria, archaea, and fungi, is sparse with most of the studies focusing on each taxa separately.

Although the importance of biofertilizers and biocontrol potential of endophytes over conventional and environment degrading chemical pesticides are well known, some drawbacks of biopesticides are responsible for our slow speed on this eco-friendly path. High production cost and limited period of activity as compared to the chemical ones along with lower potency make it difficult for the farmers to opt for it. Owing to their target-specific nature, they control a specific portion of pests in the treated area and may leave the other damage-causing pests unaffected (Kawalekar, 2013). Lesser insights are available into the overlaps present in the metabolic pathways of endophytes and host plants, which leads to the production of a particular bioactive compound (Mishra et al., 2021). More research targeted at unfurling the genetic controls involved in stress tolerance conferring potential as well as bioactive compounds accumulation capability of the microbe is to be undertaken to unfold the molecular mechanisms behind the same.

CONCLUSION

Plant and endophytes exist in close interaction with each other and provide increased productivity as a bonus. The effects and functions of these associations have not been understood fully thereby calling for a more in-depth study. It would be more beneficial if more knowledge of endophytes' ecology and their molecular interaction is made available for harnessing and application in agriculture. This research will have a progressive impact on the environment in the direction of chemical fertilizer–free cultivation and better contribution to the economy. Also, the optimization of growth conditions as well as nutrient media for the endophytes having enormous potential to be applied particularly in pharmaceutical and agricultural sectors needs to be done at the earliest. "Omics" combined with recent computational data mining tools can help unravel the functions of complex plant microbiome, which can provide us with more competent microbes as far as stress tolerance and enhancing the bioactive metabolites is concerned.

AUTHOR CONTRIBUTIONS

PS and AD conceptualized the theme of this review. SR wrote and compiled the original draft. PK, PD, and RM drafted the figures and compiled tables. All authors have made intellectual and substantial contribution and approved it for publication.

ACKNOWLEDGMENTS

SR, PK, and PD would like to acknowledge the Council of Scientific & Industrial Research, New Delhi, India, for CSIR fellowship. PS acknowledges support from the Department of Science and Technology (DST), Government of India, New Delhi. The authors would like to acknowledge the Department of Science and Technology, Government of India, for providing FIST grant (Grant No. 1196 SR/FST/LS-I/2017/4) to the Department of Microbiology, MDU, Rohtak.

REFERENCES

Abdelaziz, M. E., Kim, D., Ali, S., Fedoroff, N. V., and Al-Babili, S. (2017). The endophytic fungus *Piriformospora indica* enhances *Arabidopsis thaliana* growth and modulates Na^+/K^+ homeostasis under salt stress conditions. *Plant Sci.* 263, 107–115. doi: 10.1016/J.PLANTSCI.2017.07.006

Achari, G. A., and Ramesh, R. (2019). Colonization of Eggplant by endophytic bacteria antagonistic to *Ralstonia solanacearum*, the Bacterial Wilt Pathogen. *Proc. Natl. Acad. Sci. India Sect. B Biol. Sci.* 89, 585–593. doi: 10.1007/S40011-018-0972-2/FIGURES/3

Afzal, I., Iqrar, I., Shinwari Zabta, K., and Yasmin, A. (2017). Plant growth-promoting potential of endophytic bacteria isolated from roots of wild *Dodonaea viscosa* L. *Plant Growth Regul.* 81, 399–408. doi: 10.1007/s10725-016-0216-5/Published

Afzal, I., Shinwari, Z. K., Sikandar, S., and Shahzad, S. (2019). Plant beneficial endophytic bacteria: mechanisms, diversity, host range and genetic determinants. *Microbiol. Res.* 221, 36–49. doi: 10.1016/J.MICRES.2019.02.001

Afzal, S., Begum, N., Zhao, H., Fang, Z., Lou, L., and Cai, Q. (2017). Influence of endophytic root bacteria on the growth, cadmium tolerance and uptake of switchgrass (*Panicum virgatum* L.). *J. Appl. Microbiol.* 123, 498–510. doi: 10.1111/JAM.13505

Agisha, V. N., Eapen, J. S., Bhai, S., and Aundy, K. (2017). Detecting and monitoring endophytic colonization by *Pseudomonas putida* BP25 in black pepper (*Piper nigrum* L.) using quantitative real-time PCR exploitation of antimicrobial and growth promotive traits of *Methylobacterium* for the production and protection. *Artic. J. Spices Aromat. Crops* 26, 1–7. doi: 10.25081/josac.2017.v26.i1.812

Akbari Kiarood, S. L., Rahnama, K., Golmohammadi, M., and Nasrollanejad, S. (2020). Quorum-quenching endophytic bacteria inhibit disease caused by *Pseudomonas* syringae pv. syringae in citrus cultivars. *J. Basic Microbiol.* 60, 746–757. doi: 10.1002/JOBM.202000038

Ali, S., Charles, T. C., and Glick, B. R. (2014). Amelioration of high salinity stress damage by plant growth-promoting bacterial endophytes that contain ACC deaminase. *Plant Physiol. Biochem.* 80, 160–167. doi: 10.1016/J.PLAPHY.2014.04.003

Alibrandi, P., Cardinale, M., Rahman, M. M., Strati, F., Ciná, P., de Viana, M. L., et al. (2018). The seed endosphere of *Anadenanthera colubrina* is inhabited by a complex microbiota, including *Methylobacterium* spp. and *Staphylococcus* spp. with potential plant-growth promoting activities. *Plant Soil* 422, 81–99. doi: 10.1007/S11104-017-3182-4/FIGURES/5

Alijani, Z., Amini, J., Ashengroph, M., and Bahramnejad, B. (2019). Antifungal activity of volatile compounds produced by *Staphylococcus sciuri* strain MarR44 and its potential for the biocontrol of *Colletotrichum nymphaeae*, causal agent strawberry anthracnose. *Int. J. Food Microbiol.* 307:108276. doi: 10.1016/J.IJFOODMICRO.2019.108276

Alori, E. T., and Babalola, O. O. (2018). Microbial inoculants for improving crop quality and human health in Africa. *Front. Microbiol.* 9:2213. doi: 10.3389/FMICB.2018.02213/BIBTEX

Arora, D., Chashoo, G., Singamaneni, V., Sharma, N., Gupta, P., and Jaglan, S. (2018). *Bacillus amyloliquefaciens* induces production of a novel blennolide K in coculture of *Setophoma terrestris*. *J. Appl. Microbiol.* 124, 730–739. doi: 10.1111/JAM.13683

Arora, M., Saxena, P., Choudhary, D. K., Abdin, M. Z., and Varma, A. (2016). Dual symbiosis between *Piriformospora indica* and *Azotobacter chroococcum* enhances the artemisinin content in *Artemisia annua* L. *World J. Microbiol. Biotechnol.* 32, 19. doi: 10.1007/s11274-015-1972-5

Asghari, S., Harighi, B., Ashengroph, M., Clement, C., Aziz, A., Esmaeel, Q., et al. (2020). Induction of systemic resistance to *Agrobacterium tumefaciens* by

endophytic bacteria in grapevine. *Plant Pathol.* 69, 827–837. doi: 10.1111/PPA.13175

Aydi Ben Abdallah, R., Mokni-Tlili, S., Nefzi, A., Jabnoun-Khiareddine, H., and Daami-Remadi, M. (2016). Biocontrol of Fusarium wilt and growth promotion of tomato plants using endophytic bacteria isolated from *Nicotiana glauca* organs. *Biol. Control* 97, 80–88. doi: 10.1016/J.BIOCONTROL.2016.03.005

Babu, A. G., Shea, P. J., Sudhakar, D., Jung, I. B., and Oh, B. T. (2015). Potential use of *Pseudomonas koreensis* AGB-1 in association with *Miscanthus sinensis* to remediate heavy metal(loid)-contaminated mining site soil. *J. Environ. Manage.* 151, 160–166. doi: 10.1016/J.JENVMAN.2014.12.045

Bagde, U. S., Prasad, R., and Varma, A. (2014). Impact of culture filtrate of *Piriformospora indica* on biomass and biosynthesis of active ingredient aristolochic acid in *Aristolochia elegans* Mart. *Int. J. Biol.* 6, 29–37. doi: 10.5539/ijb.v6n1p29

Bai, F., Morimoto, Y. V., Yoshimura, S. D. J., Hara, N., Kami-Ike, N., Namba, K., et al. (2014). Assembly dynamics and the roles of FliI ATPase of the bacterial flagellar export apparatus. *Sci. Rep.* 4:6528. doi: 10.1038/srep06528

Balsanelli, E., Tadra-Sfeir, M. Z., Faoro, H., Pankievicz, V. C., de Baura, V. A., Pedrosa, F. O., et al. (2016). Molecular adaptations of *Herbaspirillum seropedicae* during colonization of the maize rhizosphere. *Environ. Microbiol.* 18, 2343–2356. doi: 10.1111/1462-2920.12887/SUPPINFO

Balsanelli, E., Tuleski, T. R., de Baura, V. A., Yates, M. G., Chubatsu, L. S., de Oliveira Pedrosa, F., et al. (2013). Maize root lectins mediate the interaction with *Herbaspirillum seropedicae* via N-Acetyl glucosamine residues of Lipopolysaccharides. *PLoS One* 8:e77001. doi: 10.1371/JOURNAL.PONE.0077001

Ban, Y., Xu, Z., Yang, Y., Zhang, H., Chen, H., and Tang, M. (2017). Effect of dark septate endophytic fungus *Gaeumannomyces cylindrosporus* on plant growth, photosynthesis and Pb tolerance of maize (*Zea mays* L.). *Pedosphere* 27, 283–292. doi: 10.1016/S1002-0160(17)60316-3

Banik, A., Mukhopadhaya, S. K., Sahana, A., Das, D., and Dangar, T. K. (2016). Fluorescence resonance energy transfer (FRET)-based technique for tracking of endophytic bacteria in rice roots. *Biol. Fertil. Soils* 52, 277–282. doi: 10.1007/S00374-015-1064-6/FIGURES/4

Barnawal, D., Bharti, N., Pandey, S. S., Pandey, A., Chanotiya, C. S., and Kalra, A. (2017). Plant growth-promoting rhizobacteria enhance wheat salt and drought stress tolerance by altering endogenous phytohormone levels and TaCTR1/TaDREB2 expression. *Physiol. Plant.* 161, 502–514. doi: 10.1111/PPL.12614

Barnawal, D., Bharti, N., Tripathi, A., Pandey, S. S., Chandan, S., and Kalra, A. (2016). ACC-deaminase-producing endophyte brachybacterium paraconglomeratum strain SMR20 ameliorates chlorophytum salinity stress via altering phytohormone generation. *J. Plant Growth Regul.* 35, 553–564. doi: 10.1007/s00344-015-9560-3

Bashir, S., Iqbal, A., Hasnain, S., and White, J. F. (2021). Screening of sunflower associated bacteria as biocontrol agents for plant growth promotion. *Arch. Microbiol.* 203, 4901–4912. doi: 10.1007/S00203-021-02463-8/FIGURES/5

Beauregard, P. B., Chai, Y., Vlamakis, H., Losick, R., and Kolter, R. (2013). Bacillus subtilis biofilm induction by plant polysaccharides. *Proc. Natl. Acad. Sci. U.S.A.* 110, E1621–E1630. doi: 10.1073/PNAS.1218984110/-/DCSUPPLEMENTAL

Bharti, N., Pandey, S. S., Barnawal, D., Patel, V. K., and Kalra, A. (2016). Plant growth promoting rhizobacteria *Dietzia natronolimnaea* modulates the expression of stress responsive genes providing protection of wheat from salinity stress. *Sci. Rep.* 6, 34768. doi: 10.1038/srep34768

Bhise, K. K., Bhagwat, P. K., and Dandge, P. B. (2017). Synergistic effect of *Chryseobacterium gleum* sp. SUK with ACC deaminase activity in alleviation of salt stress and plant growth promotion in *Triticum aestivum* L. *3 Biotech* 7, 1–13. doi: 10.1007/S13205-017-0739-0/TABLES/3

Bhutani, N., Maheshwari, R., Negi, M., and Suneja, P. (2018a). Optimization of IAA production by endophytic *Bacillus* spp. from *Vigna radiata* for their potential use as plant growth promoters. *Isr. J. Plant Sci.* 65, 83–96. doi: 10.1163/22238980-00001025

Bhutani, N., Maheshwari, R., and Suneja, P. (2018b). Isolation and characterization of plant growth promoting endophytic bacteria isolated from *Vigna radiata*-Indian Journals. *Indian J. Agric. Res.* 52, 593–603.

Bhutani, N., Maheshwari, R., Kumar, P., and Suneja, P. (2021). Bioprospecting of endophytic bacteria from nodules and roots of *Vigna radiata*, *Vigna unguiculata* and *Cajanus cajan* for their potential use as bioinoculants. *Plant Gene* 28, 100326. doi: 10.1016/J.PLGENE.2021.100326

Bilal, S., Khan, A. L., Shahzad, R., Kim, Y. H., Imran, M., Khan, M. J., et al. (2018). Mechanisms of Cr (VI) resistance by endophytic *Sphingomonas* sp. LK11 and its Cr(VI) phytotoxic mitigating effects in soybean (*Glycine max* L.). *Ecotoxicol. Environ. Saf.* 164, 648–658. doi: 10.1016/J.ECOENV.2018.08.043

Blaha, D., Prigent-Combaret, C., Mirza, M. S., and Moënne-Loccoz, Y. (2006). Phylogeny of the 1-aminocyclopropane-1-carboxylic acid deaminase-encoding gene acdS in phytobeneficial and pathogenic *Proteobacteria* and relation with strain biogeography. *FEMS Microbiol. Ecol.* 56, 455–470. doi: 10.1111/J.1574-6941.2006.00082.X

Blumer, C., and Haas, D. (2000). Mechanism, regulation, and ecological role of bacterial cyanide biosynthesis. *Arch. Microbiol.* 173, 170–177. doi: 10.1007/S002039900127

Bogas, A. C., Ferreira, A. J., Araújo, W. L., Astolfi-Filho, S., Kitajima, E. W., Lacava, P. T., et al. (2015). Endophytic bacterial diversity in the phyllosphere of Amazon *Paullinia cupana* associated with asymptomatic and symptomatic anthracnose. *Springerplus* 4, 1–13. doi: 10.1186/S40064-015-1037-0/FIGURES/8

Bonilla, A., Sarria, A. L. F., Algar, E., Muñoz Ledesma, F. J., Ramos Solano, B., Fernandes, J. B., et al. (2014). Microbe associated molecular patterns from rhizosphere bacteria trigger germination and *Papaver somniferum* metabolism under greenhouse conditions. *Plant Physiol. Biochem.* 74, 133–140. doi: 10.1016/J.PLAPHY.2013.11.012

Brígido, C., Menéndez, E., Paço, A., Glick, B. R., Belo, A., Félix, M. R., et al. (2019). Mediterranean native leguminous plants: a reservoir of endophytic bacteria with potential to enhance chickpea growth under stress conditions. *Microorganisms* 7:392. doi: 10.3390/MICROORGANISMS7100392

Bulgarelli, D., Rott, M., Schlaeppi, K., Ver Loren van Themaat, E., Ahmadinejad, N., Assenza, F., et al. (2012). Revealing structure and assembly cues for *Arabidopsis* root-inhabiting bacterial microbiota. *Nature* 488, 91–95. doi: 10.1038/nature11336

Buschart, A., Sachs, S., Chen, X., Herglotz, J., Krause, A., and Reinhold-Hurek, B. (2012). Flagella mediate endophytic competence rather than act as MAMPS in rice–*Azoarcus* sp. Strain BH72 interactions. *Mol. Plant Microbe Interact.* 25, 191–199. doi: 10.1094/MPMI-05-11-0138

Butaite, E., Baumgartner, M., Wyder, S., and Kümmerli, R. (2017). Siderophore cheating and cheating resistance shape competition for iron in soil and freshwater *Pseudomonas* communities. *Nat. Commun.* 8, 414. doi: 10.1038/s41467-017-00509-4

Canarini, A., Kaiser, C., Merchant, A., Richter, A., and Wanek, W. (2019). Root exudation of primary metabolites: mechanisms and their roles in plant responses to environmental stimuli. *Front. Plant Sci.* 10:157. doi: 10.3389/FPLS.2019.00157/BIBTEX

Carvalhais, L. C., Muzzi, F., Tan, C. H., Hsien-Choo, J., and Schenk, P. M. (2013). Plant growth in *Arabidopsis* is assisted by compost soil-derived microbial communities. *Front. Plant Sci.* 4:235. doi: 10.3389/FPLS.2013.00235/ABSTRACT

Castanheira, N. L., Dourado, A. C., Pais, I., Semedo, J., Scotti-Campos, P., Borges, N., et al. (2017). Colonization and beneficial effects on annual ryegrass by mixed inoculation with plant growth promoting bacteria. *Microbiol. Res.* 198, 47–55. doi: 10.1016/J.MICRES.2017.01.009

Castanheira, N., Dourado, A. C., Kruz, S., Alves, P. I. L., Delgado-Rodríguez, A. I., Pais, I., et al. (2016). Plant growth-promoting *Burkholderia* species isolated from annual ryegrass in Portuguese soils. *J. Appl. Microbiol.* 120, 724–739. doi: 10.1111/JAM.13025

Chaudhary, A. K., Dhakal, D., and Sohng, J. K. (2013). An insight into the "-Omics" based engineering of streptomycetes for secondary metabolite overproduction. *Biomed. Res. Int.* 2013:968518. doi: 10.1155/2013/968518

Chen, Z. J., Sheng, X. F., He, L. Y., Huang, Z., and Zhang, W. H. (2013). Effects of root inoculation with bacteria on the growth, Cd uptake and bacterial communities associated with rape grown in Cd-contaminated soil. *J. Hazard. Mater.* 244–245, 709–717. doi: 10.1016/J.JHAZMAT.2012.10.063

Cohen, A. C., Bottini, R., Pontin, M., Berli, F. J., Moreno, D., Boccanlandro, H., et al. (2015). *Azospirillum brasilense* ameliorates the response of *Arabidopsis thaliana* to drought mainly via enhancement of ABA levels. *Physiol. Plant.* 153, 79–90. doi: 10.1111/PPL.12221

Dal Cortivo, C., Barion, G., Visioli, G., Mattarozzi, M., Mosca, G., and Vamerali, T. (2017). Increased root growth and nitrogen accumulation in common

wheat following PGPR inoculation: assessment of plant-microbe interactions by ESEM. *Agric. Ecosyst. Environ.* 247, 396–408. doi: 10.1016/J.AGEE.2017.07.006

Dalal, J. M., Kulkarni, N. S., and Bodhankar, M. G. (2015). Utilization of indigenous endophytic microbes for induction of systemic resistance (ISR) in soybean (*Glycine max* (L) Merril) against challenge inoculation with *F. oxysporum*. *Res. Biotechnol.* 6, 10–25.

de Souza, R., Ambrosini, A., and Passaglia, L. M. P. (2015). Plant growth-promoting bacteria as inoculants in agricultural soils. *Genet. Mol. Biol.* 38, 401–419. doi: 10.1590/S1415-475738420150053

Depluverez, S., Devos, S., and Devreese, B. (2016). The role of bacterial secretion systems in the virulence of gram-negative airway pathogens associated with cystic fibrosis. *Front. Microbiol.* 7:1336. doi: 10.3389/FMICB.2016.01336/BIBTEX

Dheeman, S., Maheshwari, K., Dubey, R. C., Kumar, S., Baliyan, N., Dhiman, S., et al. (2019). "Harnessing beneficial *Bacillus* in Productivity improvement of food security crops of Himalayan agro-climatic zones," in *Field Crops: Sustainable Management by PGPR*, eds D. K. Maheshwari and S. Dheeman (Cham: Springer), 105–143. doi: 10.1007/978-3-030-30926-8_5

Dhole, A., Shelat, H., Vyas, R., Jhala, Y., and Bhange, M. (2016). Endophytic occupation of legume root nodules by nifH-positive non-rhizobial bacteria, and their efficacy in the groundnut (*Arachis hypogaea*). *Ann. Microbiol.* 66, 1397–1407. doi: 10.1007/S13213-016-1227-1/FIGURES/3

Dhungana, S. A., and Itoh, K. (2019). Effects of co-inoculation of indole-3-acetic acid-producing and -degrading bacterial endophytes on plant growth. *Horticulturae* 5:17. doi: 10.3390/HORTICULTURAE5010017

Dimkpa, C. (2016). Endocytobiosis and cell research microbial siderophores: production, detection and application in agriculture and environment. *Endocytobiosis Cell Res.* 27, 7–16.

Dong, C. J., Wang, L. L., Li, Q., and Shang, Q. M. (2019). Bacterial communities in the rhizosphere, phyllosphere and endosphere of tomato plants. *PLoS One* 14:e0223847. doi: 10.1371/JOURNAL.PONE.0223847

dos Santos, M. L., Berlitz, D. L., Wiest, S. L. F., Schünemann, R., Knaak, N., and Fiuza, L. M. (2018). Benefits associated with the interaction of endophytic bacteria and plants. *Braz. Arch. Biol. Technol.* 61, 1–11. doi: 10.1590/1678-4324-2018160431

Du, C., and van Wezel, G. P. (2018). Mining for microbial gems: integrating proteomics in the postgenomic natural product discovery pipeline. *Proteomics* 18:1700332. doi: 10.1002/PMIC.201700332

Dubey, A., Saiyam, D., Kumar, A., Hashem, A., Abdullah, E. F., and Khan, M. L. (2021). Bacterial root endophytes: characterization of their competence and plant growth promotion in soybean (*Glycine max* (L.) Merr.) under drought stress. *Int. J. Environ. Res. Public Health* 18:931. doi: 10.3390/IJERPH18030931

Dubey, R. C., Khare, S., Kumar, P., and Maheshwari, D. K. (2014). Combined effect of chemical fertilisers and rhizosphere-competent Bacillus subtilis BSK17 on yield of *Cicer arietinum*. *Arch. Phytopathol. Plant Prot.* 47, 2305–2318. doi: 10.1080/03235408.2013.876744

Duca, D., Lorv, J., Patten, C. L., Rose, D., and Glick, B. R. (2014). Indole-3-acetic acid in plant-microbe interactions. *Antonie Van Leeuwenhoek* 106, 85–125. doi: 10.1007/S10482-013-0095-Y/FIGURES/8

Dudeja, S. S., Giri, R., Saini, R., Suneja-Madan, P., and Kothe, E. (2012). Interaction of endophytic microbes with legumes. *J. Basic Microbiol.* 52, 248–260. doi: 10.1002/JOBM.201100063

Dudeja, S. S., Suneja-Madan, P., Paul, M., Maheswari, R., and Kothe, E. (2021). Bacterial endophytes: molecular interactions with their hosts. *J. Basic Microbiol.* 61, 475–505. doi: 10.1002/JOBM.202000657

Egamberdieva, D., Wirth, S. J., Shurigin, V. V., Hashem, A., and Abd Allah, E. F. (2017). Endophytic bacteria improve plant growth, symbiotic performance of chickpea (*Cicer arietinum* L.) and induce suppression of root rot caused by *Fusarium solani* under salt stress. *Front. Microbiol.* 8:1887. doi: 10.3389/FMICB.2017.01887/BIBTEX

Ek-Ramos, M. J., Gomez-Flores, R., Orozco-Flores, A. A., Rodríguez-Padilla, C., González-Ochoa, G., and Tamez-Guerra, P. (2019). Bioactive products from plant-endophytic gram-positive bacteria. *Front. Microbiol.* 10:463. doi: 10.3389/FMICB.2019.00463/BIBTEX

Elbeltagy, A., Nishioka, K., Suzuki, H., Sato, T., Sato, Y. I., Morisaki, H., et al. (2000). Isolation and characterization of endophytic bacteria from wild and traditionally cultivated rice varieties. *Soil Sci. Plant Nutr.* 46, 617–629. doi: 10.1080/00380768.2000.10409127

Etesami, H., Alikhani, H. A., and Hosseini, H. M. (2015). Indole-3-acetic acid (IAA) production trait, a useful screening to select endophytic and rhizosphere competent bacteria for rice growth promoting agents. *MethodsX* 2, 72–78. doi: 10.1016/J.MEX.2015.02.008

Faddetta, T., Abbate, L., Alibrandi, P., Arancio, W., Siino, D., Strati, F., et al. (2021). The endophytic microbiota of *Citrus limon* is transmitted from seed to shoot highlighting differences of bacterial and fungal community structures. *Sci. Rep.* 11:7078. doi: 10.1038/s41598-021-86399-5

Fan, B., Chen, X. H., Budiharjo, A., Bleiss, W., Vater, J., and Borriss, R. (2011). Efficient colonization of plant roots by the plant growth promoting bacterium *Bacillus amyloliquefaciens* FZB42, engineered to express green fluorescent protein. *J. Biotechnol.* 151, 303–311. doi: 10.1016/J.JBIOTEC.2010.12.022

Fan, X., Yang, R., Qiu, S., Cai, X., Zou, H., and Hu, F. (2016). The Endo-β-1,4-glucanase of *Bacillus amyloliquefaciens* is required for optimum endophytic colonization of plants. *J. Microbiol. Biotechnol.* 26, 946–952. doi: 10.4014/JMB.1512.12055

Fard, E. M., Ghabooli, M., Mehri, N., and Bakhshi, B. (2017). Regulation of miR159 and miR396 mediated by *Piriformospora indica* confer drought tolerance in rice. *J. Plant Mol. Breed.* 5, 10–18. doi: 10.22058/JPMB.2017.60864.1129

Ferchichi, N., Toukabri, W., Boularess, M., Smaoui, A., Mhamdi, R., and Trabelsi, D. (2019). Isolation, identification and plant growth promotion ability of endophytic bacteria associated with lupine root nodule grown in Tunisian soil. *Arch. Microbiol.* 201, 1333–1349. doi: 10.1007/S00203-019-01702-3/FIGURES/5

Fernández-Llamosas, H., Díaz, E., and Carmona, M. (2021). Motility, adhesion and c-di-GMP influence the endophytic colonization of rice by *Azoarcus* sp. CIB. *Microorganisms* 9:554. doi: 10.3390/MICROORGANISMS9030554

Frank, A. C., Guzmán, J. P. S., and Shay, J. E. (2017). Transmission of bacterial endophytes. *Microorganisms* 5:70. doi: 10.3390/MICROORGANISMS5040070

Gao, H., Zhou, X., Gou, Z., Zhuo, Y., Fu, C., Liu, M., et al. (2010). Rational design for over-production of desirable microbial metabolites by precision engineering. *Antonie van Leeuwenhoek* 98, 151–163. doi: 10.1007/S10482-010-9442-4/FIGURES/5

Gao, Y., Liu, Q., Zang, P., Li, X., Ji, Q., He, Z., et al. (2015). An endophytic bacterium isolated from *Panax ginseng* C.A. Meyer enhances growth, reduces morbidity, and stimulates ginsenoside biosynthesis. *Phytochem. Lett.* 11, 132–138. doi: 10.1016/J.PHYTOL.2014.12.007

Gautam, K., Tripathi, J. K., Pareek, A., and Sharma, D. K. (2019). Growth and secretome analysis of possible synergistic interaction between green algae and cyanobacteria. *J. Biosci. Bioeng.* 127, 213–221. doi: 10.1016/J.JBIOSC.2018.07.005

Ghaffari, M. R., Mirzaei, M., Ghabooli, M., Khatabi, B., Wu, Y., Zabet-Moghaddam, M., et al. (2019). Root endophytic fungus *Piriformospora indica* improves drought stress adaptation in barley by metabolic and proteomic reprogramming. *Environ. Exp. Bot.* 157, 197–210. doi: 10.1016/J.ENVEXPBOT.2018.10.002

Glassner, H., Zchori-Fein, E., Yaron, S., Sessitsch, A., Sauer, U., and Compant, S. (2018). Bacterial niches inside seeds of *Cucumis melo* L. *Plant Soil* 422, 101–113. doi: 10.1007/S11104-017-3175-3/FIGURES/7

Glick, B. R. (2012). Plant growth-promoting bacteria: mechanisms and applications. *Scientifica (Cairo)* 2012, 1–15. doi: 10.6064/2012/963401

Glick, B. R. (2014). Bacteria with ACC deaminase can promote plant growth and help to feed the world. *Microbiol. Res.* 169, 30–39. doi: 10.1016/J.MICRES.2013.09.009

Glick, B. R., Cheng, Z., Czarny, J., and Duan, J. (2007). "Promotion of plant growth by ACC deaminase-producing soil bacteria," in *New Perspect. Approaches Plant Growth-Promoting Rhizobacteria Research*, eds P. A. H. M. Bakker, J. M. Raaijmakers, G. Bloemberg, M. Höfte, P. Lemanceau, and B. M. Cooke (Dordrecht: Springer), 329–339. doi: 10.1007/978-1-4020-6776-1_8

Gond, S. K., Bergen, M. S., Torres, M. S., White, J. F., and Kharwar, R. N. (2015). Effect of bacterial endophyte on expression of defense genes in Indian popcorn against *Fusarium moniliforme*. *Symbiosis* 66, 133–140. doi: 10.1007/S13199-015-0348-9/FIGURES/5

Gorai, P. S., Ghosh, R., Mandal, S., Ghosh, S., Chatterjee, S., Gond, S. K., et al. (2021). Bacillus siamensis CNE6- a multifaceted plant growth promoting endophyte of *Cicer arietinum* L. having broad spectrum antifungal activities and host colonizing potential. *Microbiol. Res.* 252:126859. doi: 10.1016/J.MICRES.2021.126859

Gupta, G., Panwar, J., Akhtar, M. S., and Jha, P. N. (2012). Endophytic nitrogen-fixing bacteria as biofertilizer. *Sustain. Agric. Rev.* 11, 183–221. doi: 10.1007/978-94-007-5449-2_8

Hamilton, C. E., Gundel, P. E., Helander, M., and Saikkonen, K. (2012). Endophytic mediation of reactive oxygen species and antioxidant activity in plants: a review. *Fungal Divers.* 54, 1–10. doi: 10.1007/S13225-012-0158-9

Hardoim, P. R., van Overbeek, L. S., and van Elsas, J. D. (2008). Properties of bacterial endophytes and their proposed role in plant growth. *Trends Microbiol.* 16, 463–471. doi: 10.1016/J.TIM.2008.07.008

Hardoim, P. R., van Overbeek, L. S., Berg, G., Pirttilä, A. M., Compant, S., Campisano, A., et al. (2015). The hidden world within plants: ecological and evolutionary considerations for defining functioning of microbial endophytes. *Microbiol. Mol. Biol. Rev.* 79, 293–320. doi: 10.1128/MMBR.00050-14

Hazarika, D. J., Goswami, G., Gautom, T., Parveen, A., Das, P., Barooah, M., et al. (2019). Lipopeptide mediated biocontrol activity of endophytic *Bacillus subtilis* against fungal phytopathogens. *BMC Microbiol.* 19:71. doi: 10.1186/S12866-019-1440-8/FIGURES/4

Hernández-Soberano, C., Ruíz-Herrera, L. F., and Valencia-Cantero, E. (2020). Endophytic bacteria *Arthrobacter agilis* UMCV2 and *Bacillus methylotrophicus* M4-96 stimulate achene germination, in vitro growth, and greenhouse yield of strawberry (*Fragaria* × *ananassa*). *Sci. Hortic. (Amsterdam)* 261:109005. doi: 10.1016/J.SCIENTA.2019.109005

Hu, H., Gao, Y., Li, X., Chen, S., Yan, S., and Tian, X. (2020). Identification and nematicidal characterization of proteases secreted by endophytic bacteria *Bacillus cereus* BCM2. *Phytopathology* 110, 336–344. doi: 10.1094/PHYTO-05-19-0164-R/ASSET/IMAGES/LARGE/PHYTO-05-19-0164-R_F7.JPEG

Iqbal, Z., Iqbal, M. S., Hashem, A., Abd-Allah, E. F., and Ansari, M. I. (2021). Plant defense responses to biotic stress and its interplay with fluctuating dark/light conditions. *Front. Plant Sci.* 12:297. doi: 10.3389/FPLS.2021.631810/BIBTEX

Irizarry, I., and White, J. F. (2018). Bacillus amyloliquefaciens alters gene expression, ROS production and lignin synthesis in cotton seedling roots. *J. Appl. Microbiol.* 124, 1589–1603. doi: 10.1111/JAM.13744

Issa, A., Esmaeel, Q., Sanchez, L., Courteaux, B., Guise, J. F., Gibon, Y., et al. (2018). Impacts of Paraburkholderia phytofirmans strain PsJN on tomato (*Lycopersicon esculentum* L.) under high temperature. *Front. Plant Sci.* 871:1397. doi: 10.3389/FPLS.2018.01397/BIBTEX

Jan, R., Khan, M. A., Asaf, S., Lubna, Lee, I. J., and Kim, K. M. (2019). Metal resistant endophytic bacteria reduces cadmium, nickel toxicity, and enhances expression of metal stress related genes with improved growth of *Oryza sativa*, via regulating its antioxidant machinery and endogenous hormones. *Plants* 8:363. doi: 10.3390/PLANTS8100363

Jawed, K., Yazdani, S. S., and Koffas, M. A. (2019). Advances in the development and application of microbial consortia for metabolic engineering. *Metab. Eng. Commun.* 9:e00095. doi: 10.1016/J.MEC.2019.E00095

Jha, P., Panwar, J., and Jha, P. N. (2018). Mechanistic insights on plant root colonization by bacterial endophytes: a symbiotic relationship for sustainable agriculture. *Environ. Sustain.* 1, 25–38. doi: 10.1007/S42398-018-0011-5

Johnston, P. R., Sutherland, P. W., and Joshee, S. (2006). Visualising endophytic fungi within leaves by detection of (1→3)-ß-d-glucans in fungal cell walls. *Mycologist* 20, 159–162. doi: 10.1016/J.MYCOL.2006.10.003

Kandel, S. L., Joubert, P. M., and Doty, S. L. (2017a). Bacterial endophyte colonization and distribution within plants. *Microorganisms* 5:77. doi: 10.3390/MICROORGANISMS5040077

Kandel, S. L., Firrincieli, A., Joubert, P. M., Okubara, P. A., Leston, N. D., McGeorge, K. M., et al. (2017b). An in vitro study of bio-control and plant growth promotion potential of salicaceae endophytes. *Front. Microbiol.* 8:386. doi: 10.3389/FMICB.2017.00386/BIBTEX

Kandel, S. L., Herschberger, N., Kim, S. H., and Doty, S. L. (2015). Diazotrophic endophytes of poplar and willow for growth promotion of rice plants in nitrogen-limited conditions. *Crop Sci.* 55, 1765–1772. doi: 10.2135/CROPSCI2014.08.0570

Kaul, S., Sharma, T., and Dhar, M. K. (2016). "Omics" tools for better understanding the plant–endophyte interactions. *Front. Plant Sci.* 7:955. doi: 10.3389/FPLS.2016.00955/BIBTEX

Kawalekar, J. (2013). Role of biofertilizers and biopesticides for sustainable agriculture. *J. Bio Innov.* 2, 73–78.

Kawasaki, A., Donn, S., Ryan, P. R., Mathesius, U., Devilla, R., Jones, A., et al. (2016). Microbiome and exudates of the root and rhizosphere of *Brachypodium distachyon*, a model for wheat. *PLoS One* 11:e0164533. doi: 10.1371/JOURNAL.PONE.0164533

Khan, A., Sirajuddin, Zhao, X. Q., Javed, M. T., Khan, K. S., Bano, A., et al. (2016). *Bacillus pumilus* enhances tolerance in rice (*Oryza sativa* L.) to combined stresses of NaCl and high boron due to limited uptake of Na^+. *Environ. Exp. Bot.* 124, 120–129. doi: 10.1016/J.ENVEXPBOT.2015.12.011

Khan, M. A., Asaf, S., Khan, A. L., Jan, R., Kang, S. M., Kim, K. M., et al. (2020). Thermotolerance effect of plant growth-promoting *Bacillus cereus* SA1 on soybean during heat stress. *BMC Microbiol.* 20:175. doi: 10.1186/S12866-020-01822-7/FIGURES/6

Khan, M. S., Gao, J., Chen, X., Zhang, M., Yang, F., Du, Y., et al. (2020). Isolation and characterization of plant growth-promoting endophytic bacteria *Paenibacillus polymyxa* SK1 from *Lilium lancifolium*. *Biomed. Res. Int.* 2020:8650957. doi: 10.1155/2020/8650957

Khan, Z., and Doty, S. L. (2009). Characterization of bacterial endophytes of sweet potato plants. *Plant Soil* 322, 197–207. doi: 10.1007/S11104-009-9908-1/TABLES/3

Khan, Z., Rho, H., Firrincieli, A., Hung, S. H., Luna, V., Masciarelli, O., et al. (2016). Growth enhancement and drought tolerance of hybrid poplar upon inoculation with endophyte consortia. *Curr. Plant Biol.* 6, 38–47. doi: 10.1016/J.CPB.2016.08.001

Khare, E., Mishra, J., and Arora, N. K. (2018). Multifaceted interactions between endophytes and plant: developments and Prospects. *Front. Microbiol.* 9:2732. doi: 10.3389/FMICB.2018.02732/BIBTEX

Kilam, D., Saifi, M., Abdin, M. Z., Agnihotri, A., and Varma, A. (2017). Endophytic root fungus *Piriformospora indica* affects transcription of steviol biosynthesis genes and enhances production of steviol glycosides in *Stevia rebaudiana*. *Physiol. Mol. Plant Pathol.* 97, 40–48. doi: 10.1016/J.PMPP.2016.12.003

Kim, N., Jeon, H. W., Mannaa, M., Jeong, S. I., Kim, J., Kim, J., et al. (2019). Induction of resistance against pine wilt disease caused by Bursaphelenchus xylophilus using selected pine endophytic bacteria. *Plant Pathol.* 68, 434–444. doi: 10.1111/PPA.12960

Kowalski, K., Kingsley, K., Butterworth, S., Elmore, M., Brindisi, L., and White, J. (2018). *Endobiome Interference" As a Strategy to Curtail Aggressiveness of Invasive Plant Species*. Available online at: https://eco.confex.com/eco/2018/meetingapp.cgi/Paper/72836 (Accessed January 4, 2022).

Kuldau, G. A., and Yates, I. E. (2000). "Evidence for *Fusarium* endophytes in cultivated and wild plants," in *Microbial endophytes*, eds C. W. Bacon and J. F. White Jr. (New York, NY: Marcel Dekker), 85–117.

Kumar, A., Droby, S., Singh, V. K., Singh, S. K., and White, J. F. (2020). Entry, colonization, and distribution of endophytic microorganisms in plants. *Microb. Endophytes* 1–33. doi: 10.1016/B978-0-12-819654-0.00001-6

Kumar, A., Vandana, Singh, M., Singh, P. P., Singh, S. K., Singh, P. K., et al. (2016). Isolation of plant growth promoting rhizobacteria and their impact on growth and curcumin content in *Curcuma longa* L. *Biocatal. Agric. Biotechnol.* 8, 1–7. doi: 10.1016/J.BCAB.2016.07.002

Kumar, V., Jain, L., Jain, S. K., Chaturvedi, S., and Kaushal, P. (2020). Bacterial endophytes of rice (*Oryza sativa* L.) and their potential for plant growth promotion and antagonistic activities. *S. Af. J. Bot.* 134, 50–63. doi: 10.1016/J.SAJB.2020.02.017

Kusari, S., Lamshöft, M., Kusari, P., Gottfried, S., Zühlke, S., Louven, K., et al. (2014). Endophytes are hidden producers of maytansine in *Putterlickia* roots. *J. Nat. Prod.* 77, 2577–2584. doi: 10.1021/NP500219A/SUPPL_FILE/NP500219A_SI_001.PDF

Labanca, E. R. G., Andrade, S. A. L., Kuramae, E. E., and Silveira, A. P. D. (2020). The modulation of sugarcane growth and nutritional profile under aluminum stress is dependent on beneficial endophytic bacteria and plantlet origin. *Appl. Soil Ecol.* 156, 103715. doi: 10.1016/J.APSOIL.2020.103715

Lacava, P. T., Silva-Stenico, M. E., Araújo, W. L., Simionato, A. V. C., Carrilho, E., Siu, M. T., et al. (2008). Detection of siderophores in endophytic bacteria *Methylobacterium* spp. associated with *Xylella fastidiosa* subsp. pauca. *Pesqui. Agropecuária Bras.* 43, 521–528. doi: 10.1590/S0100-204X2008000400011

Lamers, J., Van Der Meer, T., and Testerink, C. (2020). How plants sense and respond to stressful environments. *Plant Physiol.* 182, 1624–1635. doi: 10.1104/PP.19.01464

Lareen, A., Burton, F., and Schäfer, P. (2016). Plant root-microbe communication in shaping root microbiomes. *Plant Mol. Biol.* 90, 575–587. doi: 10.1007/S11103-015-0417-8

Lastochkina, O., Garshina, D., Allagulova, C., Fedorova, K., Koryakov, I., and Vladimirova, A. (2020). Application of endophytic *Bacillus subtilis* and salicylic acid to improve wheat growth and tolerance under combined drought and *Fusarium* root rot stresses. *Agronomy* 10:1343. doi: 10.3390/agronomy10091343

Leonhardt, T., Sácky, J., Šimek, P., Šantrùèek, J., and Kotrba, P. (2014). Metallothionein-like peptides involved in sequestration of Zn in the Zn-accumulating ectomycorrhizal fungus *Russula atropurpurea*. *Metallomics* 6, 1693–1701. doi: 10.1039/C4MT00141A

Li, Y., Cheng, C., and An, D. (2017). Characterisation of endophytic bacteria from a desert plant *Lepidium perfoliatum* L. *Plant Prot. Sci.* 53, 32–43. doi: 10.17221/14/2016-PPS

Lima, A. S., Prieto, K. R., Santos, C. S., Paula Valerio, H., Garcia-Ochoa, E. Y., Huerta-Robles, A., et al. (2018). In-vivo electrochemical monitoring of H_2O_2 production induced by root-inoculated endophytic bacteria in *Agave tequilana* leaves. *Biosens. Bioelectron.* 99, 108–114. doi: 10.1016/J.BIOS.2017.07.039

Liscombe, D. K., and Facchini, P. J. (2008). Evolutionary and cellular webs in benzylisoquinoline alkaloid biosynthesis. *Curr. Opin. Biotechnol.* 19, 173–180. doi: 10.1016/J.COPBIO.2008.02.012

Liu, H., Zhang, L., Meng, A., Zhang, J., Xie, M., Qin, Y., et al. (2017a). Isolation and molecular identification of endophytic diazotrophs from seeds and stems of three cereal crops. *PLoS One* 12:e0187383. doi: 10.1371/JOURNAL.PONE.0187383

Liu, H., Carvalhais, L. C., Crawford, M., Singh, E., Dennis, P. G., Pieterse, C. M. J., et al. (2017b). Inner plant values: diversity, colonization and benefits from endophytic bacteria. *Front. Microbiol.* 8:2552. doi: 10.3389/FMICB.2017.02552/BIBTEX

Liu, W., Sun, Y., Shen, R., Dang, X., Liu, X., Sui, F., et al. (2018). A chemotaxis-like pathway of *Azorhizobium caulinodans* controls flagella-driven motility, which regulates biofilm formation, exopolysaccharide biosynthesis, and competitive nodulation. *Mol. Plant Microbe Interact.* 31, 737–749. doi: 10.1094/MPMI-12-17-0290-R

Liu, X., Liu, W., Sun, Y., Xia, C., Elmerich, C., and Xie, Z. (2018). A cheZ-like gene in Azorhizobium caulinodans is a key gene in the control of chemotaxis and colonization of the host plant. *Appl. Environ. Microbiol.* 84, 1827–1844. doi: 10.1128/AEM.01827-17

Lodewyckx, C., Vangronsveld, J., Porteous, F., Moore, E. R. B., Taghavi, S., Mezgeay, M., et al. (2002). Endophytic bacteria and their potential applications. *Crit. Rev. Plant Sci.* 21, 583–606. doi: 10.1080/0735-260291044377

Lòpez-Fernàndez, S., Sonego, P., Moretto, M., Pancher, M., Engelen, K., Pertot, I., et al. (2015). Whole-genome comparative analysis of virulence genes unveils similarities and differences between endophytes and other symbiotic bacteria. *Front. Microbiol.* 6:419. doi: 10.3389/FMICB.2015.00419/ABSTRACT

Lugtenberg, B., and Kamilova, F. (2009). Plant-growth-promoting rhizobacteria. *Annu. Rev. Microbiol.* 63, 541–556. doi: 10.1146/ANNUREV.MICRO.62.081307.162918

Maela, P. M. (2019). Current understanding of bacterial endophytes, their diversity, colonization and their roles in promoting plant growth. *Appl. Microbiol.* 5, 1–12. doi: 10.4172/2471-9315.1000157

Mahaffee, W. F. (1994). Endophytic colonization of *Phaseolus vulgaris* by *Pseudomonas fluorescens* strain 89B-27 and *Enterobacter asburiae* strain JM22. *Improv. Plant Product. Rhizobacteria*. Available online at: https://ci.nii.ac.jp/naid/10015091111/ (accessed March 29, 2022).

Maheshwari, R., Bhutani, N., Bhardwaj, A., and Suneja, P. (2019a). Functional diversity of cultivable endophytes from *Cicer arietinum* and *Pisum sativum*: bioprospecting their plant growth potential. *Biocatal. Agric. Biotechnol.* 20:101229. doi: 10.1016/J.BCAB.2019.101229

Maheshwari, R., Bhutani, N., and Suneja, P. (2019b). Screening and characterization of siderophore producing endophytic bacteria from *Cicer arietinum* and *Pisum sativum* plants. *J. Appl. Biol. Biotechnol.* 7, 7–14. doi: 10.7324/JABB.2019.70502

Maheshwari, R., Bhutani, N., and Suneja, P. (2020). Isolation and characterization of ACC deaminase producing endophytic *Bacillus mojavensis* PRN2 from *Pisum sativum*. *Iran. J. Biotechnol.* 18:e2308. doi: 10.30498/IJB.2020.137279.2308

Maheshwari, R., Bhutani, N., Kumar, P., and Suneja, P. (2021). Plant growth promoting potential of multifarious endophytic *Pseudomonas* lini strain isolated from *Cicer arietinum* L. *Isr. J. Plant Sci.* 1, 1–11. doi: 10.1163/22238980-BJA10047

Mao, J., Gong, M., and Guan, Q. (2019). Induced disease resistance of endophytic bacteria REB01 to bacterial blight of rice. *AIP Conf. Proc.* 2079:020017. doi: 10.1063/1.5092395

Marques, A. P. G. C., Pires, C., Moreira, H., Rangel, A. O. S. S., and Castro, P. M. L. (2010). Assessment of the plant growth promotion abilities of six bacterial isolates using *Zea mays* as indicator plant. *Soil Biol. Biochem.* 42, 1229–1235. doi: 10.1016/J.SOILBIO.2010.04.014

Martínez-Gil, M., Yousef-Coronado, F., and Espinosa-Urgel, M. (2010). LapF, the second largest *Pseudomonas putida* protein, contributes to plant root colonization and determines biofilm architecture. *Mol. Microbiol.* 77, 549–561. doi: 10.1111/J.1365-2958.2010.07249.X

Mastan, A., Vivek Babu, C. S., Hiremath, C., Srinivas, K. V. N. S., Kumar, A. N., and Kumar, J. K. (2019). Treatments with native *Coleus forskohlii* endophytes improve fitness and secondary metabolite production of some medicinal and aromatic plants. *Int. Microbiol.* 23, 345–354. doi: 10.1007/S10123-019-00108-X

Meneses, C. H. S. G., Rouws, L. F. M., Simões-Araújo, J. L., Vidal, M. S., and Baldani, J. I. (2011). Exopolysaccharide production is required for biofilm formation and plant colonization by the nitrogen-fixing endophyte *Gluconacetobacter diazotrophicus*. *Mol. Plant Microbe Interact.* 24, 1448–1458. doi: 10.1094/MPMI-05-11-0127

Meneses, C., Gonçalves, T., Alquéres, S., Rouws, L., Serrato, R., Vidal, M., et al. (2017). Gluconacetobacter diazotrophicus exopolysaccharide protects bacterial cells against oxidative stress in vitro and during rice plant colonization. *Plant Soil* 416, 133–147. doi: 10.1007/S11104-017-3201-5/FIGURES/8

Mengistu, A. A. (2020). Endophytes: colonization, behaviour, and their role in defense mechanism. *Int. J. Microbiol.* 2020:6927219. doi: 10.1155/2020/6927219

Miliute, I., Buzaite, O., Baniulis, D., Baniulis, D., and Stanys, V. (2015). Bacterial endophytes in agricultural crops and their role in stress tolerance: a review. *Zemdirb. Agric.* 102, 465–478. doi: 10.13080/z-a.2015.102.060

Minamino, T., Morimoto, Y. V., Hara, N., Aldridge, P. D., and Namba, K. (2016). The bacterial flagellar type III export gate complex is a dual fuel engine that can use Both H^+ and Na^+ for flagellar protein export. *PLoS Pathog.* 12:e1005495. doi: 10.1371/JOURNAL.PPAT.1005495

Mishra, S., Sahu, P. K., Agarwal, V., and Singh, N. (2021). Exploiting endophytic microbes as micro-factories for plant secondary metabolite production. *Appl. Microbiol. Biotechnol.* 105, 6579–6596. doi: 10.1007/S00253-021-11527-0

Mohite, B. (2013). Isolation and characterization of indole acetic acid (IAA) producing bacteria from rhizospheric soil and its effect on plant growth. *J. Soil Sci. Plant Nutr.* 13, 638–649. doi: 10.4067/S0718-95162013005000051

Montaño López, J., Duran, L., and Avalos, J. L. (2022). Physiological limitations and opportunities in microbial metabolic engineering. *Nat. Rev. Microbiol.* 20, 35–48. doi: 10.1038/s41579-021-00600-0

Monteiro, R. A., Balsanelli, E., Tuleski, T., Faoro, H., Cruz, L. M., Wassem, R., et al. (2012). Genomic comparison of the endophyte *Herbaspirillum seropedicae* SmR1 and the phytopathogen *Herbaspirillum rubrisubalbicans* M1 by suppressive subtractive hybridization and partial genome sequencing. *FEMS Microbiol. Ecol.* 80, 441–451. doi: 10.1111/J.1574-6941.2012.01309.X

Motooka, D., Fujimoto, K., Tanaka, R., Yaguchi, T., Gotoh, K., Maeda, Y., et al. (2017). Fungal ITS1 deep-sequencing strategies to reconstruct the composition of a 26-species community and evaluation of the gut mycobiota of healthy Japanese individuals. *Front. Microbiol.* 8:238. doi: 10.3389/FMICB.2017.00238/BIBTEX

Mukherjee, A., Singh, B. K., and Verma, J. P. (2020). Harnessing chickpea (*Cicer arietinum* L.) seed endophytes for enhancing plant growth attributes and bio-controlling against *Fusarium* sp. *Microbiol. Res.* 237:126469. doi: 10.1016/J.MICRES.2020.126469

Naveed, M., Mitter, B., Yousaf, S., Pastar, M., Afzal, M., and Sessitsch, A. (2013). The endophyte *Enterobacter* sp. FD17: a maize growth enhancer selected based on rigorous testing of plant beneficial traits and colonization characteristics. *Biol. Fertil. Soils* 50, 249–262. doi: 10.1007/S00374-013-0854-Y/TABLES/5

Neumann, S., Grosse, K., and Sourjik, V. (2012). Chemotactic signaling via carbohydrate phosphotransferase systems in *Escherichia coli*. *Proc. Natl. Acad. Sci. U.S.A.* 109, 12159–12164. doi: 10.1073/PNAS.1205307109/-/DCSUPPLEMENTAL

Newman, M. A., Sundelin, T., Nielsen, J. T., and Erbs, G. (2013). MAMP (microbe-associated molecular pattern) triggered immunity in plants. *Front. Plant Sci.* 4:139. doi: 10.3389/FPLS.2013.00139/BIBTEX

Nguyen, Q. T., Merlo, M. E., Medema, M. H., Jankevics, A., Breitling, R., and Takano, E. (2012). Metabolomics methods for the synthetic biology of secondary metabolism. *FEBS Lett.* 586, 2177–2183. doi: 10.1016/J.FEBSLET.2012.02.008

Nicolson, G. L. (2014). The Fluid—Mosaic Model of Membrane Structure: Still relevant to understanding the structure, function and dynamics of biological membranes after more than 40 years. *Biochim. Biophys. Acta Biomembr.* 1838, 1451–1466. doi: 10.1016/J.BBAMEM.2013.10.019

Oteino, N., Lally, R. D., Kiwanuka, S., Lloyd, A., Ryan, D., Germaine, K. J., et al. (2015). Plant growth promotion induced by phosphate solubilizing endophytic *Pseudomonas* isolates. *Front. Microbiol.* 6:745. doi: 10.3389/FMICB.2015.00745/BIBTEX

Padmaperuma, G., Kapoore, R. V., Gilmour, D. J., and Vaidyanathan, S. (2017). Microbial consortia: a critical look at microalgae co-cultures for enhanced biomanufacturing. *Crit. Rev. Biotechnol.* 38, 690–703. doi: 10.1080/07388551.2017.1390728

Palazzotto, E., and Weber, T. (2018). Omics and multi-omics approaches to study the biosynthesis of secondary metabolites in microorganisms. *Curr. Opin. Microbiol.* 45, 109–116. doi: 10.1016/J.MIB.2018.03.004

Pandey, P. K., Samanta, R., and Yadav, R. N. S. (2015). Plant beneficial endophytic bacteria from the ethnomedicinal *Mussaenda roxburghii* (Akshap) of Eastern Himalayan Province, India. *Adv. Biol.* 2015, 1–8. doi: 10.1155/2015/580510

Pankievicz, V. C. S., Camilios-Neto, D., Bonato, P., Balsanelli, E., Tadra-Sfeir, M. Z., Faoro, H., et al. (2016). RNA-seq transcriptional profiling of *Herbaspirillum seropedicae* colonizing wheat (*Triticum aestivum*) roots. *Plant Mol. Biol.* 90, 589–603. doi: 10.1007/s11103-016-0430-6

Passari, A. K., Mishra, V. K., Leo, V. V., Gupta, V. K., and Singh, B. P. (2016). Phytohormone production endowed with antagonistic potential and plant growth promoting abilities of culturable endophytic bacteria isolated from *Clerodendrum colebrookianum* Walp. *Microbiol. Res.* 193, 57–73. doi: 10.1016/J.MICRES.2016.09.006

Patel, J. K., and Archana, G. (2017). Diverse culturable diazotrophic endophytic bacteria from Poaceae plants show cross-colonization and plant growth promotion in wheat. *Plant Soil* 417, 99–116. doi: 10.1007/S11104-017-3244-7/FIGURES/5

Patel, J. K., Gohel, K., Patel, H., and Solanki, T. (2021). Wheat growth dependent succession of culturable endophytic bacteria and their plant growth promoting traits. *Curr. Microbiol.* 78, 4103–4114. doi: 10.1007/S00284-021-02668-6/FIGURES/2

Pimentel Esposito-Polesi, N., Fiori De Abreu-Tarazi, M., Vieira De Almeida, C., Tsai, S. M., and De Almeida, M. (2017). Investigation of endophytic bacterial community in supposedly axenic cultures of pineapple and orchids with evidence on abundant intracellular bacteria. *Curr. Microbiol.* 74, 103–113. doi: 10.1007/s00284-016-1163-0

Plett, J. M., and Martin, F. M. (2018). Know your enemy, embrace your friend: using omics to understand how plants respond differently to pathogenic and mutualistic microorganisms. *Plant J.* 93, 729–746. doi: 10.1111/TPJ.13802

Ponpandian, L. N., Rim, S. O., Shanmugam, G., Jeon, J., Park, Y. H., Lee, S. K., et al. (2019). Phylogenetic characterization of bacterial endophytes from four *Pinus* species and their nematicidal activity against the pine wood nematode. *Sci. Rep.* 9:12457. doi: 10.1038/s41598-019-48745-6

Pootakham, W., Mhuantong, W., Yoocha, T., Putchim, L., Sonthirod, C., Naktang, C., et al. (2017). High resolution profiling of coral-associated bacterial communities using full-length 16S rRNA sequence data from PacBio SMRT sequencing system. *Sci. Rep.* 7:2774. doi: 10.1038/s41598-017-03139-4

Qiang, X., Ding, J., Lin, W., Li, Q., Xu, C., Zheng, Q., et al. (2019). Alleviation of the detrimental effect of water deficit on wheat (*Triticum aestivum* L.) growth by an indole acetic acid-producing endophytic fungus. *Plant Soil* 439, 373–391. doi: 10.1007/S11104-019-04028-7/FIGURES/10

Qin, D., Wang, L., Han, M., Wang, J., Song, H., Yan, X., et al. (2018). Effects of an endophytic fungus *Umbelopsis dimorphaon* the secondary metabolites of host-plant *Kadsura angustifolia*. *Front. Microbiol.* 9:2845. doi: 10.3389/FMICB.2018.02845/BIBTEX

Ramanujam, B., Renuka, S., and Shylesha, A. N. (2016). Electron microscopic studies for confirmation of endophytic colonization of *Beauveria bassiana* in maize. *J. Pure Appl. Microbiol.* 10, 3017–3021. doi: 10.22207/JPAM.10.4.72

Rana, K. L., Kour, D., Kaur, T., Devi, R., Yadav, A. N., Yadav, N., et al. (2020). Endophytic microbes: biodiversity, plant growth-promoting mechanisms and potential applications for agricultural sustainability Kusam Lata Rana and Divjot Kour contributed equally to the present review. *Antonie Van Leeuwenhoek* 113, 1075–1107. doi: 10.1007/s10482-020-01429-y

Rani, S., Kumar, P., and Suneja, P. (2021). Biotechnological interventions for inducing abiotic stress tolerance in crops. *Plant Gene* 27:100315. doi: 10.1016/J.PLGENE.2021.100315

Rashid, S., Charles, T. C., and Glick, B. R. (2012). Isolation and characterization of new plant growth-promoting bacterial endophytes. *Appl. Soil Ecol.* 61, 217–224. doi: 10.1016/J.APSOIL.2011.09.011

Reimer, A., Maffenbeier, V., Dubey, M., Sentchilo, V., Tavares, D., Gil, M. H., et al. (2017). Complete alanine scanning of the *Escherichia coli* RbsB ribose binding protein reveals residues important for chemoreceptor signaling and periplasmic abundance. *Sci. Rep.* 7:8245. doi: 10.1038/s41598-017-08035-5

Reinhold-Hurek, B., and Hurek, T. (2011). Living inside plants: bacterial endophytes. *Curr. Opin. Plant Biol.* 14, 435–443. doi: 10.1016/J.PBI.2011.04.004

Ríos-Ruiz, W. F., Alfredo Valdez-Nuñez, R., Bedmar, E. J., Castellano-Hinojosa, A., Ríos-Ruiz, W. F., Valdez-Nuñez, R. A., et al. (2019). "Utilization of endophytic bacteria isolated from legume root nodules for plant growth promotion," in *Field Crops: Sustainable Management by PGPR*, eds D. K. Maheshwari and S. Dheeman (Cham: Springer), 145–176. doi: 10.1007/978-3-030-30926-8_6

Robertson-Albertyn, S., Terrazas, R. A., Balbirnie, K., Blank, M., Janiak, A., Szarejko, I., et al. (2017). Root hair mutations displace the barley rhizosphere microbiota. *Front. Plant Sci.* 8:1094. doi: 10.3389/FPLS.2017.01094/BIBTEX

Ruiz, J. A., Bernar, E. M., and Jung, K. (2015). Production of siderophores increases resistance to fusaric acid in *Pseudomonas* protegens Pf-5. *PLoS One* 10:e0117040. doi: 10.1371/JOURNAL.PONE.0117040

Saleh, D., Sharma, M., Seguin, P., and Jabaji, S. (2020). Organic acids and root exudates of *Brachypodium distachyon*: effects on chemotaxis and biofilm formation of endophytic bacteria. *Can. J. Microbiol.* 66, 562–575. doi: 10.1139/cjm-2020-0041

Samanta, D., Widom, J., Borbat, P. P., Freed, J. H., and Crane, B. R. (2016). Bacterial energy sensor aer modulates the activity of the chemotaxis kinase CheA based on the redox state of the flavin cofactor *. *J. Biol. Chem.* 291, 25809–25814. doi: 10.1074/JBC.C116.757492

Sangwan, P., Raj, K., Wati, L., and Kumar, A. (2021). Isolation and evaluation of bacterial endophytes against *Sclerospora graminicola* (Sacc.) schroet, the causal of pearl millet downy mildew. *Egypt. J. Biol. Pest Control* 31, 1–11. doi: 10.1186/S41938-021-00468-5/TABLES/4

Santoyo, G., Moreno-Hagelsieb, G., del Carmen Orozco-Mosqueda, M., and Glick, B. R. (2016). Plant growth-promoting bacterial endophytes. *Microbiol. Res.* 183, 92–99. doi: 10.1016/J.MICRES.2015.11.008

Sapre, S., Gontia-Mishra, I., and Tiwari, S. (2018). Klebsiella sp. confers enhanced tolerance to salinity and plant growth promotion in oat seedlings (*Avena sativa*). *Microbiol. Res.* 206, 25–32. doi: 10.1016/J.MICRES.2017.09.009

Sarkar, A., Pramanik, K., Mitra, S., Soren, T., and Maiti, T. K. (2018). Enhancement of growth and salt tolerance of rice seedlings by ACC deaminase-producing Burkholderia sp. MTCC 12259. *J. Plant Physiol.* 231, 434–442. doi: 10.1016/J.JPLPH.2018.10.010

Scharf, B. E., Hynes, M. F., and Alexandre, G. M. (2016). Chemotaxis signaling systems in model beneficial plant-bacteria associations. *Plant Mol. Biol.* 90, 549–559. doi: 10.1007/s11103-016-0432-4

Schmidt, R., Köberl, M., Mostafa, A., Ramadan, E. M., Monschein, M., Jensen, K. B., et al. (2014). Effects of bacterial inoculants on the indigenous microbiome and secondary metabolites of chamomile plants. *Front. Microbiol.* 5:64. doi: 10.3389/FMICB.2014.00064/ABSTRACT

Senthilkumar, M., Pushpakanth, P., Arul Jose, P., Krishnamoorthy, R., and Anandham, R. (2021). Diversity and functional characterization of endophytic *Methylobacterium* isolated from banana cultivars of South India and its impact on early growth of tissue culture banana plantlets. *J. Appl. Microbiol.* 131, 2448–2465. doi: 10.1111/JAM.15112

Sessitsch, A., Hardoim, P., Döring, J., Weilharter, A., Krause, A., Woyke, T., et al. (2011). Functional characteristics of an endophyte community colonizing rice roots as revealed by metagenomic analysis. *Mol. Plant Microbe Interact.* 25, 28–36. doi: 10.1094/MPMI-08-11-0204

Shah, A. U., Rajab, H., Jalal, A., Ajmal, M., Bangash, S. A. K., Ahmad, D., et al. (2020). Inoculation of *Brassica napus* L. genotypes with endophytic bacteria promote growth and alleviate cadmium toxicity. *APS J. Anim. Plant Sci.* 30, 1187–1193.

Shanmugam, G., Lee, S. K., and Jeon, J. (2018). Identification of potential nematicidal compounds against the pine wood nematode, *Bursaphelenchus xylophilus* through an in silico approach. *Molecules.* 23:1828. doi: 10.3390/MOLECULES23071828

Sharifazizi, M., Harighi, B., and Sadeghi, A. (2017). Evaluation of biological control of *Erwinia amylovora*, causal agent of fire blight disease of pear by antagonistic bacteria. *Biol. Control* 104, 28–34. doi: 10.1016/J.BIOCONTROL.2016.10.007

Sharma, H., Rai, A. K., Dahiya, D., Chettri, R., Nigam, P. S., Sharma, H., et al. (2021). Exploring endophytes for in vitro synthesis of bioactive compounds similar to metabolites produced in vivo by host plants. *AIMS Microbiol.* 7, 175–199. doi: 10.3934/MICROBIOL.2021012

Sharma, P., Kharkwal, A. C., Abdin, M. Z., and Varma, A. (2014). *Piriformospora indica* improves micropropagation,growth and phytochemical content of *Aloe vera* L. plants. *Symbiosis* 64, 11–23. doi: 10.1007/S13199-014-0298-7/FIGURES/8

Sharma, S. B., Sayyed, R. Z., Trivedi, M. H., and Gobi, T. A. (2013). Phosphate solubilizing microbes: sustainable approach for managing phosphorus deficiency in agricultural soils. *Springerplus* 2, 1–14. doi: 10.1186/2193-1801-2-587/FIGURES/3

Shastry, R. P., Dolan, S. K., Abdelhamid, Y., Vittal, R. R., and Welch, M. (2018). Purification and characterisation of a quorum quenching AHL-lactonase from the endophytic bacterium *Enterobacter* sp. CS66. *FEMS Microbiol. Lett.* 365:54. doi: 10.1093/FEMSLE/FNY054

Sheoran, N., Kumar, A., Munjal, V., Nadakkakath, A. V., and Eapen, S. J. (2016). *Pseudomonas putida* BP25 alters root phenotype and triggers salicylic acid signaling as a feedback loop in regulating endophytic colonization in *Arabidopsis thaliana*. *Physiol. Mol. Plant Pathol.* 93, 99–111. doi: 10.1016/J.PMPP.2016.01.008

Shi, P., Zhu, K., Zhang, Y., and Chai, T. (2016). Growth and cadmium accumulation of *Solanum nigrum* L. Seedling were enhanced by heavy metal-tolerant strains of *Pseudomonas aeruginosa*. *Water. Air Soil Pollut.* 227, 1–11. doi: 10.1007/S11270-016-3167-6/FIGURES/4

Shidore, T., Dinse, T., Öhrlein, J., Becker, A., and Reinhold-Hurek, B. (2012). Transcriptomic analysis of responses to exudates reveal genes required for rhizosphere competence of the endophyte *Azoarcus* sp. strain BH72. *Environ. Microbiol.* 14, 2775–2787. doi: 10.1111/J.1462-2920.2012.02777.X

Shinogi, T., Suzuki, T., Kurihara, T., Narusaka, Y., Park, P., Shinogi, T., et al. (2003). Microscopic detection of reactive oxygen species generation in the compatible and incompatible interactions of *Alternaria alternata* Japanese pear pathotype and host plants. *J. Gen. Plant Pathol.* 69, 7–16. doi: 10.1007/S10327-002-0013-Z

Singer, E., Bushnell, B., Coleman-Derr, D., Bowman, B., Bowers, R. M., Levy, A., et al. (2016). High-resolution phylogenetic microbial community profiling. *ISME J.* 10, 2020–2032. doi: 10.1038/ismej.2015.249

Singh, B., and Sharma, R. A. (2016). Yield enhancement of phytochemicals by *Azotobacter chroococcum* biotization in hairy roots of *Arnebia hispidissima*. *Ind. Crops Prod.* 81, 169–175. doi: 10.1016/J.INDCROP.2015.11.068

Singh, R. P., Shelke, G. M., Kumar, A., and Jha, P. N. (2015). Biochemistry and genetics of ACC deaminase: a weapon to "stress ethylene" produced in plants. *Front. Microbiol.* 6:937. doi: 10.3389/FMICB.2015.00937/BIBTEX

Singh nee' Nigam, P. (2009). "Production of bioactive secondary metabolites," in *Biotechnology for Agro-Industrial Residues Utilisation*, eds P. Singh nee' Nigam and A. Pandey (Dordrecht: Springer), 129–145. doi: 10.1007/978-1-4020-9942-7_7

Soldan, R., Mapelli, F., Crotti, E., Schnell, S., Daffonchio, D., Marasco, R., et al. (2019). Bacterial endophytes of mangrove propagules elicit early establishment of the natural host and promote growth of cereal crops under salt stress. *Microbiol. Res.* 223–225, 33–43. doi: 10.1016/J.MICRES.2019.03.008

Srinivasan, R., Kantwa, S. R., Sharma, K. K., Chaudhary, M., Prasad, M., and Radhakrishna, A. (2018). Development and evaluation of phosphate solubilising microbial inoculants for fodder production in problem soils-Indian Journals. *Range Manag. Agrofor.* 39, 77–89.

Stearns, J. C., and Glick, B. R. (2003). Transgenic plants with altered ethylene biosynthesis or perception. *Biotechnol. Adv.* 21, 193–210. doi: 10.1016/S0734-9750(03)00024-7

Stephens, E., Wolf, J., Oey, M., Zhang, E., Hankamer, B., Ross, I. L., et al. (2015). "Genetic engineering for microalgae strain improvement in relation to biocrude production systems," in *Biomass and Biofuels from Microalga*, eds N. Moheimani, M. McHenry, K. de Boer, and P. Bahri (Cham: Springer), 191–249. doi: 10.1007/978-3-319-16640-7_11

Stierle, A. A., Stierle, D. B., Decato, D., Priestley, N. D., Alverson, J. B., Hoody, J., et al. (2017). The berkeleylactones, antibiotic macrolides from fungal coculture. *J. Nat. Prod.* 80, 1150–1160. doi: 10.1021/ACS.JNATPROD.7B00133

Su, F., Jacquard, C., Villaume, S., Michel, J., Rabenoelina, F., Clément, C., et al. (2015). Burkholderia phytofirmans PsJN reduces impact of freezing temperatures on photosynthesis in *Arabidopsis thaliana*. *Front. Plant Sci.* 6:810. doi: 10.3389/FPLS.2015.00810/BIBTEX

Su, L., Shen, Z., Ruan, Y., Tao, C., Chao, Y., Li, R., et al. (2017). Isolation of antagonistic endophytes from banana roots against *Meloidogyne javanica* and their effects on soil nematode community. *Front. Microbiol.* 8:2070. doi: 10.3389/FMICB.2017.02070/BIBTEX

Suaìrez-Moreno, Z. R., Devescovi, G., Myers, M., Hallack, L., Mendonça-Previato, L., Caballero-Mellado, J., et al. (2010). Commonalities and differences in regulation of N -Acyl homoserine lactone quorum sensing in the beneficial plant-associated *Burkholderia* species cluster. *Appl. Environ. Microbiol.* 76, 4302–4317. doi: 10.1128/AEM.03086-09

Subramanian, P., Mageswari, A., Kim, K., Lee, Y., and Sa, T. (2015). Psychrotolerant endophytic *Pseudomonas* sp. strains OB155 and OS261 induced chilling resistance in tomato plants (*Solanum lycopersicum* Mill.) by activation of their antioxidant capacity. *Mol. Plant Microbe Interact.* 28, 1073–1081. doi: 10.1094/MPMI-01-15-0021-R

Suneja, P., Singh Dudeja, S., and Dahiya, P. (2016). Deciphering the phylogenetic relationships among rhizobia nodulating chickpea: a review. *J. Appl. Biol. Biotechnol.* 4, 61–070. doi: 10.7324/JABB.2016.40310

Swarnalakshmi, K., Rajkhowa, S., Dhar, D. W., Senthilkumar, M., Swarnalakshmi, K., Rajkhowa, S., et al. (2019). "Influence of endophytic bacteria on growth promotion and protection against diseases in associated plants," in *Microbial Interventions in Agriculture and Environment: Volume 3: Soil and Crop Health Management*, eds D. P. Singh and R. Prabha (Berlin: Springer). doi: 10.1007/978-981-32-9084-6_12

Tamás, M. J., Sharma, S. K., Ibstedt, S., Jacobson, T., and Christen, P. (2014). Heavy metals and metalloids as a cause for protein misfolding and aggregation. *Biomolecules* 4, 252–267. doi: 10.3390/BIOM4010252

Tang, K., Li, B., and Guo, S. (2014). An active endophytic fungus promoting growth and increasing salvianolic acid content of *Salvia miltiorrhiza*. *Mycosystema* 33, 594–600.

Tashi-Oshnoei, F., Harighi, B., and Abdollahzadeh, J. (2017). Isolation and identification of endophytic bacteria with plant growth promoting and biocontrol potential from oak trees. *For. Pathol.* 47:e12360. doi: 10.1111/EFP.12360

Taulé, C., Castillo, A., Villar, S., Olivares, F., and Battistoni, F. (2016). Endophytic colonization of sugarcane (*Saccharum officinarum*) by the novel diazotrophs *Shinella* sp. UYSO24 and *Enterobacter* sp. UYSO10. *Plant Soil* 403, 403–418. doi: 10.1007/S11104-016-2813-5

Thokchom, E., Thakuria, D., Kalita, M. C., Sharma, C. K., and Talukdar, N. C. (2017). Root colonization by host-specific rhizobacteria alters indigenous root endophyte and rhizosphere soil bacterial communities and promotes the growth of mandarin orange. *Eur. J. Soil Biol.* 79, 48–56. doi: 10.1016/J.EJSOBI.2017.02.003

Toumatia, O., Compant, S., Yekkour, A., Goudjal, Y., Sabaou, N., Mathieu, F., et al. (2016). Biocontrol and plant growth promoting properties of Streptomyces mutabilis strain IA1 isolated from a Saharan soil on wheat seedlings and visualization of its niches of colonization. *S. Afr. J. Bot.* 105, 234–239. doi: 10.1016/J.SAJB.2016.03.020

Turner, T. R., James, E. K., and Poole, P. S. (2013). The plant microbiome. *Genome Biol.* 14, 1–10. doi: 10.1186/GB-2013-14-6-209/FIGURES/1

Ullah, I., Al-Johny, B. O., Al-Ghamdi, K. M. S., Al-Zahrani, H. A. A., Anwar, Y., Firoz, A., et al. (2019). Endophytic bacteria isolated from *Solanum nigrum* L., alleviate cadmium (Cd) stress response by their antioxidant potentials, including SOD synthesis by sodA gene. *Ecotoxicol. Environ. Saf.* 174, 197–207. doi: 10.1016/J.ECOENV.2019.02.074

Van Zelm, E., Zhang, Y., and Testerink, C. (2020). Salt tolerance mechanisms of plants. *Annu Rev Plant Biol.* 71, 403–433. doi: 10.1146/ANNUREV-ARPLANT-050718-100005

Vandenkoornhuyse, P., Quaiser, A., Duhamel, M., Le Van, A., and Dufresne, A. (2015). The importance of the microbiome of the plant holobiont. *New Phytol.* 206, 1196–1206. doi: 10.1111/NPH.13312

Vasileva, E. N., Николаевна, В. Е., Akhtemova, G. A., Асановна, А. Г, Zhukov, V. A., Александрович, Ж. В, et al. (2019). Endophytic microorganisms in fundamental research and agriculture. *Ecol. Genet.* 17, 19–32. doi: 10.17816/ecogen17119-32

Verma, H., Kumar, D., Kumar, V., Kumari, M., Singh, S. K., Sharma, V. K., et al. (2021). The potential application of endophytes in management of stress from drought and salinity in crop plants. *Microorganisms* 9:1729. doi: 10.3390/MICROORGANISMS9081729

Verma, S. K., Kingsley, K., Bergen, M., English, C., Elmore, M., Kharwar, R. N., et al. (2018). Bacterial endophytes from rice cut grass (*Leersia oryzoides* L.) increase growth, promote root gravitropic response, stimulate root hair formation, and protect rice seedlings from disease. *Plant Soil* 422, 223–238. doi: 10.1007/S11104-017-3339-1/FIGURES/6

Vimal, S. R., Patel, V. K., and Singh, J. S. (2019). Plant growth promoting *Curtobacterium albidum* strain SRV4: an agriculturally important microbe to alleviate salinity stress in paddy plants. *Ecol. Indic.* 105, 553–562. doi: 10.1016/J.ECOLIND.2018.05.014

Viscardi, S., Ventorino, V., Duran, P., Maggio, A., De Pascale, S., Mora, M. L., et al. (2016). Assessment of plant growth promoting activities and abiotic stress tolerance of *Azotobacter chroococcum* strains for a potential use in sustainable agriculture. *J. Soil Sci. Plant Nutr.* 16, 848–863. doi: 10.4067/S0718-95162016005000060

Voisard, C., Keel, C., Haas, D., and Defago, G. (1989). Cyanide production by *Pseudomonas* fluorescens helps suppress black root rot of tobacco under gnotobiotic conditions. *EMBO J.* 8, 351–358. doi: 10.1002/J.1460-2075.1989.TB03384.X

Vorholt, J. A. (2012). Microbial life in the phyllosphere. *Nat. Rev. Microbiol.* 10, 828–840. doi: 10.1038/nrmicro2910

Vurukonda, S. S. K. P., Giovanardi, D., and Stefani, E. (2021). Identification, evaluation and selection of a bacterial endophyte able to colonize tomato plants, enhance their growth and control *Xanthomonas vesicatoria*, the causal agent of the spot disease. *Can. J. Plant Pathol.* 44, 1–16. doi: 10.1080/07060661.2021.1980822

Walitang, D. I., Kim, K., Madhaiyan, M., Kim, Y. K., Kang, Y., and Sa, T. (2017). Characterizing endophytic competence and plant growth promotion of bacterial endophytes inhabiting the seed endosphere of Rice. *BMC Microbiol.* 17:209. doi: 10.1186/S12866-017-1117-0/FIGURES/4

Wang, C., Wang, C., Gao, Y.-L., Wang, Y.-P., and Guo, J.-H. (2016). A consortium of three plant growth-promoting rhizobacterium strains acclimates *Lycopersicon esculentum* and confers a better tolerance to chilling stress. *J. Plant Growth Regul.* 35, 54–64. doi: 10.1007/s00344-015-9506-9

Wang, M., Weiberg, A., Dellota, E., Yamane, D., and Jin, H. (2017). Botrytis small RNA Bc-siR37 suppresses plant defense genes by cross-kingdom RNAi. *RNA Biol.* 14, 421–428. doi: 10.1080/15476286.2017.1291112

Wang, W., Wu, Z., He, Y., Huang, Y., Li, X., and Ye, B. C. (2018). Plant growth promotion and alleviation of salinity stress in *Capsicum annuum* L. by *Bacillus* isolated from saline soil in Xinjiang. *Ecotoxicol. Environ. Saf.* 164, 520–529. doi: 10.1016/J.ECOENV.2018.08.070

Wani, Z. A., Kumar, A., Sultan, P., Bindu, K., Riyaz-Ul-Hassan, S., and Ashraf, N. (2017). *Mortierella alpina* CS10E4, an oleaginous fungal endophyte of *Crocus sativus* L. enhances apocarotenoid biosynthesis and stress tolerance in the host plant. *Sci. Rep* 7:8598. doi: 10.1038/s41598-017-08974-z

War Nongkhlaw, F., and Joshi, S. (2017). Microscopic study on colonization and antimicrobial property of endophytic bacteria associated with ethnomedicinal plants of Meghalaya. *J. Microsc. Ultrastruct.* 5, 132–139. doi: 10.1016/J.JMAU.2016.09.002

White, J. F., Kingsley, K. L., Zhang, Q., Verma, R., Obi, N., Dvinskikh, S., et al. (2019). Review: endophytic microbes and their potential applications in crop management. *Pest Manag. Sci.* 75, 2558–2565. doi: 10.1002/PS.5527

White, J. F., Torres, M. S., Somu, M. P., Johnson, H., Irizarry, I., Chen, Q., et al. (2014). Hydrogen peroxide staining to visualize intracellular bacterial infections of seedling root cells. *Microsc. Res. Tech.* 77, 566–573. doi: 10.1002/JEMT.22375

Wiesel, L., Newton, A. C., Elliott, I., Booty, D., Gilroy, E. M., Birch, P. R. J., et al. (2014). Molecular effects of resistance elicitors from biological origin and their potential for crop protection. *Front. Plant Sci.* 5:655. doi: 10.3389/FPLS.2014.00655/ABSTRACT

Worsley, S. F., Macey, M. C., Prudence, S. M., Wilkinson, B., Murrell, J. C., and Hutchings, M. I. (2021). Investigating the role of root exudates in recruiting *Streptomyces* bacteria to the *Arabidopsis thaliana* microbiome. *Mol. Front. J.* 8:541. doi: 10.3389/fmolb.2021.686110

Xu, C., Ruan, H., Cai, W., Staehelin, C., and Dai, W. (2021). Identification of an exopolysaccharide biosynthesis gene in *Bradyrhizobium diazoefficiens* USDA110. *Microorganisms* 9, 2490. doi: 10.3390/MICROORGANISMS9122490

Xu, J. X., Li, Z. Y., Lv, X., Yan, H., Zhou, G. Y., Cao, L. X., et al. (2020). Isolation and characterization of *Bacillus subtilis* strain 1-L-29, an endophytic bacteria from *Camellia oleifera* with antimicrobial activity and efficient plant-root colonization. *PLoS One* 15:e0232096. doi: 10.1371/JOURNAL.PONE.0232096

Xu, L., Wang, A., Wang, J., Wei, Q., and Zhang, W. (2017). *Piriformospora indica* confers drought tolerance on *Zea mays* L. through enhancement of antioxidant activity and expression of drought-related genes. *Crop J.* 5, 251–258. doi: 10.1016/J.CJ.2016.10.002

Yan, X., Wang, Z., Mei, Y., Wang, L., Wang, X., Xu, Q., et al. (2018). Isolation, diversity, and growth-promoting activities of endophytic bacteria from tea cultivars of Zijuan and Yunkang-10. *Front. Microbiol.* 9:1848. doi: 10.3389/FMICB.2018.01848/BIBTEX

Zachow, C., Jahanshah, G., De Bruijn, I., Song, C., Ianni, F., Pataj, Z., et al. (2015). The novel lipopeptide poaeamide of the endophyte *Pseudomonas* poae RE*1-1-14 is involved in pathogen suppression and root colonization. *Mol. Plant Microbe Interact.* 28, 800–810. doi: 10.1094/MPMI-12-14-0406-R

Zeidler, D., Zähringer, U., Gerber, I., Dubery, I., Hartung, T., Bors, W., et al. (2004). Innate immunity in *Arabidopsis thaliana*: lipopolysaccharides activate nitric oxide synthase (NOS) and induce defense genes. *Proc. Natl. Acad. Sci. U.S.A.* 101, 15811–15816. doi: 10.1073/PNAS.0404536101

Zerrouk, I. Z., Benchabane, M., Khelifi, L., Yokawa, K., Ludwig-Müller, J., and Baluska, F. (2016). A *Pseudomonas* strain isolated from date-palm rhizospheres improves root growth and promotes root formation in maize exposed to salt and aluminum stress. *J. Plant Physiol.* 191, 111–119. doi: 10.1016/J.JPLPH.2015.12.009

Zhai, X., Luo, D., Li, X., Han, T., Jia, M., Kong, Z., et al. (2018). Endophyte *Chaetomium globosum* D38 promotes bioactive constituents accumulation and root production in *Salvia miltiorrhiza*. *Front. Microbiol.* 8:2694. doi: 10.3389/FMICB.2017.02694/BIBTEX

Zhang, C., Li, C., Liu, J., Lv, Y., Yu, C., Li, H., et al. (2017). The OsABF1 transcription factor improves drought tolerance by activating the transcription of COR413-TM1 in rice. *J. Exp. Bot.* 68, 4695–4707. doi: 10.1093/JXB/ERX260

Zhang, Q., Acuña, J. J., Inostroza, N. G., Mora, M. L., Radic, S., Sadowsky, M. J., et al. (2019). Endophytic bacterial communities associated with roots and leaves of plants growing in chilean extreme environments. *Sci. Rep.* 9:4950. doi: 10.1038/s41598-019-41160-x

Zheng, Y., Liang, J., Zhao, D. L., Meng, C., Xu, Z. C., Xie, Z. H., et al. (2020). The root nodule microbiome of cultivated and wild halophytic legumes showed similar diversity but distinct community structure in Yellow River delta saline soils. *Microorganisms* 8:207. doi: 10.3390/MICROORGANISMS8020207

Zhou, L., Zhang, Y., Ge, Y., Zhu, X., and Pan, J. (2020). Regulatory mechanisms and promising applications of quorum sensing-inhibiting agents in control of bacterial biofilm formation. *Front. Microbiol.* 11:2558. doi: 10.3389/fmicb.2020.589640

Ziemert, N., Alanjary, M., and Weber, T. (2016). The evolution of genome mining in microbes – a review. *Nat. Prod. Rep.* 33, 988–1005. doi: 10.1039/C6NP00025H

Zin, N. M., Ismail, A., Mark, D. R., Westrop, G., Schniete, J. K., and Herron, P. R. (2021). Adaptation to endophytic lifestyle through genome reduction by *Kitasatospora* sp. SUK42. *Front. Bioeng. Biotechnol.* 9:740722. doi: 10.3389/FBIOE.2021.740722/FULL

Zinniel, D. K., Lambrecht, P., Harris, N. B., Feng, Z., Kuczmarski, D., Higley, P., et al. (2002). Isolation and characterization of endophytic colonizing bacteria from agronomic crops and prairie plants. *Appl. Environ. Microbiol.* 68, 2198–2208. doi: doi: 10.1128/AEM.68.5.2198-2208.2002

Zúñiga, A., Poupin, M. J., Donoso, R., Ledger, T., Guiliani, N., Gutiérrez, R. A., et al. (2013). Quorum sensing and indole-3-acetic acid degradation play a role in colonization and plant growth promotion of *Arabidopsis thaliana* by *Burkholderia phytofirmans* PsJN. *Mol. Plant Microbe Interact.* 26, 546–553. doi: 10.1094/MPMI-10-12-0241-R

Conflict of Interest: The authors declare that the research was conducted in the absence of any commercial or financial relationships that could be construed as a potential conflict of interest.

Publisher's Note: All claims expressed in this article are solely those of the authors and do not necessarily represent those of their affiliated organizations, or those of the publisher, the editors and the reviewers. Any product that may be evaluated in this article, or claim that may be made by its manufacturer, is not guaranteed or endorsed by the publisher.

frontiers | Frontiers in Microbiology

ORIGINAL RESEARCH
published: 31 May 2022
doi: 10.3389/fmicb.2022.804429

Microbial Community, Fermentation Quality, and *in vitro* Degradability of Ensiling *Caragana* With Lactic Acid Bacteria and Rice Bran

Jingtao You[1†], Huan Zhang[1†], Hongfu Zhu[1], Yanlin Xue[2], Yimin Cai[3] and Guijie Zhang[1]*

[1] Department of Animal Science, Ningxia University, Yinchuan, China, [2] Inner Mongolia Key Laboratory of Microbial Ecology of Silage, Inner Mongolia Engineering Research Center of Development and Utilization of Microbial Resources in Silage, Inner Mongolia Academy of Agriculture and Animal Husbandry Science, Hohhot, China, [3] Japan International Research Center for Agricultural Science (JIRCAS), Tsukuba, Japan

OPEN ACCESS

Edited by:
Ying Ma,
University of Coimbra, Portugal

Reviewed by:
Smerjai Bureenok,
Rajamangala University of Technology Isan, Thailand
Halima Sultana,
University of Florida, United States

***Correspondence:**
Guijie Zhang
Guijiezhang@nxu.edu.cn

[†] These authors have contributed equally to this work and share first authorship

Specialty section:
This article was submitted to Microbiotechnology, a section of the journal Frontiers in Microbiology

Received: *29 October 2021*
Accepted: *26 April 2022*
Published: *31 May 2022*

Citation:
You J, Zhang H, Zhu H, Xue Y, Cai Y and Zhang G (2022) Microbial Community, Fermentation Quality, and in vitro Degradability of Ensiling Caragana With Lactic Acid Bacteria and Rice Bran. Front. Microbiol. 13:804429. doi: 10.3389/fmicb.2022.804429

This study aimed to assess the effects of microbial inoculants and growth stage on fermentation quality, microbial community, and *in vitro* degradability of *Caragana* silage from different varieties. *Caragana intermedia* (CI) and *Caragana korshinskii* (CK) harvested at the budding (BU) and blooming (BL) stages were used as raw materials to prepare silage, respectively. The silages at each growth stage were treated for ensiling alone (control), with 5% rice bran (RB), a combination of RB with commercial *Lactobacillus plantarum* (RB + LP), and a combination of RB with a selected strain *Lactobacillus plantarum* L694 (RB + L694). The results showed that the crude protein (CP) content of CI was higher than that of CK, and delay in harvest resulted in greater CP content in *Caragana* at BL stage. After 60 days of fermentation, the concentrations of lactic acid (LA) in the RB + L694 treatments were higher than those in control treatments ($p < 0.05$), while the pH, concentrations of NH_3-N, neutral detergent fiber with the addition of α-amylase (aNDF) were lower than those in control treatments ($p < 0.05$). RB + L694 treatments could decrease acid detergent fiber (ADF) content except in CIBL. In CK silages, adding RB + L694 could reduce bacterial diversity and richness ($p < 0.05$). Compared with the control, RB + L694 treatment contained higher *Lactobacillus* and *Enterobacter* ($p < 0.05$). *In vitro* NDF and DM degradability (IVNDFD and IVDMD) was mostly affected by growth period, and additive RB + l694 treatment had higher IVDMD and lower IVNDFD than other treatments ($p < 0.05$). Consequently, the varieties, growth stages, and additives could influence the fermentation process, while the blooming stage should be selected in both *Caragana*. Furthermore, the results showed that RB and *L. plantarum* could exert a positive effect on fermentation quality of *Caragana* silage by shifting bacterial community composition, and RB + L694 treatments outperformed other additives.

Keywords: *Caragana* silage, fermentation quality, conserved forage, microbial population, rice bran, *Lactobacillus*

INTRODUCTION

Caragana is a legume shrub that grows well in arid and semi-arid soils. It can be widely used to control desertification and provide ecological protection (Zhang et al., 2015). However, the overgrowth of *Caragana* may reduce the diversity of plant species and affect the ecological environment (Yang and Liu, 2019). Therefore, it is necessary to manage and effectively use *Caragana* to reduce species competition and enhance the stability of the ecosystem.

Caragana intermedia (CI) and *Caragana korshinskii* (CK) are the common cultivars in some arid regions of the world, including China. Both shrubs belong to the legume *Caragana* genus, and the fresh branches and leaves contain high-protein content and nutritional value, which can contribute to livestock production (Wang et al., 2021). Generally, the nutrient and palatability of *Caragana* are easily affected by the growth stage and the processing methods (Wang et al., 2020). Woody plants can accumulate large amounts of biomass, but the harvesting time is seasonally restricted. The natural drying process will cause nutrient loss, increase the lignin content, and reduce palatability. Therefore, silage is considered an alternative preparation and storage method that can be used as a convenient way to preserve woody forage and alleviate the problem of feed shortage in arid areas (Cai et al., 2020).

Generally, due to the low fermentation substrate of legumes, it is difficult to prepare woody plants naturally for obtaining high-quality silage (Cai et al., 2020). Ensiling shrub with lactic acid bacteria (LAB) and high sugar agricultural by-products may be an effective way to solve the fermentation problem. As a woody plant, *Broussonetia papyrifera* has high-protein content and nutritional value, which is similar to *Caragana*. Recent studies have shown that inoculated with LAB and molasses can improve the fermentation quality of *Broussonetia papyrifera* silage, change the microbial community structure, and reduce the number of harmful microorganisms (Basso et al., 2018; Du et al., 2021). Rice bran is refined to produce white rice and is also a cheap livestock feed (Shi et al., 2015). The previous study has shown that rice bran contains sugar, which can promote the growth of LAB and accelerate the fermentation of LA (Ono et al., 2014; He et al., 2020).

During ensiling, a regular succession of microbial communities occurs in the aerobic and anaerobic stages (Tao et al., 2020). For better understanding the fermentation process of ensiled, it is necessary to profile the bacterial communities (Dong et al., 2020; Ren et al., 2021). Recently, next-generation sequencing (NGS) has been widely used to study microbial communities in silage (Li et al., 2015; Zhang et al., 2017). The 16S rRNA (SSU rRNA) gene is regarded as the most widely used biomarker because it is present in the genomes of all bacteria (Grutzke et al., 2019).

The limitations of legume silage include low content of water-soluble carbohydrates (WSC) and high buffering capacity, which can result in a poor fermentation quality and nutrient loss of silage (Nkosi et al., 2016). This issue may be addressed by adding LAB and rice bran to increase WSC content and improve fermentability. Aerobic stability is an index to evaluate the difficulty of aerobic deterioration of silage. Poor aerobic stability caused dry matter (DM) and economic losses and decreased the nutrition of silages (Ferrero et al., 2019).

We hypothesized that the microbial community, fermentation quality, and *in vitro* degradability of *Caragana* silage could be improved by adding LAB and rice bran. Therefore, the purpose of this study is to investigate the microbial community, silage fermentation, aerobic stability, and *in vitro* degradability of *Caragana* prepared with LAB and rice bran.

MATERIALS AND METHODS

Materials and Silage Making

Caragana intermedia (CI) and *Caragana korshinskii* (CK) used in this experiment were planted in 2014 in an experiment field (107° E, 37° N, Yanchi, China), which was harvested at the budding stage (BU) on April 17, 2019, and the blooming stage (BL) on June 25, 2019. Both fresh shrubs were harvested from three randomly selected locations within the field as three repetitions, using hand clippers (400–700, Jingmei Linglang Trading Co., Ltd., Shenzhen, China) and leaving a stubble of 10 cm above ground.

After the cutting, the raw shrub was broken and kneaded into a slice less than 1 mm, using a kneading machine (RC-400, QuFuZhiZao Conveyor Co., Ltd., Shandong, China). The fresh shrubs were adjusted to a DM content of about 40% by adding water and then treated without additive (control) and with 5% rice bran (RB), 5% RB plus commercial LAB (*Lactobacillus plantarum* LP) inoculant (RB + LP), and 5% RB plus a selected strain *Lactobacillus plantarum* L694 (RB + L694).

The proportions of crude protein, crude fiber, crude fat, and water-soluble carbohydrates in RB are 12.8, 5.7, 16.5, and 8.58% DM, respectively, which were derived from a by-product of rice production, provided by a local feed company, and 5% of the fresh material was used for mixing with shrub samples. Strain L694 was isolated from high-moisture corn silage, which could grow under low pH conditions and produce more LA in the silage environment, provided by Sichuan Agricultural University. Strain L694 was cultured in MRS agar (HB0384, Hope Bio-Technology Co., Ltd., Qingdao, China) for 24 h for silage preparation. The plate counting method was used to determine the number of viable bacteria. The final addition amount was 3×10^5 colony-forming unit (CFU)/g of fresh weight and mixed evenly with *Caragana* sample. The commercial LAB was mixed with sterile water at an added amount of 3×10^5 CFU/g of fresh weight and uniformly sprayed on the *Caragana* sample. Silages were prepared with a laboratory-scale fermentation system with bag silos, which weigh 500 g of fresh material and then pack it into a polyethylene bag (270 mm × 300 mm; Embossed Food saver bag Co., Ltd., Chengdu, China) with a one-way exhaust valve. A vacuum packaging machine (DZ-400, Shandong Zhucheng Yizhong Machinery Co., Ltd., Zhucheng, China) was used to vacuum compress and seal the bag. There were 48 bag silos with three replicates of silage per treatment stored at room temperature (24°C–26°C) for 60 days.

Quality Analysis of Silage

The bag silos were opened on Day 60 after ensiling. 10 g silage samples were diluted with 90 ml of distilled water, filtered with four layers of cheesecloth, and stored in a refrigerator at 4 °C for 24 h. The supernatant was then measured for pH using a calibrated pH meter (PHS-3G, Mettler Toledo, Zurich, Switzerland). Before analyzing ammonia nitrogen and organic acid, a subsample of the supernatant was centrifuged at 2,500 rpm for 10 min and passed through a 0.22-μm microporous filter. The ammonia nitrogen content was analyzed according to the procedure of Broderick and Kang (1980). Organic acid was analyzed using high-performance liquid chromatography (HPLC) (KC-811 column, Shodex; Shimadzu: Japan; oven temperature 50°C; flow rate: 1 ml/min; SPD: 210 nm) as described by Tian et al. (2014).

The materials and silage samples of CI and CK were dried in a forced air oven at 105°C for 15 min and turn down to 65 °C immediately. After drying for 48 h, it was milled and passed through a 1-mm screen and then heated to 105°C until their weight was constant for the analyzed dry matter (DM). The crude protein (CP) was calculated by multiplying 6.25 with the content of nitrogen (N), which was determined using the Kjeldahl apparatus (K-360, BUCHI laboratory equipment trade Co., Ltd., Shanghai, China). NH_3-N content was determined by the phenol-sodium hypochlorite colorimetric method (Sekerka and Lechner, 1974).

Neutral detergent fiber with the addition of α-amylase (aNDF), acid detergent fiber in organic matter (ADF), and acid detergent lignin (ADL) were determined according to the methods of Van Soest et al. (1991) using an ANKOM A2000i fiber analyzer (A2000i, ANKOM Technology, New York, United States). Water-soluble carbohydrates were determined by anthrone-sulfuric acid colorimetry (Murphy, 1958).

Aerobic Stability Analysis

After 60 d of ensiling, the silages with three replicates per treatment were placed in a new polyethylene bag (270 mm × 300 mm; Embossed Food saver bag; Changyang, Chengdu, China) and stored at room temperature (24∼26°C), and each bag was portioned 500 g silages. A HOBO Pendant Temperature Data Logger (Onset Ltd., Massachusetts, United States) was put and punctured holes in the geometric center of the polyethylene bag that recorded the temperature every 30 min for each bag. Another temperature data logger was placed in the room to record room temperature. The silage was considered to have deteriorated when the silage temperature was 2°C more than the room temperature.

Bacterial Community of *Caragana*

The microbial total DNA extraction was performed according to the method of Zheng et al. (2017). Twenty grams of sample was collected, mixed with 80 ml of sterile water, and stirred at 120 rpm and 4°C for 2 h. The samples were filtered through two layers of sterile gauze and then centrifuged at 10,000 × *g* for 15 min at 4°C.

The DNA of silage was extracted by the FastDNA SPIN for Soil Kit (MP Biomedicals, Solon, United States). The final DNA concentration and purification were determined by NanoDrop 2000 UV-vis spectrophotometer (Thermo Fisher Scientific, Wilmington, United States), and DNA quality was checked by 1% agarose gel electrophoresis. The V3–V4 hypervariable regions of the bacteria 16S rRNA gene were amplified with primers 338F (5′- ACTCCTACGGGAGGCAGCAG-3′) and 806R (5′-GGACTACHVGGGTWTCTAAT-3′) by thermocycler PCR system (GeneAmp 9700, ABI, United States).

The PCR reactions were conducted using the following program: 3 min of denaturation at 95°C, 27 cycles of 30 s at 95°C, 30 s for annealing at 55°C, and 45 s for elongation at 72°C, and a final extension at 72°C for 10 min. PCR reactions were performed in triplicate 20 μL mixture containing 4 μL of 5 × FastPfu Buffer, 2 μL of 2.5 mM dNTPs, 0.8 μL of each primer (5 μM), 0.4 μL of FastPfu Polymerase, and 10 ng of template DNA. The resulted PCR products were extracted from a 2% agarose gel and further purified using the AxyPrep DNA Gel Extraction Kit (Axygen Biosciences, Union City, CA, United States) and quantified using QuantiFluor^{TM}-ST (Promega, United States) according to the manufacturer's protocol.

The reads less than 50 bp were discarding to obtained clean reads, which were clustered at the similarity of 97% into operational taxonomic units (OTUs) to investigate species diversity of all the samples by Uparse software. The OTUs were annotated by the Silva (SSU123) to obtain the composition of each sample. Alpha diversity analysis was performed using the Mothur software platform. Principal component analysis (PCA) was performed and plotted in R software (version 3.5.1).

In vitro Digestibility

The *in vitro* digestibility of dry matter (IVDMD) and NDF (IVNDFD) were measured according to Tian et al. (2014). Dried and ground silage samples (1 g, milled through a 1.0 mm screen) were incubated in the pepsin-hydrochloric acid solution for 16 h, followed by hydrolysis with a pH 4.6 cellulase–acetate buffer for 48 h, then inactivated at 90°C for 30 min, and washed with distilled water. After dried at 105°C to constant weight, the residue was weighted, and IVDMD was calculated. The content of NDF in the residue of enzymatic hydrolysis was determined, and IVNDFD was then calculated.

Statistical Analysis

Data on chemical composition, fermentation characteristics, alpha diversity, and *in vitro* degradability were analyzed via a 2 × 4 × 4 factorial design according to the model: $Yijk = \mu + Vi + Gj + Ak + (V \times G)ij + (V \times A)ik + (G \times A)jk + (V \times G \times A)ijk + eijk$, where Yij = observation; μ = overall mean; Vi = effect of varieties (i = 1,2); Gj = effect of growth stages (j = 1, 2); Ak = effect of additives (k = 1, 2, 3, 4); (V × G)ij = effect of interaction between varieties and growth stages; (V × A)ik = effect of interaction between varieties and additives; (G × A)jk = effect of interaction between growth stages and additives; (V × G × A)ijk = effect of interaction between varieties, stages, and additives, and eijk was the residual error. The model includes two varieties, two growth stages, four additives, and their interactions. Tukey's HSD was used for multiple comparisons with difference declared significant at $p < 0.05$.

RESULTS

Chemical Composition of Fresh *Caragana* Before Ensiling

Chemical composition of fresh *Caragana* before ensiling is shown in **Table 1**. The NDF content was affected by varieties, growth stage, and their interactions ($p < 0.05$). The CK had higher NDF and ADF than CI ($p < 0.05$), whereas CI contained higher CP than CK ($p < 0.05$). The fiber, CP, and WSC concentrations at the blooming stage were higher than those at the budding stage ($P < 0.05$).

TABLE 1 | Chemical composition of fresh *Caragana* before ensiling ($n = 3$).

Items[1]	Materials[2]				SEM[3]	*P*-value[4]		
	CIBU	CIBL	CKBU	CKBL		V	G	V × G
DM (%)	41.04	40.35	40.94	41.13	0.24	NS	NS	NS
CP (% DM)	12.41^{b}	14.07^{a}	10.36^{d}	11.48^{c}	0.10	**	**	NS
NDF (% DM)	70.01^{c}	71.19^{c}	73.36^{b}	77.07^{a}	0.32	**	**	**
ADF (% DM)	51.30^{c}	54.58^{b}	57.76^{ab}	59.56^{a}	0.71	**	**	NS
ADL (% DM)	16.59^{b}	20.63^{a}	18.96^{a}	19.54^{a}	0.44	NS	**	**
WSC (% DM)	1.98^{b}	3.11^{ab}	2.30^{b}	4.25^{a}	0.36	NS	**	NS

[1]DM, dry matter; CP, crude protein; NDF, neutral detergent fiber; ADF, acid detergent fiber; ADL, acid detergent lignin; WSC, water-soluble carbohydrate.
[2]CI, Caragana intermedia; CK, Caragana korshinskii; BU, budding stage; BL, blooming stage.
[3]SEM, standard error of the means.
[4]V, varieties; G, growth stage; NS, no significant.
***, $p < 0.01$.*
[a−d]Means of inoculation treatments within a row with different superscripts differ ($p < 0.05$).

Fermentation Characteristics of *Caragana* Silage

The fermentative changes in pH of silage are shown in **Figure 1**. The pH of CIBU silages treated with RB + L694 was lower than other treatments in the whole silage process ($p < 0.05$), which was 4.58 on Day 5 decreased to 4.1 at the end of ensiling. Although the pH of RB treatment group was not different from that of control group on Day 45 ($p > 0.05$), the pH value for the rest of the time was significantly higher than that of control group ($p < 0.05$). In CIBL, the initial pH value of RB + L694 treatment was 4.13, and the final pH value decreased to 3.98; furthermore, the pH of the whole silage process was significantly lower than other treatment groups ($p < 0.05$). In CKBU, pH of the whole ensiling stage in all treatment groups was lower than that in control group ($p < 0.05$). On Day 30, pH in all treatment groups decreased to 4.5 and remained at the lower level until Day 60; RB + L694 and RB treatments had the lowest final pH, which was 4.06 and 4.07. In CKBL, the RB + L694 treatment group had the lowest pH ($p < 0.05$) on Day 60, which was 3.91. In addition, during ensiling treated with CIBL and CKBL silages, pH further reduced was observed after 30 days, whereas treated with CIBU and CKBU silages pH was unchanged.

The fermentative changes in NH_3-N of silage are shown in **Figure 2**. The initial NH_3-N content in CIBU was all below 0.04 g/kg of total nitrogen (TN). On Day 60 of ensiling, the NH_3-N of the RB + L694 treatment group was 0.076 g/kg TN, which was lower than that of the other treatments ($p < 0.05$). In CIBL, the NH_3-N of the RB treatment group increased rapidly from Days 10 to 30, from 0.021 to 0.059 g/kg TN, which was higher than that of the control group ($p < 0.05$). The NH_3-N of RB + L694 on Days 45 and 60 was lower than that of other treatments ($p < 0.05$), which was 0.032 and 0.047 g/kg TN, respectively. In CKBU, the increasing trend of NH_3-N in different treatment groups was relatively slow in the first 45 days. While on Day 60, the NH_3-N in RB treatment group and RB + L694 group was lower than that in the control group ($p < 0.05$), 0.10 and 0.13 g/kg TN, respectively. There was no difference between RB + LP treatment group and control group ($p > 0.05$). The CKBL group was similar to the CIBL group, with a slower increase on days 5–10. On Day 60, the NH_3-N of RB + L694 was 0.06 g/kg TN, which was lower than that of other treatments ($p < 0.05$). In addition, the NH_3-N contents tardily increased in the first 10–30 days during ensiling and then peaked after 60 days.

As shown in **Table 2**, the lactic acid (LA), acetic acid (AA), and LA/AA contents were mainly affected by interaction between varieties, growth stage, and additives ($p < 0.01$). LA content in additive treatments was significantly higher than control group ($p < 0.05$). RB + L694 treatments significantly reduced AA content and increased LA/AA content ($p < 0.05$), compared with other treatment groups. The varieties × growth stage and varieties × additives had effects on propionic acid (PA) content. In CIBU, additives had no significant effect ($p > 0.05$).

The aerobic stability in CIBL and CKBL, and additive treatment group was significantly higher than that of control group ($p < 0.05$), and RB + L694 treatment group was the highest ($p < 0.05$). The use of additives in CKBU can reduce its aerobic stability ($p < 0.05$), while BU stage had higher aerobic stability than that of BL stage ($p < 0.05$).

Alpha Diversity of *Caragana* Silage

As shown in **Table 3**, the alpha diversity changed with varieties, growth stage, and additives. All samples had relatively high coverage (> 0.99). Both Shannon index and Simpson index were affected interactively by variety, growth period, and additives ($P < 0.01$). The varieties and additives affected interactively the indexes of Ace and Chao1 ($P < 0.01$). In addition, the indexes of Shannon, Ace, and Chao1 in additive treatment were higher than those in control treatment ($P < 0.01$). The index of Simpson in additive treatment was lower than that in control treatment ($P < 0.01$).

Principal Component Analysis of *Caragana* Silage

As shown in **Figure 3**, all fresh materials were grouped into a single category and were far away from the samples of other treatment groups. In CIBL, RB + LP silage aggregation was in the second quadrant, the distance within the group was relatively close, and the control group is clustered into one category. In CIBU, RB and RB + LP silages were clustered into one group, while control and RB + L694 silages were clustered into one

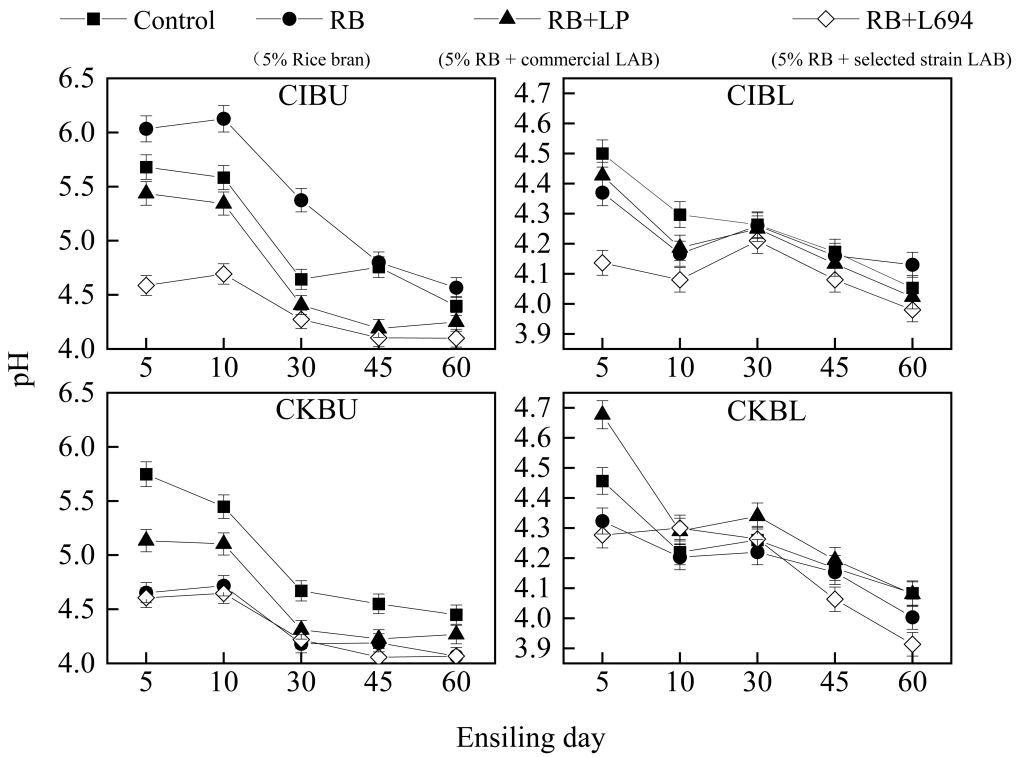

FIGURE 1 | pH dynamics of *Caragana intermedia* (CI) and *Caragana korshinskii* (CK) silages at the budding (BU) and blooming stages (BL) during ensiling. RB, 5% rice bran; LP, commercial inoculant strain *Lactobacillus plantarum*; L694, a selected strain *Lactobacillus* ($n = 3$).

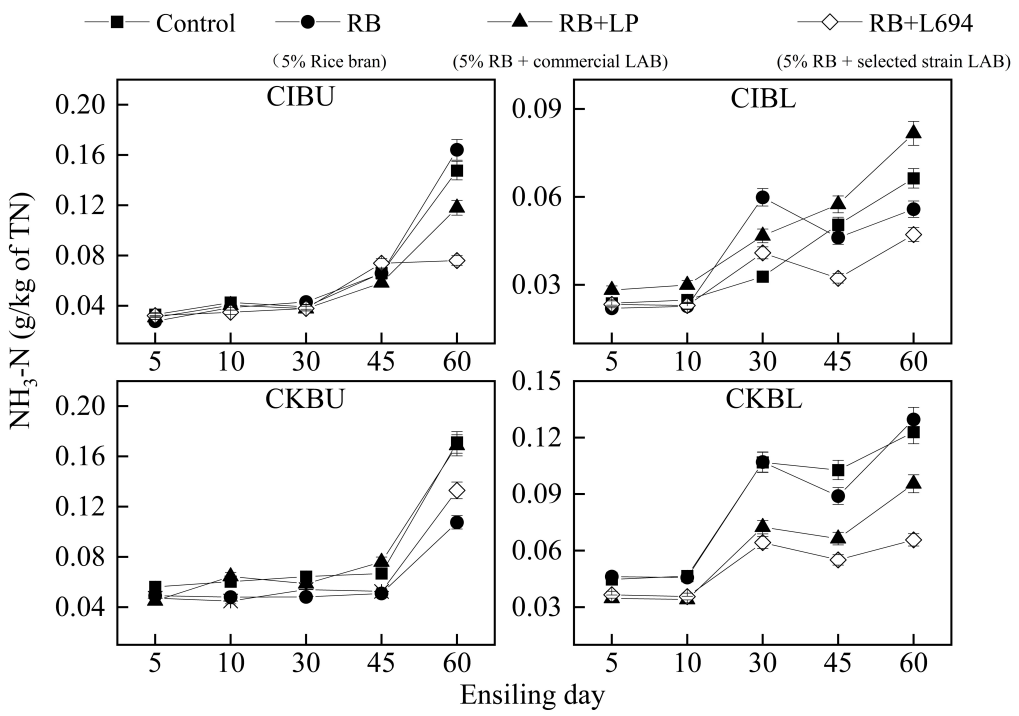

FIGURE 2 | NH_3-N dynamics of *Caragana intermedia* (CI) and *Caragana korshinskii* (CK) silages at the budding (BU) and blooming stages (BL) during ensiling. RB, 5% rice bran; LP, commercial inoculant strain *Lactobacillus plantarum*; L694, a selected strain *Lactobacillus* ($n = 3$).

TABLE 2 | Fermentation quality, IVDMD, and IVDFD of *Caragana* silages prepared without and with RB and LAB at different growth stages ($n = 3$).

Item	Material[2]	*Caragana* silage treatmen[3]				SEM[4]	*P*-value[5,6]						
		Control	RB	RB + LP	RB + L694		V	G	A	V × G	V × A	G × A	V × G × A
Lactic acid (% of DM)	CIBU	$7.32^{C\ a}$	9.47^{Ba}	8.88^{Ba}	10.66^{Aa}	0.34	**	**	**	**	**	NS	**
	CIBL	8.27^{Ba}	8.85^{ABa}	9.81^{Aa}	10.19^{Aa}								
	CKBU	5.77^{Bb}	6.65^{Bb}	9.29^{Aa}	8.64^{Ab}								
	CKBL	6.86^{Bab}	9.13^{Aa}	9.93^{Aa}	9.91^{Aa}								
Acetic acid (% of DM)	CIBU	2.13^{Aab}	1.64^{Bc}	1.83^{Bb}	1.83^{Bb}	0.06	NS	NS	**	**	**	**	**
	CIBL	2.40^{Aa}	1.91^{Bb}	2.02^{Ba}	1.67^{Cc}								
	CKBU	1.99^{Bb}	2.23^{Aa}	2.07^{ABa}	2.02^{Ba}								
	CKBL	2.12^{Aab}	1.61^{Cc}	1.90^{Bab}	1.84^{Bb}								
Propionic acid (% of DM)	CIBU	0.043^{Aa}	0.023^{Bb}	0.037^{Aa}	0.040^{Ab}	0.004	*	**	*	**	**	*	*
	CIBL	0.033^{Ab}	0.023^{Ab}	0.027^{Aa}	0.034^{Ab}								
	CKBU	0.047^{ABa}	0.053^{Aa}	0.030^{Ba}	0.053^{Aa}								
	CKBL	0.020^{Cc}	0.036^{Aab}	0.033^{ABa}	$0.027^{BC\ b}$								
LA/AA	CIBU	3.44^{Ca}	5.76^{Aa}	4.85^{Bab}	5.83^{Aa}	0.19	**	**	**	**	**	NS	**
	CIBL	3.46^{Ca}	4.63^{Bb}	4.85^{Bab}	6.09^{Aa}								
	CKBU	2.90^{Ba}	2.99^{Bc}	4.50^{Ab}	4.29^{Ab}								
	CKBL	3.24^{Ba}	5.68^{Aa}	5.23^{Aa}	5.41^{Aa}								
Aerobic stability (h)	CIBU	113.67^{Aa}	115.00^{Aa}	102.33^{Aa}	115.83^{Aa}	2.30	NS	**	**	**	**	**	**
	CIBL	36.67^{Db}	41.17^{Cc}	65.17^{Bc}	70.50^{Ac}								
	CKBU	125.17^{Aa}	115.17^{Ba}	87.17^{Db}	93.17^{Bb}								
	CKBL	36.00^{Db}	70.33^{Bb}	56.50^{Cc}	89.83^{Abc}								
In vitro digestibility[1]													
IVDMD (%DM)	CIBU	53.51^{Cb}	55.98^{Bc}	57.43^{ABb}	59.25^{Ab}	0.86	**	**	**	**	**	**	NS
	CIBL	58.40^{Ca}	63.38^{ABa}	62.55^{Ba}	66.54^{Aa}								
	CKBU	46.82^{Bc}	52.34^{Ad}	51.62^{Ac}	52.74^{Ad}								
	CKBL	46.83^{Dc}	59.61^{Ab}	53.92^{Cc}	56.49^{Bc}								
IVNDFD (%DM)	CIBU	16.87^{Ac}	16.74^{Abc}	17.63^{Ab}	16.42^{Ab}	0.29	**	**	**	NS	NS	*	NS
	CIBL	16.76^{Ac}	15.78^{Bc}	16.06^{ABc}	14.90^{Cc}								
	CKBU	19.80^{Aa}	18.85^{ABa}	19.99^{Aa}	18.26^{Ba}								
	CKBL	18.62^{Ab}	17.05^{Bb}	17.64^{Bb}	17.77^{Ba}								

[1] *IVDMD, in vitro dry matter digestibility; IVNDFD, in vitro neutral detergent fiber digestibility.*
[2] *CI, Caragana intermedia; CK, Caragana korshinskii; BU, budding stage; BL, blooming stage.*
[3] *RB, 5% rice bran; RB + LP, 5% rice bran + commercial inoculant strain Lactobacillus plantarum; RB + L694, 5% rice bran + strain Lactobacillus 694.*
[4] *SEM, standard error of the means.*
[5] *V, varieties; G, growth stage; A, additives; V × G, interaction between varieties and growth stage; V × A, interaction between varieties and additives; G × A, interaction between growth stage and additives; V × G × A, interaction between varieties, growth stage, and additives.*
[6] *NS, no significant, *$p < 0.05$; **$p < 0.01$.*
$^{A-D}$Means of inoculation treatments within a row with different superscripts differ ($p < 0.05$).
$^{a-d}$Means of variety and growth stage within a column with different superscripts differ ($p < 0.05$).

group. The samples in the two groups were close to each other, and there was little difference in species diversity. In CKBL, RB + LP, and RB + L694 were clustered into two different separate groups, and one single sample in RB treatment was far away from the other two samples, and there were great differences in species diversity. Similar to CKBL, RB + LP, and RB + L694 silages in CKBU were grouped separately, while the distance between control and RB samples was large.

Bacterial Composition Analysis of *Caragana* Silage

The fresh *Caragana* and silage had mainly five phyla and 18 genera (**Figures 4–6**). *Proteobacteria* were the main phylum in fresh *Caragana*, with 57.24% of abundance, while the most dominant phylum ($p < 0.05$) in *Caragana* silages was *Firmicutes* (50.09–98.99%). For CIBU, *Pantoea* were dominant in fresh *Caragana* (14.41%) ($p < 0.05$), and *Lactobacillus* was the most predominant epiphytic bacteria ($p < 0.05$) in RB + L694 and control silages, which was 92.34 and 89.26%, respectively. *Enterococcus* (39.44%) was the main bacteria in RB + LP silages. For CKBU, *Sphingomonas* (11.83%) and *Hymenobacter* (14.69%) were dominant in the fresh *Caragana*. The dominant bacteria of RB + L694 silage were *Lactobacillus*, with a relative abundance of 91.88%, significantly higher than that of the control group ($p < 0.05$). For CIBL, fresh *Caragana* has the most relative abundance ($p < 0.05$) of *Sphingomonas* (22.54%), same as CIBU silages. *Lactobacillus* (44.35%) was the predominant epiphytic bacteria in RB + L694, followed by *Pseudomonas* (16.75%) and *Enterococcus* (9.76%). *Lactobacillus* (77.24%) was dominant in RB + LP silage. For CKBL, *Rhodococcus* (13.72%) was dominant in the fresh *Caragana*. RB + L694 had the most

TABLE 3 | Analysis of alpha diversity of *Caragana* silage after ensiling ($n = 3$).

Items	Material	Fresh shrub	Treatment				SEM	*P*-value						
			Control	RB	RB + LP	RB + L694		V	G	A	V × G	V × A	G × A	V × G × A
Shannon	CIBU	1.91	0.91	2.06	1.64	1.47	0.069	**	**	**	*	**	*	**
	CIBL	3.15	1.59	2.72	1.66	2.23								
	CKBU	1.06	1.46	1.92	1.64	0.98								
	CKBL	2.32	1.04	0.84	3.10	0.17								
Simpson	CIBU	0.45	0.66	0.20	0.29	0.46	0.022	**	NS	**	*	**	*	**
	CIBL	0.16	0.38	0.19	0.55	0.24								
	CKBU	0.65	0.35	0.23	0.36	0.68								
	CKBL	0.35	0.53	0.70	0.08	0.95								
Ace	CIBU	490.44	137.60	258.07	206.11	259.26	8.584	NS	NS	**	**	**	*	NS
	CIBL	557.65	134.70	245.44	260.24	431.02								
	CKBU	598.49	223.85	308.87	191.37	161.39								
	CKBL	492.41	136.93	148.36	231.79	180.37								
Chao1	CIBU	486.87	130.79	202.06	201.16	261.07	8.409	**	NS	**	**	**	NS	NS
	CIBL	557.47	124.66	252.10	264.75	415.74								
	CKBU	494.67	168.78	296.79	172.35	162.48								
	CKBL	487.79	114.23	134.75	241.73	137.12								
Coverage	CIBU	0.9984	0.9993	0.9990	0.9993	0.9991	0.00	NS	**	**	NS	*	**	NS
	CIBL	0.9993	0.9995	0.9995	0.9996	0.9985								
	CKBU	0.9980	0.9992	0.9989	0.9992	0.9997								
	CKBL	0.9990	0.9995	0.9997	0.9996	0.9994								

*BU, budding stage; BL, blooming stage; CI, C. Intermedia; CK, C. korshinskii; RB, 5% rice bran; RB + LP, 5% rice bran plus commercial inoculant strain Lactobacillus plantarum; RB + L694, 5% rice bran plus strain Lactobacillus 694; V, varieties; G, growth stage; A, additives; NS, no significant, *$p < 0.05$; **$p < 0.01$.*

relative abundance ($p < 0.05$) of *Lactobacillus*, which was 98.88%. In RB + LP silage, it also appeared *Enterococcus* (10.44%), *Acetobacter* (10.77%), and *Pediococcus* (9.24%). At the genus level (**Figures 5**, **6**), the most dominant bacterial genus ($p < 0.05$) in the blooming stage silages was *Lactobacillus*, with more than 40% of abundance. However, *Enterococcus* was the most dominant genus ($p < 0.05$) in CI (9.44%) and CK (56.77%) which was treated with RB + LP, while varied microbes were observed in fresh *Caragana*.

Chemical Composition of *Caragana* Silage

The chemical compositions of *Caragana* silage are shown in **Table 4**. The varieties, growth stage, varieties × growth stage, and varieties × additives had effects on CP content ($p < 0.05$), and additives did not affect the CP content, while influenced by the interaction of the three factors. The varieties, growth stage, additives, and their interactions affected the content of aNDF, ADF, ADL, and WSC content ($p < 0.05$). The concentrations of CP, fiber, and WSC of *Caragana* silage in the blooming stage ($p < 0.05$) increased, and the CP and fiber contents in *C. intermedia* silage were higher and lower than *C. korshinskii* silage, respectively. The RB and RB + L694 treatments effectively reduced the fiber content.

In vitro Degradability of *Caragana* Silage

As shown in **Table 2**, the IVDMD was affected by varieties, growth stage, additives, and interaction between their pairwise combinations ($p < 0.01$). Compared with the control group, IVDMD content in additive treatments was significantly increased ($p < 0.05$). CI had higher IVDMD than CK ($p < 0.05$), while the budding stage had higher IVDMD than the blooming stage ($p < 0.05$). IVNDFD was mainly affected by the interaction of growth stage and additives ($p < 0.05$), added RB + L694 in *Caragana* Silage could significantly reduce the IVNDFD of CIBL, CKBU, and CKBL, and CK had higher IVNDFD ($p < 0.05$) than CK.

DISCUSSION

Chemical Composition of Fresh *Caragana* and Silage

The fresh *Caragana* had high compositions of NDF and ADF. Bai et al. (2016) reported that high CP and ash compositions are detected in Ordos *C. intermedia* (19.86 and 8.24%, respectively), but aNDF and ADF are different to this report and it is likely due to the difference in location, varieties, clipping time, and years of cultivation. It is confirmed that the nutritional value is changed in the different growth stages of *Caragana* (Chen et al., 2010). As shown in **Table 4**, the aNDF, ADF, ADL compositions of CIBL and CKBU were lower than CIBU and CKBL, which revealed that varieties and growth stage had an interaction on fiber contents of *Caragana*. The aNDF, ADF, ADL, and WSC compositions of *C. intermedia* were significantly lower than that of CK. The *Caragana* shrub generally contains higher CP, because of nitrogen fixation with rhizobia of legume (Ji et al., 2015). *Caragana* at the blooming growth

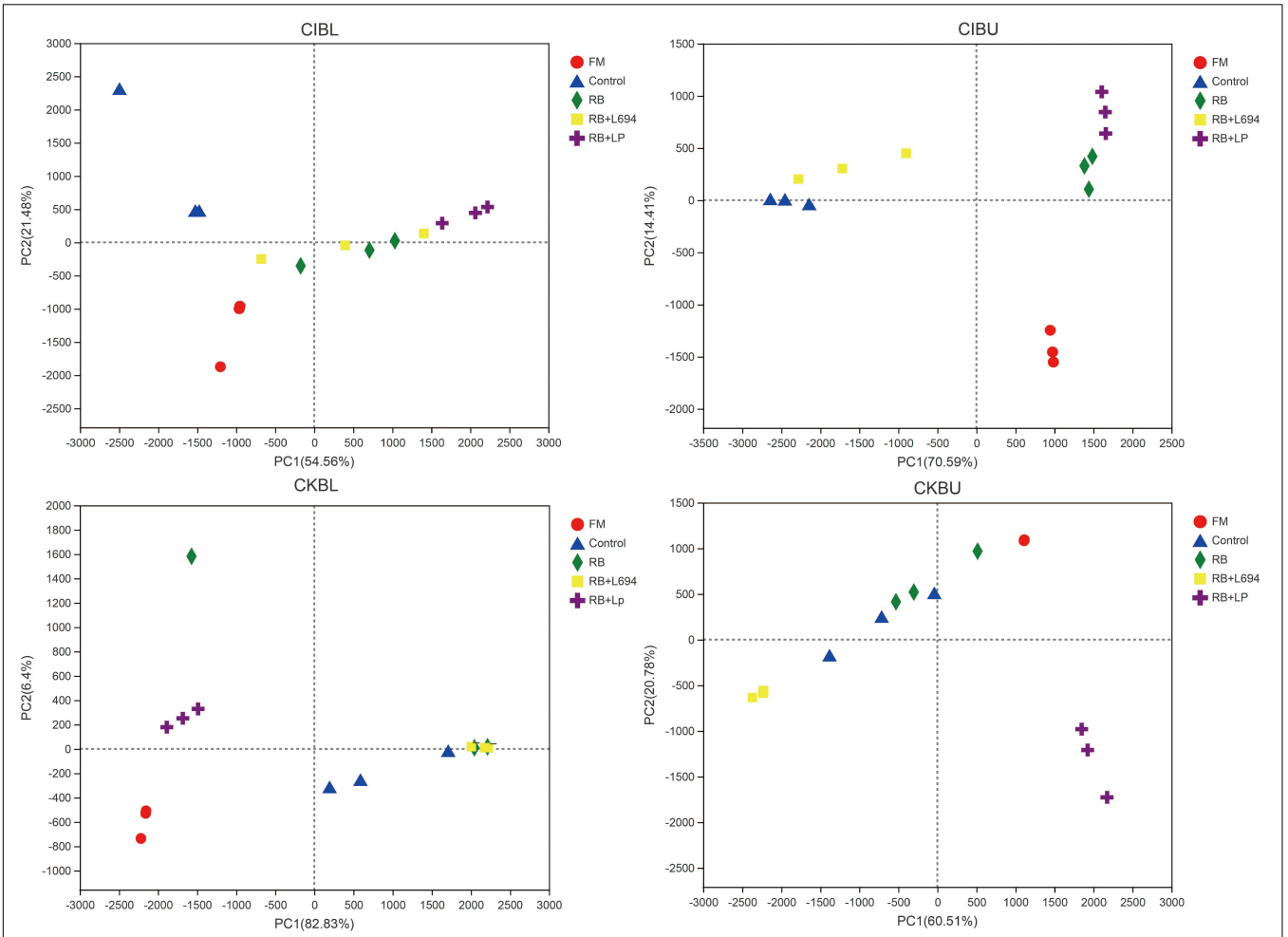

FIGURE 3 | PCA analysis of OTU level for *Caragana intermedia* (CI) and *Caragana korshinskii* (CK) silages at the budding (BU) and blooming stages (BL) after 60 days of ensiling. RB, 5% rice bran; LP, commercial inoculant strain *Lactobacillus plantarum*; L694, a selected strain *Lactobacillus* ($n = 3$).

stage contained higher WSC and CP contents than the budding growth stage, due to the accumulation of nutrients during growth process (Xie et al., 2018). Therefore, based on the above analysis, the suitable cutting time for the two varieties is the flowering period.

Low fiber contents appeared in additive groups relative to control. We attributed that the lower aNDF, ADF, and ADL content in the silage inoculated with LAB may result from fibrinolytic enzyme production by other microorganisms during silage fermentation (He et al., 2020). The use of additives had no effect on crude protein content ($p > 0.05$), and both RB and RB + L694 treatments could enhance the compositions of WSC, while reducing the compositions of ADF, aNDF, and ADL of *Caragana* silage, which is due to the carbohydrate in rice bran, provides fermentation substrates for microorganisms, thus facilitating the preservation of silage nutrients. The CIBL and CKBL silages had higher CP content and lower aNDF and ADF contents than CIBU and CKBU ($p < 0.05$). Thus, the suitable cutting time for two varieties is the blooming stage according to the above analysis, and the *C. Intermedia* harvested in the blooming stage could result in better quality silage.

Fermentation Characteristics of *Caragana* Silage

The decrease in pH is considered an important index to reflect the silage fermentation process, and the accumulation of NH_3-N during the ensiling process is commonly recognized as the indicator of protein degradation (Nkosi et al., 2010). The dynamics of pH and NH_3-N of *Caragana* silage indicate that varieties and growth stages, also rice bran and *Lactobacillus,* could influence the fermentation process.

The RB + L694 treatment exhibited lower pH and NH_3-N than control, which indicated good fermentation. It is challenging to make high-quality silage for legumes, and single or combined bacterial inoculants have been used to improve the silage fermentation by accelerating the production of LA to inhibit the growth of undesirable bacteria and fungi, thereby reducing the nutrition loss (Cai et al., 1998;

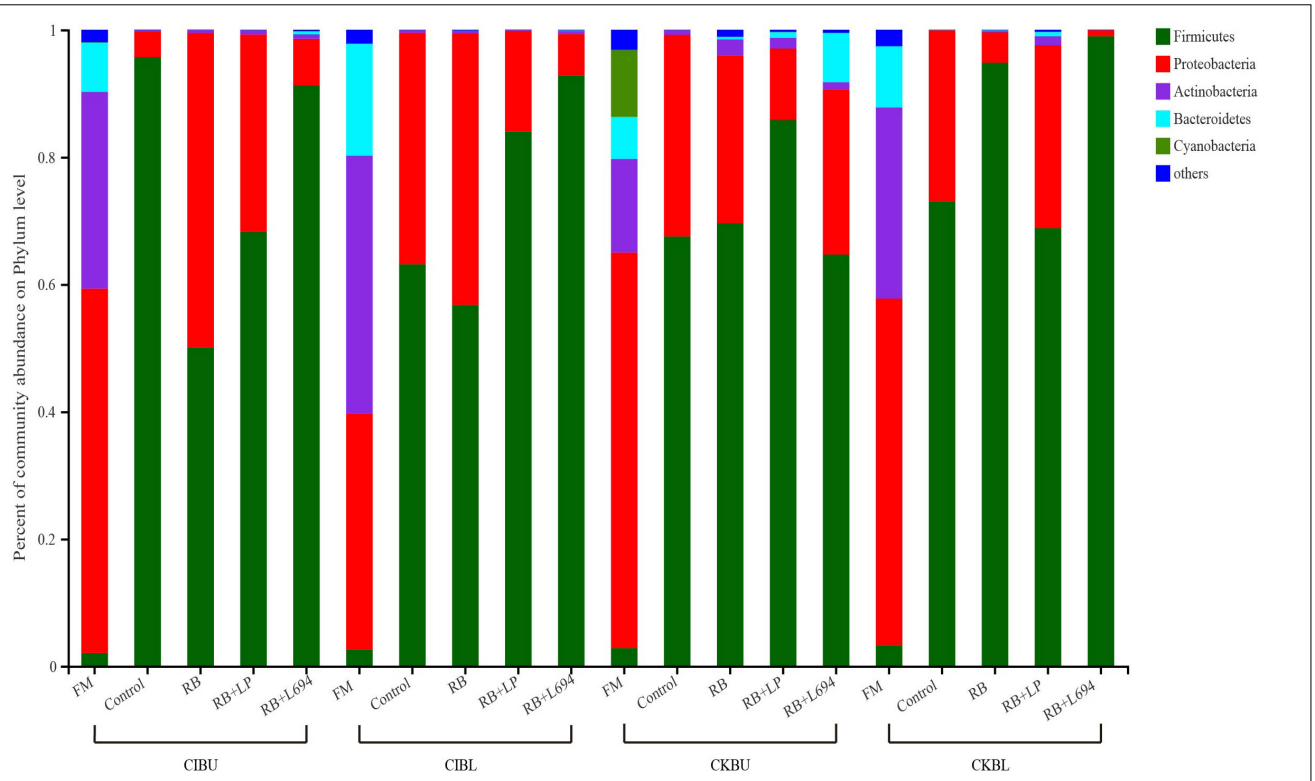

FIGURE 4 | Bacterial communities and relative abundance of *Caragana* materials and their silages at phylum level ($n = 3$).

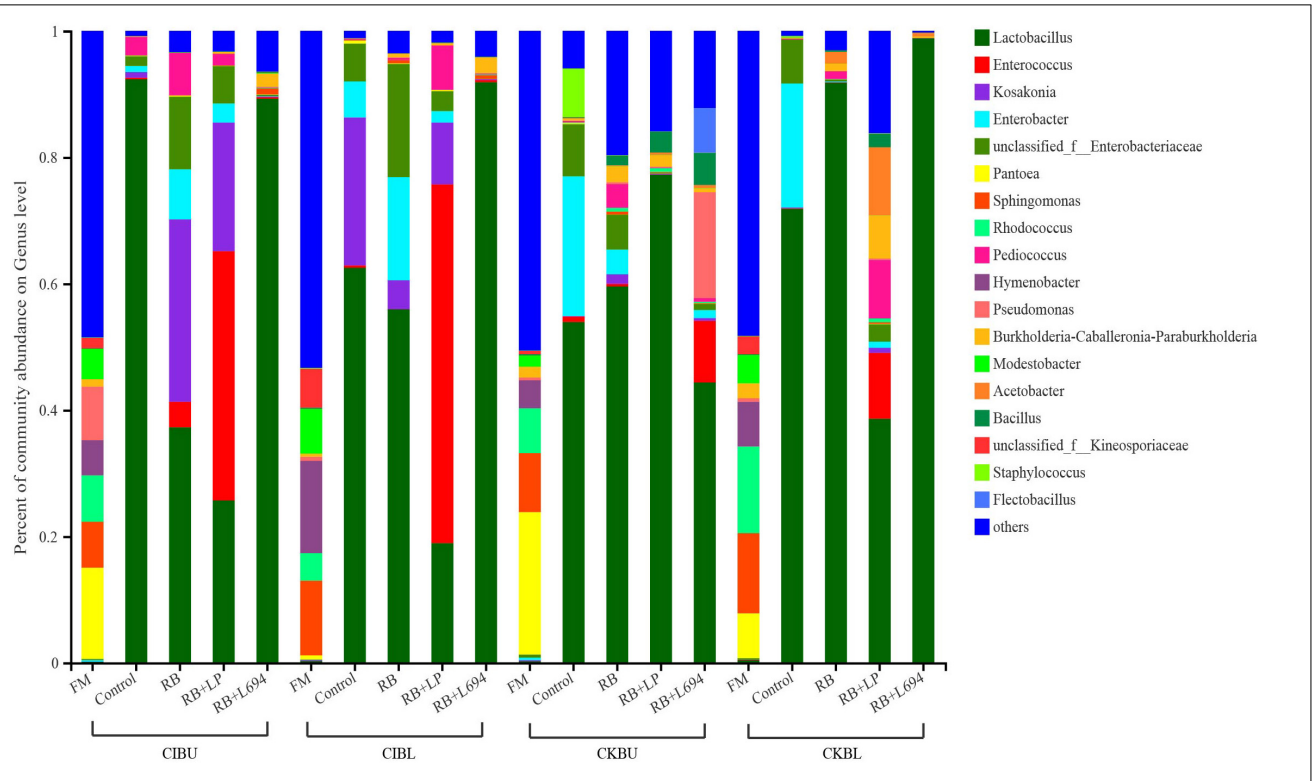

FIGURE 5 | Bacterial communities and relative abundance of *Caragana* materials and their silages at genus level ($n = 3$).

TABLE 4 | Chemical composition of *Caragana* silages prepared without and with RB and LAB at different growth stages ($n = 3$).

Item	Material[1]	*Caragana* silage treatmen[2]				SEM[3]	*P*-value[4,5]						
		Control	RB	RB + LP	RB + L694		V	G	A	V × G	V × A	G × A	V × G × A
DM (%)	CIBU	40.04	39.48	40.58	40.36	0.68	NS	NS	NS	NS	NS	NS	NS
	CIBL	39.35	41.07	41.33	39.97								
	CKBU	39.94	40.50	39.96	39.47								
	CKBL	40.46	40.82	39.85	39.65								
CP (% of DM)	CIBU	11.70^{Aa}	11.85^{Aa}	11.38^{Aa}	11.45^{Aa}	0.22	**	**	NS	**	**	**	**
	CIBL	13.19^{ABb}	14.11^{Ab}	12.57^{Bb}	13.71^{Ab}								
	CKBU	9.64^{Ac}	9.33^{Bc}	9.67^{Ab}	9.79^{Ab}								
	CKBL	9.92^{ABc}	9.50^{Bd}	11.19^{Ac}	11.09^{Ac}								
aNDFom (% of DM)	CIBU	70.34^{Ab}	65.77^{Ba}	66.05^{Bc}	65.90^{Bb}	0.89	**	**	**	**	**	**	**
	CIBL	65.62^{Ac}	56.82^{Cb}	68.80^{Aab}	61.20^{Bc}								
	CKBU	72.97^{Aab}	66.24^{Ca}	69.99^{Ba}	69.05^{Ba}								
	CKBL	75.95^{Aa}	66.10^{Ca}	66.97^{BCbc}	69.14^{Ba}								
ADFom (% of DM)	CIBU	54.58^{Ab}	50.92^{Ba}	49.66^{Bb}	49.19^{Bb}	0.76	**	**	**	**	**	**	**
	CIBL	46.73^{Bc}	42.79^{Cb}	51.57^{Aa}	45.56^{BCc}								
	CKBU	56.18^{Ab}	51.08^{Ca}	54.83^{ABa}	53.65^{Ba}								
	CKBL	59.76^{Aa}	52.40^{Ba}	51.93^{Ba}	52.82^{Ba}								
ADL (% of DM)	CIBU	20.68^{Aa}	17.90^{Ba}	15.59^{Cb}	13.73^{Cb}	0.45	**	**	**	*	**	**	**
	CIBL	15.13^{ABc}	14.49^{Bc}	14.93^{ABb}	15.54^{Aa}								
	CKBU	18.64^{Ab}	16.02^{Bb}	17.46^{Aa}	15.85^{Ba}								
	CKBL	18.75^{Ab}	16.44^{Bb}	18.56^{Aa}	16.56^{Ba}								
WSC (% of DM)	CIBU	0.33^{Cc}	0.68^{Bd}	1.23^{Ac}	1.34^{Ac}	0.08	**	**	**	**	**	**	**
	CIBL	1.16^{Cb}	2.83^{Aa}	2.37^{Ba}	2.51^{ABa}								
	CKBU	0.58^{Cc}	1.98^{Ac}	1.55^{Bc}	1.99^{Ab}								
	CKBL	2.31^{Aa}	2.57^{Ab}	1.45^{Bc}	1.72^{Bb}								

[1] *CI, Caragana intermedia; CK, Caragana korshinskii; BU, budding stage; BL, blooming stage.*
[2] *RB, 5% rice bran; RB + LP, 5% rice bran + commercial inoculant strain Lactobacillus plantarum; RB + L694, 5% rice bran + strain Lactobacillus 694.*
[3] *SEM, standard error of the means.*
[4] *V, varieties; G, growth stage; A, additives; V × G, interaction between varieties and growth stage; V × A, interaction between varieties and additives; G × A, interaction between growth stage and additives; V × G × A, interaction between varieties, growth stage, and additives.*
[5] *NS, no significant, *$p < 0.05$; **$p < 0.01$.*
[6] *DM, dry matter; CP, crude protein; aNDFom, neutral detergent fiber; ADFom, acid detergent fiber; ADL, acid detergent lignin; WSC, water-soluble carbohydrates.*
$^{A-C}$Means of inoculation treatments within a row with different superscripts differ ($p < 0.05$).
$^{a-c}$Means of variety and growth stage within a column with different superscripts differ ($p < 0.05$).

Eikmeyer et al., 2013; Bao et al., 2016; Ogunade et al., 2017; Muck et al., 2018). Treating with RB + L694 could increase the contents of LA and LA/AA and decrease pH and NH_3-N contents compared with the control group. This suggested inoculation of commercial LP or L694 with 5% rice bran at ensiling *Caragana* could improve the fermentation quality of silage.

In the current experiments, silages prepared from the budding stage exhibited low fermentation quality. Due to the low WSC content of *Caragana* in the budding stage, the fermentation substrate was less and the fermentation was incomplete, as reflected by lower LA and higher pH. It has been proved that growth stage affects aerobic losses, which tended to increase as the plants aged (Weinberg et al., 2010). The aerobic stability of additive treatment was higher than control treatment. At the blooming stage, all treated silage had higher aerobic stability than the control, and *Lactobacillus* 694 had the best effect on particularly improving aerobic stability. Therefore, the CIBL had better fermentation quality, which could improve aerobic stability by plus rice bran and a selected strain L694.

The Microbial Community of *Caragana* Silage

The high coverage value of each sample was about 0.99, indicating that most of sequencing was detected. High bacterial richness and diversity consisted in fresh *Caragana.* In our study, CK at BU and BL stages treated with RB + L694 had lower Shannon index and higher Simpson index than that of control, indicating the decrease in bacterial diversity and richness. This suggests that adding rice bran to CK silage in both growth stages can provide a basis for lactobacillus fermentation (Su et al., 2021), which can then grow rapidly under anaerobic conditions.

The fermentation quality of silage is highly dependent on the epiphytic microflora because ensiling is a bacterial-driven fermentation process. *Firmicutes* and *Proteobacteria* were the dominant microorganisms in legumes before ensiling

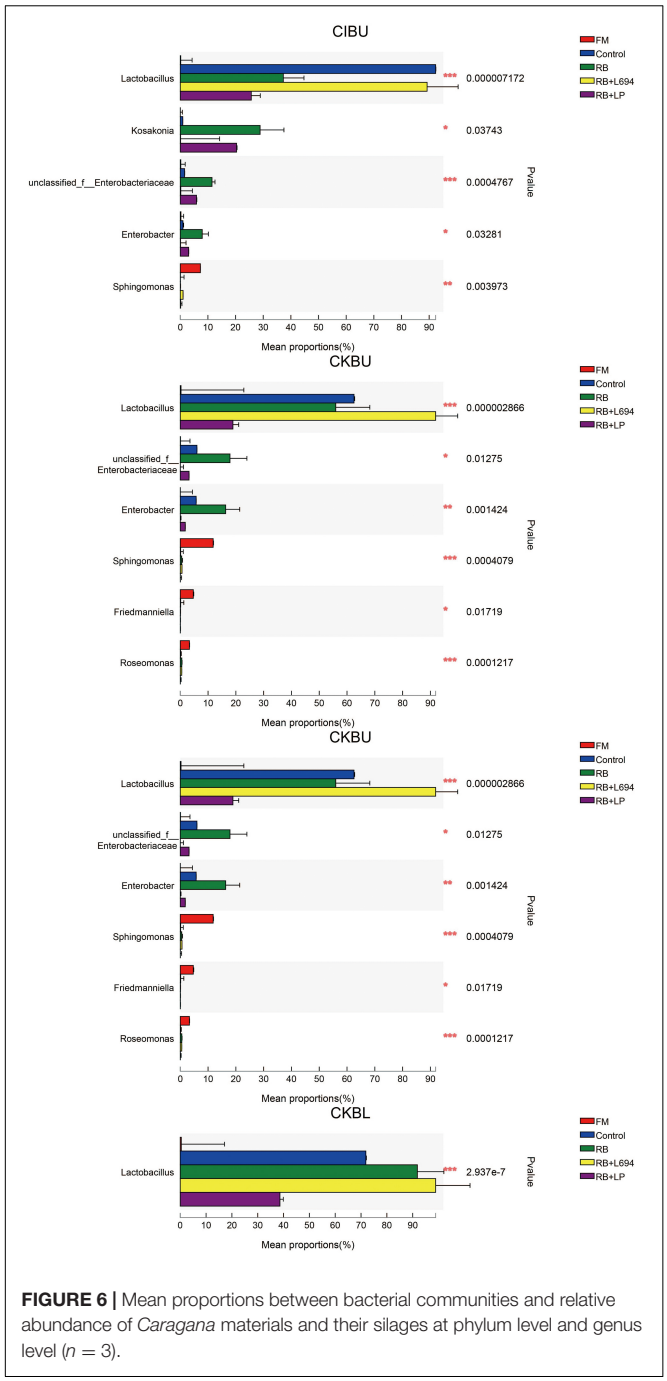

FIGURE 6 | Mean proportions between bacterial communities and relative abundance of *Caragana* materials and their silages at phylum level and genus level ($n = 3$).

(He et al., 2020). In our study, *Proteobacteria* were the dominant phylum in fresh material (57.24, 37.10, 62.12, and 54.50% for CIBU, CKBL, CIBU, and CKBL, respectively). *Proteobacteria* are gram-negative bacteria, which will compete with LAB to utilize WSC, resulting in the decreasing CP content and the increasing NH_3-N content (Madigan, 2006). *Firmicutes* as gram-positive bacteria can degrade many macromolecular compounds, such as starch, protein, and cellulose (Song et al., 2015). After silage fermentation, the bacterial community mainly evolved into *Firmicutes*, and this may be caused by an increase in *Lactobacillus* and *Enterococcus*, both of which belong to *Firmicutes*. The present findings are consistent with that of Yuan et al. (2020), who proved that *Firmicutes* increased significantly in Napier grass silage as storage period was prolonged. After 60-days fermentation, *Firmicutes* were the dominant phyla and their number increased, while the number of *Proteobacteria* decreased, which was consistent with the report of Zhang et al. (2019). The decrease in aNDF, ADF, and NH_3-N in silage might be related to this.

In order to further investigate the bacterial community during silage fermentation of *Caragana*, this experiment analyzed the changes in bacterial compositions at genus level. It showed that two growth stages could change the bacterial community of fresh material. The diversity and richness of bacteria decreased in CK silages treated with RB + L694, compared to those in the control silage.

Lactobacillus was the dominant genus in *Caragana* silage, which plays an important role in pH reduction at the later stage of ensiling (Cai et al., 1998). *Lactobacillus* abundance and fermentation quality in RB + L694 silage were higher than other silage because the exogenous *Lactobacillus* had a greater capacity to produce LA than epiphytic LAB of fresh material (Ali et al., 2020). As a kind of cumulative anaerobic bacteria mainly producing L (+)-LA, *Enterococcus* plays a positive role in improving the quality of *Caragana* silage. In this study, RB + LP treatment increased the number of *Enterococcus* in CIBU, CKBU, and CKBL. This indicated that the addition of LAB in *Caragana* silage increased the content of LA in silage and improved the fermentation quality, which was consistent with the research results of Tohno et al. (2013). Ensiling increased *Lactobacillus* and *Enterococcus* proportion in *Caragana* plant silage, which may contribute to the silage fermentation process to form an acidic environment so that most microorganisms were inhibited. This is consistent with the results reported by Cai et al. (2020). *Kosakonia* was the dominant microbe in the mulberry leaves and stylo silage and was pathogenic bacteria. The abundance of *Kosakonia* was 28.87, 20.36, 23.40, 4.58, and 9.79% in RB and RB + LP treatment of CIBU, control and RB treatment of CKBU, and RB + LP treatment of CKBU, respectively. The blooming stage of *Caragana* silage decreased *Kosakonia* abundance, indicating that undesirable microorganisms were reduced at the blooming compared with the budding growth stage. *Enterobacter* is facultative anaerobes, which is considered undesirable bacteria in silage, especially in silage with rich protein, because it can metabolize WSC and LA to produce other products, resulting in a nutrient loss in silage (Madigan, 2006). In CIBU, CKBU, and CIBL silages, *Enterobacter* was existed in untreated silage and treatments with RB silage, indicating that the LAB population did not inhibit the growth and propagation of undesirable microorganisms, and the addition of RB may promote the growth of *Enterobacter* (Keshri et al., 2019). As plant pathogens, *Pantoea* was also detected in fresh soybean and alfalfa. In our study, ensiling greatly decreases undesirable microorganisms (*Pantoea*). Thus, adding rice bran and inoculant strain *Lactobacillus* gives rise to the increase in LAB proportion and inhibits the growth of harmful bacteria in *Caragana* silage.

In vitro Degradability of *Caragana* Silage

The IVDMD at the blooming stage was higher than that in the budding stage, indicating that more DM was available in the blooming stage. The higher IVDMD of CI silage may be due to their lower fiber, because of the decomposition resistance of fiber content (Jung and Allen, 1995; Zhang et al., 2015). In this study, IVNDFD (48 h) decreased significantly with the maturation of CK ($p < 0.05$), which was similar to previous reports (Bai et al., 2016), and this may be due to the increase in ADF content with increasing maturity. The RB, RB + LP, and RB + L694 groups increased digestibility of silages, as reflected by the increasing IVDMD. Previous studies had suggested that LAB reduced DM loss in silage, and high IVDMD was detected in silage inoculated with LAB than that without LAB (Liu et al., 2016). In this study, RB + L694 group had greater IVDMD than other treatments, because RB + L694 had better inhibitive effect on DM loss.

CONCLUSION

The forage growth stage has a greater impact on fermentation quality and nutritional value of silage. Growth stage had effects on chemical composition and *in vitro* digestibility, and the suitable cutting time for two *Caragana* species is the blooming stage. Rice bran and LAB inoculants increased WSC and LA concentrations of *Caragana* silage. *L. plantarum* 694, as a screening lactic acid bacterium, performed better than commercial *L. plantarum* on fermentation quality. In the blooming stage, RB + L694 treatments for two *Caragana* species could enhance the abundance of *Lactobacillus* and inhibit the growth of harmful bacteria such as *Enterobacter* in *Caragana* silage further improving *Caragana* silage fermentation. The best fermentation group was RB + L694 treatment of CIBL, and the group that ferments best was RB + LP and RB + L694 of CKBL. This study will provide the theoretical basis for the scientific and rational utilization of *Caragana* resources.

DATA AVAILABILITY STATEMENT

The sequencing data were submitted to the NCBI Sequence Read Archive database (accession number: PRJNA815495).

AUTHOR CONTRIBUTIONS

GZ and YC designed the experiments. HZ and HFZ ensiled the *Caragana* and collected the samples. JY and HZ analyzed the data and wrote the manuscript. YX and YC helped supervise the manuscript writing. All authors read and approved the final manuscript.

FUNDING

This study was supported by the National Natural Science Foundation of China (31660694) and Top Discipline Construction Project of Pratacultural Science of Ningxia University (NXYLXK2017A01). Key Research and Development Projects of Ningxia Hui Autonomous Region (2021BBF02034, 2021BEG02042, and 2018BEB04019).

ACKNOWLEDGMENTS

The financial support from the National Natural Science Foundation of China and Ningxia University is gratefully acknowledged.

REFERENCES

Ali, N., Wang, S., Zhao, J., Dong, Z., Li, J., Nazar, M., et al. (2020). Microbial diversity and fermentation profile of red clover silage inoculated with reconstituted indigenous and exogenous epiphytic microbiota. *Bioresour. Technol.* 314:123606. doi: 10.1016/j.biortech.2020.123606

Bai, C. L., Zhao, H. P., Jia, M., and Ding, H. J. (2016). Progress on research and utilization of caragana intermedia kuang.cv.ordos. *Animal Husbandry Feed Sci.* 37, 39–40.

Bao, W., Mi, Z., Xu, H., Zheng, Y., Kwok, L. Y., Zhang, H., et al. (2016). Assessing quality of *Medicago sativa* silage by monitoring bacterial composition with single molecule, real-time sequencing technology and various physiological parameters. *Sci. Rep.* 6:28358. doi: 10.1038/srep28358

Basso, F. C., Rabelo, C. H. S., Lara, E. C., Siqueira, G. R., and Reis, R. A. (2018). Effects of *Lactobacillus buchneri* NCIMB 40788 and forage: concentrate ratio on the growth performance of finishing feedlot lambs fed maize silage. *Animal Feed Sci. Technol.* 244, 104–115. doi: 10.1016/j.anifeedsci.2018.08.008

Broderick, G. A., and Kang, J. H. (1980). Automated simultaneous determination of ammonia and total amino acids in ruminal fluid and in vitro media1. *J. Dairy Sci.* 63, 64–75. doi: 10.3168/jds.S0022-0302(80)82888-8

Cai, Y. M., Benno, Y., Ogawa, M., Ohmomo, S., Kumai, S., and Nakase, T. (1998). Influence of *Lactobacillus spp*. from an inoculant and of weissella and *Leuconostoc spp*. from forage crops on silage fermentation. *Appl. Environ. Microbiol.* 64, 2982–2987. doi: 10.1128/AEM.64.8.2982-2987.1998

Cai, Y. M., Du, Z. M., Yamasaki, S., Nguluve, D., Tinga, B., Macome, F., et al. (2020). Community of natural lactic acid bacteria and silage fermentation of corn stover and sugarcane tops in Africa. *Asian-Australasian J. Animal Sci.* 33, 1252–1264. doi: 10.5713/ajas.19.0348

Chen, X.-H., Gao, Y.-B., Zhao, T.-T., Zhu, M.-J., Ci, H.-C., and Xiao-yan, S. (2010). Morphological variations of *Caragana microphylla* populations in the *Xilingol steppe* and their relationship with environmental factors. *Acta Ecol. Sinica* 30, 50–55. doi: 10.1016/j.chnaes.2010.03.001

Dong, L. F., Zhang, H. S., Gao, Y. H., and Diao, Q. Y. (2020). Dynamic profiles of fermentation characteristics and bacterial community composition of *Broussonetia papyrifera* ensiled with perennial ryegrass. *Bioresour. Technol.* 310:123396. doi: 10.1016/j.biortech.2020.123396

Du, Z., Sun, L., Chen, C., Lin, J., Yang, F., and Cai, Y. (2021). Exploring microbial community structure and metabolic gene clusters during silage fermentation of paper mulberry, a high-protein woody plant. *Animal Feed Sci. Technol.* 275:114766. doi: 10.1016/j.anifeedsci.2020.114766

Eikmeyer, F. G., Köfinger, P., Poschenel, A., Jünemann, S., Zakrzewski, M., Heinl, S., et al. (2013). Metagenome analyses reveal the influence of the inoculant Lactobacillus buchneri CD034 on the microbial community involved in grass ensiling. *J. Biotechnol.* 167, 334–343. doi: 10.1016/j.jbiotec.2013.07.021

Ferrero, F., Tabacco, E., and Borreani, G. (2019). Effects of a mixture of monopropionine and monobutyrin on the fermentation quality and aerobic stability of whole crop maize silage. *Animal Feed Sci. Technol.* 258:114319. doi: 10.1016/j.anifeedsci.2019.114319

Grutzke, J., Malorny, B., Hammeri, J. A., Busch, A., Tausch, S. H., Tomaso, H., et al. (2019). Fishing in the soup - pathogen detection in food safety using metabarcoding and metagenomic sequencing. *Front. Microbiol.* 10:1805. doi: 10.3389/fmicb.2019.01805

He, L. W., Chen, N., Lv, H. J., Wang, C., Zhou, W., Chen, X. Y., et al. (2020). Gallic acid influencing fermentation quality, nitrogen distribution and bacterial community of high-moisture mulberry leaves and stylo silage. *Bioresour. Technol.* 295:122255. doi: 10.1016/j.biortech.2019.122255

Ji, Z., Yan, H., Cui, Q., Wang, E., Chen, W., and Chen, W. (2015). Genetic divergence and gene flow among *Mesorhizobium* strains nodulating the shrub legume Caragana. *Systematic Appl. Microbiol.* 38, 176–183. doi: 10.1016/j.syapm.2015.02.007

Jung, H. G., and Allen, M. S. (1995). Characteristics of plant cell walls affecting intake and digestibility of forages by ruminants. *J. Anim. Sci.* 73, 2774–2790. doi: 10.2527/1995.7392774x

Keshri, J., Krouptiski, Y., Abu-Fani, L., Achmon, Y., Bauer, T. S., Zarka, O., et al. (2019). Dynamics of bacterial communities in alfalfa and mung bean sprouts during refrigerated conditions. *Food Microbiol.* 84:103261. doi: 10.1016/j.fm.2019.103261

Li, L. H., Sun, Y. M., Yuan, Z. H., Kong, X. Y., Wao, Y., Yang, L. G., et al. (2015). Effect of microalgae supplementation on the silage quality and anaerobic digestion performance of *Manyflower silvergrass*. *Bioresour. Technol.* 189, 334–340. doi: 10.1016/j.biortech.2015.04.029

Liu, Q.-H., Li, X.-Y., Desta, S. T., Zhang, J.-G., and Shao, T. (2016). Effects of *Lactobacillus plantarum* and fibrolytic enzyme on the fermentation quality and in vitro digestibility of total mixed rations silage including rape straw. *J. Int. Agriculture* 15, 2087–2096. doi: 10.1016/s2095-3119(15)61233-3

Madigan, M. T. (2006). *Brock Biology of Microorganisms*. Hoboken, NJ: Pearson/Prentice Hall.

Muck, R. E., Nadeau, E. M. G., McAllister, T. A., Contreras-Govea, F. E., Santos, M. C., and Kung, L. (2018). Silage review: recent advances and future uses of silage additives. *J. Dairy Sci.* 101, 3980–4000. doi: 10.3168/jds.2017-13839

Murphy, R. P. (1958). A method for the extraction of plant samples and the determination of total soluble carbohydrates. *J. Sci. Food Agriculture* 9, 714–717. doi: 10.1002/jsfa.2740091104

Nkosi, B. D., Meeske, R., Langa, T., Motiang, M. D., Modiba, S., Mkhize, N. R., et al. (2016). Effects of ensiling forage soybean (*Glycine max* (L.) Merr.) with or without bacterial inoculants on the fermentation characteristics, aerobic stability and nutrient digestion of the silage by Damara rams. *Small Ruminant Res.* 134, 90–96. doi: 10.1016/j.smallrumres.2015.12.001

Nkosi, B. D., Meeske, R., van der Merwe, H. J., and Groenewald, I. B. (2010). Effects of homofermentative and heterofermentative bacterial silage inoculants on potato hash silage fermentation and digestibility in rams. *Animal Feed Sci. Technol.* 157, 195–200. doi: 10.1016/j.anifeedsci.2010.03.008

Ogunade, I. M., Jiang, Y., Kim, D. H., Cervantes, A. A. P., Arriola, K. G., Vyas, D., et al. (2017). Fate of *Escherichia coli* O157:H7 and bacterial diversity in corn silage contaminated with the pathogen and treated with chemical or microbial additives. *J. Dairy Sci.* 100, 1780–1794. doi: 10.3168/jds.2016-11745

Ono, H., Nishio, S., Tsurii, J., Kawamoto, T., Sonomoto, K., and Nakayama, J. (2014). Monitoring of the microbiota profile in nukadoko, a naturally fermented rice bran bed for pickling vegetables. *J. Biosci. Bioeng.* 118, 520–525. doi: 10.1016/j.jbiosc.2014.04.017

Ren, H. W., Sun, W. L., Yan, Z. H., Zhang, Y. C., Wang, Z. Y., Song, B., et al. (2021). Bioaugmentation of sweet sorghum ensiling with rumen fluid: fermentation characteristics, chemical composition, microbial community, and enzymatic digestibility of silages. *J. Clean. Product.* 294:126308. doi: 10.1016/j.jclepro.2021.126308

Sekerka, I., and Lechner, J. F. (1974). Automated simultaneous determination of water hardness, specific conductance and pH. *Anal. Lett.* 7, 399–408. doi: 10.1080/00032717408058770

Shi, C. X., Liu, Z. Y., Shi, M., Li, P., Zeng, Z. K., Liu, L., et al. (2015). Prediction of digestible and metabolizable energy content of rice bran fed to growing pigs. *Asian-Australasian J. Animal Sci.* 28, 654–661. doi: 10.5713/ajas.14.0507

Song, Z., Li, W., Liu, X., and Feng, L. (2015). Diversities of firmicutes in four hot springs in yunnan and tibet. *Biotechnology* 25, 481–486. doi: 10.16519/j.cnki.1004-311x.2015.05.0095

Su, W., Jiang, Z., Wang, C., Xu, B., Lu, Z., Wang, F., et al. (2021). Dynamics of defatted rice bran in physicochemical characteristics, microbiota and metabolic functions during two-stage co-fermentation. *Int. J. Food Microbiol.* 362:109489. doi: 10.1016/j.ijfoodmicro.2021.109489

Tao, X. X., Wang, S. R., Zhao, J., Dong, Z. H., Li, J. F., Liu, Q. H., et al. (2020). Effect of ensiling alfalfa with citric acid residue on fermentation quality and aerobic stability. *Animal Feed Sci. Technol.* 269:114622. doi: 10.1016/j.anifeedsci.2020.114622

Tian, J. P., Yu, Y. D., Yu, Z., Shao, T., Na, R. S., and Zhao, M. M. (2014). Effects of lactic acid bacteria inoculants and cellulase on fermentation quality and in vitro digestibility of *Leymus chinensis* silage. *Grassland Sci.* 60, 199–205. doi: 10.1111/grs.12059

Tohno, M., Kitahara, M., Irisawa, T., Masuda, T., Uegaki, R., Ohkuma, M., et al. (2013). Lactobacillus silagei sp. nov., isolated from orchardgrass silage. *Int. J. Systematic Evol. Microbiol.* 63, 4613–4618. doi: 10.1099/ijs.0.053124-53120

Van Soest, P. J., Robertson, J. B., and Lewis, B. A. (1991). Methods for dietary fiber, neutral detergent fiber, and nonstarch polysaccharides in relation to animal nutrition. *J. Dairy Sci.* 74, 3583–3597. doi: 10.3168/jds.S0022-0302(91)78551-2

Wang, G. H., Chen, Z. X., Shen, Y. Y., and Yang, X. L. (2021). Efficient prediction of profile mean soil water content for hillslope-scale *Caragana korshinskii* plantation using temporal stability analysis. *Catena* 206:105491. doi: 10.1016/j.catena.2021.105491

Wang, X. Y., Zheng, W. D., Ma, Y. J., Ma, J. W., Gao, Y. M., Zhang, X. Y., et al. (2020). Gasification filter cake reduces the emissions of ammonia and enriches the concentration of phosphorous in *Caragana microphylla* residue compost. *Bioresour. Technol.* 315:123832. doi: 10.1016/j.biortech.2020.123832

Weinberg, Z. G., Khanal, P., Yildiz, C., Chen, Y., and Arieli, A. (2010). Effects of stage of maturity at harvest, wilting and LAB inoculant on aerobic stability of wheat silages. *Animal Feed Sci. Technol.* 158, 29–35. doi: 10.1016/j.anifeedsci.2010.03.006

Xie, L. N., Guo, H. Y., Chen, W. Z., Liu, Z., Gu, S., and Ma, C. C. (2018). Effects of grazing on population growth characteristics of caragana stenophylla along a climatic aridity gradient. *Rangeland Ecol. Manag.* 71, 98–105. doi: 10.1016/j.rama.2017.07.005

Yang, Y., and Liu, B. R. (2019). Effects of planting *Caragana shrubs* on soil nutrients and stoichiometries in desert steppe of Northwest China. *Catena* 183:104213. doi: 10.1016/j.catena.2019.104213

Yuan, X., Li, J., Dong, Z., and Shao, T. (2020). The reconstitution mechanism of napier grass microiota during the ensiling of alfalfa and their contributions to fermentation quality of silage. *Bioresour. Technol.* 297:122391. doi: 10.1016/j.biortech.2019.122391

Zhang, H., Wu, J. W., Gao, L. J., Yu, J. D., Yuan, X. F., Zhu, W. B., et al. (2017). Aerobic deterioration of corn stalk silage and its effect on methane production and microbial community dynamics in anaerobic digestion. *Bioresour. Technol.* 250, 828–837. doi: 10.1016/j.biortech.2017.09.149

Zhang, L., Zhou, X. K., Gu, Q. C., Liang, M. Z., Mu, S. L., Zhou, B., et al. (2019). Analysis of the correlation between bacteria and fungi in sugarcane tops silage prior to and after aerobic exposure. *Bioresour. Technol.* 291:121835. doi: 10.1016/j.biortech.2019.121835

Zhang, S. J., Chaudhry, A. S., Osman, A., Shi, C. Q., Edwards, G. R., Dewhurst, R. J., et al. (2015). Associative effects of ensiling mixtures of sweet sorghum and alfalfa on nutritive value, fermentation and methane characteristics. *Animal Feed Sci. Technol.* 206, 29–38. doi: 10.1002/jsfa.9406

Zheng, M. L., Niu, D. Z., Jiang, D., Zuo, S. S., and Xu, C. C. (2017). Dynamics of microbial community during ensiling direct-cut alfalfa with and without LAB inoculant and sugar. *J. Appl. Microbiol.* 122, 1456–1470. doi: 10.1111/jam.13456

Conflict of Interest: The authors declare that the research was conducted in the absence of any commercial or financial relationships that could be construed as a potential conflict of interest.

frontiers | Frontiers in Microbiology

ORIGINAL RESEARCH
published: 02 June 2022
doi: 10.3389/fmicb.2022.813363

Optimized Ensiling Conditions and Microbial Community in Mulberry Leaves Silage With Inoculants

Xiaopeng Cui, Yuxin Yang, Minjuan Zhang, Feng Jiao, Tiantian Gan, Ziwei Lin, Yanzhen Huang, Hexin Wang, Shuang Liu, Lijun Bao, Chao Su and Yonghua Qian**

College of Animal Science and Technology, Northwest A&F University, Yangling, China

Mulberry leaves (ML) are a promising alternative fodder source due to their high protein content and the abundance of active components. A test of three inoculants in various combinations revealed that high-quality ML silage was produced at an inoculum ratio of 1:1:0 (50% *Saccharomyces cerevisiae*, 50% *Lactobacillus plantarum*, and 0% *Bacillus subtilis*). Using dry matter (DM) loss, pH, ammonia-N and amino acid contents, total antioxidant activity, and total flavonoids content to evaluate silage quality, this inoculant mixture was shown to produce high-quality silage within a range of inoculum size (5–15%), moisture contents (50–67%), ensiling temperatures (27–30°C), and ensiling duration (14–30 days). A third trial comparing silages produced after 30 days at 28°C and 50% moisture content revealed that silage E, prepared using an *L. plantarum* inoculant alone, displayed the lowest DM loss and pH, and low bacterial diversity, and it was dominated by *Lactobacillus* (88.6%), with low abundance of *Enterobacter* (6.17%). In contrast, silage B5, prepared with equal ratios of *L. plantarum* and *S. cerevisiae*, was dominated by *Enterococcus* (67.16%) and *Lactobacillus* (26.94%), with less marked yeast persistence, and reducing the DM content from 50 to 40% altered these relative abundances to 5.47 and 60.61, respectively. Control silages produced without an inoculant had the highest pH and ammonia-N content (indicative of poor quality), had the lowest antioxidant activity, had higher bacterial diversity, and were dominated by *Carnobacterium* (74.28%) and *Enterococcus* (17.3%). In summary, ensiling of ML conditions with proper inoculants yielded high-quality silage with a favorable microbial community composition.

Keywords: mulberry leaves, inoculant, ensiling conditions, ensiling characteristics, microbial community

OPEN ACCESS

Edited by:
Christopher Rensing, Fujian Agriculture and Forestry University, China

Reviewed by:
Paul James Weimer, University of Wisconsin-Madison, United States
Mao Li, Tropical Crops Genetic Resources Institute, Chinese Academy of Tropical Agricultural Sciences, China

****Correspondence:***
Chao Su
suchao503@126.com
Yonghua Qian
qyh@nwafu.edu.cn

Specialty section:
This article was submitted to Microbiotechnology, a section of the journal Frontiers in Microbiology

Received: *11 November 2021*
Accepted: *05 May 2022*
Published: *02 June 2022*

Citation:
Cui X, Yang Y, Zhang M, Jiao F, Gan T, Lin Z, Huang Y, Wang H, Liu S, Bao L, Su C and Qian Y (2022) Optimized Ensiling Conditions and Microbial Community in Mulberry Leaves Silage With Inoculants. Front. Microbiol. 13:813363. doi: 10.3389/fmicb.2022.813363

INTRODUCTION

Mulberry (*Morus alba*), which originated in China and Korea, has been cultivated in China for more than four millennia. Mulberry leaves (ML) are known for their wide adaptability (Sugiyama et al., 2016), palatability, high protein content [18–25% in dry matter (DM)], and high *in vivo* DM digestibility (75–85%; Kandylis et al., 2009), with the absence of or negligible anti-nutritional factors (Srivastava et al., 2006). In addition, as one of the Chinese traditional medicines and edible foods, ML contain a variety of components with biological activity, including 1-deoxynojirimycin (DNJ), polysaccharides, flavonoids, and polyphenols. These biologically active components have reported anti-obesity, anti-hyperglycemic, and anti-inflammatory effects (Jeszka-Skowron et al., 2014; Ren et al., 2015). Accordingly, ML can be considered as an alternative "green" additive replacing the use of

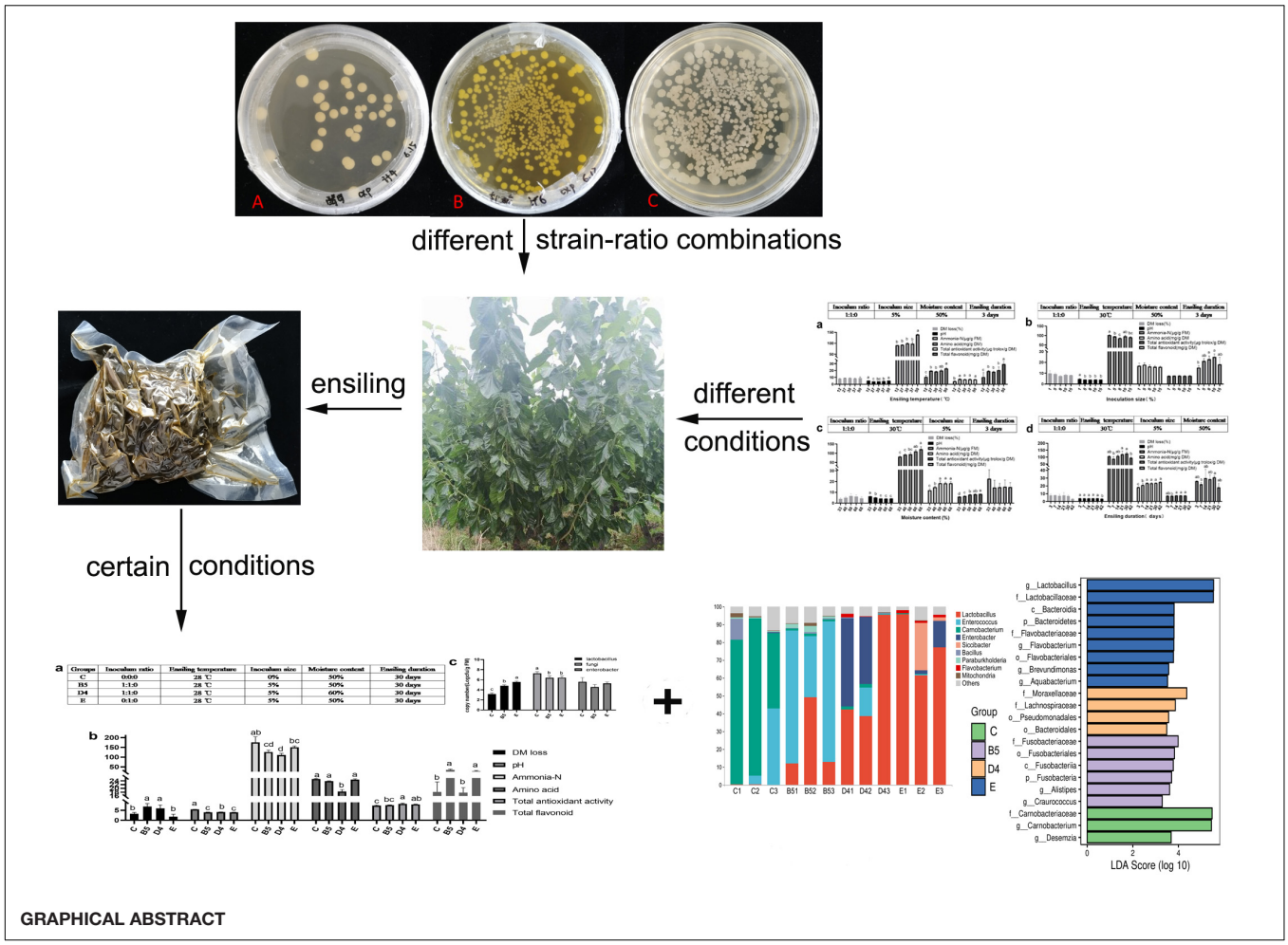

GRAPHICAL ABSTRACT

antibiotics to promote animal growth and improve the endurance and disease resistance of livestock (Zhao et al., 2015). In addition, ML are widely used in food and tea preparations in China, so they are safe for animals and human beings.

Ensiling is a traditional and effective method for the preservation of fresh forage, which can improve palatability and nutrient content and provide good nutrition for livestock throughout the year. With the gradual application of additives to improve the quality of silage fermentation, the use of bacterial inoculants, such as yeast, *Lactobacillus*, *Bacillus*, and, in particular, *Lactobacillus plantarum*, has become increasingly common practice in silage production (Yan et al., 2019; Zhao et al., 2020). Furthermore, considering that silage is the product of microbial fermentation, silage quality is likely to be strongly influenced by inoculum size and environmental factors, including temperature and moisture content. Moreover, the duration of ensiling is also closely related to the abundance of bacteria in silage (Wang et al., 2020).

As a kind of untraditional feed, ML exhibit several advantages over other forages. Hence, it is vital to explore the appropriate ensiling conditions in order to control the quality and the composition of the bacterial community of ML silage. Such knowledge is crucial to better understand the ensiling process of ML and to support its wider adoption. Therefore, in this study, optimal conditions for ML ensiling were determined by assessing fermentation characteristics and changes in the bacterial community during ensiling. The results presented in this study provide a theoretical basis and technical support for the practical implementation of ML ensiling.

MATERIALS AND METHODS

Inoculant Activation

Strains of *Saccharomyces cerevisiae* (*S. cerevisiae*, CICC 31105), *L. plantarum* (CICC 23941), and *Bacillus subtilis* (*B. subtilis*, CICC 10012) were purchased from the China Center of Industrial Culture Collection (www.china-cicc.org) and were activated referring to the manufacturer's protocols. *S. cerevisiae*, *L. plantarum*, and *B. subtilis* were grown on potato dextrose agar (PDA, Beijing Aoboxing Biotechnology Co., Ltd., Beijing, China) at 30°C for 24 h, de Man, Rogosa and Sharpe agar (MRS, Beijing Land Bridge Technology Co., Ltd., Beijing, China) at 37°C for 24 h, and Luria-Bertani (LB, consists of 1% peptone, 0.5% yeast extract, 1% sodium chloride, and 1.5–2% agar) at 37°C for 24 h,

respectively. Colony morphology of the three strains is shown in **Supplementary Figure 1**. Then, three strains were resuspended and grown in a solution of nutrient broth for 3 days at 37°C prior to application in subsequent ensiling experiments.

Silage Preparation and Experimental Design

Mulberry leaves were harvested in May 2020 at the Institute of Sericulture and Silk in Wuquan, Shaanxi Province, China. Then, they were treated with the following variables: various inoculant ratios (1:1:0, 1:0:1, 0:1:1, 1:1:1, 2:1:1, 1:2:1, 1:1:2, 2:2:1, 2:1:2, 1:2:2, and 0:0:0 exhibited by ratios of *S. cerevisiae*, *L. plantarum*, and *B. subtilis*; trial 1); various inoculum sizes (1, 5, 8, 10, and 15%); various fermentation temperatures (12, 27, 30, 37, and 50°C); various moisture contents (33, 40, 50, 60, and 67%); various ensiling duration (3, 7, 14, 21, 30, and 42 days; trial 2), which were conceived with a single-factor experimental design to determine superior conditions for ML ensiling. Subsequently, trial 3 was conducted using chosen conditions based on trials 1 and 2 to optimize ensiling conditions applied to practical promotion. Detailed experimental design is shown in the section "Results and Discussion".

After complete homogenization, each treatment mixture (approximately 30 g) was vacuum sealed in vacuum bags made with food-grade PA/PE composite material (approximately 10 × 25 cm, 16 cm thickness, No. 14914, purchased from Taobao at https://m.tb.cn/h.fG0hNxi?tk=N0lj2kuFnJQ) to enable fermentation. Three bags of each treatment were sampled to determine the dynamic profiles of ensiling characteristics and bacterial community composition. Notably, the moisture content of ML silages was controlled by the addition of sterile water to sun-dried ML, considering the limited availability of fresh ML, whose harvesting occurs from May to August every year.

Analysis of Microbial Population, Organic Acid Content, and Chemical Composition of Mulberry Leaves Silage

According to Liu et al. (2019), 5 g of the sample was immediately blended with 45 ml of sterilized saline water (0.85% NaCl), and the mixture was serially diluted from 10^{-1} to 10^{-6}. Colonies of lactic acid bacteria (LAB) were enumerated, as viable numbers of microorganisms in the samples were expressed as the colony forming unit (CFU) per gram of fresh matter on MRS agar. Five grams of each silage sample was mixed with 45 ml of distilled water, stored at 4°C for 18 h, and then filtered. The pH of this filtrate was measured using a glass electrode pH meter (PHS-25; Shanghai Ridao Co., Ltd., Shanghai, China). Crude protein content was determined using the Kjeldahl method in a Kjeltec^{TM} 8400 Auto-Analyzer (FOSS Analytical Instruments Inc., Hillerød, Denmark).

Fresh silage was dried on oven drying (DGX-9073BC-1) at 65°C for 48 h to obtain dry weight, and dry matter loss (DM loss) of ML silage was calculated by the following formula: DM loss = (fresh weight – dry weight)/dry weight. The content of ammonia-N was determined following the method by Broderick and Kang (1980). The content of water-soluble carbohydrates (WSC) was determined by referring to the anthrone method (Murphy, 2010). Contents of amino acids and alkaloids and total antioxidant capacity (DPPH) were determined using commercially available kits (AA-2-W, SWJ-2-Y, DPPH-2-D; Suzhou Keming Biological Co., Ltd.) according to the manufacturer's instructions. The content of organic acids [lactic acid (LA) and acetic acid (AA)] was measured using high-performance liquid chromatography (HPLC) [Column Kromasil C_{18} (250 mm × 4.6 mm; 5 μm); oven temperature: 30°C; mobile phase: sodium phosphate buffer solution (12.5 mM); pH: 4.0; flow rate: 1.0 ml/min; injection volume: 5 μl; using an ultraviolet detector]. Contents of total flavonoids, polysaccharides, and polyphenols were measured by ethanol extraction, phenol-sulfuric method, and the Folin-Ciocalteu method, respectively. The content of 1-deoxynojirimycin (DNJ) was determined by the enzyme-linked immune-sorbent assay using a commercial kit (ZT-20586; Fankew, Shanghai FANKEL Industrial Co., Ltd.).

Isolation of Microbial DNA and Real-Time Fluorescence Quantitative PCR for Microbial Composition

The DNA extraction was performed according to the method proposed by Liu et al. (2019). Three sample bags of each treatment (ensiling temperature and duration of trial 2 and trial 3) were taken for the analysis of microbial composition by real-time fluorescence quantitative PCR (qPCR). Approximately 10 g of the sample was mixed with 90 ml of sterile 0.85% NaCl under vigorous shaking at 120 rpm for 2 h. The mixture was filtered through four layers of cheesecloth, and the filtrate was centrifuged at 10,621 × *g* at 4°C for 10 min. The precipitate was resuspended in 1 ml of sterile 0.85% NaCl, and the microbial pellets were obtained by centrifugation at 15,294 × *g* at 4°C for 10 min. Total DNA was extracted using the OMEGA stool DNA Kit (D4015; Omega Bio-tek Inc., Norcross, GA, United States) according to the manufacturer's instructions.

Primers used in real-time qPCR performed in this study were designed for *Lactobacillus* (UF-lac: TTTAYGCGGAACAYYTR GGKGT, UR-lac: CCAAACATCACVCCRACTT), fungi (F: TGACTCAACACGGGGAAACT, R: CCAACTAAGAACGGC CATGC), and *Enterobacter* (F: ATCAGATGTGCCCAG ATGG, R: CCGTGTCTCAGTTCCAGTG) and were synthesized by Sangon Biotech (Shanghai) Co., Ltd. (Shanghai, China). Sample DNA and plasmid DNA were serially ten-fold diluted from 10^8 to 10^0 copies/μl and then employed in the real-time qPCR assay. To draw standard curves for absolute quantification of the three bacteria in the samples, low copy number samples were analyzed only when the coefficient of the standard curve regression was higher than 0.98 and the run efficiency was higher than 90%. PCR was performed using a 20-μl reaction mixture containing 10 μl of 2 × SYBR Green *Pro Taq* HS Premix, 0.4 μl of each primer (5 μM), 2 μl of template DNA, and 7.2 μl of RNase free water and was guided by 30 s of denaturation at 95°C, 40 cycles of 5 s at 95°C, 30 s for annealing at 60°C, followed with solubility curve (default setting) using Roche Light Cycler®96. For every repetition of each sample, PCR amplifications were conducted in

triplicate. The number of copies of the rRNA gene was expressed as $\log_{10}$ copy numbers/g of fresh matter (FM).

Analysis of Microbial Community

Microbial 16S rRNA gene sequencing and bioinformatic analysis were conducted by Shanghai Personal Biotechnology Co., Ltd. (Shanghai, China). Total genomic DNA was extracted using the OMEGA Soil DNA Kit (D5625-01; Omega Bio-tek Inc.) following the manufacturer's instructions and stored at –20°C until further analysis. Quantity and quality of extracted DNAs were measured using a NanoDrop ND-1000 spectrophotometer (Thermo Fisher Scientific, Waltham, MA, United States) and agarose gel electrophoresis, respectively. PCR amplifications of the V3–V4 region of the bacterial 16S rRNA gene were performed using the forward primer 338F (5′-ACTCCTACGGGAGGCAGCA-3′) and the reverse primer 806R (5′-GGACTACHVGGGTWTCTAAT-3′). Sample-specific 7-bp barcodes were incorporated into the primers for multiplex sequencing. The PCR components contained 5 μl of buffer (5 ×), 0.25 μl of Fast pfu DNA polymerase (5U/μl), 2 μl (2.5 mM) of dNTPs, 1 μl (10 μM) of each forward and reverse primer, 1 μl of DNA template, and 14.75 μl of ddH_2O. Thermal cycling consisted of initial denaturation at 98°C for 5 min, followed by 25 cycles consisting of denaturation at 98°C for 30 s, annealing at 53°C for 30 s, and extension at 72°C for 45 s, with a final extension of 5 min at 72°C. PCR amplicons were purified with Vazyme VAHTSTM DNA Clean Beads (Vazyme, Nanjing, China) and quantified using the Quant-iT PicoGreen dsDNA Assay Kit (Invitrogen, Carlsbad, CA, United States). After the individual quantification step, amplicons were pooled in equal amounts, and pair-end 2 × 250 bp sequencing was performed using the Illumina MiSeq platform according to Wang et al. (2018) with slight modification. Noisy sequences of raw tags were filtered using the QIIME 2 (2019.4) under specific filtering conditions to obtain high-quality clean tags. Sequences that contained > 10% of unknown nucleotides (N) and < 80% of bases with quality (Q-value) > 20 were removed. Paired-end clean reads were merged as raw tags using FLSAH (v1.2.7) with a minimum overlap of 10 bp and mismatch error rates of 2%. The effective tags were clustered into operational taxonomic units (OTUs) at 97% similarity using QIIME 2 dada 2. Bioinformatic analysis was performed with QIIME2 v. 2019.4 (https://docs.qiime2.org/2019.4/tutorials/) and the website at https://www.genescloud.cn. Analysis of sequencing data was mainly performed using QIIME2 and R packages (v3.2.0). The sequence data have been deposited in the NCBI database (Accession No. PRJNA782016).

Statistical Analysis

Statistical analysis was performed by the SPSS 19.0 software (IBM-SPSS Statistics, IBM Corp., Armonk, NY, United States). Data were evaluated using a one-way ANOVA followed by Fisher's multiple range tests for ensiling quality parameters and microbial counts. Significance was declared if $P < 0.05$. Additionally, data of high-throughput sequencing were analyzed using Genescloud tools, a free online platform for genomic data analysis (https://www.genescloud.cn/chart/).

TABLE 1 | Chemical and microbial composition of pre-ensiled mulberry leaves.

Characteristics	Contents
DM (%)	38.09 ± 3.80
Crude protein (%DM)	19.13 ± 1.09
Crude fiber (%DM)	27.60
Amino acid (mg/g DM)	10.40 ± 0.16
WSC (mg/g DM)	45.87 ± 2.17
Total flavonoid (mg/g DM)	20.97 ± 0.44
Polysaccharide (mg/g DM)	9.48 ± 0.19
Total polyphenol (mg/g DM)	2.67 ± 0.05
Alkaloids (μg/g DM)	566.26 ± 57.63
DNJ ($\times 10^{-4}$ ng/g DM)	9.21 ± 0.37
Lactobacillus ($\log_{10}$CFU/g FM)	2.12 ± 0.74
Fungi (log CFU/g FM)	2.81 ± 0.04
Enterobacter (log CFU/g FM)	3.09 ± 0.03

DM, dry matter; FM, fresh material.

RESULTS AND DISCUSSION

Ensiling Characteristics of Mulberry Leaves Silage Obtained With Different Inoculant Ratios (Trial 1)

Characteristics of Pre-ensiled Mulberry Leaves

Chemical composition and diversity of the microbial population of pre-ensiled ML are shown in **Table 1**. Contents of crude protein, crude fiber, and amino acid were 19.13%, 27.60%, and 10.40% DM, respectively, which were comparable with the contents in ML found by Wang et al. (2019b). ML could be an alternative supplemental feed with substantial crude protein, comparable to alfalfa, to replace conventional feed (Wang et al., 2012). According to Cai et al. (1998), a WSC content greater than 5% DM is necessary for desirable silage quality, especially for an inoculant fermentation (Muck, 2010). In this regard, the WSC content in ML (4.59% DM), although higher than that in forage soybean (1.23% DM) and lower than that in grass forage (crop corn 13.69% DM; sorghum 12.23% DM; Ni et al. (2018), was slightly sufficient for the extent and rate of an adequate fermentation and indicated some DM loss during fermentation. However, the DM content of ML (38.09%) was far higher than the minimum DM content (25%) indicated for forage to minimize the risk of effluent of nutrients (Mcdonald et al., 1991) and presumably alleviated DM loss during ensiling.

Contents of total flavonoids, polysaccharides, total polyphenols, alkaloids, and DNJ were 20.97 mg/g DM, 9.48 mg/g DM, 2.67 mg/g DM, 566.26 μg/g DM, and 9.21 μg Trolox/g DM, respectively. It is widely known that these active ingredients are beneficial to the growth and health of animals (Li et al., 2019).

In addition, the microbial load of ML was determined using real-time qPCR. Overall, the load in $\log_{10}$ CFU/g of *Lactobacillus* (2.12) was lower than that of fungi (2.81) and *Enterobacter* (3.09). Moreover, the load of *Lactobacillus* in ML in this study, as the dominant bacterial species for an exceptional fermentation, was not only below the minimum adequate number ($< 10^5$ CFU/g) known to effectively improve silage quality but also under 10^4 CFU/g, which might have contributed to reduce DM recovery

and increase ammonia concentration (Oliveira et al., 2017). Accordingly, the addition of inoculants to modulate bacterial community composition in ML is strongly advisable.

Sensory Analysis of Mulberry Leaves Silage

After ensiling at 30°C for 3 days with 5% inoculum size and 50% moisture content of ML, smell, color, and shatter value of all treatment groups changed according to the addition of different inoculant ratios compared with the control group (W), which showed less gas production, putrefactive odor, slight caking, and blue green color, all indicative of further decay of ML silage (**Table 2**). Similarly, ML silages prepared with inoculant ratios of 1:0:1 and 1:2:2 had better quality than W, since they showed less gas production, faint foul odor, and a slimy feel, which can be attributed to the activity of bacilli (Muck, 2010). Other treated groups had similar sensory evaluation profiles: low gas production, acid fragrance, loose, and faint yellow color. Collectively, when the existing population of *S. cerevisiae* and *B. subtilis* $\geq$ 60% and *S. cerevisiae* < *B. subtilis* or *L. plantarum* was absent in the inoculants, it would result in ML silage with a faint foul odor caused by spoilage bacteria with prolonged ensiling. The reasons seemed that *B. subtilis* caused the increase in pH (perhaps assisted by yeasts in some instances; Barry et al., 1980) and indole production from degradation of tryptophan, thereby accelerating spoilage of ML silage.

Ensiling Characteristics of Mulberry Leaves Silage

As presented in **Table 3**, ensiling characteristics of treated ML silage related to ammonia, pH, organic acids content, and microbial load changed greatly compared with W. DM loss mainly derived from aerobic activity at the early stage of ensiling, likely as a result of the metabolism by aerobic microorganism (e.g., yeast and bacillus) and volatile production during heterofermentation, which enabled the conversion of WSC to ethanol (Muck, 2010; Avila et al., 2014), thus resulting in DM loss (Oladosu et al., 2016) while simultaneously improving palatability. After the addition of inoculants at different ratios, an indistinctive increase in DM loss without 0:1:1 was observed compared with W, probably due to the antibacterial effect of ML on microorganisms during fermentation. Also, more DM loss was observed from *Bacillus* inoculants than from yeast inoculants. As expected, compared with W, a significant decrease in WSC, as well as in crude protein and amino acid content, was observed in treated ML silages except for treatment 1:0:1. The excessive crude protein content in ML silage obtained with the inoculant ratio of 1:0:1 might be attributed to fungal activity, since Zhao et al. (2020) reported that the crude protein content of corn straw in all fungal treatments increased, peaking on day 35.

Silage pH plays a vital role in silage quality. pH 4.2 is commonly considered as a well-fermented benchmark, particularly for high moisture silage, and a lower pH generally ensures adequate fermentation, good aerobic stability, and long preservation. However, the exact pH to inhibit these groups does vary by crop and DM content in addition to the bacterial strains present (Muck, 2010). In this study, compared with W (4.74), pH rapidly declined in ML silage ($P < 0.05$) to a relatively low value (∼4.2) at the early stages of ensiling, except for 4.99, an unfavorable pH to silages in treatment 1:0:1 due to the absence of *L. plantarum*. A similar finding (pH 4.31–4.69 for treatments compared with pH 6.07 for the control) was obtained when investigating the role of the microbiota in the fermentation of oat silage (Wang et al., 2020). In general, the pH decline is initiated by the generation of organic acids during ensiling and is greatly influenced by the acid concentration and buffering capacity of materials (Kung et al., 2018). However, the final pH of silage is also dependent on many factors (e.g., ammonia-N content; Barry et al., 1980; **Table 2** and **Supplementary Table A3**).

Lactic acid (pK_a of 3.86) is generally produced from the conversion of WSC mainly by homofermentative LAB, and it greatly contributes to a rapid decrease in the pH of silage, due to the fact that it is approximately 10–12 times stronger than other major organic acids [e.g., acetic acid (pK_a of 4.75) and propionic acid (pK_a of 4.87)] (Kung et al., 2018). Additionally, acetic acid dramatically inhibits yeast and mold growth produced by heterofermentative LAB, such as *Lactobacillus buchneri*, with a remarkable effect on improving the aerobic stability at feeding (Muck, 2010; Kung et al., 2018). As expected, treatment 1:1:0 indicated a well-preserved silage with the highest LA, AA, and LAB (**Table 3**). Moreover, both $\geq$ 50% of *L. plantarum* and the absence of *B. subtilis* were indispensable to lift the levels of LA and AA.

Ammonia-N is a common indicator of protein degradation, reflecting peptide bond hydrolysis and a higher rate of amino acid and/or peptide deamination (Li et al., 2018). In this study, over 105 μg/g FM of ammonia-N was produced in all treatments, except in treatments 1:1:0 (99.27 μg/g FM) and 0:1:1 (93.70 μg/g FM). This point might be clarified by the unfavorable role of *S. cerevisiae* and *B. subtilis* (≥50% of total addition) to silage, where bacillus has strong proteolytic activity and can decompose protein and produce ammonia. Meanwhile, the main fermentation products of yeasts are ethanol and CO_2 due to the metabolism of lactic acid (Pahlow et al., 2003; Muck, 2010). Therefore, *S. cerevisiae* and *B. subtilis* should not be applied simultaneously to ML silage, and a minimum of 50% *L. plantarum* as inoculant would probably make desirable ML silage.

TABLE 2 | Evaluation of sensory profile of mulberry leaves silage obtained with different inoculant ratios presented by *S. cerevisiae*, *L. plantarum*, and *B. subtilis* in **trial 1**.

Inoculant ratio	Gas production	Smell	Color	Shatter value
1:1:0	Remarkable	Acid fragrance	Faint yellow	Loose
1:0:1	Less	Faint foul odor	Blue green	Loose
0:1:1	Remarkable	Acid fragrance	Faint yellow	Loose
1:1:1	Remarkable	Acid fragrance	Faint yellow	Loose
2:1:1	Remarkable	Acid fragrance	Faint yellow	Loose
1:2:1	Remarkable	Acid fragrance	Faint yellow	Loose
1:1:2	Remarkable	Acid fragrance	Faint yellow	Loose
2:2:1	Remarkable	Acid fragrance	Faint yellow	Loose
2:1:2	Remarkable	Acid fragrance	Faint yellow	Loose
1:2:2	Less	Faint foul odor	Faint yellow	Loose
W(0:0:0)	Less	Putrefactive odor	Blue green	Slight caking

TABLE 3 | Ensiling parameters and chemical contents of mulberry leaves ensiled with the addition of different inoculant ratios in **trial 1**.

Treatments	DM_{loss}	Ammonia-N	pH	LA	AA	LAB	Crude protein	Amino acid	WSC
	%	μg/g FM		mg/g FM	mg/g FM	log_{10}CFU/g FM	%DM	mg/g DM	mg/g DM
1:1:0	4.53^{ab}	99.27^{de}	4.22^{b}	83.91^{a}	76.67^{a}	6.78^{a}	22.92^{b}	20.93^{b}	16.16^{b}
1:0:1	4.12^{ab}	119.47^{a}	4.99^{a}	51.97^{e}	52.42^{d}	5.38^{c}	27.85^{a}	23.69^{a}	42.60^{a}
0:1:1	5.06^{a}	93.70^{e}	4.26^{b}	70.60^{b}	65.68^{b}	4.89^{d}	22.98^{b}	21.87^{ab}	13.90^{b}
1:1:1	3.97^{ab}	105.93^{cd}	4.24^{b}	65.69^{c}	61.31^{c}	5.87^{b}	23.12^{b}	23.11^{a}	15.53^{b}
2:1:1	3.18^{ab}	106.04^{cd}	4.21^{b}	56.03^{d}	51.40^{de}	4.83^{d}	23.21^{b}	22.49^{ab}	15.57^{b}
1:2:1	4.28^{ab}	107.96^{abcd}	4.23^{b}	41.48^{f}	38.19^{f}	4.81^{d}	20.66^{bc}	22.01^{ab}	16.72^{b}
1:1:2	3.56^{ab}	109.17^{abcd}	4.25^{b}	39.69^{f}	37.58^{f}	4.20^{fg}	19.13^{c}	22.12^{ab}	16.04^{b}
2:2:1	3.02^{ab}	107.54^{bcd}	4.24^{b}	54.14^{de}	48.18^{e}	4.36^{f}	23.05^{b}	21.49^{ab}	15.23^{b}
2:1:2	3.16^{ab}	107.33^{bcd}	4.23^{b}	53.85^{de}	52.01^{d}	4.59^{e}	23.13^{b}	20.59^{b}	15.83^{b}
1:2:2	3.12^{ab}	114.98^{abc}	4.22^{b}	56.25^{d}	49.86^{de}	4.10^{g}	23.21^{b}	21.07^{b}	16.49^{b}
W	1.93^{b}	118.92^{ab}	4.74^{a}	42.16^{f}	51.18^{de}	4.01^{g}	22.72^{b}	22.56^{ab}	42.36^{a}
SEM	0.267	1.630	0.050	2.271	1.932	0.142	0.422	0.248	1.884
P-value	0.582	0.005	0.000	0.000	0.000	0.000	0.001	0.189	0.000

SEM, standard error mean. Different letters in the same column (a–g) differed (P < 0.05).

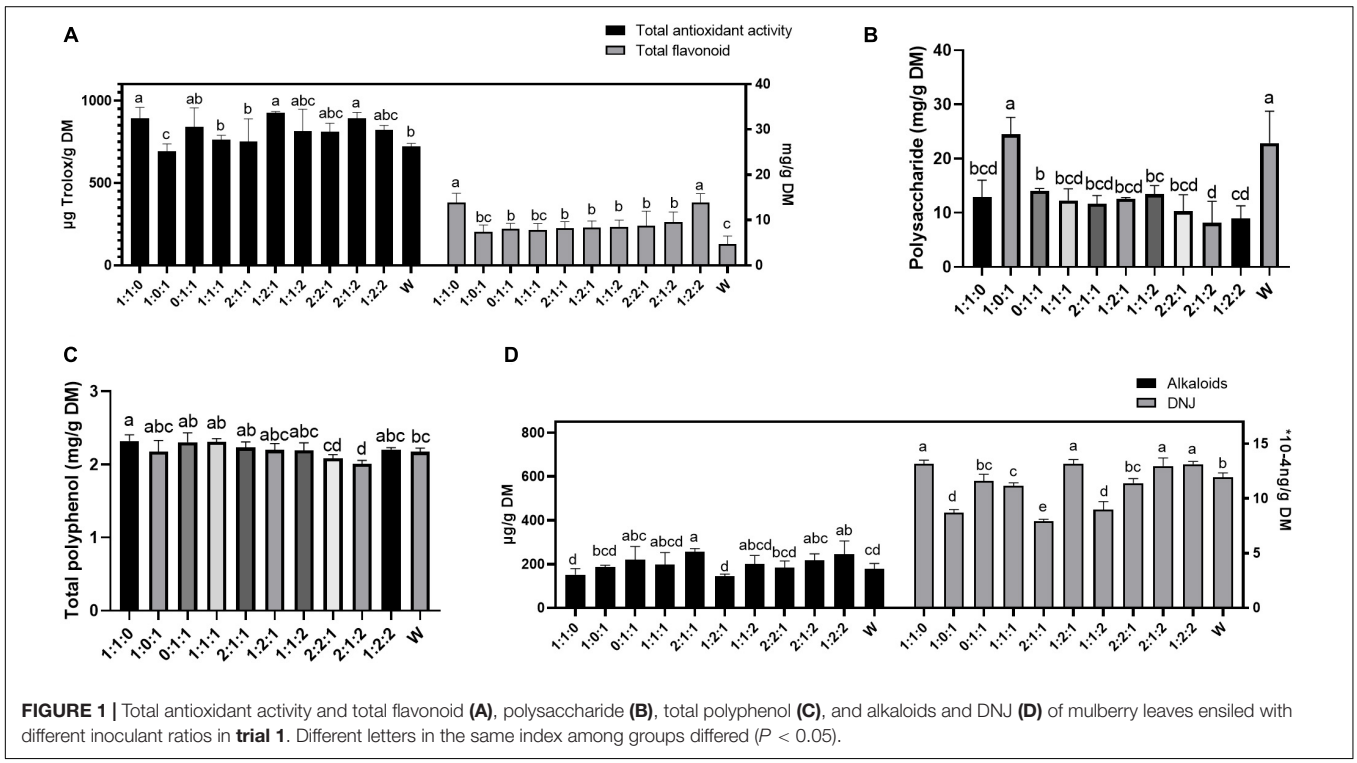

FIGURE 1 | Total antioxidant activity and total flavonoid **(A)**, polysaccharide **(B)**, total polyphenol **(C)**, and alkaloids and DNJ **(D)** of mulberry leaves ensiled with different inoculant ratios in **trial 1**. Different letters in the same index among groups differed ($P < 0.05$).

Active Ingredients and Antioxidant Activity of Mulberry Leaves Silage

As shown in **Figure 1**, there was a tendency to increase the contents of flavonoids, polyphenols, alkaloids, DNJ, and total antioxidant capacity in inoculated ML silage (1:1:0) compared with W, whereas polysaccharide content was decreased and in full accord with WSC. During the microbial fermentation, in addition to synthesizing enzymes to metabolize the ingredients of the substrate, the microorganisms also secreted some active ingredients to endow the substrate special functions, such as antioxidant properties. In addition, variation in the amount of every active ingredient depended on substrate source and inoculated bacteria (Liu et al., 2018; Li et al., 2021).

Overall, the load of both ≥ 50% of *L. plantarum* and the absence of *B. subtilis* as inoculants was sufficient to achieve successful fermentation of ML, followed by a speculation that < 1:1:0 (e.g., 0:1:0) would be a better choice than 1:1:0 to ferment ML. As reported, the outstanding inoculant ratio of 1:1:0 in trial 1 would be applied in trial 2 to test the fermentation conditions of ML silage. Synchronously, DM loss, pH, ammonia-N and amino acid contents, total antioxidant activity, and

total flavonoids content were taken as meaningful indicators of evaluating ML silage quality in trial 2 and trial 3.

Ensiling Characteristics of Mulberry Leaves Ensiled With Different Conditions (Trial 2)

It is generally assumed that ensiling temperature is a crucial factor impacting silage quality (Wang et al., 2019c). Various temperatures (12, 27, 30, 37, and 50°C) were adopted to prepare ML silage using the inoculant ratio 1:1:0. As expected (**Figure 2A** and **Table 4**), at low temperature (12°C), the pH of ML was higher, and the contents of amino acids and total flavonoids, and total antioxidant activity dramatically decreased. While fungi increased sharply, which could enhance fiber digestibility at a suitable amount in the rumen (Zhou et al., 2019) yet accompanied with nutrient loss of ML silage. And the obvious increase in undesirable Enterobacter caused putrefaction of ML silage (as observed also at 37°C). Wang et al. (2019c) reported that LAB inoculants and a relatively low ensiling temperature (15°C) could effectively improve the quality of silage of *Moringa oleifera* leaves, but the reason underlying this observation remains to be elucidated. Comparatively, a higher pH and ammonia-N content could be found in ML silage produced at higher ensiling temperature (50°C). Moreover, although the load of *Lactobacillus* was higher at 50°C, higher temperatures give bacilli an advantage over other LAB species in terms of competition for the available carbohydrates (Pahlow et al., 2003. Evidently, ensiling temperatures between 27 and 30°C could improve the quality of ML silage by ensuring low pH, lower ammonia content, and decreased number of *Enterobacter*.

In addition, the effects of different inoculum sizes (1, 5, 8, 10, and 15%) and moisture contents (33, 40, 50, 60, and 67%) on the quality of ML silage prepared with the inoculant ratio 1:1:0 were evaluated. As shown in **Figure 2B**, inoculum sizes had less effect on the quality of ML silage; a low inoculum size (1%) was not conducive to pH decrease and/or flavonoids production ($P < 0.05$). Muck (2010) reported that less than 1% of the inoculant relative to the epiphytic population produced no significant changes in fermentation. Moreover, at low moisture content of ML (33 and 40%), ensiling did not result in a decrease in pH and/or increase in amino acids content and total antioxidant activity ($P < 0.05$; **Figure 2C**). It is well known that high pH silage is undesirable, since at these conditions the activity of *Clostridium* is maintained (Emerstorfer et al., 2011), thus leading to an increase in butyric acid production (Szymanowska-Powalowska et al., 2014). Increased levels of butyric acid in silage (> 5 g/kg DM) can lead to decreased feed intake and health issues of livestock (Muck, 2010).

Duration of ensiling is another key factor for silage quality (Zeng et al., 2020). Therefore, the effect of different ensiling duration (3, 7, 14, 21, 30, and 42 days) on ML silage quality prepared with inoculant ratio 1:1:0 was evaluated. Dynamic changes in ensiling parameters and bacterial load are presented in **Figure 2D** and **Table 4**, respectively. Overall, with prolonged ensiling time, bacterial load decreased, with the lowest load of *Lactobacillus* occurring on day 42. Simultaneously, the content of amino acids in ML increased over time, peaking on day 14.

Collectively, the most promising parameters for effective ML ensiling at the initial stage in this research included the following: temperature, 27–30°C; inoculum size, 5–15%; moisture content, 50–67%, and 14–30 days of ensiling.

Ensiling Characteristics and Microbial Diversity of Mulberry Leaves Silage in Four Certain Conditions (Trial 3)

Trial 3 was set as control (C) and treatments (B5, D4, E) based on a synthesis of the preceding two experiments (**Figure 3A**). It aimed at creating a comprehensive road map to ferment ML practically and making sense of the differences and roles of the microbial community in inoculated ML silage. Changes in ensiling profiles and microbial population of ML silage are shown in **Figures 3B,C**. pH value is considered an important indicator reflecting ensiling quality. In this study, ML silage produced under B5 and E conditions had the lowest pH value ($P < 0.05$), possibly due to the heavier presence of species *Lactobacillus* quantified by PCR ($P < 0.05$), which produced more lactic acid to lower pH value in ML in accordance with Gallegos et al. (2017). High moisture content is presumably responsible to lower the acid concentration relative to the activities of LAB and yeasts (Muck, 2010), thus leading to a higher pH observed in D4 than B5 yet with the same *Lactobacillus* load. In addition, in ML produced under B5 and D4 conditions, the levels of ammonia, always indicative of protein breakdown, were remarkably reduced compared with the control, which can be attributed to a decrease in the load of *Enterobacter* (B5) as an ammonia-forming species. Notably, ML moisture content was closely related to ensiling quality, since at higher ML water

TABLE 4 | Microbial load determined by qPCR (log_{10}CFU/g FM) of ML silage produced under different ensiling temperatures and duration in **trial 2**.

	Lactobacillus	Fungi	*Enterobacter*
Fermentation temperature (°C)			
12	6.25^{a}	8.48^{a}	5.31^{a}
27	4.35^{bc}	6.83^{b}	4.37^{ab}
30	4.09^{c}	6.61^{b}	4.44^{ab}
37	5.19^{b}	7.25^{b}	5.29^{a}
50	6.69^{a}	7.28^{b}	3.61^{b}
SEM	0.293	0.193	0.219
P-value	0.000	0.002	0.036
Ensiling duration (days)			
3	5.01^{a}	6.61^{a}	5.13
7	5.03^{a}	6.76^{a}	5.14
14	4.95^{a}	6.48^{ab}	4.82
21	5.02^{a}	6.48^{ab}	4.55
30	4.80^{a}	6.38^{ab}	4.55
42	4.32^{b}	6.10^{b}	4.41
SEM	0.070	0.067	0.121
P-value	0.002	0.063	0.376

Different letters in the same column (a–c) differed ($P < 0.05$).

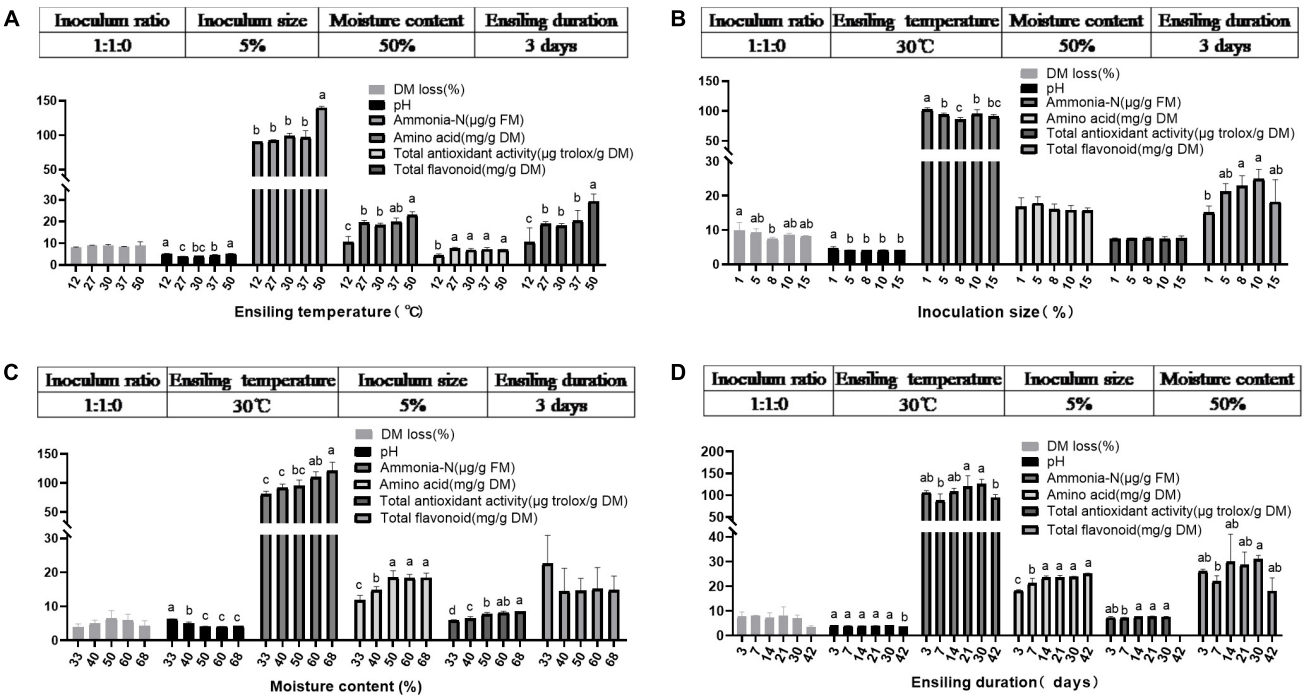

FIGURE 2 | Characteristics of ML silage under various ensiling temperatures **(A)**, various inoculum sizes **(B)**, various moisture levels **(C)**, and various ensiling duration **(D)** using the single-factor experimental method in **trial 2**. Different letters in the same index among groups differed ($P < 0.05$).

content (B5 compared with D4) a greater decrease in amino acids and flavonoids contents was observed. Compared with B5, ML produced under E condition had a remarkable decrease in DM loss ($P < 0.05$) and an increase in the load of beneficial *Lactobacillus* ($P < 0.05$). But subsequent work could elucidate exactly how changes could lead to a substantial increase in flavonoids ($P < 0.05$) in B5 and E compared with C and D4.

Shannon and Simpson indices are commonly used to reflect the α-diversity of a bacterial community. These indices were increased in ML silage prepared under conditions (B5 and D4) and decreased in E, compared with C (**Figure 4A**). It hinted that bacterial diversity in ML silages was associated with inoculants. *Lactobacillus* (100% added) helped dominate a rapid fermentation. At the same time, contributing to lower microbial diversity in ML silage with abundant *Lactobacillus* (**Figure 5A**) after fermentation. Similar results have been reported previously (Wang et al., 2019b,c), indicating that a less diverse bacterial community is established in silages where *Lactobacillus* was used as an inoculant. Dominant lactobacillus could create an acidic environment to limit the growth of other microbes (Mendez-Garcia et al., 2015), thus to lower the diversity of the bacterial community (Ogunade et al., 2016).

As shown in **Figure 4B**, the result of β-diversity analysis based on non-metric multidimensional scaling clearly reflected the between-group variance of the microbial community. ML silages produced under conditions B5 and E groups treated with different inoculants were separated from the C group. Interestingly, a distinct separation was observed among bacterial communities in the same inoculated ML silages (B5 compared to D4). This observation indicated that not only the inoculant but also the moisture content had a remarkable effect on the microbial composition of silage (Wang et al., 2019c). The variation of microbial community composition might explain the difference in silage quality (Ni et al., 2017). But the inoculated silages of whole crop maize (Parvin et al., 2010) showed less or no change in the bacterial community composition.

Most abundant bacterial communities in ML silage are shown in **Figure 5A**. Overall, Firmicutes was the most abundant phylum in all treatments, followed by Cyanobacteria and Proteobacteria. Similarly, Wang et al. (2019b) and Liu et al. (2019) reported that the dominant phyla were Firmicutes and Proteobacteria in ML and barley silages with or without inoculants. The higher abundance of Firmicutes and Proteobacteria in ML silage might be attributed to low pH and generation of anaerobic conditions toward the end of ensiling (Wang et al., 2019b). Dominant genera in each treatment were shown in **Figure 5C** (*Lactobacillus*, 88.60% in group E; *Lactobacillus*, 60.61 and *Enterobacter*, 29.91 in group D4; *Lactobacillus*, 26.94% and *Enterococcus*, 67.16% in group B5; *Enterococcus*, 17.30% and *Carnobaterium*, 74.28% in group C). Moreover, the most differentially abundant genera were *Lactobacillus* (E), *Enterobacter* (D4), *Enterococcus* (B5), and *Carnobacterium* (C) (**Figures 5B,C**). There was one further point that inoculated *S. cerevisiae* do not persist well, but inoculant of *L. plantarum* in treatments B5 and E provided higher quality silage, also with persistence in well-preserved silage (**Figures 5D,E**). It appears that inoculants fulfill their role as starter cultures that strongly influence the earliest stage of silage fermentation, after which their persistence may

A

Groups	Inoculum ratio	Ensiling temperature	Inoculum size	Moisture content	Ensiling duration
C	0:0:0	28 ℃	0%	50%	30 days
B5	1:1:0	28 ℃	5%	50%	30 days
D4	1:1:0	28 ℃	5%	60%	30 days
E	0:1:0	28 ℃	5%	50%	30 days

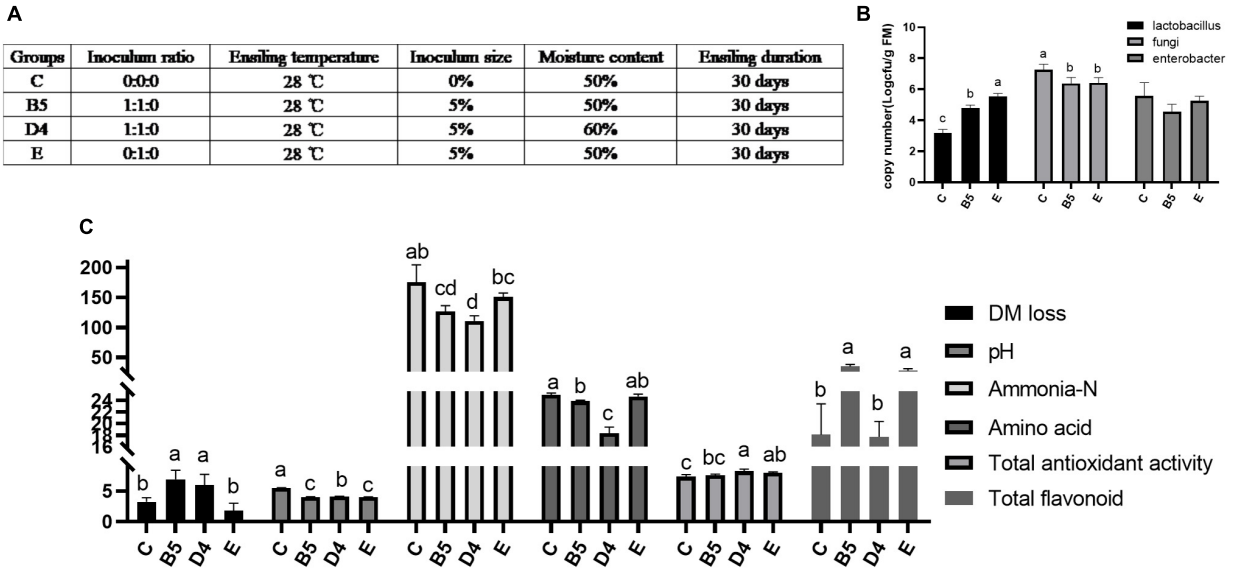

FIGURE 3 | Ensiling characteristics **(C)** and microbial load by real-time fluorescence quantitative PCR **(B)** of mulberry leaves silage in **trial 3** with experimental design **(A)**. Different letters in the same index among groups differed ($P < 0.05$).

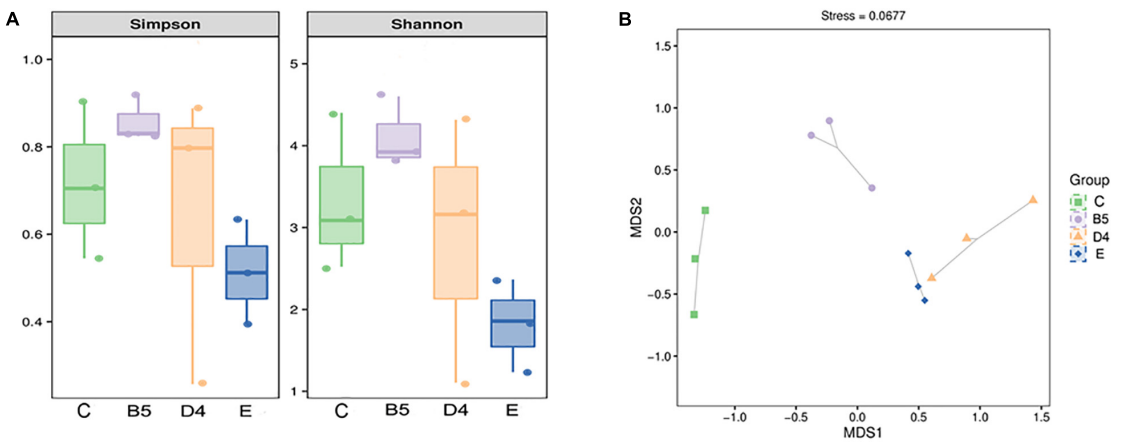

FIGURE 4 | Simpson and Shannon indices **(A)** and Bray-Curtis **(B)** based on non-metric multidimensional scaling in **trial 3**.

or may not be necessary (Stevenson et al., 2006). The well-persisted *L. plantarum* stands out in inoculated strains because of its domination, reliability, ability to use different sugars, easy adaptation to various media, and probiotic properties (Kamiloglu et al., 2020). The lower population of *S. cerevisiae* after fermentation might be present only in the earlier ensiling stage, while environmental pH was relatively high before high activities of lactobacillus, to contribute to sensory qualities of silage (Suranska et al., 2016) or to create anoxic environment for *L. plantarum* productivity or to alter the diversity of community microorganisms. Also, the populations of *Enterococcus faecium*, *Lactococcus lactis*, and *Lactobacillus delbrueckii* were determined at lower insignificant levels comparable with *S. cerevisiae* between treatments, and there were undetectable *Lactobacillus brevis*, *L. buchneri*, *Lactobacillus pentosus*, *Pediococcus pentosaceus*, and *Lactobacillus casei* (**Figure 5D**). The result dropped a hint that *E. faecium*, *L. lactis*, and *L. delbrueckii* had been working during the production of ML silage.

The genera *Lactobacillus*, *Enterococcus*, *Lactococcus*, *Weissella*, and *Pediococcus*, as common lactic acid-producing bacteria, participate positively in the evolution of LAB population during ensiling and have been widely used to improve silage quality (Chen et al., 2012; Yang et al., 2016; Ni et al., 2018). Generally, lactic acid-producing cocci (i.e., *Weissella*, *Leuconostoc*, *Pediococcus*, *Lactococcus,* and *Enterococcus*) initiate lactic fermentation at the early stages of ensiling, whereas lactic acid-producing bacilli (*Lactobacillus*) grow vigorously as pH decreases, hence becoming the dominant species at late stages of ensiling (Cai et al., 1998; Zhou et al., 2016; Liu et al., 2019). Moreover, it is known that homofermentative

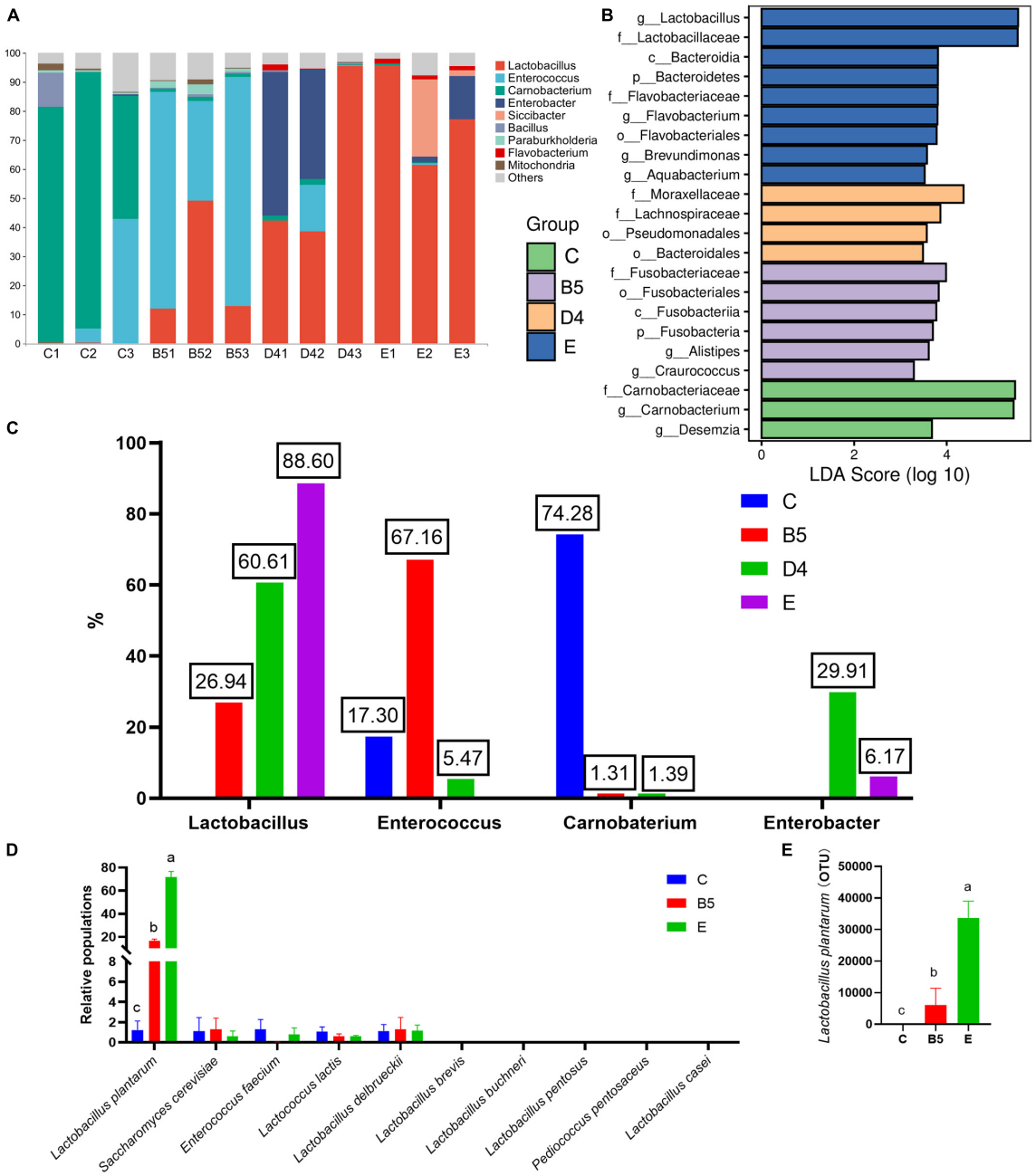

FIGURE 5 | Relative abundances of microbial communities at the genus level **(A)**, comparison of microbial variations **(B)**, percentages of main bacteria in **A (C)**, populations of individual species of lactic acid bacteria by relative quantification PCR **(D)** and 16 s sequencing **(E)** among groups of **trial 3**.

LAB can decrease the pH of silage by producing lactic acid (Oliveira et al., 2017), whereas heterofermentative LAB produced high concentrations of acetic acid, 1,2-propanediol, and other products to increase the stability of silage against deterioration by undesirable microorganisms when exposed to air (Guo et al., 2018). In this regard, the higher abundance of *Lactobacillus* in ML silage in group E, as well as after ensiling, revealed that the use of *Lactobacillus* as an inoculant was conducive to high-quality ensiling and may partly explain changes in DM loss, pH, amino acid content, and lower bacterial diversity. Cai et al. (1998) and Ogunade et al. (2016) reported that *Enterococcus* plays a pivotal role in accelerating LA fermentation and in building an anaerobic acidic environment for the development of *Lactobacillus* and to survive only at the early stages of ensiling due to its sensitivity to acid.

Interestingly, a higher abundance of *Enterococcus* was observed in ML silages with combined inoculum (**Figure 5A**),

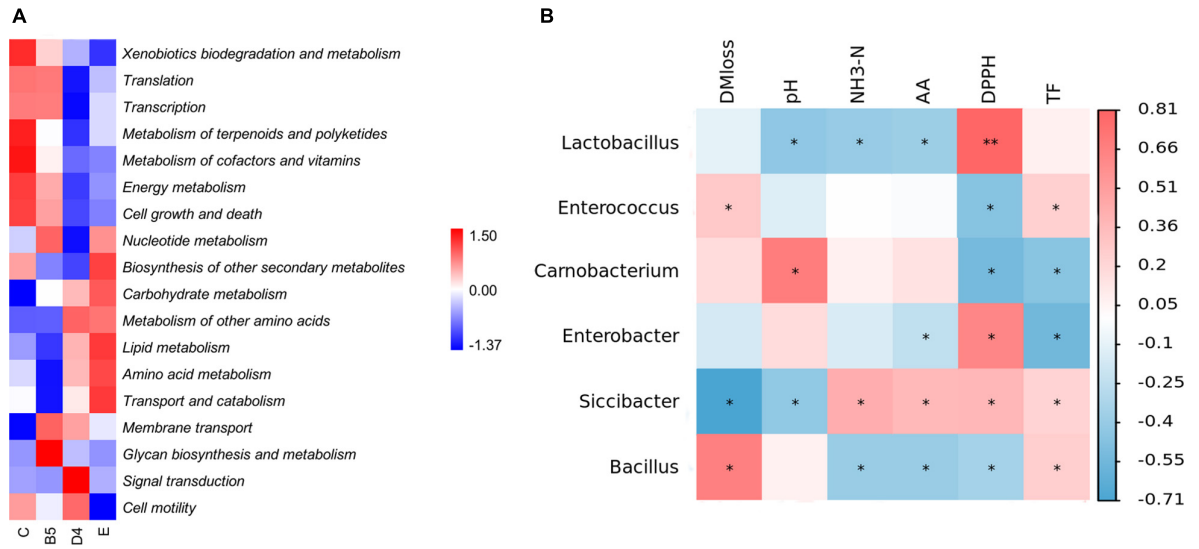

FIGURE 6 | Heatmap of 16S rRNA gene predicted functional profiles **(A)** and Pearson's correlation analysis of the bacterial community composition and ensiling parameters **(B)** in **trial 3**. *$P < 0.05$; **$P < 0.01$.

which might be explained by the different bacteria of *Alistipes* and *Craurococcus* (**Figure 5B**). The presence of *Alistipes* was significantly positively correlated with SCFAs, which are the end products of amino acid fermentation (David et al., 2013). *Craurococcus* was significantly positively correlated with total nitrogen content and negatively correlated with pH value (Rodríguez-Berbel et al., 2020); this species can degrade nutrients to produce ammonia and mitigate acidic pH, leading to a slow decrease in pH of ML silage and a higher microbial diversity except for proliferation of *Enterococcus*. This finding was consistent with increased DM loss and decreased ammonia content (B5). Moreover, the low pH value at the end of ensiling was a result of the increased abundance of *Lactobacillus*.

As the main competitors of LAB for nutrients in silage, enterobacteria produce ammonia and convert lactic acid to acetic acid alongside gas production (Muck, 2010), which reduces the energy and nutritive value of ML silage. Accordingly, increased DM loss of ML silage might be caused by the higher abundance of *Enterobacter* in group D4 due to higher moisture content, which leads to high pH and a more diverse bacterial community. Wang et al. (2019b) found that a higher abundance of *Enterobacter* could lead to relatively high levels of acetic acid and ammonia. However, pH in ML silage of group D4 was lower, which might be related to an increased proportion of *Lactobacillus*.

Carnobacterium is a Gram-positive LAB species that can metabolize arginine and various carbohydrates, frequently predominating in a range of foods, including fish, meat, and certain dairy products (Leisner et al., 2007; Mills et al., 2018). Notably, *Carnobacterium* has only been recently reported, and its roles were less described in silage. He et al. (2020a) discovered that the abundance of *Carnobacterium* was increased in control ML silage, which was consistent with the findings presented in this study. In addition, *Carnobacterium* has been found to be abundant in alfalfa silage obtained without additives and in fresh oat according to Wang et al. (2020) and Bai et al. (2020). Therefore, it could be interpreted as the change in silage pH, DM loss, and ammonia-N in group C benefited the growth of *Carnobaterium*, which was cultured to a final pH of 5.4 with an optimal growth at alkaline pH (Afzal et al., 2013) with weak acid-producing and acid-tolerance abilities; led to an increase in pH and the abundance of spoilage genera such as *Clostridium* (He et al., 2020b); or caused silage spoilage and off-odors *via* the production of spoiled metabolites (Leisner et al., 1995). Collectively, variations in microbial community composition might explain differences in silage quality, and the analysis of bacterial abundance suggested that optimized conditions for ML ensiling comprised the use of *Lactobacillus* or the combined use of *Lactobacillus* and yeast as inoculants.

The 16S rRNA gene-predicted functional profiles are shown in **Figure 6A**. Metabolism of carbohydrates, amino acids, and lipids was slightly increased in ML silage of group E along with a higher abundance of *Lactobacillus*, which contrasted with the findings obtained by Wang et al. (2019a), who found that a higher abundance of *Lactobacillus* would prompt a reduction in the metabolism of nitrogen, arginine, proline, glycine, serine, and threonine in alfalfa and stylo silage mixed with *M. oleifera* leaves. This discrepancy and decrease in DM loss previously described were related to nutrient and secondary metabolite metabolism. Consistently, the biosynthesis of other secondary metabolites was increased (E), leading to increased production of total flavonoids and improved antioxidant activity as aforementioned. The improved glycan metabolism in group B5 might be related to membrane transport, transcription, and translation, as glycans by themselves might act as signaling molecules internal to a species (Varki, 2017). Simultaneously, the higher metabolism of energy, cofactors and vitamins, terpenoids, and polyketides in group C resulting in more DM loss was likely due to abundant Carnobacteria.

To explore the relationships among ensiling properties and the roles of main bacteria acting on the fermentation process of ML, a heatmap of Pearson's correlation analysis of the bacterial community at the genus level (**Figure 6B**) and fermentation parameters was employed. Usually, metabolites are positively correlated with profitable microorganisms and negatively correlated with undesirable bacteria during ensiling based on the interaction between chemicals and microbial activity (Xu et al., 2019). *Siccibacter*, prior belonging to the genus *Cronobacter*, was reclassified as a new genus in 2014 and comprises non-pathogenic strains, isolated mainly from fruit powders, spices, herbs, and infant formula (Svobodova et al., 2017). According to the correlation analysis in this study, it was speculated that *Siccibacter* was probably linked to decreased DM loss, and similar to *Lactobacillus*, it might have the powerful ability to lower pH in ML silage than *Carnobacterium*, in spite of its small population in entire microflora. As reported, *Siccibacter turicensis* played beneficial roles in the cellulases, such as the endoglucanase (Dhakal et al., 2020), and thus, *Siccibacter* could potentially be exploited as a probiotic microbe for ML silage. For nutrient substances, *Enterobacter* correlated with decreased amino acid and total flavonoids contents. Furthermore, it was also noted that the presence of *Lactobacillus* could lead to reduced ammonia-N and improved antioxidant activity in ML silage. Besides, it was interesting to find that the relative abundance of bacteria was dissociated from their activity during ensiling.

In summary, successfully fermented ML silage should be used as livestock feed under condition E with the lowest DM loss and pH, followed by B5. Analysis of the microbial community revealed altered fermentation patterns between B5 fermented exclusively with *L. plantarum* (0:1:0) and E with combined *S. cerevisiae* and *L. plantarum* (1:1:0). Additionally, Group E, dominated by *Lactobacillus* (88.60%), exhibited less bacterial diversity and higher levels of nutrient and other secondary metabolite metabolism but depressed glycan metabolism than B5 with abundant *Enterococcus* (67.16%) and *Lactobacillus* (26.94%). In addition, the inoculant of *L. plantarum,* not *S. cerevisiae,* persists well in the well-preserved silage, which was a hint of a crucial role of *L. plantarum* acting in ML fermentation.

CONCLUSION

In conclusion, successful ensiling of ML requires inoculants and appropriate ensiling conditions, and inoculants could alter abundant bacteria, thus affecting certain metabolism to obtain glycan (B5) or small abundant secondary metabolite (E). However, the molecular mechanism of nutrient and secondary metabolite metabolism in ML silage after inoculation should be studied more deeply in the future. In this study, one further important point was the good persistence of *L. plantarum*, but not *S. cerevisiae*, in the well-preserved ML silage.

DATA AVAILABILITY STATEMENT

The datasets presented in this study can be found in online repositories. The names of the repository/repositories and accession number(s) can be found in the article/ **Supplementary Material**.

AUTHOR CONTRIBUTIONS

XC and YY contributed to the conception and design of the study. XC performed the statistical analysis and wrote the first draft of the manuscript. YY, MZ, FJ, CS, and YQ revised the manuscript. TG, ZL, YH, HW, SL, and LB helped with the experimental sections. CS and YQ provided financial support for the manuscript. All authors contributed to manuscript revision, and read and approved the submitted version.

FUNDING

This study was financially supported by the Special Program in Technology and Innovation of the Shaanxi Forestry Academy (SXLK2020-0211), China Agriculture Research System of MOF (Ministry of Finance) and MARA (Ministry of Agriculture and Rural Affairs) (CARS-18), and the Innovation-driven Program of the Shaanxi Agricultural Science and Technology (NYKJ-2021-YL(XN)31).

SUPPLEMENTARY MATERIAL

The Supplementary Material for this article can be found online at: https://www.frontiersin.org/articles/10.3389/fmicb.2022.813363/full#supplementary-material

REFERENCES

Afzal, M. I., Ariceaga, C. C., Lhomme, E., Ali, N. K., Payot, S., Burgain, J., et al. (2013). Characterization of *Carnobacterium maltaromaticum* LMA 28 for its positive technological role in soft cheese making. *Food Microbiol.* 36, 223–230. doi: 10.1016/j.fm.2013.05.008

Avila, C. L., Carvalho, B. F., Pinto, J. C., Duarte, W. F., and Schwan, R. F. (2014). The use of *Lactobacillus* species as starter cultures for enhancing the quality of sugar cane silage. *J. Dairy Sci.* 97, 940–951. doi: 10.3168/jds.2013-6987

Bai, J., Xu, D., Xie, D., Wang, M., Li, Z., and Guo, X. (2020). Effects of antibacterial peptide-producing *Bacillus subtilis* and *Lactobacillus buchneri* on fermentation, aerobic stability, and microbial community of alfalfa silage. *Bioresour. Technol.* 315, 1–9. doi: 10.1016/j.biortech.2020.123881

Barry, T. N., Menna, M. E. D., Webb, P. R., and Parleb, J. N. (1980). Some observations on aerobic deterioration in untreated silages and in silages made with formaldehyde-containing additives. *J. Sci. Food Agric.* 31, 133–146.

Broderick, G. A., and Kang, J. H. (1980). Automated simultaneous determination of ammonia and total amino acids in ruminal fluid and in vitro media. *J. Dairy Sci.* 63, 64–75. doi: 10.3168/jds.S0022-0302(80)82888-8

Cai, Y., Benno, Y., Ogawa, M., Ohmono, S., Kumai, S., and Nakase, T. (1998). Influence of *Lactobacillus* spp. from an inoculant and of *Weissella* and *Leuconostoc* spp. from forage crops on silage fermentation. *Appl. Environ. Microbiol.* 64, 2982–2987. doi: 10.1128/AEM.64.8.2982-2987.1998

Chen, M. M., Liu, Q. H., Xin, G. R., and Zhang, J. G. (2012). Characteristics of lactic acid bacteria isolates and their inoculating effects on the silage fermentation at high temperature. *Lett. Appl. Microbiol.* 56, 71–78. doi: 10.1111/lam.12018

David, L. A., Maurice, C. F., Carmody, R. N., Gootenberg, D. B., Button, J. E., Wolfe, B. E., et al. (2013). Diet rapidly and reproducibly alters the human gut microbiome. *Nature* 505, 559–563. doi: 10.1038/nature12820

Dhakal, S., Boath, J. M., Van, T. T. H., Moore, R. J., and Macreadie, I. G. (2020). *Siccibacter turicensis* from Kangaroo Scats: possible implication in cellulose digestion. *Microorganisms* 8, 1–9. doi: 10.3390/microorganisms8050635

Emerstorfer, F., Hein, W., Resch, R., Poetsch, E. M., Zitz, U., and Kneifel, W. (2011). Application of plant-based antimicrobials for the growth inhibition of clostridia in pressed beet pulp silage. *J. Sci. Food. Agric.* 91, 2038–2044. doi: 10.1002/jsfa.4416

Gallegos, D., Wedwitschka, H., Moeller, L., Zehnsdorf, A., and Stinner, W. (2017). Effect of particle size reduction and ensiling fermentation on biogas formation and silage quality of wheat straw. *Bioresour. Technol.* 245, 216–224. doi: 10.1016/j.biortech.2017.08.137

Guo, X. S., Ke, W. C., Ding, W. R., Ding, L. M., Xu, D. M., Wang, W. W., et al. (2018). Profiling of metabolome and bacterial community dynamics in ensiled *Medicago sativa* inoculated without or with *Lactobacillus plantarum* or *Lactobacillus buchneri*. *Sci. Rep.* 8, 1–10. doi: 10.1038/s41598-017-18348-0

He, L., Chen, N., Lv, H., Wang, C., Zhou, W., Chen, X., et al. (2020a). Gallic acid influencing fermentation quality, nitrogen distribution and bacterial community of high-moisture mulberry leaves and stylo silage. *Bioresour. Technol.* 295, 1–32. doi: 10.1016/j.biortech.2019.122255

He, L., Lv, H., Wang, C., Zhou, W., Pian, R., Zhang, Q., et al. (2020b). Dynamics of fermentation quality, physiochemical property and enzymatic hydrolysis of high-moisture corn stover ensiled with sulfuric acid or sodium hydroxide. *Bioresour. Technol.* 298, 1–7. doi: 10.1016/j.biortech.2019.122510

Jeszka-Skowron, M., Flaczyk, E., Jeszka, J., Krejpcio, Z., Król, E., and Buchowski, M. S. (2014). Mulberry leaf extract intake reduces hyperglycaemia in streptozotocin (STZ)-induced diabetic rats fed high-fat diet. *J. Funct. Foods* 8, 9–17.

Kamiloglu, A., Kaban, G., and Kaya, M. (2020). Technological properties of autochthonous *Lactobacillus plantarum* strains isolated from sucuk (Turkish dry-fermented sausage). *Braz. J. Microbiol.* 51, 1279–1287. doi: 10.1007/s42770-020-00262-9

Kandylis, K., Hadjigeorgiou, I., and Harizanis, P. (2009). The nutritive value of mulberry leaves (*Morus alba*) as a feed supplement for sheep. *Trop. Anim. Health Prod.* 41, 17–24. doi: 10.1007/s11250-008-9149-y

Kung, L. Jr., Shaver, R. D., Grant, R. J., and Schmidt, R. J. (2018). Silage review: interpretation of chemical, microbial, and organoleptic components of silages. *J. Dairy Sci.* 101, 4020–4033. doi: 10.3168/jds.2017-13909

Leisner, J. J., Greer, G. G., Dilts, B. D., and Stiles, M. E. (1995). Effect of growth of selected lactic acid bacteria on storage life of beef stored under vacuum and in air. *Int. J. Food Microbiol.* 26, 231–243. doi: 10.1016/0168-1605(94)00133-q

Leisner, J. J., Laursen, B. G., Prevost, H., Drider, D., and Dalgaard, P. (2007). *Carnobacterium*: positive and negative effects in the environment and in foods. *FEMS Microbiol. Rev.* 31, 592–613. doi: 10.1111/j.1574-6976.2007.00080.x

Li, J., Shi, L., Xu, S., Gu, S., Wen, X., Xu, D., et al. (2021). Optimal fermentation time for *Nigrospora*-fermented tea rich in bostrycin. *J. Sci. Food Agric.* 101, 2483–2490. doi: 10.1002/jsfa.10874

Li, Q., Liu, F., Liu, J., Liao, S., and Zou, Y. (2019). Mulberry leaf polyphenols and fiber induce synergistic antiobesity and display a modulation effect on gut microbiota and metabolites. *Nutrients* 11, 1–19. doi: 10.3390/nu11051017

Li, X., Tian, J., Zhang, Q., Jiang, Y., Wu, Z., and Yu, Z. (2018). Effects of mixing red clover with alfalfa at different ratios on dynamics of proteolysis and protease activities during ensiling. *J. Dairy Sci.* 101, 8954–8964. doi: 10.3168/jds.2018-14763

Liu, B., Huan, H., Gu, H., Xu, N., Shen, Q., and Ding, C. (2019). Dynamics of a microbial community during ensiling and upon aerobic exposure in lactic acid bacteria inoculation-treated and untreated barley silages. *Bioresour. Technol.* 273, 212–219. doi: 10.1016/j.biortech.2018.10.041

Liu, X., Cheng, J., Zhang, G., Ding, W., Duan, L., Yang, J., et al. (2018). Engineering yeast for the production of breviscapine by genomic analysis and synthetic biology approaches. *Nat. Commun.* 9, 1–10. doi: 10.1038/s41467-018-02883-z

Mcdonald, P., Henderson, A. R., and Heron, S. J. E. (1991). *The Biochemistry of Silage*, 2nd Edn. Marlow: Chalcombe Publications.

Mendez-Garcia, C., Pelaez, A. I., Mesa, V., Sanchez, J., Golyshina, O. V., and Ferrer, M. (2015). Microbial diversity and metabolic networks in acid mine drainage habitats. *Front. Microbiol.* 6:475. doi: 10.3389/fmicb.2015.00475

Mills, J., Horvath, K. M., Reynolds, A. D., and Brightwell, G. (2018). Farm and abattoir sources of *Carnobacterium* species and implications for lamb meat spoilage. *J. Appl. Microbiol.* 125, 142–147. doi: 10.1111/jam.13748

Muck, R. E. (2010). Silage microbiology and its control through additives. *R. Bras. Zootec.* 39, 183–191.

Murphy, R. P. (2010). A method for the extraction of plant samples and the determination of total soluble carbohydrates. *J. Sci. Food Agric.* 9, 714–717.

Ni, K., Wang, F., Zhu, B., Yang, J., Zhou, G., Pan, Y., et al. (2017). Effects of lactic acid bacteria and molasses additives on the microbial community and fermentation quality of soybean silage. *Bioresour. Technol.* 238, 706–715. doi: 10.1016/j.biortech.2017.04.055

Ni, K., Zhao, J., Zhu, B., Su, R., Pan, Y., Ma, J., et al. (2018). Assessing the fermentation quality and microbial community of the mixed silage of forage soybean with crop corn or sorghum. *Bioresour. Technol.* 265, 563–567. doi: 10.1016/j.biortech.2018.05.097

Ogunade, I. M., Jiang, Y., Kim, D. H., Cervantes, A. A. P., Arriola, K. G., Vyas, D., et al. (2016). Fate of *Escherichia coli* O157:H7 and bacterial diversity in corn silage contaminated with the pathogen and treated with chemical or microbial additives. *J. Dairy Sci.* 100, 1–15.

Oladosu, Y., Rafii, M. Y., Abdullah, N., Magaji, U., Hussin, G., Ramli, A., et al. (2016). Fermentation quality and additives: a case of rice straw silage. *Biomed. Res. Int.* 2016, 1–14. doi: 10.1155/2016/7985167

Oliveira, A. S., Weinberg, Z. G., Ogunade, I. M., Cervantes, A. A. P., Arriola, K. G., Jiang, Y., et al. (2017). Meta-analysis of effects of inoculation with homofermentative and facultative heterofermentative lactic acid bacteria on silage fermentation, aerobic stability, and the performance of dairy cows. *J. Dairy Sci.* 100, 4587–4603. doi: 10.3168/jds.2016-11815

Pahlow, G., Muck, R. E., Driehuis, F., Elferink, S. J. W. H. O., and Spoelstra, S. F. (2003). Microbiology of ensiling. *Microbiology* 42, 31–93.

Parvin, S., Wang, C., Li, Y., and Nishino, N. (2010). Effects of inoculation with lactic acid bacteria on the bacterial communities of Italian ryegrass, whole crop maize, guinea grass and rhodes grass silages. *Anim. Feed Sci. Technol.* 160, 160–166.

Ren, C., Zhang, Y., Cui, W., Lu, G., Wang, Y., Gao, H., et al. (2015). A polysaccharide extract of mulberry leaf ameliorates hepatic glucose metabolism and insulin signaling in rats with type 2 diabetes induced by high fat-diet and streptozotocin. *Int. J. Biol. Macromol.* 72, 951–959. doi: 10.1016/j.ijbiomac.2014.09.060

Rodríguez-Berbel, N., Ortega, R., Lucas-Borja, M. E., Solé-Benet, A., and Miralles, I. (2020). Long-term effects of two organic amendments on bacterial communities of calcareous mediterranean soils degraded by mining. *J. Environ. Manag.* 271, 1–14. doi: 10.1016/j.jenvman.2020.110920

Srivastava, S., Kapoor, R., Thathola, A., and Srivastava, R. P. (2006). Nutritional quality of leaves of some genotypes of mulberry (*Morus alba*). *Int. J. Food Sci. Nutr.* 57, 305–313. doi: 10.1080/09637480600801837

Stevenson, D. M., Muck, R. E., Shinners, K. J., and Weimer, P. J. (2006). Use of real time PCR to determine population profiles of individual species of lactic acid bacteria in alfalfa silage and stored corn stover. *Appl. Microbiol. Biotechnol.* 71, 329–338. doi: 10.1007/s00253-005-0170-z

Sugiyama, M., Katsube, T., Koyama, A., and Itamura, H. (2016). Effect of solar radiation on the functional components of mulberry (*Morus alba* L.) leaves. *J. Sci. Food Agric.* 96, 3915–3921. doi: 10.1002/jsfa.7614

Suranska, H., Vranova, D., and Omelkova, J. (2016). Isolation, identification and characterization of regional indigenous Saccharomyces cerevisiae strains. *Braz. J. Microbiol.* 47, 181–190. doi: 10.1016/j.bjm.2015.11.010

Svobodova, B., Vlach, J., Junkova, P., Karamonova, L., Blazkova, M., and Fukal, L. (2017). Novel method for reliable identification of *Siccibacter* and *Franconibacter* strains: from "Pseudo-Cronobacter" to new Enterobacteriaceae genera. *Appl. Environ. Microbiol.* 83, 1–33. doi: 10.1128/AEM.00234-17

Szymanowska-Powalowska, D., Orczyk, D., and Leja, K. (2014). Biotechnological potential of *Clostridium butyricum* bacteria. *Braz. J. Microbiol.* 45, 892–901.

Varki, A. (2017). Biological roles of glycans. *Glycobiology* 27, 3–49.

Wang, S., Zhao, J., Dong, Z., Li, J., Kaka, N. A., and Shao, T. (2020). Sequencing and microbiota transplantation to determine the role of microbiota on the fermentation type of oat silage. *Bioresour. Technol.* 309, 1–10. doi: 10.1016/j.biortech.2020.123371

Wang, W. X., Yang, H. J., Bo, Y. K., Ding, S., and Cao, B. H. (2012). Nutrient composition, polyphenolic contents, and in situ protein degradation kinetics of leaves from three mulberry species. *Livest. Sci.* 146, 203–206.

Wang, Y., Chen, X., Wang, C., He, L., Zhou, W., Yang, F., et al. (2019b). The bacterial community and fermentation quality of mulberry (*Morus alba*) leaf silage with or without *Lactobacillus casei* and sucrose. *Bioresour. Technol.* 293, 1–8. doi: 10.1016/j.biortech.2019.122059

Wang, Y., He, L., Xing, Y., Zhou, W., Pian, R., Yang, F., et al. (2019c). Bacterial diversity and fermentation quality of *Moringa oleifera* leaves silage prepared with lactic acid bacteria inoculants and stored at different temperatures. *Bioresour. Technol.* 284, 349–358.

Wang, C., He, L., Xing, Y., Zhou, W., Yang, F., Chen, X., et al. (2019a). Fermentation quality and microbial community of alfalfa and stylo silage mixed with *Moringa oleifera* leaves. *Bioresour. Technol.* 284, 240–247.

Wang, Y., Wang, C., Zhou, W., Yang, F. Y., Chen, X. Y., and Zhang, Q. (2018). Effects of Wilting and *Lactobacillus plantarum* addition on the fermentation quality and microbial community of *Moringa oleifera* leaf silage. *Front Microbiol* 9:1817. doi: 10.3389/fmicb.2018.01817

Xu, D., Ding, W., Ke, W., Li, F., Zhang, P., and Guo, X. (2019). Modulation of metabolome and bacterial community in whole crop corn silage by Inoculating homofermentative *Lactobacillus plantarum* and heterofermentative *Lactobacillus buchneri*. *Front. Microbiol.* 9:3299. doi: 10.3389/fmicb.2018.03299

Yan, Y., Li, X., Guan, H., Huang, L., Ma, X., Peng, Y., et al. (2019). Microbial community and fermentation characteristic of Italian ryegrass silage prepared with corn stover and lactic acid bacteria. *Bioresour. Technol.* 279, 166–173. doi: 10.1016/j.biortech.2019.01.107

Yang, J., Tan, H., and Cai, Y. (2016). Characteristics of lactic acid bacteria isolates and their effect on silage fermentation of fruit residues. *J. Dairy Sci.* 99, 5325–5334. doi: 10.3168/jds.2016-10952

Zeng, T., Li, X., Guan, H., Yang, W., Liu, W., Liu, J., et al. (2020). Dynamic microbial diversity and fermentation quality of the mixed silage of corn and soybean grown in strip intercropping system. *Bioresour. Technol.* 313, 1–8. doi: 10.1016/j.biortech.2020.123655

Zhao, X., Li, L., Luo, Q., Ye, M., Luo, G., and Kuang, Z. (2015). Effects of mulberry (*Morus alba* L.) leaf polysaccharides on growth performance, diarrhea, blood parameters, and gut microbiota of early-weanling pigs. *Livest. Sci.* 177, 88–94.

Zhao, X., Wang, F., Fang, Y., Zhou, D., Wang, S., Wu, D., et al. (2020). High-potency white-rot fungal strains and duration of fermentation to optimize corn straw as ruminant feed. *Bioresour. Technol.* 312, 1–9. doi: 10.1016/j.biortech.2020.123512

Zhou, R., Wu, J., Zhang, L., Liu, L., Casper, D. P., Jiao, T., et al. (2019). Effects of oregano essential oil on the ruminal pH and microbial population of sheep. *PLoS One* 14:e0217054. doi: 10.1371/journal.pone.021?7054

Zhou, Y., Drouin, P., and Lafreniere, C. (2016). Effect of temperature (5–25°C) on epiphytic lactic acid bacteria populations and fermentation of whole-plant corn silage. *J. Appl. Microbiol.* 121, 657–671. doi: 10.1111/jam.13198

Conflict of Interest: The authors declare that the research was conducted in the absence of any commercial or financial relationships that could be construed as a potential conflict of interest.

Publisher's Note: All claims expressed in this article are solely those of the authors and do not necessarily represent those of their affiliated organizations, or those of the publisher, the editors and the reviewers. Any product that may be evaluated in this article, or claim that may be made by its manufacturer, is not guaranteed or endorsed by the publisher.

frontiers | Frontiers in Microbiology

TYPE Original Research
PUBLISHED 28 July 2022
DOI 10.3389/fmicb.2022.840318

OPEN ACCESS

EDITED BY
Christopher Rensing,
Fujian Agriculture and Forestry University, China

REVIEWED BY
Anukool Vaishnav,
Agroscope, Switzerland
Fenglong Wang,
Tobacco Research Institute (CAAS), China

*CORRESPONDENCE
Zhiping Wang
wangzp@syau.edu.cn
Yuanhua Wu
wuyh09@syau.edu.cn

SPECIALTY SECTION
This article was submitted to Microbiotechnology, a section of the journal Frontiers in Microbiology

RECEIVED 21 December 2021
ACCEPTED 05 July 2022
PUBLISHED 28 July 2022

CITATION
Liu H, Jiang J, An M, Li B, Xie Y, Xu C, Jiang L, Yan F, Wang Z and Wu Y (2022) *Bacillus velezensis* SYL-3 suppresses *Alternaria alternata* and tobacco mosaic virus infecting *Nicotiana tabacum* by regulating the phyllosphere microbial community. *Front. Microbiol.* 13:840318. doi: 10.3389/fmicb.2022.840318

Bacillus velezensis SYL-3 suppresses *Alternaria alternata* and tobacco mosaic virus infecting *Nicotiana tabacum* by regulating the phyllosphere microbial community

He Liu[1], Jun Jiang[1], Mengnan An[1], Bin Li[2], Yunbo Xie[2], Chuantao Xu[1,3], Lianqiang Jiang[4], Fangfang Yan[5], Zhiping Wang[1]* and Yuanhua Wu[1]*

[1]Liaoning Key Laboratory of Plant Pathology, College of Plant Protection, Shenyang Agricultural University, Shenyang, China, [2]Sichuan Province Tobacco Company, Chengdu, China, [3]Sichuan Province Tobacco Company, Luzhou, China, [4]Sichuan Province Tobacco Company, Xichang, China, [5]Sichuan Province Tobacco Company, Panzhihua, China

The occurrence of plant diseases is closely associated with the imbalance of plant tissue microecological environment. The regulation of the phyllosphere microbial communities has become a new and alternative approach to the biological control of foliar diseases. In this study, *Bacillus velezensis* SYL-3 isolated from Luzhou exhibited an effective inhibitory effect against *Alternaria alternata* and tobacco mosaic virus (TMV). The analysis of phyllosphere microbiome by PacBio sequencing indicated that SYL-3 treatment significantly altered fungal and bacterial communities on the leaves of *Nicotiana tabacum* plants and reduced the disease index caused by *A. alternata* and TMV. Specifically, the abundance of *P. seudomo*, *Sphingomonas*, *Massilia*, and *Cladosporium* in the SYL-3 treatment group increased by 19.00, 9.49, 3.34, and 12.29%, respectively, while the abundances of *Pantoea*, *Enterobacter*, *Sampaiozyma*, and *Rachicladosporium* were reduced. Moreover, the abundance of beneficial bacteria, such as *Pseudomonas* and *Sphingomonas,* was negatively correlated with the disease indexes of *A. alternata* and TMV. The PICRUSt data also predicted the composition of functional genes, with significant differences being apparent between SYL-3 and the control treatment group. Further functional analysis of the microbiome also showed that SYL-3 may induce host disease resistance by motivating host defense-related pathways. These results collectively indicate that SYL-3 may suppress disease progression caused by *A. alternata* or TMV by improving the microbial community composition on tobacco leaves.

KEYWORDS

***Bacillus velezensis* SYL-3, *Alternaria alternata*, tobacco mosaic virus, *Nicotiana tabacum*, phyllosphere microbial community**

Introduction

Microorganisms are ubiquitous in nature and influence everyday life in various harmful as well as beneficial ways (Morelli and Pellegrino, 2021). Currently, biological control using microorganisms and their metabolites has been used as a potentially effective, sustainable, and alternative method (Zhang N. et al., 2017). The microorganisms such as the genera *Bacillus*, *Pseudomonas*, *Trichoderma*, as well as *Streptomyces* have been reported to effectively inhibit the occurrence and pathogenesis of plant diseases caused by various pathogenic fungi, bacteria, and viruses (Ashrafi et al., 2021; Gao et al., 2021; Jiang et al., 2021; Sánchez-Montesinos et al., 2021). The major *Bacillus* spp. that has been applied in biological control are *B. subtilis*, *B. megaterium*, *B. amyloliquefaciens*, and *B. velezensis* (Wang Y. et al., 2020; Zeng et al., 2021). *Bacillus* is a well-known producer of a wide array of antagonistic compounds with different structures, namely, peptides, lipopeptides, bacteriocins, and polyketide compounds (Fira et al., 2018). For instance, the *B. amyloliquefaciens* PPL strain can suppress the infection of cucumber mosaic virus as well as upregulate plant defense-related genes by producing fengycin (Kang et al., 2021). *B. velezensis* AR1 has been reported to resist *Alternaria* leaf spots caused by *Alternaria sesami* and improve plant physiological traits by inducing resistance in the host (Bayisa, 2020). Bacillomycin D and fengycin produced by *B. amyloliquefaciens* LYZ69 can effectively inhibit anthracnose of *Medicago sativa* (Hu et al., 2021).

In addition to the beneficial rhizosphere microorganisms that have been well investigated in their roles in the management of plant diseases (Wang et al., 2021; Zhuang et al., 2021), some lines of research indicate that phyllosphere microbial communities, namely, those of bacteria, fungi, and protozoa are also closely related to plant health as well as disease progression (Gu et al., 2010; Yang et al., 2017). The next-generation sequencing techniques are extensively applied for comprehensive analysis of the structure of microbial communities such as phyllosphere microbiome (Zhou et al., 2018; Vu et al., 2019). The sequences of 16S ribosomal RNA or the internal transcribed spacer (ITS) are currently used for amplification to analyze phyllosphere bacterial or fungal communities, respectively, (Vorholt, 2012). Recent studies indicated that the application of beneficial microorganisms, as well as microbial pesticides, can regulate the microbial community composition of the phyllosphere, thereafter promoting plant fitness and alleviating symptoms (Vorholt, 2012; Podolich et al., 2015). For example, foliar application of *B. megaterium* PB50 improved plant growth under various stress conditions by changing the structure of phyllosphere microbiota during the reproductive stage of rice (Arun et al., 2020). *B. amyloliquefaciens* B1408 was reported to promote plant growth and suppress cucumber fusarium wilt disease by changing the microbial community composition in the rhizosphere (Han et al., 2018). Studies also showed that *Pseudomonas putida* KT2440 can drastically reduce necrosis on the leaves of *Nicotiana benthamiana* by influencing the microbial composition of the rhizosphere and phyllosphere (Bernal et al., 2017).

The yield and quality of crops are affected by many factors, among which the occurrence of diseases is usually the dominant one (Pan et al., 2021). *Alternaria alternata* is a facultative saprophytic fungus infecting over 400 species of host plants and ubiquitously causes leaf spot or leaf blight by synthesizing various kinds of mycotoxin, which pose threats to food safety and human health (Liu et al., 2020; Huang et al., 2021). Epidemiological studies also demonstrated that *A. alternata* released a large number of fungal spores in the atmosphere, making the disease hard to prevent and control (Woudenberg et al., 2015). Tobacco mosaic virus (TMV) is also a well-investigated plant virus with broad host ranges and causes significant economic losses in agriculture (Roossinck, 2015). The two pathogens above are ubiquitous and serious, causing huge losses to crop yield and agricultural economy every year (Wang et al., 2017; Chen et al., 2020). Traditional management methods, such as seedling grafting, crop rotation, and chemical strategies, have been suggested to control tobacco diseases, but these approaches are not economical, reliable, or environmentally friendly (Zhang et al., 2020).

Compared with in-depth research on the role of root colonization microbiota in plant health (Palmieri et al., 2016; Shi et al., 2016, 2017), few studies have been conducted on the potential interactions between phyllosphere microbial communities and plant diseases. In this study, the newly identified *B. velezensis* SYL-3 showed a significant inhibitory effect on *A. alternata* and TMV. In addition, a microbiome high-throughput sequencing was performed and the results suggested that SYL-3 can reduce the incidence of tobacco leaf diseases probably by promoting the phyllosphere microbial community structure, which provided a valuable theoretical basis for the biological control of tobacco diseases.

Materials and methods

Biomaterials and growth conditions

Biocontrol strain SYL-3 and *A. alternata* were isolated from tobacco leaves in Luzhou (105°26′E, 28°52′N), Sichuan Province of China, which were isolated and stored on the potato dextrose agar (PDA) and Luria–Bertani (LB) medium (Solarbio, Beijing, China) at 4°C, respectively, and were activated at 28°C for subsequent experiments. TMV virions were purified from pCB-TMV-SY (no. MG516107) inoculated *N. benthamiana* leaves according to Gooding's method and diluted to 20 μg/mL with 10 mM phosphate-buffered saline. The *Nicotiana glutinosa* and *Nicotiana tabacum* cv. NC89 plants were cultivated at the 26°C

growth chamber and were treated at the fifth to seventh leaf stage for subsequent experiments.

Bacterial identification

The strain SYL-3 was identified by Gram staining, morphology, physiological, and biochemical tests according to Bergey's Manual of Determinative Bacteriology (Brenner et al., 2005). Further identification of SYL-3 was confirmed by the analysis of 16S rRNA and *gyrA* gene sequences. Genomic DNA was isolated according to the standard phenol:chloroform procedure. The 16S rRNA gene was amplified by PCR with the bacterial universal primer pair 27F:5′-AGTTTGATCMTGGCTCAG-3′ and 1492R:5′-GGTTACCTTGTTACGACTT-3′ (Marchesi et al., 1998). Primer pair *gyrA*-F:5′-CAGTCAGGAAATGCGTACGTCCTT-3′ and *gyrA*-R:5′-CAAGGTAATGCTCCAGGCATTGCT-3′ was used to amplify the partial gene sequence of *gyrA* (Yang et al., 2017; Zhang X. et al., 2017; Dhruw et al., 2020; Wu et al., 2021). The obtained PCR products were sequenced (Sangon Biotech Co., Ltd) and BLAST alignment was performed in GenBank according to sequence homology. Then, phylogenetic analysis was performed using MEGA7.0 by the neighbor-joining method with 1,000 bootstrap replications.

The colonization of the SYL-3 strain

Bacillus competent cell preparation and electrotransformation were performed according to a previous study (Wang B. et al., 2020). SYL-3 was transformed with a pGFP78 plasmid that was kindly provided by Prof. Wang Qi from China Agricultural University. The SYL-3 expressing GFP was designated as SYL-3-*gfp* and incubated in a 100 mL of LB agar medium (containing 50 μg/mL of ampicillin and tetracycline) at 28°C, 180 r/min. Then, *N. tabacum* cv. NC89 plants were treated with SYL-3-*gfp* bacterial suspension (10^9 CFU/mL), and the colonization of SYL-3-*gfp* strain on tobacco leaves was detected based on fluorescence signal. The GFP fluorescence was photographed under ultraviolet illumination by a B-100AP longwave-UV lamp (Ultra-Violet Products, Upland, CA, United States.) and laser scanning confocal microscope (Olympus Co., Ltd, Japan, FV3000).

Effects of SYL-3 on pathogenic microorganisms

The inhibitory effect of SYL-3 against *A. alternata* was determined using *in vitro* antagonism assay as previously described (Ren et al., 2012). Briefly, a fungus plug measuring 5 mm in diameter was placed at the center of the PDA, and 1 μL of bacterial culture (10^9 CFU/mL) was deposited on both sides of the fungus block. All tests were performed in triplicate. The plates were incubated at 28°C for 4 days, at which time the antifungal efficacy of treatments was evaluated and recorded. Leaves of *N. glutinosa* at the same position were inoculated with 100 μg TMV virions and treated with SYL-3 bacterial suspension (10^9 CFU/mL) or ningnanmycin (An et al., 2019) at 12 h post-inoculation. Meanwhile, leaves inoculated with TMV virions (100 μg) and treated with sterile water only were served as control treatments. The local lesion numbers were recorded 3–4 days post-inoculation.

Plot test

Plot experiments with four treatments, namely, SYL-3 bacterial suspension, ningnanmycin (8% water, Deqiang Biology Co., Ltd., China), dimethachlon (40% wettable powder, Jiangxi Heyi Chemical Co., Ltd., China), and sterile water were conducted in Luzhou planting field (105°26′E, 28°52′N) using tobacco variety Yunyan No. 87. Those two pesticide treatments were served as positive control groups and water treatment was used as blank control. Each agent treated 60 tobacco plants per treatment and consisted of three biologically independent replicates. The concentration of the bacterial suspension is 10^9 CFU/mL, and dimethachlon and ningnanmycin were diluted to 36 μg/mL and 75 μg/mL in the field experiment, respectively. Each plant was treated with about 30 mL of bacterial suspension and the leaves were sprayed evenly on both sides, at 0, 7, and 14 days, respectively.

Disease incidence estimating, sample collection, and phyllosphere microbe elution

A random sampling method was used to select five points in each plot, and four tobacco plants were selected at each point and marked to investigate the disease index on 16 June 2021 (before SYL-3 application), 23 June 2021 (7 days after SYL-3 application), 30 June 2021 (14 days after SYL-3 application), and 7 July 2021 (21 days after SYL-3 application), respectively. The degrees of disease infection (*r*) were classified into six grades (0, 1, 3, 5, 7, and 9) as previously described (Sama et al., 2019). The mean disease index of diseased tobacco plants was calculated by the following equation:

$$\textbf{\textit{Disease index}}(\%) = [\sum(\boldsymbol{r} \times \boldsymbol{ni})/(\boldsymbol{nt} \times \boldsymbol{R})] \times \mathbf{100}$$

where *r* represents the degree of disease infection, *ni* represents the number of infected plants corresponding to the grade of *r*, *nt* represents the total number of tested plants, and *R* represents the value of the highest degree of disease infection among the

plants. The disease control rate was calculated according to the following equation:

$$\textit{Disease control rate}\,(\%) = (Ci - Ti)/Ci \times 100$$

Ci represents the disease index of control and *Ti* represents the disease index of the treatments. After the fourth disease investigation, five fields were selected by random sampling method in SYL-3 bacterial suspension and blank control-treated plots. Twenty randomly selected tobacco plants and four leaves per plant were collected from each treatment group. Thereafter, 10 g of each sample was vibrated in 100 mL of sterile water at 170 r/min for 30 min and then under ultrasonic conditions for 5 min. The vibration and ultrasonic operations were repeated three times. Finally, the supernatant was transferred to 50 mL centrifuge tubes, centrifuged at 12,000 r/min for 10 min to collect the precipitated microorganisms, and quickly placed in liquid nitrogen for subsequent experiments.

DNA extraction, amplification, and sequencing of phyllosphere microbe

Total DNA of phyllosphere microbial samples was extracted from samples using the Microbial DNA Extraction Kit (UltraClean® Microbial DNA Kit, MoBio, United States) according to the instructions. Using the extracted DNA as a template for PCR reaction, the V3–V4 region of the bacterial 16S rRNA gene and the ITS1 region of the fungal 18S rRNA gene were amplified with respective primer pairs combined with adapter sequences and barcode sequences (The bacterial 16S rRNA primer sequences: Forward primer, 5′-AGTTTGATCMTGGCTCAG-3′; reverse primer, 5′-GGTTACCTTGTTACGACTT-3′; the fungi ITS1 primer sequences: Forward primer, 5′-CTTGGTCATTTAGAGGAAGTAA-3′; reverse primer, 5′-GCTGCGTTCTTCATCGATGC-3′). The Quant-iT^{TM} dsDNA HS reagent (Thermo Fisher Scientific, Waltham, MA, United States) was used to quantify and pool all PCR products. High-throughput sequencing was carried out on the PacBio sequencing platform (Biomarker Technologies Co. Ltd, China). The SMRT Cell method (Jones and Kustka, 2017) was used to sequence marker genes, and then circular consensus sequencing (CCS) was filtered by UCHIME v4.2[1] software to acquire Optimization-CCS. The sequence was clustered by operational taxonomic units (USEARCH v10.0)[2] at a 97% similarity level, then the species composition of samples can be revealed by species annotation and richness analysis (RDP Classifier v2.2)[3]. Alpha diversity, Beta diversity, and significant species difference analysis were carried out by MOTHUR (version v1.30)[4] to discover the differences between samples. The raw reads generated by PacBio sequencing were submitted to the Sequence Read Archive database at NCBI (SRA)[5], with the SRA BioProject accession number [PRJNA790673 (Bacterial communities 16s rRNA sequencing results)] and [PRJNA790671 (Fungal communities ITS sequencing results)].

Functional gene prediction

The PICRUSt software was used to infer the functional gene composition in the samples by comparing the species composition information obtained from the 16S sequencing data, thus analyzing the functional differences between different samples or subgroups (Parks et al., 2014). The differences and changes in the metabolic pathways of microbial community functional genes among samples of different groups were predicted through the difference analysis of the KEGG metabolic pathways (Wilkinson et al., 2017).

Statistical analysis

All data and Spearman correlation analysis were analyzed using the SPSS 20.0 program (SPSS Inc., Chicago, IL, United States), and the one-way analysis of variance with Duncan's test was used to assign significance as $P < 0.05$, using SparCC algorithm for correlation analysis. The correlation between the sample and other species at a certain taxonomic level can be achieved through Pearson's correlation network analysis. The network diagram of species correlation was generated by Python (Maucher et al., 2011). A linear discriminant analysis and effect size (LEfSe) was performed to identify microbial communities' biomarkers with statistical differences between different treatments (Segata et al., 2011).

Results

Identification and colonization of biocontrol strain SYL-3

The strain SYL-3 was identified by morphological, physiological, and biochemical tests, along with genetic homology analysis. The results showed that the colony of SYL-3 was milky white, dim, and opaque, with a bulged center and wrinkled edges (**Figure 1A**). SYL-3 was Gram-positive (**Figure 1B**) and rod-shaped (**Figure 1C**). Based on the

1 http://drive5.com/usearch/manual/uchime_algo.htm

2 http://www.drive5.com/usearch/

3 https://sourceforge.net/projects/rdp-classifier/

4 http://www.mothur.org/

5 http://www.ncbi.nlm.nih.gov/Traces/sra

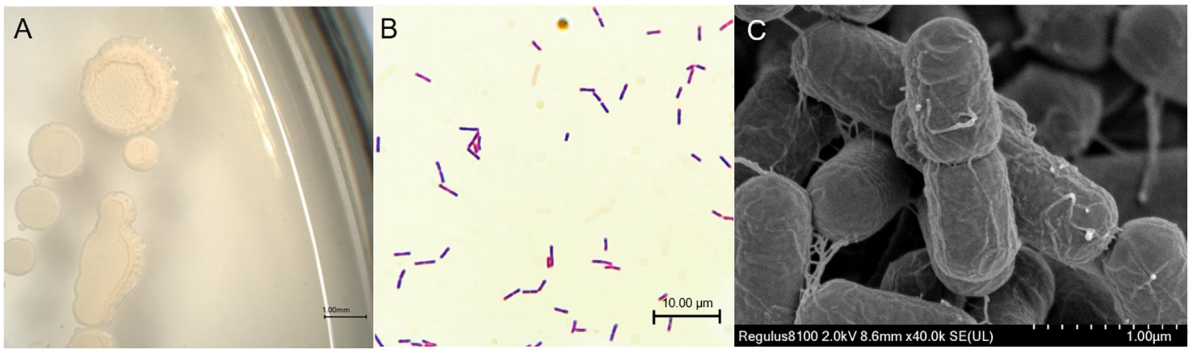

FIGURE 1
Morphological identification of SYL-3. **(A)** Morphology observation of SYL-3 on LB agar medium. **(B)** Observation of the strain SYL-3 after Gram staining. **(C)** Scanning electron micrographs of the strain SYL-3.

physiological and biochemical characteristics (Table 1), SYL-3 was preliminarily identified as *Bacillus* sp. Sequence alignments and phylogenetic analysis were conducted using sequences of 16S rRNA and *gyrA* gene of SYL-3. The results indicated that the 16S rRNA gene of SYL-3 was most closely related to *B. velezensis* B04 (MW418038.1), *B. velezensis* BKS104 (MW577624.1), and *B. velezensis* TB918 (CP069430.1) with 99.28, 99.10, and 99.10% sequence identity, respectively, and showed comparatively lower sequence similarity with *Bacillus safensis* U17 (CP015611.1) and *B. cellulasensis* GLB197 (CP018574.1; Figure 2A). In addition, sequencing of *gyrA* of SYL-3 showed high sequence similarity with *B. velezensis* LG37 (CP023341.1), *B. velezensis* ANSB01E (CP036518.1), and *B. velezensis* LDO2 (CP029034.1), with 99.30% sequence identity, respectively, while distantly related to *B. amyloliquefaciens* strain HM618 (CP029466.1) and *B. amyloliquefaciens* strain 9001 (KT736040.1; Figure 2B). Taken altogether, strain SYL-3 was identified as a strain of *B. velezensis*.

TABLE 1 Physiological and biochemical characteristics of SYL-3 strain.

Test index	Results (±)
Voges-Proskauer test	+
Citrate	−
Propionate	−
D-Xylose	+
L-Arabinose	+
D-Mannitol	+
Gelatin liquefaction	+
7%NaCl	+
PH5.7	+
Nitrate reduction	+
Starch hydrolysis	+

"+" Positive; "−" negative.

Affirming the colonization ability of biocontrol strains on host plants would lay a foundation for using the strains for disease control in the field. The GPF fluorescence expressed from SYL-3-*gfp* can be observed by fluorescence microscopy, indicating that the strain was successfully transformed with the plasmid expressing GFP (Supplementary Figure 1A). By UV light irradiation, we observed that the SYL-3-*gfp* strain evenly covered the surface of tobacco leaves 2 days after the bacterial suspension was sprayed (Supplementary Figure 1B). Furthermore, the SYL-3-*gfp* was observed around tobacco leaf epidermal cells as well as in the vascular tissue on the fourth day after treatment (Supplementary Figures 1C,D). The results confirmed the good colonization ability of SYL-3 on tobacco leaves.

SYL-3 exhibited a significant inhibitory effect against *A. alternata* and tobacco mosaic virus

To clarify the inhibitory effect of SYL-3 on *A. alternata*, we conducted an antibacterial test using *in vitro* confrontation method. The results showed that SYL-3 significantly reduced the mycelium growth of *A. alternata* by 71.33% ± 3.22 (Figure 3A). To clarify the effect of SYL-3 on the infection of TMV in plants, we assessed the inhibitory activity of SYL-3 bacterial suspension against TMV by investigating the number of necrotic spots on the inoculated leaves. It showed that SYL-3 reduced the necrotic spots by 87.77% ± 2.81 compared with the control treatment, suggesting a strong anti-TMV effect (Figures 3B,C).

The field plot experiments were conducted in the selected tobacco planting field with perennially occurring foliar disease caused by *A. alternata* or TMV. We thereafter used the disease index of tobacco leaves to determine the inhibitory effect of SYL-3 on these diseases. The results showed that SYL-3 significantly suppressed the disease progression of

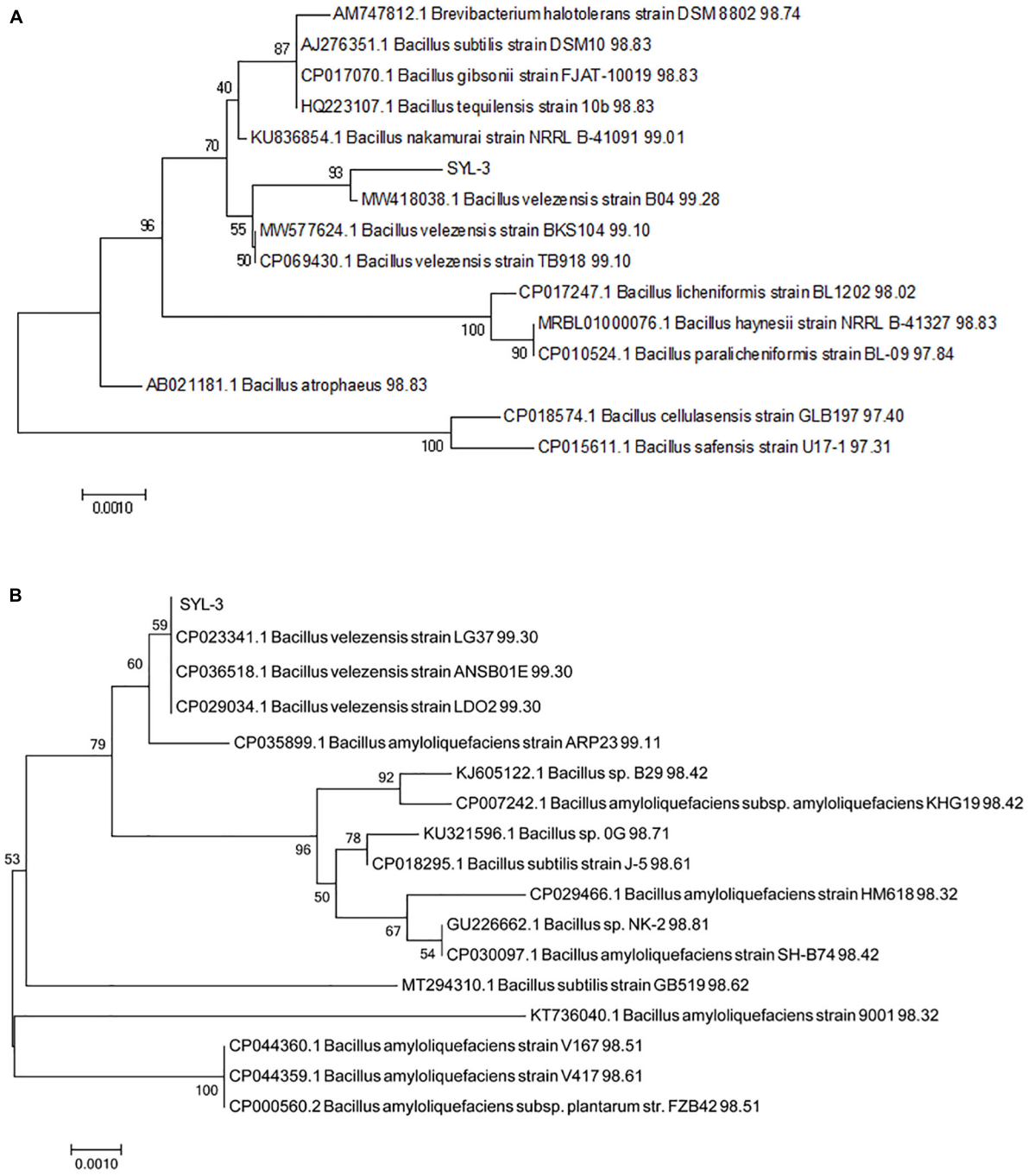

FIGURE 2
Phylogenetic analysis of strain SYL-3 based on the sequences of 16s rRNA **(A)** and *gyrA* **(B)**. The tree was constructed using the neighbor-joining algorithm with 1,000 bootstrap replications.

A. alternata and reduced the respective disease index from 1.96 (control treatment) to 0.66 on day 21 after treatment (Figure 4A). Meanwhile, the disease index of *A. alternata* after dimethachlon treatment was 0.91. In addition, SYL-3 treatment also markedly suppressed mosaic leaf symptoms caused by TMV and lowered the disease index from 8.89 (control treatment) to 2.83 (Figure 4B). In contrast, the disease index after ningnanmycin treatment was down to 4.78. The inhibitory rates of SYL-3 against *A. alternata* and TMV were determined as 50.72% ± 3.63 and 68.11% ± 0.14, respectively, (Figures 4C,D), which was comparatively higher than that of dimethachlon or ningnanmycin. These results collectively indicated an effective

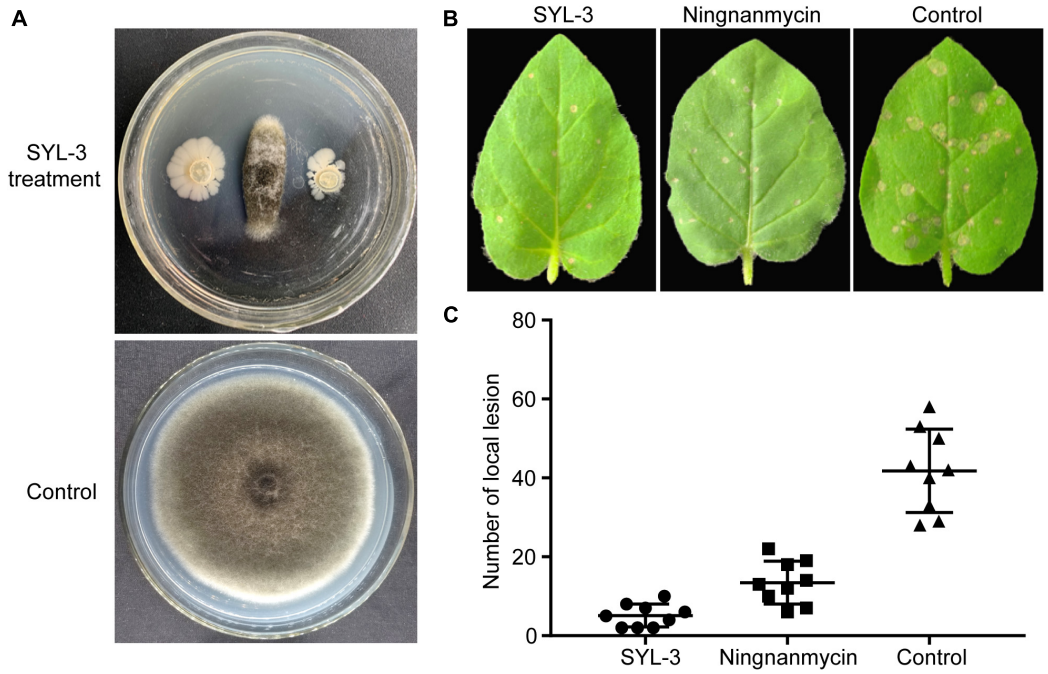

FIGURE 3
Antagonistic activities of SYL-3 against *A. alternata* and TMV. **(A)** Effects of SYL-3 on the mycelial growth of *A. alternata in vitro*. **(B)** Effects of SYL-3 or ningnanmycin on the necrotic lesions caused by TMV on *N. glutinosa* leaves. **(C)** Scatter plot of the necrotic lesions on *N. glutinosa* leaves treated with SYL-3, ningnanmycin, and sterile water (control).

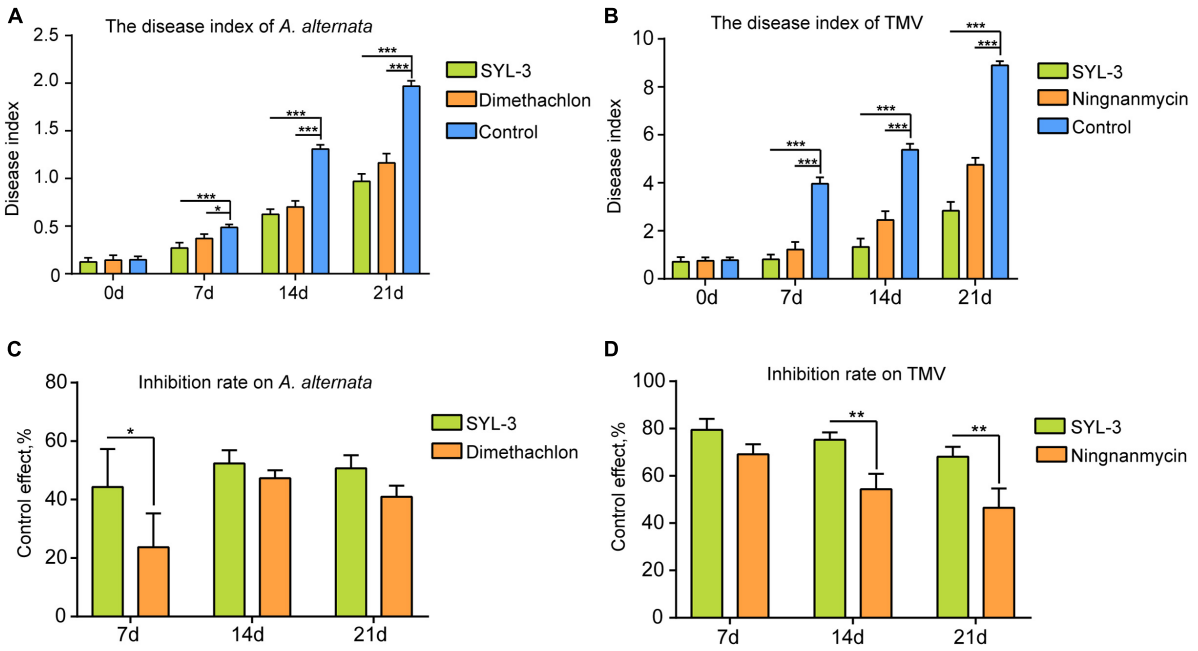

FIGURE 4
Plant disease index of *A. alternata* and TMV and control effect of SYL-3. **(A, B)** The disease index of *A. alternata* and TMV treated with SYL-3 on different days. **(C, D)** Inhibition rate on *A. alternata* and TMV treated with SYL-3 on different days (*$p < 0.05$, ** $p < 0.01$, and *** $p < 0.001$).

inhibitory effect of SYL-3 against *A. alternata* and TMV *in planta* as well as in the field.

Analysis of 16S rRNA and ITS1 sequencing data

Currently, many studies on microbial diversity are mainly based on the conserved region of nucleic acid sequences that encode ribosomal RNA as well as the ITS region (Zhuang et al., 2020). In this study, results of high-throughput sequencing analysis showed that 43,370 and 55,459 CCS were collected for SYL-3 and control treatment, respectively. A total of 38,097 and 53,599 high-quality optimization-CCS for bacteria were obtained after filtering the low-quality reads, chimeras, and attachment sequences, accounting for 88% and 97% of the total reads the number of these two treatments, respectively. Furthermore, there were 17,995 and 23,119 optimization-CCS obtained from SYL-3 and control treatment groups through ITS sequencing analysis, which accounted for about 96% and 99% of the total CCS (**Table 2**). The amount of sequencing data indicated that it was sufficient to reflect the species diversity in these samples.

Phyllosphere microbial community structure affected by SYL-3

The changes in the structure and composition of the phyllosphere microbial community are closely correlated with the impact of the external environment on the host plant (Vogel et al., 2020). At the genus level, we analyzed the phyllosphere microbial community structure in the control and SYL-3-treated groups on day 21 after treatment. The results showed the top 10 abundant kinds of the bacterial and fungal genus and revealed the effect of SYL-3 treatment on the phyllosphere microbial community structure of tobacco (**Figures 5A,B**). The abundances of *Pseudomonas*, *Sphingomonas*, and *Massilia* in the SYL-3 treatment group were increased by 19.00, 9.49, and 3.34%, respectively, compared with that of the control group (**Supplementary Table 1**), becoming the dominant genus of the bacterial community (**Figure 5A**). In contrast, the relative abundance of *Pantoea* decreased by 4.99% after SYL-3 treatment compared with the control group (**Supplementary Table 1**). The results of LEfSe analysis also indicated that *Pseudomonas* and *Sphingomonas* abundance were significantly increased compared with the control group (**Figure 5C**). Meanwhile, SYL-3 also affected the community structure of phyllosphere fungi, among which the abundance level of *Cladosporium* was markedly increased by 12.29% compared with the control group (**Figures 5B,D** and **Supplementary Table 1**). The abundance value of *Filobasidium* was also increased by 3.38%. On the contrary, the dominant fungus species *Sampaiozyma* decreased by 14.91% after SYL-3 treatment (**Supplementary Table 1**).

Phyllosphere microbial community diversity affected by SYL-3

A rarefaction curve can be used to reflect the sequencing amount of microbiome samples (Wang et al., 2012). Here, the rarefaction curve of 16S rRNA and ITS1 sequencing gradually flattens out, indicating that the amount of sequencing data was sufficient to reflect the species diversity in samples (**Supplementary Figure 2**). In addition, to further elucidate the effects of SYL-3 on the diversity of tobacco phyllosphere microbial communities, we first analyzed the microbial community by using the diversity index. The results showed that the bacteria species richness (Chao1 and Ace index measure) and species diversity (Shannon index; Grice et al., 2009) of tobacco phyllosphere were significantly increased after SYL-3 treatment (**Table 3**). In contrast, the SYL-3 treatment resulted in a decrease in the Chao1 index of fungal diversity compared with that of the control treatment (**Table 3**). A principal coordinate analysis based on the Bray–Curtis algorithm was performed on phyllosphere microbial community samples. For fungal and bacterial communities, the spots representing the SYL-3 (red) or control (blue) treatment samples were separated (**Figure 6A**). In the total variance of the data set, the first two major components together comprised 94.93% and 86.77% of the total bacterial and fungal communities, respectively. In addition, the first principal component (PC1) was the most important, accounting for 86.15% and 55.77% of the total variation of bacterial (**Figure 6A**) and fungal communities (**Figure 6B**), respectively. These results revealed that phyllosphere microbial diversity significantly changed after SYL-3 treatment.

Correlation between phyllosphere microbial community structure and disease incidence

After 21 days of SYL-3 treatment, correlation analysis was performed between the abundance of dominant bacteria in tobacco phyllosphere and the disease index of common diseases. The results showed that the increase in the abundance of *Pseudomonas* and *Sphingomonas* in the phyllosphere microbes was negatively correlated ($P < 0.05$) with the disease index caused by *A. alternata* and TMV after SYL-3 treatment (**Figure 7**). In addition, analysis of phyllosphere microbial correlation community network showed that the relative abundance of *Pseudomonas* and *Sphingomonas* was positively correlated with the abundance of beneficial bacteria such as *Stenotrophomonas* and *Methylobacterium* (**Supplementary Figure 3**). Such correlation results suggested that changes in the population structure of *Pseudomonas* and *Sphingomonas* may indirectly affect the occurrence of plant diseases by SYL-3 treatment.

TABLE 2 Statistics of sample sequencing data processing result.

Treatment	16s rRNA			ITS		
	Barcode-CCS	Optimization-CCS	Effective%	Barcode-CCS	Optimization-CCS	Effective%
SYL-3	43370 ± 860.97	38097 ± 969.32	87.84 ± 3.76	18838 ± 1375.95	17995 ± 1247.74	95.53 ± 1.14
Control	55459 ± 2342.28	53599 ± 2342.65	96.65 ± 0.50	23442 ± 264.52	23119 ± 201.80	98.62 ± 0.77

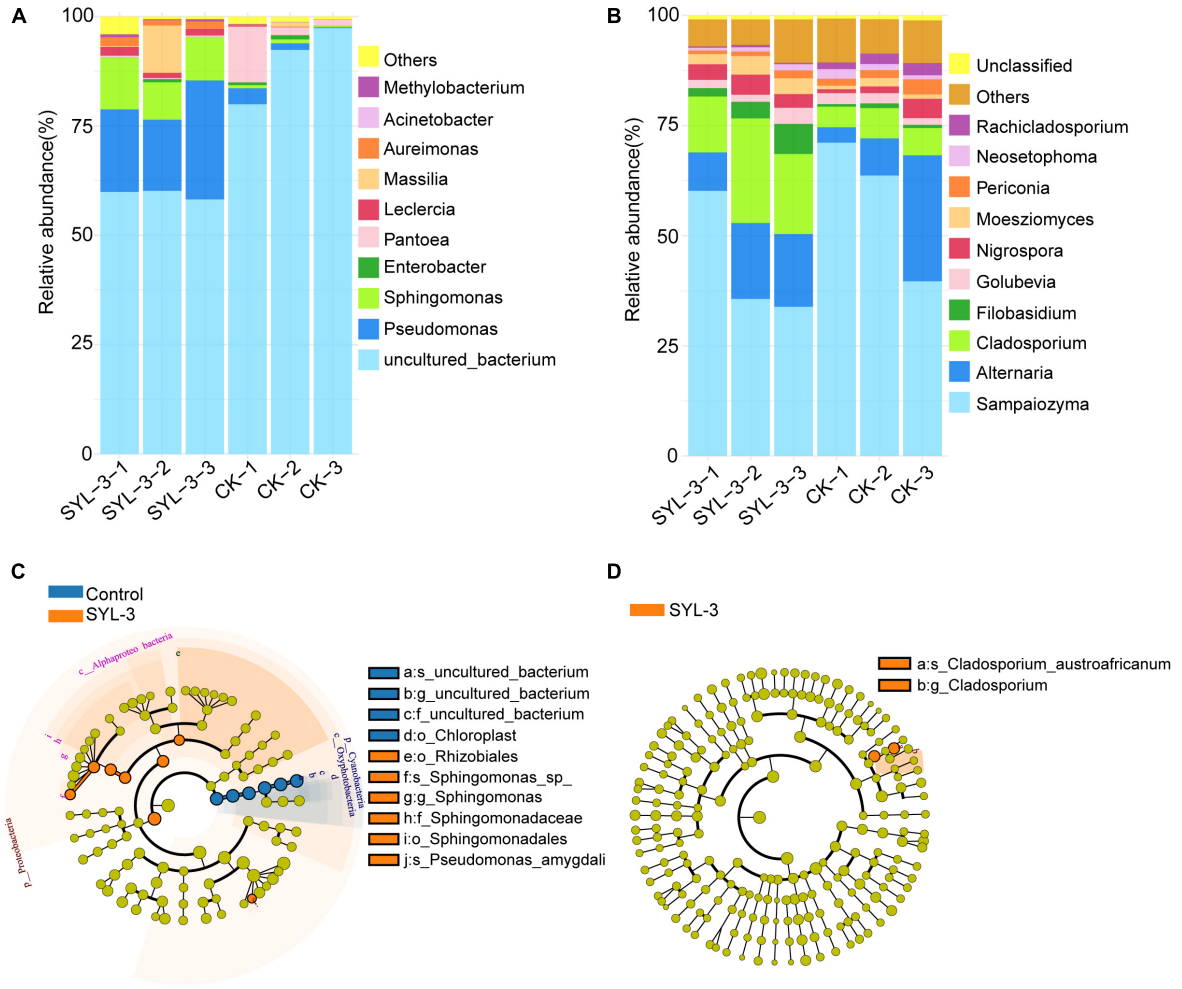

FIGURE 5
Comparative analysis of the phyllosphere dominant microbial taxa in samples collected from SYL-3 and the control treatment group. Relative abundance of several dominant bacterial genera **(A)** and fungal genera **(B)**. Comparison of microbial variations based on the LEfSe analysis of bacterial community **(C)** and fungal community **(D)** in the SYL-3 treatment and control treatment. Differences are represented by the color of the taxa (orange represents the SYL-3 treatment, blue represents the control treatment, and yellow represents the species with no significant difference).

Function of tobacco phyllosphere microbial community affected by SYL-3

PICRUSt software was used to predict the composition of functional genes in the samples by comparing the species composition information obtained from the 16S sequencing data of phyllosphere microorganisms. Then, the differences in metabolic pathways of functional genes in microbial communities between SYL-3 and control-treated samples were analyzed by KEGG (Figure 8). The KEGG metabolic pathways such as gene replication and repair, translation, nucleotide metabolism, energy metabolism, vitamin and cofactor metabolism, and the biosynthesis of other

TABLE 3 Statistics of alpha diversity index of phyllosphere microbial community.

Treatment	Community characteristics					
	Bacterial community			Fungal community		
	ACE	Chao1	Shannon	ACE	Chao1	Shannon
SYL-3	65.14 ± 3.00	65.47 ± 3.91	1.49 ± 0.13	147.26 ± 4.47	140.71 ± 4.44	2.05 ± 0.26
Control	59.22 ± 7.48	58.33 ± 8.81	0.60 ± 0.31	144.65 ± 22.66	140.94 ± 18.78	1.84 ± 0.22

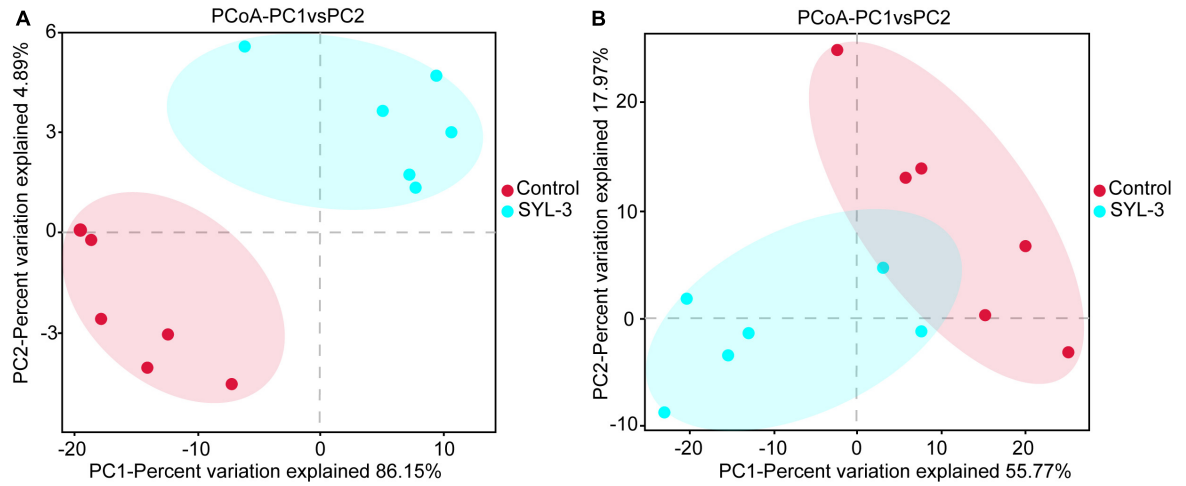

FIGURE 6
Taxonomic beta-diversity of phyllosphere microbial community as indicated by principal coordinates analysis (PCoA) plots. **(A)** PCoA analysis of bacterial community. **(B)** PCoA analysis of fungal community.

secondary metabolites were enriched after SYL-3 treatment compared with that of the control treatment. In contrast, the enrichment of pathways such as cell motility, membrane transport, and signal transduction decreased after SYL-3 treatment.

Discussion

Understanding the structure and dynamics of microbial communities is of great significance due to their effects on plant health (Gobbi et al., 2020). Previous investigations in biological control have mainly focused on soil microbial communities and revealed their critical roles in crop disease management (Palmieri et al., 2016; Shi et al., 2016, 2017). As many foliar pathogens colonize on leaf surfaces before infection, the regulation of the phyllosphere microbial community has become a new subject in biological control (Vorholt, 2012). In this study, the potential relationship among the newly isolated beneficial *B. velezensis* strain SYL-3, the phyllosphere microbial community of tobacco, and the occurrence of two ubiquitous plant diseases was investigated using microbiome high-throughput sequencing approaches.

Among the reported beneficial microorganisms and biological agents, *Bacillus* spp. has been widely applied in the management of various plant diseases (Shafi et al., 2017; Yang et al., 2020; Zhou et al., 2021). Here, phylogenetic analysis indicated that SYL-3 showed high sequence identity and clustered closely with species *B. velezensis*. Previous investigations reported that *B. velezensis* produced a variety of metabolites, regulating the microbial community structure, and can effectively inhibit a variety of crop diseases. For instance, *B. velezensis* FZB42 efficiently antagonizes *Phytophthora sojae* by producing bacilysin (Han et al., 2021). *B. velezensis* B-4 is effective in controlling *Sclerotinia sclerotiorum* by synthesizing non-ribosomal peptide synthetases, polyketide synthases, and lantipeptide synthesis proteins (Zhu et al., 2020). *B. velezensis* T052-76 can control sweet potato foot-rot disease caused by *Plenodomus destruens* by altering the structure of the indigenous bacterial community (Mateus et al., 2019).

Our results showed that SYL-3 significantly affected the relative abundance of foliar bacterial communities compared with those of the fungus. Especially, the genera of *Sphingomonas* and *Pseudomonas* increased observably and became the dominant bacterial genera under SYL-3 treatment.

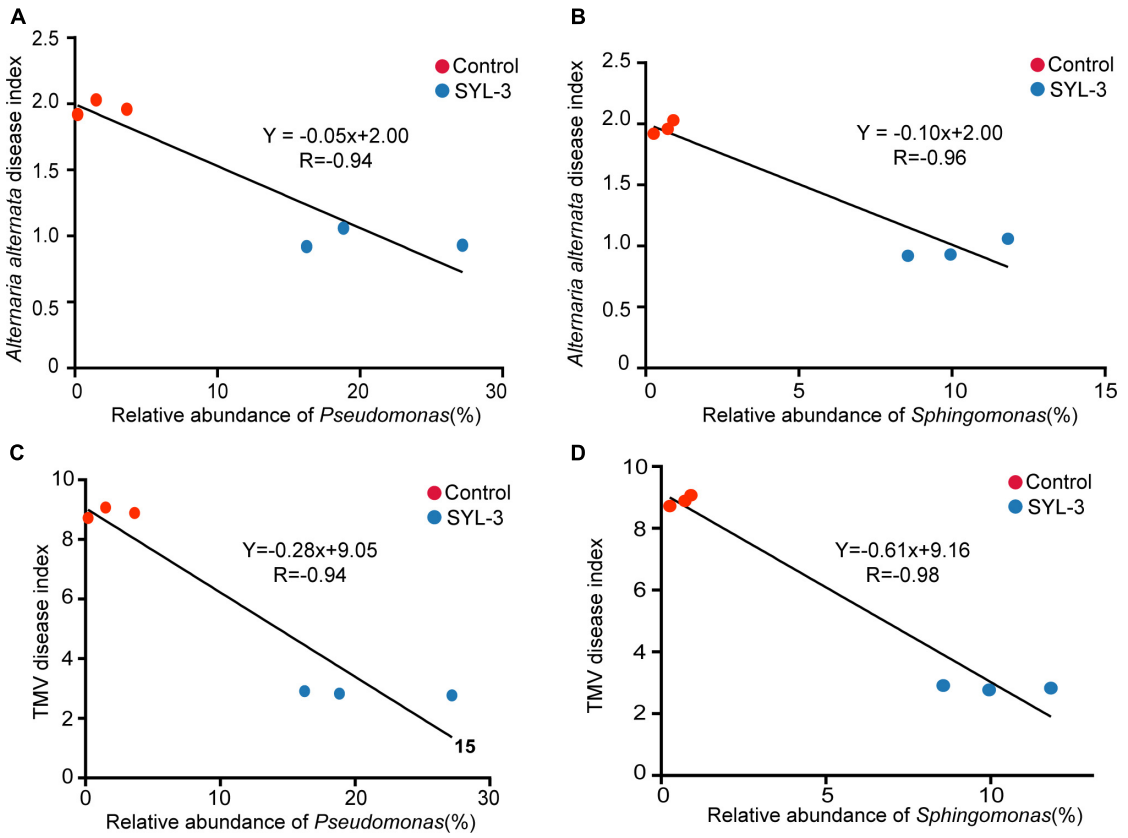

FIGURE 7
The correlation between the abundance of *Pseudomonas* and *Sphingomonas* and the disease index of *A. alternata* **(A, B)** and TMV **(C, D)**.

Sphingomonas sp. is a Gram-negative, rod-shaped aerobic bacterium that possesses multifaceted functions ranging from improving plant fitness to protecting plants from diseases (Innerebner et al., 2011; Asaf et al., 2020). The researchers demonstrated that the foliar bacterium *Sphingomonas* sp. could protect plants against the leaf-pathogenic *Pseudomonas syringae* through substrate competition (Vogel et al., 2012). The lesion coverage rate (LCR) of angular leaf spot of cucumber was correlated negatively with the abundance of *Sphingomonas* in the phyllosphere microbial community (Luo et al., 2019). *Sphingomonas* isolated from tomato leaves had strong *in vitro* antifungal activity against *B. solani*, one of the tomato pathogens (Enya et al., 2007). Herein, our research indicated that the abundance of *Sphingomonas* was negatively (r = –0.96) associated with *A. alternata* disease index, which was consistent with earlier reports. *Pseudomonas* sp. is a Gram-negative bacterium, which has been reported to inhibit plant diseases caused by *Ralstonia solanacearum*, *Phytophthora capsici*, and *Rhizoctonia solani* (Li, 2018; Shi, 2019), as well as induce host systemic resistance and improve morphological and biochemical traits of crops (Kumar Yadav et al., 2021). Here, the abundance of *Pseudomonas* was negatively correlated with the TMV disease index (r = –0.94; **Figure 7C**), which is also consistent with previous reports that the *Pseudomonas* can inhibit the incidence of TMV in tomato plants and induce plant resistance (Gupta et al., 2021). Additionally, the results showed that *B. velezensis* could be detected but not as the dominant strain in the phyllosphere (**Supplementary Table 1**). Nevertheless, based on the good colonization capability of SYL-3, we reasonably speculate that SYL-3 treatment can exhibit a sustainable regulatory effect on phyllosphere microbial communities as well as plant pathogens.

Changes in fungal communities in the treatment groups were not as dramatic as those in bacterial communities, with only a significant increase in the abundance of *Cladosporium*. Studies have shown that *Cladosporium* produced secondary metabolites like phenylacetic acid, p-hydroxyphenyl acetic acid, and p-hydroxyphenyl ethanol, exhibiting good antibacterial and antifungal activities (Hwang et al., 2001; Kim et al., 2004; Ding et al., 2008). It has been reported that the volatile organic compounds (VOCs) produced by *Cladosporium* could promote the growth and development of tobacco as well as improve its disease resistance (Paul and Park, 2013).

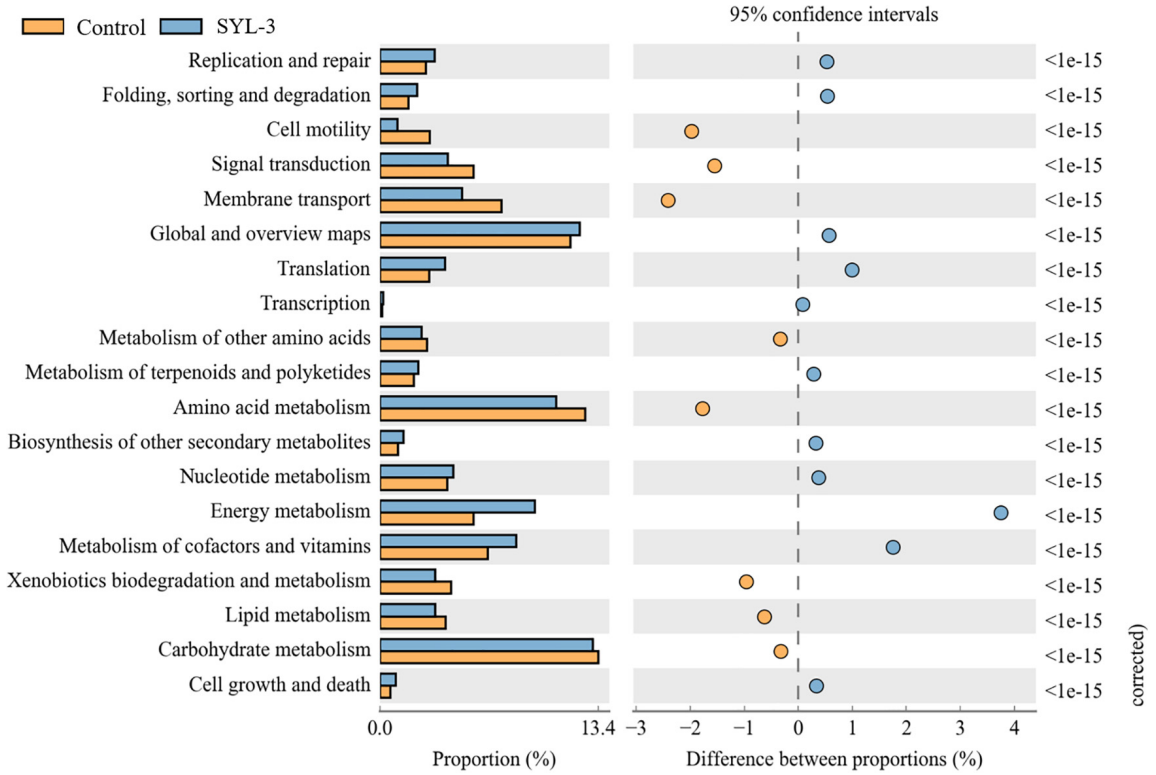

FIGURE 8
Metagenomes predicted by PICRUSt show significant differences in the functionality between SYL-3 treatment samples and controls.

Additionally, *Cladosporium* conidia can induce hypersensitive responses when in contact with tobacco leaves, activating defense responses in tobacco cells (Mattos et al., 2018). Likewise, metagenomic functional analysis of the PICRUSt predictions conducted in this study also confirmed that pathways for the biosynthesis of secondary metabolites were enriched in the treatment groups (**Figure 8**), which suggested that the decrease in the incidence of tobacco diseases in the treatment group may also be associated with the increase in the abundance of *Cladosporium*. Taken together, SYL-3 treatment induced the colonization of *Sphingomonas*, *Pseudomonas*, *Cladosporium*, etc. in foliar microorganisms, and then the beneficial microflora above contributed to inhibiting the occurrence and progression of diseases (**Figures 5**, **7**). However, considering which microorganism was the one playing a leading role in the disease-inhibiting event, or whether it was the result of the synergistic effect of multiple microorganisms, we still need further research on the isolation and culture of phyllosphere microorganisms.

Microbial diversity was identified as a key factor in preventing diseases and can be implemented as a biomarker in plant protection strategies (Berg et al., 2017). Several studies indicated that a relationship has been found between microbial diversity and root disease suppression. For example, traditional crop rotation reduces the outbreak potential of pathogenic microorganisms by enhancing the overall microbial diversity in the soil (Mazzola, 2004). *B. amyloliquefaciens* FZB42, as a commercial and efficient plant strengthener, can resist *R. solani* by enhancing the overall microbial diversity (Erlacher et al., 2014). *B. subtilis* Tpb55 can effectively inhibit *Phytophthora parasitica* var. *nicotianae* by increasing bacterial diversity in tobacco rhizosphere soil (You et al., 2014). In this study, the alpha diversity of the microbial community in the SYL-3 treatment group was significantly increased, and the beta diversity of the microbial community was significantly spatially differentiated. And through the microbial correlation network analysis, it was also found that due to the increase in the diversity of phyllosphere microbes, the correlation between microbes also increased, which may lead to the formation of new homeostasis between plants and phyllosphere microbes. This is consistent with the conclusion of previous studies that greater microbial diversity has a more beneficial impact on crop resistance to pathogens (Shi et al., 2017; Han et al., 2018).

Validating the function of the microbiome is the key to revealing their relationship with the environment (Escalas et al., 2019). Inferring functions based on the diversity of bacteria at present is difficult since bacteria often transfer genes and exhibit a high degree of dependence and redundancy (Klindworth et al., 2013). Currently, PICRUSt analysis is widely explored

to acquire functional insights into the microbial community (Langille et al., 2013). This study found that several pathways that are significantly enriched after treatment, such as cofactors and vitamin metabolism pathways, are related to the promotion of plant resistance by microbial treatment (Sun et al., 2021). Studies have shown that DNA damage repair pathways mainly determine genome integrity and plant survival (Raina et al., 2021). Meanwhile, the biosynthesis of secondary metabolites of microorganisms is recognized as a rich source of biomolecules with potential medicinal applications (Li and Tan, 2017). Therefore, SYL-3 application significantly affected the function of the phyllosphere microbiome. At the same time, it indicated that SYL-3 may indirectly increase host resistance through the induction of host critical genes or pathways from the transcriptional level of some common resistance indicator genes and content of active oxygen (data not shown). Thus, it also showed the potential application value of SYL-3 as a resistance inducer for a wider range of other plant disease control.

In this study, SYL-3 belonging to *B. velezensis* was isolated and identified with a robust inhibitory effect on the infection of *A. alternata* and TMV. SYL-3 increased the abundance of several beneficial microorganisms such as *Pseudomonas*, *Sphingomonas*, and *Massilia* as well as enhanced the overall diversity of the phyllosphere microorganisms, which largely contributed to the induction of resistance against *A. alternata* or TMV. This work will improve the understanding of action modes on biocontrol for SYL-3 and provide a potential sustainable management strategy for plant diseases caused by *A. alternata* and TMV.

Data availability statement

The original contributions presented in this study are publicly available. This data can be found here: The raw reads generated by PacBio sequencing were submitted to the Sequence Read Archive database at NCBI (SRA; http://www.ncbi.nlm.nih.gov/Traces/sra), with the SRA BioProject accession numbers [PRJNA790673 (Bacterial communities 16s rRNA sequencing results)] and [PRJNA790671 (Fungal communities ITS sequencing results)].

Author contributions

ZW, YW, and HL conceived and designed the experiments, carried out the transcriptome analysis, and analyzed the data. HL, JJ, MA, BL, and YX performed the main experiments. HL and JJ contributed equally. CX, LJ, and HL cultivated *N. benthamiana* plants and *N. tabacum* cv. NC89 and treated samples for transcriptome sequencing. HL, MA, FY, JJ, and ZW prepared reagents, materials, and analysis tools. ZW, JJ, and HL prepared the figures and tables. HL wrote the original draft. ZW, YW, BL, and CX reviewed drafts of the manuscript. All authors reviewed and approved the manuscript.

Funding

This research was funded by Key Scientific and Technological Projects of the Sichuan Branch of China National Tobacco Company (SCYC202113) and Key Scientific and Technological Projects of the Liaoning Branch of China National Tobacco Company (2021210000200014).

Conflict of interest

BL, YX, CX, LJ, and FY were employed by Sichuan Province Tobacco Company.

The remaining authors declare that the research was conducted in the absence of any commercial or financial relationships that could be construed as a potential conflict of interest.

Publisher's note

Supplementary material

The Supplementary Material for this article can be found online at: https://www.frontiersin.org/articles/10.3389/fmicb.2022.840318/full#supplementary-material

SUPPLEMENTARY FIGURE 1
Colonization of SYL-3-*gfp* strain on tobacco leaves. **(A)** Confocal microscope observation of SYL-3-*gfp* strain. **(B)** UV irradiation observation of the distribution of SYL-3-*gfp* strain on the leaf surface 2 days after spraying. **(C, D)** Confocal microscopy observation of the colonization of SYL-3-*gfp* in leaf epidermal cells and vascular tissue.

SUPPLEMENTARY FIGURE 2
Sample rarefaction curve. **(A)** Rarefaction curve for bacteria in samples. **(B)** Rarefaction curve for fungus in samples.

SUPPLEMENTARY FIGURE 3
Pearson's correlation network analyses at genus level of phyllosphere microbial communities in SYL-3 treatment. Circles represent species, the size of the circle represents the abundance, the edges represent the correlation between the two species, the thickness of the edge represents the strength of the correlation and the color of the line: orange represents the positive correlation and green represents the negative correlation.

References

An, M., Zhou, T., Guo, Y., Zhao, X., and Wu, Y. (2019). Molecular regulation of host defense responses mediated by biological anti-TMV agent Ningnanmycin. *Viruses* 11:815. doi: 10.3390/v11090815

Arun, K. D., Sabarinathan, K. G., Gomathy, M., Kannan, R., and Balachandar, D. (2020). Mitigation of drought stress in rice crop with plant growth-promoting abiotic stress-tolerant rice phyllosphere bacteria. *J. Basic Microbiol.* 60, 768–786. doi: 10.1002/jobm.202000011

Asaf, S., Numan, M., Khan, A. L., and Al-Harrasi, A. (2020). *Sphingomonas*: from diversity and genomics to functional role in environmental remediation and plant growth. *Crit. Rev. Biotechnol.* 40, 138–152. doi: 10.1080/07388551.2019.1709793

Ashrafi, J., Rahnama, K., Babaeizad, V., Ramezanpour, S. S., and Keel, C. (2021). Induction of wheat resistance to STB by the endophytic fungus *serendipita Indica* and *pseudomonas Protegens*. *Iran. J. Biotechnol*. 19:e2762. doi: 10.30498/IJB.2021.2762

Bayisa, R. A. (2020). Enhancing resistance of *Sesamum indicum* against *Alternaria sesami* through *Bacillus velezensis* AR1. *Pest Manag. Sci.* 76, 3577–3586. doi: 10.1002/ps.5890

Berg, G., Köberl, M., Rybakova, D., Müller, H., Grosch, R., and Smalla, K. (2017). Plant microbial diversity is suggested as the key to future biocontrol and health trends. *FEMS Microbiol. Ecol.* 93:fix050. doi: 10.1093/femsec/fix050

Bernal, P., Allsopp, L. P., Filloux, A., and Llamas, M. A. (2017). The *Pseudomonas putida* T6SS is a plant warden against phytopathogens. *ISME J.* 11, 972–987. doi: 10.1038/ismej.2016.169

Brenner, D. J., Krieg, N. R., and Staley, J. R. (2005). *Bergey's Manual of Systematic Bacteriology*. Berlin: Springer.

Chen, Q., Cai, L., Wang, H., Cai, L., Goodwin, P., Ma, J., et al. (2020). Fungal composition and diversity of the tobacco leaf phyllosphere during curing of leaves. *Front. Microbiol.* 11:554051. doi: 10.3389/fmicb.2020.554051

Dhruw, C., Husain, K., Kumar, V., and Sonawane, V. (2020). Novel xylanase producing *Bacillus* strain X2: molecular phylogenetic analysis and its application for production of *xylooligosaccharides*. *3 Biotech* 10:328. doi: 10.1007/s13205-020-02322-1

Ding, L., Qin, S., Li, F., Chi, X., and Laatsch, H. (2008). Isolation, antimicrobial activity, and metabolites of fungus *Cladosporium* sp. associated with red alga *Porphyra yezoensis*. *Curr. Microbiol.* 56, 229–235. doi: 10.1007/s00284-007-9063-y

Enya, J., Shinohara, H., Yoshida, S., Tsukiboshi, T., Negishi, H., and Suyama, K. (2007). Culturable leaf-associated bacteria on tomato plants and their potential as biological control agents. *Microb. Ecol.* 53, 524–536. doi: 10.1007/s00248-006-9085-1

Erlacher, A., Cardinale, M., Grosch, R., Grube, M., and Berg, G. (2014). The impact of the pathogen *Rhizoctonia solani* and its beneficial counterpart *Bacillus amyloliquefaciens* on the indigenous lettuce microbiome. *Front. Microbiol.* 5:175. doi: 10.3389/fmicb.2014.00175

Escalas, A., Hale, L., Voordeckers, J. W., Yang, Y., Firestone, M. K., Alvarez-Cohen, L., et al. (2019). Microbial functional diversity: from concepts to applications. *Ecol. Evol.* 9, 12000–12016. doi: 10.1002/ece3.5670

Fira, D., Dimkić, I., Berić, T., Lozo, J., and Stanković, S. (2018). Biological control of plant pathogens by *Bacillus* species. *J. Biotechnol.* 285, 44–55. doi: 10.1016/j.jbiotec.2018.07.044

Gao, L., Ma, J., Liu, Y., Huang, Y., Mohamad, O. A. A., Jiang, H., et al. (2021). Diversity and biocontrol potential of cultivable endophytic bacteria associated with halophytes from the west Aral sea basin. *Microorganisms* 9:1448. doi: 10.3390/microorganisms9071448

Gobbi, A., Kyrkou, I., Filippi, E., Ellegaard-Jensen, L., and Hansen, L. H. (2020). Seasonal epiphytic microbial dynamics on grapevine leaves under biocontrol and copper fungicide treatments. *Sci. Rep.* 10:681. doi: 10.1038/s41598-019-56741-z

Grice, E. A., Kong, H. H., Conlan, S., Deming, C. B., Davis, J., and Young, A. C. (2009). Topographical and temporal diversity of the human skin microbiome. *Science* 324, 1190–1192. doi: 10.1126/science.1171700

Gu, L., Bai, Z., Jin, B., Hu, Q., Wang, H., Zhuang, G., et al. (2010). Assessing the impact of fungicide enostroburin application on bacterial community in wheat phyllosphere. *J. Environ. Sci.* 22, 134–141. doi: 10.1016/s1001-0742(09)60084-x

Gupta, A., Verma, J., Srivastava, A., Srivastava, S., and Prasad, V. (2021). A comparison of induced antiviral resistance by the phytoprotein CAP-34 and isolate P1f of the rhizobacterium *Pseudomonas putida*. *3 Biotech* 11:509. doi: 10.1007/s13205-021-03057-3

Han, L., Wang, Z., Li, N., Wang, Y., Feng, J., and Zhang, X. (2018). *Bacillus amyloliquefaciens* B1408 suppresses fusarium wilt in cucumber by regulating the rhizosphere microbial community. *Appl. Soil Ecol.* 136, 55–66. doi: 10.1016/j.apsoil.2018.12.011

Han, X., Shen, D., Xiong, Q., Bao, B., Zhang, W., Dai, T., et al. (2021). The plant beneficial rhizobacterium *Bacillus velezensis* FZB42 controls the soybean pathogen *Phytophthora sojae* due to bacilysin production. *Appl. Environ. Microbiol.* 87:e0160121. doi: 10.1128/AEM.01601-21

Hu, J., Zheng, M., Dang, S., Shi, M., Zhang, J., and Li, Y. (2021). Biocontrol potential of *Bacillus amyloliquefaciens* LYZ69 against anthracnose of alfalfa (*Medicago sativa*). *Phytopathology* 111, 1338–1348. doi: 10.1094/PHYTO-09-20-0385-R

Huang, K., Tang, J., Zou, Y., Sun, X., Lan, J., Wang, W., et al. (2021). Whole genome sequence of *Alternaria alternata*, the causal agent of black spot of kiwifruit. *Front. Microbiol.* 12:713462. doi: 10.3389/fmicb.2021.713462

Hwang, B., Lim, S., Kim, B., Lee, J., and Moon, S. (2001). Isolation and in vivo and in vitro antifungal activity of phenylacetic acid and sodium phenylacetate from *Streptomyces humidus*. *Appl. Environ. Microbiol.* 67, 3739–3745. doi: 10.1128/AEM.67.8.3739-3745.2001

Innerebner, G., Knief, C., and Vorholt, J. A. (2011). Protection of *Arabidopsis thaliana* against leaf-pathogenic *Pseudomonas syringae* by *Sphingomonas* strains in a controlled model system. *Appl. Environ. Microbiol.* 77, 3202–3210. doi: 10.1128/AEM.00133-11

Jiang, M., Xu, X., Song, J., Li, D., Han, L., Sun, X., et al. (2021). *Streptomyces botrytidirepellens* sp. nov., a novel actinomycete with antifungal activity against *Botrytis cinerea*. *Int. J. Syst. Evol. Microbiol.* 71. doi: 10.1099/ijsem.0.005004

Jones, B. M., and Kustka, A. B. (2017). A quantitative SMRT cell sequencing method for ribosomal amplicons. *J. Microbiol. Methods* 135, 77–84. doi: 10.1016/j.mimet.2017.01.017

Kang, B. R., Park, J. S., and Jung, W. J. (2021). Antiviral activity by lecithin-induced fengycin lipopeptides as a potent key substrate against cucumber mosaic virus. *Microb. Pathog.* 155:104910. doi: 10.1016/j.micpath.2021.104910

Kim, Y., Cho, J., Kuk, J., Moon, J., Cho, J., and Kim, Y. (2004). Identification and antimicrobial activity of phenylacetic acid produced by *Bacillus licheniformis* isolated from fermented soybean, Chungkook-Jang. *Curr. Microbiol.* 48, 312–317. doi: 10.1007/s00284-003-4193-3

Klindworth, A., Pruesse, E., Schweer, T., Peplies, J., Quast, C., Horn, M., et al. (2013). Evaluation of general 16S ribosomal RNA gene PCR primers for classical and next-generation sequencing-based diversity studies. *Nucleic Acids Res.* 41:e1. doi: 10.1093/nar/gks808

Kumar Yadav, V., Krishna Jha, R., Kaushik, P., Altalayan, F. H., Al Balawi, T., and Alam, P. (2021). Traversing arbuscular mycorrhizal fungi and *Pseudomonas fluorescens* for carrot production under salinity. *Saudi J. Biol. Sci.* 28, 4217–4223. doi: 10.1016/j.sjbs.2021.06.025

Langille, M. G., Zaneveld, J., Caporaso, J. G., McDonald, D., Knights, D., Reyes, J. A., et al. (2013). Predictive functional profiling of microbial communities using 16S rRNA marker gene sequences. *Nat. Biotechnol.* 31, 814–821. doi: 10.1038/nbt.2676

Li, B. D. (2018). *The Study of the Control Effects of Two Biological Control Agents (Paenibacillus polymyxa and Pseudomonas fluorescens) on Tobacco Bacterial Wilt*. Master's thesis. Chongqing: Southwest University.

Li, Y., and Tan, H. (2017). Biosynthesis and molecular regulation of secondary metabolites in microorganisms. *Sci. China Life Sci.* 60, 935–938. doi: 10.1007/s11427-017-9115-x

Liu, H., Chen, J., Xia, Z., An, M., and Wu, Y. (2020). Effects of ε-poly-l-lysine on vegetative growth, pathogenicity, and gene expression of *Alternaria alternata* infecting *Nicotiana tabacum*. *Pestic. Biochem. Physiol.* 163, 147–153. doi: 10.1016/j.pestbp.2019.11.005

Luo, L., Zhang, Z., Wang, P., Han, Y., Jin, D., Su, P., et al. (2019). Variations in phyllosphere microbial community along with the development of angular leaf-spot of cucumber. *AMB Express* 9:76. doi: 10.1186/s13568-019-0800-y

Marchesi, J. R., Sato, T., Weightman, A. J., Martin, T. A., Fry, J. C., Hiom, S. J., et al. (1998). Design and evaluation of useful bacterium-specific PCR primers that amplify genes coding for bacterial 16S rRNA. *Appl. Environ. Microbiol.* 64, 795–799. doi: 10.1128/AEM.64.2.795-799.1998

Mateus, J. R., Marques, J. M., Dal'Rio, I., Vollú, R. E., Coelho, M. R. R., and Seldin, L. (2019). Response of the microbial community associated with sweet

potato (*Ipomoea batatas*) to *Bacillus safensis* and *Bacillus velezensis* strains. *Antonie Van Leeuwenhoek* 112, 501–512. doi: 10.1007/s10482-018-1181-y

Mattos, B. B., Montebianco, C., Romanel, E., da Franca, T., Bernabé, R. B., Simas-Tosin, F., et al. (2018). A peptidogalactomannan isolated from *Cladosporium herbarum* induces defense-related genes in BY-2 tobacco cells. *Plant Physiol. Biochem*. 126, 206–216. doi: 10.1016/j.plaphy.2018.02.023

Maucher, M., Kracher, B., Kühl, M., and Kestler, H. A. (2011). Inferring Boolean network structure via correlation. *Bioinformatics* 27, 1529–1536. doi: 10.1093/bioinformatics/btr166

Mazzola, M. (2004). Assessment and management of soil microbial community structure for disease suppression. *Annu. Rev. Phytopathol.* 42, 35–59. doi: 10.1146/annurev.phyto.42.040803.140408

Morelli, L., and Pellegrino, P. (2021). A critical evaluation of the factors affecting the survival and persistence of beneficial bacteria in healthy adults. *Benef. Microbes* 12, 15–25. doi: 10.1094/PHYTO-09-16-0330-RVW

Palmieri, D., Vitullo, D., De Curtis, F., and Lima, G. (2016). A microbial consortium in the rhizosphere as a new biocontrol approach against *Fusarium* decline of chickpea. *Plant Soil* 412, 425–439. doi: 10.1007/s11104-016-3080-1

Pan, Z., Munir, S., Li, Y., He, P., He, P., and Wu, Y. (2021). Deciphering the *Bacillus amyloliquefaciens* B9601-Y2 as a potential antagonist of tobacco leaf mildew pathogen during flue-curing. *Front. Microbiol.* 12:683365. doi: 10.3389/fmicb.2021.683365

Parks, D. H., Tyson, G. W., Hugenholtz, P., and Beiko, R. G. (2014). STAMP: statistical analysis of taxonomic and functional profiles. *Bioinformatics* 30, 3123–3124. doi: 10.1093/bioinformatics/btu494

Paul, D., and Park, K. (2013). Identification of volatiles produced by *Cladosporium cladosporioides* CL-1, a fungal biocontrol agent that promotes plant growth. *Sensors* 13, 13969–13977. doi: 10.3390/s131013969

Podolich, O., Ardanov, P., Zaets, I., Pirttilä, A. M., and Kozyrovska, N. (2015). Reviving of the endophytic bacterial community as a putative mechanism of plant resistance. *Plant Soil* 388, 367–377. doi: 10.1007/s11104-014-2235-1

Raina, A., Sahu, P. K., Laskar, R. A., Rajora, N., Sao, R., Khan, S., et al. (2021). Mechanisms of genome maintenance in plants: playing it safe with breaks and bumps. *Front. Genet.* 12:675686. doi: 10.3389/fgene.2021.675686

Ren, X., Zhang, N., Cao, M., Wu, K., and Huang, Q. (2012). Biological control of tobacco black shank and colonization of tobacco roots by a *Paenibacillus polymyxa* strain C5. *Biol. Fertil. Soils* 48, 613–620. doi: 10.1007/s00374-011-0651-4

Roossinck, M. J. (2015). Plants, viruses, and the environment: ecology and mutualism. *Virology* 479-480, 271–277. doi: 10.1016/j.virol.2015.03.041

Sama, A., Mha, B., Ysm, A., Nan, B., and Ae, C. (2019). Biological control of root rot in lettuce caused by *Exserohilum rostratum* and *Fusarium oxysporum* via induction of the defense mechanism. *Biol. Control* 128, 76–84. doi: 10.1016/j.biocontrol.2018.09.014

Sánchez-Montesinos, B., Santos, M., Moreno-Gavíra, A., Marín-Rodulfo, T., Gea, F. J., and Diánez, F. (2021). Biological control of fungal diseases by *Trichoderma aggressivum* f. *europaeum* and its compatibility with fungicides. *J. Fungi* 7:598. doi: 10.3390/jof7080598

Segata, N., Izard, J., Waldron, L., Gevers, D., Miropolsky, L., Garrett, W. S., et al. (2011). Metagenomic biomarker discovery and explanation. *Genome Biol.* 12:R60. doi: 10.1186/gb-2011-12-6-r60

Shafi, S., Kamili, A. N., Shah, M. A., Bandh, S. A., and Dar, R. (2017). Dynamics of bacterial class *Bacilli* in the deepest valley lake of Kashmir-the Manasbal Lake. *Microb. Pathog.* 104, 78–83. doi: 10.1016/j.micpath.2017.01.018

Shi, L., Du, N., Shu, S., Sun, J., Li, S., and Guo, S. (2017). *Paenibacillus polymyxa* NSY50 suppresses *Fusarium* wilt in cucumbers by regulating the rhizospheric microbial community. *Sci. Rep.* 7:41234. doi: 10.1038/srep41234

Shi, L., Du, N., Yuan, Y., Shu, S., Sun, J., and Guo, S. (2016). Vinegar residue compost as a growth substrate enhances cucumber resistance against the Fusarium wilt pathogen *Fusarium oxysporum* by regulating physiological and biochemical responses. *Environ. Sci. Pollut. Res. Int.* 23, 18277–18287. doi: 10.1007/s11356-016-6798-7

Shi, M. D. (2019). *Mechanism research of Pseudomonas koreensis GS and Molecular Regulatory Mechanism of Streptomyces pactum Act12 on the Biocontrol Effect of Pseudomonas koreensis GS*. Master's thesis. Shaanxi: Northwest A&F University.

Sun, D., Qu, J., Huang, Y., Lu, J., and Yin, L. (2021). Analysis of microbial community diversity of muscadine grape skins. *Food Res. Int.* 145:110417. doi: 10.1016/j.foodres.2021.110417

Vogel, C., Innerebner, G., Zingg, J., Guder, J., and Vorholt, J. A. (2012). Forward genetic *in planta* screen for identification of plant-protective traits of *Sphingomonas* sp. strain Fr1 against *Pseudomonas syringae* DC3000. *Appl. Environ. Microbiol.* 78, 5529–5535. doi: 10.1128/AEM.00639-12

Vogel, M. A., Mason, O. U., and Miller, T. E. (2020). Host and environmental determinants of microbial community structure in the marine phyllosphere. *PLoS One* 15:e0235441. doi: 10.1371/journal.pone.0235441

Vorholt, J. A. (2012). Microbial life in the phyllosphere. *Nat. Rev. Microbiol.* 10, 828–840. doi: 10.1038/nrmicro2910

Vu, V. H., Li, X., Wang, M., Liu, R., Zhang, G., Liu, W., et al. (2019). Dynamics of fungal community during silage fermentation of elephant grass (*Pennisetum purpureum*) produced in northern Vietnam. *Asian-Australas. J. Anim. Sci.* 32, 996–1006. doi: 10.5713/ajas.18.0708

Wang, B., Wan, C., and Zeng, H. (2020). Colonization on cotton plants with a GFP labeled strain of *Bacillus axarquiensis*. *Curr. Microbiol.* 77, 3085–3094. doi: 10.1007/s00284-020-02071-7

Wang, J., Wang, Y., Zhao, T., Dai, P., and Li, X. (2017). Characterization of the pathogen causing a new bacterial vein rot disease in tobacco in China. *Crop Prot.* 92, 93–98. doi: 10.1016/j.cropro.2016.10.025

Wang, Y., Sheng, H. F., He, Y., Wu, J. Y., Jiang, Y. X., Tam, N. F., et al. (2012). Comparison of the levels of bacterial diversity in freshwater, intertidal wetland, and marine sediments by using millions of illumina tags. *Appl. Environ. Microbiol.* 78, 8264–8271. doi: 10.1128/AEM.01821-12

Wang, Y., Zhang, C., Liang, J., Wang, L., Gao, W., Jiang, J., et al. (2020). Surfactin and fengycin B extracted from *Bacillus pumilus* W-7 provide protection against potato late blight via distinct and synergistic mechanisms. *Appl. Microbiol. Biotechnol.* 104, 7467–7481. doi: 10.1007/s00253-020-10773-y

Wang, Z., Li, Y., Zhao, Y., Zhuang, L., Yu, Y., Wang, M., et al. (2021). A microbial consortium-based product promotes potato yield by recruiting rhizosphere bacteria involved in nitrogen and carbon metabolisms. *Microb. Biotechnol.* 14, 1961–1975. doi: 10.1111/1751-7915.13876

Wilkinson, T. J., Cowan, A. A., Vallin, H. E., Onime, L. A., Oyama, L. B., Cameron, S. J., et al. (2017). Characterization of the microbiome along the gastrointestinal tract of growing Turkeys. *Front. Microbiol.* 8:1089. doi: 10.3389/fmicb.2017.01089

Woudenberg, J. H., Seidl, M. F., Groenewald, J. Z., de Vries, M., Stielow, J. B., Thomma, B. P., et al. (2015). *Alternaria* section *Alternaria*: species, *formae speciales* or pathotypes? *Stud. Mycol.* 82, 1–21. doi: 10.1016/j.simyco.2015.07.001

Wu, X., Jiang, Q., Wang, Z., Xu, Y., Chen, W., Sun, J., et al. (2021). Diversity, enzyme production and antibacterial activity of *Bacillus* strains isolated from sesame-flavored liquor Daqu. *Arch. Microbiol.* 203, 5831–5839. doi: 10.1007/s00203-021-02552-8

Yang, F., Zhang, R., Wu, X., Xu, T., Ahmad, S., Zhang, X., et al. (2020). An endophytic strain of the genus *Bacillus* isolated from the seeds of maize (*Zea mays* L.) has antagonistic activity against maize pathogenic strains. *Microb. Pathog.* 142:104074. doi: 10.1016/j.micpath.2020.104074

Yang, H., Li, J., Xiao, Y., Gu, Y., Liu, H., Liang, Y., et al. (2017). An integrated insight into the relationship between soil microbial community and tobacco bacterial wilt disease. *Front. Microbiol.* 8:2179. doi: 10.3389/fmicb.2017.02179

You, C., Zhang, L. M., Ji, S. G., Gao, J. M., Zhang, C. S., and Kong, F. Y. (2014). Impact of biocontrol agent *Bacillus subtilis* on bacterial communities in tobacco rhizospheric soil. *Ying Yong Sheng Tai Xue Bao* 25, 3323–3330.

Zeng, Y., Liu, H., Zhu, T., Han, S., and Li, S. (2021). Preparation of nanomaterial wettable powder formulations of antagonistic bacteria from *Phellodendron chinense* and the biological control of brown leaf spot disease. *Plant Pathol. J.* 37, 215–231. doi: 10.5423/PPJ.OA.02.2021.0020

Zhang, N., Pan, R. H., Shen, Y. F., Yuan, J., Wang, L., Luo, X., et al. (2017). Development of a novel bio-organic fertilizer for plant growth promotion and suppression of rhizome rot in ginger. *Biol. Control* 114, 97–105. doi: 10.1016/j.biocontrol.2017.08.001

Zhang, Q., Geng, Z., Li, D., and Ding, Z. (2020). Characterization and discrimination of microbial community and co-occurrence patterns in fresh and strong flavor style flue-cured tobacco leaves. *Microbiologyopen* 9:e965. doi: 10.1002/mbo3.965

Zhang, X., Zhou, Y., Li, Y., Fu, X., and Wang, Q. (2017). Screening and characterization of endophytic *Bacillus* for biocontrol of grapevine downy mildew. *Crop Prot.* 96, 173–179. doi: 10.1016/j.cropro.2017.02.018

Zhou, L., Song, C., Muñoz, C. Y., and Kuipers, O. P. (2021). *Bacillus cabrialesii* BH5 protects tomato plants against *Botrytis cinerea* by production of specific antifungal compounds. *Front. Microbiol.* 12:707609. doi: 10.3389/fmicb.2021.707609

Zhou, L., Wang, Y., Xie, Z., Zhang, Y., Malhi, S. S., Guo, Z., et al. (2018). Effects of lily/maize intercropping on rhizosphere microbial community and yield of *Lilium davidii* var. *unicolor*. *J. Basic Microbiol.* 58, 892–901. doi: 10.1002/jobm.201800163

Zhu, Z., Peng, Q., Man, Y., Li, Z., Zhou, X., Bai, L., et al. (2020). Analysis of the antifungal properties of *Bacillus velezensis* B-4 through a bioassay and complete-genome sequencing. *Front. Genet.* 11:703. doi: 10.3389/fgene.2020.00703

Zhuang, L., Li, Y., Wang, Z., Yu, Y., Zhang, N., Yang, C., et al. (2021). Synthetic community with six *Pseudomonas* strains screened from garlic rhizosphere microbiome promotes plant growth. *Microb. Biotechnol.* 14, 488–502. doi: 10.1111/1751-7915.13640

Zhuang, W., Yu, X., Hu, R., Luo, Z., Liu, X., Zheng, X., et al. (2020). Diversity, function and assembly of mangrove root-associated microbial communities at a continuous fine-scale. *NPJ Biofilms Microbiomes* 6:52. doi: 10.1038/s41522-020-00164-6

Advantages of publishing in Frontiers

OPEN ACCESS
Articles are free to read for greatest visibility and readership

FAST PUBLICATION
Around 90 days from submission to decision

HIGH QUALITY PEER-REVIEW
Rigorous, collaborative, and constructive peer-review

TRANSPARENT PEER-REVIEW
Editors and reviewers acknowledged by name on published articles

Frontiers
Avenue du Tribunal-Fédéral 34
1005 Lausanne | Switzerland

Visit us: www.frontiersin.org
Contact us: frontiersin.org/about/contact

REPRODUCIBILITY OF RESEARCH
Support open data and methods to enhance research reproducibility

DIGITAL PUBLISHING
Articles designed for optimal readership across devices

FOLLOW US
@frontiersin

IMPACT METRICS
Advanced article metrics track visibility across digital media

EXTENSIVE PROMOTION
Marketing and promotion of impactful research

LOOP RESEARCH NETWORK
Our network increases your article's readership